Synthesis of Fused N-Heterocycles via Tandem Alkenyl/Alkynyl Cyclization Reactions

A dissertation submitted in partial fulfillment for the degree of

Doctor of Philosophy

Submitted by

Pallav Jyoti Arandhara

Roll No.: 196122103

Under the Supervision of

Prof. Anil K. Saikia

Department of Chemistry

Indian Institute of Technology Guwahati

Guwahati–781039, Assam, India

July 2025

Dedicated to

My Beloved Parents

Indian Institute of Technology Guwahati
Department of Chemistry
North Guwahati,
Guwahati – 781039, India
e-mail: p.jyoti@iitg.ac.in

Pallav Jyoti Arandhara
Research Scholar

Declaration

I do hereby declare that the work presented in this thesis, titled ***"Synthesis of Fused N-Heterocycles via Tandem Alkenyl/Alkynyl Cyclization Reactions"*** is the result of my own research conducted in the Department of Chemistry, Indian Institute of Technology Guwahati, Assam, India, under the supervision of Prof. Anil K. Saikia. I have submitted this thesis to the Department of Chemistry, Indian Institute of Technology Guwahati for the award of the degree of Doctor of Philosophy.

Wherever the work of others has been cited, proper acknowledgements have been made in accordance with standard scientific practices. To the best of my knowledge, I also declare that this thesis has not been submitted elsewhere for any degree, diploma, or equivalent qualification at any institute or university.

Pallav jyoti Arandhara

Date: 21st July 2025
Place: IIT Guwahati

Pallav Jyoti Arandhara
Roll No.: 196122103

Indian Institute of Technology Guwahati
Department of Chemistry
North Guwahati,
Guwahati – 781039, India
Phone: +91 (361)2582316
Fax: +91 (361)2690762
e-mail: asaikia@iitg.ac.in

Dr. Anil K. Saikia, FRSC
Professor

Certificate

This is to certify that Mr. Pallav Jyoti Arandhara has been working under my supervision as a regular registered Ph.D. student since January 2020. The thesis entitled *"**Synthesis of Fused N-Heterocycles via Tandem Alkenyl/Alkynyl Cyclization Reactions**"* is an original record of the research carried out in the Department of Chemistry, Indian Institute of Technology Guwahati, Assam, India. I am forwarding the thesis for the award of the degree of Doctor of Philosophy in Chemistry at this institute. I also certify that Pallav has fulfilled all the requirements as per the institute's regulations regarding the investigations embodied in his thesis, and the work has not been submitted elsewhere for any degree.

Date: 21st July 2025
Place: IIT Guwahati

Prof. Anil K. Saikia
Thesis Supervisor

~Acknowledgments~

The journey of a Ph.D. is never a solitary endeavor—it is shaped and supported by the presence, guidance, and kindness of many individuals whose contributions, in different forms, have made this achievement possible. As I reach the culmination of this important chapter in my life, it is a pleasant aspect that now I have taken this opportunity to express my heartfelt gratitude to each one who has been a part of this journey directly or indirectly.

First and foremost, I express my sincere thanks and deepest appreciation to my research supervisor, ***Prof. Anil Kumar Saikia****, for his mentorship, guidance, and encouragement throughout my research period. His expertise, patience, and constructive feedback have been instrumental in shaping the direction and quality of this thesis.*

I am also truly grateful to the members of my doctoral committee ***Prof. Aditya Narayan Panda*** *(Chairperson),* ***Prof. Shyam Prosad Biswas*** *and* ***Prof. Dipankar Srimani*** *for their timely evaluation of my annual progress, thoughtful feedback, and valuable suggestions, which have greatly contributed to the quality and clarity of my thesis. I extend my sincere thanks to all the faculty and staff members of the Department of Chemistry, IIT Guwahati for their kind cooperation, and readiness to help whenever needed.*

I sincerely express gratitude to the ***University Grants Commission*** *(UGC), India, for the financial support throughout my doctoral studies, and IIT Guwahati for providing all the necessary facilities that enabled my research. I am also thankful to the Central Instrument Facility (CIF) and NECBH, IIT Guwahati, for the instrument facilities like NMR and HRMS.*

I truly acknowledge all the members of the IITG staff in general, for their valuable services. In particular, my heartfelt thanks go to ***Mr. Imdadul Islam*** *(Technical Superintendent, Department of Chemistry),* ***Dr. Kh. Kesho Singh*** *(Technical Superintendent, CIF),* ***Mr. Bhaskar Jyoti Hazarika*** *(Instrument Operator, HRMS CIF),* ***Dr. Babulal Das*** *(Technical Officer, CIF), and* ***Dr. K. K. Senapati*** *(Sr. Technical Officer, Department of Chemistry) for their frequent help whenever needed during my tenure. Again, I'm indebted to all my fellow operators of NMR (Department of Chemistry) and HRMS (CIF) and also SCXRD operators (Department of Chemistry) and NMR operators (NECBH) for their kind assistance in sample analysis and data collection.*

I consider myself lucky to have shared this journey with such a fantastic group of colleagues. I would like to express my deepest gratitude to all my past and present lab mates, who have been an integral part, making this journey both productive and memorable. Their constant support, insightful discussions, and cheerful companionship have made the lab a motivating and enjoyable place to work in. Among them, I owe special thanks to ***Archana****, who holds a truly special place. Her presence has been nothing short of a blessing, she has stood by me like her own, offering not just help, but genuine care, patience, and encouragement at every step. In moments of doubt and difficulty, she was the one who kept me going. I can say with complete honesty that without her, this journey would have been incredibly difficult. Her unwavering support has been a pillar of strength for me, and I will always remain deeply grateful for everything she has done. She is, in every sense, one of the key reasons behind the successful completion of this thesis. I am also indebted to all my seniors:* ***Dr. Upasana Borthakur****,* ***Dr. Namita Devi****,* ***Malay Das****,* ***Dr. Archana Kumari Sahu****,* ***Dr. Bipin Kumar Behera****,* ***Dr. Sudip Shit****,* ***Dr. Subhamoy Biswas*** *and* ***Dr. Bikoshita Porashar*** *for their guidance, support and suggestions during my earlier phase in the lab. I want to heartily appreciate all my juniors* ***Hunmoina****,* ***Ankita****,* ***Chinmayee*** *and* ***Manas*** *for their constant support, help and for maintaining a friendly environment in the lab.*

I am deeply grateful to my friends, seniors, and juniors both on and off campus for their constant support, care, and encouragement throughout this journey. Their presence and kind words meant a lot to me and helped me stay strong during challenging times. I wish to thank ***Dr. Chiranjib Gogoi****,* ***Dr. Nikita Chakraborty****,* ***Dr. Raktim Gogoi****,* ***Dr. Pranjyoti Saikia****,* ***Dr. Hemanat Boruah****,* ***Dr. Indraneel Debnath****,* ***Dr. Somnath Paik****,* ***Dr. Monuranjan Gogoi****,* ***Dr. Bubul Das****,* ***Dr. Jagnyesh K. Satpathy****,* ***Rabu****,* ***Sukesh****,* ***Anjela****,* ***Mithu****,* ***Ujjwal****,* ***Neichoi****,* ***Prangan****,* ***Hirok****,* ***Nandan****,* ***Rahul****,* ***Sangay****,* ***Partha****,* ***Gunanka****,* ***Suravi****,* ***Hemanta****,* ***Satyendra****,* ***Amrit****,* ***Hrishikesh****,* ***Asish****,* ***Manash****,* ***Imran****,* ***Rohit****,* ***Kritanjali****,* ***Kaushik****,* ***Anol****.*

The role of a teacher in shaping one's academic journey and personal growth is truly invaluable. I feel immensely fortunate to have been guided by inspiring and dedicated mentors. I would like to express my profound gratitude to all my respected teachers from these formative years for their unwavering support, insightful guidance, and the lasting impact they have had on my academic path.

I would also like to thank the Central Gym, IIT Guwahati for helping me stay physically and mentally balanced throughout this journey. The discipline and motivation I

found there made a significant difference during challenging times. Special mention to Mr. ***Mridul Ray*** *(Gym trainer),* ***Mr. Riju Mahato*** *(Junior Superintendent),* ***Prof. Charudatt Y. Kadolkar*** *(Department of Physics),* ***Prof. Prabir Barooah*** *(Department of EEE),* ***Suvendu****, and* ***Surya****, whose constant motivation, friendly encouragement, and shared dedication truly inspired me and kept me going. My heartfelt thanks also goes to my Kapili hostel mates specially* ***Ayush****,* ***Sahil****,* ***Kalpa****,* ***Bishwa****,* ***Satyajit****,* ***Dinabandhu****,* ***Mrinal****,* ***Subham****,* ***Arijit****, whose friendship, constant support, and positive energy created a homely environment that kept me going every day.*

With immense appreciation, I thank my mother ***Malaya Arandhara****, my father* ***Pradip K. Arandhara****, my sister* ***Pinky*** *and my beloved niece* ***Kiskindhya*** *(Emon), whose unwavering support, unconditional love, and constant faith in me have been the foundation of my strength throughout this journey. Their endless encouragement, patience, and belief in my abilities kept me motivated during the most challenging times.*

I bow in gratitude to the ***Almighty God****, whose divine grace and blessings have guided me through every step of this journey. I am truly thankful for the wisdom, patience, and resilience I have been granted, and I humbly acknowledge His presence in all that I have achieved.*

Sincerely,

Pallav

Contents

Abstract

The contents of the present thesis, titled "***Synthesis of Fused N-Heterocycles via Tandem Alkenyl/Alkynyl Cyclization Reactions***" is divided into five chapters, each based on the outcomes of the experimental work/studies carried out during the Ph.D. research period.

Chapter 1 covers an overview of heterocyclic compounds, with a primary focus on *N*-heterocycles, importance of fused *N*-heterocyclic compounds, tandem reactions, and the utility and reactivity of alkenes and alkynes. This briefly discusses tandem reactions and their applications in constructing diverse fused *N*-heterocycles. It also emphasizes the reactivity and use of alkenes and alkynes in acid-, base-, or metal-catalyzed/promoted tandem or cascade reactions for synthesizing highly functionalized fused *N*-heterocycles. Overall, this chapter aims to provide a comprehensive insight into tandem strategies, the role of alkene/alkyne functionalities, and their significance in the synthesis of complex *N*-heterocycles within the field of organic chemistry.

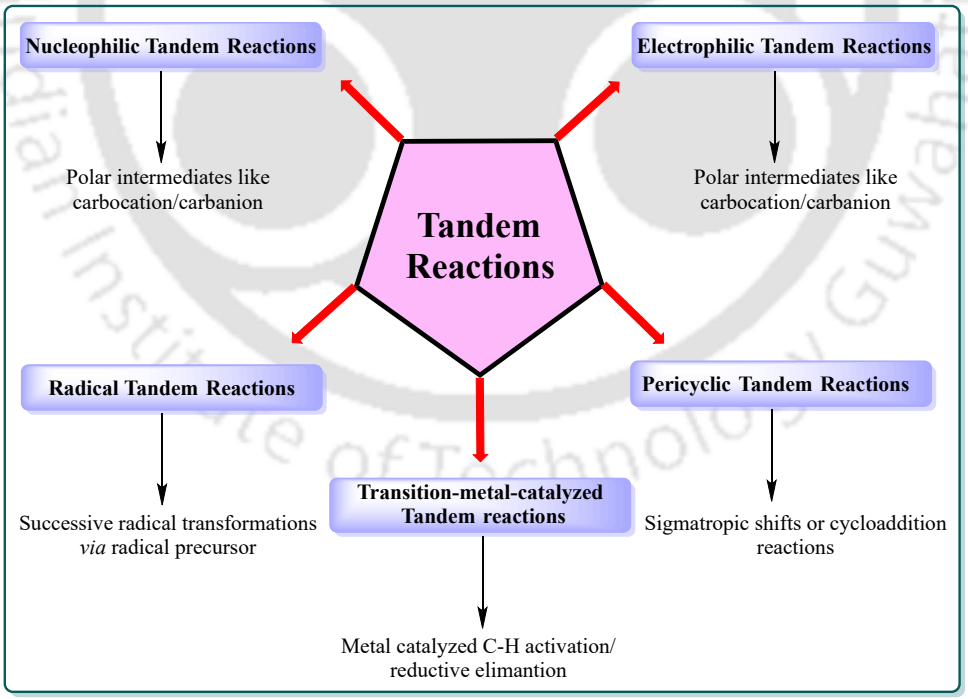

Chapter 2 describes an efficient transition-metal-free one-pot synthesis of dihydro[1,2,3]triazolo-pyrimidoisoindolone and dihydro[1,2,3]triazolo-diazepinoisoindolone scaffolds from *N*-alkynyl-3-hydroxyisoindolinones and sodium azide (NaN_3), utilizing

the reactive intermediate *N*-acyliminium ion and Huisgen reaction. The reaction is mediated by an inexpensive Lewis acid borontrifluoride diethyl etherate ($BF_3{\cdot}OEt_2$) in *N*,*N*-dimethylformamide (DMF) at 130 °C. The protocol provides a simple route for the synthesis of functionalized 1,2,3-triazole-fused *N*-heterocycles in moderate to good yields. The methodology can further be extended towards the synthesis of its thione derivative dihydro[1,2,3]triazolo-pyrimidoisoindolthione *via* thionation of amide.

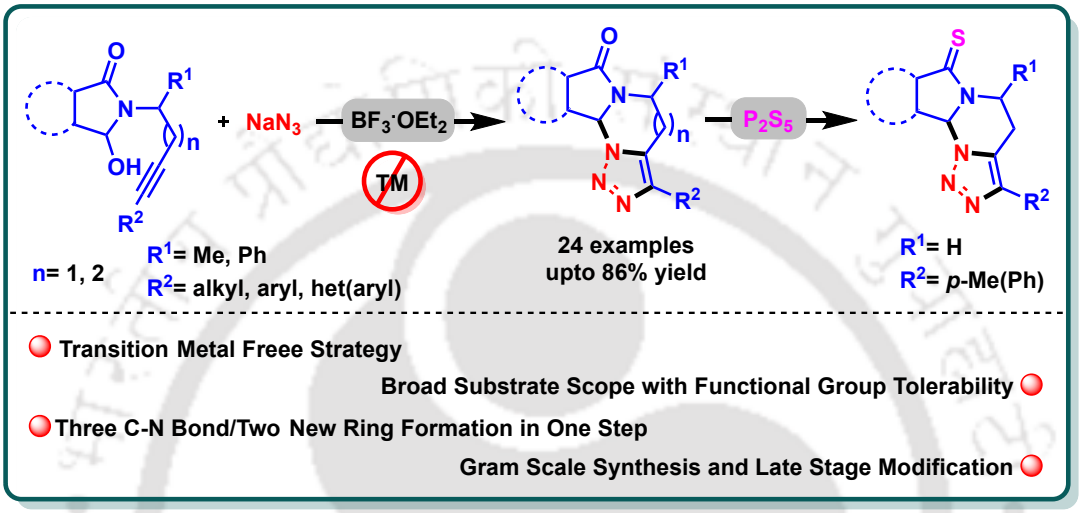

Org. Biomol. Chem. **2023**, *21*, 8772–8781.

Chapter 3 outlines the streamlined synthesis of structurally fused 6-iminoisoindoloindolones *via* a cascade reaction in remarkable yields. The reaction proceeds through intermolecular tandem alkynyl cyclization reaction of 2-alkynylanilines with 2-formylbenzaldehydes for the construction of iminoisoindoloindolone derivatives under the catalytic action of a Lewis acid. The protocol utilizes trimethylsilyl trifluoromethanesulfonate (TMSOTf) as a Lewis acid which effectively activates the nitrile group and H_2O as a nucleophile under open air condition. The methodology can be further utilized for the synthesis of bioactive isoindoloindolone as well as unprecedented diphenylbenzopyrrolizinoisoquinolinone derivatives in good yields.

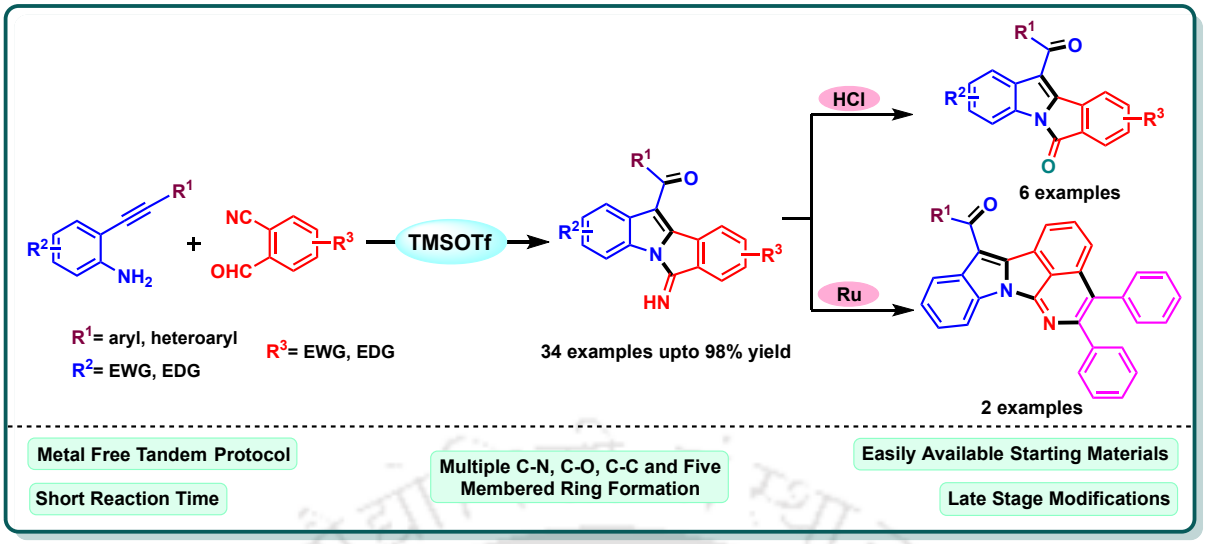

J. Org. Chem. **2024**, *89*, 12128–12142.

Chapter 4 highlights a facile and efficient synthesis of structurally diverse pseudoindoxyls *via* indole-assisted Michael/Domino reaction of 2-nitrobenzylidenemalonates and indoles. The reaction is promoted by an inorganic base giving good to excellent yields. The reaction proceeds *via* Michael addition followed by nucleophilic addition-elimination and hydrolysis, where eco-friendly H_2O acts as an oxygen source in a cascade fashion. The developed methodology is a transition-metal-free novel and sustainable approach for the construction of pseudoindoxyl scaffolds with various functional group compatibility. The synthetic utility of the protocol was demonstrated by late-stage functionalization of the products, and photophysical properties have also been studied for some synthesized compounds.

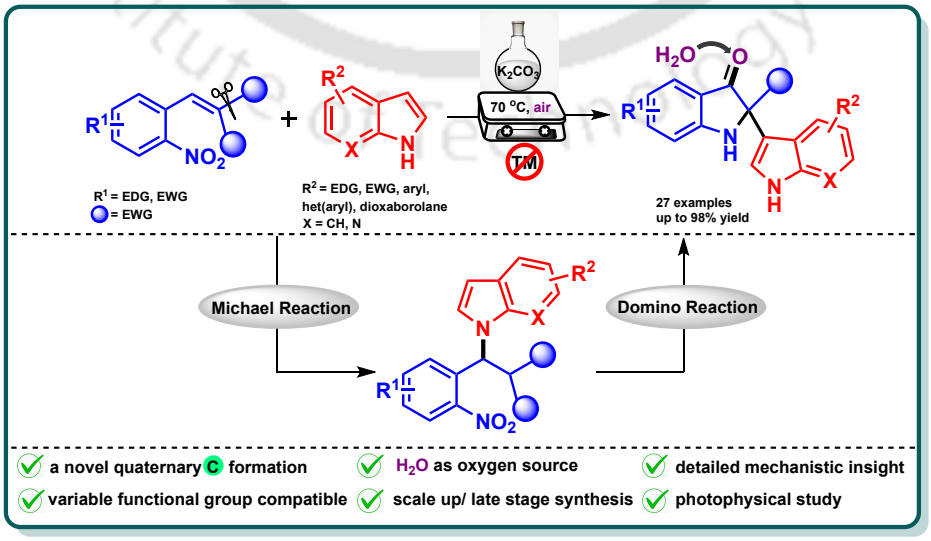

Org. Lett. **2025**, *27*, 6641–6647.

Chapter 5 represents a highly efficient and substrate-dependent methodology utilizing 2-alkynylcyclopropanes as a key substrate which undergoes tandem annulation with 2-azidobenzonitriles and 2-azidobenzaldehydes separately under Lewis acidic condition to provide 1,6-naphthyridine and isochromeno[4,3-*c*]quinoline frameworks, respectively, in excellent yields. Utilizing only a Lewis acid and easily available starting materials, it proficiently constructs highly fused *N*-heterocycles promising simplicity and advancement in the proposed protocol.

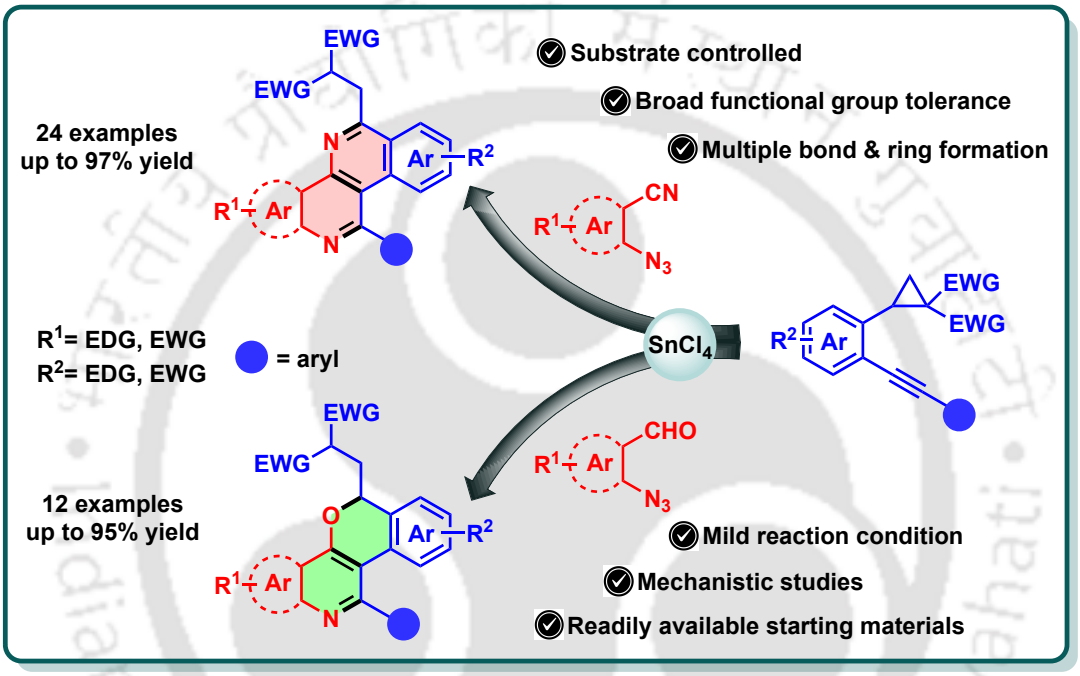

Manuscript Under Communication.

Chapter 6 summarizes the key outcomes of the thesis, which focuses on the efficient and practical synthesis of diverse fused *N*-heterocycles of biological relevance. Various 1,2,3-triazole-fused isoindolone, isoindoloindolone, pseudoindoxyl, 1,6-naphthyridine, as well as isochromenoquinoline based frameworks were developed through metal-free, Lewis acid-catalyzed/mediated, and base-promoted reactions. The methods are straightforward, scalable, and follow a tandem reaction pathway. The structural features of these compounds offer opportunities for further modifications, biological evaluations, and potential applications in drug discovery and catalysis. The chapter also highlights future directions to expand the scope and impact of the present works.

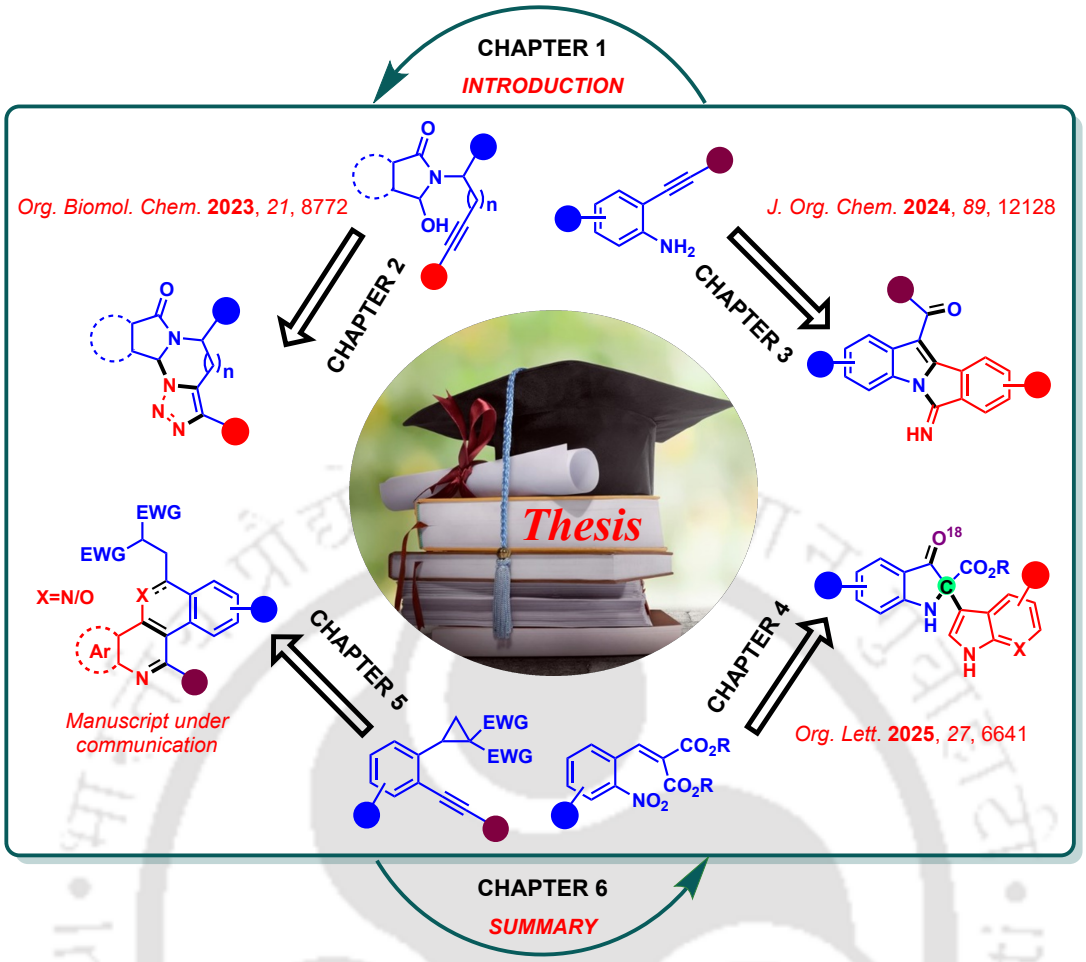
CHAPTER 1
INTRODUCTION
Org. Biomol. Chem. 2023, 21, 8772
J. Org. Chem. 2024, 89, 12128
CHAPTER 2
CHAPTER 3
Thesis
Manuscript under communication
Org. Lett. 2025, 27, 6641
CHAPTER 5
CHAPTER 4
CHAPTER 6
SUMMARY

List of Abbreviations

DFT	Discrete Fourier Transform	$Pd(OAc)_2$	Palladium(II) acetate
TBHP	*tert*-Butyl hydroperoxide	CH_3CN	Acetonitrile
DMF	*N*,*N*-Dimethylformamide	KO^tBu	Potassium *tert*-butoxide
LED	Light Emitting Diode	$BF_3{\cdot}OEt_2$	Boron trifluoride diethyl etherate
AgOTf	Silver trifluoromethanesulfonate	$Cu(OAc)_2$	Copper(II) acetate
AcOH	Acetic acid	MAO-B	Monoamine oxidase B
MCR	Multicomponent reaction	TMSOTf	Trimethylsilyl trifluoromethanesulfonate
Me	Methyl	Ph	Phenyl
COSY	Correlated Spectroscopy	nOe	Nuclear Overhauser Effect
HRMS	High-Resolution Mass Spectrometry	NMR	Nuclear Magnetic Resonance
CCDC	Cambridge Crystallographic Data Centre	ORTEP	Oak Ridge Thermal Ellipsoid Plot Program
$CDCl_3$	Deuterated chloroform	XRD	X-ray Diffraction
TLC	Thin Layer Chromatography	Q-TOF	Quadrupole Time-of-Flight
DIAD	Diisopropyl azodicarboxylate	$NaBH_4$	Sodium borohydride
$NaHCO_3$	Sodium bicarbonate	Na_2SO_4	Sodium sulfate
P_2S_5	Phosphorus pentasulfide	EtOAc	Ethyl acetate
EWG	Electron withdrawing group	EDG	Electron donating group
THF	Tetrahydrofuran	PIDA	Phenyliodine(III) diacetate
DCE	1,2-Dichloroethene	DCM	Dichloromethane
TfOH	Trifluoromethanesulfonic acid	*p*-TsOH	*p*-Toluenesulfonic acid
t-BuCN	*tert*-Butyl cyanide	$K_2S_2O_8$	Potassium persulfate
^{t}Bu	*tert*-butyl	HCl	Hydrochloric acid

t-AmOH	*tert*-Amyl alcohol	rt	Room temperature
NH_4Cl	Ammonium chloride	mp	Melting point
DMSO	Dimethyl sulfoxide	CueO	Copper efflux oxidase
H_2O_2	Hydrogen peroxide	CAN	Ceric ammonium nitrate
K_2CO_3	Potassium carbonate	NaH	Sodium hydride
DBU	1,8-Diazabicyclo[5.4.0]undec-7-ene	K_3PO_4	Potassium phosphate tribasic Potassium
TEMPO	2,2,6,6-Tetramethylpiperidine-1-oxyl	BHT	Butylated Hydroxytoluene
OLEDs	Organic Light Emitting Diodes	UV	Ultraviolet
EtOH	Ethanol	NaOH	Sodium hydroxide
HIV	Human immunodeficiency virus	DMA	Dimethylacetamide
DAC	Donor-Acceptor cyclopropane	ACP	2-Alkynylcyclopropane
$SnCl_4$	Tin(IV) chloride	$TiCl_4$	Titanium tetrachloride

Abbreviations for intensities of NMR signals

s	singlet	t	triplet
d	doublet	q	quartet
dd	doublet of doublet	m	multiplet
ddd	doublet of doublet of doublet	brs	broad signal
dt	doublet of triplet	Hz	Hertz
td	triplett of doublet	MHz	Mega-Hertz

General Information and Instrumentation

All chemicals were of reagent grade (AR grade) and used as purchased without further purification. Silica gel (60–120 mesh size) was used for column chromatography. Reactions were monitored by TLC on silica gel GF254 (0.25 mm). Melting points were recorded in an open capillary tube and are uncorrected. Fourier transform-infrared (FT-IR) spectra were recorded as neat liquids or KBr pellets. NMR spectra were recorded in $CDCl_3$ with tetramethylsilane as the internal standard for ^{1}H (600 MHz, 500 MHz, and 400 MHz) or $^{13}C\{^{1}H\}$ (150 MHz, 125 MHz, and 100 MHz) NMR. $^{19}F\{^{1}H\}$ NMR spectra were recorded at 470 MHz and chemical shifts are relative to hexafluorobenzene in $CDCl_3$ at δ = -164.9 ppm (external reference). Chemical shifts (δ) are reported in ppm with abbreviations, s = singlet, d = doublet, dd = doublet of doublets, ddd = doublet of doublets of doublets, dt = doublet of triplets, t = triplet, q = quartet, m = multiplet, brs = broad singlet and spin-spin coupling constants (J) are given in Hz. Structural assignments were made with additional information from single crystal XRD experiments. HRMS spectra were recorded using a Q-TOF mass spectrometer.

Bruker APEX-II CCD diffractometer was used to collect intensity data for X-ray crystallographic studies. The instrument is equipped with a fine focus 1.75 kW sealed tube Mo Kα radiation (λ = 0.71073 Å). APEX4 software was used for data acquisition as well as data integration and reduction. Multi-scan empirical absorption corrections were employed to the data using the same program. Structures were solved by direct methods using SHELXL-2019 software and refined with full-matrix least-squares on F2 using SHELXL-2019/1.[1] Structural illustrations have been drawn with ORTEP-3 for Windows.[2]

[1]Sheldrick, G. M. SHELXS-2014, Program for the crystal structure solution; University of Göttingen: Göttingen, Germany, **2014**.

[2]Farrugia, L. J. *WinGX* and *ORTEP* for *Windows*: an update. *J. Appl. Cryst.* **2012**, *45*, 849–854.

Chapter 1

An Overview of *N*-Heterocyclic Compounds and Tandem Reactions with Special Emphasis on Alkenes and Alkynes

Contents

Abstract: This chapter covers an overview of heterocyclic compounds, with a primary focus on *N*-heterocycles, importance of fused *N*-heterocyclic compounds, tandem reactions, and the utility and reactivity of alkenes and alkynes. This briefly discusses tandem reactions and their applications in constructing diverse fused *N*-heterocycles. It also emphasizes the reactivity and use of alkenes and alkynes in acid-, base-, or metal-catalyzed/promoted tandem or cascade reactions for synthesizing highly functionalized fused *N*-heterocycles. Overall, this chapter aims to provide a comprehensive insight into tandem strategies, the role of alkene/alkyne functionalities, and their significance in the synthesis of complex *N*-heterocycles within the field of organic chemistry.

1.1 Introduction to Heterocyclic Compounds

Heterocyclic compounds stand for a foundational class of organic molecules containing ring structures composed of carbon atoms and at least one heteroatom, typically nitrogen, oxygen, or sulfur. These heteroatoms introduce unique electronic and steric properties to the ring, significantly affecting the reactivity, stability, and overall behavior of the molecules. Based on their degree of saturation and π-conjugation, heterocycles are commonly divided into aromatic and aliphatic categories.[1] Aromatic heterocycles such as pyrrole (**1**), furan (**2**), thiophene (**3**), and pyrazine (**4**) (*Figure 1.1.1*) are stabilized through delocalized π-electron systems and conform to Hückel's rule, which accounts for their broad synthetic utility.

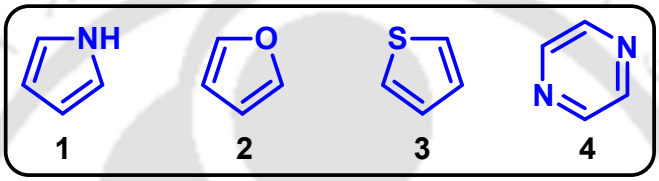

Figure 1.1.1. *Some examples of aromatic heterocyclic compounds.*

However, aliphatic heterocycles like tetrahydrofuran (**5**), tetrahydrothiophene (**6**), piperidine (**7**), and imidazolidine (**8**) (*Figure 1.1.2*), in contrast, exhibit saturated or partially saturated structures and offer different reactivity profiles compared to their aromatic counterparts. They represent a cornerstone in medicinal chemistry due to their structural diversity and wide-range of biological activities.

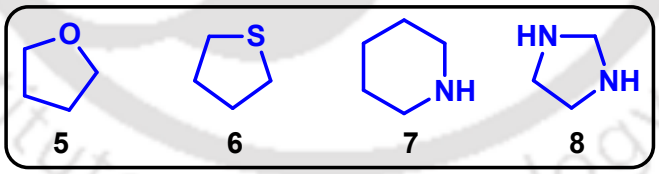

Figure 1.1.2. *Some examples of aliphatic heterocyclic compounds.*

These compounds, characterized by rings containing heteroatoms like nitrogen, oxygen, or sulfur, form the backbone of essential biomolecules such as DNA, RNA, and vitamins, and are integral to modern drug design.[2] Their synthetic versatility enables applications across multiple therapeutic domains, such as triazine and benzimidazole derivatives exhibit antimicrobial, antifungal, and antibacterial properties,[3a,b] while chalcone-based heterocycles and pyrimidine analogues demonstrate anti-inflammatory and anticonvulsant effects.[3c,d] Notably, phenanthroquinolizidine alkaloids and coumarin derivatives have shown potent anticancer activity by disrupting cell prolif-

eration in various cancer cell lines.[4] Additionally, heterocycles like 1,3,4-thiadiazoles and oxadiazoles contribute to antiviral, antidiabetic, and herbicidal applications, highlighting their adaptability in addressing emerging health challenges.[5] The pharmacological significance of these compounds is further underscored by their role in developing targeted therapies.

1.1.1 Introduction to *N*-Heterocyclic Compounds

Among heterocycles, nitrogen-containing heterocycles (*N*-heterocycles) are a key group of organic compounds that have one or more nitrogen atoms in their ring structure. They have unique chemical and biological properties and also play a central role in both natural and synthetic chemistry due to their enormous medicinal and industrial applications.[6] These scaffolds are widespread in nature and are integral to vital biomolecules such as nucleic acids, vitamins, and antibiotics, as well as many synthetic pharmaceuticals.[7] Their ability to form diverse interactions like hydrogen bonding and π-stacking that enables them to bind selectively to enzymes and receptors. This leads to their strong bioactivity and makes them valuable in drug discovery and medicinal chemistry. Statistically, about 60% of FDA-approved small-molecule drugs contain *N*-heterocyclic scaffolds due to their efficiency in modulating biological targets,[8a] which is significantly higher than those containing sulfur (26%) or fluorine (13%).[8b] These compounds exhibit a broad spectrum of pharmacological effects, including anticancer, antimicrobial, anti-inflammatory, and antiviral properties, making them invaluable in drug discovery and medicinal chemistry.[9] For example, pyrimidine (**9**) ring in DNA; pyrazoline **(10)** ring in compounds exhibiting anticancer, antimicrobial, and antitubercular activities; pyrrole (**11**) ring in heme (the oxygen-carrying component of hemoglobin); pyrazole (**12**) ring in anti-inflammatory agents; pyridine (**13**) ring in antitubercular and antihypertensive drugs; and 1,2,4-triazole (**14**) rings in antifungal and anticancer agents (*Figure 1.1.1.1*).

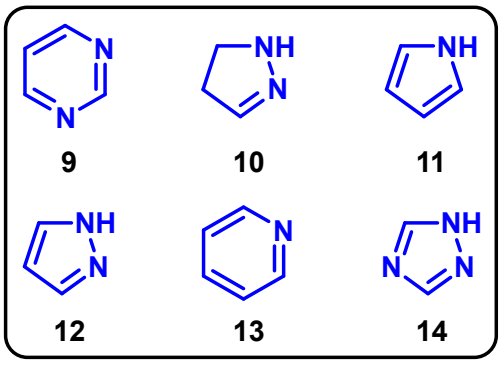

Figure 1.1.1.1. *Some biologically important N-heterocycles.*

All of these illustrate the broad utility and essential nature of *N*-heterocycles across scientific fields. Beyond biology and medicine, *N*-heterocycles also serve as building blocks in materials science and catalysis.[6,10] Their structural diversity and ability to interact selectively with biological molecules underscore the crucial role of *N*-heterocycles in advancing human health and technology.

1.1.2 Introduction to Fused *N*-Heterocycles

Fused nitrogen-containing heterocycles are a prominent subclass of *N*-heterocyclic compounds in which two or more rings share common atoms, forming rigid and often planar systems with extended conjugation. These fused systems, particularly those integrating aromatic or partially aromatic nitrogen heterocycles, are structurally complex and exhibit enhanced chemical stability, biological activity, and electronic versatility. Such characteristics make them invaluable in pharmaceuticals, agrochemicals, dyes, and functional materials.[11] From a pharmacological standpoint, fused *N*-heterocycles are the core frameworks of several natural products and drug molecules. For instance, indole (**15**), quinoline (**16**), benzazepine (**17**), pyrido[1,2-*a*]pyrimidine (**18**), and indoline (**19**) derivatives (*Figure 1.1.2.1*) are found in a variety of clinical agents with wide-ranging therapeutic properties such as anticancer (e.g., camptothecin), antimicrobial (e.g., ciprofloxacin), antitumor (e.g., berberine), antimalarial (e.g., chloroquine), anti-inflammatory (e.g., indomethacin), and CNS-active drugs (e.g., clozapine) etc.[12] Their reactivity often results from their planarity and ability to engage in π–π stacking, hydrogen bonding, and metal chelation within biological targets such as DNA, enzymes, and receptors.

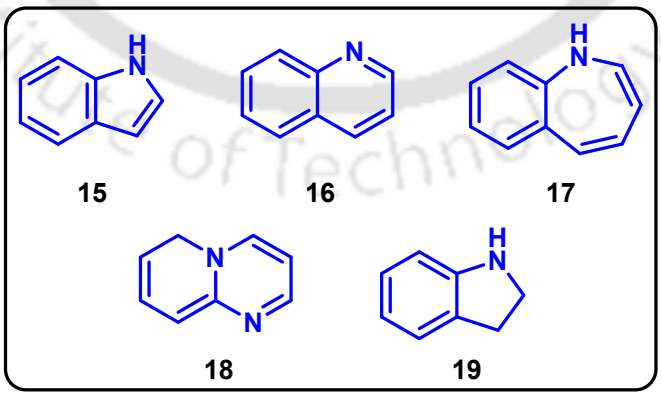

Figure 1.1.2.1. *Representative structures of biologically important fused N-heterocycles.*

1.1.3 Importance of Triazole Fused *N*-Heterocycle, Isoindoloindole, Pseudoindoxyl, 1,6-Naphthyridine, and Isochromeno[4,3-*c*]quinoline Scaffolds

Triazole-fused *N*-heterocycles are an important subgroup of *N*-heterocyclic compounds characterized by a five-membered aromatic ring composed of two carbon atoms and three nitrogen atoms. The two main isomers, 1,2,3-triazole and 1,2,4-triazole, can be fused with various carbocyclic or heterocyclic systems, creating versatile molecular frameworks. They are attractive candidates for drug design and materials science due to their structural diversity and ease of functionalization.[13] Triazole-fused *N*-heterocycles are recognized for their wide-range of biological effects. They serve as key scaffolds in many pharmaceuticals, such as anticancer, antifungal, antibacterial, antiviral, anticonvulsant, and anti-inflammatory agents.[14] For example, triazolobenzodiazepines (**20**) can be used as therapeutic agents in the treatment of depression,[15a] whereas triazolobenzodiazepine adinazolam (**21**) is also known as an antidepressant.[15b] Again, estazolam (**22**) is a tranquilizer medication of the triazolobenzodiazepine (TBZD) class[15c] (*Figure 1.1.3.1*).

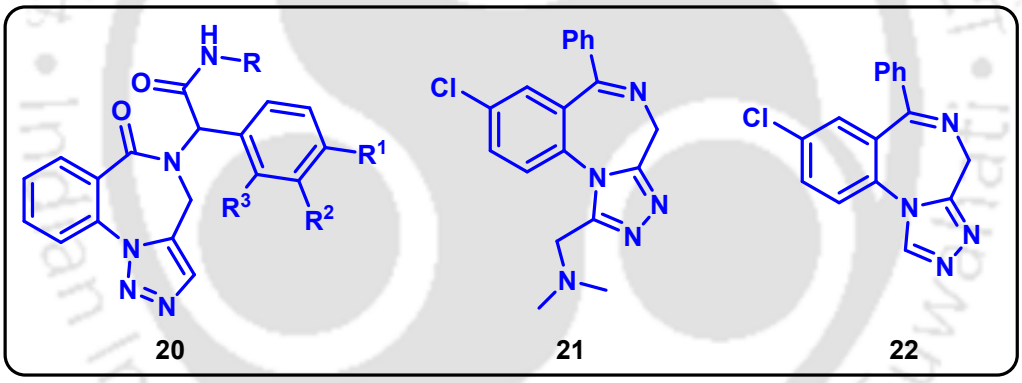

Figure 1.1.3.1. *Examples of bioactive triazole fused N-heterocycles.*

Similarly, isoindoloindoles, commonly referred to as isoindolinones, are bicyclic structures consisting of a benzene ring fused to a five-membered ring containing nitrogen. This core is present in various natural products and synthetic drugs, with notable pharmaceutical relevance.[16] They are highly valued for their multifunctional bioactivity. Recent studies have demonstrated that derivatives of isoindolinones can act as potent inhibitors of human carbonic anhydrase (hCA) isoforms I and II, with some compounds showing stronger inhibition than the standard drug acetazolamide.[17] Isoindolinones have been explored as antiviral agents, including activity against SARS-CoV-2 protease, and as scaffolds for enzyme inhibition relevant to diseases, including glaucoma, diabetes, and Alzheimer's disease.[18] Again, many synthetic pharmaceutical molecules containing isoindolinones are HIV-1 reverse transcriptase inhibitors (**23**),[19a]

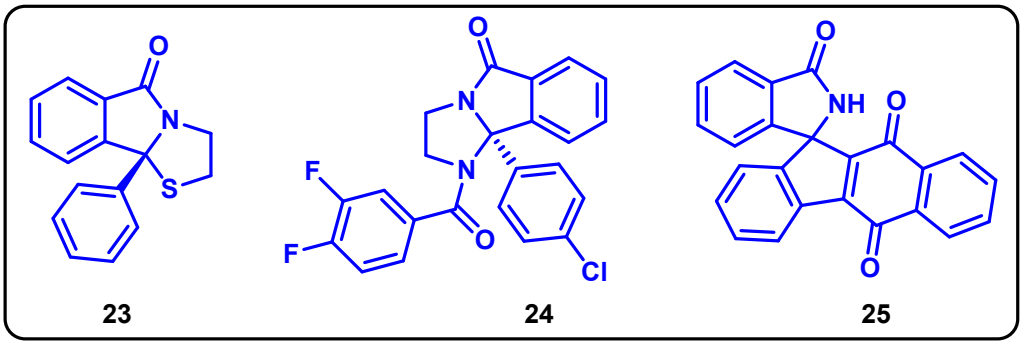

Figure 1.1.3.2. *Examples of bioactive isoindolinones.*

muscarinic acetylcholine receptor modulators (**24**),[19b] and anticancer agents (**25**)[19c] (*Figure 1.1.3.2*).

On the other hand, pseudoindoxyls are a unique subclass of oxygenated indole alkaloids, distinguished by a spirocyclic core structure. They are found in natural products such as mitragynine pseudoindoxyl, a metabolite of the kratom plant, and have attracted attention for their complex architecture and biological properties.[20] Mitragynine pseudoindoxyl demonstrates strong antinociceptive effects with reduced risks of tolerance, dependence, respiratory depression, and gastrointestinal side effects.[21] In addition to this, pseudoindoxyls are notable for their potent analgesic (pain-relieving) properties, often acting as mu-opioid receptor agonists with a favorable side effect profile compared to traditional opioids. Beyond analgesia, pseudoindoxyl derivatives have shown neuroprotective effects and the ability to inhibit monoamine oxidase B (MAO-B), indicating their potential for treating neurodegenerative diseases like Alzheimer's and Parkinson's disease.[22] Since 1947, several natural products containing the pseudoindoxyl scaffold have been isolated, some of which exhibit significant biological activity, for example, duocarmycin (**26**) (antitumour antibiotic activity),[23a] (–)-isatisine A (**27**) (anti-HIV activity),[23b] and rupicoline (**28**) (anti-cholinesterasic activity)[23c] (*Figure 1.1.3.3*).

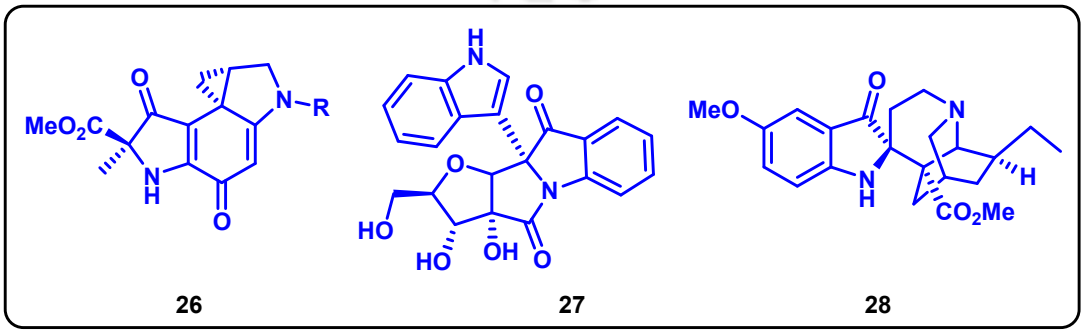

Figure 1.1.3.3. *Examples of bioactive pseudoindoxyls.*

Besides, 1,6-naphthyridine is a bicyclic heterocycle consisting of two fused pyridine rings, with nitrogen atoms located at the 1- and 6- positions. This scaffold is a part of the broader naphthyridine family, which is structurally related to naphthalene but with nitrogen substitution, and is widely explored in medicinal chemistry and also exhibits broad pharmacological properties.[24] Naturally derived naphthyridines, such as aaptamine display cytotoxic, antimicrobial, and neurological activities, further highlighting the scaffold's versatility.[25] Over the last few decades, the 1,6-naphthyridine structure has become important as a bicyclic aromatic core. These molecules have proven useful as inhibitors for various disorders, such as inhibitor for HIV integrase (**29**),[26a] phosphodiesterase 10A (PDE10A) (**30**),[26b] and FGF Receptor-1 Tyrosine Kinase (**31**)[26c] (*Figure 1.1.3.4*). Thus, they are versatile scaffolds with validated applications in oncology, immunology, and infectious diseases.

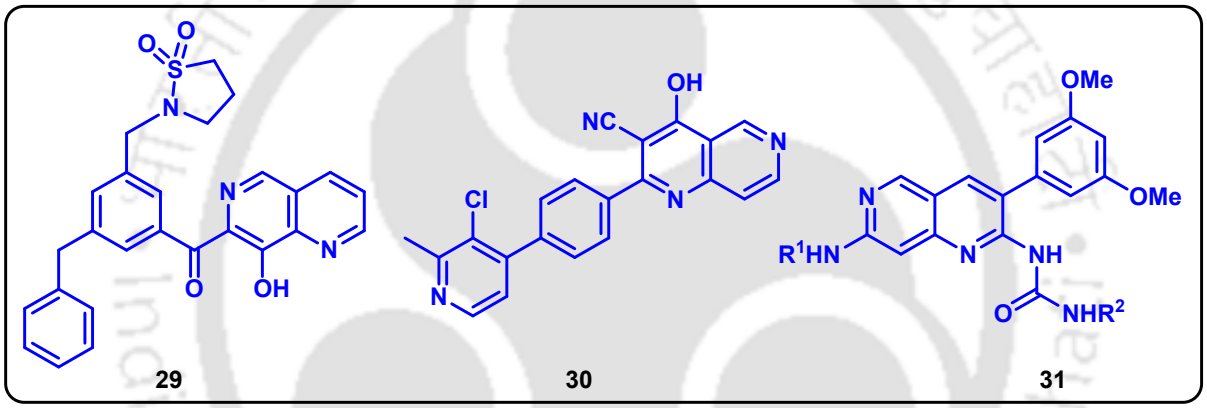

Figure 1.1.3.4. *Examples of bioactive 1,6-naphthyridines.*

Again, quinoline, a heterocyclic aromatic compound, has long served as a key framework in both medicinal and material chemistry because of its structural versatility and bioactive properties.[27] Among its derivatives, pyrano[3,2-*c*]quinoline (analogous to isochromeno[4,3-*c*]quinoline) has emerged as a privileged framework, combining quinoline's inherent stability with a fused pyran ring that enhances binding affinity and pharmacological potential.[28] For instance, huajiaosimuline (**32**) shows cytotoxicity against cancer cells,[29a] 5-phenyl-pyrano[3,2-*c*]quinoline-6-chloro-tacrine hybrid (**33**) demonstrates inhibitory activity against both acetylcholinesterase (AChE) and butyrylcholinesterase (BChE).[29b] Additionally, compound **34**, isolated from a Chaetomium funicola strain, acts as an inhibitor of metallo-β-lactamases[29c] (*Figure 1.1.3.5*).

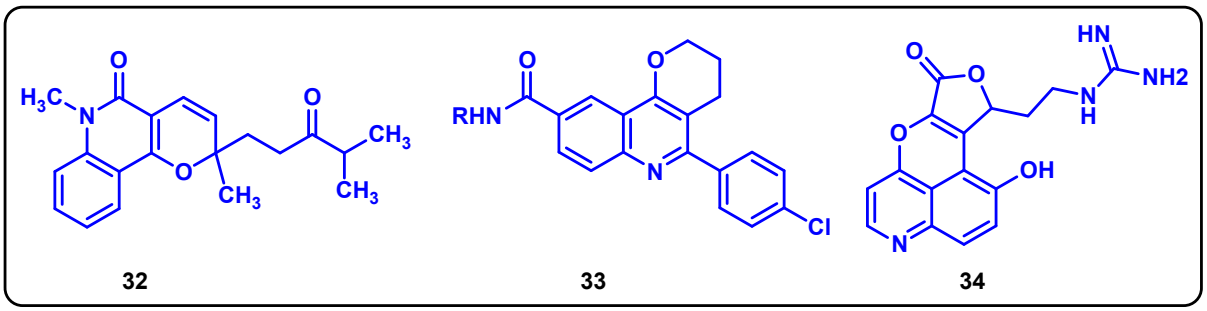

Figure 1.1.3.5. *Examples of bioactive pyrano[3,2-c]quinolines.*

Each of these scaffolds- triazole-fused *N*-heterocycles, isoindoloindoles, pseudoindoxyls, 1,6-naphthyridines, and isochromeno[4,3-*c*]quinolines are valued in drug discovery for their unique structures, stability, and bioactivity, though their synthesis is challenging due to the need for precise regioselectivity and ring closure. Traditional methods such as electrophilic substitution and metal-catalyzed annulations often have drawbacks like harsh conditions and poor atom economy, motivating the exploration of tandem reaction strategies. Therefore, this thesis emphasizes the importance of tandem reactions, which streamline the synthesis of these heterocyclic systems and will be explored in detail, especially highlighting the reactivity of alkenyl and alkynyl functionalities in tandem strategies for constructing fused *N*-heterocycles.

1.2 An Overview of Tandem Reactions in Organic Synthesis

1.2.1 Introduction to Tandem Reactions

Tandem reactions, also called domino or cascade reactions, are powerful synthetic strategies in modern organic chemistry that enable the efficient formation of intricate heterocyclic frameworks in a one-pot synthetic operation. These sequences involve multiple bond-forming events without isolating intermediates, enabling high atom economy, reduced waste, and structural complexity with operational simplicity.[30] Tandem reactions have significantly advanced the synthesis of heterocycles, which serve as essential structural units in natural products, pharmaceuticals, and agrochemicals.[31] By streamlining reaction sequences, tandem reactions enhance atom and step economy, reduce reagent and solvent use, lower energy consumption, and minimize waste production, making them well aligned with the principles of green chemistry.[32] Beyond their operational simplicity and efficiency, tandem reactions offer access to molecular frameworks that are often challenging to obtain *via* traditional stepwise synthesis. Whether deliberately designed or discovered accidentally, tandem reactions

modernize complex syntheses and offer profound insight into reactivity and molecular design. As a result, they remain vital in developing efficient, economical, and environmentally sustainable synthetic methodologies for constructing structurally diverse and functionally rich heterocycles, advancing the synthesis of biologically active scaffolds, underscoring their role in both medicinal chemistry and industrial applications.[33]

In 1917, Robert Robinson introduced the first cascade reaction, enabling the total synthesis of the alkaloid tropinone (**39**).[34] This notable one-pot and single-step process combined succinaldehyde (**35**), acetone dicarboxylic acid (**36**), and methylamine hydrochloride (**37**), yielding the bridged bicyclic alkaloid tropinone in 42% yield. The transformation proceeds *via* key steps including condensation of methylamine with dialdehyde to generate a cyclic iminium intermediate (**38**), followed by a double Mannich reaction and subsequent decarboxylation (*Scheme 1.2.1.1*). Leveraging fundamental mechanistic insight and molecular symmetry, this strategy efficiently generated four bonds and two rings in a single operation, demonstrating the power of synthetic strategies to construct complex molecular scaffolds from simple precursors, through the principles of synthetic and retrosynthetic design.

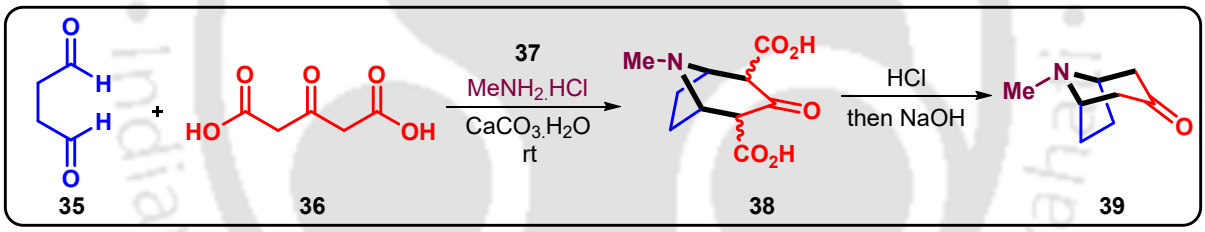

Scheme 1.2.1.1. *Robinson's tropinone synthesis.*

1.2.2 Classification of Tandem Reactions

Classifying tandem or cascade reactions poses a challenge due to their mechanistic diversity and wide variety of steps involved. Nevertheless, they are typically categorized based on the fundamental mechanistic theme that focuses on the initiating step or dominant reaction type. Despite differing opinions on classification criteria, one widely accepted reference categorization is by K. C. Nicolaou, who categorizes tandem reactions reflecting their key mechanistic pathways into different categories[35] as shown in *Figure 1.2.2.1.* They are as follows:

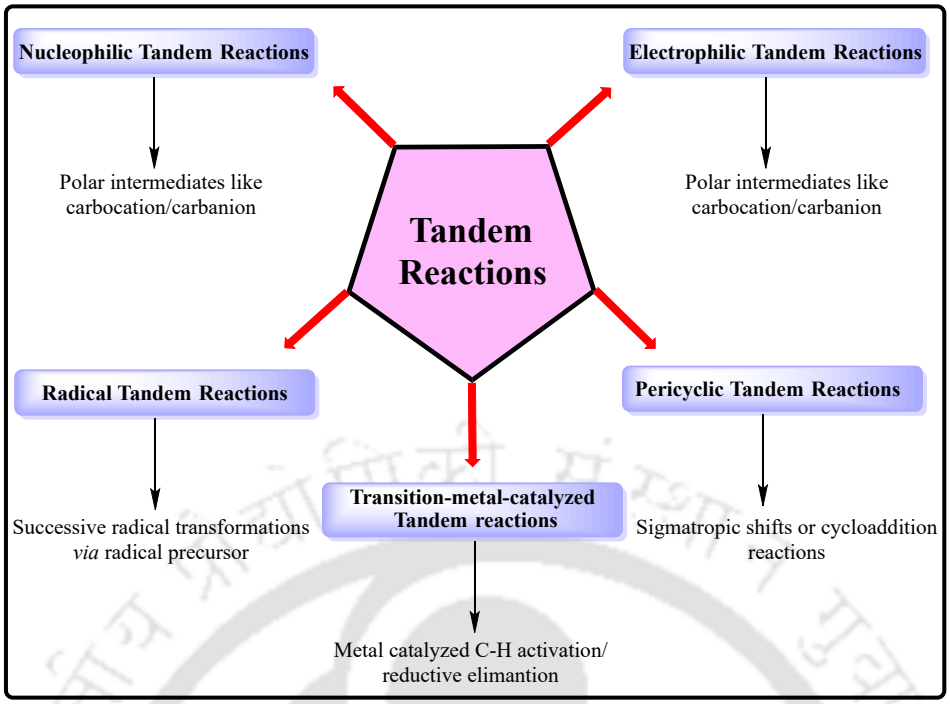

Figure 1.2.2.1. *Classification of tandem reactions.*

- Nucleophilic tandem reactions (involving polar intermediates like carbocations or carbanions)
- Electrophilic tandem reactions (involving polar intermediates like carbocations or carbanions, similar to the earlier one)
- Radical tandem reactions (based on successive radical transformations)
- Pericyclic tandem reactions (concerted mechanisms such as sigmatropic shifts or cycloadditions) and
- Transition-metal-catalyzed tandem reactions (where a single metal catalyst facilitates multiple steps including C–H activation and reductive elimination).

Despite the debates over classification criteria, the synthetic value of these reactions is universally bound to their efficiency, quantified by the extent of bond formation and the molecular complexity achieved in a single synthetic operation. These reactions are gaining notable attention from synthetic organic chemists due to their novel avenues of research as well as new reaction development, minimizing waste generation and excluding additional expenditure.

1.2.3 Representative Examples of Tandem Reactions for the Synthesis of Fused *N*-Heterocycles

Saikia and his group developed a temperature-dependent divergent cascade reaction between 2-aminobenzonitriles **40** and donor–acceptor cyclopropanes **41** for the selective synthesis of tetrahydropyrroloquinolinones **42** and dihydrobenzoazepines **43** using $SnCl_4$ as a Lewis acid (*Scheme 1.2.3.1*).[36] At lower temperature (0 °C), the reaction proceeds through nucleophilic ring-opening, followed by intramolecular nucleophilic attack of the amine on the ester group and subsequent C–C bond cleavage, yield dihydrobenzoazepines. In contrast, elevating the reaction temperature to 80 °C leads to the formation of a lactam intermediate, which subsequently undergoes enolization, C–N bond cleavage, and a final 1,3-hydrogen shift to furnish tetrahydropyrroloquinolinone scaffolds.

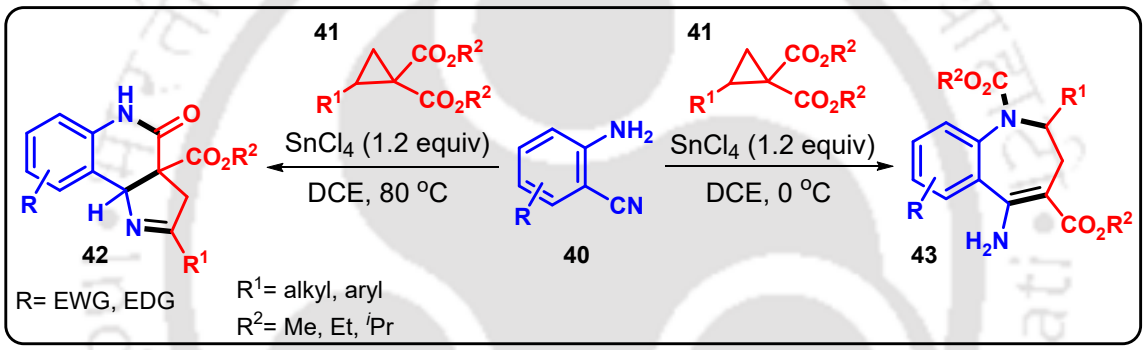

Scheme 1.2.3.1. *$SnCl_4$-mediated synthesis of tetrahydropyrroloquinolinones and dihydrobenzoazepines.*

An unusual tandem protocol has been introduced by Baidya and co-workers for the construction of functionalized indazole scaffolds **46** from aryne precursor **45** and *N*-alkyl-*N*-nitrosamides **44** under ambient conditions (*Scheme 1.2.3.2*).[37]

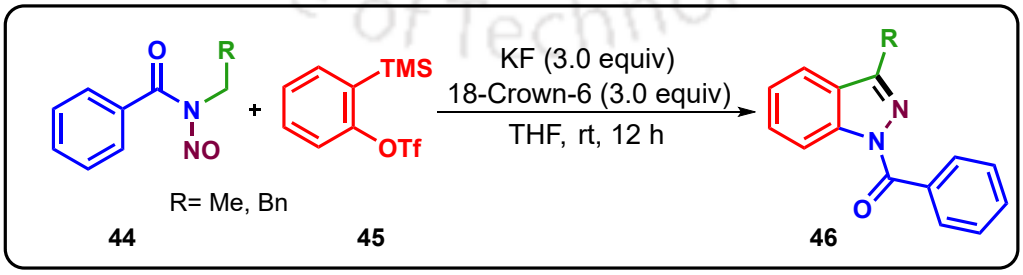

Scheme 1.2.3.2. *Aryne-assisted synthesis of indazoles.*

This metal-free transformation proceeds *via* aryne σ-insertion into the *N*–*N* bond of *N*-nitrosamides, followed by C(sp³)–H functionalization, achieving regioselective indazole

formation in high yields. Further, mechanistic insights from DFT calculations support the proposed tandem annulation pathway.

Li and colleagues reported a transition-metal-free domino annulation strategy involving 1,2-benzdiyne precursors **47** that proceeds through a unique nucleophilic–ene cascade process for the construction of a variety of benzo-fused *N*-heterocycles **49** (*Scheme 1.2.3.3*).[38] This approach utilizes rationally designed aryne precursors with different leaving groups, enabling the efficient generation of 1,2-aryne intermediates that undergo sequential nucleophilic addition and ene-type cyclization to deliver a range of polycyclic compounds.

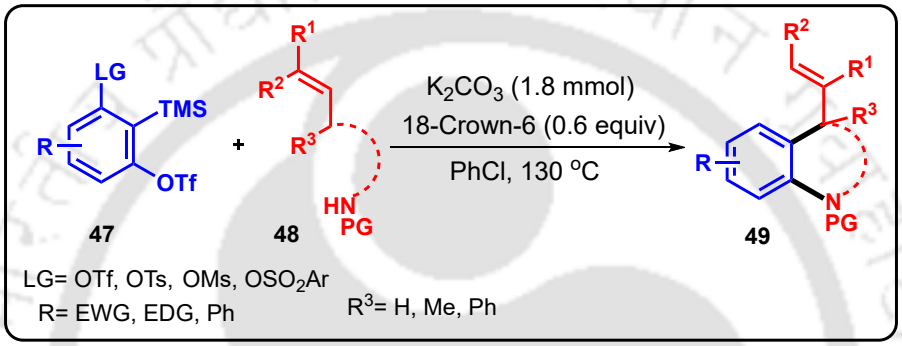

Scheme 1.2.3.3. *Transition-metal-free synthesis of fused N-heterocycles.*

Dabiri and his group established a $Pd(OAc)_2$-catalyzed cascade methodology for the synthesis of hydroxyisoindolo[1,2-*b*]quinazolinone derivatives **52** from aryl-quinazolinones **50** and aldehydes **51** (*Scheme 1.2.3.4*).[39] This one-pot protocol proceeds *via* sequential dehydrogenative coupling of the aldehyde with the quinazolinone core, followed by intramolecular annulation to construct the fused tetracyclic scaffold.

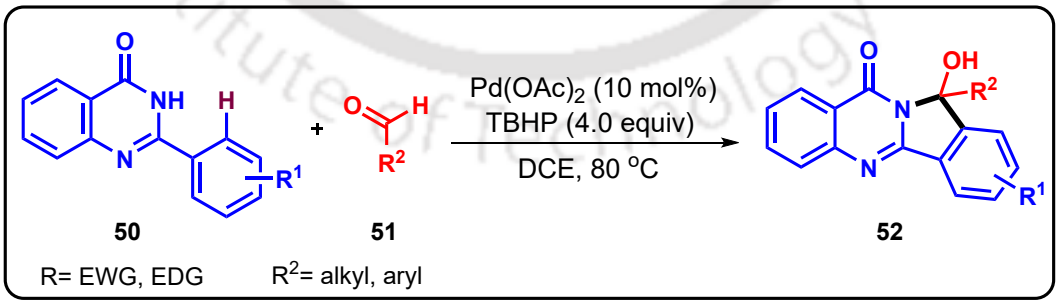

Scheme 1.2.3.4. *Pd-catalyzed synthesis of hydroxyisoindoloquinazolinones.*

Volla and his team developed a Rh(II)-catalyzed diastereoselective tandem transannulation approach for the synthesis of tricyclic 2-imidazolone derivatives **55** from *N*-sulfonyl-1,2,3-triazoles **54** and 4-vinyl benzoxazinanones **53** (*Scheme 1.2.3.5*).[40] This

reaction proceeds *via* O–H insertion of Rh-azavinyl carbenes, followed by an intramolecular rearrangement to furnish the fused *N*-heterocycles.

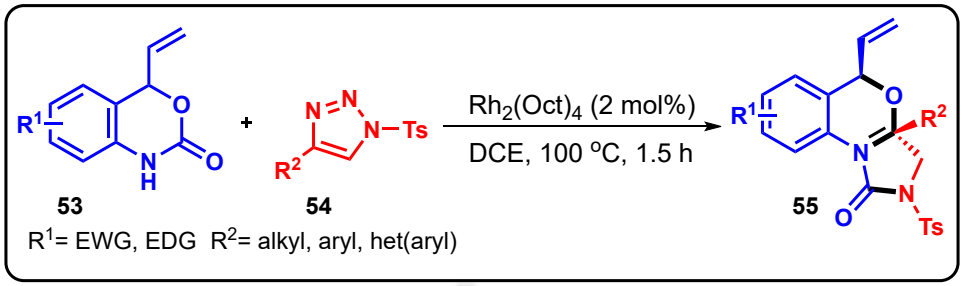

Scheme 1.2.3.5. *Rh-catalyzed synthesis of 2-imidazolones.*

Yu and co-workers developed a TBHP-promoted cascade strategy for the construction of phenanthridine-6-carboxamide derivatives **58** from aryl isonitriles **56** and formamides **57** (*Scheme 1.2.3.6*).[41] In this metal-free process, TBHP acts as an oxidant to facilitate the reaction between aryl isonitriles and formamides. The reaction proceeds through the addition of formamide-derived radicals to aryl isonitriles, followed by intramolecular aromatic cyclization to form C–C bonds, producing phenanthridinecarboxamides in good yields.

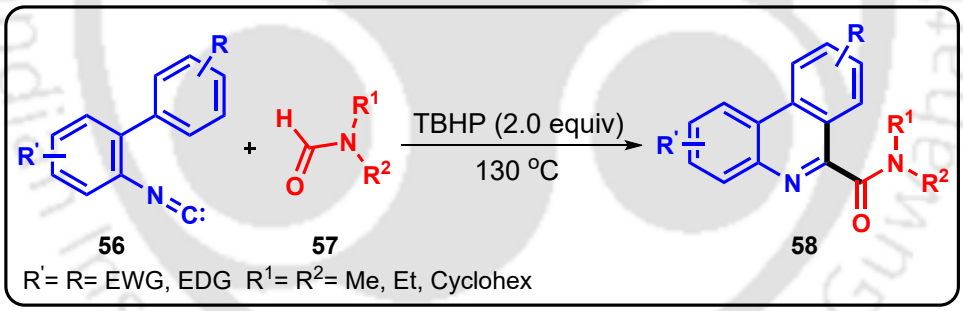

Scheme 1.2.3.6. *TBHP-promoted synthesis of phenanthridine 6-carboxamides.*

Prajapati and colleagues reported a green and efficient approach for the synthesis of tetrahydroquinazoline derivatives **62** from 2-naphthyl amine **59**,

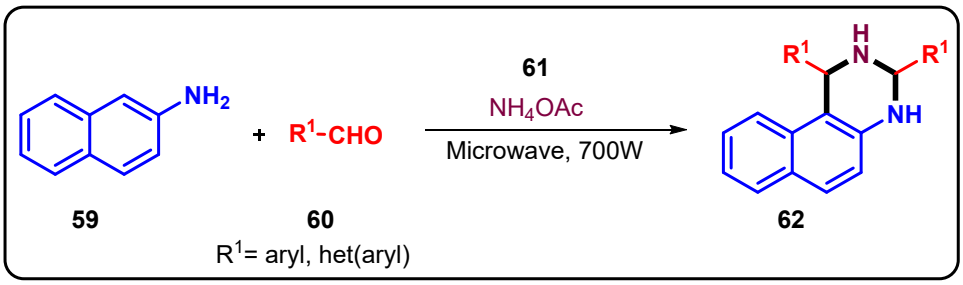

Scheme 1.2.3.7. *Microwave-assisted synthesis of tetrahydroquinazolines.*

aryl aldehydes **60** and ammonium acetate **61** as a nitrogen source under microwave irradiation (*Scheme 1.2.3.7*).[42] This catalyst- and solvent-free strategy proceeds *via* an aza-Diels–Alder reaction, where the *in situ* generation of both the diene and dienophile enables efficient cyclization to afford the tetrahydroquinazoline frameworks.

A one-pot tandem strategy has been established by Zhang and his group for constructing 2,3-disubstituted 4-aminoquinolines **66** *via* a three-component reaction involving azidobenzaldehydes **63**, *α*-fluoro-*β*-ketoesters **64**, and amines **65** using triphenylphosphine (PPh_3) in CH_3CN (*Scheme 1.2.3.8*).[43] The transformation proceeds *via* sequential Mannich reaction, aza-Wittig reaction, and dehydrofluorinative aromatization, achieving the fused 4-aminoquinoline moieties in good yields.

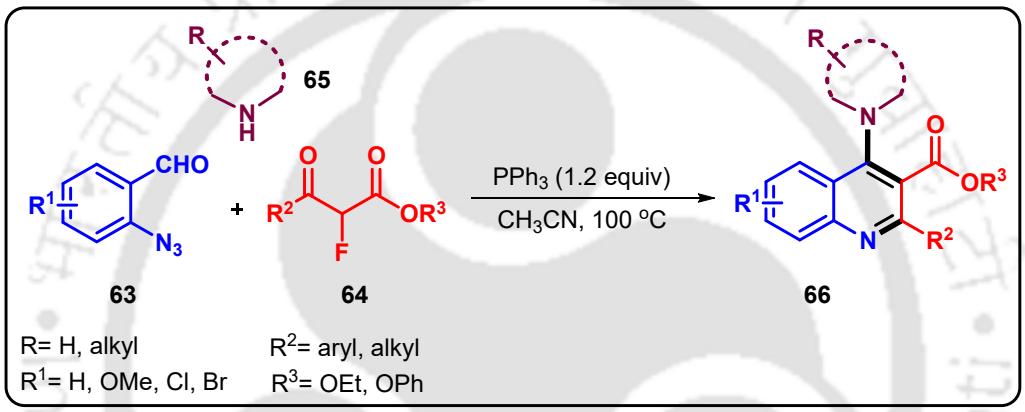

Scheme 1.2.3.8. *PPh_3-mediated synthesis of 4-aminoquinolines.*

Dash and co-workers established a potassium *tert*-butoxide-mediated tandem protocol for the efficient synthesis of rutaecarpine alkaloid analogues **69** from readily available 2-aminobenzonitriles **67** and indole-2-carbaldehydes **68** (*Scheme 1.2.3.9*).[44]

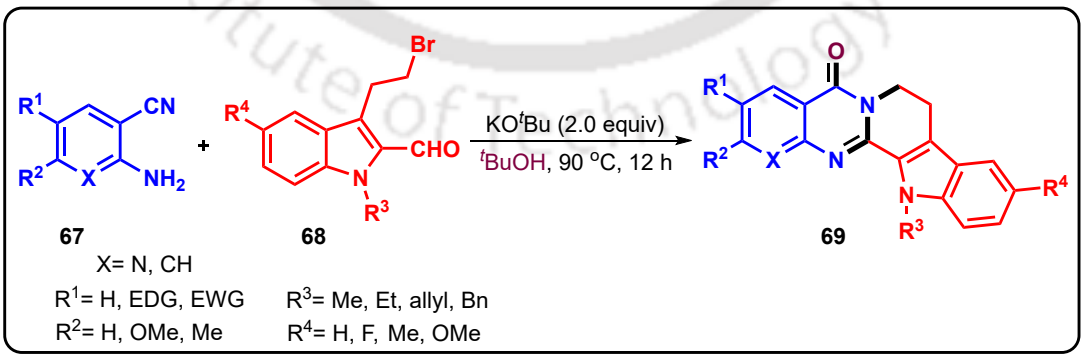

Scheme 1.2.3.9. *KO^{t}Bu-mediated synthesis of rutaecarpine analogues.*

This base-mediated transformation proceeds *via* sequential imine formation followed by radical-driven quinazolinone formation, oxidation, and cyclization to furnish

polycyclic *N*-heterocyclic frameworks. This KO^{t}Bu-mediated, additive-free method exhibits broad substrate scope and efficiently delivers rutaecarpine analogues, making it suitable for time- and step-efficient large-scale synthesis.

1.3 Alkenyl/Alkynyl Functionalities in Organic Synthesis

Alkenes and alkynes, characterized by carbon–carbon double (C=C) and triple (C≡C) bonds respectively, are fundamental unsaturated hydrocarbons in organic chemistry. Their unique electronic structure imparts distinct chemical reactivity, such as the ability to undergo addition, cycloaddition, and functional group transformation reactions, making them fundamental in synthetic organic chemistry for the construction of diverse and complex molecular frameworks. In organic synthesis, alkenyl and alkynyl functionalities are invaluable. The π-bonds present in alkenyl and alkynyl moieties not only serve as reactive sites for numerous transformations but also disclose rigidity and planarity to molecular scaffolds, influencing the physical and chemical properties of target molecules.[45] Due to their versatility, alkenyl and alkynyl functionalities are widely employed as key intermediates in the synthesis of natural products, pharmaceuticals, and advanced functional materials. For example, transition-metal-catalyzed cross-coupling reactions, such as the Heck, Sonogashira, and Suzuki reactions, frequently utilize alkenyl and alkynyl substrates to form carbon–carbon bonds with high precision and efficiency.[46] Thus, the strategic incorporation and utilization of alkenyl and alkynyl groups remain dominant in modern organic synthesis, facilitating the efficient and rapid construction of structurally diverse and functionally rich compounds.

1.3.1 Introduction to Alkenyl/Alkynyl Functionalities as Synthetic Precursors in Tandem Reactions

Alkenes and alkynes have emerged as versatile synthetic precursors in tandem reactions due to their intrinsic reactivity and ability to take part in multiple bond-formation. This facilitates the efficient formation of complex molecular frameworks under a single set of conditions through sequential transformations. Their π-systems can be readily activated by transition metals, Brønsted or Lewis acids, enabling diverse transformations including cyclization, functionalization with high atom- and step-economy.[47] In particular, alkynes serve as key intermediates in tandem processes such as cyclization and nucleophilic additions, which are widely employed in constructing of complex heterocycles and natural product analogues.[48] Similarly, alkenes can mimic

alkynes, undergoing cycloaddition/rearrangement strategies, offering streamlined access to a broad array of fused and bridged ring systems.[49]

In tandem or cascade transformations, these functionalities serve as reactive centers that initiate or propagate cyclization sequences, thereby enabling the formation of structurally complex frameworks from simple precursors. The reactivity of alkenes in cyclization processes often relies on their activation *via* electrophilic catalysis or radical initiation. Upon activation, the π-bond becomes susceptible to intramolecular nucleophilic attack, enabling the formation of five- or six-membered cyclic frameworks through various processes such as hydroamination, haloetherification, or oxacyclization. Alkynes, in contrast, exhibit an even broader spectrum of reactivity due to their linear geometry, greater polarizability, and higher energy π-orbitals. They are particularly well-suited for cyclization reactions under the influence of transition metals like gold, silver, copper, or platinum, or Lewis/Brønsted acids, which coordinate to the triple bond and make it an electrophilic site. However, the alkenyl/alkynyl functionalities act either as a nucleophile (a more common case) or an electrophile (a less common case) depending on the coupling partner used (either electrophile/nucleophile) and undergo cyclization/annulation reaction in a tandem manner for the construction of structurally diverse heterocycles (*Scheme 1.3.1.1*).

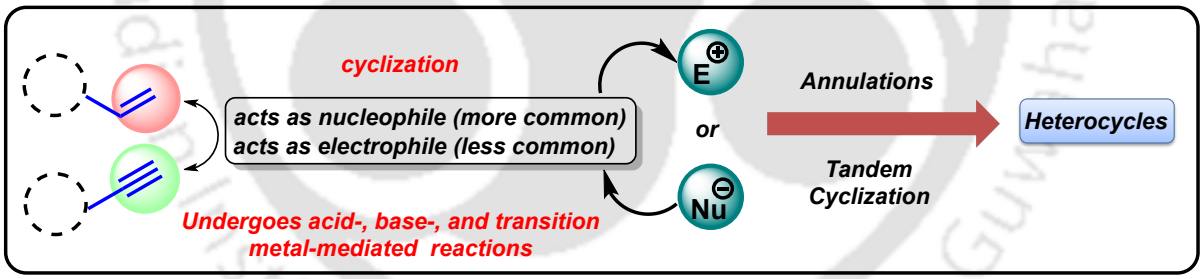

Scheme 1.3.1.1. *General reactivity of alkenes/alkynes towards heterocycles.*

Besides, alkenyl and alkynyl functionalities are valuable building blocks in tandem reaction pathways for the efficient synthesis of fused *N*-heterocycles. Their π-rich nature enables activation by transition metals or acids, facilitating key steps such as cyclization, annulation, and heteroatom incorporation, etc.[50] The reactions involving alkenyl or alkynyl groups often proceed *via* tandem mechanisms, where several bonds are formed in a single synthetic step, delivering complex *N*-fused frameworks with excellent regio- and stereoselectivity.

The strategic incorporation of alkenes or alkynes in tandem protocols not only simplifies synthetic routes but also enables rapid synthesis of diverse bioactive fused *N*-heterocyclic scaffolds from easily accessible starting materials.

1.3.2 Representative Examples of Tandem Alkenyl Cyclization for fused *N*-Heterocycle Synthesis

Tandem cyclization strategies involving alkenyl functionalities have emerged as powerful approaches for the efficient construction of fused *N*-heterocyclic frameworks. These transformations typically proceed through sequential bond formation initiated by the activation of the alkenyl group, leading to the swift synthesis of a wide range of functionalized fused *N*-heterocyclic compounds from simple precursors. The following representative examples highlight the synthetic versatility and efficiency of alkenyl-tethered substrates in accessing extensive fused *N*-heterocycles.

Saikia and his group reported an efficient tandem protocol for the synthesis of tetrahydroquinazolines **72** from readily accessible 2-aminobenzonitriles **70** with alkylidene malonates **71** using $SnCl_4$ as a Lewis acid (*Scheme 1.3.2.1*).[51] The transformation initiates with a 1,4-conjugate addition of the amino group to the electron-deficient alkene, followed by an unprecedented rearrangement and an intramolecular Mannich type reaction to deliver the tetrahydroquinazoline frameworks.

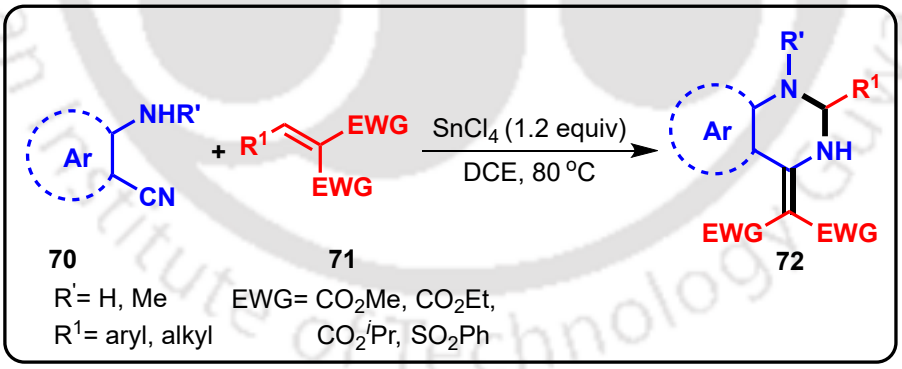

Scheme 1.3.2.1. *$SnCl_4$-mediated synthesis of tetrahydroquinazolines.*

Xiao and co-workers established a Brønsted acid-catalyzed tandem Diels–Alder/ aromatization protocol for the synthesis of tetrahydrocarbazoles **74** from 2-vinylindoles **73** (*Scheme 1.3.2.2*).[52] This developed method proceeds *via* an initial Brønsted acid-activated [4+2] cycloaddition followed by subsequent aromatization to generate structurally fused *N*-heterocycles. Utilizing TFA as a catalyst under mild conditions,

this metal-free method shows broad substrate scope in high yields, offering a concise route to biologically relevant fused polycyclic scaffolds.

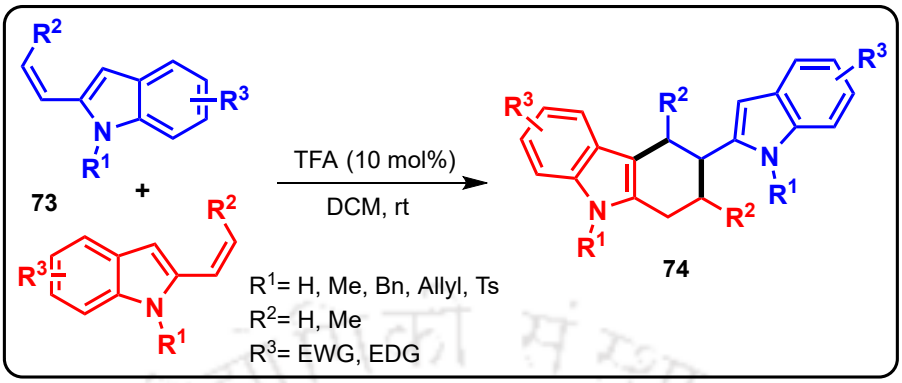

Scheme 1.3.2.2. *Brønsted acid-catalyzed synthesis of tetrahydrocarbazoles.*

Xu and colleagues developed a base-mediated, transition-metal-free tandem [3+2] cycloaddition followed by reductive cyclization strategy for the synthesis of pyrroloquinolone scaffolds **77** from nitrochalcones **75** and methylene isocyanides **76** (*Scheme 1.3.2.3*).[53] In this method, the nitro group is converted into an electrophilic nitroso intermediate *via* an *in situ* generated dihydropyrroline intermediate, which behaves as an internal reductant. This nitroso intermediate then undergoes intramolecular C–N bond formation through Cadogan reductive cyclization, affording the fused *N*-heterocyclic compounds.

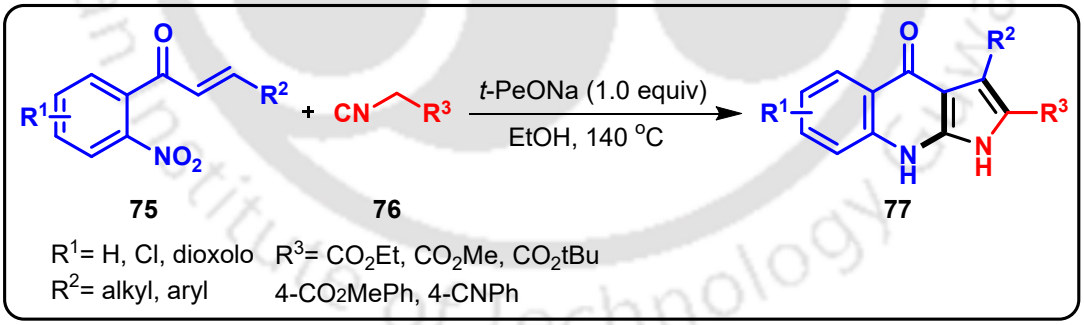

Scheme 1.3.2.3. *Base-mediated synthesis of pyrroloquinolones.*

Yang *et al.* demonstrated a Pd(II)-catalyzed enantioselective oxidative tandem cyclization methodology for constructing indoline derivatives **79** from *N*-(2-allylaryl)amides **78** using molecular oxygen as the oxidant and (–)-sparteine as the chiral ligand (*Scheme 1.3.2.4*).[54] This transformation features consecutive C–N and C–C bond formation under green oxidative conditions. Catalyzed by a chiral Pd(II)/(–)-sparteine complex, the reaction proceeds with excellent enantioselectivity, delivering the products in moderate to good yields.

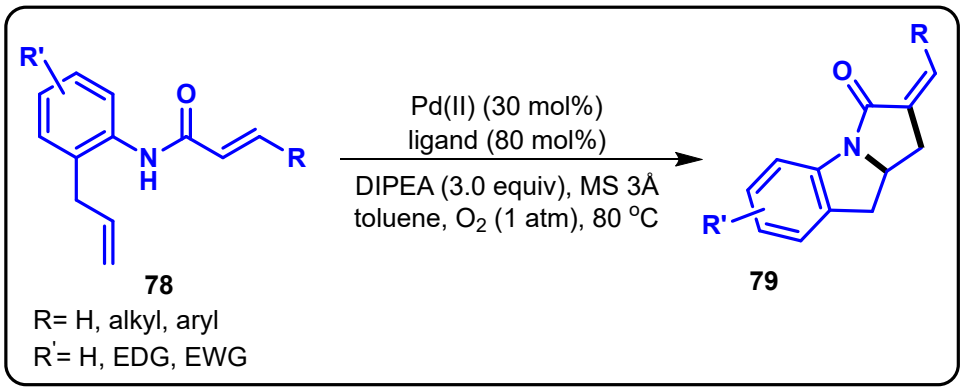

Scheme 1.3.2.4. *Pd(II)-catalyzed synthesis of indolines.*

Xiao and co-workers devised an organocatalytic multiple tandem strategy for the asymmetric synthesis of enantioenriched tetrahydrocarbazoles **82** from 2-vinylindoles **80** with α,β-unsaturated aldehydes **81** (*Scheme 1.3.2.5*).[55] This transformation proceeds *via* the formation of an activated iminium intermediate, catalyzed by a chiral secondary amine, which subsequently undergoes an enantioselective Friedel–Crafts-type alkylation with a nucleophilic indole. Subsequently, intramolecular conjugate addition, [1,3]-hydrogen shift, and finally hydrolysis leads to the desired tetrahydrocarbazole scaffold.

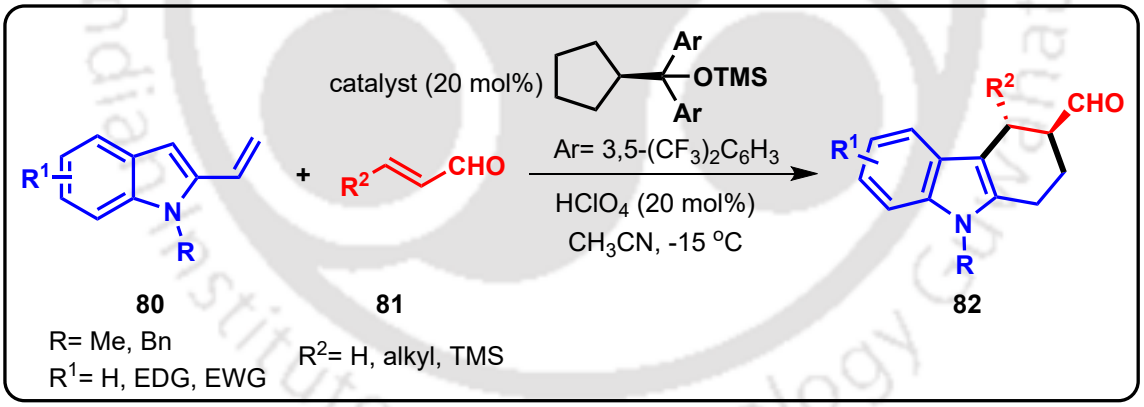

Scheme 1.3.2.5. *Organocatalytic synthesis of tetrahydrocarbazoles.*

Saikia and co-workers developed a stereoselective tandem aza-Prins–Ritter/Friedel–Crafts type protocol for the synthesis of azabicyclic derivatives **84** from endocyclic *N*-acyliminium ion precursors **83** (*Scheme 1.3.2.6*).[56] The reaction proceeds *via* the *in situ* generation of an *N*-acyliminium ion in the presence of a Lewis acid, which undergoes an aza-Prins-type cyclization followed by an intermolecular Ritter or Friedel–Crafts reaction to form structurally fused amido and phenyl-substituted azabicyclic derivatives.

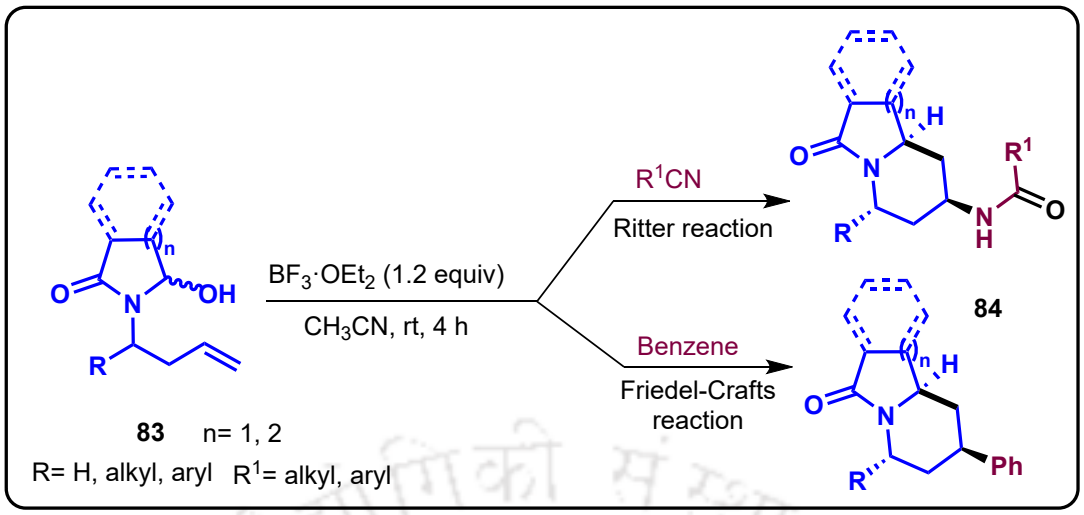

Scheme 1.3.2.6. *Lewis acid-mediated synthesis of azabicyclic derivatives.*

A visible-light-mediated oxidative tandem strategy has been disclosed by Zheng and colleagues for the construction of *N*-arylindoles **86** from styryl anilines **85** using a photocatalyst under mild aerobic conditions (*Scheme 1.3.2.7*).[57] This protocol employs a 18W white LED light and silica gel as an additive, enabling sequential oxidation *via* $[Ru(bpz)_3](PF_6)_2$, electrophilic addition, further oxidation of benzylic radical, and finally aromatization to construct the indole moiety.

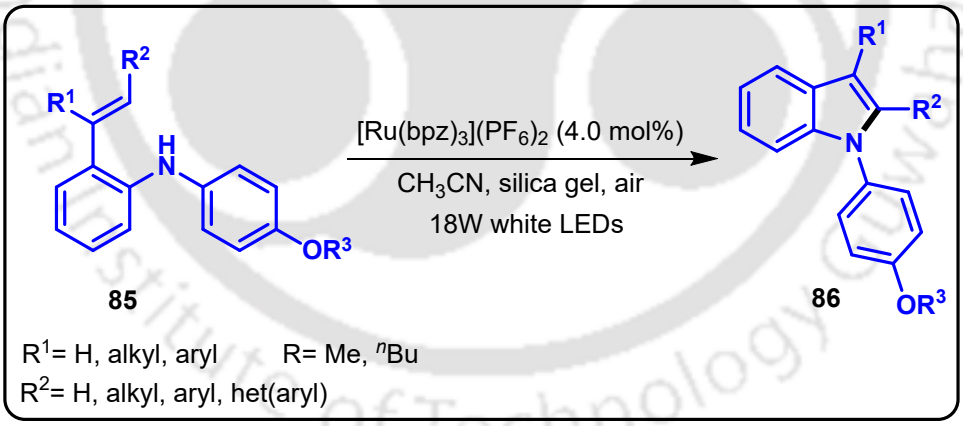

Scheme 1.3.2.7. *Photocatalytic synthesis of N-arylindoles.*

Adimurthy and co-workers developed a copper-catalyzed C–H functionalization methodology for the synthesis of imidazopyridines **91** and 2-phenylimidazoisoquinolines **90** from pyridines **87** or isoquinolines **88** with vinyl azides **89** (*Scheme 1.3.2.8*).[58] The reaction proceeds *via* 2*H*-azirine formation from vinyl azide, which later undergoes C–N bond cleavage under the catalytic influence of Cu(I). Further, cyclization, subsequent C–N reductive elimination of Cu(III) intermediate, and finally oxidation afforded the imidazo-fused heterocycles.

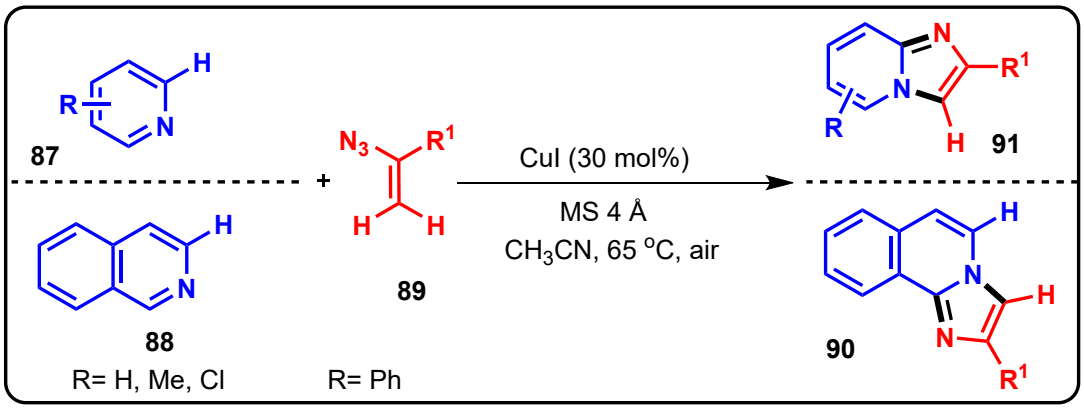

Scheme 1.3.2.8. *Cu-catalyzed synthesis of imidazo-fused heterocycles.*

Xiao et al. reported a Brønsted acid-catalyzed one-pot multicomponent strategy for the chemo- and regioselective synthesis of tetrahydrocarboline **95** and tetrahydroquinoline **96** derivatives from aldehydes **92**, *p*-methoxyaniline **93**, and 2-vinylindoles **94** (*Scheme 1.3.2.9*).[59] The reaction exhibits a chemo- and regioselectivity switch depending on the substituents present on the indole component, even under similar reaction conditions. This practical tandem approach is catalyzed by Brønsted acid, 3,5-dinitrobenzoic acid (DNBA) to generate structurally diverse and biologically important *N*-heterocycles in good yields.

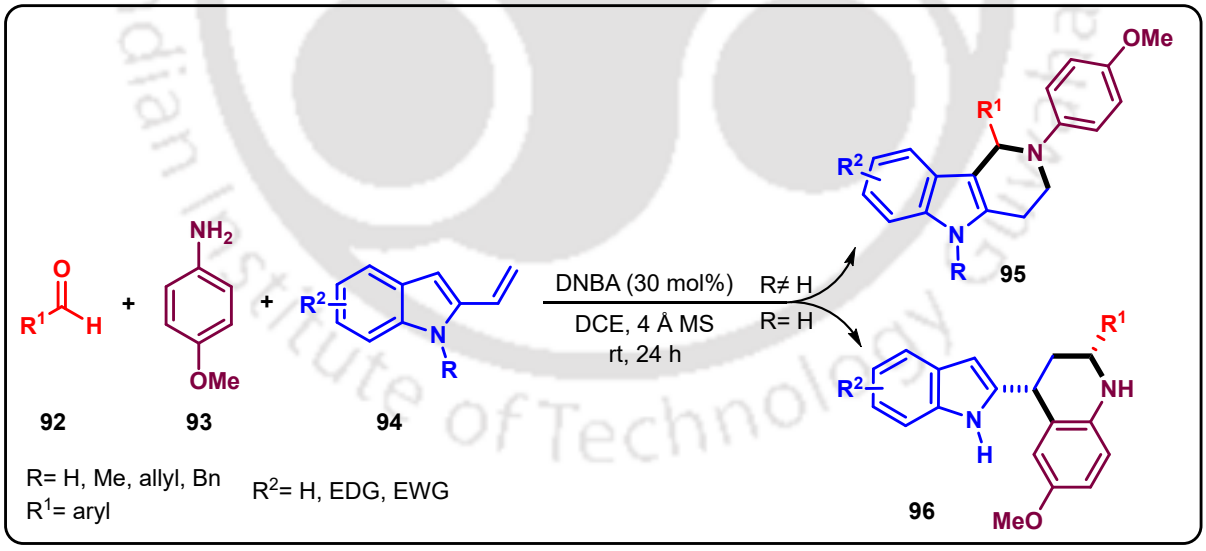

Scheme 1.3.2.9. *DNBA-catalyzed synthesis of tetrahydrocarbolines and tetrahydroquinolines.*

Hajra and his group disclosed a Fe(III)-catalyzed tandem reaction between 2-aminopyridines **97** and nitroolefins **98** for constructing of imidazopyridines derivatives **99** (*Scheme 1.3.2.10*).[60] The mechanism initially involves Michael addition of the aminopyridine to the nitroolefin, followed by intramolecular cyclization and subse-

quent denitration to form the fused *N*-heterocyclic core. The developed methodology utilizes non-hazardous and less expensive catalyst and also the starting materials can be prepared easily. The drug zolimidine, used for the treatment of peptic ulcers, can also be synthesized using this strategy.

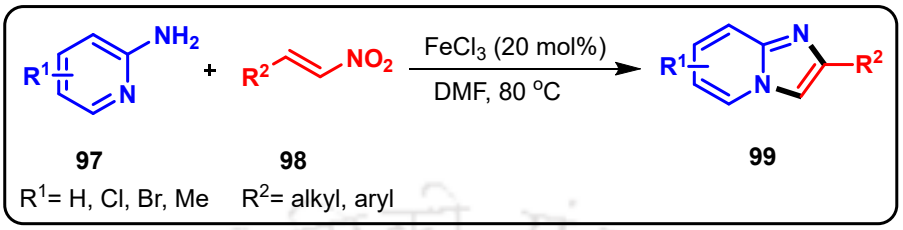

Scheme 1.3.2.10. *Fe(III)-catalyzed synthesis of imidazopyridines.*

1.3.3 Representative Examples of Tandem Alkynyl Cyclization for Fused *N*-Heterocycle Synthesis

Like alkene, tandem cyclization approaches involving alkynyl functionalities have also emerged as efficient methods for constructing fused *N*-heterocycles. The intrinsic reactivity of the triple bond allows tandem sequences that lead to multiple bond formations in a single step. The following representative examples illustrate how alkynyl-tethered substrates can strategically be employed to achieve a wide variety of fused *N*-heterocyclic systems.

Saikia and co-workers developed a $BF_3{\cdot}OEt_2$-promoted tandem benzannulation/ intramolecular Friedel–Crafts reaction involving 2-alkynylanilines **100** and 2-alkynylbenzaldehydes **101** for the synthesis of π-extended dihydrobenzo[*a*]indenocarbazoles **102** (*Scheme 1.3.3.1*).[61] This transition-metal-free protocol proceeds *via* Lewis acid-mediated imine formation, followed by sequential nucleophilic attacks from the alkyne groups to generate alkenyl carbocation. Later, intramolecular Friedel–Crafts

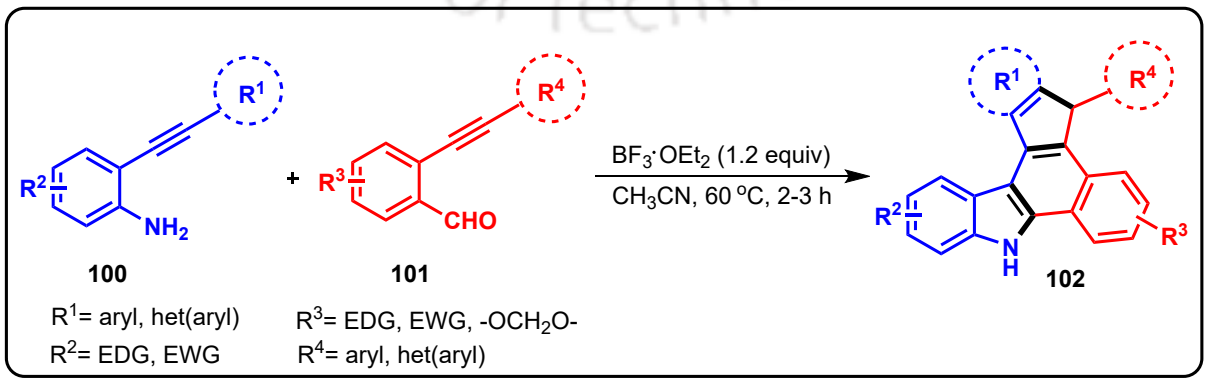

Scheme 1.3.3.1. *$BF_3{\cdot}OEt_2$-promoted synthesis of dihydrobenzo[a]indenocarbazoles.*

cyclization in the alkenyl carbocation and finally *via* 1,5-hydrogen shift leads to achieve the highly π-extended fused *N*-heterocyclic scaffolds in moderate to good yields.

A palladium-catalyzed cascade strategy has been disclosed by Jin and co-workers for the construction of cyclopenta-fused acenaphthoindole derivatives **104** from *N*-alkyl indole precursors **103** (*Scheme 1.3.3.2*).[62] This efficient one-pot reaction proceeds *via* sequential indolization followed by peri-C–H annulation and finally a *N*-dealkylation step, delivering the fused polycyclic indole scaffolds in good yields.

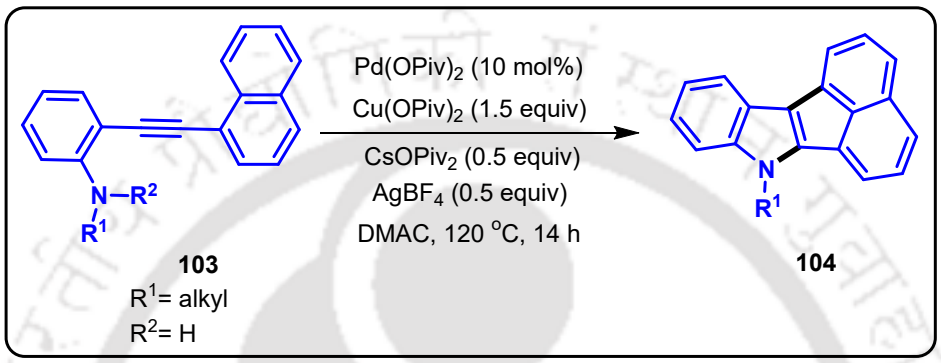

Scheme 1.3.3.2. *Pd-catalyzed synthesis of cyclopenta-fused acenaphtho[1,2-b]indoles.*

Zhan and colleagues demonstrated a silver(I) triflate-catalyzed tandem strategy for synthesizing *N*-fused pyrroloindole derivatives **107** through sequential Friedel–Crafts alkylation and C–N bond formation between 3-substituted 1*H*-indoles **105** and propargyl alcohols **106** (*Scheme 1.3.3.3*).[63] This ligand-free approach proceeds through initial activation of propargyl alcohols by AgOTf, which undergo C–C bond formation *via* Friedel–Crafts reaction at the C–2 position of the indole ring. Subsequent Ag-mediated N–C coupling with the propargyl moiety facilitates cyclization, yielding the tricyclic *N*-heterocycles with excellent chemoselectivity.

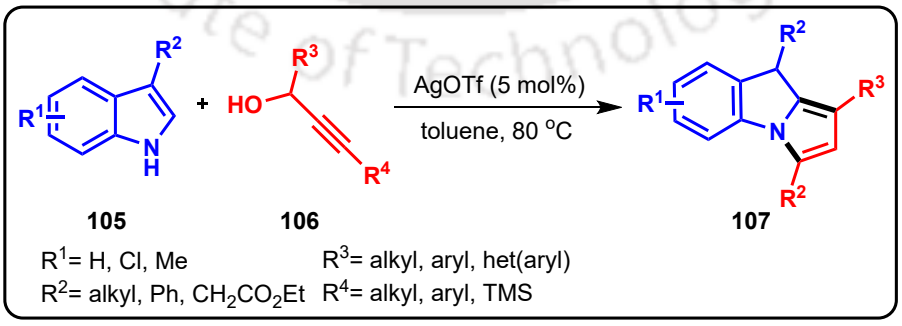

Scheme 1.3.3.3. *AgOTf-catalyzed synthesis of pyrroloindoles.*

Balci and his group explored a base-mediated tandem reaction involving *N*-propargylated pyrrole- and indole-carbaldehydes **108** with various amines **109**, resulting

in diverse fused *N*-heterocyclic compounds pyrrolo- and indolo-pyrazinones **110** (*Scheme 1.3.3.4*).[64] Alkylamines and benzylamines afforded the corresponding pyrazinone derivatives, while reactions with allylamine and propargylamine led to pyrazine products **111**. Notably, in the case of allylamine and propargylamine, the reaction involves the unexpected cleavage of the allyl or propargyl group from the nitrogen atom.

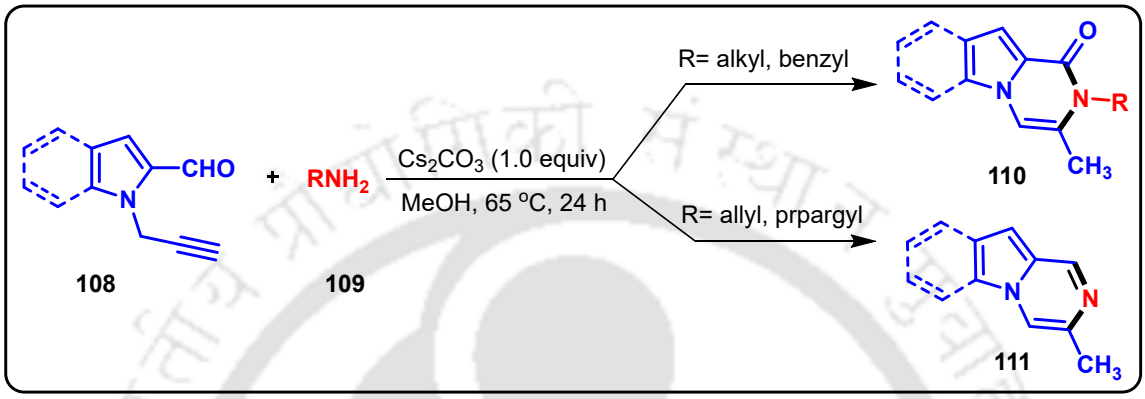

Scheme 1.3.3.4. *Base-mediated synthesis of pyrazinones and pyrazines.*

The same group developed a versatile and concise synthetic strategy for constructing pyrazolo-pyrrolo-pyrazines **113** and pyrazolo-pyrrolo-diazepines **114** from *N*-propargyl pyrazole precursors **112** (*Scheme 1.3.3.5*).[65] Their approach involves the initial formation of *a*,*β*-alkynyl ketones, which subsequently transformed into pyrazole derivatives through reaction with hydrazine monohydrate. The $AuCl_3$-catalyzed method selectively produces 7-membered diazepines from internal alkynes *via* 7-endo-dig cyclization, while terminal alkynes form 6-membered pyrazines *via* 6-*exo-dig* pathway. In contrast, NaH-mediated cyclization exclusively yields 6-membered pyrazines regardless of the alkyne substitution, *via* allene intermediate, which undergoes intramolecular 6-exo-trig cyclization.

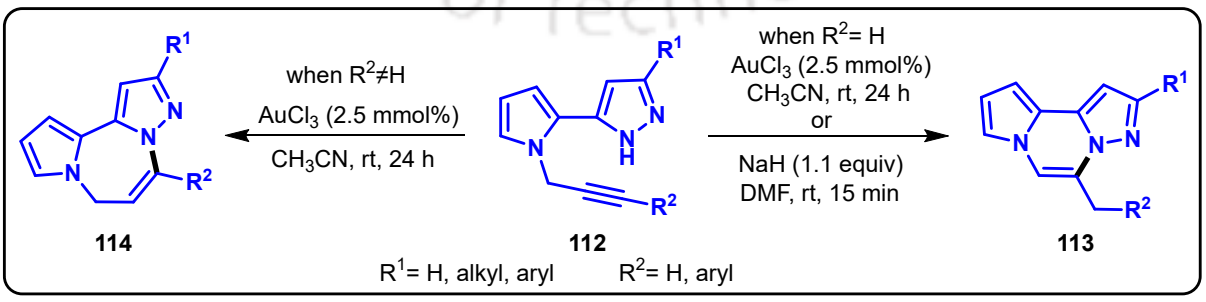

Scheme 1.3.3.5. *$AuCl_3$-catalyzed NaH-promoted synthesis of pyrazolo-pyrrolo-pyrazines/diazepines.*

Saikia and co-worker reported a tandem stereoselective method for synthesizing substituted pyrroloisoindolones/pyridoisoindolones **116** from *N*-homopropargyl imides **115** (*Scheme 1.3.3.6*).[66] The developed protocol proceeds through a key *N*-acyliminium ion intermediate, formed *via* the regioselective reduction of *N*-homopropargyl imide, under the action of triflic acid (TfOH). Further, intramolecular aza-Prins cyclization, nucleophilic attack by water, and finally tautomerization leads to afford the highly diastereoselective tricyclic azo compounds in good yields.

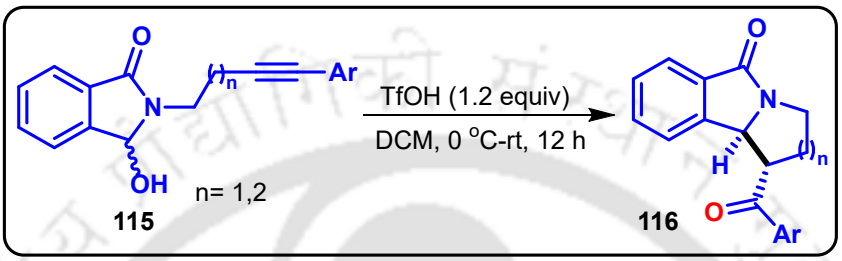

Scheme 1.3.3.6. *TfOH-mediated synthesis of pyrroloisoindolones and pyridoisoindolones.*

Li and his group established a metal-free strategy for the synthesis of benzo-fused cyclopentaazepinones **119** *via* a decarbonylative radical cascade annulation between *N*-arylpropiolamides **117** and aldehydes **118** under aerobic conditions (*Scheme 1.3.3.7*).[67] This transformation involves the auto-oxidation of aldehydes to generate carbonyl radical intermediate, which later forms homoalkyl radical intermediate *via* decarbonylation. Later, sequential [3+2]/[5+2] annulations with the alkyne moiety of *N*-arylpropiolamides forms the fused azepinone framework. The reaction proceeds in the absence of a metal catalyst, enabling the construction of complex *N*-heterocycles in moderate to good yields.

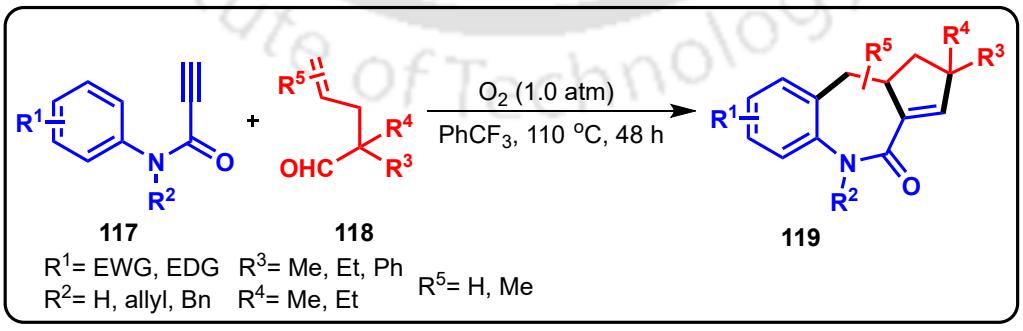

Scheme 1.3.3.7. *Dioxygen (O_2)-promoted synthesis of benzocyclopentaazepinones.*

An efficient method was demonstrated by Chuang *et al.* for synthesizing benzo-fused naphthoazepinediones **121** through electrophilic carbocyclization of 1,4-naph-

thoquinones **120** (*Scheme 1.3.3.8*).[68] This Ag(I)-catalyzed reaction proceeds *via* a regioselective 7-*endo-dig* cyclization, forming new carbon–carbon bonds under mild conditions. Additionally, treatment with iodine (I_2) selectively affords 13-iodo-substituted benzazepine derivatives **122** *via* a distinct electrophilic pathway. The protocol shows wide compatibility with functional groups and provides a straightforward approach to construct fused azepine frameworks in good to excellent yields.

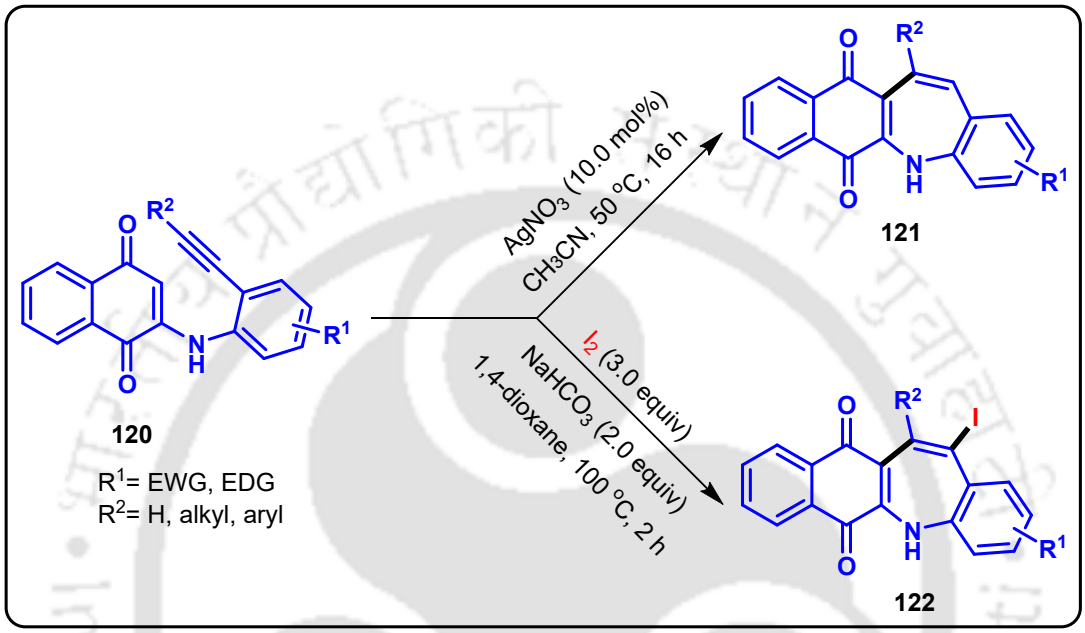

Scheme 1.3.3.8. *Ag(I)/I_2-promoted synthesis of benzazepines.*

Liang and colleagues devised a copper-catalyzed tandem annulation method for constructing benzo-fused imidazoisoquinolines **125** from *o*-alkynylbenzonitriles **123** and 2-iodoanilines **124** (*Scheme 1.3.3.9*).[69] The developed protocol proceeds *via* the sequential formation of three C–N bonds, involving the cleavage of one C–I bond and two N–H bonds in the presence of $Cu(OAc)_2$ and KO^{t}Bu, delivering the fused *N*-heterocycles in moderate to good yields. This methodology provides an efficient route for the

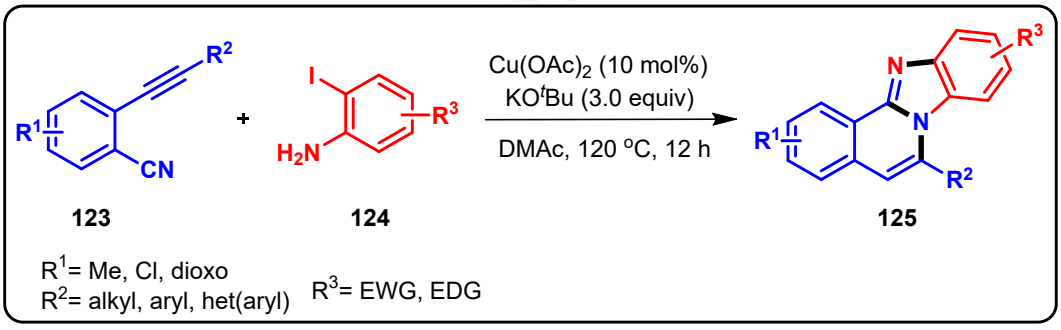

Scheme 1.3.3.9. *Copper-catalyzed synthesis of benzoimidazoisoquinolines.*

synthesis of isoquinoline-fused benzimidazoles which have diverse importance in pharmaceuticals, natural products, and functional materials.

Kwon and co-workers reported a phosphine-catalyzed α-umpolung–aldol reaction for the construction of benzo[*b*]azepin-3-ones **128** (*Scheme 1.3.3.10*).[70] This transformation involves an intermolecular cyclization between 2-sulfonamidobenzaldehyes **126** and ynones **127**, proceeding through an α-umpolung addition catalyzed by PPh_2Et, followed by an aldol reaction. The reaction delivers benzo fused azepinones in good to excellent yields under mild conditions, with exclusive *E*-configuration.

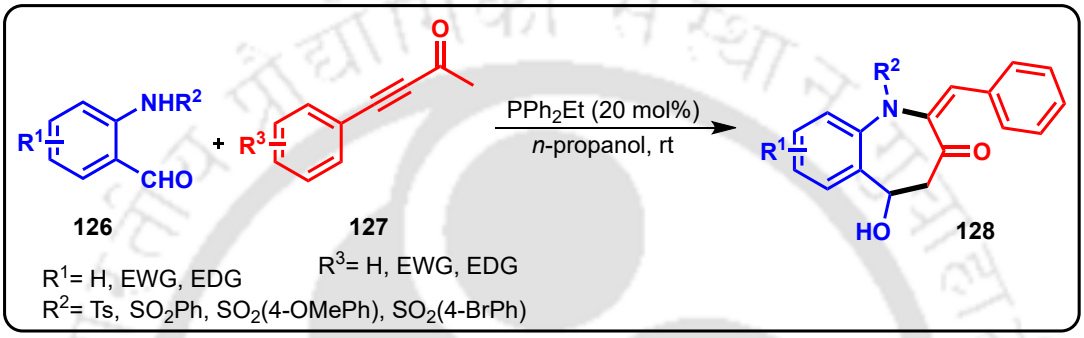

Scheme 1.3.3.10. *Phosphine-catalyzed synthesis of benzoazepinones.*

1.4 Summary

In summary, the above presented literature methods highlight the strategic use of alkenes and alkynes in tandem reactions for constructing fused *N*-heterocycles. These alkenyl and alkynyl precursors show diverse reactivity under various reaction conditions, such as different reagents, additives, temperatures, and reaction times, and with a range of coupling partners. The reactive and versatile double and triple bonds in these molecules enable them to take part in efficient tandem processes, leading to the formation of complex and biologically important fused *N*-heterocyclic frameworks in a practical and streamlined manner.

1.5 Objectives of the Present Work

The objectives of this research work are to develop efficient and straightforward synthetic methods to access a variety of fused *N*-heterocycles with significant biological importance. These methods rely on tandem reactions involving alkenyl or alkynyl precursors, which react with diverse coupling partners such as azides, cyanobenzaldehydes, indoles, azidobenzonitriles and azidobenzaldehydes. Our strategies are driven

by either acid- or base-catalyzed/mediated pathway to construct a range of bioactive compounds, including triazole-fused *N*-heterocycles, isoindoloindoles, pseudoindoxyls, 1,6-naphthyridines, and isochromenoquinolines in good to excellent yields. The overall goal of these works is to unveil advanced and innovative synthetic approaches that can contribute to the fields of natural product chemistry, drug discovery, and material science.

1.6 References

1. Katritzky, A. R.; Ramsden, C. A.; Scriven, E. F. V; Taylor, R. J. K. *Comprehensive Heterocyclic Chemistry III*; Elsevier: Oxford, **2008**.

2. (a) Al-Mulla, A. *Der Pharm. Chem.* **2017**, *9*, 141–147; (b) Saini, M. S.; Kumar, A.; Dwivedi, J.; Singh, R. *Int. J. Pharm. Sci. Res.* **2013**, *4*, 66–77; (c) Qadir, T.; Amin, A.; Sharma, P. K.; Jeelani, I.; Abe, H. *Open J. Med. Chem.* **2022**, *16*, 1–28; (d) Arora, P.; Arora, V.; Lamba, H. S.; Wadhwa, D. *Int. J. Pharm. Sci. Res.* **2012**, *3*, 2947–2954; (e) Kabir, E.; Uzzaman, M. A. *Results Chem.* **2022**, *12*, 1–25.

3. (a) Elnima, E. I.; Zubair, M. U.; Al-Badr, A. A. *Antimicrob. Agents Chemother.* **1981**, *19*, 29–32; (b) Liu, H.; Long, S.; Rakesh, K. P.; Zha, G. F. *Eur. J. Med. Chem.* **2020**, *185*, 111804; (c) Santosh, R.; Selvam, M. K.; Kanekar, S. U.; Nagaraja, G. K. *ChemistrySelect* **2018**, *3*, 6338–6343; (d) El-Hashash, M. A.; Rizk, S. A.; Atta-Allah, S. R. *Molecules* **2015**, *20*, 22069–22083.

4. (a) Liu, Y.; Qing, L.; Meng, C.; Shi, J.; Yang, Y.; Wang, Z.; Han, G.; Wang, Y.; Ding, J.; Meng, L-H.; Wang, Q. *J. Med. Chem.* **2017**, *60*, 2764–2779; (b) Rawat, A.; Reddy, A. V. B. *Eur. J. Med. Chem. Rep.* **2022**, *5*, 100038.

5. (a) Kumar, D.; Aggarwal, N.; Kumar, V.; Chopra, H.; Marwaha, R. K.; Sharma, R. *Future Med. Chem.* **2024**, *16*, 563–581; (b) Atmaram, U. A.; Roopan, S. M. *Appl. Microbiol. Biotechnol.* **2022**, *106*, 3489–3505; (c) Sharma, S.; Majee, C.; Mazumder, R.; Mazumder, A.; Taygi, P. K.; Singh, S. K. *Indian J. Pharm. Educ. Res.* **2025**, *59*, s25–s45; (d) Gour, V. K.; Yahya, S.; Shahar Yar, M. *Arch. Pharm.* **2024**, *357*, 2300328.

6. Amin, A.; Qadir, T.; Sharma, P. K.; Jeelani, I.; Abe, H. *Open J. Med. Chem.* **2022**, *16*, e187410452209010.

7. (a) Kerru, N.; Gummidi, L.; Maddila, S.; Gangu, K. K.; Jonnalagadda, S. B. *Molecules* **2020**, *25*, 1909; (b) HM, A. B.; Dubey, S. *Paving the Path to Discoveries and Unlocking the Secrets of N-Heterocycles* **2024**, 64.

8. (a) Vitaku, E.; Smith, D. T.; Njardarson, J. T. *J. Med. Chem.* **2014**, *57*, 10257–10274; (b) Ilardi, E. A.; Vitaku, E.; Njardarson, J. T. *J. Med. Chem.* **2014**, *57*, 2832–2842.

9. (a) Dinodia, M. *Mini-Rev. Org. Chem.* **2023**, *20*, 735–747; (b) Majee, S.; Shilpa; Sarav, M.; Banik, B. K.; Ray, D. *Pharmaceuticals* **2023**, *16*, 873; (c) Jampilek, J. *Molecules* **2019**, *24*, 3839.

10. (a) Sun, K.; Shan, H.; Ma, R.; Wang, P.; Neumann, H.; Lu, G. P.; Beller, M. *Chem. Sci.* **2022**, *13*, 6865–6872; (b) Takasao, G.; Maity, B.; Dutta, S.; Kancherla, R.; Rueping, M.; Cavallo, L. *ACS Catal.* **2025**, *15*, 5915–5927.

11. (a) Ledade, P. V.; Lambat, T. L.; Gunjate, J. K.; Chopra, P. K.; Bhute, A. V.; Lanjewar, M. R.; Kadu, P. M.; Dongre, U. J.; Mahmood, S. H. *Curr. Org. Chem.* **2023**, *27*, 206–222; (b) Biswas, T.; Mittal, R. K.; Sharma, V.; Kanupriya; Mishra, I. *Med. Chem.* **2024**, *20*, 369–384; (c) Nitha, P. R.; Soman, S.; John, J. *Mater. Adv.* **2021**, *2*, 6136–6168; (d) Fusco, S.; Maglione, C.; Velardo, A.; Piccialli, V.; Liguori, R.; Peluso, A.; Rubino, A.; Centore, R. *Eur. J. Org. Chem.* **2016**, *2016*, 1772–1780.

12. (a) Biswal, S.; Sahoo, U.; Sethy, S.; Kumar, H. K. S.; Banerjee, M. *Asian J. Pharm. Clin. Res.* **2012**, *5*, 1–6; (b) Kumar, S.; Bawa, S.; Gupta, H. *Mini Rev. Med. Chem.* **2009**, *9*, 1648–1654; (c) Liu, D.; Meng, X.; Wu, D.; Qiu, Z.; Luo, H. *Front. Pharmacol.* **2019**, *10*, 9; (d) Mane, U. R.; Mohanakrishnan, D.; Sahal, D.; Murumkar, P. R.; Giridhar, R.; Yadav, M. R. *Eur. J. Med. Chem.* **2014**, *79*, 422–435; (e) Pathare, B.; Bansode, T. *Results Chem.* **2021**, *3*, 100200.

13. (a) Sathish Kumar, S.; Kavitha, H. P. *Mini-Rev. Org. Chem.* **2013**, *10*, 40–65; (b) Gao, H.; Zhang, Q.; Jean'ne, M. S. *J. Mater. Chem. A.* **2020**, *8*, 4193–4216.

14. (a) Dheer, D.; Singh, V.; Shankar, R. *Bioorg. Chem.* **2017**, *71*, 30–54; (b) Matin, M. M.; Matin, P.; Rahman, M. R.; Ben Hadda, T.; Almalki, F. A.; Mahmud, S.; Ghoneim, M. M.; Alruwaily, M.; Alshehri, S. *Front. Mol. Biosci.* **2022**, *9*, 864286; (c) Haider, S.; Alam, M. S.; Hamid, H. *Inflamm. Cell Signal* **2014**, *1*, e95.

15. (a) Belhassan, A.; Zaki, H.; Benlyas, M.; Lakhlifi, T.; Bouachrine, M. *Heliyon* **2019**, *5*, e02446; (b) Lahti, R. A.; Sethy, V. H.; Barsuhn, C.; Hester, J. B. *Neuropharmacology* **1983**, *22*, 1277–1282; (c) Fischer, J.; Ganellin, C. R. *Chem. Int.* **2010**, *32*, 12–15.

16. (a) Speck, K.; Magauer, T. *Beilstein J. Org. Chem.* **2013**, *9*, 2048–2078; (b) He, Y.; Li, H.; Song, L.; Chen, L.; Liu, S. *New J. Chem.* **2024**, *48*, 7754–7760.

17. Yazıcıoğlu, Y. S.; Elmas, Ş.; Kılıç, Z.; Çelik, M.; Bakan, B.; Atmaca, U.; Bayrak, S. *J. Biochem. Mol. Toxicol.* **2025**, *39*, e70261.

18. Liu, J.; Wang, L.; Guo, N.; Teng, Y. O.; Yu, P. *J. Chem. Pharm. Res.* **2014**, *6*, 256–263.

19. (a) Mertens, A.; Zilch, H.; Koenig, B.; Schaefer, W.; Poll, T.; Kampe, W.; Seidel, H.; Leser, U.; Leinert, H. *J. Med. Chem.* **1993**, *36*, 2526–2535; (b) McGowan, K. M.; Nance, K. D.; Cho, H. P.; Bridges, T. M.; Conn, P. J.; Jones, C. K.; Lindsley, C. W. *Bioorg. Med. Chem. Lett.* **2017**, *27*, 1356–1359; (c) Sharma, S.; Oh, Y.; Mishra, N. K.; De, U.; Jo, H.; Sachan, R.; Kim, H. S.; Jung, Y. H.; Kim, I. S. *J. Org. Chem.* **2017**, *82*, 3359–3367.

20. (a) Dhote, P. S.; Patel, P.; Vanka, K.; Ramana, C. V. *Org. Biomol. Chem.* **2021**, *19*, 7970–7994; (b) Angyal, P.; Hegedüs, K.; Mészáros, B. B.; Daru, J.; Dudás, Á.; Galambos, A. R.; Essmat, N.; Al-Khrasani, M.; Varga, S.; Soós, T. *Angew. Chem. Int. Ed.* **2023**, *62*, e202303700; (c) Angyal, P.; Hegedüs, K.; Mészáros, B. B.; Daru, J.; Dudás, Á.; Galambos, A. R.; Essmat, N.; Al-Khrasani, M.; Varga, S.; Soós, T. *Angew. Chem. Int. Ed.* **2023**, *62*, e202303700.

21. Váradi, A.; Marrone, G. F.; Palmer, T. C.; Narayan, A.; Szabó, M. R.; Le Rouzic, V.; Grinnell, S. G.; Subrath, J. J.; Warner, E.; Kalra, S.; Hunkele, A. *J. Med. Chem.* **2016**, *59*, 8381–8397.

22. Perumal, K.; Lee, J.; Annes, S. B.; Ramesh, S.; Rangarajan, T. M.; Mathew, B.; Kim, H. *RSC Adv.* **2023**, *13*, 24925–24935.

23. (a) Gomi, K.; Kobayashi, E.; Miyoshi, K.; Ashizawa, T.; Okamoto, A.; Ogawa, T.; Katsumata, S.; Mihara, A.; Okabe, M.; Hirata, T. *Jpn. J. Cancer Res.* **1992**, *83*, 113–120; (b) Liu, J. F.; Jiang, Z. Y.; Wang, R. R.; Zheng, Y. T.; Chen, J. J.; Zhang, X. M.; Ma, Y. B. *Org. Lett.* **2007**, *9*, 4127–4129; (c)

Andrade, M. T.; Lima, J. A.; Pinto, A. C.; Rezende, C. M.; Carvalho, M. P.; Epifanio, R. A. *Bioorg. Med. Chem.* **2005**, *13*, 4092–4095.

24. (a) Oliveras, J. M.; Puig de la Bellacasa, R.; Estrada-Tejedor, R.; Teixidó, J.; Borrell, J. I. *Pharmaceuticals* **2021**, *14*, 1029; (b) Kulikova, L. N.; Raesi, G. R.; Levickaya, D. D.; Purgatorio, R.; Spada, G. L.; Catto, M.; Altomare, C. D.; Voskressensky, L. G. *Molecules* **2023**, *28*, 1662.

25. Chabowska, G.; Barg, E.; Wójcicka, A. *Molecules* **2021**, *26*, 4324.

26. (a) Zhuang, L.; Wai, J. S.; Embrey, M. W.; Fisher, T. E.; Egbertson, M. S.; Payne, L. S.; Guare, J. P.; Vacca, J. P.; Hazuda, D. J.; Felock, P. J.; Wolfe, A. L.; Stillmock, K. A.; Witmer, M. V.; Moyer, G.; Schleif, W. A.; Gabryelski, L. J.; Leonard, Y. M.; Lynch, J. J.; Michelson, S. R.; Young, S. D. *J. Med. Chem.* **2003**, *46*, 453–456; (b) Bauer, U.; Giordanetto, F.; Bauer, M.; O'Mahony, G.; Johansson, K. E.; Knecht, W.; Hartleib-Geschwindner, J.; Carlsson, E. T.; Enroth, C. *Bioorg. Med. Chem. Lett.* **2012**, *22*, 1944–1948; (c) Thompson, A. M.; Connolly, C. J.; Hamby, J. M.; Boushelle, S.; Hartl, B. G.; Amar, A. M.; Kraker, A. J.; Driscoll, D. L.; Steinkampf, R. W.; Patmore, S. J.; Vincent, P. W. *J. Med. Chem.* **2000**, *43*, 4200–4211.

27. (a) Michael, J. P. *Nat. Prod. Rep.* **2003**, *20*, 476–493; (b) Michael, J. P. *Nat. Prod. Rep.* **2001**, *18*, 543–559.

28. (a) Upadhyay, K. D.; Shah, A. K. *Anti-Cancer Agents Med. Chem.* **2019**, *19*, 1285–1292; (b) Heydari, Z.; Mohammadi-Khanaposhtani, M.; Imanparast, S.; Faramarzi, M. A.; Mahdavi, M.; Ranjbar, P. R.; Larijani, B. *Med. Chem.* **2019**, *15*, 8–16; (c) Upadhyay, K. D.; Dodia, N. M.; Khunt, R. C.; Chaniara, R. S.; Shah, A. K. *ACS Med. Chem. Lett.* **2018**, *9*, 283–288.

29. (a) Chen, I. S.; Wu, S. J.; Tsai, I. L. *J. Nat. Prod.* **1994**, *57*, 1206–1211; (b) Di Pietro, O.; Vicente-García, E.; Taylor, M. C.; Berenguer, D.; Viayna, E.; Lanzoni, A.; Sola, I.; Sayago, H.; Riera, C.; Fisa, R.; Clos, M. V.; Pérez, B.; Kelly, J. M.; Lavilla, R.; Muñoz-Torrero, D. *Eur. J. Med. Chem.* **2015**, *105*, 120; (c) Payne, D. J.; Hueso-Rodríguez, J. A.; Boyd, H.; Concha, N. O.; Janson, C. A.; Gilpin, M.; Bateson, J. H.; Cheever, C.; Niconovich, N. L.; Pearson, S.; Rittenhouse, S.; Tew, D.; Díez, E.; Pérez, P.; Fuénte, J.; Rees, M.; Rivera-Sagredo, A. *Antimicrob. Agents Chemother.* **2002**, *46*, 1880.

30. (a) Tietze, L. F. *Chem. Rev.* **1996**, *96*, 115–136; (b) Nicolaou, K. C.; Montagnon, T.; Snyder, S. A. *Chem. Commun.* **2003**, 551–564; (c) Wasilke, J.-C.; Obrey, S. J.; Baker, R. T.; Bazan, G. C. *Chem. Rev.* **2005**, *105*, 1001–1020; (d) Patil, N. T.; Yamamoto, Y. *Synlett.* **2007**, *2007*, 1994–2005.

31. (a) Ardkhean, R.; Caputo, D. F. J.; Morrow, S. M.; Shi, H.; Xiong, Y.; Anderson, E. A. *Chem. Soc. Rev.* **2016**, *45*, 1557–1569; (b) Tietze, L. F.; Modi, A. *Med. Res. Rev.* **2000**, *20*, 304–322; (c) Clavier, H.; Pellissier, H. *Adv. Synth. Catal.* **2012**, *354*, 3347–3403; (d) Bunce, R. A. *Tetrahedron* **1995**, *51*, 13103–13159.

32. (a) Nicolaou K. C.; Chen, J. S. *Chem. Soc. Rev.* **2009**, *38*, 2993–3009; (b) Tiwari, G.; Kumar, M.; Chauhan, A. N. S.; Erande, R. D. *Org. Biomol. Chem.* **2022**, *20*, 3653–3674.

33. (a) Ihara, M. *Arkivoc*, **2006**, *7*, 416–438; (b) Liao, J.; Yang, X.; Ouyang, L.; Lai, Y.; Huang, J.; Luo, R. *Org. Chem. Front.* **2021**, *8*, 1345–1363; (c) Fathi Vavsari, V.; Balalaie, S. *Curr. Org. Chem.* **2017**, *21*, 1393–1426.

34. (a) Robinson, R. *J. Chem. Soc.* **1917**, *111*, 762–768; (b) Robinson, R. *J. Chem. Soc.* **1917**, *111*, 876–899.

35. Nicolaou, K. C.; Edmonds, D. J.; Bulger, P. G. *Angew. Chem. Int. Ed.* **2006**, *45*, 7134–7186.

36. Porashar, B.; Biswas, S.; Sahu, A. K.; Chutia, A.; Saikia, A. K. *Org. Lett.* **2022**, *24*, 9038–9042.

37. Sureshbabu, P.; Bhajammanavar, V.; Choutipalli, V. S. K.; Subramanian, V.; Baidya, M. *Chem. Commun.* **2022**, *58*, 1187–1190.

38. Xu, H.; He, J.; Shi, J.; Tan, L.; Qiu, D.; Luo, X; Li, Y. *J. Am. Chem. Soc.* **2018**, *140*, 3555–3559.

39. Dabiri, M.; Lehi, N. F.; Movahed, S. K; Khavasi, H. R. *Eur. J. Org. Chem.* **2019**, *2019*, 2933–2940.

40. Pal, K.; Sontakke, G. S; Volla, C. M. *Org. Lett.* **2019**, *21*, 3716–3720.

41. Feng, X.; Zhu, H.; Wang, L.; Jiang, Y.; Cheng, J.; Yu, J. T. *Org. Biomol. Chem.* **2014**, *12*, 9257–9263.

42. Bhuyan, D.; Sarma, R.; Dommaraju, Y; Prajapati, D. *Green Chem.* **2014**, *16*, 1158–1162.

43. Zhang, X.; Ma, X.; Qiu, W.; Awad, J.; Evans, J.; Zhang, W. *Adv. Synth. Catal.* **2020**, *362*, 5513–5517.

44. Basak, S. J.; Dash, J. *J. Org. Chem.* **2024**, *89*, 233–244.

45. (a) Arora, A. *Hydrocarbons (Alkanes, Alkenes and Alkynes)*; Discovery Publishing House: New Delhi, **2006**; (b) March, J. *Advanced Organic Chemistry: Reactions, Mechanisms, and Structure*; McGraw-Hill: New York, **1977**; (c) Clayden, J.; Greeves, N.; Warren, S.; Wothers, P. *Organic Chemistry*; Oxford University Press: Oxford, **2001**; (d) Abozenadah, H.; Bishop, A.; Bittner, S.; Lopez, O.; Wiley, C.; Flatt, P. M. *Consumer Chemistry: How Organic Chemistry Impacts Our Lives*; Western Oregon University: Monmouth, OR, **2017**.

46. Nicolaou, K.C.; Bulger, P. G.; Sarlah, D. *Angew. Chem. Int. Ed.* **2005**, *44*, 4442–4489.

47. (a) Alabugin, I. V.; Gonzalez-Rodriguez, E.; Kawade, R. K.; Stepanov, A. A.; Vasilevsky, S. F. *Molecules* **2019**, *24*, 1036; (b) Sun, K.; Wang, X.; Li, C.; Wang, H.; Li, L. *Org. Chem. Front.* **2020**, *7*, 3100–3119; (c) Ha, S.; Lee, Y.; Kwak, Y.; Mishra, A.; Yu, E.; Ryou, B.; Park, C. M. *Nat. Commun.* **2020**, *11*, 2509.

48. (a) Shaw, R.; Singh, A.; Althagafi, I.; Pratap, R.; Yadav, D. K. *RSC Adv.* **2025**, *15*, 12202–12245; (b) Michelet, V.; Toullec, P. Y.; Genêt, J. P. *Angew. Chem. Int. Ed.* **2008**, *47*, 4268–4315; (c) Hong, F. L.; Ye, L. W. *Acc. Chem. Res.* **2020**, *53*, 2003–2019.

49. (a) Denmark, S. E.; Thorarensen, A. *Chem. Rev.* **1996**, *96*, 137–166; (b) Nicolaou, K. C.; Snyder, S. A.; Montagnon, T.; Vassilikogiannakis, G. *Angew. Chem. Int. Ed.* **2002**, *41*, 1668–1698; (c) Mohamed, R. K.; Mondal, S.; Gold, B.; Evoniuk, C. J.; Banerjee, T.; Hanson, K.; Alabugin, I. V. *J. Am. Chem. Soc.* **2015**, *137*, 6335–6349.

50. Zeng, X. *Chem. Rev.* **2013**, *113*, 6864–6900.

51. Porashar, B.; Behera, B. K.; Phukon, H.; Saikia, A. K. *Chem. Commun.* **2024**, *60*, 4358–4361.

52. Chen, C. B.; Wang, X. F.; Cao, Y. J.; Cheng, H. G.; Xiao, W. J. *J. Org. Chem.* **2009**, *74*, 3532–3535.

53. Lin, Z.; Hu, Z.; Zhang, X.; Dong, J.; Liu, J. B.; Chen, D. Z.; Xu, X. *Org. Lett.* **2017**, *19*, 5284–5287.

54. Yip, K. T.; Yang, M.; Law, K. L.; Zhu, N. Y.; Yang, D. *J. Am. Chem. Soc.* **2006**, *128*, 3130–3131.

55. Cao, Y. J.; Cheng, H. G.; Lu, L. Q.; Zhang, J. J.; Cheng, Y.; Chen, J. R.; Xiao, W. J. *Adv. Synth. Catal.* **2011**, *353*, 617–623.

56. Indukuri, K.; Unnava, R.; Deka, M. J.; Saikia, A. K. *J. Org. Chem.* **2013**, *78*, 10629–10641.

57. Maity, S.; Zheng, N. *Angew. Chem. Int. Ed.* **2012**, *51*, 9562.

58. Donthiri, R. R.; Pappula, V.; Reddy, N. N. K.; Bairagi, D.; Adimurthy, S. *J. Org. Chem.* **2014**, *79*, 11277–11284.

59. Cheng, H. G.; Chen, C. B.; Tan, F.; Chang, N. J.; Chen, J. R.; Xiao, W. J. *Eur. J. Org. Chem.* **2010**, *2010*, 4976–4980.

60. Santra, S.; Bagdi, A. K.; Majee, A.; Hajra, A. *Adv. Synth. Catal.* **2013**, *355*, 1065–1070.

61. Chutia, A.; Arandhara, P. J.; Saikia, A. K. *J. Org. Chem.* **2024**, *89*, 11542–11557.

62. Jin, T.; Suzuki, S.; Ho, H. E.; Matsuyama, H.; Kawata, M; Terada, M. *Org. Lett.* **2021**, *23*, 9431–9435.

63. Hao, L.; Pan, Y.; Wang, T.; Lin, M.; Chen, L.; Zhan, Z. P. *Adv. Synth. Catal.* **2010**, *352*, 3215– 3222.

64. Sari, O.; Seybek, A. F.; Kaya, S.; Menges, N.; Erdem, S. S.; Balci, M. *Eur. J. Org. Chem.* **2019**, 5261–5274.

65. Basceken, S.; Balci, M. *J. Org. Chem.* **2015**, *80*, 3806–3814.

66. Das, M; Saikia A. K. *J. Org. Chem.* **2018**, *83*, 6178–6185.

67. Li, Y.; Li, J.-H. *Org. Lett.* **2018**, *20*, 5323–5326.

68. Sie, C.-Y.; Chuang, C.-P. *Org. Biomol. Chem.* **2018**, *16*, 5483–5491.

69. Liu, X.; Deng, G.; Liang, Y. *Tetrahedron Lett.* **2018**, *59*, 2844–2847.

70. Zhang, K.; Cai, L.; Hong, S.; Kwon, O. *Org. Lett.* **2019**, *21*, 5143–5146.

Chapter 2

Synthesis of 1,2,3-Triazole-Fused *N*-Heterocycles from *N*-Alkynyl Hydroxyisoindolinones and Sodium Azide *via* the Huisgen Reaction

Contents

Abstract: This chapter describes an efficient transition-metal-free one-pot synthesis of dihydro[1,2,3]triazolo-pyrimidoisoindolone and dihydro[1,2,3]triazolo-diazepinoisoindolone scaffolds from *N*-alkynyl-3-hydroxyisoindolinones and sodium azide (NaN_3), utilizing the reactive intermediate *N*-acyliminium ion and Huisgen reaction. The reaction is mediated by an inexpensive Lewis acid borontrifluoride diethyl etherate ($BF_3{\cdot}OEt_2$) in *N*,*N*-dimethylformamide (DMF) at 130 °C. The protocol provides a simple route for the synthesis of functionalized 1,2,3-triazole-fused *N*-heterocycles in moderate to good yields. The methodology can further be extended towards the synthesis of its thione derivative dihydro[1,2,3]triazolo-pyrimidoisoindolthione *via* thionation of amide.

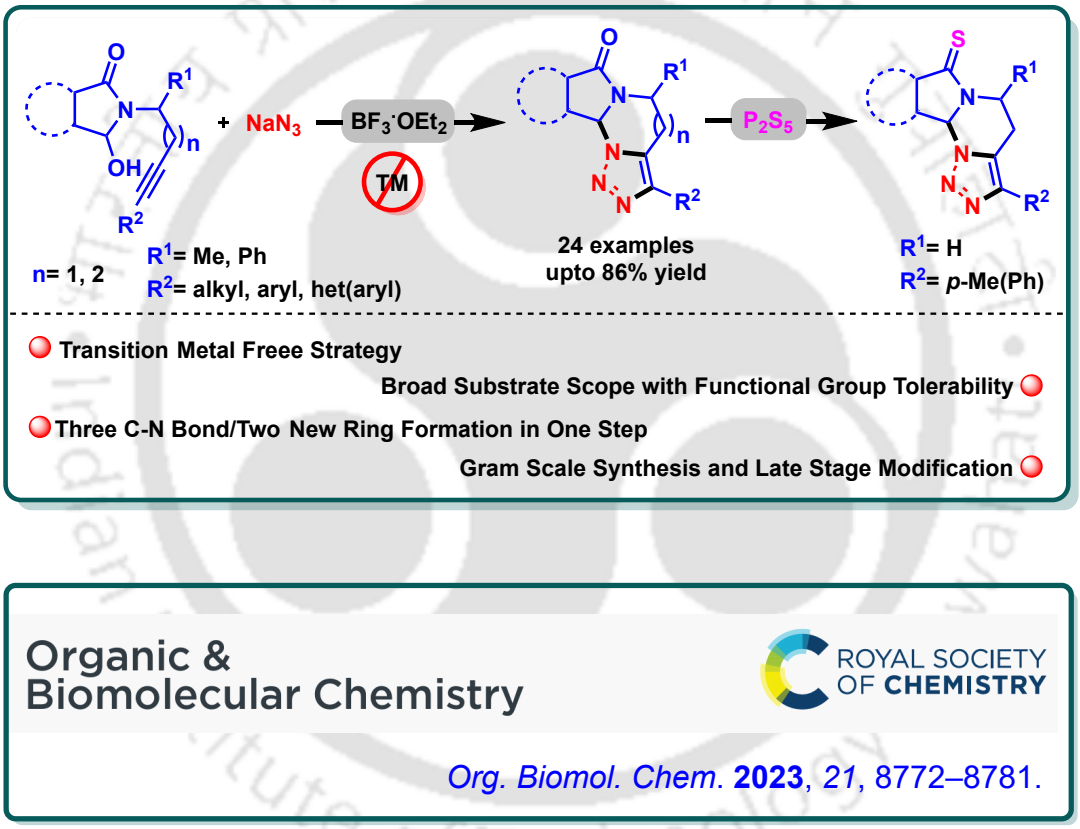

2.1 Introduction

Structurally diverse nitrogen heterocyclic compounds are important motifs in drug development and related fields. Therefore, enormous efforts have been given to design new and innovative synthetic methodologies for the synthesis of such compounds.[1] Among them, triazole-fused *N*-heterocycles are an important class of compounds known for their diverse biological activities and structural complexity.[2] For example, [1,2,3]triazolo[1,5-*a*]-quinoxalin-4(5*H*)-one (**I**) and its analogous tricyclic system **II** have been found to possess important biological activities such as agonists for the G-protein-coupled niacin receptor 109A,[3] and inhibitors for the benzodiazepine receptor and adenosine receptors.[4] Indolo[3,2-*e*][1,2,3]triazolo[1,5-*a*]pyrimidine derivative **III** possess antitumor activity (*Figure 2.1.1*).[5] In these triazole-fused *N*-heterocycles, a triazole ring is integrated with another nitrogen-containing heterocycle, resulting in unique electronic and steric properties. The fusion of triazole with other nitrogen-containing rings enhances molecular rigidity, stability, and pharmacological potential. These frameworks are widely explored in medicinal chemistry, agrochemicals, and material science.

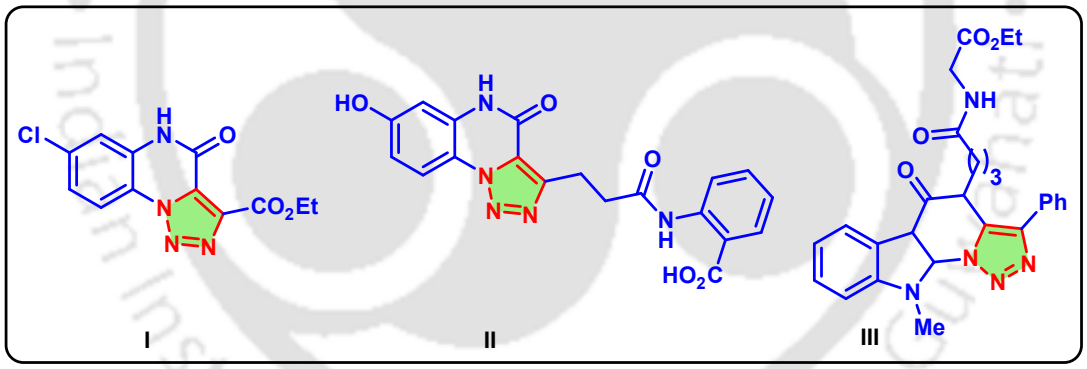

Figure 2.1.1. *Examples of bioactive triazole fused N-heterocycles.*

2.2 Literature Survey on the Synthesis of 1,2,3-Triazole Fused *N*-Heterocycles

Various synthetic strategies, including cycloaddition and tandem reactions, have been developed to access these fused heterocyclic systems efficiently. One-pot tandem reactions have been intensively studied and demonstrated as a powerful tool in organic synthesis.[6] A wide range of 1,2,3-triazole-fused *N*-heterocyclic compounds have been synthesized through diverse methodologies employing a variety of starting materials, reagents, and catalysts.

Here, a few examples for the synthesis of 1,2,3-triazole fused *N*-heterocycles have been presented:

An interesting example regarding the synthesis of [1,2,3]-triazole-fused 1,4-benzodiazepinone derivatives **3** was reported by Martin *et al.* in the presence of sodium triacetoxyborohydride, $NaBH(OAc)_3$, and glacial AcOH (*Scheme 2.2.1*).[7] The [1,2,3]-triazolo-1,4-benzodiazepine scaffolds were prepared from 2-azidobenzaldehydes **1** *via* reductive amination with propargylamine (**2**), followed by thermally induced, intramolecular Huisgen cycloaddition reaction.

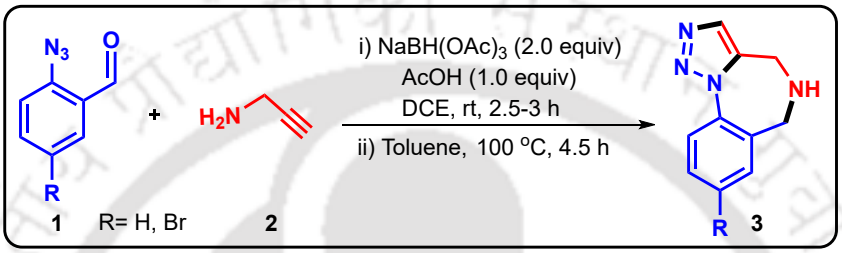

Scheme 2.2.1. *$NaBH(OAc)_3$-mediated synthesis of 1,2,3-triazole-fused 1,4-benzodiazepine.*

Similarly, Ganai and co-workers described a copper-catalyzed tandem Ullmann C-N coupling followed by azide-alkyne cycloaddition in DMF in the presence of K_2CO_3 to form substituted [1,2,3]-triazole-fused 1,4-benzodiazepine derivatives **6** (*Scheme 2.2.2*).[8] The reaction proceeds *via* the interaction between *o*-azidobenzylbromide **4** and *N*-propargylated aniline **5** derivatives.

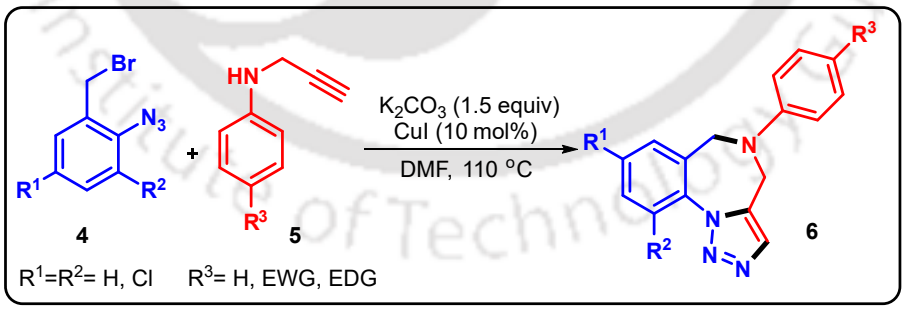

Scheme 2.2.2. *Copper-catalyzed synthesis of 1,2,3-triazole-fused 1,4-benzodiazepines.*

Pan and co-workers established the first azide-alkene cycloaddition of benzylazides *in situ* generated from the corresponding *ortho*-substituted benzyl bromides **7** and sodium azide **8** (*Scheme 2.2.3*).[9] This catalyst-free reaction proceeds smoothly at room temperature in DMF to afford the fused [1,2,3]-triazole-fused tricyclic frameworks **9** in moderate to good yields.

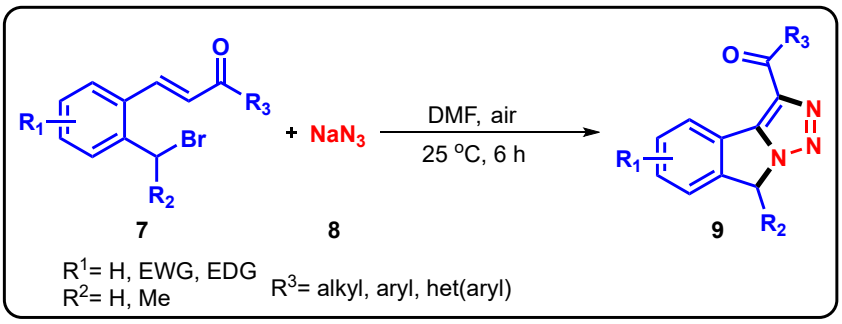

Scheme 2.2.3. *Catalyst free synthesis of 1,2,3-triazole-fused tricyclic frameworks.*

Akritopoulou- Zanze *et al.* reported a two-step synthesis of fused dihydrotriazolo[1,5-*a*]pyrazinone derivatives **15** and triazolobenzodiazepine derivatives **16** using Ugi/ alkyne-azide cycloaddition reaction in sequence (*Scheme 2.2.4*).[10] The reaction proceeds *via* Ugi MCR among aldehyde **10**, amine **11**, isocyanide **12**, and acid **13** to from an Ugi adduct **14**, which undergoes intramolecular alkyne-azide cyclization to access these highly functionalized heterocycles.

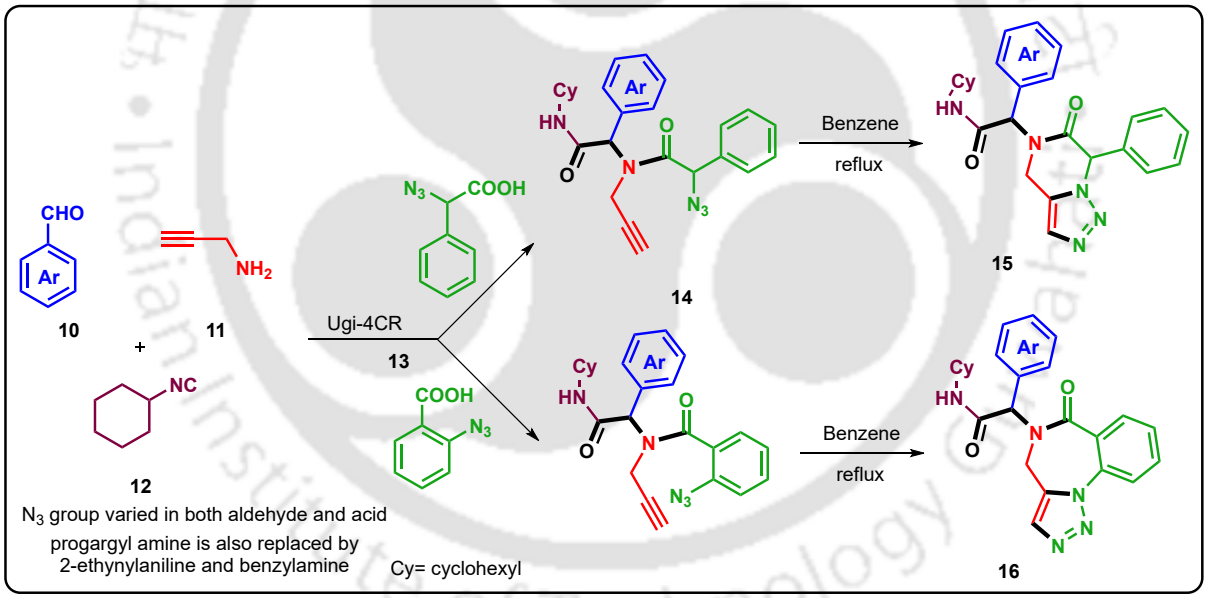

Scheme 2.2.4. *Two-step synthesis of dihydrotriazolo-pyrazinones and triazolo-benzodiazepines.*

Eycken and co-workers developed another Ugi 4-component and azide-alkyne cycloaddition/Ullmann coupling strategy for the efficient synthesis of triazolo[1,5-*a*][1,4]benzodiazepinone scaffolds **22** (*Scheme 2.2.5*).[11] This Cu-catalyzed tandem reaction proceeds *via* the [3+2] cycloaddition between NaN_3 and Ugi-product **21** derived from *o*-bromobenzaldehyde **17**, amine **18**, isocyanide **19**, and propiolic acid **20** derivatives.

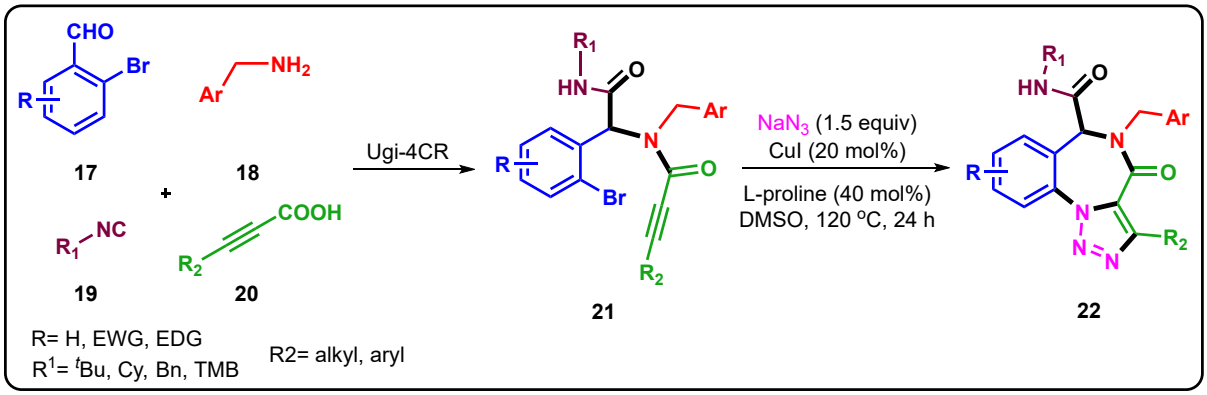

Scheme 2.2.5. *Cu-catalyzed synthesis of triazolo-benzodiazepinones.*

Balasubramanian *et al.* have reported the synthesis of 1,2,3- triazolo-benzoxazepine derivatives **25** *via* Cu(I)-catalyzed 1,3-dipolar cycloaddition of azido-alkynes **24** derived from salicylaldehyde **23** (*Scheme 2.2.6*).[12] The azido-alkynes were synthesized from the corresponding salicylaldehyde in three steps. The cycloaddition reaction was performed with a copper sulfate solution in ethanol under refluxing conditions to afford the [1,2,3]-triazolo[5,1-*c*][1,4]benzoxazepine derivatives in good yields.

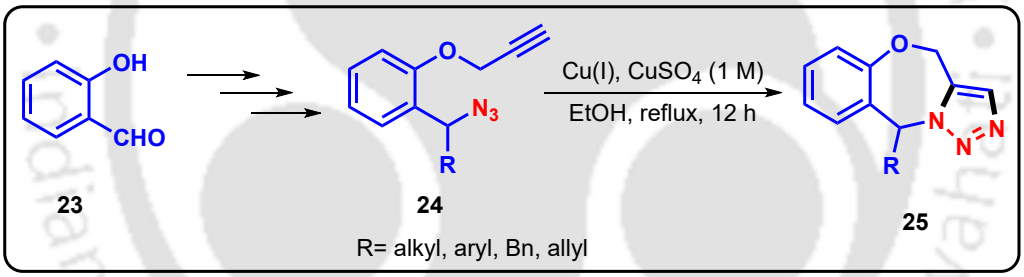

Scheme 2.2.6. *Cu(I)-catalyzed synthesis of triazolo-benzoxazepines.*

Chowdhury and his group demonstrated an efficient palladium-copper-catalyzed heteroannulation reaction of *o*-iodobenzyl azide **26** and acetylene derivatives **27** for the construction of isoindolotriazoles **28**. The reaction proceeds through carbon-carbon bond formation followed by cycloaddition (*Scheme 2.2.7*).[13]

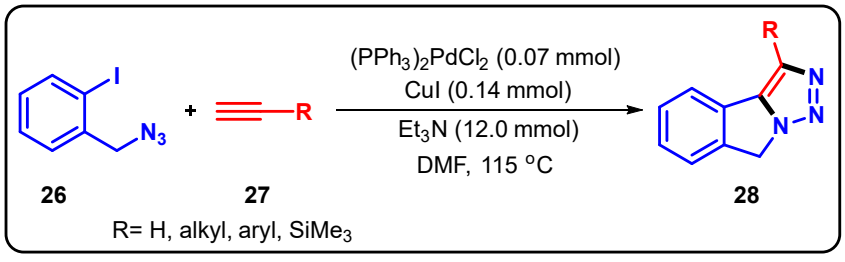

Scheme 2.2.7. *Pd/Cu-catalyzed synthesis of isoindolotriazoles.*

The developed methodology is operationally simple and convenient for the cycloaddition strategy of azide to the internal alkynes.

The same group has also reported the synthesis of [1,2,3]triazolo[5,1-*c*][1,4]benzoxazines **31** from 1-azido-2-(prop-2-ynyloxy)benzene **29** with aryl/vinyl iodides **30** using the same catalytic system i.e., palladium–copper (*Scheme 2.2.8*).[14] This one-pot protocol operates through carbon–carbon bond formation followed by intramolecular cycloaddition of aromatic azide with alkyne, generated *in situ* under palladium-copper catalysis.

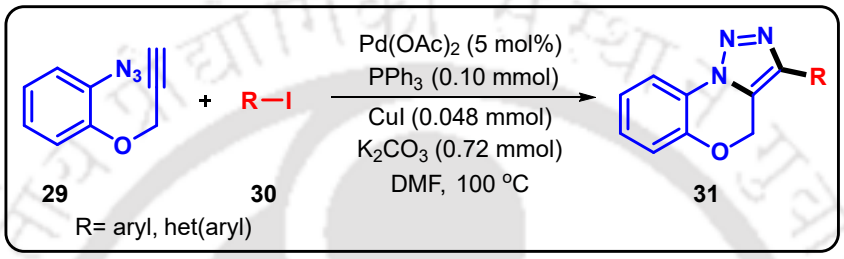

Scheme 2.2.8. *Pd/Cu-catalyzed synthesis of triazolo-benzoxazines.*

2.3 Present Work

The above literature survey suggests that the synthesis of 1,2,3-triazole fused-*N*-heterocycles *via N*-acyliminium ion intermediates, followed by the Huisgen reaction, have not been much explored yet. *N*-acyliminium ions are powerful reactive intermediates and have been utilized for the construction of a range of structurally diverse compounds *via* intra- and intermolecular nucleophilic addition (*Scheme 2.3.1a*).[15]

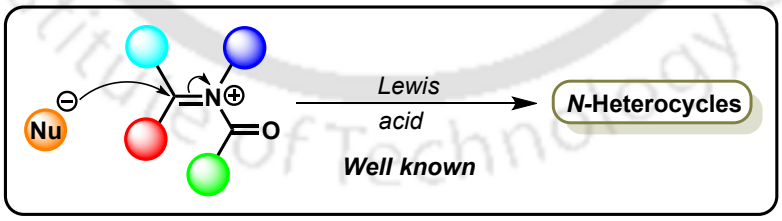

Scheme 2.3.1a. *Previous reports on N-acyliminium ion.*

On the other hand, the Huisgen reaction, a 1,3-dipolar cycloaddition reaction, is one of the atom-economical thermal [3 + 2]-cycloaddition type reactions of alkynes with azides, and has been investigated widely in organic synthesis (*Scheme 2.3.1b*).[16] Intramolecular azide-alkyne cycloaddition reactions have also been reported.[17] 1,2,3-triazoles are commonly prepared by the Huisgen 1,3-dipolar cycloaddition of azides with alkynes.

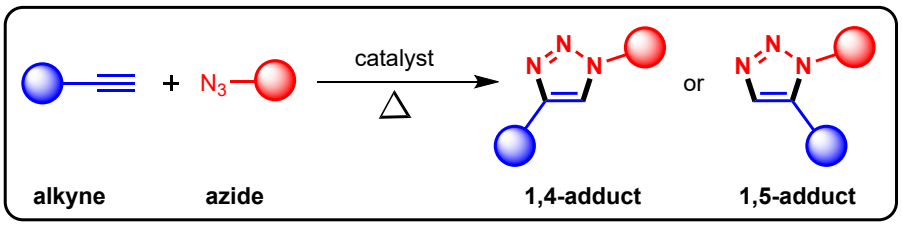

Scheme 2.3.1b. *Previous reports on Huisgen reaction.*

Keeping these considerations in mind, we sought to develop a methodology for the synthesis of triazole fused *N*-heteocyclic scaffolds by integrating *N*-acyliminium ion chemistry with the Huisgen reaction. Herein, we report an *N*-acyliminium ion-initiated direct transformation of *N*-alkynyl hydroxyisoindolinones **32** and sodium azide **33** into triazolo-pyrimidoisoindolone and triazolo-diazepinoisoindolone derivatives **34** in moderate to good yields (*Scheme 2.3.1c*). The reaction involves the *in situ* generation of the *N*-acyliminium ion intermediate, which undergoes a nucleophilic attack by the azide ion, followed by a [3 + 2]-intramolecular azide–alkyne cycloaddition reaction. Importantly, the reaction proceeds without the involvement of any transition metal catalyst.

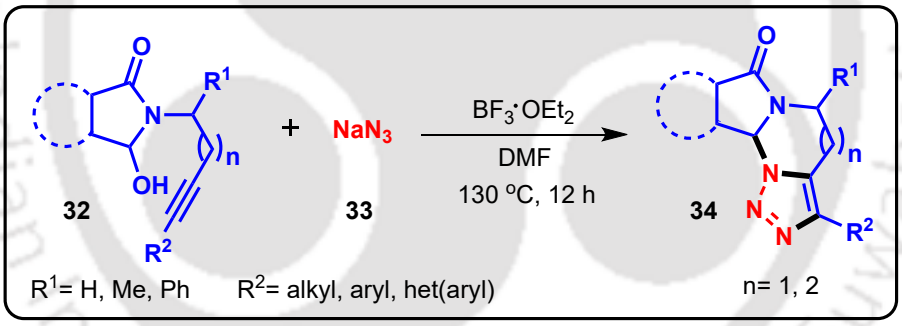

Scheme 2.3.1c. *Synthesis of 1,2,3-triazole-fused N-heterocycles via N-acyliminium ion and the Huisgen reaction.*

Thus, in this chapter, a concise synthesis of dihydro[1,2,3]triazolo-pyrimidoisoindolones and dihydro[1,2,3]triazolo-diazepinoisoindolones from *N*-alkynyl hydroxyisoindolinones and sodium azide *via* an azide-alkyne cycloaddition reaction is presented.

2.4 Results and Discussion

2.4.1 Optimization of the Reaction

To start with, *N*-alkynyl amido alcohol **32a** was treated with sodium azide **33** (2.0 equiv) in the presence of 1.2 equiv of borontrifluoride etherate ($BF_3{\cdot}OEt_2$)

in dimethylformamide (DMF) at 110 °C for 12 h and dihydro[1,2,3]triazolo-pyrimidoisoindolone **34a** was obtained with 50% yield (*Table 2.4.1.1*, entry 1).

Table 2.4.1.1. *Optimization of the reaction*[a]

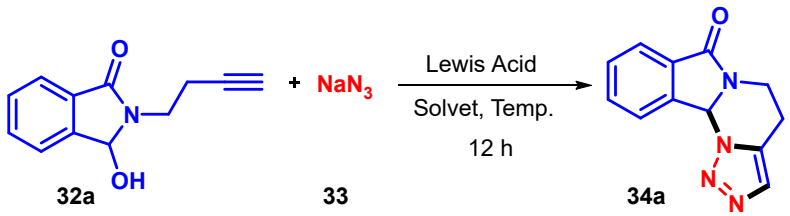

Entry[a]	Lewis acid (equiv)	Solvent	Temp (°C)	Yield (%)[b]
1.	$BF_3{\cdot}OEt_2$ (1.2)	DMF	110	50
2.	$BF_3{\cdot}OEt_2$ (1.2)	DMSO	110	35
3.	$BF_3{\cdot}OEt_2$ (1.2)	toluene	110	-[c]
4.	$BF_3{\cdot}OEt_2$ (1.2)	Dioxane	110	45
5.	$BF_3{\cdot}OEt_2$ (1.2)	Acetonitrile	80	-[c]
6.	$BF_3{\cdot}OEt_2$ (1.5)	DMF	110	65
7.	$BF_3{\cdot}OEt_2$ (2.0)	DMF	110	73
8.	$BF_3{\cdot}OEt_2$ (3.0)	DMF	110	69
9.	**$BF_3{\cdot}OEt_2$ (2.0)**	**DMF**	**130**	**84**
10.	$BF_3{\cdot}OEt_2$ (2.0)	DMF	150	80
11.	$BF_3{\cdot}OEt_2$ (2.0)	DMF	130	82[d]
12.	$InCl_3$ (0.2)	DMF	130	40
13.	TMSOTf (1.2)	DMF	130	44
14.	$FeCl_3$ (1.2)	DMF	130	-[c]
15.	$In(OTf)_3$ (0.2)	DMF	130	N.R.
16.	$Bi(OTf)_3$ (0.2)	DMF	130	N.R.
17.	$Sc(OTf)_3$ (0.2)	DMF	130	N.R.
18.	AgOTf (0.2)	DMF	130	N.R.

[a]**32a** (0.5 mmol), **33** (1.0 mmol), solvent 4.0 mL, N_2 atmosphere. [b]Isolated yield, [c]Decomposed product, [d]Reaction was continued for 18 h, N.R.= no reaction.

The reaction was also screened with other solvents such as dimethyl sulfoxide (DMSO), toluene, dioxane, and acetonitrile (*Table 2.4.1.1*, entries 2–5). The reaction in DMSO and dioxane gave 35% and 45% yields, respectively, whereas in toluene and acetonitrile, the reaction resulted in a decomposed product. Among all, DMF was found to be the most suitable solvent for the transformation. To increase the efficiency of our strategy, the reaction was screened with different stoichiometries of the reagent. Increasing the amount of $BF_3{\cdot}OEt_2$ to 1.5 and 2.0 equiv increased the yield of the product to 65% and 73% (*Table 2.4.1.1*, entries 6 and 7), respectively. Further increasing the reagent amount to 3.0 equiv did not lead to any improvement in the yield (*Table 2.4.1.1*, entry 8). When the temperature was raised to 130 °C, the yield was favorably increased to 84% (*Table 2.4.1.1*, entry 9). In contrast, the same reaction at 150 °C gave a comparatively lower yield of 80% (*Table 2.4.1.1*, entry 10). The reaction was also continued for 18 h to check the yield, but it resulted in a slightly lower yield of 82% (*Table 2.4.1.1*, entry 11). Keeping the temperature constant at 130 °C, the reaction was screened with other Lewis acids such as $InCl_3$, TMSOTf, $FeCl_3$, $In(OTf)_3$, $Bi(OTf)_3$, $Sc(OTf)_3$ and AgOTf (*Table 2.4.1.1*, entries 12–18), but all of them were found to be inefficient in providing a better yield of the desired product. Therefore, 2.0 equiv of $BF_3{\cdot}OEt_2$ in DMF at 130 °C were found to be the optimal conditions for the reaction.

2.4.2 Substrate Scope

With the established optimal conditions in hand, the reaction was explored with various *N*-substituted amido alcohols, as shown in *Scheme 2.4.2.1*. It was observed that both terminal (R^2 = H) and internal (R^2 = alkyl, aryl, heteroaryl) alkynes gave moderate to good yields. The substituents on the aromatic ring of the alkynyl part had a promising effect on the yield of the reaction. Electron-donating groups on the aromatic ring gave higher yields (*Scheme 2.4.2.1*, **34j**–**34m**) compared to electron-withdrawing groups on the aromatic ring (*Scheme 2.4.2.1*, **34c**–**34i**). This might be due to the electronic effect of the substituent groups, where electron-donating groups increase the electron density on the alkyne group; conversely, electron-withdrawing groups reduce the electron density over the alkyne group. Alkyl and heteroaryl substituted alkyne substrates also worked well, furnishing the corresponding products **34n** and **34o** in 69% and 70% yields, respectively (*Scheme 2.4.2.1*).

The reaction was also successfully carried out with naphthalene-, hexahydro-, and tetrahydro-substituted *N*-amido alcohol, which furnished the corresponding products in 68%, 57% and 68% yields, respectively (*Scheme 2.4.2.1*, **34p**–**34r**). Alkyl and aryl

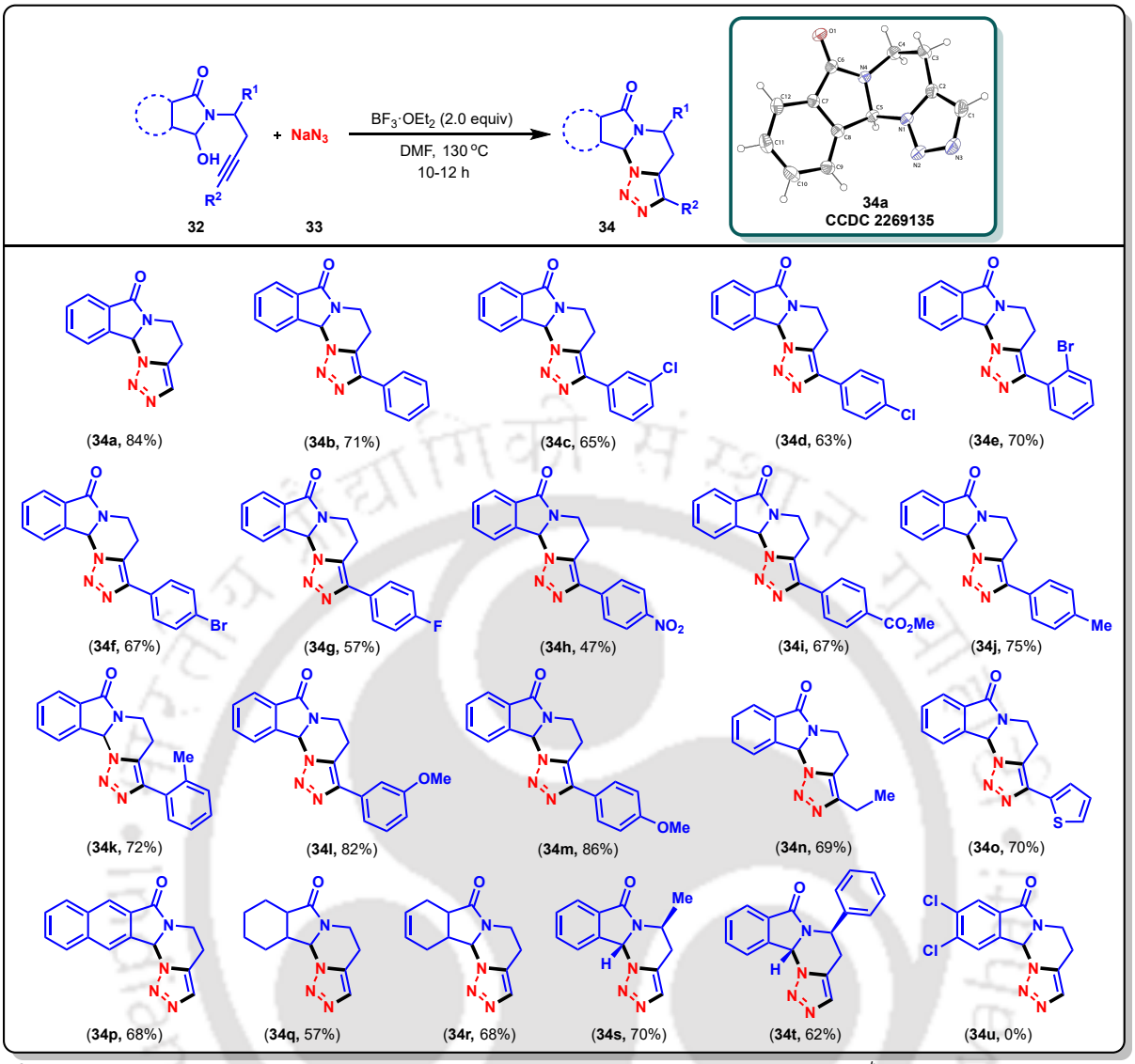

[a]Reaction condition: **32** (0.5 mmol, 1.0 equiv), **33** (1.0 mmol, 2.0 equiv), DMF 4.0 mL, N_2 atmosphere. [b]Isolated yield of the product.

Scheme 2.4.2.1. *Scope of synthesis of dihydro[1,2,3]triazolo-pyrimidoisoindolones.*[a,b]

substitution (R^1 = Me, Ph) at the 1-position of the alkyl side chain also provided the desired products in good yields (*Scheme 2.4.2.1*, **34s** and **34t**). Unfortunately, the substrate having an electron-withdrawing group in the aromatic ring of the *N*-alkynyl amido alcohol **32u** could not produce product **34u** but decomposed under the reaction conditions.

Furthermore, the strategy can be extended to the synthesis of structurally complex seven-membered ring systems, dihydro[1,2,3]triazolo-diazepinoisoindolones (*Scheme 2.4.2.2*, **34v**–**34y**).

The structure of the compounds **34a**–**34y** was determined by NMR, IR spectroscopy, COSY and nOe experiments for compounds **34s**, **34t**, High resolution mass spectrometry (HRMS), and finally by X-ray crystallographic analysis of compound **34a**.

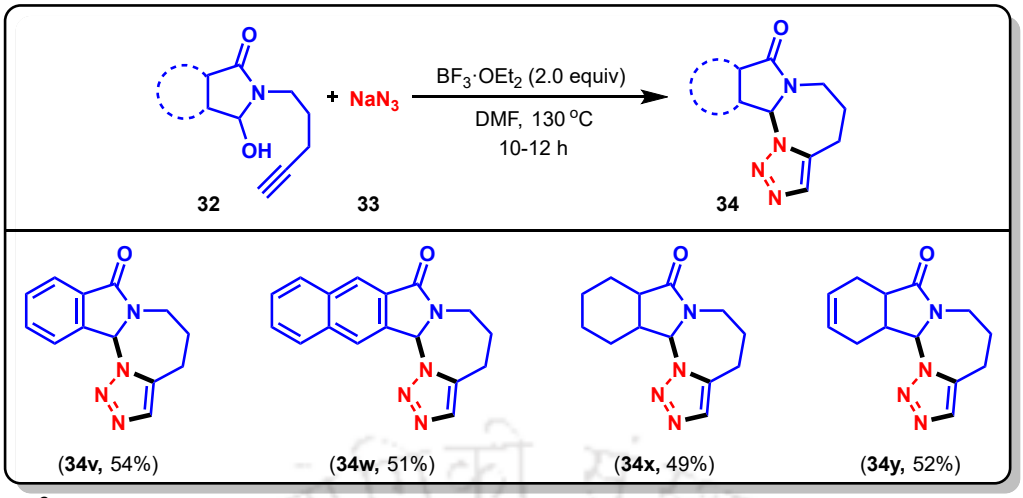

[a]Reaction condition: **32** (0.5 mmol, 1.0 equiv), **33** (1.0 mmol, 2.0 equiv), DMF 4.0 mL, N_2 atmosphere. [b]Isolated yield of the product.

Scheme 2.4.2.2. *Scope of synthesis of dihydro[1,2,3]triazolo-diazepinoisoindolone derivatives.*[a,b]

2.4.3 Gram-Scale Synthesis

In order to check the scalability of the methodology, a gram scale reaction was carried out. Compound **32a** (1.00 g, 4.97 mmol) was treated with sodium azide **33** (646 mg, 9.94 mmol) under the standard reaction conditions to provide a 64% (719 mg) yield of the corresponding product **34a** (*Scheme 2.4.3.1*).

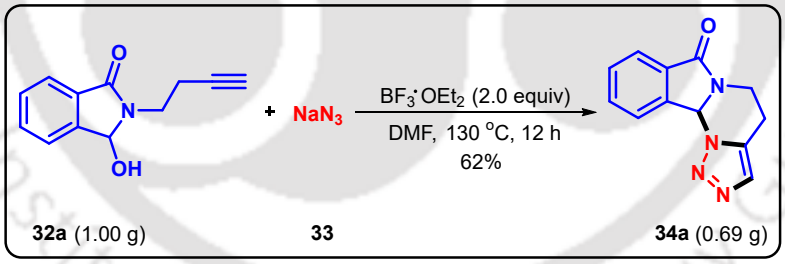

Scheme 2.4.3.1. *Gram-scale synthesis.*

2.4.4 Control Experiments

To explore the mechanism of the reaction, some control experiments were carried out. In order to confirm the *in situ* generation of intermediate **B** (*Scheme 2.4.4.1*), substrate **32a** (1.0 equiv) was subjected to react with sodium azide **33** (2.0 equiv) in the presence of $BF_3{\cdot}OEt_2$ in DMF at room temperature for 6 h. The azide-substituted intermediate **B** was isolated with 71% yield (*Scheme 2.4.4.1a*), which was confirmed by NMR and HRMS analysis. Furthermore, a reaction was performed with the isolated intermediate **B** in DMF at 130 °C, which resulted in 80% yield of the

desired product **34a** *via* the Huisgen reaction (*Scheme 2.4.4.1b*). These experiments suggest that the reaction might be proceeding through intermediate **B**.

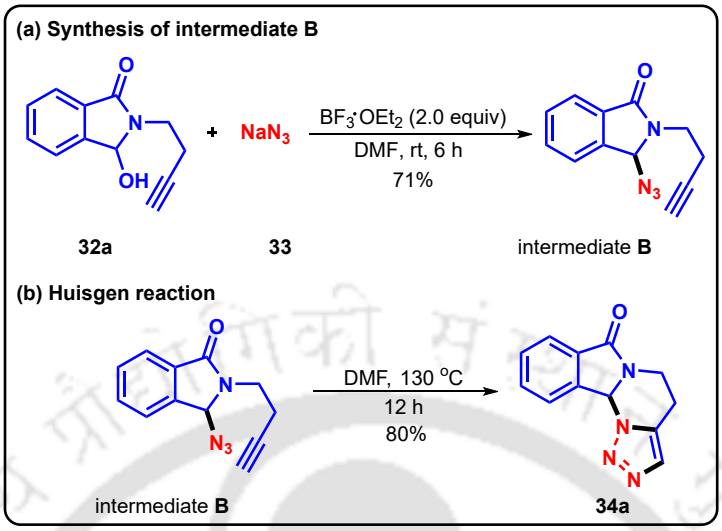

Scheme 2.4.4.1. *Control experiments.*

2.4.5 Plausible Mechanism

From the above control experiments and previous literature reports,[17] a plausible mechanism is proposed. Initially, the amido alcohol **32** under Lewis acidic conditions generates *N*-acyliminium ion **A**, which is attacked by sodium azide *via* a nucleophilic addition reaction to give intermediate **B**. Finally, an intramolecular [3 + 2] Huisgen cycloaddition, intermediate **B** furnishes the final product **34** (*Scheme 2.4.5.1*).

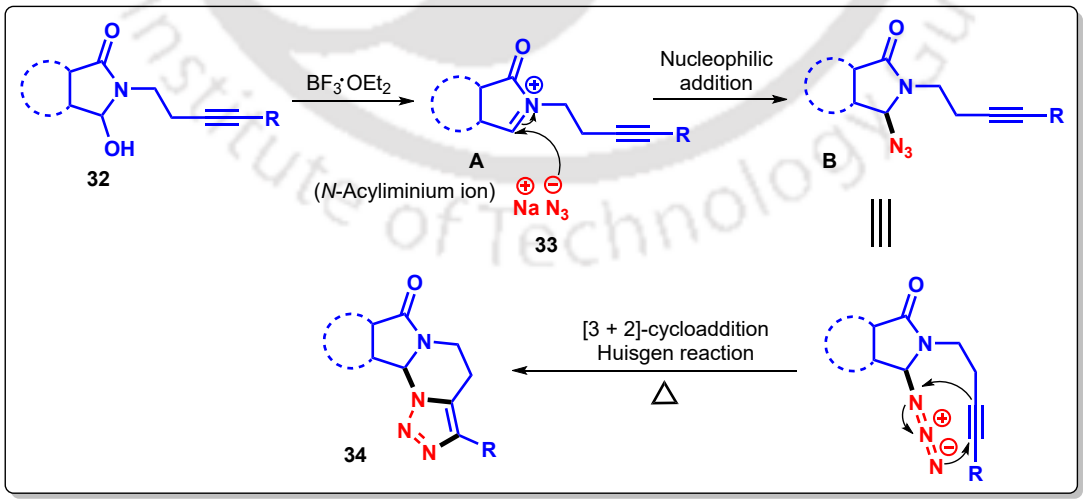

Scheme 2.4.5.1. *Plausible mechanism for the reaction.*

2.4.6 Post-synthetic Application

In an attempt to convert pyrimidoisoindol-2-one into pyrimidoisoindol-2-thione, compound **34j** (1.0 equiv) was treated with phosphorus pentasulfide (P_2S_5) (1.0 equiv) in toluene under reflux condition, affording product **35j** in 68% yield (*Scheme 2.4.6.1*).

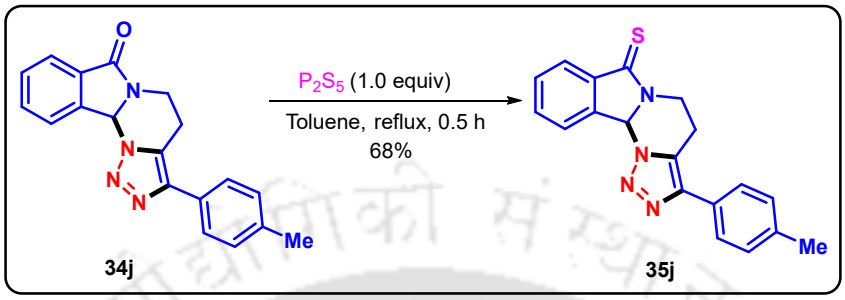

Scheme 2.4.6.1. *Scope of synthesis of pyrimidoisoindol-2-thione.*

2.5 Crystallographic Description

The structure of all compounds was confirmed from standard spectroscopic experiments and finally by *X*-ray crystallographic analysis of compound **34a** (*Figure 2.5.1*).

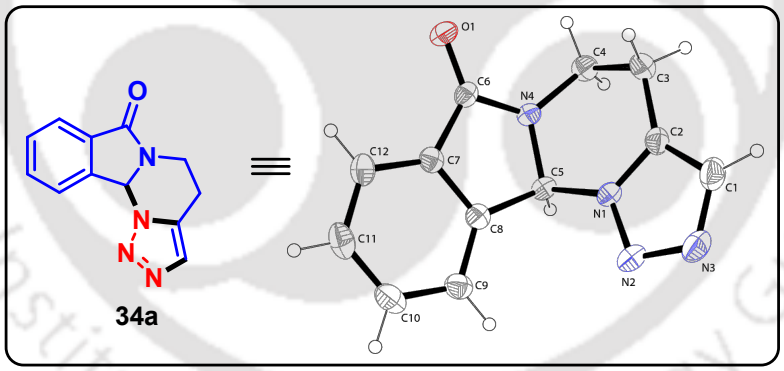

Figure 2.5.1. *ORTEP diagram of compound **34a**, thermal ellipsoids are drawn on 30% probability level.*

Single crystal X-ray diffraction of compound **34a** was obtained by slow evaporation of hexane and ethyl acetate solution (9:1). The detailed data collection and structure refinement are summarized in *Table 2.5.1*, where CCDC **2269135** of **34a** contains the supplementary crystallographic data

Table 2.5.1. *Crystal parameters of compound* ***34a***

Compound 34a	CCDC 2269135
Formula	$C_{12}H_{10}N_4O$
Formula weight	244.26
T/K	298(2)
Crystal system	monoclinic
Space group	P 21
a/Å	10.0470(8)
b/Å	4.9832(4)
c/Å	11.8477(10)
a/°	90
β/°	104.242(2)
γ/°	90
V/Å^3	574.98(8)
Z	2
Abs. Coeff./mm^{-1}	0.100
Abs. Correction	multi-scan
GOF on F^2	0.715
Final R indices [$I > 2\sigma(I)$]	$R1 = 0.0357$ $wR2 = 0.1020$
R indices [all data]	$R1 = 0.0405$ $wR2 = 0.1103$

2.6 Conclusion

In conclusion, we have developed a transition-metal-free one-pot synthesis of dihydro[1,2,3]triazolo-pyrimidoisoindolone and dihydro[1,2,3]triazolo-diazepinoisoindolone derivatives from *N*-alkynyl-3-hydroxyisoindolinones utilizing the reactive intermediate *N*-acyliminium ion and Huisgen reaction. The reaction is mediated by an inexpensive Lewis acid and is compatible with a variety of functional groups, giving

moderate to good yields. The versatility of this protocol is demonstrated by its scalability and modification to the corresponding thione derivative

2.7 Experimental Section

2.7.1 Reaction Procedure

2.7.1.1 General Experimental Procedure for the Synthesis of Starting Materials

The starting materials **32a**, **32b**, **32d**, **32f**, **321g**, **32j**, **32k**, **32m**, and **32n** were synthesized according to the literature reports, and the spectroscopic data of the compounds are in good agreement with the literature data.[18]

2.7.1.1.1 General Experimental Procedure for the Synthesis of Compounds 32c, 32e, 32h, 32i, 32l and 32o–32y

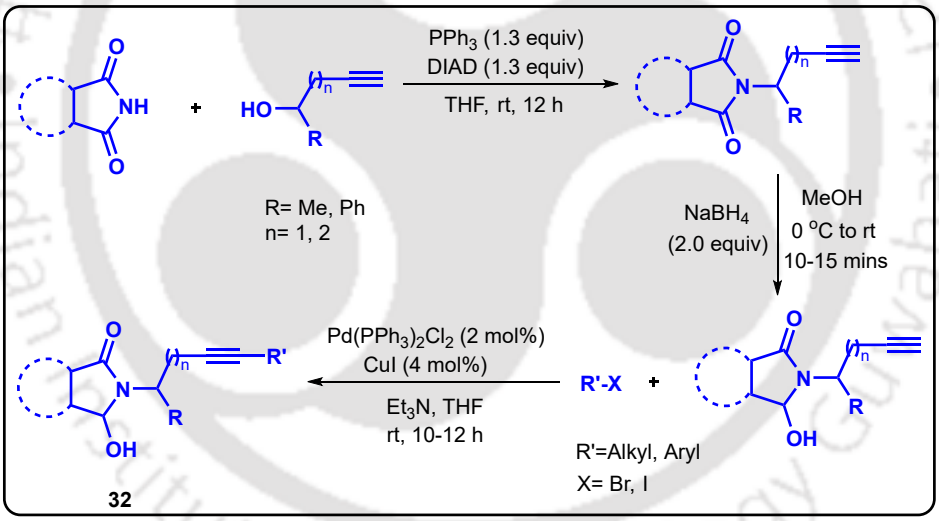

To a suspension of substituted pthalimide derivative (3.4 mmol, 1.3 equiv) and PPh_3 (3.4 mmol, 1.3 equiv) in THF under N_2 atmosphere was added substituted alcohol derivative (2.6 mmol, 1 equiv), followed by DIAD (3.4 mmol, 1.3 equiv) dropwise at 0 °C under nitrogen atmosphere. The reaction mixture was allowed to stir at 0 °C for 5 min, which was then warmed to room temperature. The progress of the reaction was monitored by TLC analysis. After completion of the reaction, the reaction mixture was quenched with brine solution and the aqueous layer was extracted with ethyl acetate (3 × 15 mL). The combined organic layers were further washed with brine, followed by drying over anhydrous Na_2SO_4. The organic phase was concentrated using a rotary

evaporator to give the crude product, which was then subjected to column chromatography over silica gel to provide the corresponding *N*-substituted isoindolinone product. Subsequently, to an ice-cold solution of *N*-substituted isoindolinone (1.5 mmol, 1.0 equiv) in methanol, $NaBH_4$ (3 mmol, 2.0 equiv) was added slowly in open air condition. The reaction was allowed to stir at the same temperature until the starting material was entirely consumed, as evident by TLC analysis. After completion of the reaction, the solvent was removed under reduced pressure and diluted with saturated $NaHCO_3$ solution. The aqueous layer was extracted with ethyl acetate (3 × 15 mL), and the combined organic layers were further washed with brine, followed by drying over anhydrous Na_2SO_4. The organic phase was concentrated in a rotary evaporator to give the crude product, which was then subjected to column chromatography over silica gel to provide the desired product *N*-substituted amido alcohol derivatives. Next, to a mixture of $Pd(PPh_3)_2Cl_2$ (0.018 mmol, 2.0 mol%) and CuI (0.036 mmol, 4.0 mol%) under inert atmosphere, triethylamine (4.5 mmol, 5.0 equiv) was added, followed by the dropwise addition of iodobenzene (0.9 mmol, 1 equiv). The reaction mixture was stirred for 10 min at room temperature, after which the corresponding amido alcohol (1.0 mmol, 1.1 equiv) dissolved in THF (5 mL) was added dropwise over a period of 5 min. The reaction mixture was then allowed to stir for 10-12 h (monitored by TLC analysis) before filtering through a pad of celite. The solids were washed with ethyl acetate, and the combined filtrates were concentrated in a rotary evaporator. The crude product was then purified by column chromatography over silica gel to provide the corresponding product **32**.

2.7.1.2 General Experimental Procedure for the Synthesis of Compounds 34a-34t and 34v-34y

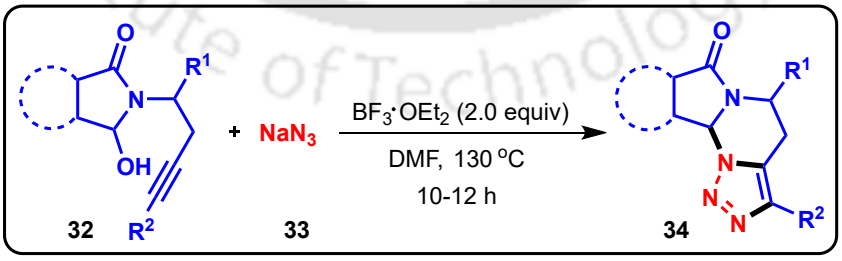

To a stirred solution of *N*-alkynyl hydroxyisoindolinones **32** (0.5 mmol, 1.0 equiv) and sodium azide **33** (1 mmol, 2.0 equiv) in DMF (4 ml) was added $BF_3{\cdot}OEt_2$ (1 mmol, 2.0 equiv) dropwise at 0 °C under nitrogen atmosphere. Then the mixture was allowed to stir at room temperature for 5–10 min, followed by heating at 130 °C in an oil bath, and the reaction was monitored by TLC. After completion of the reaction (10–

12 h), the reaction mixture was allowed to cool at room temperature and then diluted with ethyl acetate, saturated $NaHCO_3$, and brine solution. The organic phase was extracted with ice water (3 × 10 mL). The combined organic extracts were dried over anhydrous Na_2SO_4 and concentrated using a rotary evaporator. The crude product was subjected to column chromatography over silica gel to provide the corresponding product **34**.

2.7.1.3 Experimental Procedure for the Gram-scale Synthesis of Compound 34a

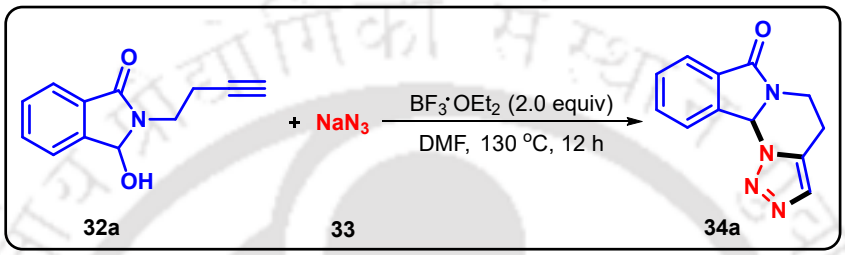

To a stirred solution of 2-(but-3-yn-1-yl)-3-hydroxyisoindolinone (**32a**) (1.00 g, 4.97 mmol, 1 equiv) and sodium azide **33** (646 mg, 9.94 mmol, 2 equiv) in DMF (12 ml) was added $BF_3{\cdot}OEt_2$ (1.23 ml, 9.94 mmol, 2 equiv) dropwise at 0 °C under nitrogen atmosphere. The reaction mixture was allowed to stir at room temperature for 5–10 min followed by heating at 130 °C in an oil bath for 12 h. The reaction was monitored by TLC, and after completion of the reaction, the reaction was allowed to cool at room temperature and then diluted with ethyl acetate, saturated $NaHCO_3$, and brine solution. The organic phase was extracted with ice water (3 × 20 mL). The combined organic extracts were dried over anhydrous Na_2SO_4 and concentrated using a rotary evaporator. The crude product was subjected to column chromatography over silica gel to provide the corresponding product **34a** with 64% yield (719 mg).

2.7.1.4 Experimental Procedure for Control Experiments

2.7.1.4.1 Experimental Procedure for the Synthesis of Intermediate B (a)

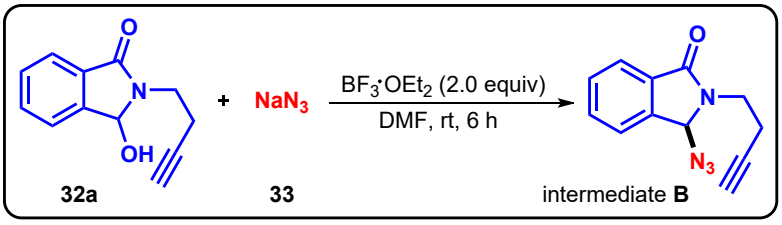

To a stirred solution of 2-(but-3-yn-1-yl)-3-hydroxyisoindolinone **32a** (0.25 mmol, 1 equiv) and sodium azide **33** (0.5 mmol, 2 equiv) in DMF (2 ml) was added $BF_3{\cdot}OEt_2$ (0.5 mmol, 2 equiv) dropwise at 0 °C under nitrogen atmosphere. The reaction mixture was then allowed to stir at room temperature and monitored by TLC. After completion of the reaction, the reaction mixture was diluted with ethyl acetate, saturated $NaHCO_3$ and brine solution. The organic phase was extracted with ice water (3 × 10 mL). The combined organic extracts were dried over Na_2SO_4 and concentrated using rotary evaporator. The crude product was subjected to column chromatography over silica gel to give the corresponding intermediate **B** in 71% yield, which was confirmed by ^1H, $^{13}C\{^1H\}$ and HRMS analysis.

2.7.1.4.2 Experimental Procedure for the Synthesis of 34a from Intermediate B (b)

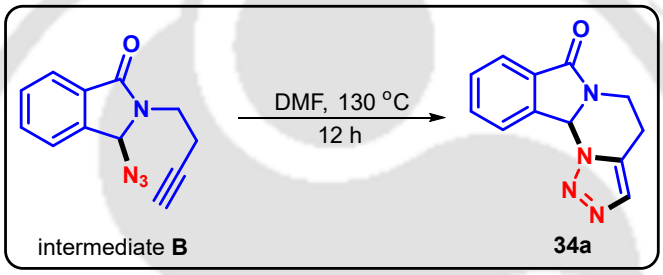

The compound **B** (0.18 mmol, 1.0 equiv) was dissolved in DMF (2.0 ml) and the reaction mixture was allowed to stir at 130 °C under nitrogen atmosphere. The progress of the reaction was monitored by TLC, and after completion of the reaction, the reaction mixture was allowed to cool to room temperature and then diluted with ethyl acetate. The organic phase was extracted with ice water (3 × 10 mL). The combined organic extracts were dried over anhydrous Na_2SO_4 and concentrated using rotary evaporator. The crude product was subjected to column chromatography over silica gel to give the corresponding product **34a** in 80% yield.

2.7.1.5 Experimental Procedure for the Synthesis of Compound 35j

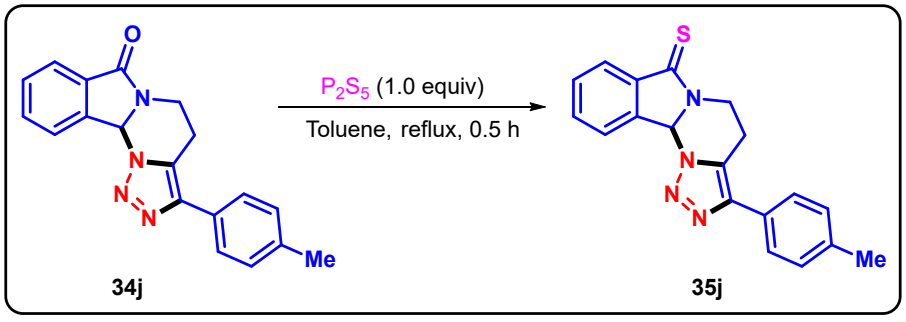

To a stirred solution of P_2S_5 (71 mg, 0.32 mmol, 1.0 equiv) in toluene (3.0 mL), compound **34j** (100 mg, 0.32 mmol, 1.0 equiv) dissolved in toluene was added slowly to the reaction mixture at room temperature. The reaction mixture was then refluxed under nitrogen atmosphere in an oil bath for 0.5 h. The reaction was monitored by TLC, and after the completion of the reaction, the reaction mixture was poured into water and extracted with EtOAc (3 × 10 mL). The combined organic layers were washed with water and dried over anhydrous Na_2SO_4. The solvent was removed under reduced pressure, and the crude product was then purified using column chromatography over silica gel to get the corresponding product **35j** in 68% yield.

2.8 References

1. (a) Quin, L. D.; Tyrell, J. *Fundamentals of Heterocyclic Chemistry: Importance in Nature and in the Synthesis of Pharmaceuticals*; Wiley: **2010**; (b) Joule, J. A.; Mills, K. *Heterocyclic Chemistry*; Wiley: **2010**; (c) Katritzky, A. R.; Zhang, Y.; Singh, S. K. *Heterocycles.* **2003**, *60*, 1225–1239.

2. (a) Alvarez, R.; Velazquez, S.; San-Felix, A.; Aquaro, S.; De Clercq, E.; Perno, C. F. N.; Karlsson, A.; Balzarini, J.; Camarasa, M. J. *J. Med. Chem.* **1994**, *37*, 4185–4194; (b) Brik, A.; Muldoon, J.; Lin, Y. C.; Elder, J. H.; Goodsell, D. S.; Olson, A. J.; Fokin, V. V.; Sharpless, K. B.; Wong, C. H. *ChemBioChem* **2003**, *4*, 1246–1248; (c) Alagarsamy, V.; Solomon, V. R.; Murugan, M. *Bioorg. Med. Chem.* **2007**, *15*, 4009–4015; (d) Bertelli, L.; Biagi, G.; Giorgi, I.; Livi, O.; Manera, C.; Scartoni, V.; Lucacchini, A.; Giannaccini, G.; Barili, P. L. *Eur. J. Med. Chem.* **2000**, *35*, 333–341.

3. Shen, H. C.; Ding, F.-X.; Deng, Q. L.; Wilsie, L. C.; Krsmanovic, M. L.; Taggart, A. K.; Carballo-Jane, E.; Ren, N.; Cai, T.-Q.; Wu, T.-J.; Wu, K. K.; Cheng, K.; Chen, Q.; Wolff, M. S.; Tong, X. C.; Holt, T. G.; Waters, M. G.; Hammond, M. L.; Tata, J. R.; Colletti, S. L. *J. Med. Chem.* **2009**, *52*, 2587–2602.

4. (a) Biagi, G.; Giorgi, I.; Livi, O.; Scartoni, V.; Betti, L.; Giannaccini, G.; Trincavelli, M. L. *Eur. J. Med. Chem.* **2002**, *37*, 565–571; (b) Bertelli, L.; Biagi, G.; Giorgi, I.; Manera, C.; Livi, O.; Scarton, V.; Betti, L.; Giannaccini, G.; Trincavelli, L.; Barili, P. L. *Eur. J. Med. Chem.* **1998**, *33*, 113–122.

5. Lauria, A.; Patella, C.; Dattolo, G.; Almerico, A. M. *J. Med. Chem.* **2008**, *51*, 2037–2046.

6. (a) Nicolaou, K. C.; Montagnon, T.; Snyder, S. A. *Chem. Commun.* **2003**, 551–564; (b) Parsons, P. J.; Penkett, C. S.; Shell, A. J. *Chem. Rev.* **1996**, *96*, 195–206; (c) Pellissier, H. *Adv. Synth. Catal.* **2019**, *361*, 1733–1755.

7. Donald, J. R.; Martin, S. F. *Org. Lett.* **2011**, *13*, 852–855.

8. Majumdar, K. C.; Ganai, S. *Tetrahedron Lett.* **2013**, *54*, 6192–6195.

9. Xie, Y. Y.; Wang, Y. C.; He, Y.; Hu, D. C.; Wang, H. S.; Pan, Y. M. *Green Chem.* **2017**, *19*, 656–659.

10. Akritopoulou-Zanze, I.; Gracias, V.; Djuric, S. W. *Tetrahedron Lett.* **2004**, *45*, 8439–8441.

11. Vachhani, D. D.; Kumar, A.; Modha, S. G.; Sharma, S. K.; Parmar, V. S.; Van der Eycken, E. V. *Eur. J. Org. Chem.* **2013**, *2013*, 1223–1227.

12. Chandrasekhar, S.; Seenaiah, M.; Kumar, A.; Reddy, C. R.; Mamidyala, S. K.; Kumar, C. G.; Balasubramanian, S. *Tetrahedron Lett.* **2011**, *52*, 806–808.

13. Chowdhury, C.; Mandal, S. B.; Achari, B. *Tetrahedron Lett.* **2005**, *46*, 8531–8534.

14. Chowdhury, C.; Sasmal, A. K.; Dutta, P. K. *Tetrahedron Lett.* **2009**, *50*, 2678–2681.

15. (a) Wu, P.; Nielsen, T. E. *Chem. Rev.* **2017**, *117*, 7811–7856; (b) Yazici, A.; Pyne, S. G. *Org. Lett.* **2013**, *15*, 5878–5881; (c) Andna, L.; Miesch, L. *Org. Lett.* **2018**, *20*, 3430–3433; (d) Krishna, Y.; Tanaka, F. *Org. Lett.* **2021**, *23*, 1874–1879.

16. (a) Johansson, R.; Beke-Somfai, T.; Stålsmeden, A. S.; Kann, N. *Chem. Rev.* **2016**, *116*, 14726–14768; (b) Rostovtsev, V. V.; Green, L. G.; Fokin, V. V.; Sharpless, K. B. *Angew. Chem. Int. Ed.* **2002**, *41*, 2596–2599.

17. (a) Oliva, A. I.; Christmann, U.; Font, D.; Cuevas, F.; Ballester, P.; Buschmann, H.; Torrens, A.; Yenes, S.; Pericàs, M. A. *Org. Lett.* **2008**, *10*, 1617–1619; (b) Vekariya, R. H.; Liu, R.; Aubé, J. *Org. Lett.* **2014**, *16*, 1844–1847; (c) Li, R.; Jansen, D. J.; Datta, A. *Org. Biomol. Chem.* **2009**, *7*, 1921–1930.

18. (a) Das, M.; Saikia, A. K. *J. Org. Chem.* **2018**, *83*, 6178–6185; (b) Sahu, A. K.; Unnava, R.; Shit, S.; Saikia, A. K. *J. Org. Chem.* **2020**, *85*, 1961–1971.

2.9 Characterization Data

2-(4-(3-Chlorophenyl)but-3-yn-1-yl)-3-hydroxyisoindolin-1-one (32c):

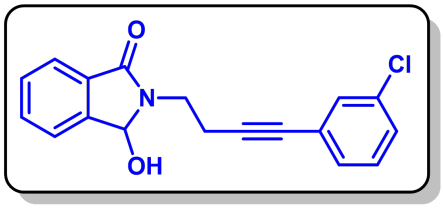

White solid; R_f (Hexane/EtOAc, 3:2) 0.45; mp 155–157 °C. Yield 264 mg, 85%; ^{1}H NMR (500 MHz, $CDCl_3$) δ 7.62–7.60 (m, 2 H), 7.58–7.55 (m, 1 H), 7.45 (t, J = 7.5 Hz, 1 H), 7.28–7.26 (m, 1 H), 7.24–7.22 (m, 1 H), 7.19–7.15 (m, 2 H), 5.93 (d, J = 11.0 Hz, 1 H), 4.01 (d, J = 11.5 Hz, 1 H), 3.67–3.62 (m, 1 H), 3.59–3.54 (m, 1 H), 2.74–2.71 (m, 2 H); ^{13}C{^{1}H} NMR (125 MHz, $CDCl_3$) δ 167.9, 144.2, 134.3, 132.7, 131.6, 131.4, 130.0, 129.9, 129.7, 128.4, 125.2, 123.7, 123.5, 88.6, 38.4, 19.6; IR (KBr, neat) 3357, 2920, 1678, 1470, 1417, 1206, 1060, 747, 696 cm^{-1}; HRMS (ESI) calcd. for $C_{18}H_{15}ClNO_2$ $(M + H)^+$ 312.0786, found 312.0788.

2-(4-(2-Bromophenyl)but-3-yn-1-yl)-3-hydroxyisoindolin-1-one (32e):

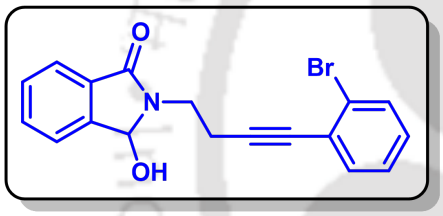

Brown solid; R_f (Hexane/EtOAc, 3:2) 0.45; mp 121–123 °C. 266 mg, 75%; ^{1}H NMR (500 MHz, $CDCl_3$) δ 7.63–7.59 (m, 2 H), 7.55 (t, J = 7.0 Hz, 1 H), 7.49 (d, J = 8.0 Hz, 1 H), 7.44 (t, J = 7.0 Hz, 1 H), 7.36–7.34 (m, 1 H), 7.20–7.17 (m, 1 H), 7.11–7.08 (m, 1 H), 6.05 (d, J = 7.5 Hz, 1 H), 3.97 (s, 1 H), 3.73–3.67 (m, 1 H), 3.64–3.58 (m, 1 H), 2.83–2.79 (m, 2 H); ^{13}C{^{1}H} NMR (125 MHz, $CDCl_3$) δ 167.8, 144.3, 133.7, 132.6, 132.5, 131.5, 130.0, 129.3, 127.2, 125.5, 125.5, 123.6, 123.5, 92.3, 82.6, 81.1, 38.3, 19.8; IR (KBr, neat) 3338, 2923, 1678, 1469, 1362, 1208, 1127, 1055, 748, 697 cm^{-1}; HRMS (ESI) calcd. for $C_{18}H_{15}BrNO_2$ $(M + H)^+$ 356.0281, found 356.0285.

3-Hydroxy-2-(4-(4-nitrophenyl)but-3-yn-1-yl)isoindolin-1-one (32h):

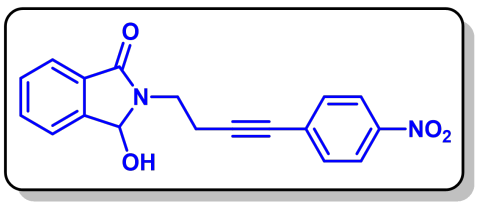

Brown solid; R_f (Hexane/EtOAc, 3:2) 0.55; mp 233–235 °C. Yield 248 mg, 77%; ^{1}H NMR (500 MHz, $CDCl_3$/DMSO–d_6) δ 8.08 (d, J = 9.0 Hz, 2 H), 7.74 (d, J = 7.5 Hz, 1 H), 7.58 (d, J = 7.0 Hz, 1 H), 7.53 (t, J = 7.5 Hz, 1 H), 7.47–7.43 (m, 3 H), 5.88 (d, J = 10.0 Hz, 1 H), 5.50 (d, J = 10.0 Hz, 1 H), 3.94–3.89 (m, 1 H), 3.76–3.70 (m, 1 H), 2.89–2.79 (m, 2 H); ^{13}C{^{1}H} NMR (125 MHz, $CDCl_3$/DMSO–d_6) δ 167.4, 146.9, 144.7, 132.5, 132.3, 131.9, 130.7, 129.7, 123.6, 123.5, 123.2, 93.6, 82.2,

80.6, 38.4, 19.8; IR (KBr, neat) 3257, 2919, 1672, 1513, 1340, 1275, 1261, 852, 750 cm^{-1}; HRMS (ESI) calcd. for $C_{18}H_{15}N_2O_4$ $(M + H)^+$ 323.1026, found 326.1033.

Methyl 4-(4-(1-hydroxy-3-oxoisoindolin-2-yl)but-1-yn-1-yl)benzoate (32i):

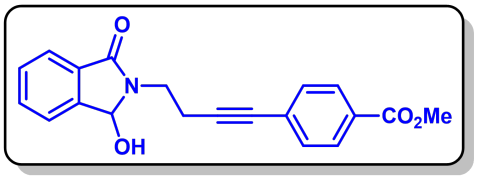

Grey solid; R_f (Hexane/EtOAc, 3:2) 0.45; mp 149–151 °C. Yield 241 mg, 72%; ^{1}H NMR (500 MHz, $CDCl_3$) δ 7.90 (d, J = 8.0 Hz, 2 H), 7.66 (d, J = 7.5 Hz, 1 H), 7.62–7.56 (m, 2 H), 7.47 (t, J = 7.5 Hz, 1 H), 7.36 (d, J = 8.0 Hz, 2 H), 5.95 (d, J = 8.0 Hz, 1 H), 3.89 (s, 3 H), 3.78–3.72 (m, 1 H), 3.68–3.62 (m, 1 H), 3.57 (d, J = 10.5 Hz, 1 H), 2.81–2.77 (m, 2 H); ^{13}C{^{1}H} NMR (125 MHz, $CDCl_3$) δ 167.7, 166.8, 144.1, 132.7, 131.7, 131.6, 130.2, 129.7, 129.5, 128.2, 123.6, 90.7, 82.6, 81.9, 52.4, 38.7, 19.8; IR (KBr, neat) 3342, 2922, 1680, 1433, 1276, 1110, 747, 613 cm^{-1}; HRMS (ESI) calcd. for $C_{20}H_{18}NO_4$ $(M + H)^+$ 336.1230, found 336.1241.

3-Hydroxy-2-(4-(3-methoxyphenyl)but-3-yn-1-yl)isoindolin-1-one (32l):

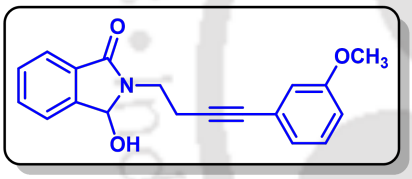

Brown solid; R_f (Hexane/EtOAc, 3:2) 0.50; mp 106–108 °C. Yield 205 mg, 67%; ^{1}H NMR (500 MHz, $CDCl_3$) δ 7.60 (t, J = 8.5 Hz, 2 H), 7.55 (t, J = 7.0 Hz, 1 H), 7.44 (t, J = 7.5 Hz, 1 H), 7.15 (t, J = 8 Hz, 1 H), 6.90 (d, J = 7.5 Hz, 1 H), 6.84–6.80 (m, 2 H), 5.96 (d, J = 11.0 Hz, 1 H), 3.99 (d, J = 11.0 Hz, 1 H), 3.74 (s, 3 H), 3.70–3.64 (m, 1 H), 3.61–3.55 (m, 1 H), 2.74–2.71 (m, 2 H); ^{13}C{^{1}H} NMR (125 MHz, $CDCl_3$) δ 167.8, 159.5, 144.2, 132.6, 131.5, 130.0, 129.5, 124.5, 124.3, 123.6, 123.4, 116.7, 114.7, 87.1, 82.5, 82.3, 55.4, 38.6, 19.6; IR (KBr, neat) 3331, 2921, 1679, 1603, 1423, 1285, 1205, 1047, 747, 690 cm^{-1}; HRMS (ESI) calcd. for $C_{19}H_{18}NO_3$ $(M + H)^+$ 308.1281, found 308.1290.

3-Hydroxy-2-(4-(thiophen-2-yl)but-3-yn-1-yl)isoindolin-1-one (32o):

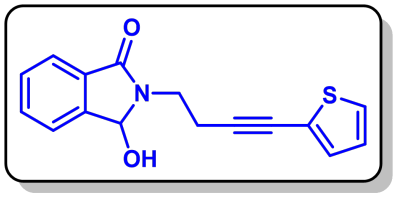

Off white solid; R_f (Hexane/EtOAc, 3:2) 0.50; mp 126–128 °C. Yield 161 mg, 57%; ^{1}H NMR (500 MHz, $CDCl_3$) δ 7.61–7.55 (m, 3 H), 7.44 (t, J = 7.0 Hz, 1 H), 7.16–7.15 (m, 1 H), 7.06 (d, J = 3.5 Hz, 1 H), 6.90 (dd, J = 5.5, 4 Hz, 1 H), 5.93 (d, J = 11.0 Hz, 1 H), 4.11 (d, J = 11.5 Hz, 1 H), 3.65–3.52 (m, 2 H), 2.79–2.68 (m, 2 H); ^{13}C{^{1}H} NMR (125 MHz, $CDCl_3$) δ 167.8, 144.2, 132.6, 131.7, 131.4, 130.0, 127.0, 126.7, 123.6, 123.5, 123.5,

91.3, 82.6, 75.6, 38.4, 19.9; IR (KBr, neat) 3322, 2925, 1677, 1423, 1206, 1058, 746, 697 cm^{-1}; HRMS (ESI) calcd. for $C_{16}H_{14}NO_2S$ $(M + H)^+$ 284.0740, found 284.0747.

2-(But-3-yn-1-yl)-3-hydroxy-2,3-dihydro-1*H*-benzo[*f*]isoindol-1-one (32p):

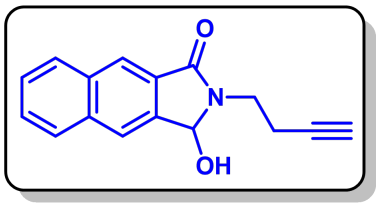

White solid; R_f (Hexane/EtOAc, 3:2) 0.50; mp 161–163 °C. Yield 248 mg, 66%; ^1H NMR (500 MHz, $CDCl_3$) δ 7.99 (s, 1 H), 7.96 (s, 1 H), 7.89 (d, J = 8.5 Hz, 1 H), 7.74 (d, J = 8.0 Hz, 1 H), 7.58–7.55 (m, 1 H), 7.49–7.45 (m, 1 H), 6.06 (s, 1 H), 3.78–3.72 (m, 1 H), 3.66–3.60 (m, 1 H), 2.60–2.57 (m, 2 H), 1.97 (t, J = 2.5 Hz, 1 H); $^{13}C\{^1H\}$ NMR (125 MHz, $CDCl_3$) δ 167.56, 139.2, 135.5, 133.8, 129.8, 128.8, 128.7, 128.2, 127.23, 124.0, 123.1, 82.5, 81.9, 70.4, 38.7, 18.6; IR (KBr, neat) 3295, 2922, 2179, 1677, 1422, 1277, 1258, 1047, 750, 438 cm^{-1}; HRMS (ESI) calcd. for $C_{16}H_{14}NO_2$ $(M + H)^+$ 252.1019, found 252.1022.

2-(But-3-yn-1-yl)-3-hydroxyoctahydro-1*H*-isoindol-1-one (32q):

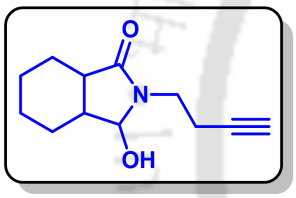

Brown gummy; R_f (Hexane/EtOAc, 3:2) 0.40. Yield 158 mg, 51%; ^1H NMR (500 MHz, $CDCl_3$) δ 4.84 (s, 1 H), 3.59–3.53 (m, 1 H), 3.50–3.43 (m, 1 H), 2.81–2.78 (m, 1 H), 2.50–2.47 (m, 2 H), 2.24–2.20 (m, 1 H), 2.06–2.03 (m, 2 H), 1.82–1.77 (m, 1 H), 1.58–1.49 (m, 3 H), 1.25–1.08 (m, 4 H); $^{13}C\{^1H\}$ NMR (125 MHz, $CDCl_3$) δ 176.9, 87.7, 83.0, 70.5, 41.6, 40.3, 38.9, 26.5, 23.5, 23.4, 23.1, 18.6; IR (KBr, neat) 3309, 2928, 1701, 1449, 1374, 1260, 1076, 749, 636 cm^{-1}; HRMS (ESI) calcd. for $C_{12}H_{18}NO_2$ $(M + H)^+$ 208.1332, found 208.1332.

2-(But-3-yn-1-yl)-3-hydroxy-2,3,3*a*,4,7,7*a*-hexahydro-1*H*-isoindol-1-one (32r):

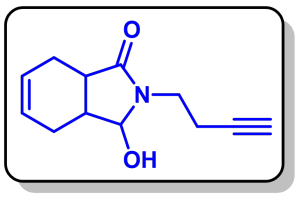

Brown gummy; R_f (Hexane/EtOAc, 3:2) 0.40. Yield 218 mg, 71%; ^1H NMR (500 MHz, $CDCl_3$) δ 5.76–5.67 (m, 2 H), 4.88 (d, J = 5.0 Hz, 1 H), 4.44 (d, J = 6.0 Hz, 1 H), 3.54–3.49 (m, 1 H), 3.44–3.39 (m, 1 H), 2.95–2.91 (m, 1 H), 2.45–2.42 (m, 2 H), 2.39–2.34 (m, 2 H), 2.27–2.20 (m, 2 H), 1.99 (t, J = 3 Hz, 1 H), 1.90–1.84 (m, 1 H); $^{13}C\{^1H\}$ NMR (125 MHz, $CDCl_3$) δ 177.5, 126.6, 125.4, 88.6, 82.23, 70.3, 39.6, 39.0, 37.5, 24.6, 22.3, 18.2; IR (KBr, neat) 3294, 2925, 2179, 1687, 1431, 1260, 1077, 685, 654 cm^{-1}; HRMS (ESI) calcd. for $C_{12}H_{16}NO_2$ $(M + H)^+$ 206.1176, found 206.1179.

3-Hydroxy-2-(pent-4-yn-2-yl)isoindolin-1-one (32s):

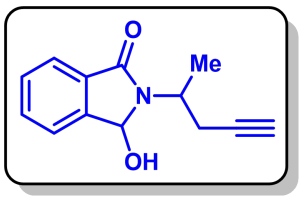

White solid; R_f (Hexane/EtOAc, 3:2) 0.50; mp 93–95 °C. Yield 197 mg, 61%; ^{1}H NMR (500 MHz, $CDCl_3$) δ 7.67 (t, J = 7.0 Hz, 1 H), 7.56–7.53 (m, 2 H), 7.48–7.45 (m, 1 H), 5.97–5.93 (m, 1 H), 4.44–4.27 (m, 1 H), 3.41–3.26 (m, 1 H), 2.87–2.77 (m, 1 H), 2.66–2.58 (m, 1 H), 2.00–1.96 (m, 1 H), 1.50–1.47 (m, 3 H); ^{13}C{^{1}H} NMR (125 MHz, $CDCl_3$) δ 167.5, 167.4, 144.1, 144.0, 132.5, 132.5, 131.9, 131.8, 130.1, 130.0, 123.5, 123.5, 123.4, 123.3, 82.2, 81.9, 70.8, 70.6, 47.8, 47.3, 25.4, 24.2, 19.4, 18.1; IR (KBr, neat) 3296, 2926, 1673, 1415, 1362, 1210, 1052, 747, 697, 641 cm^{-1}; HRMS (ESI) calcd. for $C_{13}H_{14}NO_2$ $(M + H)^+$ 216.1019, found 216.1023.

3-Hydroxy-2-(1-phenylbut-3-yn-1-yl)isoindolin-1-one (32t, diastereomeric mixture, 1:1):

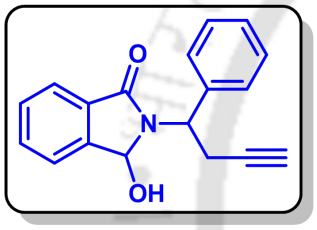

Pale yellow solid; R_f (Hexane/EtOAc, 3 : 2) 0.55; mp 141–143 °C. Yield 216 mg, 52%; ^{1}H NMR (400 MHz, $CDCl_3$) δ 7.77–7.74 (m, 1 H), 7.57–7.45 (m, 5 H), 7.38–7.27 (m, 3 H), 5.93 (d, J = 10.0 Hz, 0.5 H), 5.68–5.61 (m, 1 H), 5.23 (dd, J = 10.0 Hz and 5.6 Hz, 0.5 H), 3.63–3.55 (m, 0.5 H), 3.41–3.33 (m, 0.5 H), 3.08–3.03 (m, 1 H), 3.02–2.99 (m, 0.5 H), 2.80 (d, J = 11.6 Hz, 0.5 H), 1.98–1.95 (m, 1 H); ^{13}C{^{1}H} NMR (125 MHz, $CDCl_3$) δ 167.7, 167.4, 144.0, 143.9, 140.0, 138.2, 132.7, 132.6, 131.9, 131.4, 130.2, 130.1, 129.0, 128.9, 128.4, 128.2, 128.2, 127.8, 123.9, 123.7, 123.5, 123.3, 81.9, 70.9, 70.8, 55.8, 54.4, 22.9, 22.6; IR (KBr, neat) 3294, 2919, 1675, 1407, 1359, 1208, 1132, 1056, 747, 697 cm^{-1}; HRMS (ESI) calcd. for $C_{18}H_{16}NO_2$ $(M + H)^+$ 278.1176, found 278.1183.

2-(But-3-yn-1-yl)-5,6-dichloro-3-hydroxyisoindolin-1-one (32u):

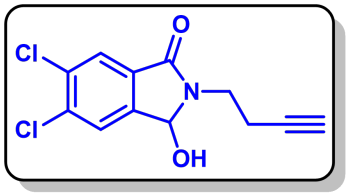

White solid; R_f (Hexane/EtOAc, 3:2) 0.45; mp 151–153 °C. Yield 271 mg, 67%; ^{1}H NMR (500 MHz, $CDCl_3$/DMSO–d_6) δ 7.73 (d, J = 5.0 Hz, 1 H), 7.61 (d, J = 5.5 Hz, 1 H), 6.21–6.18 (m, 1 H), 5.86–5.83 (m, 1 H), 4.63 (s, 1 H), 3.80–3.73 (m, 1 H), 3.56–3.50 (m, 1 H), 1.94–1.92 (m, 1 H); ^{13}C{^{1}H} NMR (125 MHz, $CDCl_3$/DMSO–d_6) δ 165.2, 144.0, 136.4, 134.0, 131.7, 125.8, 125.0, 81.5, 81.2, 70.2, 38.4, 18.3; IR (KBr, neat) 3396, 2923, 2259, 1695, 1532, 1347, 998, 824, 761, 628 cm^{-1}; HRMS (ESI) calcd. for $C_{12}H_9Cl_2KNO_2$ $(M + K)^+$ 307.9642, found 307.9662.

3-Hydroxy-2-(pent-4-yn-1-yl)isoindolin-1-one (32v):

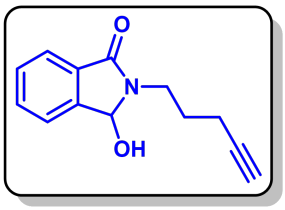

Brown solid; R_f (Hexane/EtOAc, 3:2) 0.45; mp 116–118 °C. Yield 197 mg, 61%; ^{1}H NMR (500 MHz, $CDCl_3$) δ 7.60–7.54 (m, 3 H), 7.44 (t, J = 7.5 Hz, 1 H), 5.76 (s, 1 H), 3.69 (s, 1 H), 3.55–3.49 (m, 1 H), 3.48–3.42 (m, 1 H), 2.24–2.20 (m, 2 H), 1.93 (t, J = 2.5 Hz, 1 H), 1.89–1.82 (m, 2 H); ^{13}C{^{1}H} NMR (125 MHz, $CDCl_3$) δ 167.9, 144.1, 132.5, 131.7, 130.0, 123.5, 123.5, 83.7, 82.3, 69.3, 38.8, 27.2, 16.5; IR (KBr, neat) 3294, 2926, 1677, 1424, 1315, 1206, 1128, 1054, 748, 697 cm^{-1}; HRMS (ESI) calcd. for $C_{13}H_{14}NO_2$ $(M + H)^+$ 216.1019, found 216.1026.

3-Hydroxy-2-(pent-4-yn-1-yl)-2,3-dihydro-1*H*-benzo[*f*]isoindol-1-one (32w):

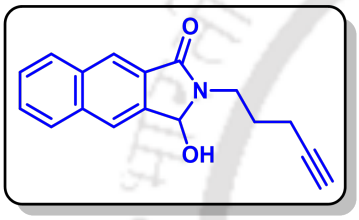

White solid; R_f (Hexane/EtOAc, 3:2) 0.50; mp 128–130 °C. Yield 207 mg, 52%; ^{1}H NMR (500 MHz, $CDCl_3$/DMSO–d_6) δ 8.17 (s, 1 H), 7.99 (s, 1 H), 7.90 (t, J = 8.5 Hz, 2 H), 7.56–7.48 (m, 2 H), 5.91 (d, J = 10.5 Hz, 1 H), 5.19 (d, J = 10.5 Hz, 1 H), 3.80–3.74 (m, 1 H), 3.63–3.58 (m, 1 H), 2.29–2.25 (m, 2 H), 2.00–1.92 (m, 2 H), 1.91 (t, J = 2.5 Hz, 1 H); ^{13}C{^{1}H} NMR (125 MHz, $CDCl_3$/DMSO-d_6) δ 167.2, 139.9, 135.3, 133.7, 129.8, 129.5, 128.6, 127.7, 126.8, 123.2, 122.8, 83.7, 81.9, 68.9, 39.0, 27.2, 16.4; IR (KBr, neat) 3298, 2918, 1679, 1456, 1319, 1229, 1159, 1024, 767, 642 cm^{-1} HRMS (ESI) calcd. for $C_{17}H_{16}NO_2$ $(M + H)^+$ 266.1176, found 266.1173.

3-Hydroxy-2-(pent-4-yn-1-yl)octahydro-1*H*-isoindol-1-one (32x, diastereomeric mixture, 1:4):

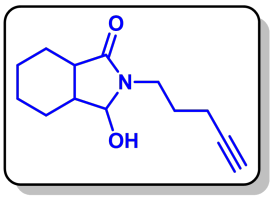

Brown gummy; R_f (Hexane/EtOAc, 3:2) 0.50. Yield 232 mg, 70% ^{1}H NMR (500 MHz, $CDCl_3$) δ 5.14 (s, 1 H, minor), 4.68 (s, 1 H, major), 4.45 (d, J = 7.0 Hz, 1 H, major), 4.04 (d, J = 7.0 Hz, 1 H, minor), 3.48–3.39 (m, 1 H), 3.30–3.24 (m, 1 H), 2.76 (d, J = 5.0 Hz, 1 H), 2.37–2.34 (m, 1 H), 2.20–2.15 (m, 3 H), 1.90–1.92 (m, 1 H), 1.82–1.71 (m, 3 H), 1.52–1.46 (m, 3 H), 1.25–1.14 (m, 1 H), 1.11–0.95 (m, 2 H) ^{13}C{^{1}H} NMR (125 MHz, $CDCl_3$)δ 177.1, 176.6, 87.2, 84.7, 83.9, 83.7, 69.3, 69.1, 41.3, 41.2, 39.9, 39.1, 38.9, 37.5, 26.9, 26.8, 26.6, 24.3, 23.4, 23.3, 23.2, 23.1, 22.3, 16.5, 16.4; IR (KBr, neat) 3295, 2932, 1665, 1446, 1259, 1119, 1026, 847, 744, 636, 522 cm^{-1}; HRMS (ESI) calcd. for $C_{13}H_{20}NO_2$ $(M + H)^+$ 222.1489, found 222.1488.

3-Hydroxy-2-(pent-4-yn-1-yl)-2,3,3*a*,4,7,7*a*-hexahydro-1*H*-isoindol-1-one (32y):

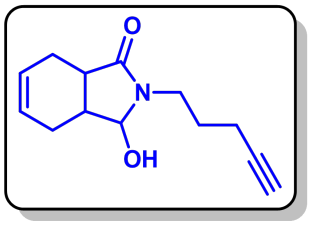

Brown gummy; R_f (Hexane/EtOAc, 3:2) 0.50. Yield 184 mg, 56%; ^{1}H NMR (500 MHz, $CDCl_3$) δ 5.78–5.72 (m, 2 H), 4.74 (s, 1 H), 3.72 (s, 1 H), 3.51–3.46 (m, 1 H), 3.33–3.28 (m, 1 H), 2.95–2.91 (m, 1 H), 2.42–2.36 (m, 2 H), 2.26–2.18 (m, 4 H), 1.98 (t, J = 2.5 Hz, 1 H), 1.83–1.72 (m, 3 H); ^{13}C{^{1}H} NMR (125 MHz, $CDCl_3$) δ 177.3, 127.2, 125.5, 88.9, 83.8, 69.4, 39.9, 39.4, 37.9, 26.8, 24.9, 22.6, 16.3; IR (KBr, neat) 3293, 2950, 2905, 1669, 1434, 1259, 1149, 1057, 849, 647 cm^{-1} HRMS (ESI) calcd. for $C_{13}H_{18}NO_2$ $(M + H)^+$ 220.1332, found 220.1330.

4,5-Dihydro-[1,2,3]triazolo[1',5':3,4]pyrimido[2,1-*a*]isoindol-7(11b*H*)-one (34a):

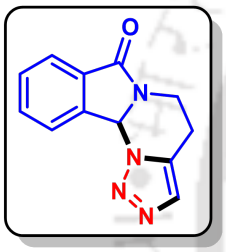

Yellow solid; R_f (Hexane/EtOAc, 1:4) 0.45; mp 188-190 °C. Yield 95 mg, 84%; ^{1}H NMR (500 MHz, $CDCl_3$) δ 8.22 (d, J = 7.5 Hz, 1 H), 7.86 (d, J = 7.5 Hz, 1 H), 7.69 (t, J = 7.5 Hz, 1 H), 7.59 (t, J = 7.5 Hz, 1 H), 7.51 (s, 1 H), 6.73 (s, 1 H), 4.78–4.74 (m, 1 H), 3.41–3.34 (m, 1 H), 3.07–2.93 (m, 2 H); ^{13}C{^{1}H} NMR (125 MHz, $CDCl_3$) δ 167.8, 140.1, 133.3, 131.8, 131.7, 131.1, 130.9, 126.0, 124.2, 70.8, 35.7, 21.4; IR (KBr, neat) 2920, 1710, 1455, 1404, 1296, 1129, 748 cm^{-1}; HRMS (ESI) calcd. for $C_{12}H_{11}N_4O$ $(M + H)^+$ 227.0927, found 227.0937.

3-Phenyl-4,5-dihydro-[1,2,3]triazolo[1',5':3,4]pyrimido[2,1-*a*]isoindol-7(11b*H*)-one (34b):

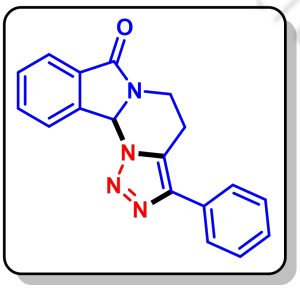

Off white solid; R_f (Hexane/EtOAc, 3:2) 0.55; mp 211–213 °C. Yield 107 mg, 71%; ^{1}H NMR (400 MHz, $CDCl_3$) δ 8.28 (d, J = 7.6 Hz, 1 H), 7.90 (d, J = 7.6 Hz, 1 H), 7.75–7.68 (m, 3 H), 7.62 (t, J = 7.6 Hz, 1 H), 7.44 (t, J = 7.6 Hz, 2 H), 7.36–7.32 (m, 1 H), 6.80 (s, 1 H), 4.86–4.81 (m, 1 H), 3.46–3.39 (m, 1 H), 3.21–3.18 (m, 2 H); ^{13}C{^{1}H} NMR (125 MHz, $CDCl_3$) δ 167.9, 143.4, 140.2, 133.4, 131.9, 131.1, 131.0, 129.1, 128.3, 128.1, 126.7, 126.1, 124.3, 70.9, 35.7, 22.9; IR (KBr, neat) 2924, 1712, 1466, 1403, 1293, 1211, 1118, 746 cm^{-1}; HRMS (ESI) calcd. for $C_{18}H_{15}N_4O$ $(M + H)^+$ 303.1240, found 303.1265.

3-(3-Chlorophenyl)-4,5-dihydro-[1,2,3]triazolo[1',5':3,4]pyrimido[2,1-*a*]isoindol-7(11*bH*)-one (34c):

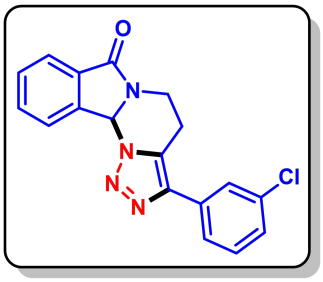

Brown solid; R_f (Hexane/EtOAc, 3:2) 0.50; mp 223–225 °C. Yield 109 mg, 65%; ^{1}H NMR (500 MHz, $CDCl_3$) δ 8.25 (d, J = 7.5 Hz, 1 H), 7.88 (d, J = 8 Hz, 1 H), 7.73–7.69 (m, 2 H), 7.61 (t, J = 7.5 Hz, 1 H), 7.55 (d, J= 8 Hz, 1 H), 7.35 (t, J = 7.5 Hz, 1 H), 7.29 (d, J = 8.0 Hz, 1 H), 6.78 (s, 1 H), 4.85–4.81 (m, 1 H), 3.45–3.39 (m, 1 H), 3.19–3.16 (m, 2 H); ^{13}C{^{1}H} NMR (125 MHz, $CDCl_3$) δ 167.8, 142.1, 140.0, 135.1, 133.4, 132.7, 131.8, 131.1, 130.4, 128.6, 128.3, 126.6, 126.1, 124.6, 124.3, 70.9, 35.5, 22.8; IR (KBr, neat) 3745, 2955, 2917, 1699, 1469, 1275, 750 cm^{-1} HRMS (ESI) calcd. for $C_{18}H_{14}ClN_4O$ (M + H)$^+$ 337.0851, found 337.0848.

3-(4-Chlorophenyl)-4,5-dihydro-[1,2,3]triazolo[1',5':3,4]pyrimido[2,1-*a*]isoindol-7(11*bH*)-one (34d):

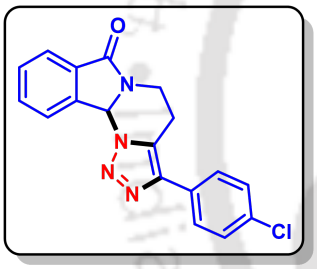

Brown solid; R_f (Hexane/EtOAc, 3:2) 0.50; mp 241–243 °C. Yield 106 mg, 63%; ^{1}H NMR (400 MHz, $CDCl_3$) δ 8.23 (d, J = 7.6 Hz, 1 H), 7.87 (d, J = 7.6 Hz, 1 H), 7.70 (t, J = 7.6 Hz, 1 H), 7.62–7.59 (m, 3 H), 7.38 (d, J =8.8 Hz, 2 H), 6.77 (s, 1 H), 4.84–4.79 (m, 1 H), 3.45–3.37 (m, 1 H), 3.17–3.13 (m, 2 H); ^{13}C{^{1}H} NMR (125 MHz, $CDCl_3$) δ 167.9, 142.4, 140.1, 134.2, 133.4, 131.8, 131.1, 129.5, 129.4, 128.2, 127.8, 126.1, 124.3, 70.9, 35.6, 22.8; IR (KBr, neat) 2924, 1712, 1491, 1411, 1274, 1211, 827, 750 cm^{-1}; HRMS (ESI) calcd. for $C_{18}H_{14}N_4O$ (M + H)$^+$ 337.0851, found 337.0859.

3-(2-Bromophenyl)-4,5-dihydro-[1,2,3]triazolo[1',5':3,4]pyrimido[2,1-*a*]isoindol-7(11*bH*)-one (34e):

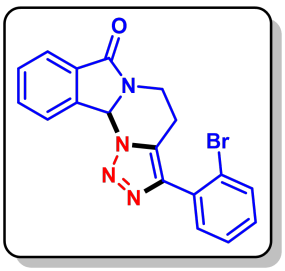

Brown solid; R_f (Hexane/EtOAc, 3:2) 0.50; mp 173–175 °C. Yield 133 mg, 70%; ^{1}H NMR (500 MHz, $CDCl_3$) δ 8.30 (d, J = 7.0 Hz, 1 H), 7.92 (d, J = 6.0 Hz, 1 H), 7.76–7.73 (m, 1 H), 7.66–7.63 (m, 2 H), 7.43–7.37 (m, 2 H), 7.29–7.27 (m, 1 H), 6.83 (s, 1 H), 4.81–4.76 (m, 1 H), 3.45–3.39 (m, 1 H), 3.09–2.94 (m, 2 H); ^{13}C{^{1}H} NMR (125 MHz, $CDCl_3$) δ 167.8, 143.4, 140.0, 133.3, 133.3, 132.5, 131.9, 131.8, 131.0, 130.5, 130.0, 127.7, 126.0, 124.2, 123.4, 70.9,

35.7, 22.6; IR (KBr, neat) 3747, 2958, 2928, 1713, 1469, 1275, 1003, 750 cm^{-1}; HRMS (ESI) calcd. for $C_{18}H_{14}BrN_4O$ $(M + H)^+$ 381.0346, found 381.0357.

3-(4-Bromophenyl)-4,5-dihydro-[1,2,3]triazolo[1',5':3,4]pyrimido[2,1-*a*]isoindol-7(11*bH*)-one (34f):

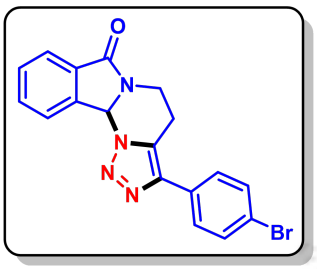

Brown solid; R_f (Hexane/EtOAc, 3:2) 0.50; mp 235–237 °C. Yield 127 mg, 67%; ^{1}H NMR (500 MHz, $CDCl_3$) δ 8.25 (d, J = 7.5 Hz, 1 H), 7.89 (d, J = 7.5 Hz, 1 H), 7.72 (t, J = 7.5 Hz, 1 H), 7.62 (t, J = 7.5 Hz, 1 H), 7.58–7.54 (m, 4 H), 6.79 (s, 1 H), 4.86–4.81 (m, 1 H), 3.45–3.39 (m, 1 H), 3.18–3.15 (m, 2 H); ^{13}C{^{1}H} NMR (125 MHz, $CDCl_3$) δ 167.9, 142.5, 140.1, 133.4, 132.3, 131.8, 131.1, 129.9, 128.3, 128.1, 126.1, 124.3, 122.3, 70.9, 35.6, 22.8; IR (KBr, neat) 2925, 1709, 1466, 1343, 1233, 1156, 827, 745 cm^{-1}; HRMS (ESI) calcd. for $C_{18}H_{14}BrN_4O$ $(M + H)^+$ 381.0346, found 381.0350.

3-(4-Fluorophenyl)-4,5-dihydro-[1,2,3]triazolo[1',5':3,4]pyrimido[2,1-*a*]isoindol-7(11*bH*)-one (34g):

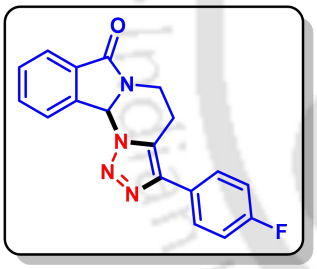

Off white solid; R_f (Hexane/EtOAc, 3:2) 0.55; mp 225–227 °C. Yield 91 mg, 57%; ^{1}H NMR (500 MHz, $CDCl_3$) δ 8.24 (d, J = 8 Hz, 1 H), 7.88 (d, J = 8 Hz, 1 H), 7.70 (t, J = 7.5 Hz, 1 H), 7.67–7.64 (m, 2 H), 7.61 (t, J = 7.5 Hz, 1 H), 7.13–7.09 (m, 2 H), 6.78 (s, 1 H), 4.84–4.80 (m, 1 H), 3.44–3.38 (m, 1 H), 3.16–3.13 (m, 2 H); ^{13}C{^{1}H} NMR (125 MHz, $CDCl_3$) δ 167.8, 162.7 (d, J = 246.3 Hz), 142.6, 140.1, 133.3, 131.8, 131.0, 128.4, 128.3, 127.9, 127.1, 127.1, 126.1, 124.2, 116.1 (d, J = 21.5) 70.9, 35.5, 22.7; ^{19}F NMR (470 MHz, C_6F_6/$CDCl_3$) δ 48.33 (s, -F); IR (KBr, neat) 2922, 1713, 1507, 1395, 1233, 1154, 838, 739 cm^{-1}; HRMS (ESI) calcd. for $C_{18}H_{14}FN_4O$ $(M + H)^+$ 321.1146, found 321.1144.

3-(4-Nitrophenyl)-4,5-dihydro-[1,2,3]triazolo[1',5':3,4]pyrimido[2,1-*a*]isoindol-7(11*bH*)-one (34h):

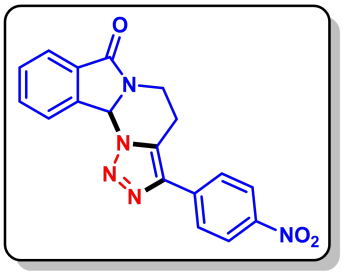

Pale yellow solid; R_f (Hexane/EtOAc, 3:2) 0.60; mp 228–230 °C. Yield 81 mg, 47%; ^{1}H NMR (500 MHz, $CDCl_3$) δ 8.28–8.23 (m, 3 H), 7.89–7.87 (m, 3 H), 7.71 (t, J = 7.5 Hz, 1 H), 7.61 (t, J = 7.5 Hz, 1 H), 6.82 (s, 1 H), 4.87–4.83 (m, 1 H), 3.48–3.42 (m, 1 H), 3.24–3.21 (m, 2 H); ^{13}C{^{1}H} NMR (125 MHz, $CDCl_3$) δ 167.7, 147.3, 141.3, 139.8, 137.3, 133.4, 131.7, 131.2, 129.8, 126.8, 126.0, 124.4, 124.3, 70.9, 35.3, 22.9; IR (KBr, neat) 2922, 1713, 1463, 1346, 1296, 1206, 855, 720 cm^{-1}; HRMS (ESI) calcd. for $C_{18}H_{14}N_5O_3$ $(M + H)^+$ 348.1091, found 348.1099.

Methyl-4-(7-oxo-4,5,7,11*b*-tetrahydro-[1,2,3]triazolo[1',5':3,4]pyrimido[2,1-*a*]isoindol-3-yl)benzoate (34i):

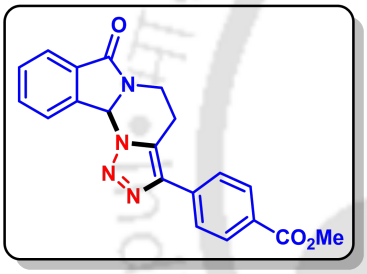

Brown solid; R_f (Hexane/EtOAc, 3:2) 0.50; mp 222–224 °C. Yield 121 mg, 67%; ^{1}H NMR (500 MHz, $CDCl_3$) δ 8.25 (d, J = 8 Hz, 1 H), 8.08 (d, J = 8. Hz, 2 H), 7.89 (d, J = 75 Hz, 1 H), 7.78 (d, J = 8. Hz, 2 H), 7.71 (t, J = 7.5 Hz, 1 H), 7.62 (t, J = 7.5 Hz, 1 H), 6.80 (s, 1 H), 4.86–4.82 (m, 1 H), 3.92 (s, 3 H), 3.47–3.41 (m, 1 H), 3.23–3.20 (m, 2 H); ^{13}C{^{1}H} NMR (125 MHz, $CDCl_3$) δ 167.8, 166.9, 142.4, 140.0, 135.3, 133.4, 131.8, 131.1, 130.4, 129.6, 129.1, 126.2, 126.1, 124.3, 70.9, 52.4, 35.5, 23.0; IR (KBr, neat) 3750, 2925, 1713, 1466, 1274, 1112, 749 cm^{-1}; HRMS (ESI) calcd. for $C_{20}H_{17}N_4O_3$(M + H)$^+$ 361.1295, found 361.1314.

3-(*p*-Tolyl)-4,5-dihydro-[1,2,3]triazolo[1',5':3,4]pyrimido[2,1-*a*]isoindol-7(11*bH*)-one (34j):

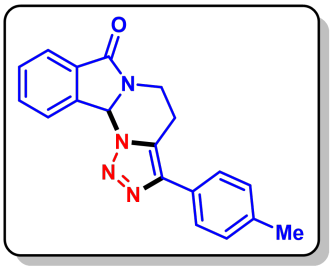

Brown solid; R_f (Hexane/EtOAc, 3:2) 0.45; mp 192–194 °C. Yield 118 mg, 75%; ^{1}H NMR (500 MHz, $CDCl_3$) δ 8.25 (d, J = 7.5 Hz, 1 H), 7.88 (d, J = 7.5 Hz, 1 H), 7.70 (t, J = 8 Hz, 1 H), 7.62–7.56 (m, 3 H), 7.23 (d, J = 8 Hz, 2 H), 6.77 (s, 1 H), 4.83–4.78 (m, 1 H), 3.43–3.37 (m, 1 H), 3.16–3.14 (m, 2 H), 2.36 (s, 3 H); ^{13}C{^{1}H} NMR (125 MHz, $CDCl_3$) δ 167.8, 143.4, 140.1, 138.1, 133.3, 131.8, 130.9, 129.7, 128.0, 127.7, 126.5, 126.1, 124.2,

70.8, 35.6, 22.8, 21.5; IR (KBr, neat) 2921, 1708, 1463, 1346, 1241, 1211, 822, 741 cm^{-1}; HRMS (ESI) calcd. for $C_{19}H_{17}N_4O$ $(M + H)^+$ 317.1397, found 317.1395.

3-(*o*-Tolyl)-4,5-dihydro-[1,2,3]triazolo[1',5':3,4]pyrimido[2,1-*a*]isoindol-7(11*bH*)-one (34k):

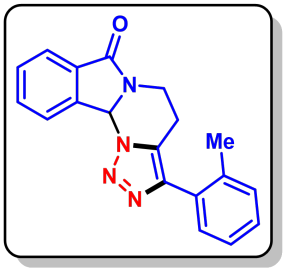

Pale yellow solid; R_f (Hexane/EtOAc, 3:2) 0.45; mp 218–220 °C. Yield 114 mg, 72%; ^{1}H NMR (500 MHz, $CDCl_3$) δ 8.30 (d, J = 7.5 Hz, 1 H), 7.92 (d, J = 7.5 Hz, 1 H), 7.76–7.73 (m, 1 H), 7.64 (t, J = 7.5 Hz, 1 H), 7.30–7.28 (m, 2 H), 7.24–7.18 (m, 2 H), 6.81 (s, 1 H), 4.81–4.77 (m, 1 H), 3.42–3.36 (m, 1 H), 3.03–2.89 (m, 2 H), 2.35 (s, 3 H); ^{13}C{^{1}H} NMR (125 MHz, $CDCl_3$) δ 168.0, 144.1, 140.2, 137.7, 133.4, 131.9, 131.1, 131.0, 129.9, 129.7, 129.2, 128.8, 126.1, 126.0, 124.3, 71.0, 35.9, 22.1, 20.7; IR (KBr, neat) 2924, 1713, 1466, 1402, 1276, 1003, 748 cm^{-1}; HRMS (ESI) calcd. for $C_{19}H_{17}N_4O$ $(M + H)^+$ 317.1397, found 317.1386.

3-(3-Methoxyphenyl)-4,5-dihydro-[1,2,3]triazolo[1',5':3,4]pyrimido[2,1-*a*]isoindol-7(11*bH*)-one (34l):

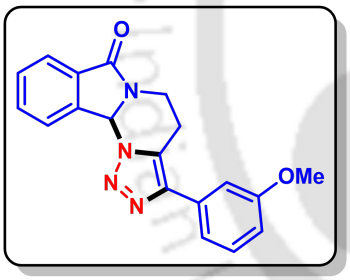

Off white solid; R_f (Hexane/EtOAc, 3:2) 0.50; mp 178–180 °C. Yield 136 mg, 82%; ^{1}H NMR (500 MHz, $CDCl_3$) δ 8.22 (d, J = 8 Hz, 1 H), 7.85 (d, J = 8 Hz, 1 H), 7.70–7.66 (m, 1 H), 7.58 (t, J = 7.5 Hz, 1 H), 7.31–7.28 (m, 2 H), 7.17 (d, J = 7.5 Hz, 1 H), 6.86–6.84 (m, 1 H), 6.74 (s, 1 H), 4.80–4.75 (m, 1 H), 3.82 (s, 3 H), 3.42–3.36 (m, 1 H), 3.15–3.12 (m, 2 H); ^{13}C{^{1}H} NMR (125 MHz, $CDCl_3$) δ 167.8, 160.2, 143.2, 140.1, 133.3, 132.2, 131.8, 131.0, 130.1, 128.2, 126.1, 124.2, 118.8, 114.1, 112.0, 70.9, 55.5, 35.6, 22.9; IR (KBr, neat) 2960, 2919, 1713, 1469, 855, 750 cm^{-1}; HRMS (ESI) calcd. for $C_{19}H_{17}N_4O_2$ $(M + H)^+$ 333.1346, found 333.1350.

3-(4-Methoxyphenyl)-4,5-dihydro-[1,2,3]triazolo[1',5':3,4]pyrimido[2,1-*a*]isoindol-7(11*bH*)-one (34m):

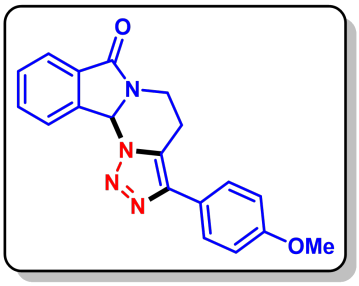

Brown solid; R_f (Hexane/EtOAc, 3:2) 0.50; mp 206–208 °C. Yield 143 mg, 86%; ^{1}H NMR (500 MHz, $CDCl_3$) δ 8.25 (d, J = 7.5 Hz, 1 H), 7.88 (d, J = 7.5 Hz, 1 H), 7.71 (t, J = 7.5 Hz, 1 H), 7.62–7.59 (m, 3 H), 6.96 (d, J = 8.5 Hz, 2 H), 6.77 (s, 1 H), 4.83–4.79 (m, 1 H), 3.83 (s, 3 H), 3.43–3.37 (m, 1 H), 3.16–3.13 (m, 2 H); ^{13}C{^{1}H} NMR (125 MHz, $CDCl_3$) δ 167.9, 159.7, 143.3, 140.2, 133.4, 131.9, 131.0, 128.0, 127.3, 126.1, 124.3, 123.6, 114.6, 70.9, 55.6, 35.7, 22.8; IR (KBr, neat) 2922, 1707, 1466, 1348, 1277, 1115, 835, 747 cm^{-1}; HRMS (ESI) calcd. for $C_{19}H_{17}N_4O_2$(M + H)$^+$ 333.1346, found 333.1328.

3-Ethyl-4,5-dihydro-[1,2,3]triazolo[1',5':3,4]pyrimido[2,1-*a*]isoindol-7(11*bH*)-one (34n):

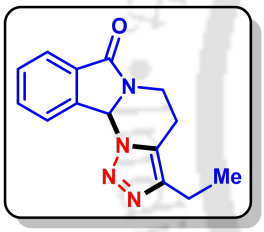

Pale yellow solid; R_f (Hexane/EtOAc, 3:2) 0.45; mp 179–181 °C. Yield 121 mg, 69%; ^{1}H NMR (500 MHz, $CDCl_3$) δ 8.22 (d, J = 7.5 Hz, 1 H), 7.86 (d, J = 7.5 Hz, 1 H), 7.69 (t, J = 7.5 Hz, 1 H), 7.59 (t, J = 7.5 Hz, 1 H), 6.69 (s, 1 H), 4.80–4.75 (m, 1 H), 3.39–3.33 (m, 1 H), 2.94–2.84 (m, 2 H), 2.72–2.57 (m, 2 H), 1.22 (t, J = 7.5 Hz, 3 H); ^{13}C{^{1}H} NMR (125 MHz, $CDCl_3$) δ 167.9, 145.2, 140.2, 133.2, 131.8, 130.9, 127.6, 126.0, 124.1, 70.7, 35.7, 21.1, 18.5, 13.7; IR (KBr, neat) 3747, 2958, 2922, 1710, 1461, 1411, 1277, 750 cm^{-1}; HRMS (ESI) calcd. for $C_{14}H_{15}N_4O$(M + H)$^+$ 255.1240, found 255.1253.

3-(Thiophen-2-yl)-4,5-dihydro-[1,2,3]triazolo[1',5':3,4]pyrimido[2,1-*a*]isoindol-7(11*bH*)-one (34o):

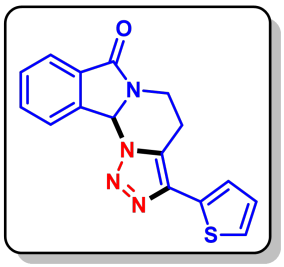

Brown solid; R_f (Hexane/EtOAc, 3:2) 0.55; mp 189–191 °C. Yield 108 mg, 70%; ^{1}H NMR (500 MHz, $CDCl_3$) δ 8.73 (d, J = 8 Hz, 1 H), 8.38 (d, J = 7.5 Hz, 1 H), 8.21 (t, J = 7.5 Hz, 1 H), 8.11 (t, J = 7.5 Hz, 1 H), 7.81–7.77 (m, 2 H), 7.59–7.57 (m, 1 H), 7.26 (s, 1 H), 5.36–5.31 (m, 1 H), 3.98–3.92 (m, 1 H), 3.70–3.56 (m, 2 H); ^{13}C{^{1}H} NMR (125 MHz, $CDCl_3$) δ 167.7, 139.9, 139.1, 133.3, 132.9, 131.8, 131.0, 127.9, 127.3, 126.1, 125.4, 124.2, 124.2, 70.8, 35.4,

22.3; IR (KBr, neat) 3070, 2925, 1711, 1468, 1403, 1290, 961, 739 cm^{-1}; HRMS (ESI) calcd. for $C_{16}H_{13}N_4OS$ $(M + H)^+$ 309.0805, found 309.0811.

4,5-Dihydro-[1,2,3]triazolo[1',5':3,4]pyrimido[2,1-*a*]benzo[*f*]isoindol-7 (13*bH*)-one (34p):

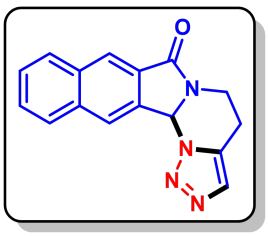

Brown solid; R_f (Hexane/EtOAc, 1:4) 0.55; mp 237–239 °C. Yield 94 mg, 68%; ^{1}H NMR (500 MHz, $CDCl_3$) δ 8.66 (s, 1 H), 8.34 (s, 1 H), 8.00 (t, J = 9.5 Hz, 2 H), 7.65–7.58 (m, 2 H), 7.53 (s, 1 H), 6.86 (s, 1 H), 4.83–4.79 (m, 1 H), 3.44–3.38 (m, 1 H), 3.09–2.98 (dt, J = 12.8, 5.5 Hz, 2 H); ^{13}C{^{1}H} NMR (125 MHz, $CDCl_3$) δ 167.6, 135.6, 134.2, 134.0, 131.8, 131.2, 129.8, 129.2, 128.8, 128.5, 127.9, 126.0, 125.0, 70.8, 35.8, 21.4; IR (KBr, neat) 3745, 2925, 1711, 1456, 1398, 1276, 750, 474 cm^{-1}; HRMS (ESI) calcd. for $C_{16}H_{13}N_4O$ $(M + H)^+$ 277.1084, found 277.1092.

4,5,7a,8,9,10,11,11a-Octahydro-[1,2,3]triazolo[1',5':3,4]pyrimido[2,1-*a*]isoindol-7(11*bH*)-one (34q):

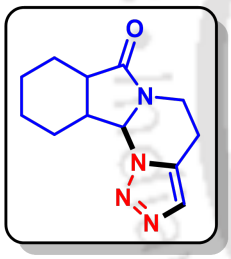

Off white solid; R_f (Hexane/EtOAc, 1:4) 0.40; mp 118–120 °C. Yield 66 mg, 57%; ^{1}H NMR (500 MHz, $CDCl_3$) δ 7.51 (s, 1 H), 5.56 (d, J = 3.5 Hz, 1 H), 4.47–4.43 (m, 1 H), 3.15–3.09 (m, 1 H), 3.05–3.00 (m, 1 H), 2.98–2.90 (m, 2 H), 2.50 (q, J = 7 Hz, 1 H), 2.03–1.97 (m, 1 H), 1.91–1.74 (m, 4 H), 1.68–1.61 (m, 1 H), 1.54–1.47 (m, 1 H), 1.44–1.36 (m, 1 H); ^{13}C{^{1}H} NMR (125 MHz, $CDCl_3$) δ 177.0, 132.2, 131.5, 75.1, 40.9, 38.3, 36.0, 25.9, 24.3, 23.1, 23.0, 20.7; IR (KBr, neat) 3457, 2928, 1707, 1452, 1417, 1261, 750, 468 cm^{-1}; HRMS (ESI) calcd. for $C_{12}H_{17}N_4O$ $(M + H)^+$ 233.1397, found 233.1417.

4,5,7*a*,8,11,11*a*-Hexahydro-[1,2,3]triazolo[1',5':3,4]pyrimido[2,1-*a*]isoindol-7(11*bH*)-one (34r):

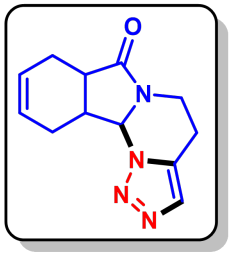

Pale yellow solid; R_f (Hexane/EtOAc, 1:4) 0.45; mp 85–87 °C. Yield 78 mg, 68%; ^{1}H NMR (500 MHz, $CDCl_3$) δ 7.51 (s, 1 H), 5.94 (d, J = 2.5 Hz, 2 H), 5.51 (d, J = 4 Hz, 1 H), 4.46–4.42 (m, 1 H), 3.24–3.19 (m, 1 H), 3.12–3.06 (m, 1 H), 2.97–2.94 (m, 2 H), 2.85–2.81 (m, 1 H), 2.66–2.60 (m, 1 H), 2.53–2.48 (m, 1 H), 2.44–2.31 (m, 2 H); ^{13}C{^{1}H} NMR (125 MHz, $CDCl_3$) δ 176.6, 131.9, 131.4, 128.0, 126.3, 39.9, 37.6, 35.8, 25.2, 23.4, 20.7; IR (KBr, neat) 3473, 2922, 1702, 1458, 1427

1398, 1232, 985, 692 cm^{-1}; HRMS (ESI) calcd. for $C_{12}H_{15}N_4O$ $(M + H)^+$ 231.1240, found 231.1246.

(5*S,11*bR**)-5-Methyl-4,5-dihydro-[1,2,3]triazolo[1',5':3,4]pyrimido[2,1-*a*]isoindol-7(11*bH*)-one (34s):**

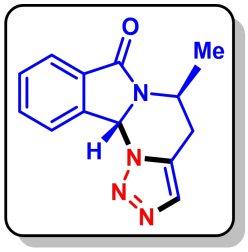

Pale yellow solid; R_f (Hexane/EtOAc, 1:4) 0.40; mp 154–156 °C. Yield 84 mg, 70%; ^{1}H NMR (400 MHz, $CDCl_3$) δ 8.19 (d, J = 7.6 Hz, 1 H), 7.81 (d, J = 7.6 Hz, 1 H), 7.67–7.63 (m, 1 H), 7.57–7.53 (m, 1 H), 7.50 (s, 1 H), 6.69 (s, 1 H), 5.05 (t, J = 6.8 Hz, 1 H), 3.07 (dd, J = 16.0, 6.0 Hz, 1 H), 2.86 (d, J = 16.4 Hz, 1 H), 1.35 (d, J = 7.2 Hz, 3 H); ^{13}C{^{1}H} NMR (125 MHz, $CDCl_3$) δ 167.5, 140.0, 133.2, 132.0, 131.9, 130.9, 130.8, 126.0, 124.2, 67.8, 41.3, 27.2, 18.1; IR (KBr, neat) 3269, 2922, 1709, 1543, 1394, 1218, 1077, 984, 749 cm^{-1}; HRMS (ESI) calcd. for $C_{13}H_{13}N_4O$ $(M + H)^+$ 241.1084, found 241.1093.

(5*R,11*bR**)-5-Phenyl-4,5-dihydro-[1,2,3]triazolo[1',5':3,4]pyrimido[2,1-*a*]isoindol-7(11*bH*)-one (34t):**

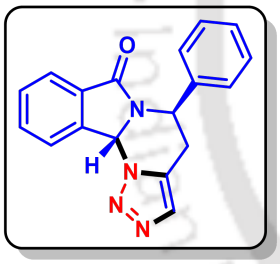

Brown solid; R_f (Hexane/EtOAc, 1:4) 0.45; mp 203–205 °C. Yield 94 mg, 62%; ^{1}H NMR (400 MHz, $CDCl_3$) δ 8.21 (d, J = 7.6 Hz, 1 H), 7.95 (d, J = 7.6 Hz, 1 H), 7.74–7.69 (m, 2 H), 7.64 (t, J = 7.6, 1 H), 7.37–7.32 (m, 3 H), 7.28–7.26 (m, 2 H), 6.35 (s, 1 H), 6.14 (d, J = 6.4 Hz, 1 H), 3.68 (d, J = 16.8 Hz, 1 H), 3.40 (dd, J = 16.8, 6.8 Hz, 1 H); ^{13}C{^{1}H} NMR (125 MHz, $CDCl_3$) δ 167.4, 139.9, 136.8, 133.4, 131.7, 131.3, 131.2, 131.0, 129.5, 128.8, 127.3, 126.2, 124.4, 68.00, 47.8, 24.0; IR (KBr, neat) 2923, 1711, 1453, 1387, 1239, 1214, 1125, 984, 748,699 cm^{-1}; HRMS (ESI) calcd. for $C_{18}H_{15}N_4O$ $(M + H)^+$ 303.1240, found 303.1251.

5,6-Dihydro-4*H*-[1,2,3]triazolo[1',5':3,4][1,3]diazepino[2,1-*a*]isoindol-8(12*bH*)-one (34v):

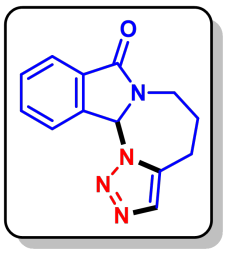

Pale yellow solid; R_f (Hexane/EtOAc, 1:4) 0.40; mp 126–128 °C. Yield 65 mg, 54%; ^{1}H NMR (500 MHz, $CDCl_3$) δ 7.98 (d, J = 8 Hz, 1 H), 7.87 (d, J = 7.5 Hz, 1 H), 7.67 (t, J = 7.5 Hz, 1 H), 7.59 (t, J = 7.5 Hz, 1 H), 7.46 (s, 1 H), 6.72 (s, 1 H), 4.70–4.65 (m, 1 H), 3.33–3.27 (m, 1 H), 2.99–2.86 (m, 2 H), 2.11–2.03 (m, 2 H); ^{13}C{^{1}H} NMR (125 MHz, $CDCl_3$) δ 168.2, 139.0, 137.3, 133.1, 132.7, 131.4, 130.7, 126.8, 124.1, 74.5, 42.2, 25.6, 21.5; IR (KBr, neat) 3501, 2925, 1708, 1424, 1409,

1296, 1143, 827, 744 cm^{-1}; HRMS (ESI) calcd. for $C_{13}H_{13}N_4O$ $(M + H)^+$ 241.1084, found 241.1104.

5,6-Dihydro-4*H*-[1,2,3]triazolo[1',5':3,4][1,3]diazepino[2,1-*a*]benzo[*f*]isoindol-8(14*bH*)-one (34w):

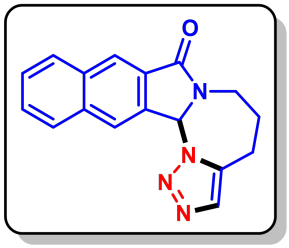

White solid; R_f (Hexane/EtOAc, 1:4) 0.50; mp 175–177 °C. Yield 74 mg, 51%; ^{1}H NMR (400 MHz, $CDCl_3$) δ 8.39 (d, J = 10.0 Hz, 2 H), 7.99 (t, J = 9.2 Hz, 2 H), 7.65–7.57 (m, 2 H), 7.46 (s, 1 H), 6.89 (s, 1 H), 4.74–4.68 (m, 1 H), 3.37–3.30 (m, 1 H), 2.92–2.87 (m, 2 H), 2.23–2.13 (m, 1 H), 2.10–2.03 (m, 1 H); ^{13}C{^{1}H} NMR (125 MHz, $CDCl_3$) δ 168.2, 137.1, 135.5, 134.1, 133.5, 133.1, 129.8, 129.3, 128.6, 128.2, 127.8, 126.5, 124.8, 74.8, 41.9, 25.6, 21.2; IR (KBr, neat) 3351, 2923, 1703, 1640, 1423, 1240, 1092, 775, 631 cm^{-1}; HRMS (ESI) calcd. for $C_{17}H_{15}N_4O$ $(M + H)^+$ 291.1240, found 291.1240.

5,6,8*a*,9,10,11,12,12*a*-Octahydro-4*H*-[1,2,3]triazolo[1',5':3,4][1,3]diazepino[2,1-*a*]isoindol-8(12*bH*)-one (34x):

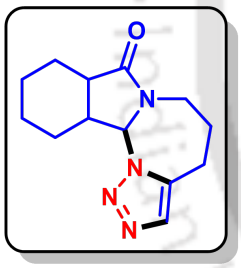

Pale yellow solid; R_f (Hexane/EtOAc, 1:4) 0.40; mp 97–99 °C. Yield 60 mg, 49%; ^{1}H NMR (500 MHz, $CDCl_3$) δ 7.42 (s, 1 H), 5.22 (s, 1 H), 4.56–4.51 (m, 1 H), 3.87–3.82 (m, 1 H), 3.12–3.01 (m, 2 H), 2.75–2.67 (m, 2 H), 2.21–2.17 (m, 1 H), 2.04–2.00 (m, 1 H), 1.98–1.93 (m, 1 H), 1.71 (d, J = 13.5 Hz, 1 H), 1.64–1.61 (m, 2 H), 1.56–1.50 (m, 1 H), 1.33–1.24 (m, 1 H), 1.21–1.05 (m, 2 H); ^{13}C{^{1}H} NMR (125 MHz, $CDCl_3$) δ 175.6, 137.8, 133.5, 78.4, 44.1, 39.1, 35.9, 27.6, 26.2,23.8, 22.8, 22.7, 22.6; IR (KBr, neat) 3456, 2929, 1704, 1429, 1260, 1206, 815, 740 cm^{-1}; HRMS (ESI) calcd. for $C_{13}H_{19}N_4O$ $(M + H)^+$ 247.1553, found 247.1557.

4,5,7*a*,8,11,11*a*-Hexahydro-[1,2,3]triazolo[1',5':3,4]pyrimido[2,1-*a*]isoindol-7(11*bH*)-one (34y):

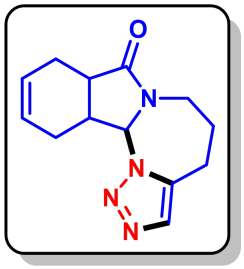

Pale yellow solid; R_f (Hexane/EtOAc, 1:4) 0.45; mp 80–82 °C. Yield 63 mg, 52%; ^{1}H NMR (500 MHz, $CDCl_3$) δ 7.45 (s, 1 H), 5.81–5.77 (m, 1 H), 5.74–5.70 (m, 1 H), 5.33 (s, 1 H), 4.56–4.51 (m, 1 H), 4.00–3.95 (m, 1 H), 3.12 (dd, J = 15.5, 6.5 Hz, 1 H), 3.09–3.03 (m, 1 H), 2.86 (t, J = 8.0 Hz, 1 H), 2.79–2.73 (m, 1 H), 2.58 (d, J = 19.0 Hz, 1 H), 2.50–2.44 (m, 1 H), 2.36–2.29 (m, 1 H), 2.00–1.95 (m, 1 H), 1.93–1.86 (m, 1 H), 1.70–1.66 (m, 1 H); ^{13}C{^{1}H} NMR (125

MHz, $CDCl_3$) δ 176.2, 137.8, 133.6, 126.4, 124.0, 79.2, 44.3, 37.1, 32.7, 26.1, 25.0, 22.7, 21.5; IR (KBr, neat) 3460, 2919, 1704, 1429, 1263, 1153, 825, 689 cm^{-1}; HRMS (ESI) calcd. for $C_{13}H_{17}N_4O$ $(M + H)^+$ 245.1397, found 245.1399.

3-Azido-2-(but-3-yn-1-yl)isoindolin-1-one (intermediate B):

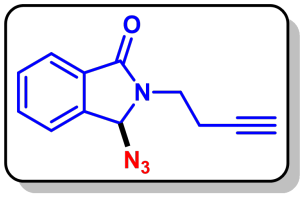

Yellow gummy; R_f (Hexane/EtOAc, 3:1) 0.50. Yield 40 mg, 71%; ^1H NMR (500 MHz, $CDCl_3$) δ 7.87 (d, J = 7.5 Hz, 1 H), 7.66 (t, J = 7.5 Hz, 1 H), 7.61–7.56 (m, 2 H), 5.76 (s, 1 H), 4.04–3.99 (m, 1 H), 3.63–3.57 (m, 1 H), 2.71–2.56 (m, 2 H), 2.01 (t, J = 2.5 Hz, 1 H); $^{13}C\{^1H\}$ NMR (125 MHz, $CDCl_3$) δ 167.5, 140.4, 132.9, 131.9, 130.7, 124.2, 123.4, 81.5, 74.8, 70.7, 39.4, 18.7; IR (KBr, neat) 3299, 2923, 2101, 1705, 1404, 1209, 1134, 1026, 744, 642 cm^{-1}; HRMS (ESI) calcd. for $C_{12}H_{11}N_4O$ $(M + H)^+$ 227.0927, found 227.0936.

3-(*p*-Tolyl)-4,5-dihydro-[1,2,3]triazolo[1',5':3,4]pyrimido[2,1-*a*]isoindole-7(11*bH*)-thione (35j):

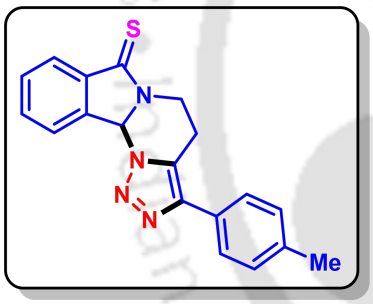

Dark brown solid; R_f (Hexane/EtOAc, 3:1) 0.50; mp 163–165 °C. Yield 71 mg, 68%; ^1H NMR (500 MHz, $CDCl_3$) δ 8.22 (d, J = 7.5 Hz, 1 H), 8.05 (d, J = 7.5 Hz, 1 H), 7.69 (t, J = 7.5 Hz, 1 H), 7.59 (dd, J = 17.5, 7.5 Hz, 3 H), 7.23 (d, J = 8.0 Hz, 2 H), 6.92 (s, 1 H), 5.50–5.45 (m, 1 H), 3.70–3.63 (m, 1 H), 3.32–3.17 (m, 2 H), 2.37 (s, 3 H); $^{13}C\{^1H\}$ NMR (125 MHz, $CDCl_3$) δ 195.3, 143.3, 139.1, 138.2, 138.2, 133.0, 131.1, 129.8, 127.9, 127.7, 126.5, 125.9, 125.2, 76.2, 39.8, 22.0, 21.5; IR (KBr, neat) 2955, 2922, 1715, 1466, 1352, 1187, 1082, 822, 759, 424 cm^{-1}; HRMS (ESI) calcd. for $C_{19}H_{17}N_4S$ $(M + H)^+$ 333.1168, found 333.1184.

2.10 Representative Spectra

^{1}H spectrum of compound **34a** (500 MHz, $CDCl_3$)

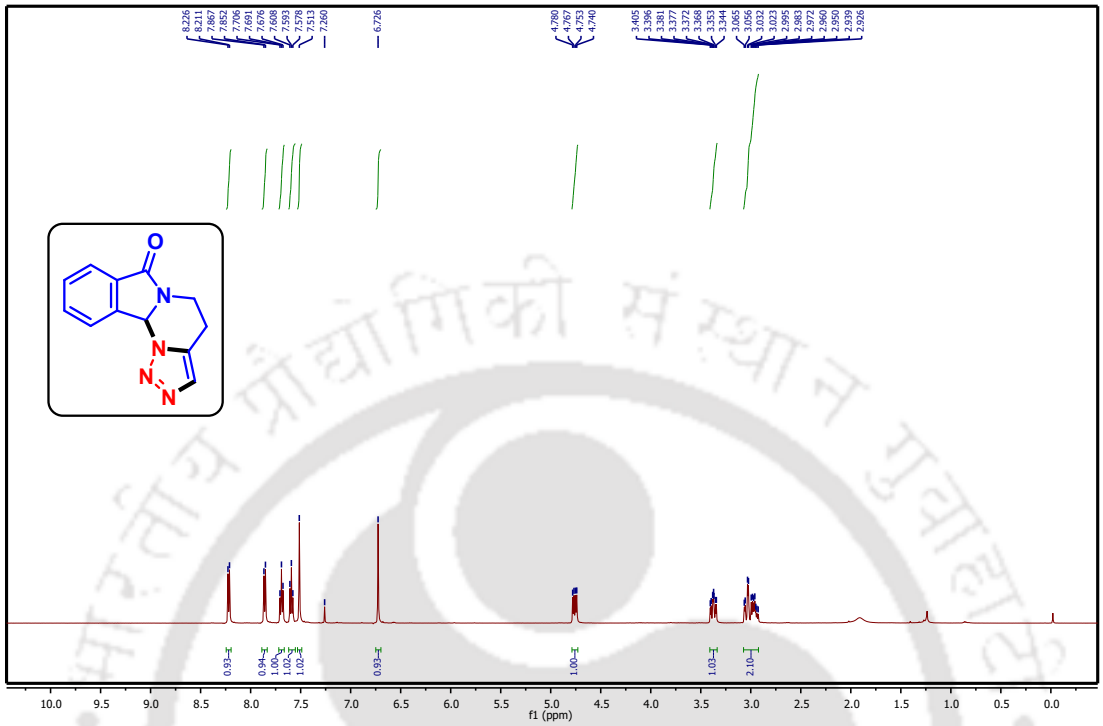

^{13}C{^{1}H} spectrum of compound **34a** (125 MHz, $CDCl_3$)

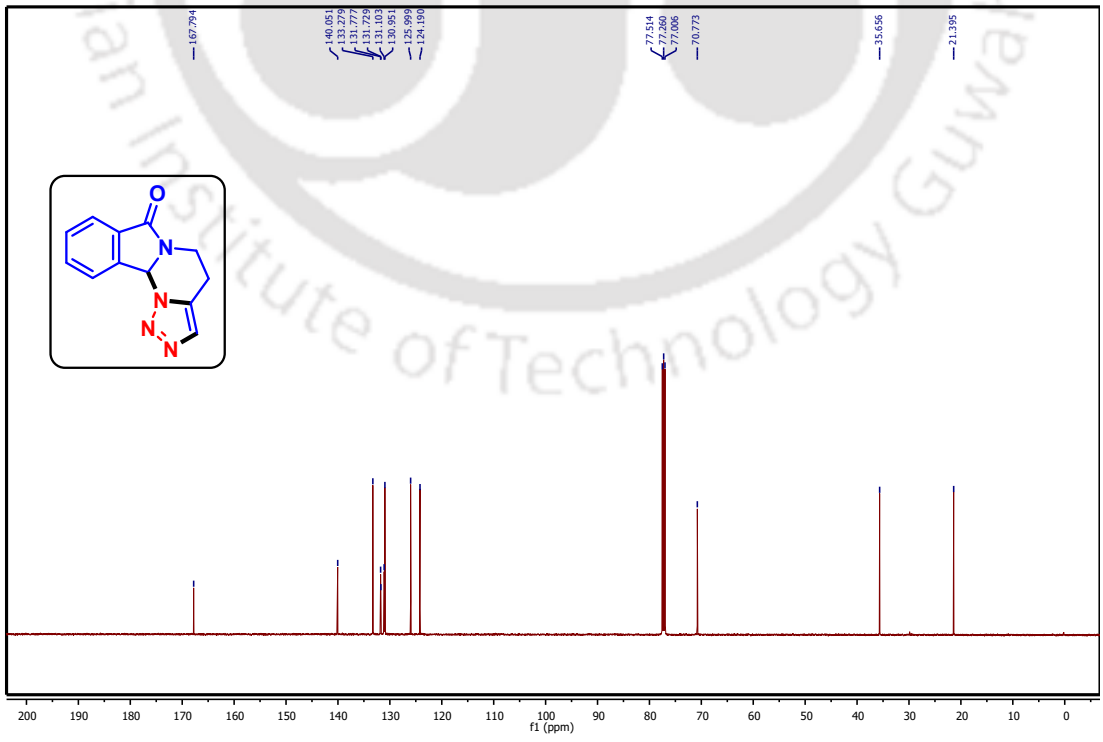

^{1}H spectrum of compound **34i** (500 MHz, $CDCl_3$)

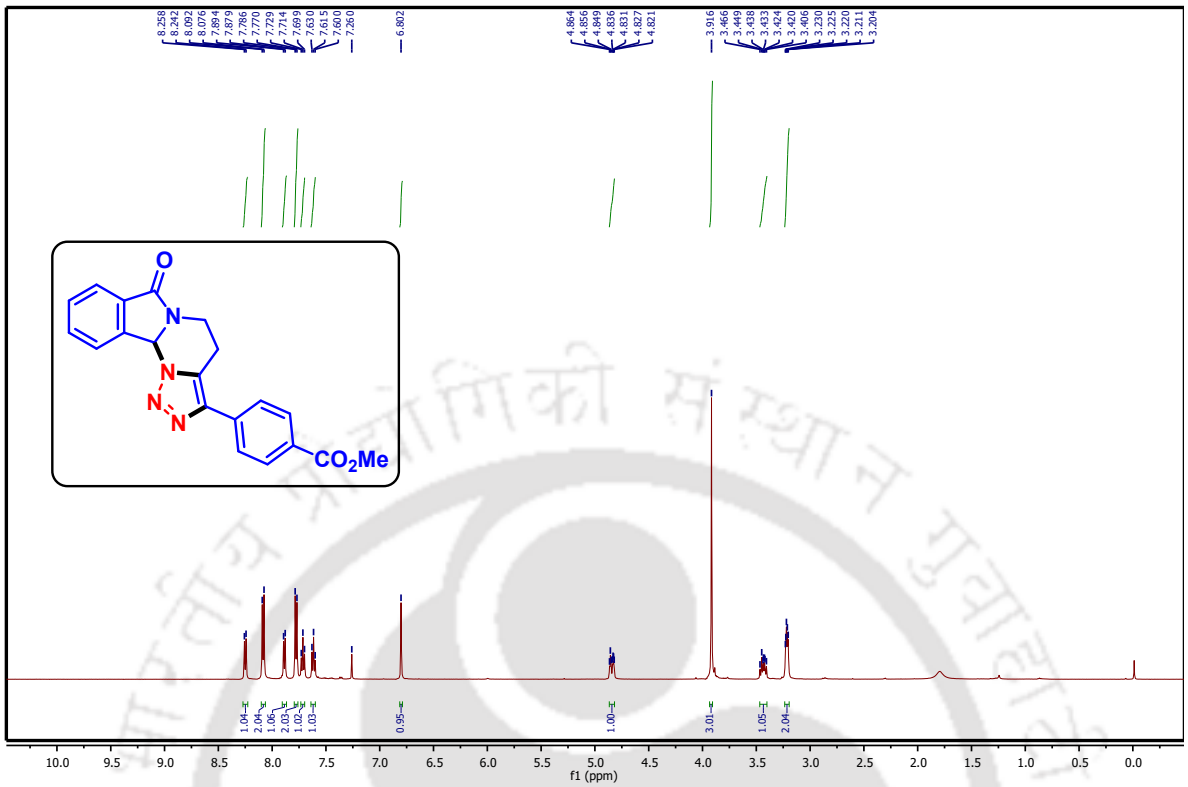

^{13}C{^{1}H} spectrum of compound **34i** (125 MHz, $CDCl_3$)

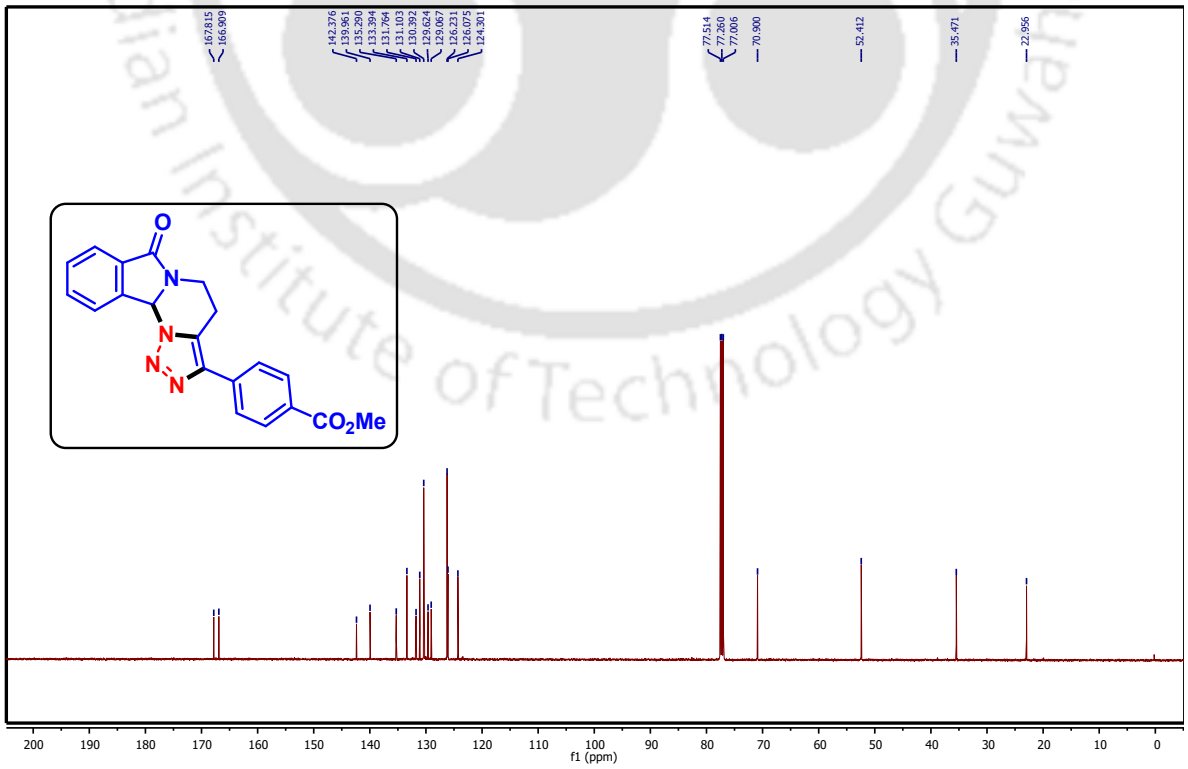

^{1}H spectrum of compound **34o** (500 MHz, $CDCl_3$)

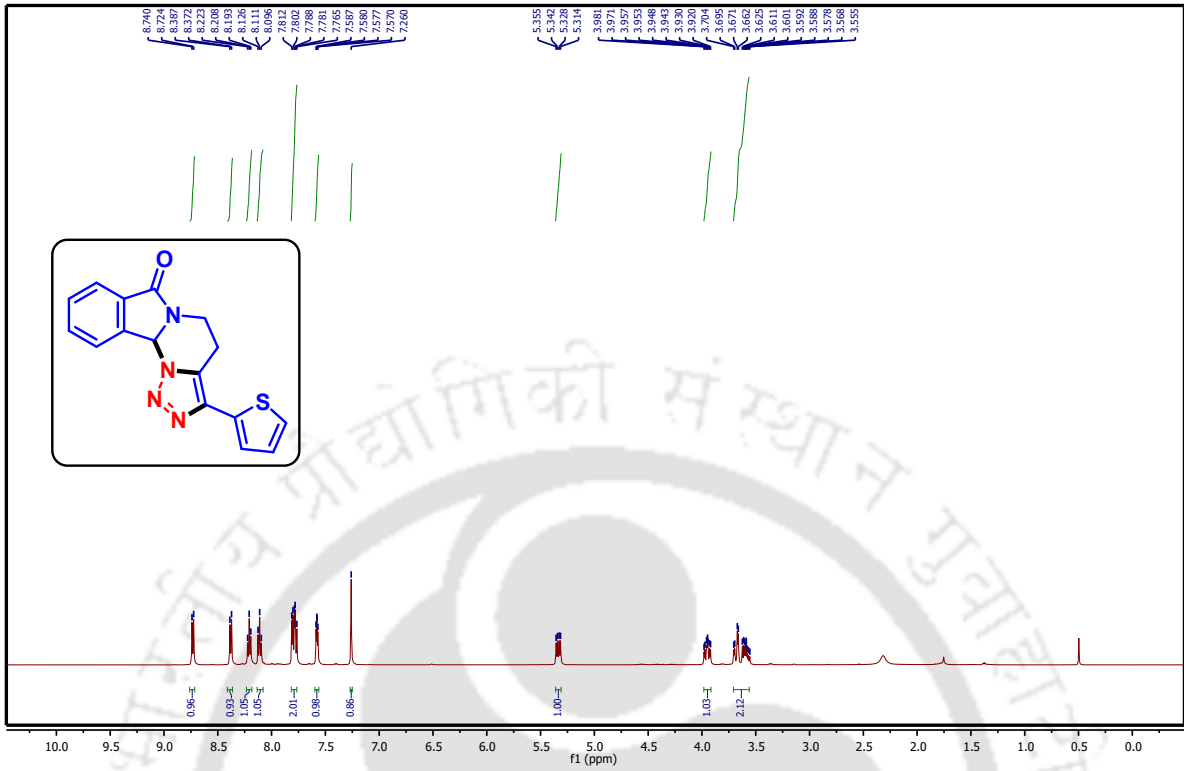

^{13}C{^{1}H} spectrum of compound **34o** (125 MHz, $CDCl_3$)

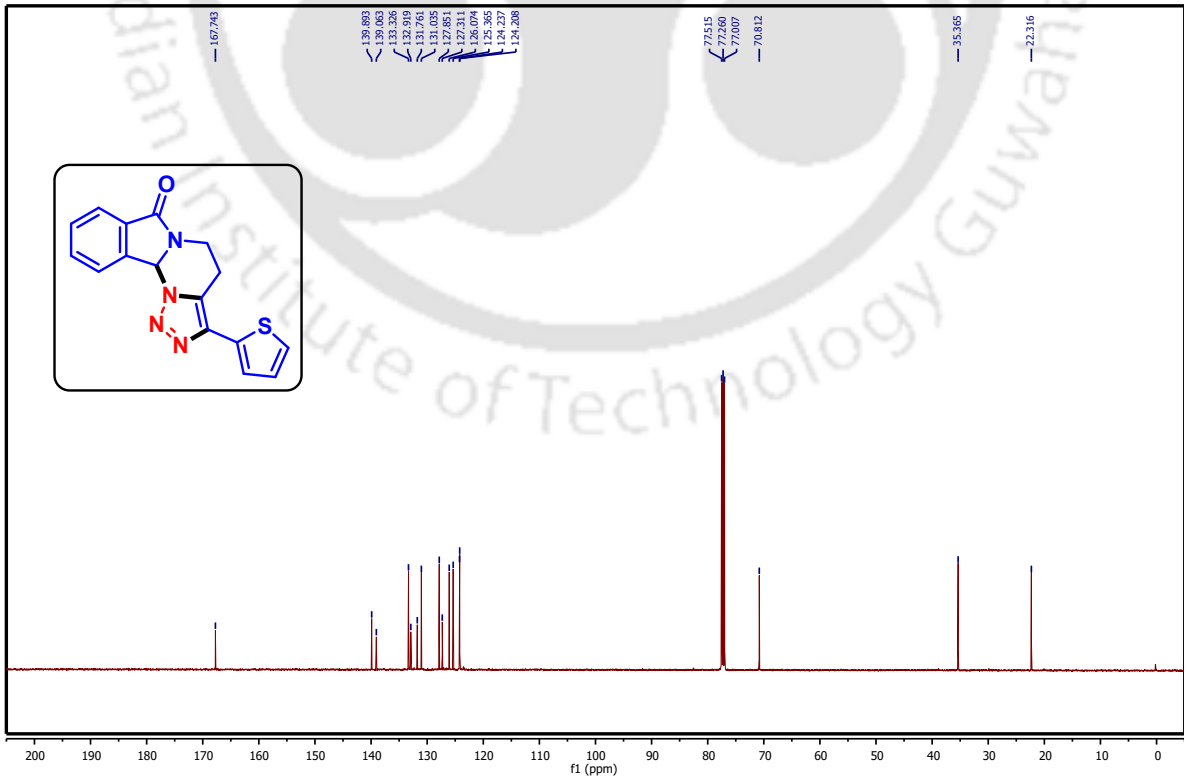

^{1}H spectrum of compound **34q** (500 MHz, $CDCl_3$)

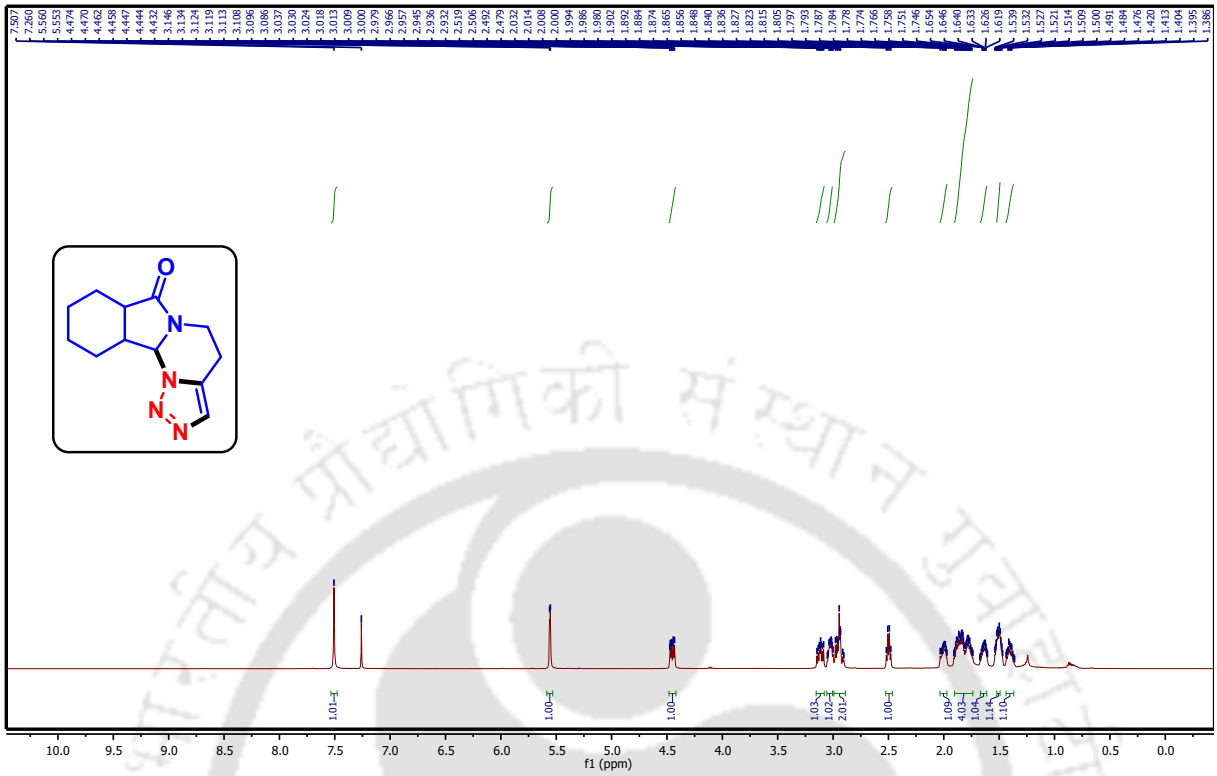

^{13}C{^{1}H} spectrum of compound **34q** (125 MHz, $CDCl_3$)

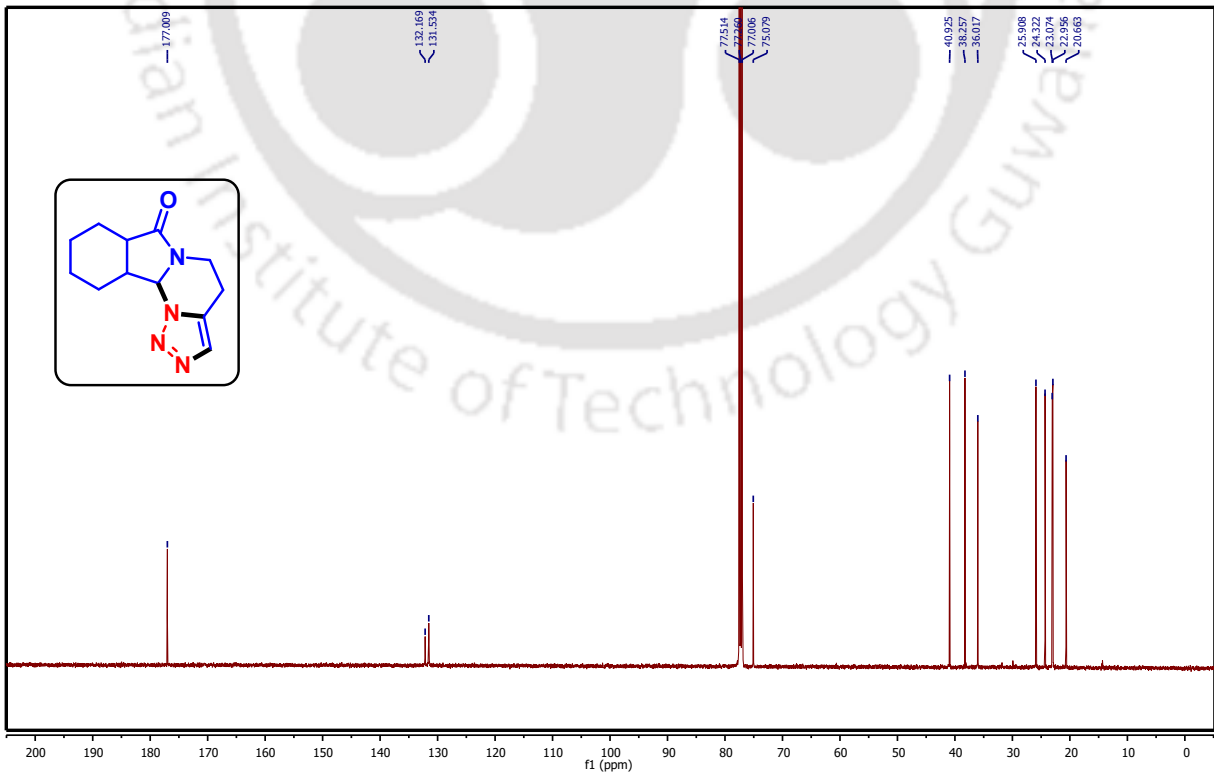

^{1}H spectrum of compound **34t** (400 MHz, $CDCl_3$)

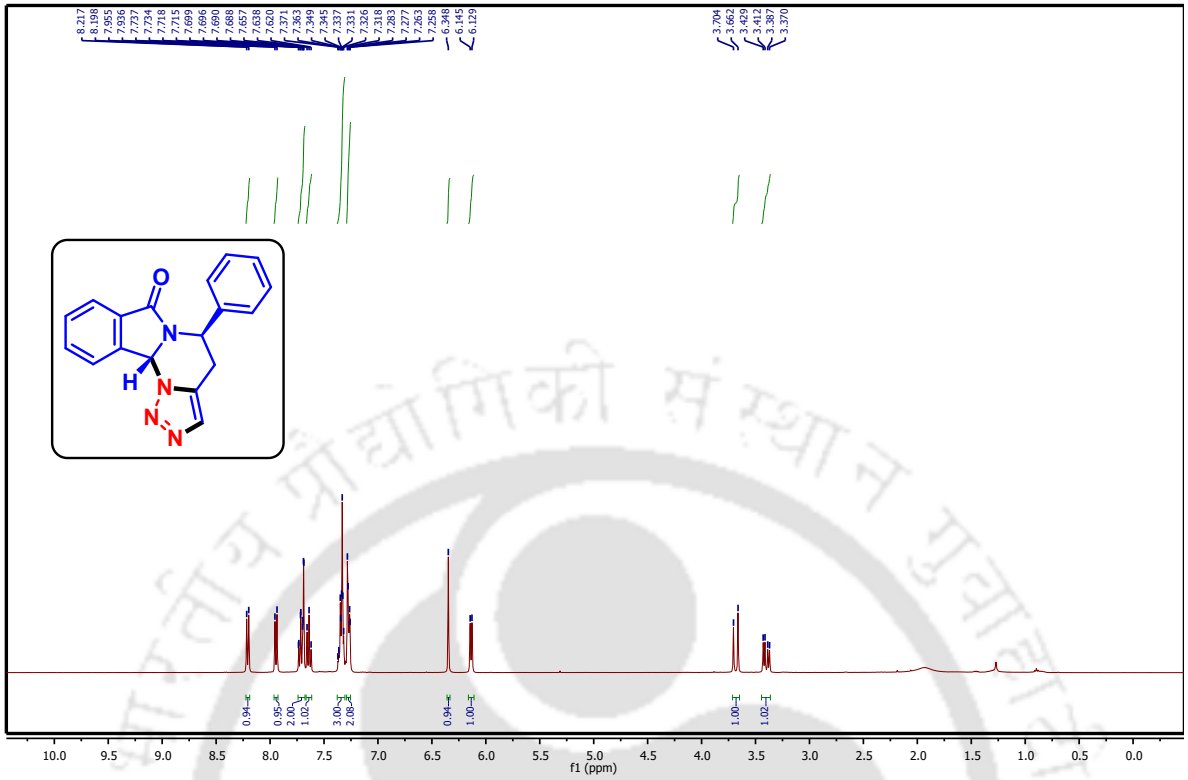

^{13}C{^{1}H} spectrum of compound **34t** (125 MHz, $CDCl_3$)

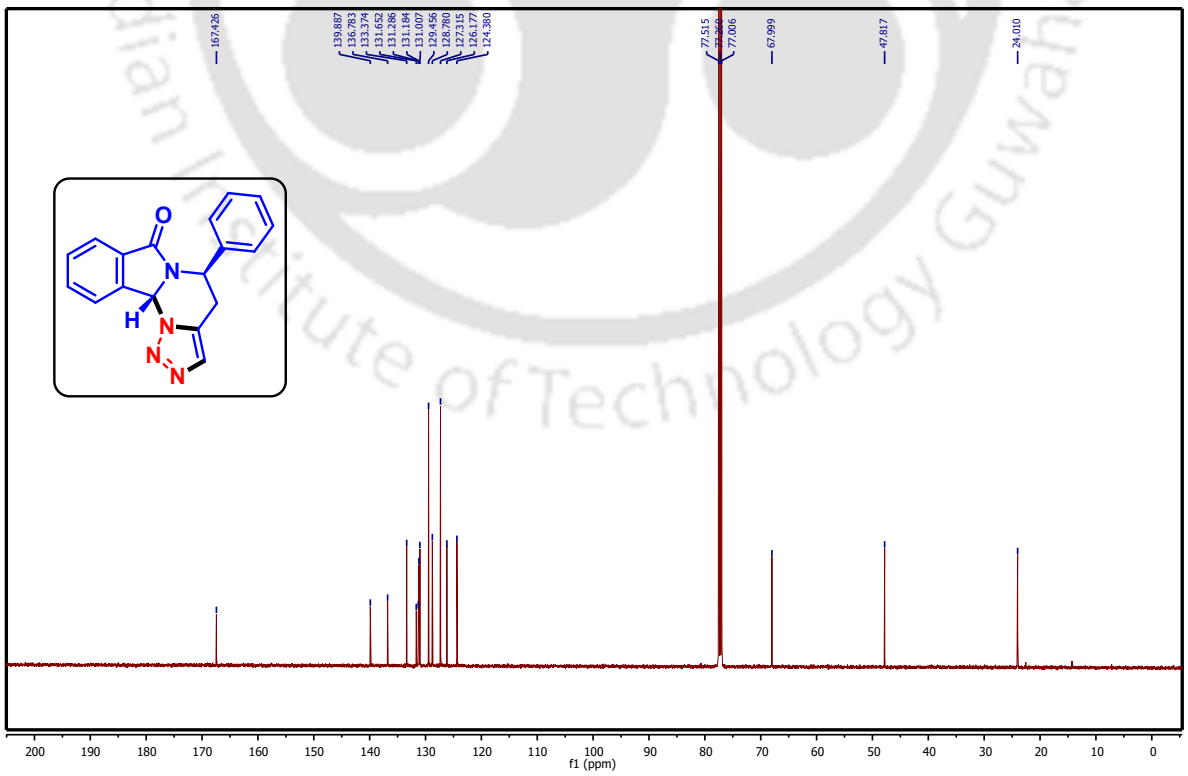

COSY spectrum of compound **34t** (400 MHz, $CDCl_3$)

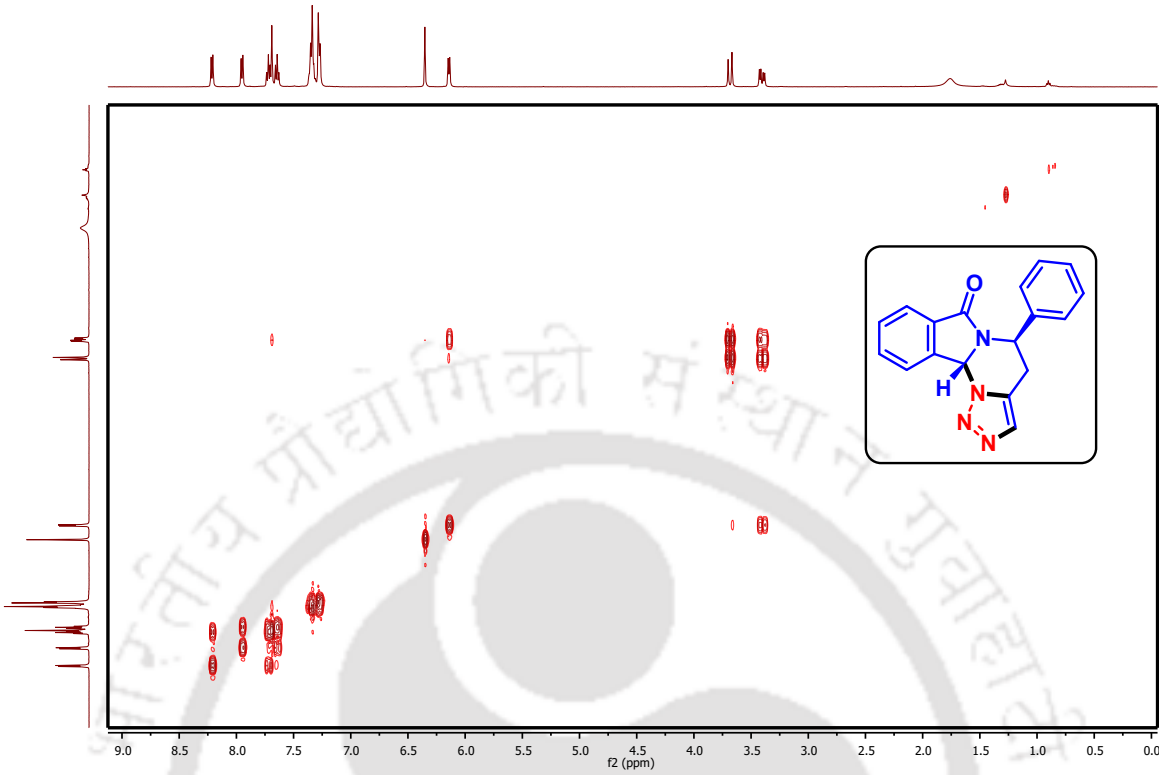

NOESY spectrum of compound **34t** (400 MHz, $CDCl_3$)

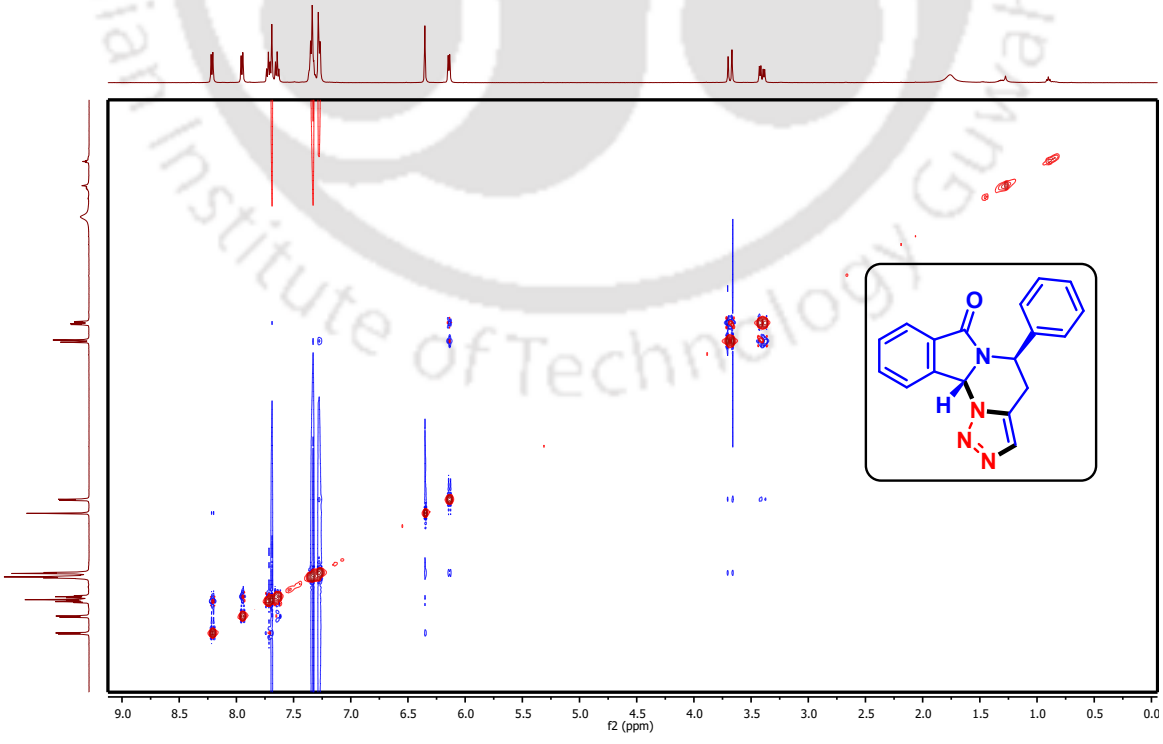

^{1}H spectrum of intermediate **34v** (500 MHz, $CDCl_3$)

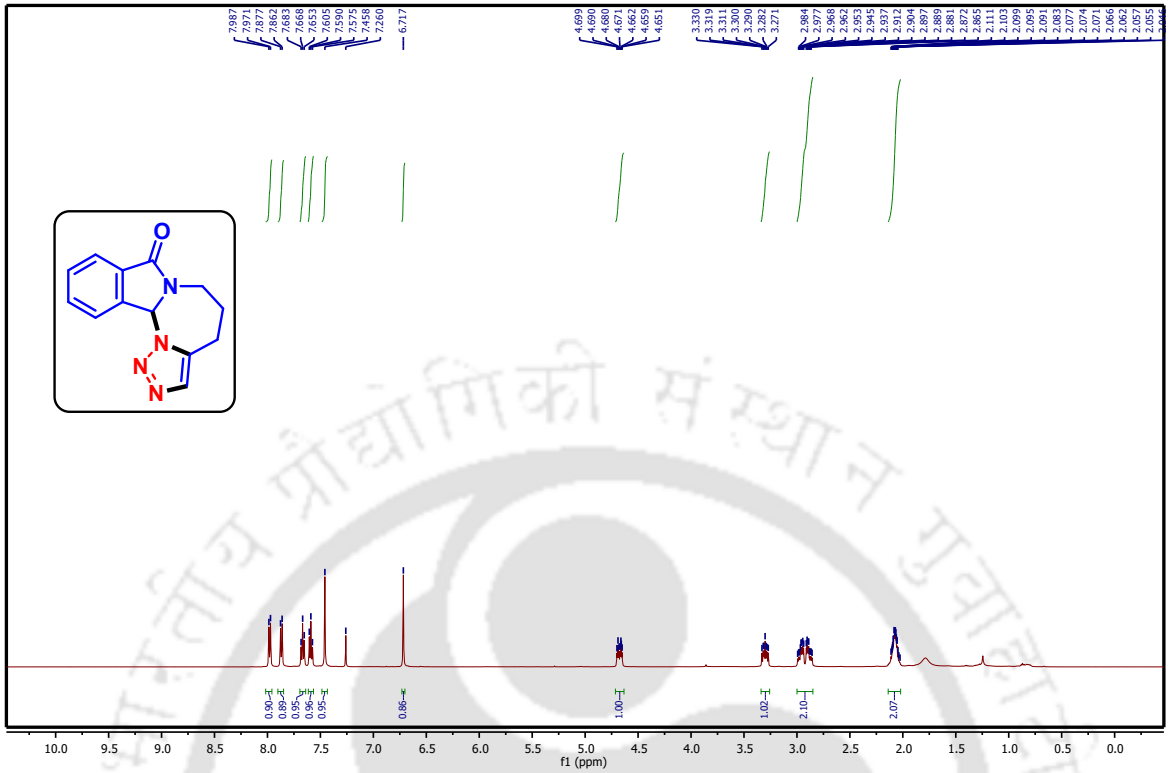

^{13}C{^{1}H} spectrum of intermediate **34v** (125 MHz, $CDCl_3$)

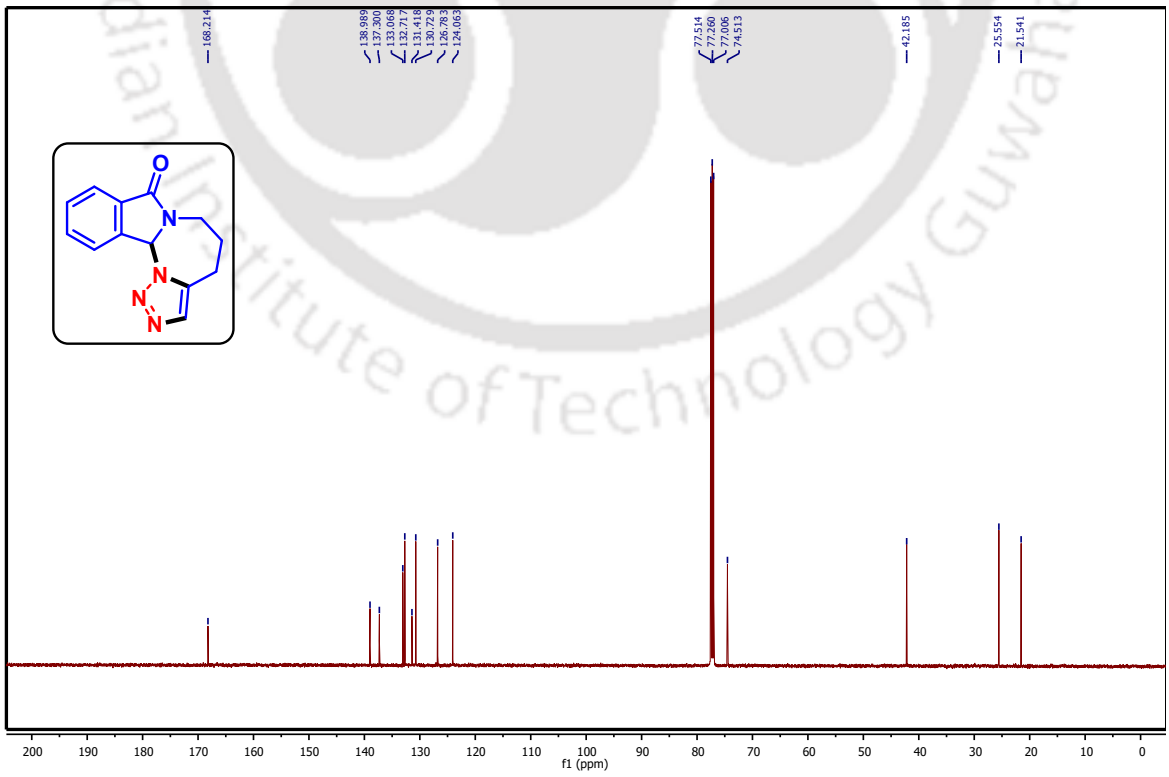

^{1}H spectrum of intermediate **B** (500 MHz, $CDCl_3$)

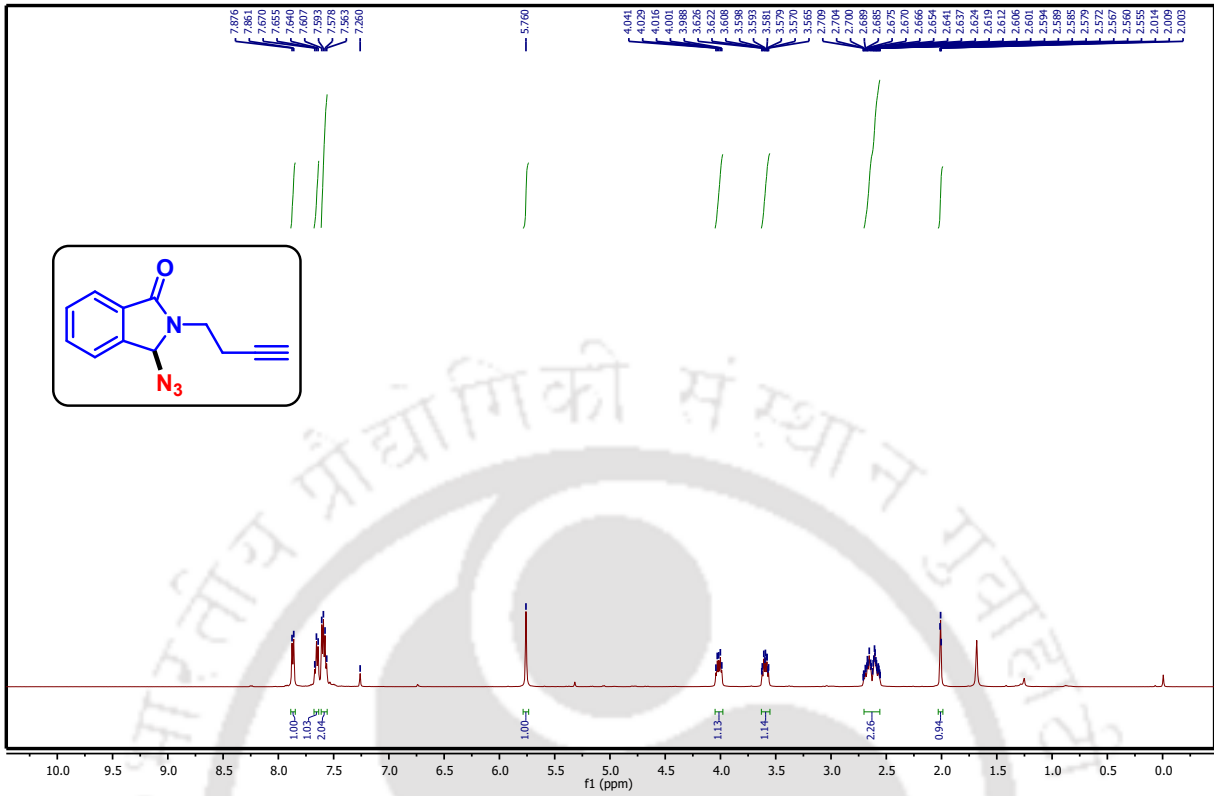

^{13}C{^{1}H} spectrum of intermediate **B** (125 MHz, $CDCl_3$)

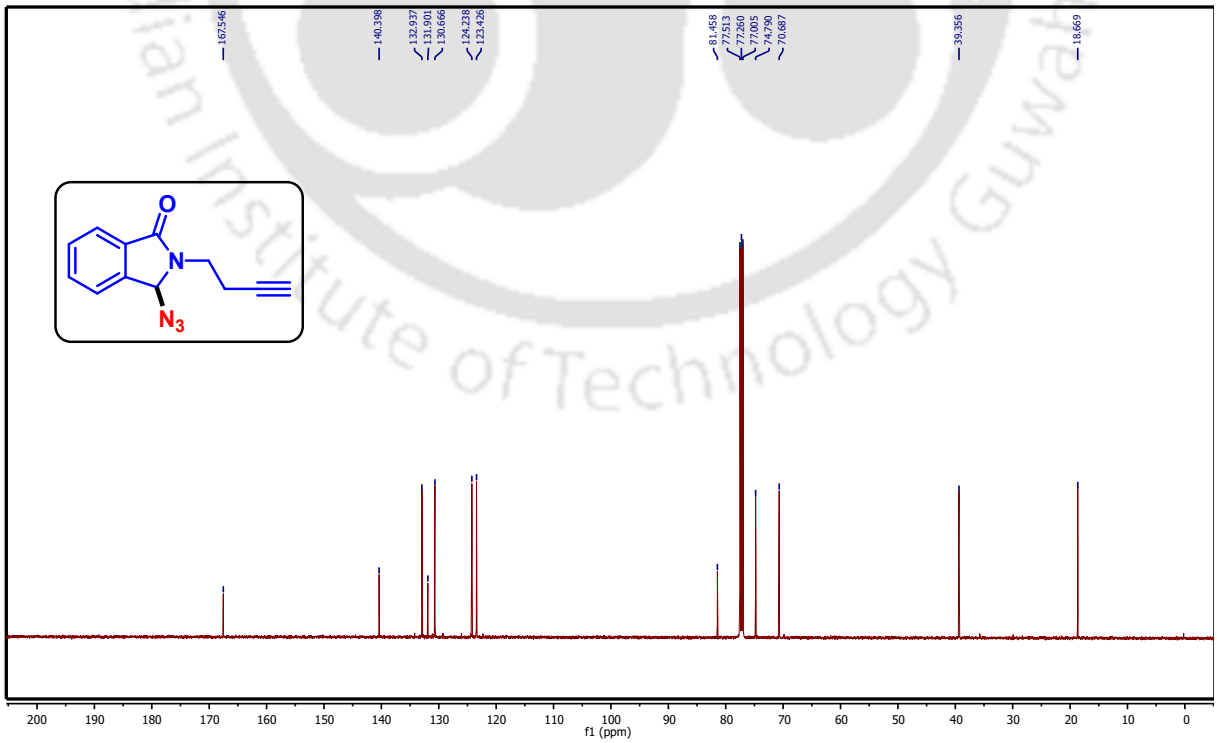

^{1}H spectrum of compound **35j** (500 MHz, $CDCl_3$)

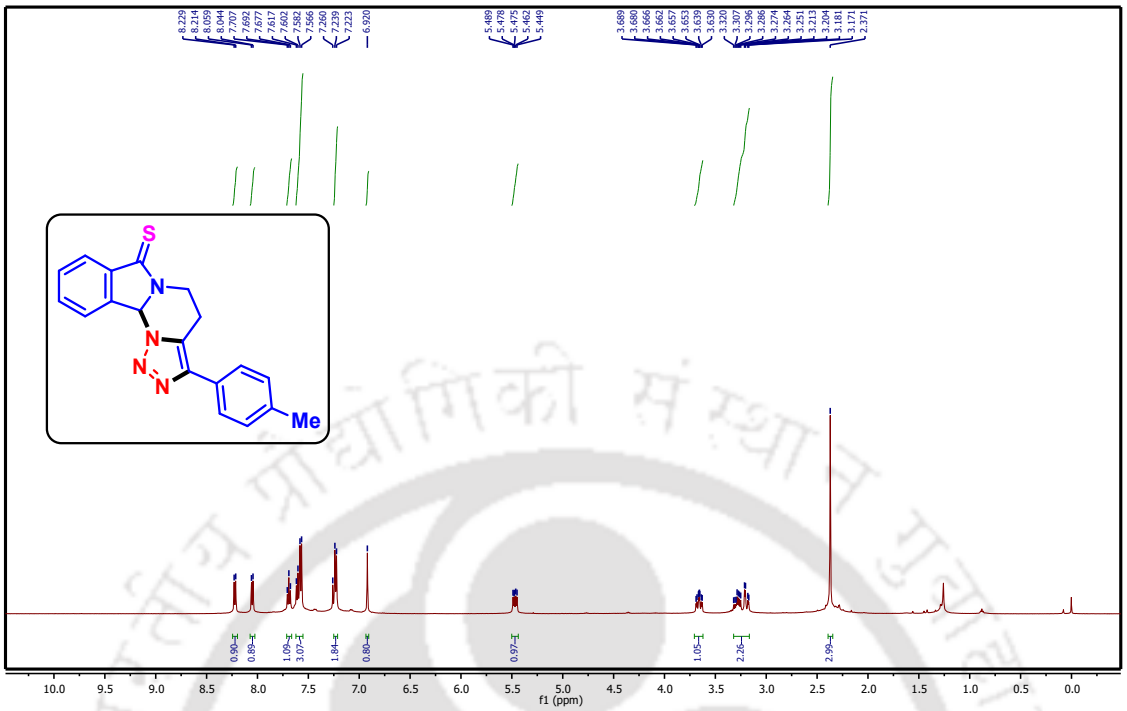

^{13}C{^{1}H} spectrum of compound **35j** (125 MHz, $CDCl_3$)

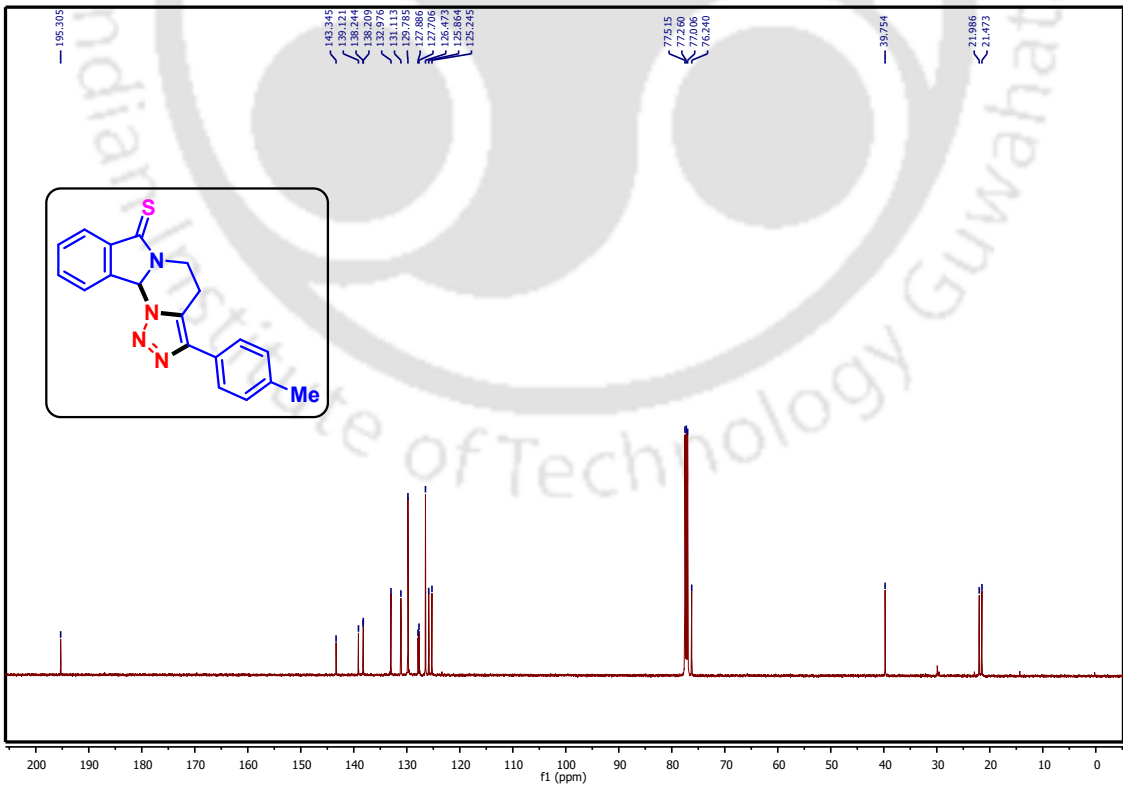

Chapter 3

A Lewis Acid-Catalyzed Cascade Synthesis of Fused *N*-Heterocycles from 2-Alkynylanilines and 2-Formylbenzonitriles: Unveiling Iminoisoindoloindolone and Its Derivatives

Contents

Abstract: This chapter outlines the streamlined synthesis of structurally fused 6-iminoisoindoloindolones *via* a cascade reaction in remarkable yields. The reaction proceeds through intermolecular tandem alkynyl cyclization reaction of 2-alkynylanilines with 2-formylbenzaldehydes for the construction of iminoisoindoloindolone derivatives under the catalytic action of a Lewis acid. The protocol utilizes trimethylsilyl trifluoromethanesulfonate (TMSOTf) as a Lewis acid which effectively activates the nitrile group and H_2O as a nucleophile under open air condition. The methodology can be further utilized for the synthesis of bioactive isoindoloindolone as well as unprecedented diphenylbenzopyrrolizinoisoquinolinone derivatives in good yields.

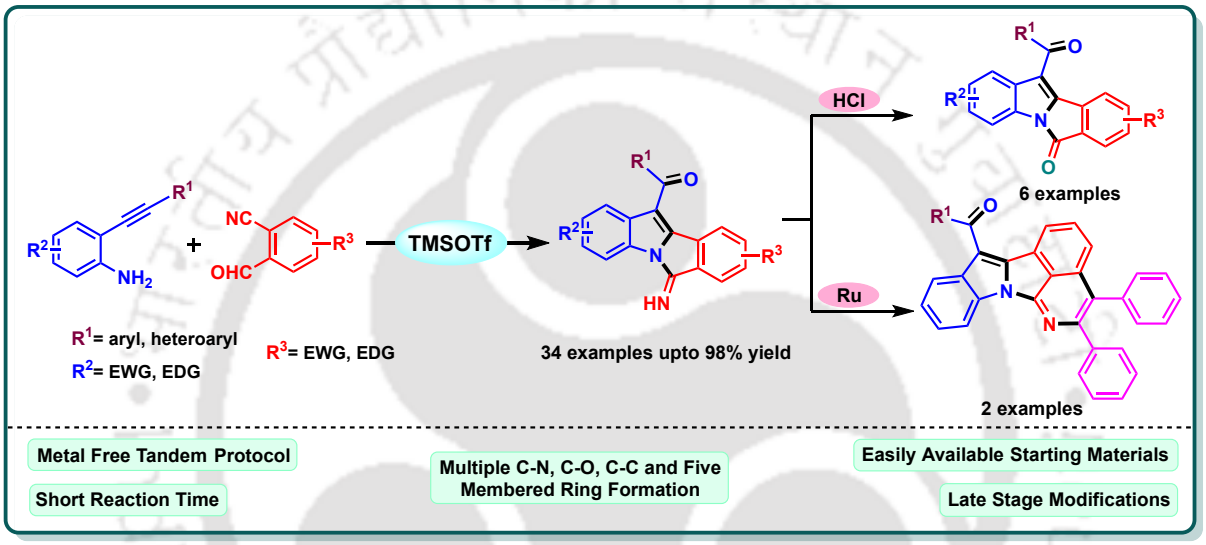

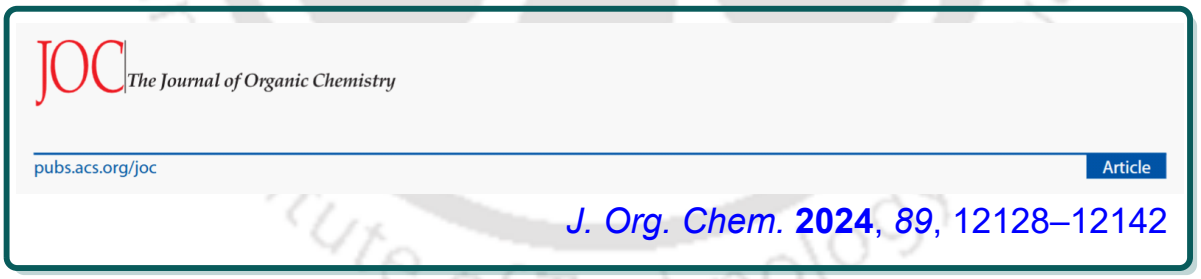

3.1 Introduction

Multifused *N*-heterocyclic compounds represent some of the most versatile and significant heterocyclic scaffolds, abundant in natural products with diverse medicinal importance and widespread natural occurrence.[1] Their pivotal roles in pharmaceutical industry and material science have garnered considerable attention in recent years. Among the plethora of fused *N*-heterocyclic motifs, indole-fused polycyclic scaffolds stand out for their prevalence in numerous heterocyclic compounds, exhibiting remarkable physiological and biological activities across natural products, medicines, and agrochemicals.[2] The past few years have witnessed a surge in interest towards synthesizing indole derivatives, driven by the potential to design polycyclic structures incorporating multiple fused heterocyclic scaffolds, thus offering avenues for creating novel heterocycles with both chemical and biomedical implications.[3] These compounds have emerged as privileged backbones not only for bioactive materials but also for electronic materials.[4] Of particular note is the 6*H*-isoindolo[2,1-*a*]indol-6-one, an analogue of the pyrrolo[1,2-*a*]indole, characterized by a tetracyclic fused indole and isoindoline ring system, serving as a core structure for numerous biologically active compounds.[5]

Due to their notable anticancer activity **I**,[6a] affinity for the hNK1 receptor **II**,[6b] melatonin binding site MT3 **III**,[6c] role as hepatitis C virus (HCV) inhibitors **IV**,[6d] and utility as precursors for the synthesis of NorA pump inhibitors **V**[6e] (*Figure 3.1.1*), multifused *N*-heterocyclic compounds have attained momentous recognition. Consequently, there has been a surge of interest among synthetic organic chemists in devising efficient methodologies for synthesizing fused polycyclic indoles.[7]

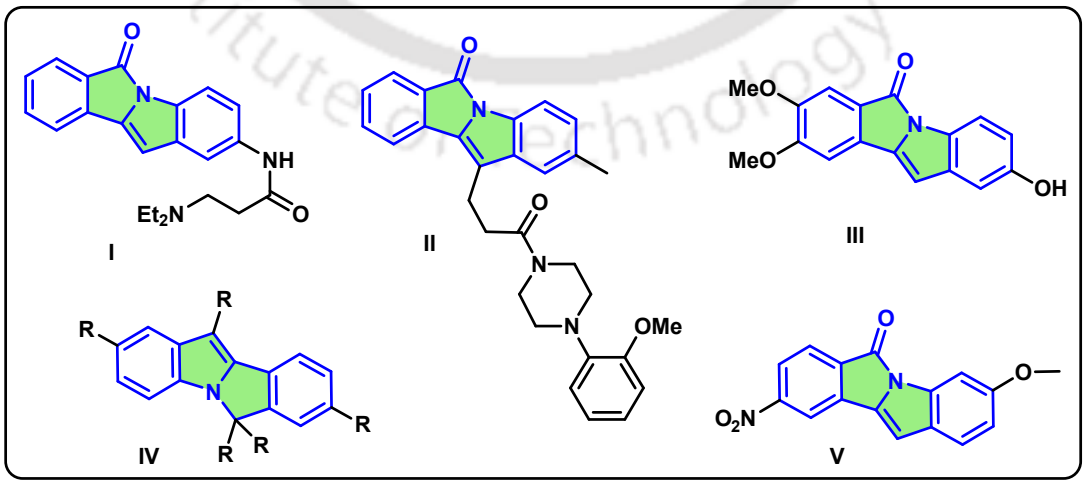

Figure 3.1.1. *Examples of bioactive fused 6H-isoindolo[2,1-a]indole derivatives.*

3.2 Literature Survey on the Synthesis of Substituted Isoindoloindoles

Due to the biologically interesting applications of isoindoloindoles (a class of polycyclic indoles), enormous efforts have designed numerous synthetic approaches[8] for constructing this class of compounds, with a diverse array of strategies reported for synthesizing fused polycyclic indoles and their analogues.

Here, a few examples for the synthesis of isoindoloindole derivatives have been presented:

Park and colleagues introduced a $Pd(OAc)_2$ and PPh_3-catalyzed regiodivergent 5-exo-dig cyclization reaction, through alkyne-directed C–H activation of *N*-alkynylindoles **1**. In this approach, an ortho-aryl palladium species was added to the α-position of an ynamine, affording (*Z*)-6-alkylidene/benzylidene-6*H*-isoindolo[2,1-*a*]indoles **2** (*Scheme 3.2.1*).[9]

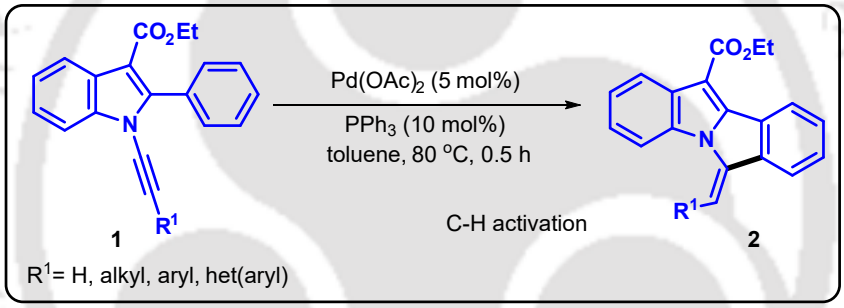

Scheme 3.2.1. *PPh_3-catalyzed synthesis of 6H-isoindolo[2,1-a]indoles.*

In another approach, the Huang group disclosed a catalyst-controlled regioselective intramolecular C–H/N–H cross-dehydrogenative-coupling (CDC) reaction of *ortho*-alkenylated 2-phenylindole **5**, where a $Pd(OAc)_2$ catalyst favored 6-alkylidene-6*H*-isoindo[2,1-*a*]indoles **6** (*Scheme 3.2.2*).[10] The CDC reaction of 2-phenyl-1*H*-indole derivatives **3** with alkenes **4** forms the alkenylated starting precursor after mono-olefination.

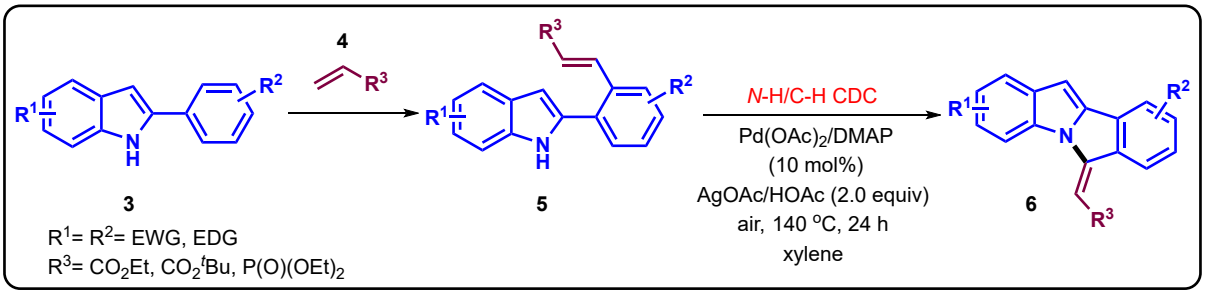

Scheme 3.2.2. *$Pd(OAc)_2$-catalyzed synthesis of 6H-isoindo[2,1-a]indoles.*

Koós and co-workers have recently developed a one-step tandem Pd-catalyzed strategy for the synthesis of isoindolo[2,1-*a*]indol-6-ones **9**, involving aminocarbonylation followed by an intramolecular C–H activation-based cross-coupling (*Scheme 3.2.3*).[11] This method utilizes aryl dibromides **8** and indoles **7** to generate *N*-(2′-bromoaroyl)indoles *in situ*, which then undergo C–H activation to form biologically significant tetracyclic isoindoloindole scaffolds. Importantly, the transformation proceeds efficiently under a standard catalytic system with *ex situ* generation of gaseous CO.

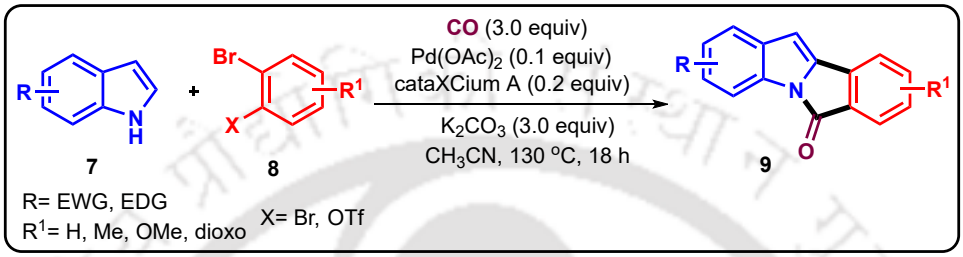

Scheme 3.2.3. *Pd-catalyzed synthesis of isoindolo[2,1-a]indol-6-ones.*

Maurya and group reported a facile synthesis of 11-aryl-6*H*-isoindolo[2,1-*a*]-indol-6-ones **11** *via* hypervalent iodine(III) (PIDA)-promoted intramolecular cascade oxidative cyclization of ortho-(1-arylethynyl)-*N*-arylbenzamides **10** at room temperature in trifluoroethanol (*Scheme 3.2.4*).[12]

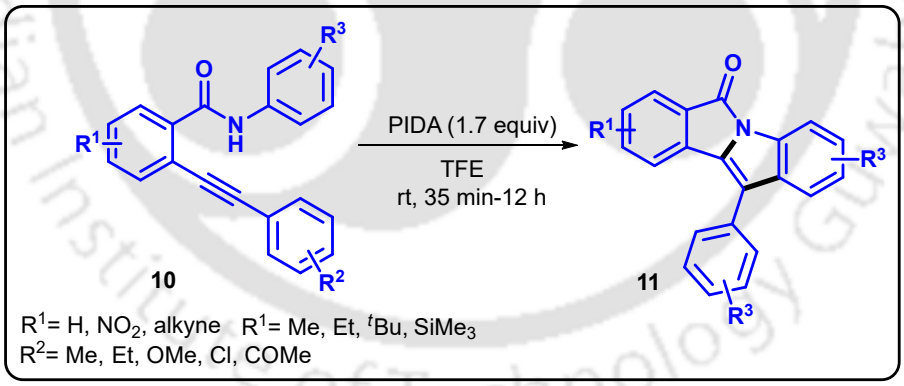

Scheme 3.2.4. *PIDA-promoted synthesis of 6H-isoindolo[2,1-a]-indolones.*

Shi and co-workers developed a CuI-catalyzed radical cascade cyclization of alkyne tethered to the aniline precursors **12** in the presence of di-*tert*-butyl peroxide (DTBP) in *t*-BuCN at 140 °C, providing *N*-fused polycyclic indoles **13** *via* intramolecular N-H/C-H annulation (*Scheme 3.2.5*).[13] Mechanistic studies suggest the involvement of a vinyl radical in this reaction, with the transformation likely proceeding through an amidyl-radical-initiated cascade pathway.

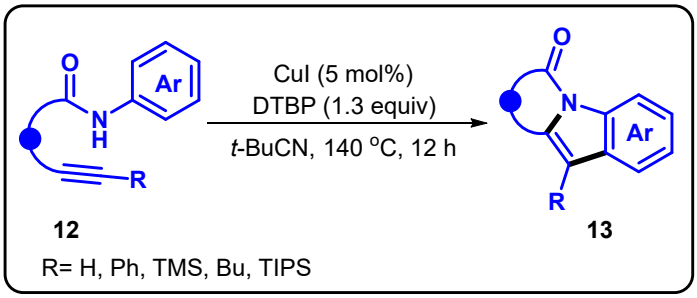

Scheme 3.2.5. *CuI-catalyzed synthesis of polycyclic indoles.*

Roy and co-workers demonstrated a Pd-catalyzed annulation of indole-*N*-arylated aldoximes **14** for the synthesis of indolo[1,2-*a*] indoles **15** (*Scheme 3.2.6*).[14] The reaction proceeds *via* $Pd(OAc)_2$-catalyzed two sequential dehydrogenative C–H activation of iminyl hydrogen with the indole C3-H and C2-H bond using $K_2S_2O_8$ as an oxidant.

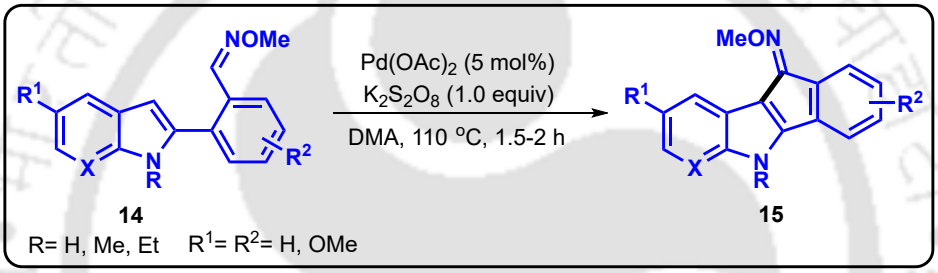

Scheme 3.2.6. *$Pd(OAc)_2$-catalyzed synthesis of indolo[1,2-a]indoles.*

Hua and co-workers reported a copper-catalyzed intramolecular arylative cyclization of *N*-(2-cyanophenyl)indoles **16** with diaryliodonium salts **17** for the synthesis of fused polycyclic indole derivatives **18** (*Scheme 3.2.7*).[15] In this reaction, Cu(I) species generated after reduction or disproportion of $Cu(OTf)_2$ undergo oxidative addition to diaryliodonium salt which acts as an aryl reagent.

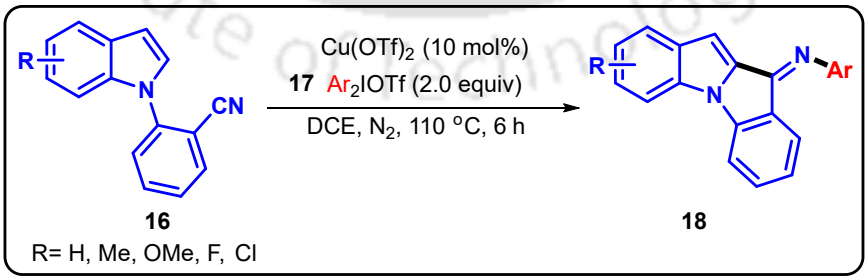

Scheme 3.2.7. *$Cu(OTf)_2$-catalyzed synthesis of polycyclic indoles.*

Cheng and co-workers described an elegant synthesis of 10*H*-indolo[1,2-*a*]indol-10-one derivatives **21** based on the Rh-catalyzed [4 + 1] annulation reaction between aroyl sulfoxonium ylides **19** and anthranils **20** (*Scheme 3.2.8*).[16] The reaction begins with

an unprecedented [4 + 1] annulation to form *N*-(2-formylphenyl)indolones, involving sequential ortho-C-H amination of aroyl sulfoxonium ylides by anthranils and N-H insertion into a carbene, followed by Aldol condensation to form the second indole ring.

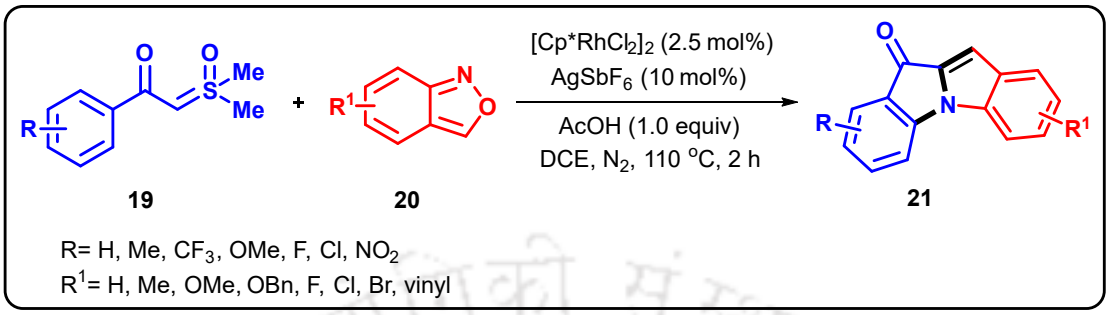

Scheme 3.2.8. *Rh-catalyzed synthesis of indolo[1,2-a]indolones.*

3.3 Present Work

From the above literature reports, it is evident that most of the strategies rely on indole-based compounds as starting materials, alongside expensive metal catalysts and often multistep processes.[17] These approaches can be categorized by dissecting individual bonds within the isoindoloindole skeleton. The prevailing protocols predominantly involve in C–N-lactam bond formation[18] and isoindolo ring formation *via* C–C coupling.[19] Alternatively, some methods employ condensation reactions[20] or Heck coupling[21] to construct the indole ring. Consequently, there is a notable gap in the exploration of divergent and simplified methods for synthesizing these compounds from readily available acyclic starting materials in a manner that maximizes atom economy, presenting a highly promising avenue for further research and development.[22]

Besides, several literature reports show that amine and aldehyde derivatives couple in the presence of an acid to form various *N*-heterocycles, mainly *via* condensation reactions (*Scheme 3.3.1a*). From that point of view, it was expected that 2-alkynylaniline would undergo condensation reaction with 2-formylbenzonitrile under Lewis acidic condition to form a tetracyclic indole moiety (*Scheme 3.3.1b*). Instead, the

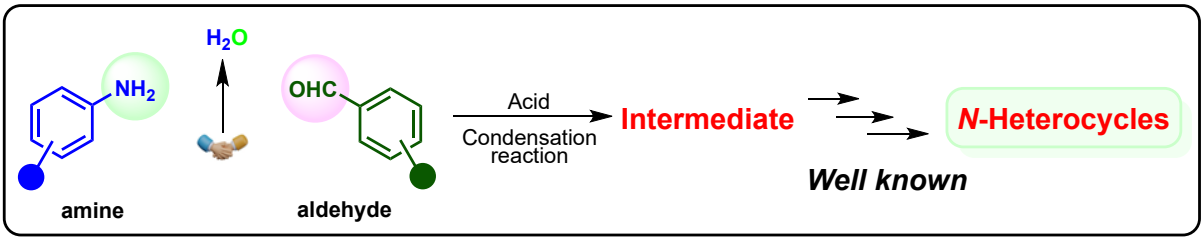

Scheme 3.3.1a. *Previous reports on the reactivity of amine with aldehyde.*

reaction surprisingly underwent nucleophilic attack by amine on the Lewis acid-activated nitrile in the initial step.

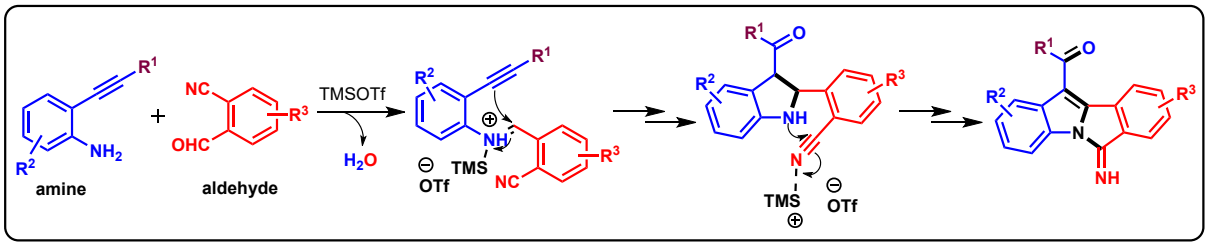

Scheme 3.3.1b. *Our hypothesis on the reactivity of amine with aldehyde to form iminoisoindoloindolone.*

Thus, this chapter describes a straightforward synthesis of fused 6-imino-6*H*-isoindolo[2,1-*a*]indolone and its derivatives **24** from 2-alkynylanilines **22** and 2-formylbenzonitriles **23** in excellent yields (*Scheme 3.3.1c*). The reaction progresses in a cascade fashion under the catalytic action of TMSOTf.

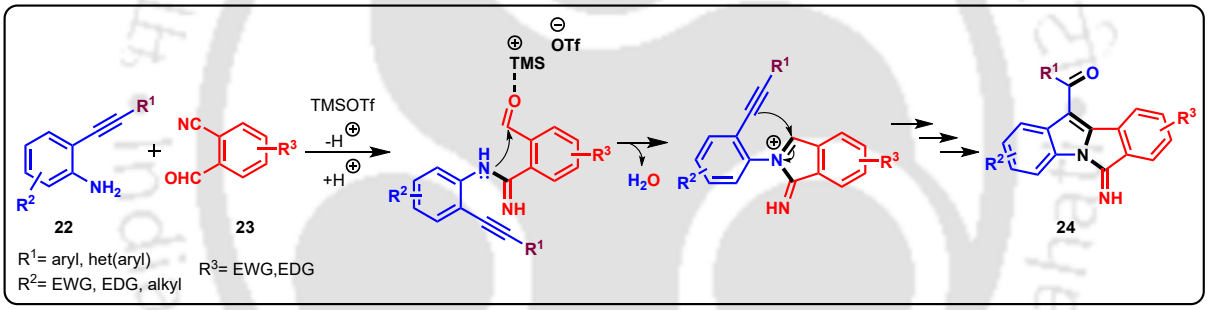

Scheme 3.3.1c. *Synthesis of iminoisoindoloindolones via nucleophilic attack by amine on the Lewis acid-activated nitrile.*

3.4 Results and Discussion

3.4.1 Optimization of the Reaction

We commenced our study using 2-(phenylethynyl)aniline (**22aa**) and 2-formylbenzonitrile (**23a**) as model substrates. In the first attempt, compounds **22aa** (1.0 equiv) and **23a** (1.1 equiv) were reacted with $BF_3{\cdot}OEt_2$ (0.2 equiv) in 1,2-DCE at 0 °C to room temperature. After 12 h, the desired product **24aa** was obtained in 35% yield with partial consumption of the starting materials (*Table 3.4.1.1,* entry 1). NMR (^{1}H and ^{13}C{^{1}H}) spectroscopy and HRMS confirmed the product as (6-imino-6*H*-isoindolo[2,1-*a*]indol-11-yl)(phenyl)methanone (**24aa**), and the structure was further validated by single-crystal X-ray analysis. To improve the yield, we repeated the reaction at 80

°C under the same reaction conditions. This resulted in 74% yield of **24aa** in just 30 min with complete consumption of the starting materials (*Table 3.4.1.1,* entry 2).

Table 3.4.1.1. *Optimization of the reaction*[a]

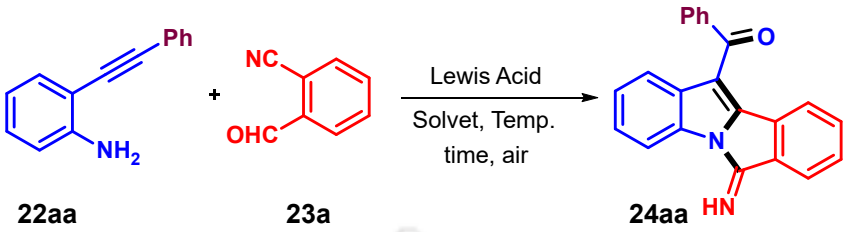

22aa **23a** **24aa**

Entry[a]	Lewis acid (equiv)	Solvent	Temp (°C)	Time (h)	Yield (%)[b]
1.	$BF_3{\cdot}OEt_2$ (0.2)	1,2-DCE	rt	12.0	35
2.	$BF_3{\cdot}OEt_2$ (0.2)	1,2-DCE	80	0.50	74
3.	$In(OTf)_3$ (0.2)	1,2-DCE	80	12.0	N.R.
4.	$Bi(OTf)_3$ (0.2)	1,2-DCE	80	12.0	N.R.
5.	$TiCl_4$ (0.2)	1,2-DCE	80	0.50	59
6.	$SnCl_4$ (0.2)	1,2-DCE	80	0.50	65
7.	$FeCl_3$ (1.2)	1,2-DCE	80	12.0	N.R.
8.	$InCl_3$ (0.2)	1,2-DCE	80	12.0	N.R.
9.	TMSOTf (0.2)	1,2-DCE	80	0.25	83
10.	TfOH (0.2)	1,2-DCE	80	0.25	67
11.	*p*-TsOH (0.2)	1,2-DCE	80	0.25	70
12.	TMSOTf (0.2)	1,2-DCE	100	0.25	73
13.	**TMSOTf (0.2)**	**1,2-DCE**	**70**	**0.25**	**89**
14.	TMSOTf (0.5)	1,2-DCE	70	0.25	87
15.	TMSOTf (0.2)	DCM	40	0.50	55
16.	TMSOTf (0.2)	Toluene	110	0.50	63
17.	TMSOTf (0.2)	CH_3CN	80	12.0	N.R.
18.	TMSOTf (0.2)	DMF	120	2.0	-[c]

[a]**22aa** (0.3 mmol), **23a** (0.33 mmol), solvent 2.0 mL. [b]Isolated yield, [c]Decomposed product, N.R.= no reaction.

Encouraged by this, we examined other Lewis acids such as $In(OTf)_3$, $Bi(OTf)_3$, $TiCl_4$, $SnCl_4$, $FeCl_3$, $InCl_3$, and TMSOTf (*Table 3.4.1.1,* entries 3–9). $In(OTf)_3$ and $Bi(OTf)_3$ did not afford the product (*Table 3.4.1.1,* entries 3 and 4), while $TiCl_4$ and $SnCl_4$ gave moderate yields of 59% and 65% respectively (entries 5 and 6). $FeCl_3$ and $InCl_3$ were found to be ineffective towards this protocol (*Table 3.4.1.1,* entries 7 and 8). Notably, TMSOTf gave a better result, producing the target iminoisoindoloindolone in 83% yield within just 15 min (*Table 3.4.1.1,* entry 9). Brønsted acids such as TfOH and *p*-TsOH were also implemented, but both of them were incapable of improving the yield of the reaction (*Table 3.4.1.1,* entries 10 and 11). From all of these points of view, TMSOTf was found to be the suitable reagent for this conversion. Increasing the temperature up to 100 °C leads to lowering the yield to 73% (*Table 3.4.1.1,* entry 12) owing to the formation of some decomposed byproducts. On the contrary, decreasing the temperature to 70 °C favorably facilitates up to 89% yield of the desired product (*Table 3.4.1.1,* entry 13). Changing the equivalency of TMSOTf from 0.2 to 0.5 equiv results in a slight decrease in yield to 87% (*Table 3.4.1.1,* entry 14). The methodology was also screened with different solvents such as DCM, toluene, CH_3CN, and DMF (*Table 3.4.1.1,* entries 15–18). In DCM and toluene, the reaction delivered comparatively lower yields of 55% and 63%, respectively (*Table 3.4.1.1,* entries 15 and 16). Moreover, in CH_3CN, the reaction did not afford the desired product (*Table 3.4.1.1,* entry 17), and in DMF, decomposed byproducts were obtained (*Table 3.4.1.1,* entry 18). Acquiring all these data, it was evident that TMSOTf (0.2 equiv) in 1,2-DCE at 70 °C were established to be the optimized condition for this transformation.

3.4.2 Substrate Scope

The substrate range of the reaction was extensively investigated under the established optimal conditions with substituted 2-alkynylanilines **22** and substituted 2-formylbenzonitriles **23**. The protocol was primarily scrutinized by varying the alkyne side chain of 2-ethynylanilines **22a** (R^1) (*Scheme 3.4.2.1*) with both electron-withdrawing as well as electron-donating groups on different positions of the phenyl ring. Moderately electron-withdrawing groups like –Cl, –Br, and –F at the *para*-position of the aromatic ring furnished their respective products **24ab**, **24ad**, and **24af** with good yields of 77%, 80%, and 81%, respectively. The introduction of a –Cl group at the *meta*-position of the aromatic ring proved effective, providing an impressive 82% yield of its product **24ac**. The sterically hindered *ortho*-substituted ethynylanilines **22ae** and **22ak** also provided good yields of **24ae** and **24ak** in 75% and 90%, respectively. The strategy was also screened with strong electron-withdrawing

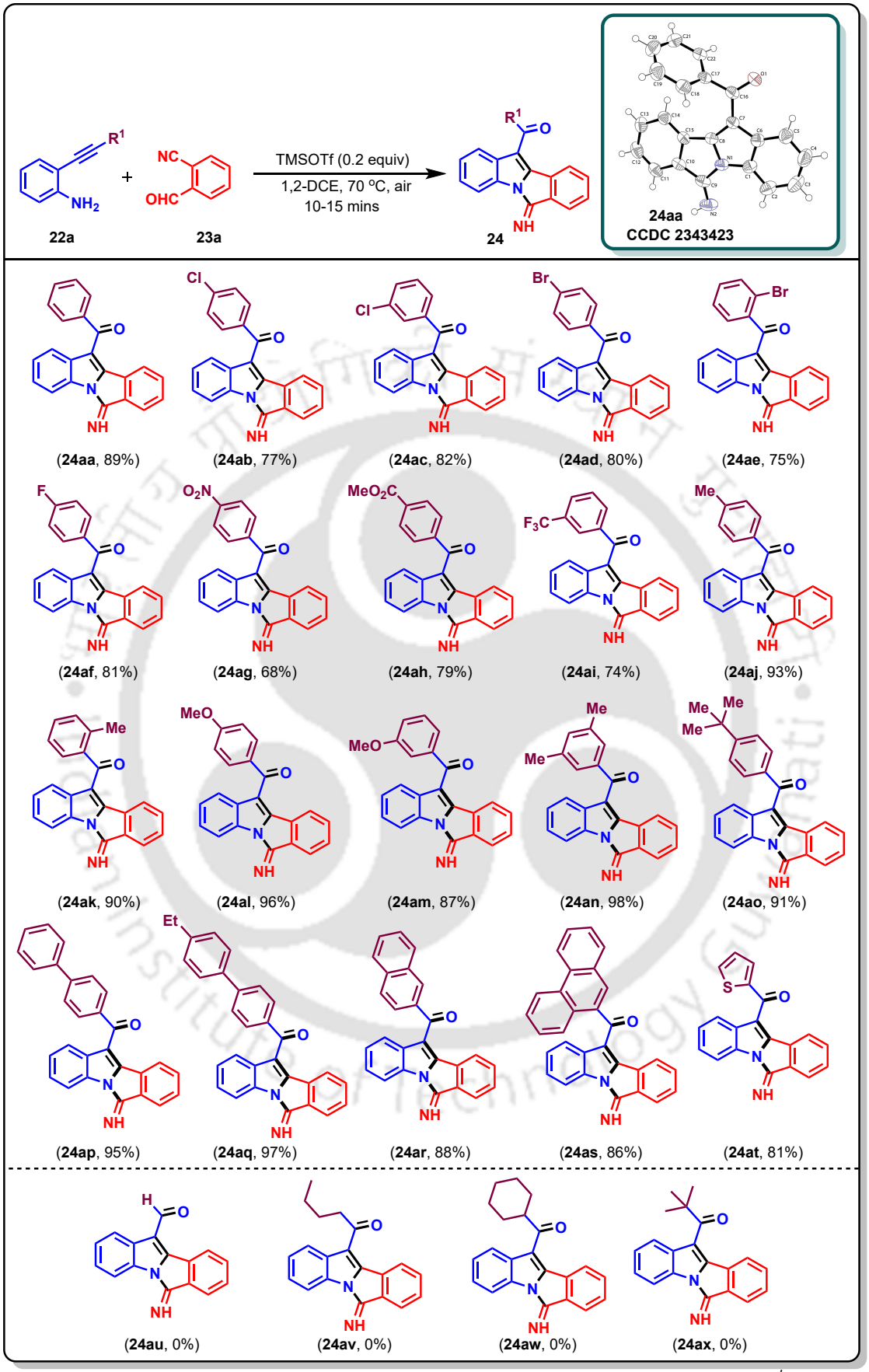

[a]Reaction condition: **22a** (0.52 mmol, 1.0 equiv), **23a** (0.57 mmol, 1.1 equiv), solvent 4.0 mL. [b]Isolated yield of the product.

Scheme 3.4.2.1. *Scope of different functionalized 2-ethynylanilines.*[a,b]

groups such as $-NO_2$, $-CO_2Me$, and $-CF_3$ at both *para* and *meta*-positions and all of them worked well providing the desired iminoisoindoloindolones **24ag**, **24ah**, and **24ai** in moderate to good yields (68–79%). Similarly, electron-donating groups like –Me, –OMe, and bulky electron-donating group $-^tBu$ at *para*-position of the aromatic ring were also introduced, and they were able to afford their corresponding products **24aj**, **24al**, and **24ao** in 93%, 96%, and 91% yields, respectively. Again, incorporating an electron-donating –OMe group at *meta*-position led to 87% yield of its respective product **24am**. The reaction with two –Me groups at both the *meta*-positions of the aromatic ring efficiently furnished its corresponding iminoisoindoloindolone **24an** with an outstanding 98% yield. Furthermore, aromatic groups like 1,1′-biphenyl and ethyl-substituted 1,1′-biphenyl rings at 2-alkynyl position exhibited comparable reactivity towards this transformation, affording excellent yields of 95% and 97% of their respective products **24ap** and **24aq**. Even fused and bulky rings like naphthalene and phenanthrene progressed favorably under the developed protocol, affording structurally hindered products **24ar** and **24as** in good yields of 88% and 86%, respectively. Heterocyclic ring like thiophene was also compatible with this strategy, providing an admirable 81% yield of its corresponding product **24at**. Unfortunately, reactions involving terminal alkyne **22au**, *n*-butyl **22av**, cyclohexyl **22aw**, and *tert*-butyl group **22ax** at the alkynyl side chain failed to proceed to provide their respective products **24au**, **24av**, **24aw**, and **24ax**. Instead, these substrates decomposed to a complex mixture under the proposed reaction conditions. This could be attributed to the instability of the carbocation generated during the reaction.

To further discover the efficacy of our protocol, the reaction was examined by varying 2-(phenylethynyl)aniline **22b** (R^2) (*Scheme 3.4.2.2*). Moderately electron-withdrawing groups like –Cl, –Br, and –F at the 4-position of the 2-ethynylaniline afforded their corresponding products **24ba**, **24bc**, and **24bd** in commendable yields of 90%, 90%, and 87%, respectively. Altering the site of electron-withdrawing group –Cl to the 5-position, the strategy comfortably furnished its respective product **24bb** in 75% yield. Highly electron-withdrawing groups like $-CO_2Me$ and $-CF_3$ at the 4-position furnished moderate yields of 71% and 77% of their corresponding products **24be** and **24bf**, respectively. Moreover, electron-donating groups like –Me and –OMe, bulky electron-donating group $-^tBu$, and long-chain electron-donating group $-^nBu$ at the 4-position proceeded smoothly and furnished their products **24bg**, **24bi**, **24bj**, and **24bk** respectively in exceptional yields (91–95%). Besides, an electron-donating –Me group at the 5-position of the aromatic ring resulted in its corresponding product **24bh** in 90% yield.

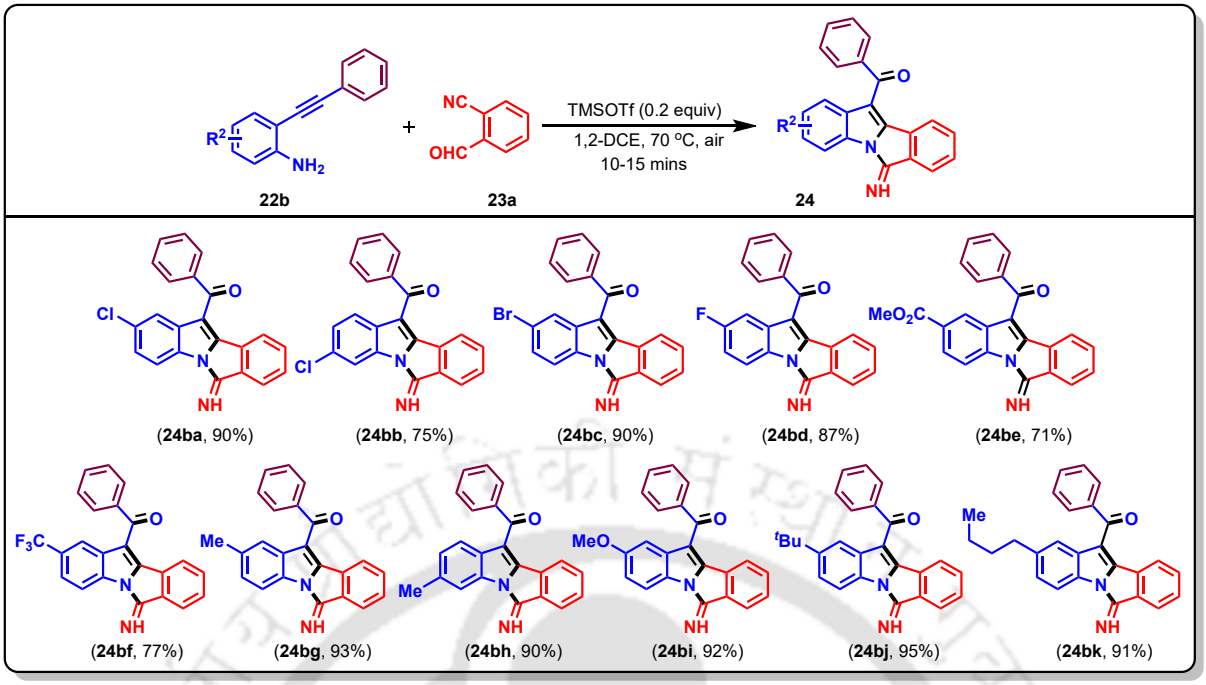

[a]Reaction condition: **22b** (0.52 mmol, 1.0 equiv), **23a** (0.57 mmol, 1.1 equiv), solvent 4.0 mL. [b]Isolated yield of the product.

Scheme 3.4.2.2. *Scope of different functionalized 2-(phenylethynyl)anilines.*[a,b]

The strategy was also screened with a variety 2-formylbenzonitriles **23** (R^3) (*Scheme 3.4.2.3*). Electron-withdrawing groups like –Br and –F at 4- and 5-positions and electron-donating group like –Me at 6-position of the aromatic ring were found to be effective toward this methodology, providing their corresponding products **24cb**, **24cc**, and **24cd**, in 72%, 77%, and 88% yields, respectively.

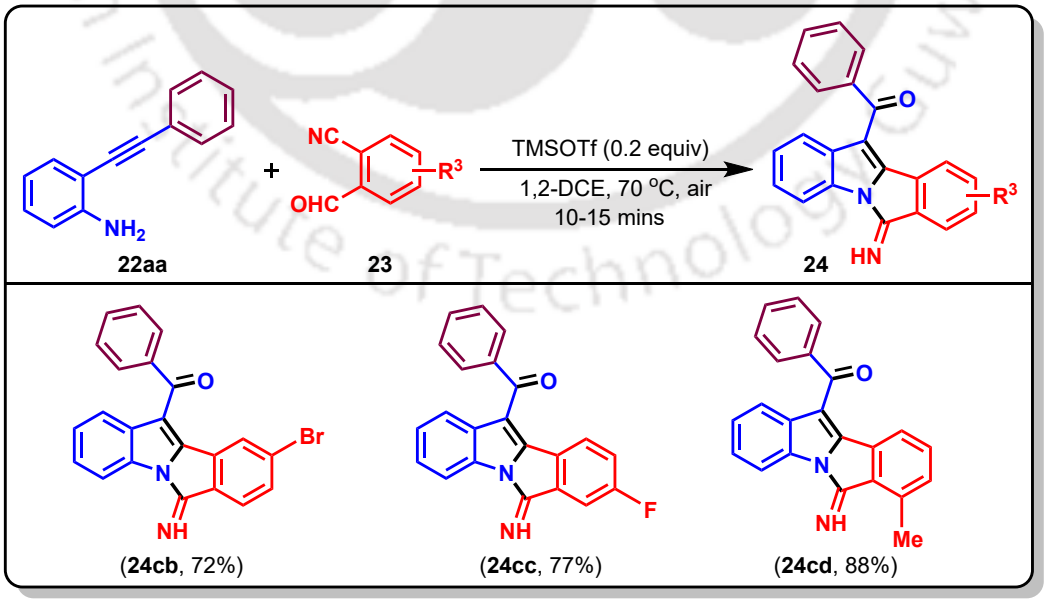

[a]Reaction condition: **22aa** (0.52 mmol, 1.0 equiv), **23** (0.57 mmol, 1.1 equiv), solvent 4.0 mL. [b]Isolated yield of the product.

Scheme 3.4.2.3. *Scope of different functionalized 2-formylbenzonitriles.*[a,b]

The structure of the compounds **24ab–24at**, **24ba–24bk**, and **24cb-24cd** was determined by NMR, IR spectroscopy, HRMS, and finally by X-ray crystallographic analysis of the compound **24aa**.

3.4.3 Gram-Scale Synthesis

To assess the scalability of the methodology, a gram-scale reaction was carried out using compounds **22aa** (1.00 g, 5.18 mmol) and **23a** (0.75 g, 5.70 mmol) under the standard reaction conditions (*Scheme 3.4.3.1*). The reaction afforded 1.36g of product **24aa** in 81% yield, highlighting its suitability for scale-up synthesis of the iminoisoindoloindolone moiety

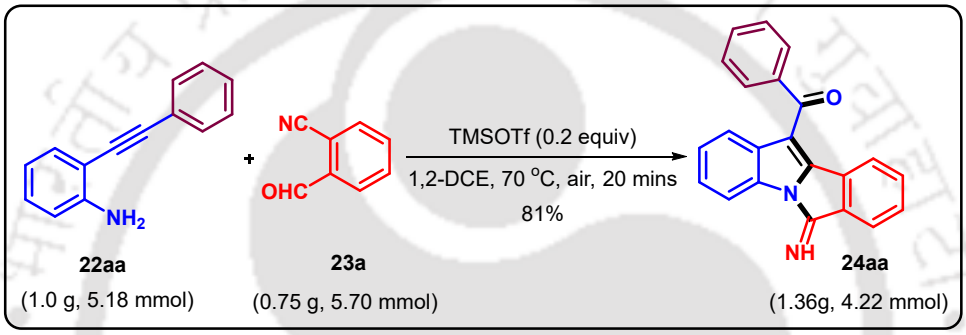

Scheme 3.4.3.1. *Gram-scale synthesis.*

3.4.4 Control Experiments

In order to investigate the reaction pathway, additionally, some control experiments were carried out (*Scheme 3.4.4.1*). Initially, 2-(phenylethynyl)aniline (**22aa**) was subjected to react with 2-formylbenzonitrile (**23a**) in the presence of TMSOTf (0.2 equiv) in 1,2-DCE:H_2O (4:1) at room temperature (*Scheme 3.4.4.1a*). Unfavorably, the reaction could not yield the desired iminoisoindoloindolone moiety and converted to some decomposed products within 10 min of the reaction. This indicates that external water constrains the reaction by quenching the action of Lewis acid instead of accelerating the nucleophilic attack by water.

Another experiment was implemented between **22aa** and **23a** keeping the standard reaction conditions under N_2 atmosphere (*Scheme 3.4.4.1b*). In contrast to the open-air reaction, the said protocol produced a relatively lower yield of 55% of its corresponding product (6-imino-6*H*-isoindolo[2,1-*a*]indol-11-yl)(phenyl)methanone (**24aa**). This can be attributed to the fact that under N_2 atmosphere, oxidative aromatization is limited to some extent to provide a better yield of the desired product.

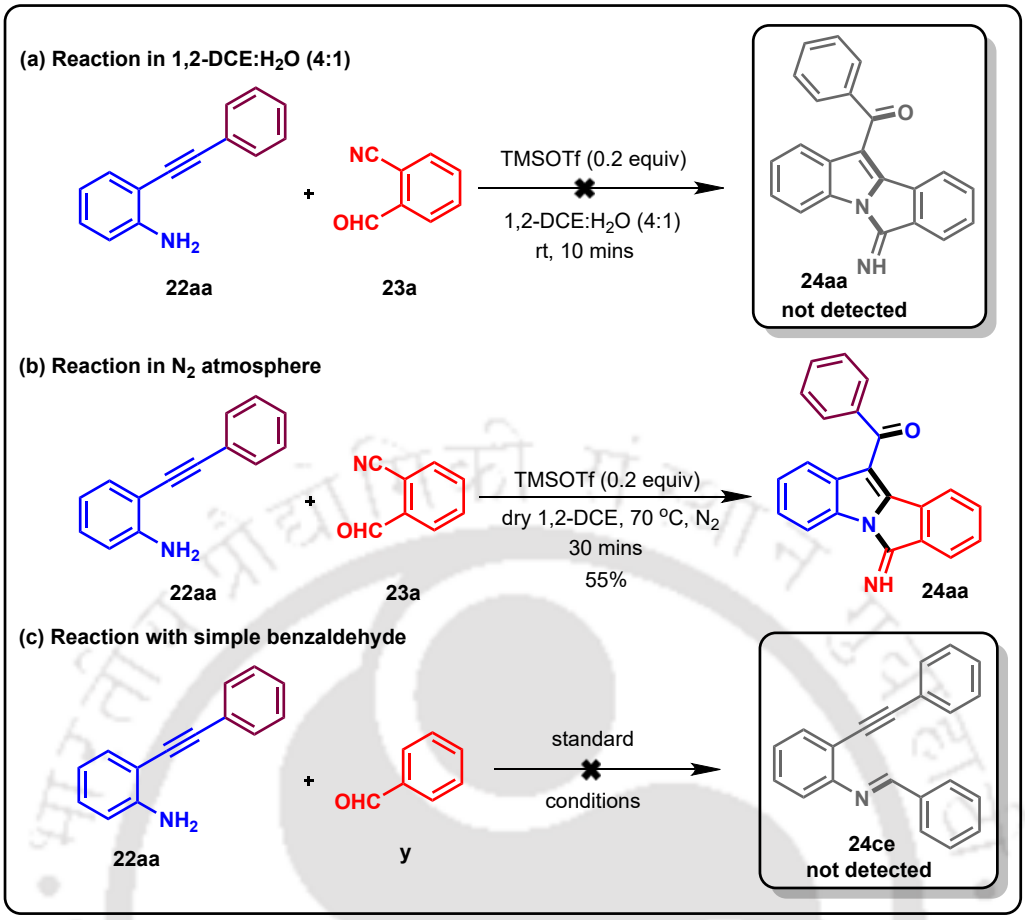

Scheme 3.4.4.1. *Control experiments.*

Again a reaction was conducted between **22aa** and simple benzaldehyde **y** using the proposed reaction conditions (*Scheme 3.4.4.1c*). However, the reaction did not produce compound **24ce** even after 12 h of the reaction; instead, starting materials were recovered in 96% yield.

3.4.5 Plausible Mechanism

On the basis of our control experiments, a plausible mechanism has been presented (*Scheme 3.4.5.1*). The reaction starts with the nucleophilic attack by amine of **22** on the Lewis acid-activated nitrile of **23** to form intermediate **A**, which was confirmed by HRMS. Then, the intramolecular amine and aldehyde condensation resulted in the formation of intermediate **B**, which after nucleophilic attack by the alkyne group leads to the formation of carbocation intermediate **C**. The intermediate **C** is attacked by water to form enol intermediate **D**, which after keto–enol tautomerization forms intermediate **E**. Finally, intermediate **E** undergoes oxidative aromatization,[23] to furnish product **24**.

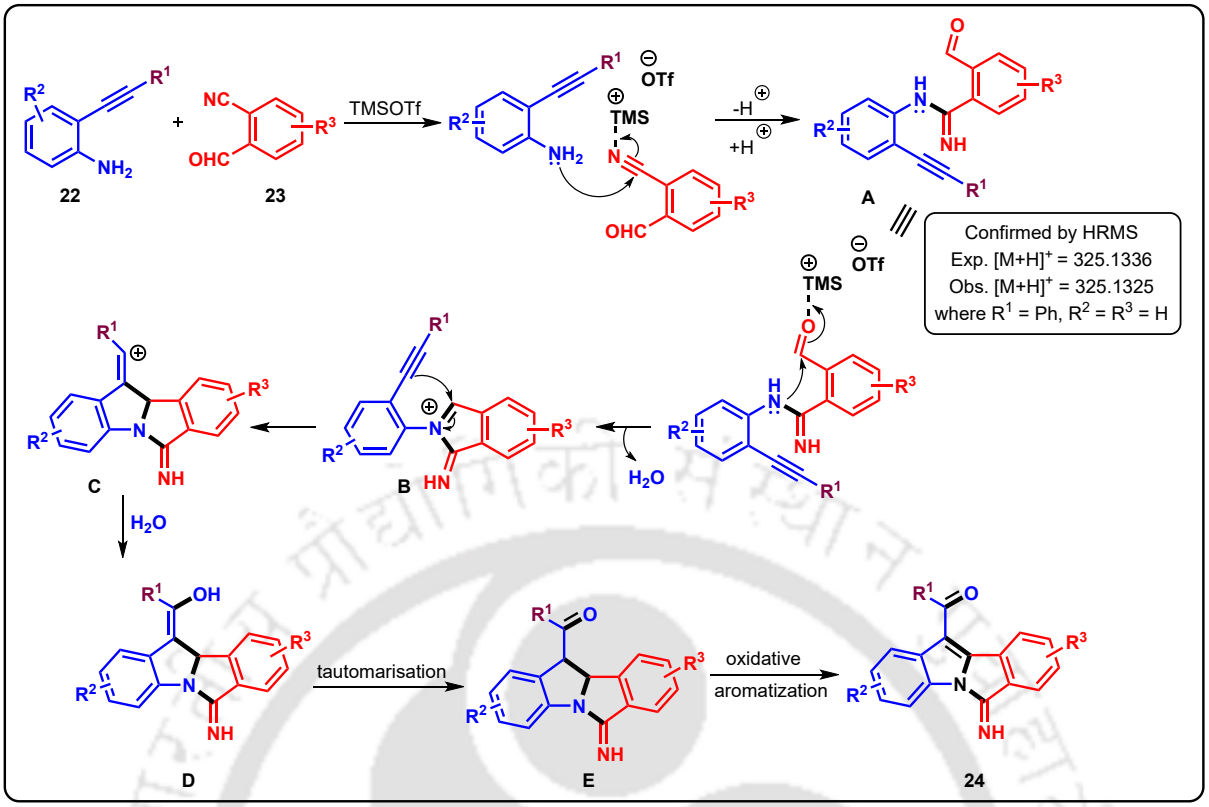

Scheme 3.4.5.1. *Plausible mechanism for the reaction*

3.4.6 Post-synthetic Application

This method offers a practical route to synthesize 11-benzoyl-6*H*-isoindolo[2,1-*a*]indol-6-one derivatives **25**, which show potential for antibacterial, antitumor, and anticancer applications, as well as use as valuable intermediates in organic synthesis.

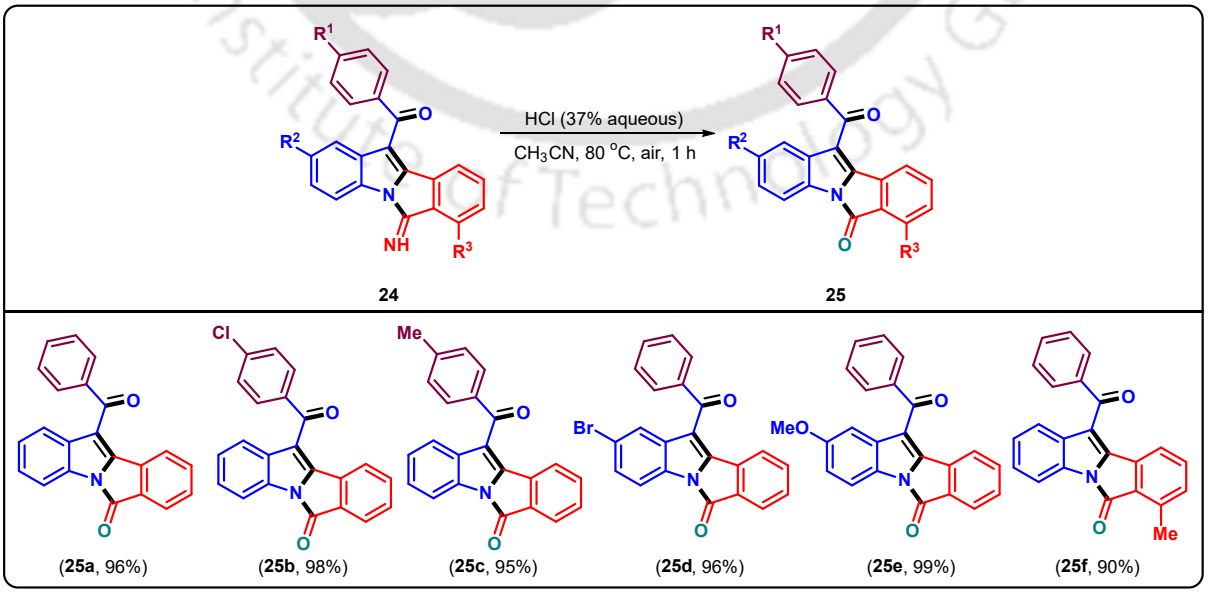

Scheme 3.4.6.1. *Scope of synthesis of isoindolo[2,1-a]indolones.*

Starting from compound **24**, the reaction involves treatment with 37% aqueous HCl in acetonitrile at 80 °C. This moderately elevated temperature promotes the transformation, providing compounds **25a**–**25f** in excellent yields (90–99%), as shown in *Scheme 3.4.6.1*. The significance of isoindolo[2,1-*a*]indolones lies in their broad pharmacological relevance and utility in synthetic organic chemistry.[24]

This synthetic strategy not only enables the preparation of isoindolo[2,1-*a*]indolone derivatives but also allows the novel synthesis of diphenylbenzopyrrolizinoisoquinolinone derivatives **27** (*Scheme 3.4.6.2*). In this transformation, compound **24** reacts with 1,2-diphenylethyne (**26**) in the presence of Ru(*p*-cymene)$_2$Cl$_2$ and Cu(OAc)$_2$ in *t*-AmOH at 120 °C.[25] After 12 h, products **27a** and **27b** were obtained in moderate to good yields of 63% and 67%, respectively. These late-stage products are relatively stable in air due to their rigid as well as highly fused ring systems, which offer steric protection to the reactive sites.

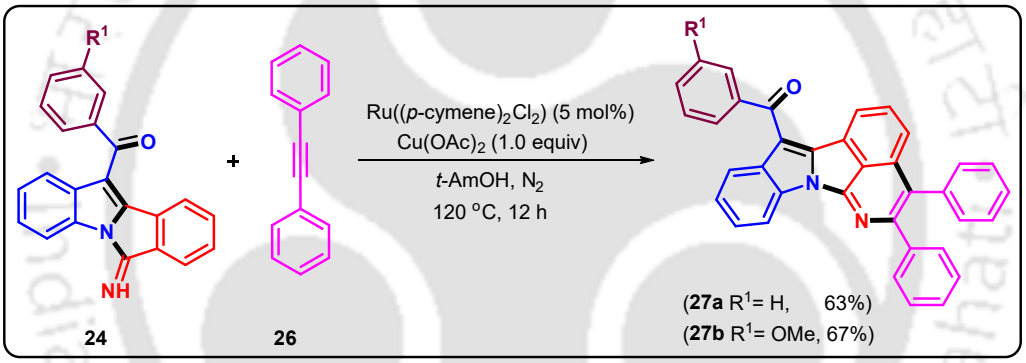

Scheme 3.4.6.2. *Scope of synthesis of diphenylbenzopyrrolizinoisoquinolinones.*

3.5 Crystallographic Description

The structure of all compounds was confirmed from standard spectroscopic experiments and finally by *X*-ray crystallographic analysis of compound **24aa** (*Figure 3.5.1*).

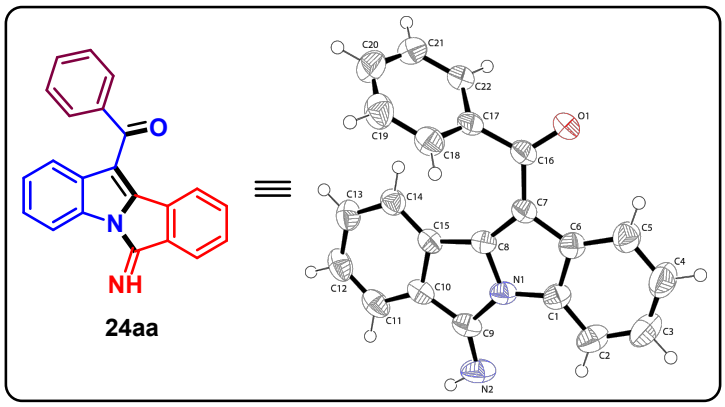

Figure 3.5.1. *ORTEP diagram of compound* ***24aa****, thermal ellipsoids are drawn on 50% probability level.*

Single crystal X-ray diffraction of compound **24aa** was obtained by slow evaporation of hexane and ethyl acetate solution (9:1). The detailed data collection and structure refinement are summarized in *Table 3.5.1,* where CCDC **2343423** of **24aa** contains the supplementary crystallographic data.

Table 3.5.1. *Crystal parameters of compound* ***24aa***

Compound 24aa	**CCDC 2343423**
Formula	$C_{22}H_{14}N_2O$
Formula weight	322.35
T/K	297(2)
Crystal system	Triclinic
Space group	P-1
a/Å	8.2941(9)
b/Å	9.8304(11)
c/Å	9.9245(11)
a/°	92.042(3)
β/°	95.291(3)
γ/°	96.115(3)
V/Å^3	800.31(15)
Z	2
Abs. Coeff./mm^{-1}	0.083

Compound 24aa	CCDC 2343423
Abs. Correction	none
GOF on F^2	1.158
Final R indices [$I > 2\sigma(I)$]	$R1 = 0.0500$ $wR2 = 0.1012$
R indices [all data]	$R1 = 0.0618$ $wR2 = 0.1081$

3.6 Conclusion

In conclusion, a Lewis acid-catalyzed cascade reaction enabling the efficient synthesis of 6-iminoisoindoloindolones in high yields has been developed, demonstrating the versatility of this approach. The use of TMSOTf to activate the nitrile group further expanded its utility, allowing access to both isoindoloindolone and novel diphenylbenzopyrrolizinoisoquinolinone derivatives. The reaction features broad substrate scope with excellent functional group compatibility, offering a concise route to these highly fused *N*-heterocycles.

3.7 Experimental Section

3.7.1 Reaction Procedure

3.7.1.1 General Experimental Procedure for the Synthesis of Starting Materials

The starting materials **22aa**–**22ap**, **22ar**–**22ax**, **22ba**–**22bj**, and **22bl** were synthesized according to the literature reports, and the spectroscopic data of the compounds are in good agreement with the literature data.[26]

3.7.1.1.1 General Experimental Procedure for the Synthesis of Compounds 22aq and 22bk

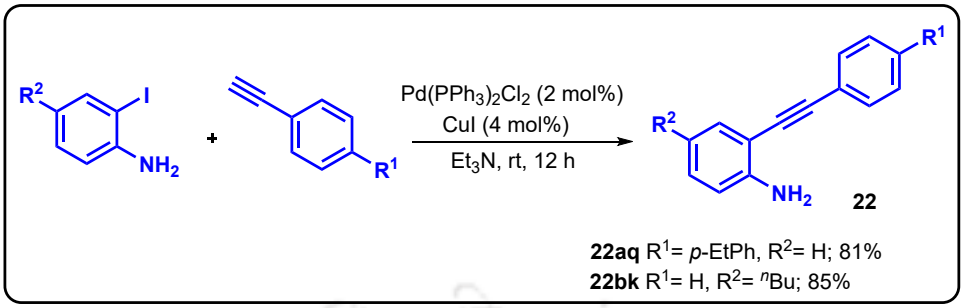

To a stirred suspension of $PdCl_2(PPh_3)_2$ (0.02 mmol, 2 mol %) and CuI (0.04 mmol, 4 mol %) in trimethylamine, Et_3N (5.0 mmol, 5.0 equiv) under a nitrogen atmosphere was added 2-iodoaniline derivative (1.0 mmol, 1.0 equiv), and the reaction mixture was stirred for 10 min. Eventually, terminal alkyne derivative (1.1 mmol, 1.1 equiv) was added to the reaction mixture, and the mixture was allowed to stir at room temperature. The progress of the reaction was monitored by TLC (using hexane/ ethyl acetate = 9:1 as eluents). After completion of the reaction (12 h), the excess triethylamine was evaporated using a rotary evaporator, and the reaction mixture was washed with saturated NH_4Cl and brine solution. The aqueous phase was extracted with ethyl acetate (3 × 10 mL). The combined organic layers were then dried over Na_2SO_4 and concentrated using a rotary evaporator. The resulting crude product underwent column chromatography over silica gel to isolate the corresponding product **22**.

3.7.1.2 General Experimental Procedure for the Synthesis of Compounds 24aa-24at, 24ba-24bk, and 24cb-24cd

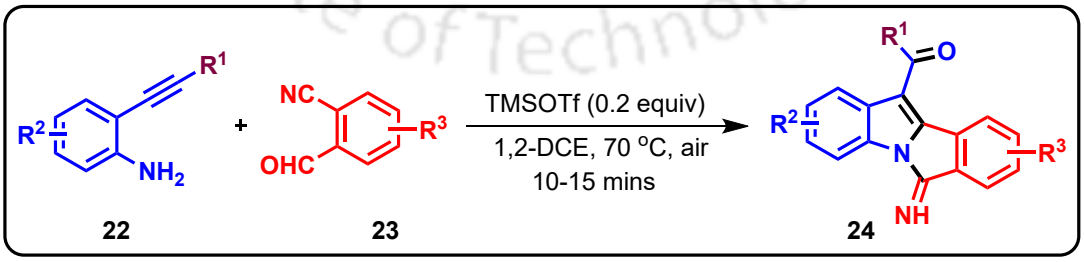

To a stirred solution of 2-alkynylaniline derivative **22** (0.52 mmol, 1.0 equiv) and 2-formylbenzonitrile derivative **23** (0.57 mmol, 1.1 equiv) in 1,2-DCE (4 mL), TMSOTf (0.1 mmol, 0.2 equiv) was added dropwise at 0 °C under air atmosphere. The mixture was then stirred at room temperature for 5–10 min before being heated to 70 °C in

an oil bath. The progress of the reaction was monitored by TLC (using hexane/ethyl acetate = 3:1 as eluents). After completion of the reaction (10–15 min), the reaction mixture was cooled to room temperature. The solvent was removed under vacuo in a rotary evaporator, and then the residue was diluted with ethyl acetate, saturated $NaHCO_3$, and brine solution. The aqueous phase was extracted with ethyl acetate (3 × 10 mL), and the combined organic extracts were dried over anhydrous Na_2SO_4 and concentrated using a rotary evaporator. The resulting crude product was purified by column chromatography over silica gel to yield the desired product **24**.

3.7.1.3 Experimental Procedure for the Gram-scale Synthesis of Compound 24aa

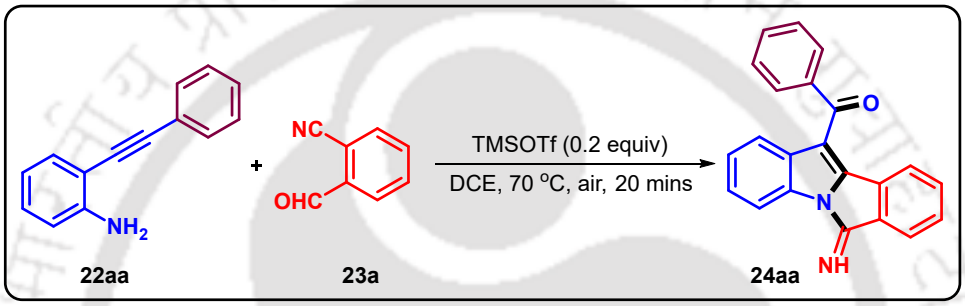

To a stirred solution of 2-(phenylethynyl)aniline (**22aa**) (1.0 g, 5.18 mmol, 1.0 equiv) and 2-formylbenzonitrile (**23a**) (0.75 g, 5.70 mmol, 1.1 equiv) in 1,2-DCE (20 mL), TMSOTf (0.19 mL, 1.04 mmol, 0.2 equiv) was added dropwise at 0 °C under air atmosphere. The mixture was then stirred at room temperature for 5 min before being heated to 70 °C in an oil bath. The progress of the reaction was monitored by TLC (using hexane/ethyl acetate = 3:1 as eluents). After completion of the reaction (15 min), the reaction mixture was cooled to room temperature. The solvent was removed under vacuo in a rotary evaporator, and then the residue was diluted with ethyl acetate, saturated $NaHCO_3$, and brine solution. The aqueous phase was extracted with ethyl acetate (3 × 15 mL), and the combined organic extracts were dried over anhydrous Na_2SO_4 and concentrated using a rotary evaporator. The resulting crude product was purified by column chromatography over silica gel to afford the desired product **24aa** in 81% yield (1.36 g).

3.7.1.4 Experimental Procedure for Control Experiments

3.7.1.4.1 Experimental Procedure for the Reaction in 1,2-DCE:H_2O (4:1) (a)

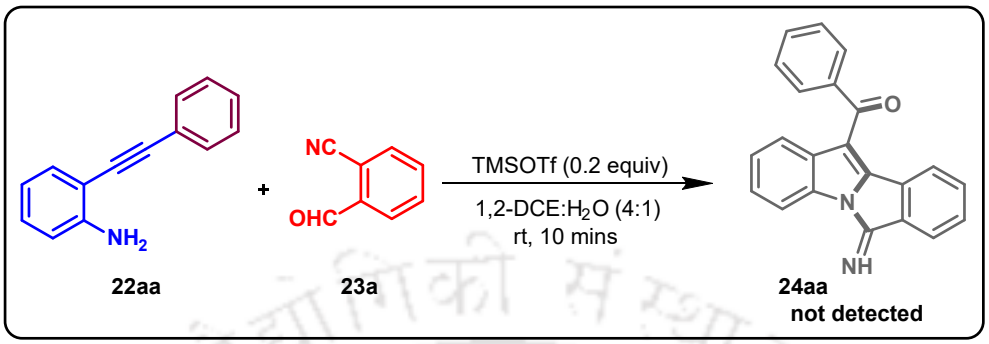

To a stirred solution of 2-(phenylethynyl)aniline (**22aa**) (0.52 mmol, 1.0 equiv) and 2-formylbenzonitrile (**23a**) (0.57 mmol, 1.1 equiv) in 1,2-DCE:H_2O (4:1, 5 mL), TMSOTf (0.1 mmol, 0.2 equiv) was added dropwise at 0 °C under air atmosphere. To our dismay, the reaction resulted in various decomposed products within a brief 10 min window, ultimately failing to produce the desired iminoisoindoloindolone moiety **24aa**.

3.7.1.4.2 Experimental Procedure for the Reaction in N_2 atmosphere (b)

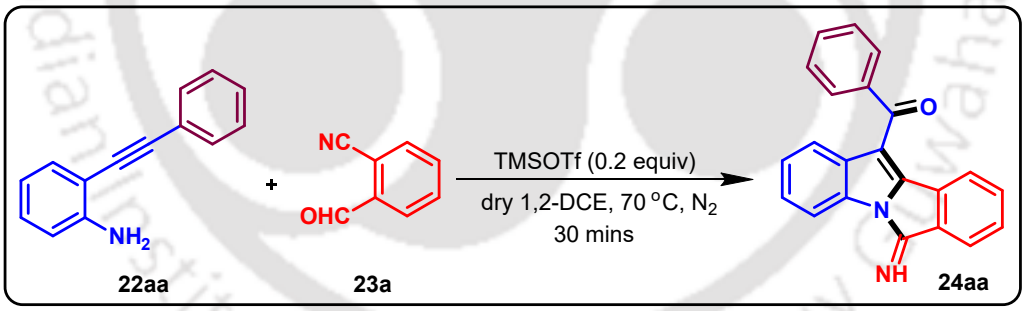

To a stirred solution of 2-(phenylethynyl)aniline (**22aa**) (0.52 mmol, 1.0 equiv) and 2-formylbenzonitrile (**23a**) (0.57 mmol, 1.1 equiv) in dry 1,2-DCE (4 mL), TMSOTf (0.1 mmol, 0.2 equiv) was added dropwise at 0 °C under nitrogen atmosphere. The reaction mixture was then stirred at room temperature for 5 min before being heated to 70 °C in an oil bath. The progress of the reaction was monitored by TLC (using hexane/ethyl acetate = 3:1 as eluents). After completion of the reaction (25 min), the reaction mixture was cooled to room temperature. The solvent was removed under vacuo in a rotary evaporator, and then the residue was diluted with ethyl acetate, saturated $NaHCO_3$, and brine solution. The aqueous phase was extracted with ethyl acetate (3 × 10 mL), and the combined organic extracts were dried over anhydrous

Na_2SO_4 and concentrated using a rotary evaporator. The resulting crude product was purified by column chromatography over silica gel to get the desired product **24aa** in 55% yield.

3.7.1.4.3 Experimental Procedure for the Reaction with Benzaldehyde (c)

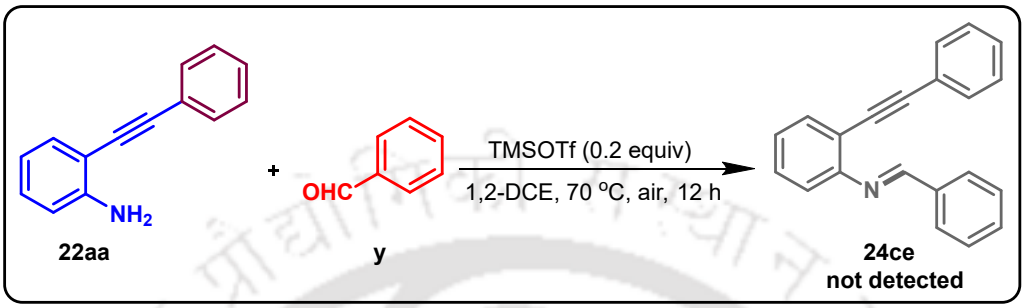

To a stirred solution of 2-(phenylethynyl)aniline (**22aa**) (0.52 mmol, 1.0 equiv) and benzaldehyde **y** (0.57 mmol, 1.1 equiv) in 1,2-DCE, (4 mL), TMSOTf (0.1 mmol, 0.2 equiv) was added dropwise at 0 °C under air atmosphere. The reaction mixture was stirred at room temperature for 5 min and then heated to 70 °C in an oil bath. The progress of the reaction was monitored by TLC (using hexane/ethyl acetate = 3:1 as eluents). Even after 12 h, the reaction did not proceed, and the starting materials remained unchanged.

3.7.1.5 General Experimental Procedure for the Synthesis of Compounds 25a–25f

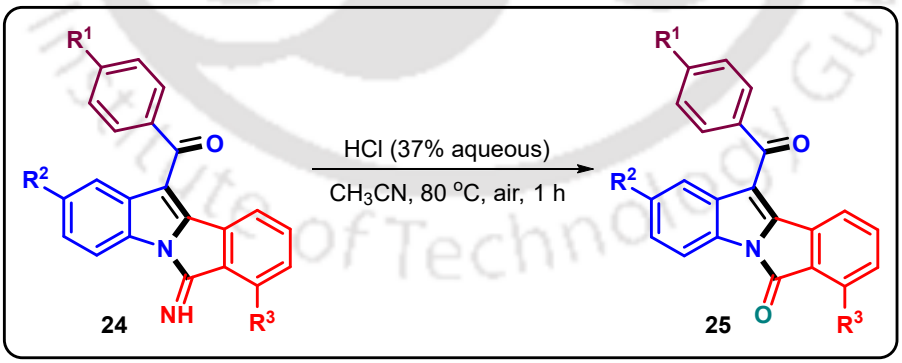

To a stirred solution of (6-imino-6*H*-isoindolo[2,1-*a*]indol-11-yl)(phenyl)methanone derivative **24** (0.15 mmol, 1 equiv) in acetonitrile (3.0 mL) was added conc. HCl (37% aqueous, 37.5 μL) dropwise under air atmosphere. The reaction was then allowed to stir at 80 °C and monitored *via* TLC (using hexane/ethyl acetate = 9:1 as eluents). After completion of the reaction (1 h), the reaction mixture was allowed to cool to room temperature. Then, the solvent was removed under vacuo in a rotary evaporator,

and the reaction mixture was washed with saturated $NaHCO_3$ and brine solution. The aqueous phase was extracted with ethyl acetate (3 × 10 mL), and the combined organic extracts were dried over anhydrous Na_2SO_4 and concentrated using a rotary evaporator. The crude product was subjected to column chromatography over silica gel to get the product **25**.

3.7.1.6 General Experimental Procedure for the Synthesis of Compounds 27a and 27b

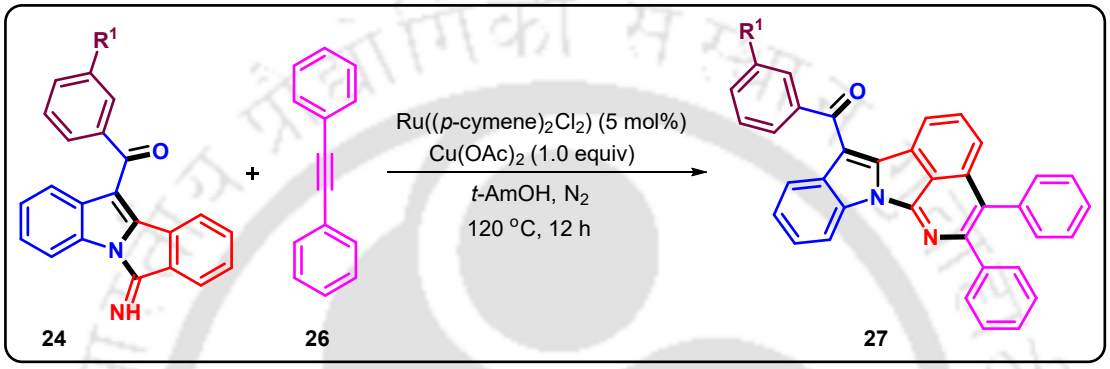

To a stirred suspension of (6-imino-6*H*-isoindolo[2,1-*a*]indol-11-yl)(phenyl) methanone derivative **24** (0.1 mmol, 1 equiv), Ru((*p*-cymene)$_2$Cl$_2$) (0.005 mmol, 5 mol %), $Cu(OAc)_2$ (0.1 mmol, 1 equiv), and 1,2-diphenylethyne **26** (0.12 mmol, 1.2 equiv), *tert*-amyl alcohol (*t*-AmOH) (1 mL) was added under nitrogen atmosphere in a sealed tube. Then, the reaction mixture was allowed to stir for 12 h at 120 °C. The progress of the reaction was monitored by TLC (using hexane/ethyl acetate = 17:1 as the eluents). After completion of the reaction, the reaction mixture was allowed to filter through Celite and washed with ethyl acetate. The combined organic layers were then dried over Na_2SO_4 and concentrated using a rotary evaporator. The resulting crude product underwent column chromatography over silica gel to isolate the product **27**.

3.8 References

1. (a) Boussard, M.-F.; Truche, S.; Rousseau-Rojas, A.; Briss, S.; Descamps, S.; Droual, M.; Wierzbicki, M.; Ferry, G.; Audinot, V.; Delagrange, P.; Boutin, J. A. *Eur. J. Med. Chem.* **2006**, *41*, 306–320; (b) Guillaumel, J.; Léonce, S.; Pierré, A.; Renard, P.; Pfeiffer, B.; Arimondo, P. B.; Monneret, C. *Eur. J. Med. Chem.* **2006**, *41*, 379–386; (c) Ambrus, J. I.; Kelso, M. J.; Bremner, J. B.; Ball, A. R.; Casadei, G.; Lewis, K. *Bioorg. Med. Chem. Lett.* **2008**, *18*, 4294–

4297; (d) Fotso, S.; Mahmud, T.; Zabriskie, T. M.; Santosa, D. A.; Sulastri; Proteau, P. J. *J. Nat. Prod.* **2008**, *71*, 61–65.

2. (a) Lu, P.; Zhuang, W.; Lu, L.; Liu, A.; Chen, Y.; Wu, C.; Zhang, X.; Huang, Q. *J. Org. Chem.* **2022**, *87*, 10967–10981; (b) Ciccolini, C.; Mari, G.; Gatti, F. G.; Gatti, G.; Giorgi, G.; Mantellini, F.; Favi, G. *J. Org. Chem.* **2020**, *85*, 11409–11425; (c) Zheng, L.; Hua, R. *Front. Chem.* **2020**, *8*, 580355.

3. (a) Mondal, D.; Kalar, P. L.; Kori, S.; Gayen, S.; Das, K. *Curr. Org. Chem.* **2020**, *24*, 2665–2693; (b) Liu, H.; Dömling, A. *J. Org. Chem.* **2009**, *74*, 6895–6898.

4. (a) D. U. Lee, J. S. Bae, H. Nam, S. G. Hong, D. H. Lee, S. S. Kim, *Korean Patent* **2010**, 2010113204; (b) D. S. Kim, S. H. Lee, J. H. Park, S. Y. Moon, J. U. Ju, J. H. Byun, B. R. Park, D. H. Oh, B. S. Lee, D. H. Kim, D. H. Choi, G. M. Lee, *Korean Patent* **2013**, 2013126399.

5. (a) Guillaumel, J.; Leonce, S.; Pierre, A.; Renard, P.; Pfeiffer, B.; Arimondo, P. B.; Monneret, C. *Eur. J. Med. Chem.* **2006**, *41*, 379–386; (b) Ambrus, J. I.; Kelso, M. J.; Bremner, J. B.; Ball, A. R.; Casadei, G.; Lewis, K. *Bioorg. Med. Chem. Lett.* **2008**, *18*, 4294–4297.

6. (a) Kaur Bhatia, R. *Curr. Top. Med. Chem.* **2017**, *17*, 189–207; (b) Dinnell, K.; Chicchi, G. G.; Dhar, M. J.; Elliott, J. M.; Hollingworth, G. J.; Kurtz, M. M.; Ridgill, M. P.; Rycroft, W.; Tsao, K.-L.; Williams, A. R.; Swain, C. J. *Bioorg. Med. Chem. Lett.* **2001**, *11*, 1237–1240; (c) Boussard, M. F.; Truche, S.; Rousseau-Rojas, A.; Briss, S.; Descamps, S.; Droual, M.; Wierzbicki, M.; Ferry, G.; Audinot, V.; Delagrange, P.; Boutin, J. A. *Eur. J. Med. Chem.* **2006**, *41*, 306–320; (d) T. Hudyma, X. Zheng, F. He, M. Ding, C. Bergstrom, P. Hewawasam, S. Martin, R. G. Gentles, *US Patent* **2006**, 20060046983 A1; (e) Samosorn, S.; Bremner, J. B.; Ball, A.; Lewis, K. *Bioorg. Med. Chem.* **2006**, *14*, 857–865.

7. (a) Zhou, F.; Jin, H.; Zhang, Y.; Li, J.; Walsh, P. J.; Lin, S. *Org. Lett.* **2023**, *25*, 7132–7136; (b) Udayanga, D. M. N.; Le, N.; Schwirian, E. N.; Donnadieu, B.; Nash, K.; Collier, W.; Webster, C. E.; Cui, X. *Org. Lett.* **2023**, *25*, 8745–8750; (c) Wang, Y.; Xie, F.; Lin, B.; Cheng, M.; Liu, Y. *Chem. - Eur. J.* **2018**, *24*, 14302–14315.

8. (a) Wang, Z.; Addepalli, Y.; He, Y. *Org. Lett.* **2018**, *20*, 644–647; (b) Guo, S.; Pan, R.; Guan, Z.; Li, P.; Cai, L.; Chen, S.; Lin, A.; Yao, H. *Org. Lett.* **2019**, *21*, 6320–6324; (c) Yang, S.; An, X.-D.; Qiu, B.; Liu, R.-B.; Xiao, J. *Org. Lett.* **2021**, *23*, 9100–9105.

9. Alam, K.; Hong, S. W.; Oh, K. H.; Park, J. K. *Angew. Chem.* **2017**, *129*, 13572–13576.

10. Liu, A.; Han, Q.; Zhang, X.; Li, B.; Huang, Q. *Org. Lett.* **2019**, *21*, 6839–6843.

11. Čarný, T.; Markovič, M.; Gracza, T.; Koóš, P. *J. Org. Chem.* **2019**, *84*, 12499–12507.

12. Dev, K.; Maurya, R. *RSC Adv.* **2015**, *5*, 13102–13106.

13. Liu, Y. H.; Song, H.; Zhang, C.; Liu, Y. J.; Shi, B. F. *Chin. J. Chem.* **2020**, *38*, 1545–1552.

14. Hazra, S.; Mondal, B.; De, R. N.; Roy, B. *RSC Adv.* **2015**, *5*, 22480–22489.

15. Zhang, L.; Wang, Y.; Zheng, L.; Guo, B.; Hua, R. *Tetrahedron.* **2017**, *73*, 395–402.

16. Wu, X.; Xiao, Y.; Sun, S.; Yu, J. T.; Cheng, J. *Org. Lett.* **2019**, *21*, 6653–6657.

17. (a) Jadhav, A. S.; Pankhade, Y. A.; Anand, R. V. *J. Org. Chem.* **2018**, *83*, 8615–8626; (b) Gharpure, S. J.; Shelke, Y. G. *Org. Lett.* **2017**, *19*, 5406–5409; (c) Cai, J.; Wu, B.; Rong, G.; Zhang, C.; Qiu, L.; Xu, X. *Org. Lett.* **2018**, *20*, 2733–2736.

18. (a) Yoo, J. M.; Ho, S. L.; Cho, C. S. *Synlett* **2016**, *27*, 1383–1386; (b) Huang, Q.; Han, Q.; Fu, S.; Yao, Z.; Su, L.; Zhang, X.; Lin, S.; Xiang, S. *J. Org. Chem.* **2016**, *81*, 12135–12142; (c) Guo, S.; Tao, L.; Wang, F.; Fan, X. *Chem. Asian J.* **2016**, *11*, 3090–3096.

19. (a) Dwight, T. A.; Rue, N. R.; Charyk, D.; Josselyn, R.; DeBoef, B. *Org. Lett.* **2007**, *9*, 3137–3139; (b) Kandukuri, S. R.; Oestreich, M. *J. Org. Chem.* **2012**, *77*, 8750–8755; (c) Kandukuri, S. R.; Schiffner, J. A.; Oestreich, M. *Angew. Chem., Int. Ed.* **2012**, *51*, 1265–1269.

20. (a) Duncanson, P.; Cheong, Y.-K.; Motevalli, M.; Griffiths, D. V. *Org. Biomol. Chem.* **2012**, *10*, 4266–4279; (b) Wang, L.; Sun, M.; Ding, M. *Eur. J. Org. Chem.* **2017**, *2017*, 2568–2578.

21. (a) Kim, G.; Kim, J. H.; Kim, W.; Kim, Y. A. *Tetrahedron Lett.* **2003**, *44*, 8207–8209; (b) García, A.; Rodríguez, D.; Castedo, L.; Saá, C.; Domínguez, D. *Tetrahedron Lett.* **2001**, *42*, 1903–1905.

22. (a) Okada, T.; Sakai, A.; Hinoue, T.; Satoh, T.; Hayashi, Y.; Kawauchi, S.; Chandrababunaidu, K.; Miura, M. *J. Org. Chem.* **2018**, *83*, 5639–5649; (b) Zhou, X.; Pan, Y.; Li, X. *Angew. Chem., Int. Ed.* **2017**, *56*, 8163–8167; (c) Kaufmann, J.; Jäckel, E.; Haak, E. *Angew. Chem., Int. Ed.* **2018**, *57*, 5908–5911.

23. (a) Zhang, C.; Zhang, L.; Jiao, N. *Green Chem.* **2012**, *14*, 3273–3276; (b) Zou, Y.-Q.; Lu, L.-Q.; Fu, L.; Chang, N.-J.; Rong, J.; Chen, J.-R.; Xiao, W.-J. *Angew. Chem., Int. Ed.* **2011**, *50*, 7171–7175; (c) Chen, S.; Xia, Y.; Jin, S.; Lei, H.; You, K.; Deng, G. J. *J. Org. Chem.* **2022**, *87*, 3212–3222; (d) Dagar, A.; Bae, G. H.; Lee, J. H.; Kim, I. *J. Org. Chem.* **2019**, *84*, 6916–6927.

24. (a) Kadam, H. K.; Tilve, S. G. *ARKIVOC* **2015**, *2015*, 524–539; (b) Marković, M.; Koós, P.; Čarný, T.; Gracza, T. *Tetrahedron Lett.* **2020**, *61*, No. 152370; (c) Samosorn, S.; Bremner, J. B.; Ball, A.; Lewis, K. *Bioorg. Med. Chem.* **2006**, *14*, 857–865; (d) Kadam, H. K.; Tilve, S. G. *Eur. J. Org. Chem.* **2013**, *2013*, 4280–4284.

25. (a) Wang, L.; Ackermann, L. *Org. Lett.* **2013**, *15*, 176–179; (b) Ackermann, L.; Lygin, A. V. *Org. Lett.* **2012**, *14*, 764–767.

26. (a) Luo, W.; Chen, Q.; Mo, X.; Jiang, J.; Xie, P. *Org. Chem. Front.* **2024**, *11*, 1112–1117; (b) Punjajom, K.; Ruengsangtongkul, S.; Tummatorn, J.; Paiboonsombat, P.; Ruchirawat, S.; Thongsornkleeb, C. *J. Org. Chem.* **2023**, *88*, 6736–6749; (c) Yang, L.; Ma, Y.; Song, F.; You, J. *Chem. Commun.* **2014**, *50*, 3024–3026; (d) Ishida, T.; Kikuchi, S.; Yamada, T. *Org. Lett.* **2013**, *15*, 3710–3713; (e) Wang, Y.; Zhou, Y.; Ma, X.; Song, Q. *Org. Lett.* **2021**, *23*, 5599–5604.

3.9 Characterization Data

2-((4'-Ethyl-[1,1'-biphenyl]-4-yl)ethynyl)aniline (22aq):

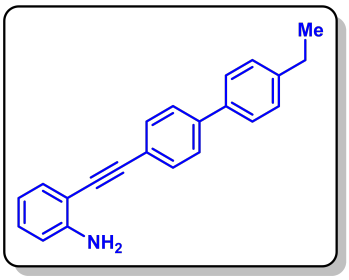

Grey solid; R_f (Hexane/EtOAc, 9:1) 0.45; mp 173–175 °C. Yield 240 mg, 81%; ^{1}H NMR (500 MHz, $CDCl_3$) δ 7.60 (s, 4 H), 7.55 (d, J = 8.0 Hz, 2 H), 7.40 (d, J = 8.0 Hz, 1 H), 7.30 (d, J = 8.0 Hz, 2 H), 7.16 (t, J = 7.5 Hz, 1 H), 6.76–6.73 (m, 2 H), 4.27 (s, 2 H), 2.72 (q, J = 7.5 Hz, 2 H), 1.30 (t, J = 7.5 Hz, 3 H); ^{13}C{^{1}H} NMR (125 MHz, $CDCl_3$) δ 148.0, 144.1, 141.1, 137.9, 132.4, 132.1, 129.9, 128.6, 127.2, 127.1, 122.1, 118.2, 114.6, 108.3, 94.9, 86.7, 28.8, 15.8; IR (KBr, neat) 3476, 2984, 1738, 1612, 1373, 1239, 1046, 822, 742, 634 cm^{-1}; HRMS (ESI) calcd. for $C_{22}H_{20}N$ $(M + H)^+$ 298.1591, found 298.1537.

4-Butyl-2-(phenylethynyl)aniline (22bk):

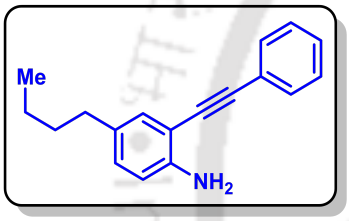

Dark brown liquid; R_f (Hexane/EtOAc, 9:1) 0.55. Yield 212 mg, 85%; ^{1}H NMR (500 MHz, $CDCl_3$) δ 7.54 (dd, J = 8.0, 2.5 Hz, 2 H), 7.38–7.33 (m, 3 H), 7.21 (s, 1 H), 6.98 (d, J = 8.5 Hz, 1 H), 6.68 (d, J = 8.0 Hz, 1 H), 4.12 (s, 2 H), 2.51 (t, J = 8.0 Hz, 2 H), 1.60–1.54 (m, 2 H), 1.39–1.32 (m, 2 H), 0.94 (t, J = 7.5 Hz, 3 H); ^{13}C{^{1}H} NMR (125 MHz, $CDCl_3$) δ 145.7, 132.8, 131.9, 131.7, 130.3, 128.6, 128.3, 123.7, 114.8, 108.2, 94.6, 86.4, 34.8, 34.0, 22.5, 14.2; IR (KBr, neat) 3379, 2926, 1617, 1501, 1311, 1255, 1154, 819, 754, 689, 576 cm^{-1}; HRMS (ESI) calcd. for $C_{18}H_{20}N$ $(M + H)^+$ 250.1591, found 250.1603.

(6-Imino-6*H*-isoindolo[2,1-*a*]indol-11-yl)(phenyl)methanone (24aa):

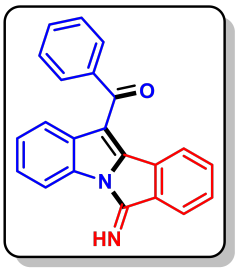

Brown Solid; R_f (Hexane/EtOAc, 3:1) 0.5; mp 178–180 °C. Yield 149 mg, 89%; ^{1}H NMR (500 MHz, $CDCl_3$) δ 8.97 (s, 1 H), 8.15 (s, 1 H), 7.91 (d, J = 7.5 Hz, 2 H), 7.65–7.59 (m, 2 H), 7.50 (t, J = 7.5 Hz, 2 H), 7.45 (d, J = 8.0 Hz, 1 H), 7.37–7.32 (m, 4 H), 7.15 (t, J = 7.5 Hz, 1 H); ^{13}C{^{1}H} NMR (125 MHz, $CDCl_3$) δ 192.1, 158.5, 144.3, 140.1, 133.7, 133.2, 132.9, 132.8, 132.3, 132.2, 129.7, 129.5, 128.9, 126.1, 125.0, 123.9, 123.0, 122.5, 114.4, 113.5; IR (KBr, neat) 3268, 2923, 1729, 1604, 1445, 1365, 1271, 1037, 872, 746, 697 cm^{-1}; HRMS (ESI) calcd. for $C_{22}H_{15}N_2O$ $(M + H)^+$ 323.1179, found 323.1190.

(4-Chlorophenyl)(6-imino-6*H*-isoindolo[2,1-*a*]indol-11-yl)methanone (24ab):

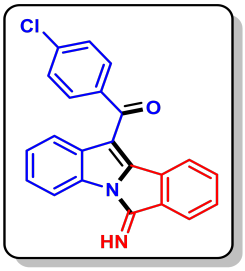

Yellow Solid; R_f (Hexane/EtOAc, 3:1) 0.5; mp 202–204 °C. Yield 142 mg, 77%; ^{1}H NMR (500 MHz, $CDCl_3$) δ 8.13 (d, J = 8.0 Hz, 1 H), 7.86 (d, J = 8.5 Hz, 2 H), 7.62 (d, J = 6.0 Hz, 1 H), 7.53 (d, J = 6.0 Hz, 1 H), 7.48 (d, J = 8.0 Hz, 2 H), 7.42–7.38 (m, 2 H), 7.35 (dd, J = 18.0, 8.5 Hz, 2 H), 7.15 (t, J = 7.5 Hz, 1 H); ^{13}C{^{1}H} NMR (125 MHz, $CDCl_3$) δ 190.6, 158.4, 144.6, 139.3, 138.3, 133.7, 133.2, 132.9, 132.2, 132.0, 131.1, 129.9, 129.2, 126.2, 125.0, 123.9, 122.8, 122.6, 113.9, 113.7; IR (KBr, neat) 3384, 2923, 1637, 1554, 1444, 1274, 1028, 994, 824, 745 cm^{-1}; HRMS (ESI) calcd. for $C_{22}H_{14}ClN_2O$ $(M + H)^+$ 357.0789, found 357.0785.

(3-Chlorophenyl)(6-imino-6*H*-isoindolo[2,1-*a*]indol-11-yl)methanone (24ac):

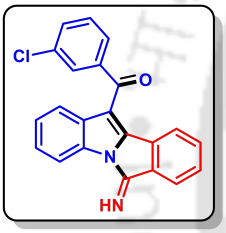

Orange Solid; R_f (Hexane/EtOAc, 3:1) 0.55; mp 167–169 °C. Yield 155 mg, 84%; ^{1}H NMR (500 MHz, $CDCl_3$) δ 9.03 (s, 1 H), 8.16 (s, 1 H), 7.90 (s, 1 H), 7.78 (d, J = 8.0 Hz, 1 H), 7.66 (s, 1 H), 7.61 (d, J = 8.0 Hz, 1 H), 7.53 (s, 1 H), 7.46–7.43 (m, 3 H), 7.38 (t, J = 8.5 Hz, 2 H), 7.17 (t, J = 8.0 Hz, 1 H); ^{13}C{^{1}H} NMR (125 MHz, $CDCl_3$) δ 190.5, 158.5, 144.8, 141.7, 135.2, 133.3, 133.0, 132.8, 132.2, 131.9, 131. 4, 130.2, 130.0, 129.4, 127.8, 126.3, 125.0, 124.0, 122.8, 122.6, 113.8, 113.7; IR (KBr, neat) 3268, 2983, 1738, 1446, 1372, 1239, 1044, 844, 742, 467 cm^{-1}; HRMS (ESI) calcd. for $C_{22}H_{14}ClN_2O$ $(M + H)^+$ 357.0789, found 357.0819.

(4-Bromophenyl)(6-imino-6*H*-isoindolo[2,1-*a*]indol-11-yl)methanone (24ad):

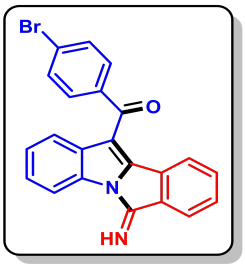

Yellow Solid; R_f (Hexane/EtOAc, 3:1) 0.5; mp 188–190 °C. Yield 166 mg, 80%; ^{1}H NMR (500 MHz, $CDCl_3$) δ 9.01 (s, 1 H), 8.14 (s, 1 H), 7.79 (d, J = 8.0 Hz, 2 H), 7.65 (d, J = 8.0 Hz, 3 H), 7.56 (d, J = 7.0 Hz, 1 H), 7.42 (t, J = 6.0 Hz, 2 H), 7.37–7.33 (m, 2 H), 7.15 (t, J = 7.5 Hz, 1 H); ^{13}C{^{1}H} NMR (125 MHz, $CDCl_3$) δ 190.5, 158.3, 144.4, 138.5, 133.0, 132.7, 132.1, 132.0, 131.9, 131.7, 131.0, 129.7, 127.7, 126.0, 124.8, 123.7, 122.6, 122.3, 113.7, 113.4; IR (KBr, neat) 3278, 2925, 1636, 1585, 1445, 1274, 1172, 1032, 934, 837, 746 cm^{-1}; HRMS (ESI) calcd. for $C_{22}H_{14}BrN_2O$ $(M + H)^+$ 401.0284, found 401.0306.

(2-Bromophenyl)(6-imino-6*H*-isoindolo[2,1-*a*]indol-11-yl)methanone (24ae):

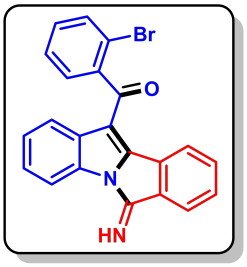

Yellow Solid; R_f (Hexane/EtOAc, 3:1) 0.5; mp 183–185 °C. Yield 156 mg, 75%; ^{1}H NMR (500 MHz, $CDCl_3$) δ 9.08 (s, 1 H), 8.15 (d, J = 8.0 Hz, 1 H), 7.95 (d, J = 8.0 Hz, 1 H), 7.73 (d, J = 8.0 Hz, 1 H), 7.65 (d, J = 7.5 Hz, 1 H), 7.50–7.47 (m, 3 H), 7.46–7.43 (m, 2 H), 7.31 (t, J = 7.5 Hz, 1 H), 7.07 (t, J = 7.5 Hz, 1 H), 6.91 (d, J = 8.0 Hz, 1 H); ^{13}C{^{1}H} NMR (125 MHz, $CDCl_3$) δ 190.9, 158.7, 146.0, 143.1, 133.8, 133.6, 133.3, 133.2, 132.2, 131.7, 131.4, 130.3, 128.9, 128.1, 126.1, 126.0, 124.3, 122.5, 122.1, 119.6, 114.3, 113.7; IR (KBr, neat) 3197, 2922, 1728, 1532, 1468, 1306, 1053, 1026, 936, 740, 714 cm^{-1}; HRMS (ESI) calcd. for $C_{22}H_{14}BrN_2O$ $(M + H)^+$ 401.0284, found 401.0309.

(4-Fluorophenyl)(6-imino-6*H*-isoindolo[2,1-*a*]indol-11-yl)methanone (24af):

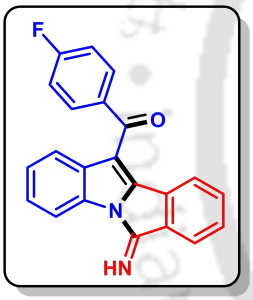

Brown Solid; R_f (Hexane/EtOAc, 3:1) 0.45; mp 210–212 °C. Yield 143 mg, 81%; ^{1}H NMR (500 MHz, $CDCl_3$) δ 8.96 (s, 1 H), 8.13 (d, J = 8.5 Hz, 1 H), 7.97–7.94 (m, 2 H), 7.64–7.62 (m, 1 H), 7.48–7.46 (m, 1 H), 7.41–7.38 (m, 3 H), 7.34 (t, J = 7.5 Hz, 1 H), 7.20–7.14 (m, 3 H); ^{13}C{^{1}H} NMR (125 MHz, $CDCl_3$) δ 190.4, 165.8 (d, J = 252.9 Hz), 158.4, 144.3, 136.3 (d, J = 3.1 Hz), 133.7, 133.2, 132.8, 132.3, 132.2, 132.2, 132.1, 129.8, 126.2, 124.4 (d, J = 124.4 Hz), 122.8, 122.6, 116.0 (d, J = 21.6 Hz), 114.1, 113.7; ^{19}F NMR (470 MHz, C_6F_6/$CDCl_3$) δ 108.7 (s, –F); IR (KBr, neat) 3280, 2925, 1640, 1599, 1445, 1241, 1153, 1032, 935, 847, 747, 604 cm^{-1}; HRMS (ESI) calcd. for $C_{22}H_{14}FN_2O$ $(M + H)^+$ 341.1085, found 341.1089.

(6-Imino-6*H*-isoindolo[2,1-*a*]indol-11-yl)(4-nitrophenyl)methanone (24ag):

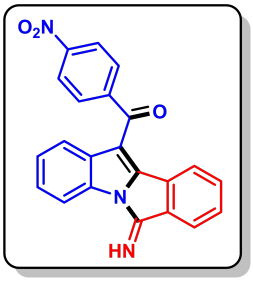

Red Solid; R_f (Hexane/EtOAc, 3:1) 0.45; mp 208–210 °C. Yield 134 mg, 70%; ^{1}H NMR (500 MHz, $CDCl_3$/DMSO-d_6) δ 9.10 (s, 1 H), 8.14 (s, 1 H), 7.87–7.81 (m, 2 H), 7.65 (s, 1 H), 7.49– 7.47 (m, 1 H), 7.45–7.43 (m, 2 H), 7.41–7.37 (m, 2 H), 7.35–7.28 (m, 2 H), 7.17–7.10 (m, 1 H); ^{13}C{^{1}H} NMR (125 MHz, $CDCl_3$/DMSO-d_6) δ 190.6, 158.6, 144.5, 139.2, 138.2, 133.2, 132.8, 132.1, 131.9, 131.0, 130.9, 129.9, 129.1, 126.2, 126.1, 124.8, 123.9, 123.8, 122.7, 113.8; IR (KBr, neat)

3288, 2924, 1728, 1522, 1343, 1247, 1032, 937, 854, 749, 717 cm^{-1}; HRMS (ESI) calcd. for $C_{22}H_{14}N_3O_3$ $(M + H)^+$ 368.1030, found 368.1058.

Methyl 4-(6-imino-6*H*-isoindolo[2,1-*a*]indole-11-carbonyl)benzoate (24ah):

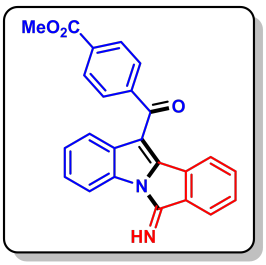

Pale Yellow Solid; R_f (Hexane/EtOAc, 3:1) 0.5; mp 207–209 °C. Yield 158 mg, 80%; ^{1}H NMR (500 MHz, $CDCl_3$) δ 9.03 (s, 1 H), 8.19–8.14 (m, 2 H), 7.95 (d, J = 8.5 Hz, 2 H), 7.66–7.64 (m, 1 H), 7.58–7.56 (m, 1 H), 7.42–740 (m, 2 H), 7.34 (d, J = 7.5 Hz, 1 H), 7.30 (d, J = 8.5 Hz, 1 H), 7.13 (d, J = 7.5 Hz, 1 H), 3.98 (s, 3 H); ^{13}C{^{1}H} NMR (125 MHz, $CDCl_3$) δ 191.3, 166.6, 158.5, 145.0, 143.8, 133.7, 133.3, 133.0, 132.2, 131.9, 130.1, 130.0, 129.4, 126.3, 125.13, 124.0, 122.8, 122.6, 114.0, 113.7, 52.7; IR (KBr, neat) 3268, 2925, 1726, 1639, 1551, 1444, 1275, 1112, 1033, 934, 747 cm^{-1}; HRMS (ESI) calcd. for $C_{24}H_{17}N_2O_3$ $(M + H)^+$ 381.1234, found 381.1259.

(6-Imino-6*H*-isoindolo[2,1-*a*]indol-11-yl)(3-(trifluoromethyl)phenyl) methanone (24ai):

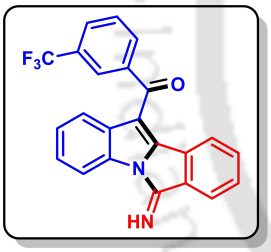

Dark Brown Solid; R_f (Hexane/EtOAc, 3:1) 0.45; mp 169–171 °C. Yield 150 mg, 74%; ^{1}H NMR (500 MHz, $CDCl_3$) δ 8.19–8.16 (m, 2 H), 8.09 (d, J = 8.0 Hz, 1 H), 7.90 (d, J = 8.0 Hz, 1 H), 7.68–7.64 (m, 2 H), 7.59–7.57 (m, 1 H), 7.44–7.41 (m, 2 H), 7.36 (t, J = 7.5 Hz, 1 H), 7.30 (d, J = 8.5 Hz, 1 H), 7.15 (t, J = 7.5 Hz, 1 H); ^{13}C{^{1}H} NMR (125 MHz, $CDCl_3$) δ 190.4, 158.5, 145.1, 140.6, 133.7, 133.3, 133.02, 132.8, 132.1, 131.8, 131.6 (q, J = 32.7 Hz), 130.1, 129.50, 129.3(q, J = 3.6 Hz), 126.5 (q, J = 3.9 Hz), 126.4, 125.0, 124.1, 122.8, 122.7, 122.6, 113.8, 113.7; ^{19}F NMR (470 MHz, C_6F_6/$CDCl_3$) δ 65.9 (s, –F); IR (KBr, neat) 3265, 2924, 1770, 1605, 1536, 1445, 1320, 1245, 1116, 938, 743 cm^{-1}; HRMS (ESI) calcd. for $C_{22}H_{14}F_3N_2O$ $(M + H)^+$ 391.1053, found 391.1082.

(6-Imino-6*H*-isoindolo[2,1-*a*]indol-11-yl)(*p*-tolyl)methanone (24aj):

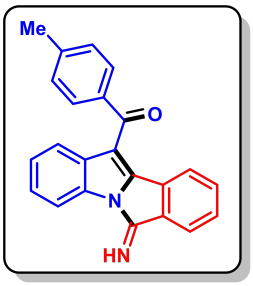

Dark Grey Solid; R_f (Hexane/EtOAc, 3:1) 0.5; mp 153–155 °C. Yield 162 mg, 93%; ^{1}H NMR (500 MHz, $CDCl_3$) δ 8.93 (s, 1 H), 8.12 (d, J = 8.0 Hz, 1 H), 7.83 (d, J = 8.0 Hz, 2 H), 7.62–7.60 (m, 1 H), 7.46 (d, J = 8.0 Hz, 1 H), 7.42–7.40 (m, 1 H), 7.37–7.33 (m, 3 H), 7.30 (d, J = 8.0 Hz, 2 H), 7.15 (t, J = 7.5 Hz, 1 H), 2.47 (s, 3 H); ^{13}C{^{1}H} NMR (125 MHz, $CDCl_3$) δ 191.7, 158.4, 144.0, 143.8, 137.3, 133.8, 133.2, 132.7, 132.4, 132.3, 129.8, 129.6, 129.5, 126.1, 124.9, 123.7, 123.0, 122.4, 114.5, 113.5, 22.0; IR (KBr, neat) 3273, 2920, 1634, 1605, 1556, 1445, 1257, 1174, 1033, 934, 746 cm^{-1}; HRMS (ESI) calcd. for $C_{23}H_{17}N_2O$ $(M + H)^+$ 337.1335, found 337.1315.

(6-Imino-6*H*-isoindolo[2,1-*a*]indol-11-yl)(*o*-tolyl)methanone (24ak):

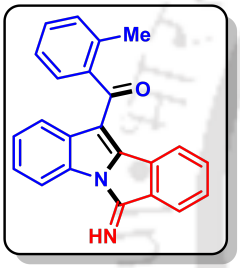

Yellow Solid; R_f (Hexane/EtOAc, 3:1) 0.5; mp 177–179 °C. Yield 157 mg, 90%; ^{1}H NMR (500 MHz, $CDCl_3$) δ 8.12 (d, J = 8.0 Hz, 1 H), 7.60 (s, 1 H), 7.46 (t, J = 7.5 Hz, 3 H), 7.39–7.35 (m, 3 H), 7.32–7.25 (m, 2 H), 7.18 (d, J = 8.0 Hz, 1 H), 7.09 (t, J = 7.5 Hz, 1 H), 2.42 (s, 3 H); ^{13}C{^{1}H} NMR (125 MHz, $CDCl_3$) δ 193.9, 158.6, 145.0, 141.4, 136.2, 133.7, 133.0, 132.3, 131.8, 131.5, 130.8, 129.9, 128.3, 126.4, 126.1, 125.6, 124.1, 122.7, 122.4, 119.6, 115.4, 113.5, 19.8; IR (KBr, neat) 3280, 2922, 1734, 1605, 1444, 1363, 1246, 1028, 934, 745, 643 cm^{-1}; HRMS (ESI) calcd. for $C_{23}H_{17}N_2O$ $(M + H)^+$ 337.1335, found 337.1341.

(6-Imino-6*H*-isoindolo[2,1-*a*]indol-11-yl)(4-methoxyphenyl)methanone (24al):

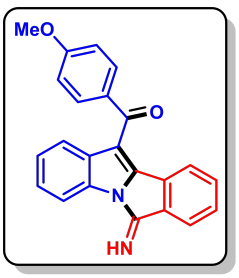

Yellow Solid; R_f (Hexane/EtOAc, 3:1) 0.55; mp 199–201 °C. Yield 176 mg, 96%; ^{1}H NMR (500 MHz, $CDCl_3$) δ 8.11 (d, J = 8.5 Hz, 1 H), 7.93 (d, J = 8.5 Hz, 2 H), 7.62–7.60 (m, 1 H), 7.49 (d, J = 8.0 Hz, 1 H), 7.42–7.40 (m, 1 H), 7.36–7.31 (m, 3 H), 7.16 (t, J = 8.5 Hz, 1 H), 6.97 (d, J = 8.5 Hz, 2 H), 3.89 (s, 3 H); ^{13}C{^{1}H} NMR (125 MHz, $CDCl_3$) δ 190.5, 163.7, 158.4, 143.5, 133.8, 133.2, 132.7, 132.5, 132.5, 132.4, 132.1, 129.5, 126.0, 124.8, 123.7, 123.0, 122.4, 114.6, 114.1, 113.5, 55.7; IR (KBr, neat) 3274, 2932, 1600, 1570, 1445, 1254, 1167, 1026, 943, 746, 606 cm^{-1}; HRMS (ESI) calcd. for $C_{23}H_{17}N_2O_2$ $(M + H)^+$ 353.1285, found 353.1269.

(6-Imino-6*H*-isoindolo[2,1-*a*]indol-11-yl)(3-methoxyphenyl)methanone (24am):

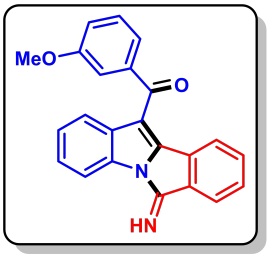

Dark Grey Solid; R_f (Hexane/EtOAc, 3:1) 0.5; mp 175–177 °C. Yield 159, 87%; ^{1}H NMR (500 MHz, $CDCl_3$) δ 8.13 (d, J = 8.0 Hz, 1 H), 7.62 (s, 1 H), 7.49 (t, J = 7.0 Hz, 2 H), 7.45 (s, 1 H), 7.39 (d, J = 7.5 Hz, 1 H), 7.37–7.35 (m, 3 H), 7.33 (d, J = 7.5 Hz, 1 H), 7.19–7.14 (m, 2 H), 3.83 (s, 3 H); ^{13}C{^{1}H} NMR (125 MHz, $CDCl_3$) δ 191.7, 160.1, 158.4, 144.3, 141.4, 133.7, 133.2, 132.8, 132.3, 132.2, 129.9, 129.7, 126.2, 125.0, 123.9, 123.1, 122.5, 122.3, 119.6, 114.4, 113.5, 113.4, 55.7; IR (KBr, neat) 3259, 2938, 1604, 1445, 1364, 1260, 1153, 1030, 772, 746, 644 cm^{-1}; HRMS (ESI) calcd. for $C_{23}H_{17}N_2O_2$ $(M + H)^+$ 353.1285, found 353.1283.

(3,5-Dimethylphenyl)(6-imino-6*H*-isoindolo[2,1-*a*]indol-11-yl)methanone (24an):

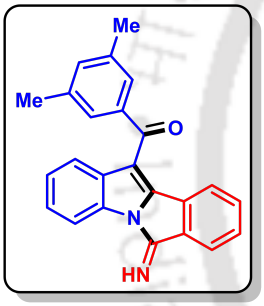

Yellow Solid; R_f (Hexane/EtOAc, 3:1) 0.6; mp 229–231 °C. Yield 178 mg, 98%; ^{1}H NMR (500 MHz, $CDCl_3$) δ 8.22 (d, J = 8.5 Hz, 1 H), 7.76 (s, 1 H), 7.55 (s, 2 H), 7.51 (d, J = 8.0 Hz, 1 H), 7.41 (d, J = 7.0 Hz, 2 H), 7.38 (d, J = 7.0 Hz, 2 H), 7.29 (s, 2 H), 7.19 (t, J = 7.5 Hz, 1 H), 2.38 (s, 6 H); ^{13}C{^{1}H} NMR (125 MHz, $CDCl_3$) δ 192.3, 158.4, 144.1, 140.0, 138.6, 134.6, 133.8, 133.3, 133.0, 132.5, 132.4, 129.8, 127.3, 126.4, 125.0, 124.1, 123.2, 122.9, 115.2, 113.7, 21.5; IR (KBr, neat) 3267, 2923, 1729, 1604, 1445, 1364, 1246, 1172, 1054, 865, 743 cm^{-1}; HRMS (ESI) calcd. for $C_{24}H_{19}N_2O$ $(M + H)^+$ 351.1492, found 351.1518.

(4-(Tert-butyl)phenyl)(6-imino-6*H*-isoindolo[2,1-*a*]indol-11-yl)methanone (24ao):

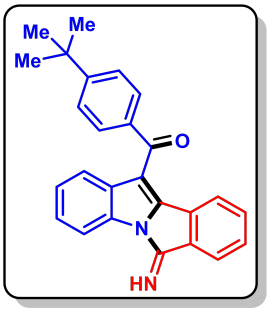

Orange Solid; R_f (Hexane/EtOAc, 3:1) 0.55; mp 166–168 °C. Yield 179 mg, 91%; ^{1}H NMR (500 MHz, $CDCl_3$) δ 8.13 (d, J = 8.5 Hz, 1 H), 7.87 (d, J = 8.5 Hz, 2 H), 7.58 (t, J = 8.0 Hz, 2 H), 7.52 (d, J = 8.0 Hz, 2 H), 7.36–7.31 (m, 2 H), 7.30–7.27 (m, 1 H), 7.19–7.15 (m, 2 H), 1.40 (s, 9 H); ^{13}C{^{1}H} NMR (125 MHz, $CDCl_3$) δ 191.7, 158.3, 156.7, 144.0, 137.4, 133.7, 133.2, 132.5, 132.3, 132.3, 129.5, 129.5, 126.0, 125.8, 124.9, 123.8, 123.0, 122.4, 114.6, 113.5, 35.4, 31.4; IR (KBr, neat) 3265, 2962, 1770, 1605, 1471, 1445, 1364,

1248, 1036, 846, 746 cm^{-1}; HRMS (ESI) calcd. for $C_{26}H_{23}N_2O$ $(M + H)^+$ 379.1805, found 379.1779.

[1,1'-Biphenyl]-4-yl(6-imino-6*H*-isoindolo[2,1-*a*]indol-11-yl)methanone (24ap):

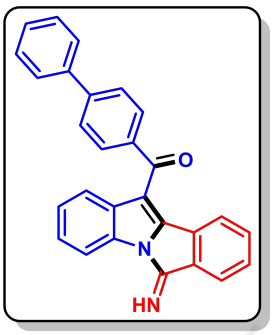

Yellow Solid; R_f (Hexane/EtOAc, 3:1) 0.55; mp 217–219 °C. Yield 197 mg, 95%; ^1H NMR (500 MHz, $CDCl_3$) δ 8.16 (d, J = 8.5 Hz, 1 H), 8.00 (d, J = 8.0 Hz, 2 H), 7.73 (d, J = 8.0 Hz, 2 H), 7.68 (d, J = 7.5 Hz, 2 H), 7.63–7.61 (m, 1 H), 7.52–7.48 (m, 3 H), 7.47–7.45 (m, 1 H), 7.42 (d, J = 7.5 Hz, 1 H), 7.37–7.34 (m, 3 H), 7. 17 (t, J = 7.5 Hz, 1 H); $^{13}C\{^1H\}$ NMR (125 MHz, $CDCl_3$) δ 191.5, 158.4, 145.6, 144.2, 140.1, 138.7, 133.7, 133.2, 132.8, 132.3, 132.2, 130.2, 129.7, 129.2, 128.4, 127.5, 127.4, 126.1, 125.0, 123.8, 123.0, 122.5, 114.5, 113.6; IR (KBr, neat) 3270, 2919, 1770, 1604, 1558, 1445, 1247, 1033, 935, 848, 743 cm^{-1}; HRMS (ESI) calcd. for $C_{28}H_{19}N_2O$ $(M + H)^+$ 399.1492, found 399.1490.

(4'-Ethyl-[1,1'-biphenyl]-4-yl)(6-imino-6*H*-isoindolo[2,1-*a*]indol-11-yl)methanone (24aq):

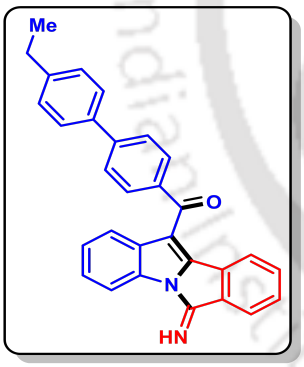

Dark Brown Solid; R_f (Hexane/EtOAc, 3:1) 0.55; mp 221–223 °C. Yield 215 mg, 97%; ^1H NMR (400 MHz, $CDCl_3$) δ 8.94 (s, 1 H), 8.16 (d, J = 8.0 Hz, 1 H), 8.00 (d, J = 8.4 Hz, 2 H), 7.73 (d, J = 8.4 Hz, 2 H), 7.62 (d, J = 8.4 Hz, 3 H), 7.54 (d, J = 8.0 Hz, 1 H), 7.47–7.44 (m, 1 H), 7.38–7.35 (m, 3 H), 7.34 (s, 1 H), 7.32 (s, 1 H), 7.20–7.16 (m, 1 H), 2.73 (q, J = 7.6 Hz, 2 H), 1.30 (t, J = 7.6 Hz, 3 H); $^{13}C\{^1H\}$ NMR (125 MHz, $CDCl_3$) δ 191.4, 158.3, 145.5, 144.7, 144.1, 138.3, 137.3, 133.7, 133.1, 132.6, 132.2, 130.2, 129.6, 128.7, 127.3, 127.1, 126.1, 124.9, 123.8, 123.0, 122.4, 114.4, 113.5, 28.7, 15.7; IR (KBr, neat) 3283, 2927, 1770, 1605, 1554, 1445, 1368, 1246, 1048, 829, 747 cm^{-1}; HRMS (ESI) calcd. for $C_{30}H_{23}N_2O$ $(M + H)^+$ 427.1805, found 427.1828.

(6-Imino-6*H*-isoindolo[2,1-*a*]indol-11-yl)(naphthalen-2-yl)methanone (24ar):

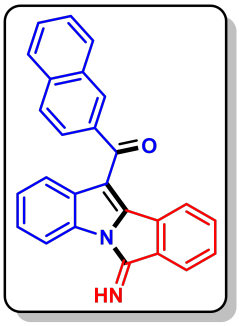

Yellow Solid; R_f (Hexane/EtOAc, 3:1) 0.5; mp 201–203 °C. Yield 170 mg, 88%; ^{1}H NMR (500 MHz, $CDCl_3$) δ 8.44 (s, 1 H), 8.16 (d, J = 8.0 Hz, 1 H), 8.02 (d, J = 7.5 Hz, 1 H), 7.97 (d, J = 8.5 Hz, 1 H), 7.93 (d, J = 8.5 Hz, 1 H), 7.87 (d, J = 8.2 Hz, 1 H), 7.64–7.60 (m, 2 H), 7.54 (t, J = 7.5 Hz, 1 H), 7.49 (d, J = 7.5 Hz, 1 H), 7.41 (d, J = 8.0 Hz, 1 H), 7.35–7.32 (m, 2 H), 7.30 (d, J = 7.5 Hz, 1 H), 7.11 (t, J = 8.0 Hz, 1 H); ^{13}C{^{1}H} NMR (125 MHz, $CDCl_3$) δ 191.7, 158.4, 144.3, 137.1, 135.6, 134.4, 133.7, 133.2, 132.8, 132.7, 132.3, 131.3, 129.7, 129.7, 128.7, 128.5, 128.1, 127.0, 126.1, 125.4, 124.9, 123.8, 123.0, 122.5, 114.5, 113.6; IR (KBr, neat) 3270, 2993, 1770, 1615, 1551, 1467, 1371, 1245, 1127, 1048, 747 cm^{-1}; HRMS (ESI) calcd. for $C_{26}H_{17}N_2O$ $(M + H)^+$ 373.1335, found 373.1325.

(6-Imino-6*H*-isoindolo[2,1-*a*]indol-11-yl)(phenanthren-9-yl)methanone (24as):

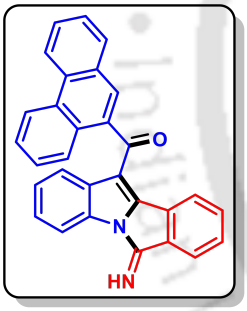

Pale Yellow Solid; R_f (Hexane/EtOAc, 3:1) 0.5; mp 213–215 °C. Yield 189 mg, 86%; ^{1}H NMR (500 MHz, $CDCl_3$) δ 8.80 (dd, J = 18.5, 8.5 Hz, 2 H), 8.36 (d, J = 8.0 Hz, 1 H), 8.20 (d, J = 8.5 Hz, 1 H), 8.06 (s, 1 H), 7.90 (d, J = 7.5 Hz, 1 H), 7.84 (d, J = 7.5 Hz, 1 H), 7.78 (t, J = 7.5 Hz, 1 H), 7.75–7.71 (m, 2 H), 7.64–7.60 (m, 2 H), 7.43–7.36 (m, 2 H), 7.29 (t, J = 7.5 Hz, 1 H), 7.10 (d, J = 8.0 Hz, 1 H), 6.96 (t, J = 7.5 Hz, 1 H); ^{13}C{^{1}H} NMR (125 MHz, $CDCl_3$) δ 192.9, 158.7, 145.6, 137.5, 133.7, 133.4, 133.2, 132.4, 131.8, 131.7, 131.1, 130.7, 130.1, 130.0, 129.3, 128.9, 128.7, 127.7, 127.6, 127.4, 126.7, 126.2, 125.9, 124.2, 123.3, 123.0, 122.9, 122.6, 116.0, 113.7; IR (KBr, neat) 3288, 2924, 1770, 1661, 1542, 1444, 1363, 1247, 1128, 1064, 747 cm^{-1}; HRMS (ESI) calcd. for $C_{30}H_{18}N_2NaO$ $(M + Na)^+$ 445.1312, found 445.1309.

(6-Imino-6*H*-isoindolo[2,1-*a*]indol-11-yl)(thiophen-2-yl)methanone (24at):

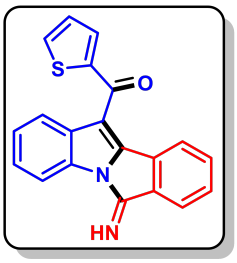

Grey Solid; R_f (Hexane/EtOAc, 3:1) 0.45; mp 181–183 °C. Yield 138 mg, 81%; ^{1}H NMR (500 MHz, $CDCl_3$) δ 8.13 (d, J = 8.0 Hz, 1 H), 7.77 (dd, J = 8.5, 3.5 Hz, 2 H), 7.70 (d, J = 8.0 Hz, 1 H), 7.63 (d, J = 7.0 Hz, 1 H), 7.54 (d, J = 7.0 Hz, 1 H), 7.42–7.34 (m, 3 H), 7.21 (d, J = 7.5 Hz, 1 H), 7.14 (t, J = 4.5 Hz, 1 H); ^{13}C{^{1}H} NMR (125 MHz, $CDCl_3$) δ 182.9, 158.2, 145.1, 143.1, 134.5, 134.2, 133.5, 133.0, 132.6, 132.1, 131.8, 129.5, 128.0, 126.1, 124.5, 123.6, 122.6, 122.3, 114.2, 113.4; IR (KBr, neat) 3281, 2924, 1727, 1661, 1605, 1561, 1414, 1384, 1249, 1050,744 cm^{-1}; HRMS (ESI) calcd. for $C_{20}H_{13}N_2OS$ $(M + H)^+$ 329.0743, found 329.0735.

(2-Chloro-6-imino-6*H*-isoindolo[2,1-*a*]indol-11-yl)(phenyl)methanone (24ba):

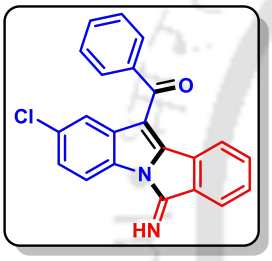

Brown Solid; R_f (Hexane/EtOAc, 3:1) 0.5; mp 162–164 °C. Yield 167 mg, 90%; ^{1}H NMR (500 MHz, $CDCl_3$) δ 8.00 (d, J = 8.5 Hz, 1 H), 7.83 (d, J = 7.0 Hz, 2 H), 7.61–7.55 (m, 2 H), 7.46 (t, J = 7.5 Hz, 2 H), 7.41 (s, 1 H), 7.32 (t, J = 7.5 Hz, 1 H), 7.28 (d, J = 7.5 Hz, 1 H), 7.24–7.20 (m, 2 H), 7.12 (d, J = 7.5 Hz, 1 H); ^{13}C{^{1}H} NMR (125 MHz, $CDCl_3$) δ 191.5, 158.2, 145.1, 139.9, 133.4, 133.1, 132.9, 132.0, 131.5, 130.0, 129.6, 129.4, 129.0, 128.8, 128.5, 126.4, 125.2, 122.6, 114.5, 113.7; IR (KBr, neat) 3278, 2924, 1770, 1637, 1552, 1445, 1247, 1023, 898,751, 598 cm^{-1}; HRMS (ESI) calcd. for $C_{22}H_{14}ClN_2O$ $(M + H)^+$ 357.0789, found 357.0800.

(3-Chloro-6-imino-6*H*-isoindolo[2,1-*a*]indol-11-yl)(phenyl)methanone (24bb):

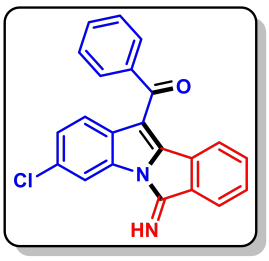

Orange Solid; R_f (Hexane/EtOAc, 3:1) 0.5; mp 173–175 °C. Yield 139 mg, 75%; ^{1}H NMR (500 MHz, $CDCl_3$/DMSO–d_6) δ 9.10 (s, 1 H), 8.05 (d, J = 9.0 Hz, 1 H), 7.86 (d, J = 8.0 Hz, 2 H), 7.63 (s, 2 H), 7.51–7.47 (m, 3 H), 7.39–7.28 (m, 3 H), 7.16 (d, J = 8.0 Hz, 1 H); ^{13}C{^{1}H} NMR (125 MHz, $CDCl_3$/DMSO–d_6) δ 191.6, 158.7, 145.1, 139.8, 133.3, 133.1, 132.9, 131.9, 131.5, 130.0, 129.5, 129.4, 129.0, 128.7, 126.3, 125.1, 122.6, 122.5, 114.5, 113.5; IR (KBr, neat) 3288, 2924, 1770, 1659, 1599, 1445, 1247, 1063, 809, 751, 692 cm^{-1}; HRMS (ESI) calcd. for $C_{22}H_{14}ClN_2O$ $(M + H)^+$ 357.0789, found 357.0800.

(2-Bromo-6-imino-6*H*-isoindolo[2,1-*a*]indol-11-yl)(phenyl)methanone (24bc):

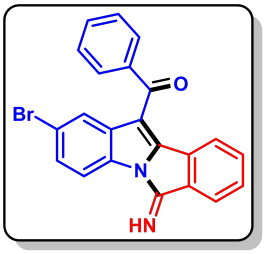

Brown Solid; R_f (Hexane/EtOAc, 3:1) 0.5; mp 181–183 °C. Yield 187 mg, 90%; ^{1}H NMR (400 MHz, $CDCl_3$) δ 7.99 (d, J = 8.4 Hz, 1 H), 7.88 (d, J = 8.0 Hz, 2 H), 7.67–7.63 (m, 2 H), 7.60 (d, J = 7.2 Hz, 1 H), 7.51 (t, J = 7.6 Hz, 2 H), 7.41 (d, J = 9.2 Hz, 1 H), 7.37–7.30 (m, 1 H), 7.13 (d, J = 7.6 Hz, 1H); ^{13}C{^{1}H} NMR (125 MHz, $CDCl_3$) δ 191.5, 158.3, 144.9, 139.8, 133.8, 133.4, 133.18, 132.9, 131.9, 131.8, 130.1, 129.5, 129.1, 129.0, 125.6, 125.2, 122.6, 117.3, 114.9, 113.5; IR (KBr, neat) 3422, 2985, 1735, 1714, 1444, 1373, 1239, 1045, 751, 609, 528 cm^{-1}; HRMS (ESI) calcd. for $C_{22}H_{14}BrN_2O$ $(M + H)^+$ 401.0284, found 401.0283.

(2-Fluoro-6-imino-6*H*-isoindolo[2,1-*a*]indol-11-yl)(phenyl)methanone (24bd):

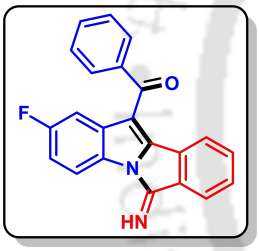

Yellow Solid; R_f (Hexane/EtOAc, 3:1) 0.5; mp 170–172 °C. Yield 154 mg, 87%; ^{1}H NMR (500 MHz, $CDCl_3$) δ 8.96 (s, 1 H), 8.08 (dd, J = 9.0, 4.5 Hz, 1 H), 7.88 (d, J = 7.0 Hz, 2 H), 7.66–7.61 (m, 2 H), 7.52 (t, J = 7.5 Hz, 2 H), 7.40–7.34 (m, 2 H), 7.28 (d, J = 7.5 Hz, 1 H), 7.15 (dd, J = 9.5, 2.5 Hz, 1 H), 7.09–7.04 (m, 1 H); ^{13}C{^{1}H} NMR (125 MHz, $CDCl_3$) δ 191.7, 160.0 (d, J = 238.6 Hz), 158.4, 145.6, 140.0, 133.4, 133.2 (d, J = 10.5 Hz), 133.1, 132.9, 132.2, 120.0, 129.7, 129.4, 129.0, 125.2, 122.5, 114.4 (d, J = 9.3 Hz), 114.1, 113.9, 109.0 (d, J = 25.5 Hz); ^{19}F NMR (470 MHz, C_6F_6/$CDCl_3$) δ 121.5 (s, –F); IR (KBr, neat) 3256, 2924, 1770, 1614, 1538, 1471, 1446, 1247, 1038, 1022, 750 cm^{-1}; HRMS (ESI) calcd. for $C_{22}H_{14}FN_2O$ $(M + H)^+$ 341.1085, found 341.1083.

Methyl 11-benzoyl-6-imino-6*H*-isoindolo[2,1-*a*]indole-2-carboxylate (24be):

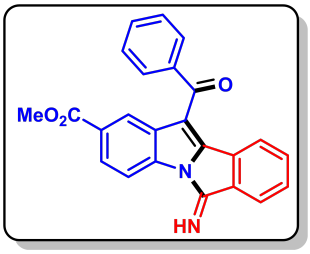

Pale Yellow Solid; R_f (Hexane/EtOAc, 3:1) 0.5; mp 167–169 °C. Yield 140 mg, 71%; ^{1}H NMR (500 MHz, $CDCl_3$) δ 8.34 (s, 1 H), 8.23–8.19 (m, 2 H), 8.06 (d, J = 8.0 Hz, 1 H), 7.92 (d, J = 8.0 Hz, 2 H), 7.67 (s, 2 H), 7.52 (s, 2 H), 7.30–7.36 (m, 3 H), 3.88 (s, 3 H); ^{13}C{^{1}H} NMR (125 MHz, $CDCl_3$) δ 191.6, 167.4, 158.3, 145.0, 139.7, 135.7, 133.3, 133.1, 132.1, 130.9, 130.2, 129.6, 129.1, 127.7, 125.9, 125.3, 125.2, 122.8, 114.7, 113.3, 52.3; IR (KBr, neat)

3290, 2924, 1716, 1606, 1467, 1437, 11241, 1112, 905, 764, 699 cm^{-1}; HRMS (ESI) calcd. for $C_{24}H_{17}N_2O_3$ $(M + H)^+$ 381.1234, found 381.1244.

(6-Imino-2-(trifluoromethyl)-6*H*-isoindolo[2,1-a]indol-11-yl)(phenyl) methanone (24bf):

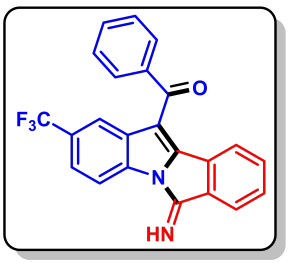

Grey Solid; R_f (Hexane/EtOAc, 3:1) 0.45; mp 197–199 °C. Yield 156 mg, 77%; ^{1}H NMR (500 MHz, $CDCl_3$) δ 8.25 (d, J = 8.5 Hz, 1 H), 7.89 (d, J = 7.5 Hz, 2 H), 7.81 (s, 1 H), 7.67 (t, J = 7.0 Hz, 2 H), 7.58 (d, J = 8.5 Hz, 1 H), 7.52 (t, J = 7.5 Hz, 2 H), 7.41 (t, J = 7.5 Hz, 1 H), 7.35 (t, J = 8.0 Hz, 1 H), 7.17 (d, J = 7.5 Hz, 1 H); ^{13}C{^{1}H} NMR (125 MHz, $CDCl_3$) δ 191.5, 158.3, 145.3, 139.7, 134.6, 133.3, 133.1, 132.1, 131.9, 130.3, 129.5, 129.1, 126.2 (q, J = 32.1 Hz), 125.4, 123.8, 123.6, 123.1 (q, J = 3.6 Hz), 122.8, 120.5 (q, J = 4.1 Hz), 114.3, 113.9; ^{19}F NMR (470 MHz, C_6F_6/$CDCl_3$) δ 64.5 (s, –F); IR (KBr, neat) 3283, 2985, 1737, 1642, 1445, 1372, 1238, 1102, 1045, 900, 752 cm^{-1}; HRMS (ESI) calcd. for $C_{22}H_{14}F_3N_2O$ $(M + H)^+$ 391.1053, found 391.1024.

(6-Imino-2-methyl-6*H*-isoindolo[2,1-*a*]indol-11-yl)(phenyl)methanone (24bg):

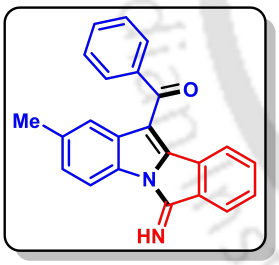

Dark Brown Solid; R_f (Hexane/EtOAc, 3:1) 0.55; mp 199–201 °C. Yield 162 mg, 93%; ^{1}H NMR (500 MHz, $CDCl_3$) δ 7.99 (d, J = 8.0 Hz, 1 H), 7.91 (d, J = 7.5 Hz, 2 H), 7.62 (t, J = 8.0 Hz, 2 H), 7.50 (t, J = 7.5 Hz, 2 H), 7.35–7.28 (m, 3 H), 7.15 (t, J = 10.0 Hz, 2 H), 2.36 (s, 3 H); ^{13}C{^{1}H} NMR (125 MHz, $CDCl_3$) δ 192.1, 158.3, 144.2, 140.2, 133.8, 133.6, 132.9, 132.7, 132.6, 132.4, 131.4, 129.6, 128.9, 127.5, 124.8, 123.0, 122.5, 114.2, 113.1, 21.8; IR (KBr, neat) 3237, 2922, 1770, 1606, 1544, 1446, 1247, 1036, 905, 804, 751 cm^{-1}; HRMS (ESI) calcd. for $C_{23}H_{17}N_2O$ $(M + H)^+$ 337.1335, found 337.1329.

(6-Imino-3-methyl-6*H*-isoindolo[2,1-*a*]indol-11-yl)(phenyl)methanone (24bh):

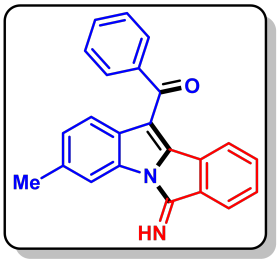

Yellow Solid; R_f (Hexane/EtOAc, 3:1) 0.55; mp 251–253 °C. Yield 157 mg, 90%; ^{1}H NMR (500 MHz, $CDCl_3$) δ 7.94 (s, 1 H), 7.90 (d, J = 7.5 Hz, 2 H), 7.62 (d, J = 7.0 Hz, 2 H), 7.49 (d, J = 7.5 Hz, 2 H), 7.36–7.34 (m, 3 H), 7.29 (d, J = 8.0 Hz, 1 H), 6.97 (d, J = 8.5 Hz, 1 H), 2.47 (s, 3 H); ^{13}C{^{1}H} NMR (125 MHz, $CDCl_3$) δ 192.1, 158.6, 143.8, 140.2, 136.7, 133.6, 132.9, 132.8, 132.4, 130.7, 130.0, 129.5, 128.9, 125.4, 124.9, 122.6, 122.5, 114.5, 113.7, 22.0; IR (KBr, neat) 3587, 2985, 1737, 1714, 1444, 1372, 1238, 1045, 847, 750, 634 cm^{-1}; HRMS (ESI) calcd. for $C_{23}H_{16}N_2NaO$ $(M + Na)^+$ 359.1155, found 359.1155.

(6-Imino-2-methoxy-6*H*-isoindolo[2,1-*a*]indol-11-yl)(phenyl)methanone (24bi):

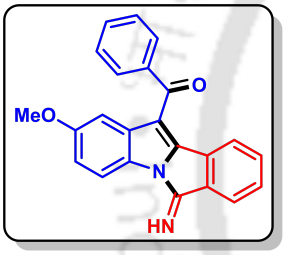

Red Solid; R_f (Hexane/EtOAc, 3:1) 0.55; mp 211–213 °C. Yield 168 mg, 92%; ^{1}H NMR (500 MHz, $CDCl_3$) δ 8.01 (d, J = 8.5 Hz, 1 H), 7.90 (d, J = 7.5 Hz, 2 H), 7.62 (t, J = 6.5 Hz, 2 H), 7.51 (t, J = 7.5 Hz, 2 H), 7.35–7.28 (m, 2 H), 7.13 (d, J = 7.5 Hz, 1 H), 7.00 (s, 1 H), 6.95 (dd, J = 8.5, 2.5 Hz, 1 H), 3.73 (s, 3 H); ^{13}C{^{1}H} NMR (125 MHz, $CDCl_3$) δ 192.1, 158.2, 156.9, 144.7, 140.3, 133.6, 133.3, 132.8, 132.7, 132.4, 129.6, 129.5, 128.9, 128.0, 124.8, 122.5, 115.2, 114.3, 114.1, 105.7, 55.8; IR (KBr, neat) 3280, 2995, 1770, 1634, 1471, 1247, 1206, 1040, 809, 761, 749 cm^{-1}; HRMS (ESI) calcd. for $C_{23}H_{17}N_2O_2$ $(M + H)^+$ 353.1285, found 353.1283.

(2-(Tert-butyl)-6-imino-6*H*-isoindolo[2,1-*a*]indol-11-yl)(phenyl)methanone (24bj):

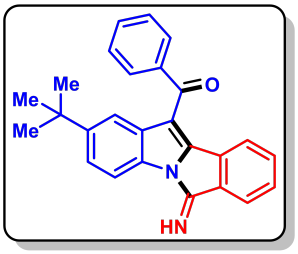

Dark Brown Solid; R_f (Hexane/EtOAc, 3:1) 0.55; mp 111–113 °C. Yield 187 mg, 95%; ^{1}H NMR (500 MHz, $CDCl_3$) δ 8.02 (d, J = 8.5 Hz, 1 H), 7.91 (d, J = 8.0 Hz, 2 H), 7.65–7.60 (m, 2 H), 7.51 (t, J = 8.0 Hz, 2 H), 7.47 (s, 1 H), 7.41 (d, J = 8.5 Hz, 1H), 7.34–7.30 (m, 3 H), 1.29 (s, 9 H); ^{13}C{^{1}H} NMR (125 MHz, $CDCl_3$) δ 192.2, 158.2, 146.9, 144.4, 140.3, 133.8, 132.7, 132.6, 132.4, 132.2, 131.3, 129.6, 129.5, 128.8, 124.9, 124.0, 122.4, 119.5, 114.4, 112.8,

35.0, 31.7; IR (KBr, neat) 3283, 2960, 1770, 1641, 1551, 1364, 1471, 1246, 1057, 954, 750 cm^{-1}; HRMS (ESI) calcd. for $C_{26}H_{23}N_2O$ $(M + H)^+$ 379.1805, found 379.1790.

(2-Butyl-6-imino-6*H*-isoindolo[2,1-*a*]indol-11-yl)(phenyl)methanone (24bk):

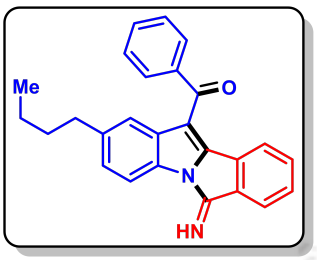

Yellow Solid; R_f (Hexane/EtOAc, 3:1) 0.5; mp 142–144 °C. Yield 179 mg, 91%; ^1H NMR (500 MHz, $CDCl_3$) δ 8.03 (d, J = 8.5 Hz, 1 H), 7.92 (d, J = 7.5 Hz, 2 H), 7.64 (t, J = 7.5 Hz, 2 H), 7.50 (t, J = 7.5 Hz, 2 H), 7.38–7.30 (m, 3 H), 7.19 (t, J = 9.0 Hz, 2 H), 2.61 (t, J = 8.0 Hz, 2 H), 1.60–1.53 (m, 2 H), 1.36–1.29 (m, 2 H), 0.90 (t, J = 7.5 Hz, 3 H); $^{13}C\{^1H\}$ NMR (125 MHz, $CDCl_3$) δ 192.1, 158.3, 144.2, 140.2, 138.8, 133.8, 132.9, 132.8, 132.5, 132.5, 131.6, 129.6, 128.9, 127.1, 124.8, 122.6, 122.5, 114.4, 113.1, 35.9, 34.2, 22.4, 14.2; IR (KBr, neat) 3278, 2953, 1770, 1637, 1551, 1470, 1363, 1247, 1034, 750, 699 cm^{-1}; HRMS (ESI) calcd. for $C_{26}H_{22}N_2NaO$ $(M + Na)^+$ 401.1625, found 401.1619.

(9-Bromo-6-imino-6*H*-isoindolo[2,1-*a*]indol-11-yl)(phenyl)methanone (24cb):

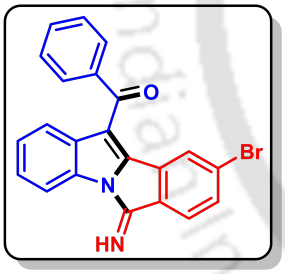

Dark Brown Solid; R_f (Hexane/EtOAc, 3:1) 0.5; mp 144–146 °C. Yield 150 mg, 72%; ^1H NMR (500 MHz, $CDCl_3$/DMSO–d_6) δ 9.34 (s, 1 H), 8.04 (s, 1 H), 7.74 (d, J = 7.5 Hz, 2 H), 7.54 (t, J = 7.5 Hz, 1 H), 7.50 (d, J = 7.0 Hz, 1 H), 7.40 (t, J = 8.0 Hz, 3 H), 7.31 (d, J = 6.5 Hz, 2 H), 7.22 (t, J = 7.5 Hz, 1 H), 7.04 (d, J = 8.0 Hz, 1 H); $^{13}C\{^1H\}$ NMR (125 MHz, $CDCl_3$/DMSO–d_6) δ 191.5, 158.2, 144.9, 139.8, 133.8, 133.1, 132.8, 131.8, 131.8, 130.7, 130.0, 129.4, 129.0, 128.9, 125.5, 125.1, 122.6, 117.2, 114.9, 113.3; IR (KBr, neat) 3260, 2920, 1770, 1604, 1549, 1426, 1247, 1055, 819, 747, 697 cm^{-1}; HRMS (ESI) calcd. for $C_{22}H_{14}BrN_2O$ $(M + H)^+$ 401.0284, found 401.0283.

(8-Fluoro-6-imino-6*H*-isoindolo[2,1-*a*]indol-11-yl)(phenyl)methanone (24cc):

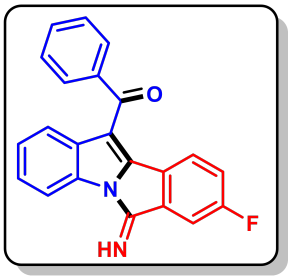

Red Solid; R_f (Hexane/EtOAc, 3:1) 0.5; mp 174–176 °C. Yield 136 mg, 77%; ^{1}H NMR (500 MHz, $CDCl_3$) δ 8.09 (d, J = 8.0 Hz, 1 H), 7.89 (d, J = 7.0 Hz, 1 H), 7.64 (t, J = 7.5 Hz, 1 H), 7.51 (t, J = 7.5 Hz, 2 H), 7.44 (dd, J = 8.5, 5.0 Hz, 1 H), 7.39 (d, J = 8.0 Hz, 1 H), 7.34 (t, J = 7.5 Hz, 2 H), 7.15 (d, J = 7.5 Hz, 1 H), 7.07 (t, J = 8.5 Hz, 1 H); ^{13}C{^{1}H} NMR (125 MHz, $CDCl_3$) δ 191.8, 163.6 (d, J = 250.5 Hz), 157.1, 143.5, 139.8, 132.7, 132.5 (d, J = 162.9 Hz), 129.3, 128.8, 128.7, 128.3 (d, J = 3.0 Hz), 126.7 (d, J = 8.4 Hz), 126.0, 124.8, 123.8, 122.9, 119.6 (d, J = 22.6 Hz), 114.0, 113.3, 110.2 (d, J = 24.9 Hz); ^{19}F NMR (470 MHz, C_6F_6/$CDCl_3$) δ 127.3 (s, –F) IR (KBr, neat) 3273, 2990, 1770, 1661, 1639, 1556, 1470, 1247, 1037, 749, 694 cm^{-1}; HRMS (ESI) calcd. for $C_{22}H_{14}FN_2O$ $(M + H)^+$ 341.1085, found 341.1109.

(6-Imino-7-methyl-6*H*-isoindolo[2,1-*a*]indol-11-yl)(phenyl)methanone (24cd):

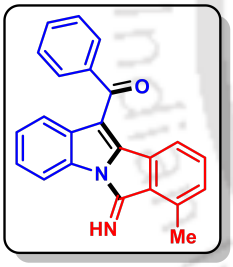

Red Solid; R_f (Hexane/EtOAc, 3:1) 0.45; mp 162–164 °C. Yield 154 mg, 88%; ^{1}H NMR (500 MHz, $CDCl_3$) δ 8.90 (s, 1 H), 8.08 (d, J = 8.0 Hz, 1 H), 7.88 (d, J = 8.0 Hz, 2 H), 7.61 (t, J = 7.5 Hz, 1 H), 7.48 (t, J = 7.5 Hz, 2 H), 7.40 (d, J = 8.0 Hz, 1 H), 7.29 (t, J = 7.5 Hz, 1 H), 7.23 (d, J = 7.5 Hz, 1 H), 7.16–7.10 (m, 2 H), 7.03 (d, J = 7.5 Hz, 1 H), 2.62 (s, 3 H); ^{13}C{^{1}H} NMR (125 MHz, $CDCl_3$) δ 192.0, 158.8, 143.9, 140.2, 136.4, 133.0, 132.8, 132.7, 132.7, 132.2, 132.2, 129.4, 128.8, 125.8, 123.6, 123.0, 122.8, 113.5, 113.2, 18.8; IR (KBr, neat) 3349, 3053, 1770, 1637, 1550, 1363, 1244, 1036, 936, 746, 696 cm^{-1}; HRMS (ESI) calcd. for $C_{23}H_{17}N_2O$ $(M + H)^+$ 337.1335, found 337.1310.

11-Benzoyl-6*H*-isoindolo[2,1-*a*]indol-6-one (25a):

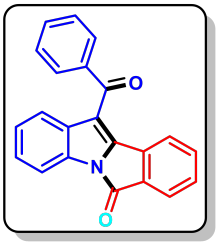

Yellow Solid; R_f (Hexane/EtOAc, 4:1) 0.5; mp 153–155 °C. Yield 46.5 mg, 96%; ^{1}H NMR (500 MHz, $CDCl_3$) δ 7.93 (dd, J = 14.0, 8.0 Hz, 3 H), 7.76–7.74 (m, 1 H), 7.65 (t, J = 7.0 Hz, 1 H), 7.51 (t, J = 8.0 Hz, 2 H), 7.40 (d, J = 8.0 Hz, 1 H), 7.36–7.34 (m, 2 H), 7.32 (d, J = 7.5 Hz, 1 H), 7.16– 7.11 (m, 2 H); ^{13}C{^{1}H} NMR (125 MHz, $CDCl_3$) δ 191.7, 163.0, 142.4, 139.4, 134.5, 133.9, 133.7, 133.4, 133.1, 132.5, 130.4,

129.5, 129.0, 127.2, 125.6, 124.9, 124.7, 123.2, 117.0, 113.4; IR (KBr, neat) 3063, 2928, 1743, 1645, 1468, 1359, 1280, 1035, 905,748, 696 cm^{-1}; HRMS (ESI) calcd. for $C_{22}H_{14}NO_2$ $(M + H)^+$ 324.1019, found 324.1031.

11-(4-Chlorobenzoyl)-6*H*-isoindolo[2,1-*a*]indol-6-one (25b):

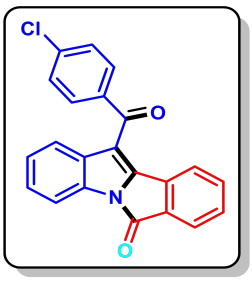

Pale Yellow Solid; R_f (Hexane/EtOAc, 4:1) 0.45; mp 209–211 °C. Yield 52 mg, 98%; ^{1}H NMR (500 MHz, $CDCl_3$) δ 7.98 (d, J = 8.0 Hz, 1 H), 7.89 (d, J = 8.5 Hz, 2 H), 7.80 (d, J = 7.0 Hz, 1 H), 7.50 (d, J = 8.0 Hz, 2 H), 7.45 (t, J = 7.5 Hz, 1 H), 7.40 (t, J = 7.0 Hz, 1 H), 7.37–7.33 (m, 3 H), 7.17 (t, J = 7.5 Hz, 1 H); ^{13}C{^{1}H} NMR (125 MHz, $CDCl_3$) δ 190.4, 163.1, 142.7, 139.9, 137.5, 134.7, 133.9, 133.7, 133.2, 132.3, 131.1, 130.7, 129.4, 127.3, 125.8, 124.9, 124.9, 123.0, 116.7, 113.6; IR (KBr, neat) 2924, 2854, 1748, 1644, 1590, 1444, 1358, 1190, 1014, 934, 747 cm^{-1}; HRMS (ESI) calcd. for $C_{22}H_{13}ClNO_2$ $(M + H)^+$ 358.0629, found 358.0629.

11-(4-Methylbenzoyl)-6*H*-isoindolo[2,1-*a*]indol-6-one (25c):

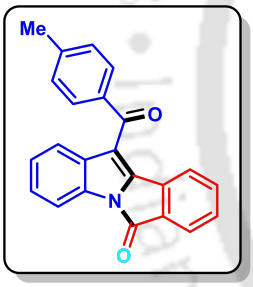

Yellow Solid; R_f (Hexane/EtOAc, 4:1) 0.5; mp 203–205 °C. Yield 48 mg, 95%; ^{1}H NMR (500 MHz, $CDCl_3$) δ 7.97 (d, J = 8.0 Hz, 1 H), 7.85 (d, J = 7.5 Hz, 2 H), 7.78 (d, J = 7.5 Hz, 1 H), 7.42 (d, J = 8.0 Hz, 1 H), 7.38 (t, J = 8.0 Hz, 2 H), 7.35 (d, J = 7.5 Hz, 1 H), 7.31 (d, J = 8.0 Hz, 2 H), 7.23 (d, J = 7.0 Hz, 1 H), 7.16 (t, J = 8.0 Hz, 1 H), 2.47 (s, 3 H); ^{13}C{^{1}H} NMR (125 MHz, $CDCl_3$) δ 191.4, 163.1, 144.4, 142.1, 136.6, 134.5, 134.0, 133.8, 133.2, 132.6, 130.3, 129.9, 129.7, 127.2, 125.6, 124.9, 124.7, 123.2, 117.3, 113.5, 22.0; IR (KBr, neat) 2925, 2855, 1745, 1606, 1566, 1444, 1394, 1228, 1177, 1039, 753 cm^{-1}; HRMS (ESI) calcd. for $C_{23}H_{16}NO_2$ $(M + H)^+$ 338.1176, found 338.1195.

11-Benzoyl-2-bromo-6*H*-isoindolo[2,1-*a*]indol-6-one (25d):

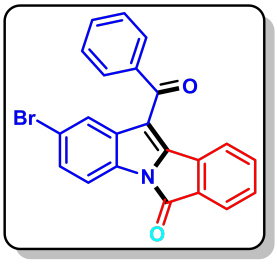

Pale Yellow Solid; R_f (Hexane/EtOAc, 4:1) 0.45; mp 201–203 °C. Yield 58 mg, 96%; ^{1}H NMR (500 MHz, $CDCl_3$) δ 7.91 (d, J = 7.5 Hz, 2 H), 7.83 (d, J = 8.5 Hz, 1 H), 7.77 (d, J = 7.5 Hz, 1 H), 7.68 (t, J = 7.5 Hz, 1 H), 7.62 (s, 1 H), 7.53 (t, J = 7.5 Hz, 2 H), 7.45 (d, J = 6.5 Hz, 1 H), 7.40–7.34 (m, 2 H), 6.99 (d, J = 6.0 Hz, 1 H); ^{13}C{^{1}H} NMR (125 MHz, $CDCl_3$) δ 191.2, 162.8, 143. 1, 139.1, 134.7, 134.1, 133.7, 133.6, 133.5, 131.8, 130.8, 130.1, 129.5, 129.2, 125.9, 125.8, 125.2, 118.2, 116.1, 114.6; IR (KBr, neat) 2924, 2853, 1743, 1638, 1551, 1442,

1365, 1231, 1216, 763, 749 cm^{-1}; HRMS (ESI) calcd. for $C_{22}H_{13}BrNO_2$ $(M + H)^+$ 402.0124, found 402.0129.

11-Benzoyl-2-methoxy-6*H*-isoindolo[2,1-*a*]indol-6-one (25e):

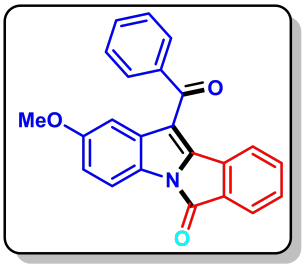

Red Solid; R_f (Hexane/EtOAc, 4:1) 0.5; mp 205–207 °C. Yield 52 mg, 99%; ^{1}H NMR (500 MHz, $CDCl_3$) δ 7.92 (d, J = 6.0 Hz, 2 H), 7.82 (d, J = 8.5 Hz, 1 H), 7.74–7.72 (m, 1 H), 7.65 (t, J = 7.0 Hz, 1 H), 7.52 (t, J = 7.5 Hz, 2 H), 7.34–7.29 (m, 2 H), 6.95–6.92 (m, 3 H), 3.73 (s, 3 H); ^{13}C{^{1}H} NMR (125 MHz, $CDCl_3$) δ 191.9, 162.9, 157.4, 143.0, 139.5, 134.3, 134.0, 133.8, 133.5, 133.4, 130.3, 129.5, 129.0, 127.8, 125.5, 124.8, 116.8, 115.7, 114.0, 106.2, 55.8; IR (KBr, neat) 2924, 2856, 1740, 1643, 1465, 1363, 1260, 1091, 1040, 749 cm^{-1}; HRMS (ESI) calcd. for $C_{23}H_{16}NO_3$ $(M + H)^+$ 354.1125, found 354.1142.

11-Benzoyl-7-methyl-6*H*-isoindolo[2,1-*a*]indol-6-one (25f):

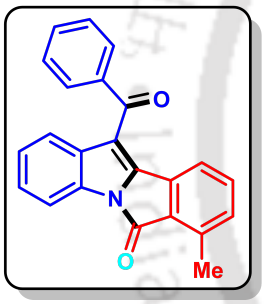

Yellow Solid; R_f (Hexane/EtOAc, 4:1) 0.55; mp 208–210 °C. Yield 45.5 mg, 90%; ^{1}H NMR (500 MHz, $CDCl_3$) δ 7.96 (d, J = 8.0 Hz, 1 H), 7.92 (d, J = 7.0 Hz, 2 H), 7.64 (t, J = 7.5 Hz, 1 H), 7.50 (t, J = 8.0 Hz, 2 H), 7.38 (d, J = 8.0 Hz, 1 H), 7.32 (t, J = 7.5 Hz, 1 H), 7.22 (d, J = 7.5 Hz, 1 H), 7.14 (t, J = 8.0 Hz, 1 H), 7.10 (d, J = 7.5 Hz, 1 H), 7.02 (d, J = 7.5 Hz, 1 H), 2.67 (s, 3 H); ^{13}C{^{1}H} NMR (125 MHz, $CDCl_3$) δ 191.9, 164.0, 142.2, 140.3, 139.5, 134.2, 134.1, 133.3, 133.1, 133.0, 132.5, 130.4, 129.6, 129.0, 127.0, 124.6, 123.1, 122.8, 116.4, 113.3, 17.6; IR (KBr, neat) 2924, 2853, 1736, 1455, 1366, 1277, 126, 1231, 1040, 749 cm^{-1}; HRMS (ESI) calcd. for $C_{23}H_{16}NO_2$ $(M + H)^+$ 338.1176, found 338.1195.

(2,3-Diphenylbenzo[5,6]pyrrolizino[1,2,3-*ij*]isoquinolin-7-yl) (phenyl)methanone (27a):

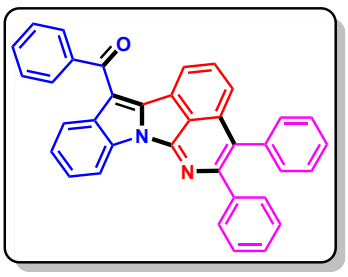

Black Solid; R_f (Hexane/EtOAc, 17:1) 0.5; mp 178–180 °C. Yield 31 mg, 63%; ^{1}H NMR (500 MHz, $CDCl_3$) δ 7.90 (d, J = 7.0 Hz, 2 H), 7.82 (d, J = 7.5 Hz, 1 H), 7.63 (t, J = 7.5 Hz, 1 H), 7.52 (t, J = 7.5 Hz, 2 H), 7.41–7.34 (m, 3 H), 7.24–7.19 (m, 4 H), 7.14 (d, J = 7.8 Hz, 2 H), 7.10–7.07 (m, 4 H), 7.04 (d, J = 7.5 Hz, 1 H), 6.71 (t, J = 8.0 Hz, 1 H), 6.06 (d, J = 7.5 Hz, 1 H); ^{13}C{^{1}H} NMR (125 MHz, $CDCl_3$) δ 191.9, 148.1, 146.4, 143.7, 141.8, 140.5, 140.1, 139.0, 135.5, 134.5, 133.7, 133.1, 132.7, 132.6, 130.8, 129.7,

129.3, 129.1, 129.1, 128.9, 127.5, 127.22, 127.2, 126.7, 124.7, 124.5, 124.3, 123.1, 121.2, 113.6; IR (KBr, neat) 2924, 2854, 1741, 1711, 1645, 1445, 1359, 1086, 1021, 798, 749 cm^{-1}; HRMS (ESI) calcd. for $C_{36}H_{23}N_2O$ $(M + H)^+$ 498.1805, found 498.1817.

(2,3-Diphenylbenzo[5,6]pyrrolizino[1,2,3-*ij*]isoquinolin-7-yl)(3-methoxyphenyl)methanone (27b):

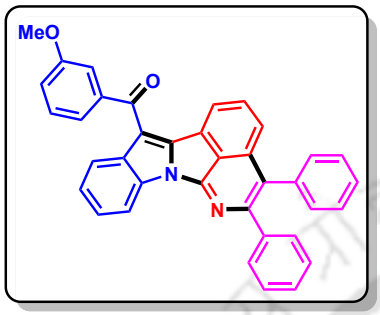

Black Solid; R_f (Hexane/EtOAc, 17:1) 0.55; mp 161–163 °C. Yield 35 mg, 67%; ^{1}H NMR (500 MHz, $CDCl_3$) δ 7.82 (d, J = 7.5 Hz, 1 H), 7.50 (d, J = 7.5 Hz, 1 H), 7.43–7.41 (m, 2 H), 7.40 (s, 1 H), 7.39–7.35 (m, 2 H), 7.24–7.21 (m, 3 H), 7.19 (d, J = 6.0 Hz, 2 H), 7.17 (s, 1 H), 7.14 (d, J = 8.0 Hz, 1 H), 7.10–7.07 (m, 4 H), 7.04 (d, J = 7.5 Hz, 1 H), 6.71 (t, J = 7.5 Hz, 1 H), 6.06 (d, J = 7.5 Hz, 1 H), 3.85 (s, 3 H); ^{13}C{^{1}H} NMR (125 MHz, $CDCl_3$) δ 191.5, 160.2, 148.1, 146.4, 143.7, 141.7, 141.7, 140.1, 139.0, 135.5, 134.5, 133.7, 133.1, 132.6, 130.8, 130.2, 129.7, 129.3, 128.9, 127.5, 127.2, 127.2, 126.7, 124.7, 124.5, 124.4, 123.1, 121.7, 121.3, 119.5, 113.6, 113.0, 55.8; IR (KBr, neat) 2924, 2853, 1742, 1630, 1541, 1470, 1366, 1266, 1032, 748, 699 cm^{-1}; HRMS (ESI) calcd. for $C_{37}H_{25}N_2O_2$ $(M + H)^+$ 529.1911, found 529.1921.

3.10 Representative Spectra

^{1}H spectrum of compound **24aa** (500 MHz, $CDCl_3$)

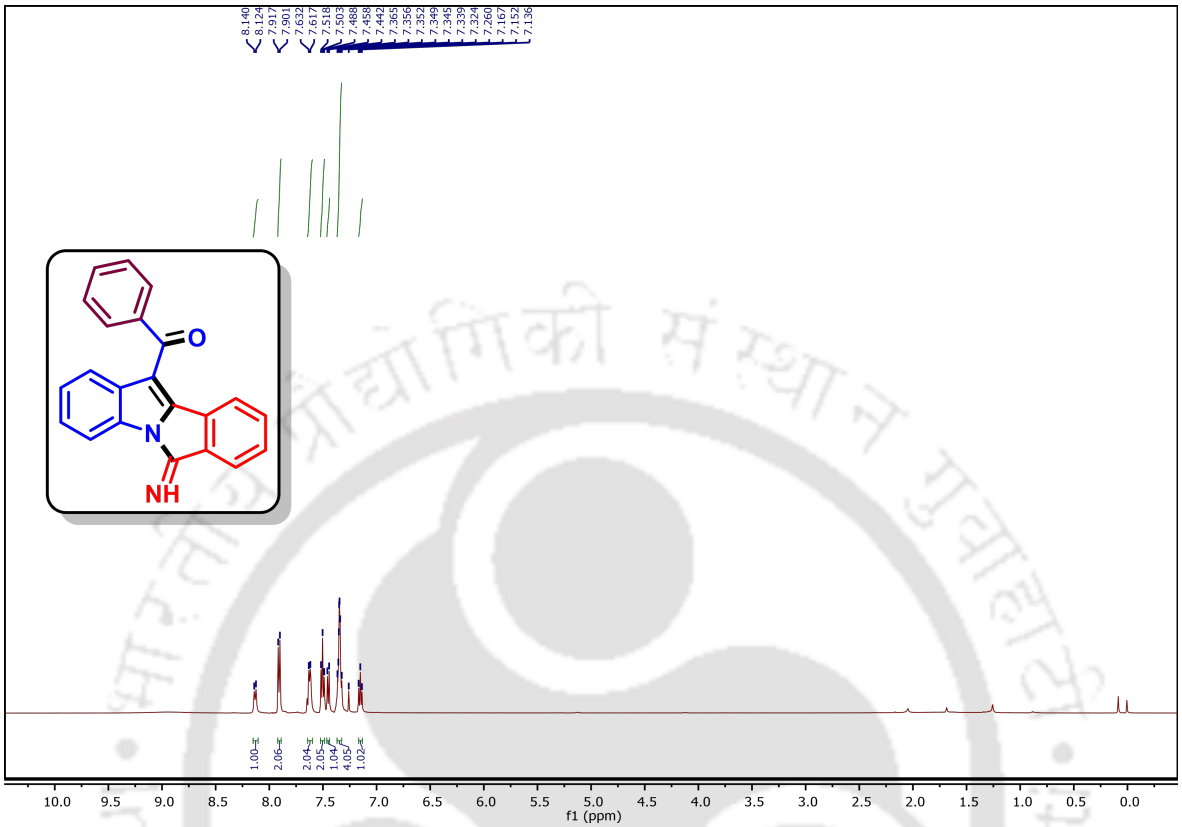

^{13}C{^{1}H} spectrum of compound **24aa** (125 MHz, $CDCl_3$)

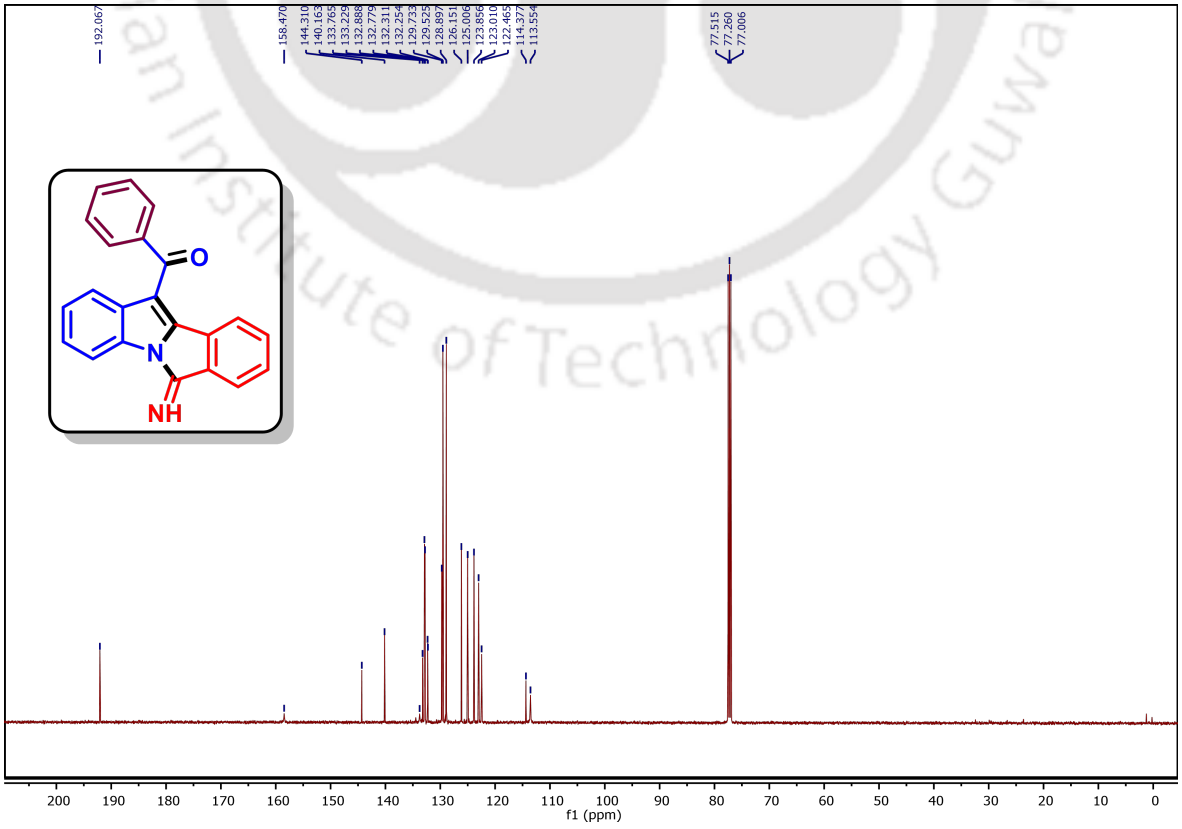

^{1}H spectrum of compound **24aj** (500 MHz, $CDCl_3$)

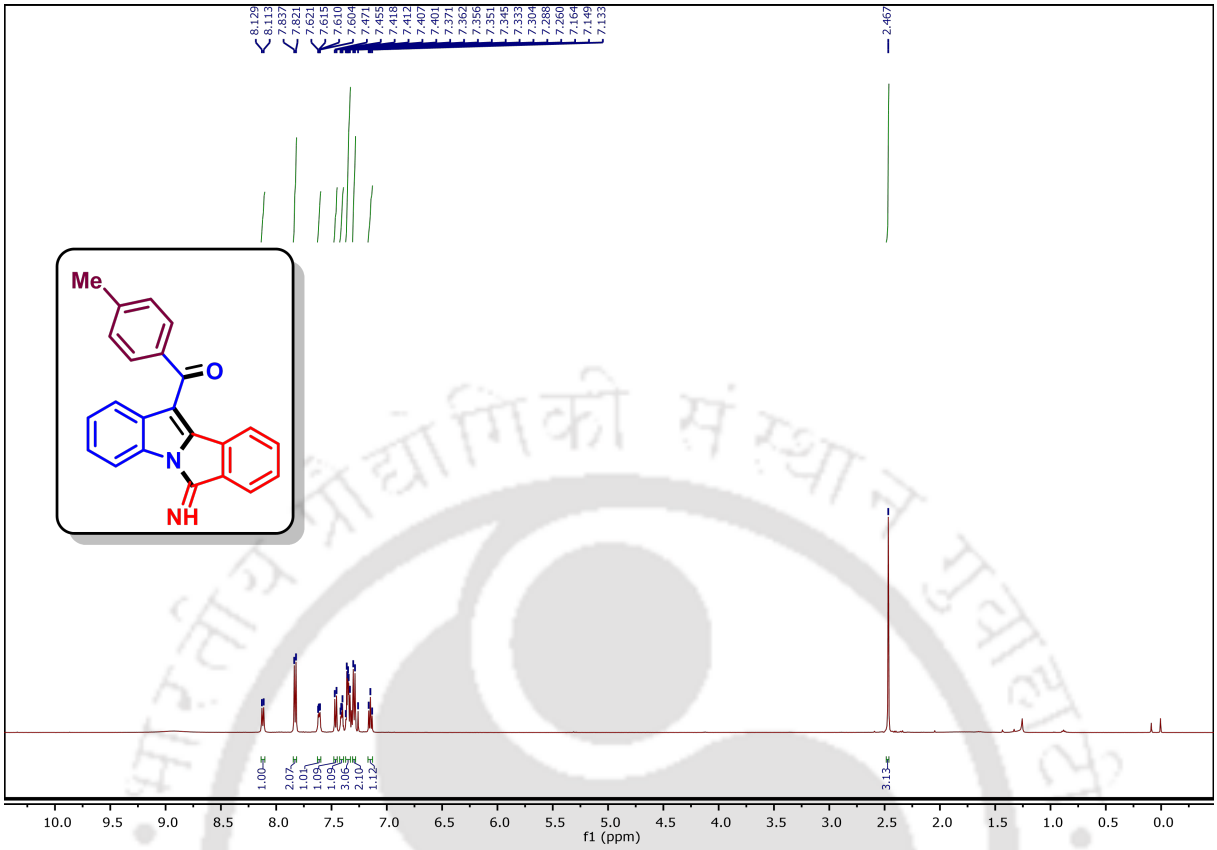

^{13}C{^{1}H} spectrum of compound **24aj** (125 MHz, $CDCl_3$)

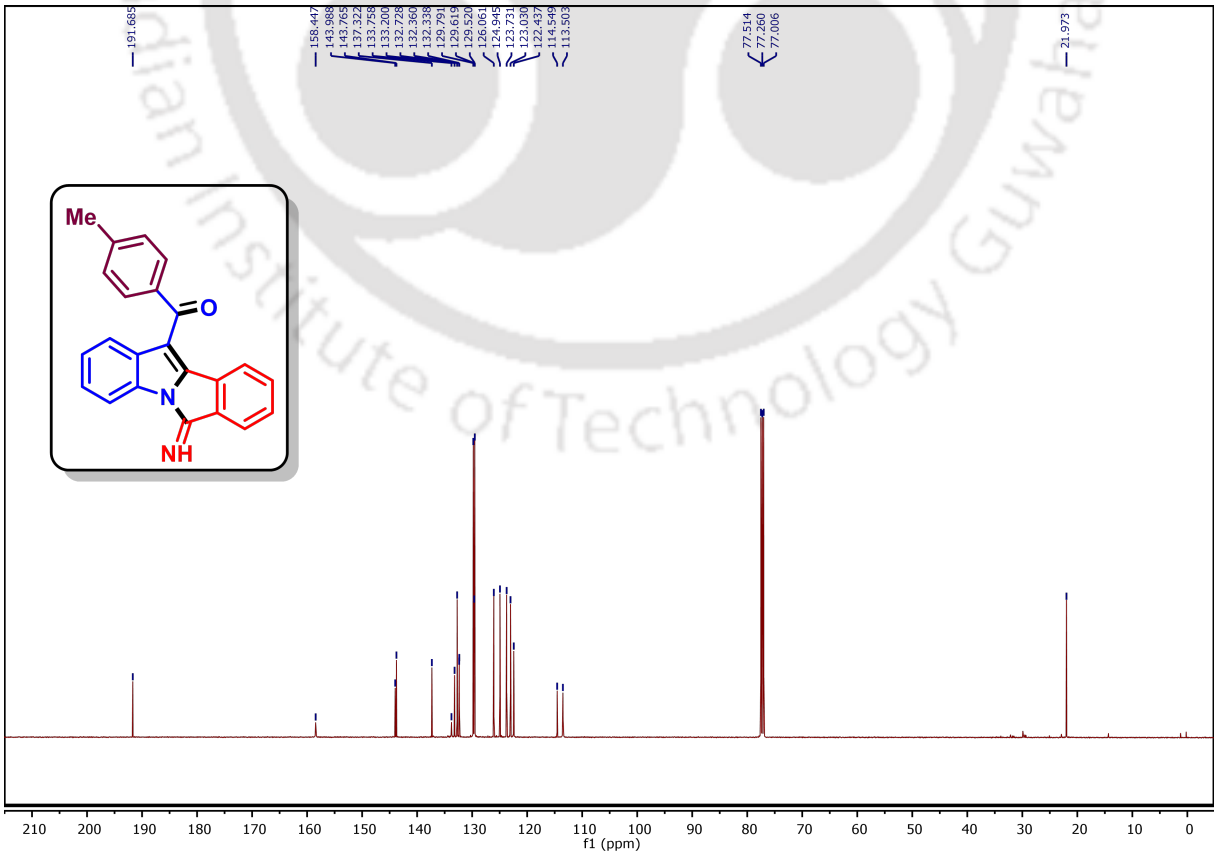

^{1}H spectrum of compound **24aq** (400 MHz, $CDCl_3$)

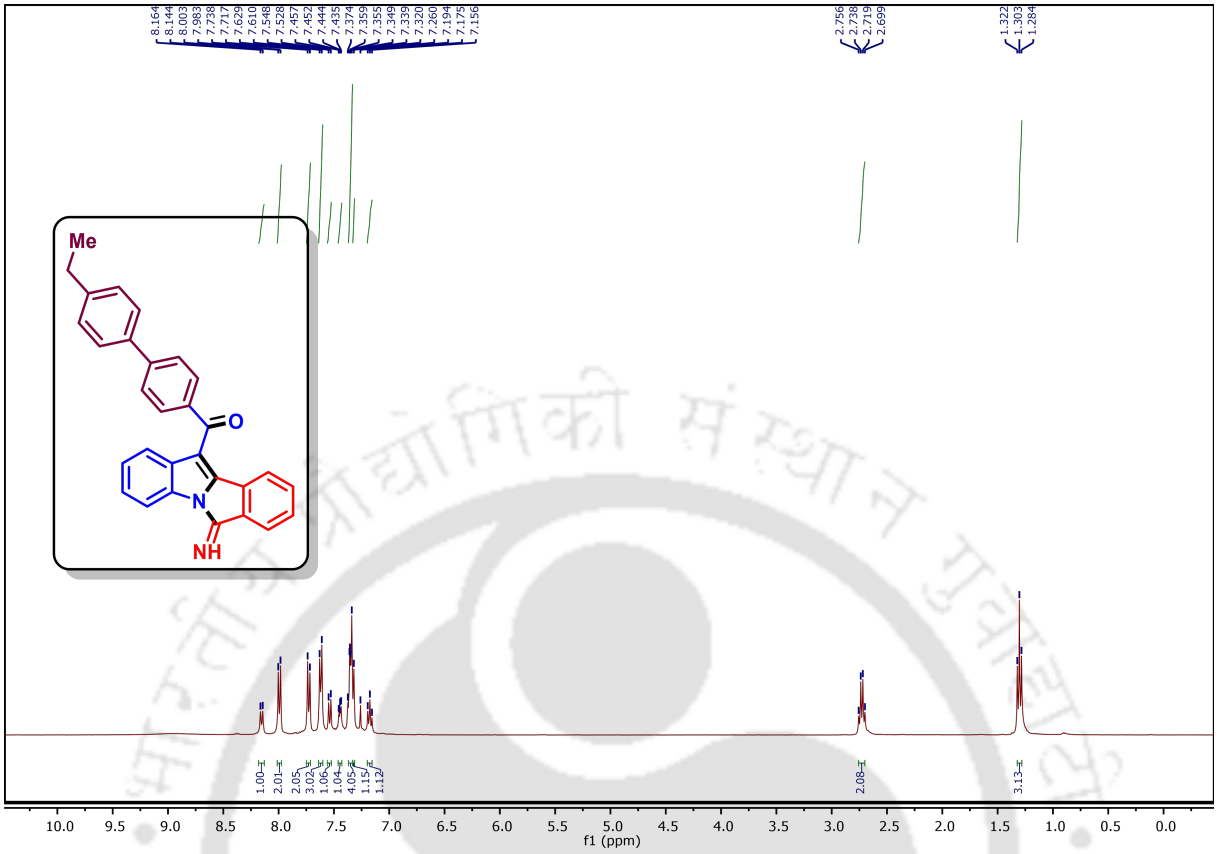

^{13}C{^{1}H} spectrum of compound **24aq** (125 MHz, $CDCl_3$)

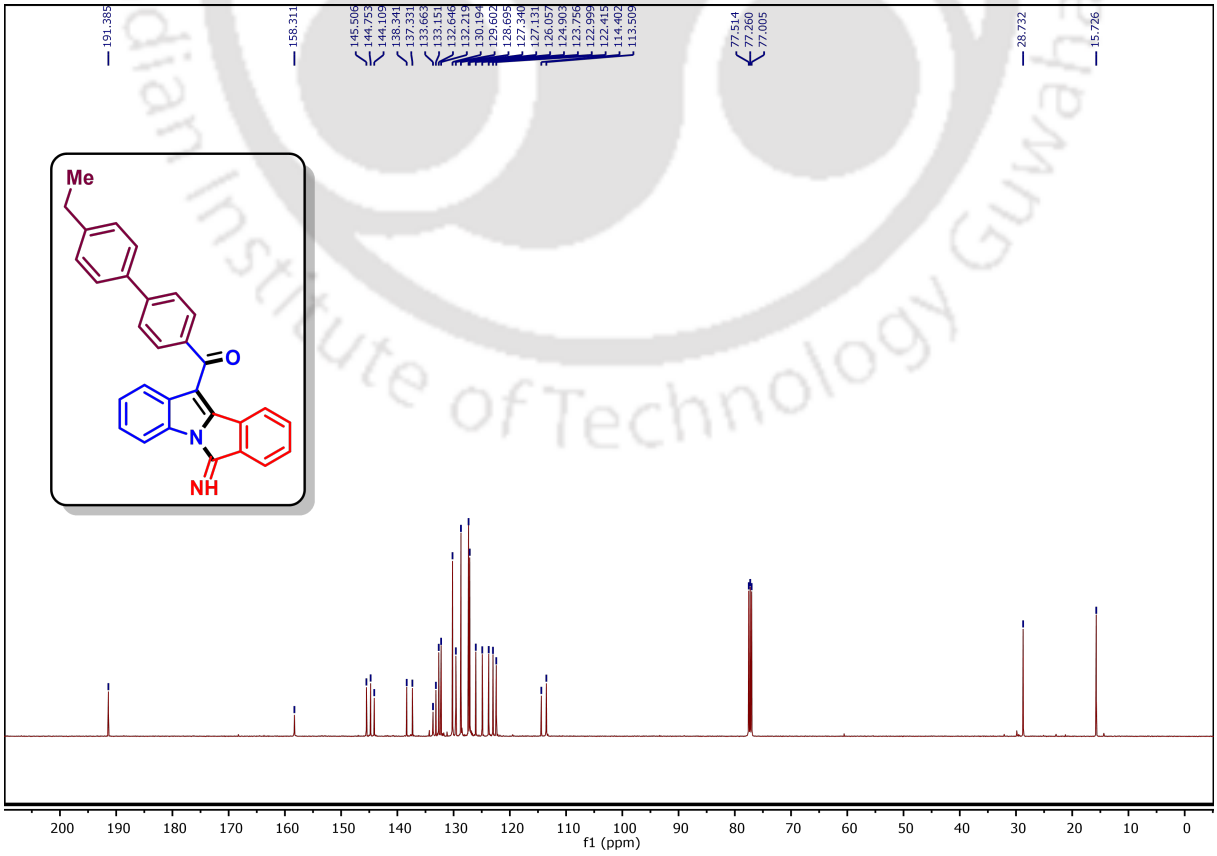

^{1}H spectrum of compound **24bc** (400 MHz, $CDCl_3$)

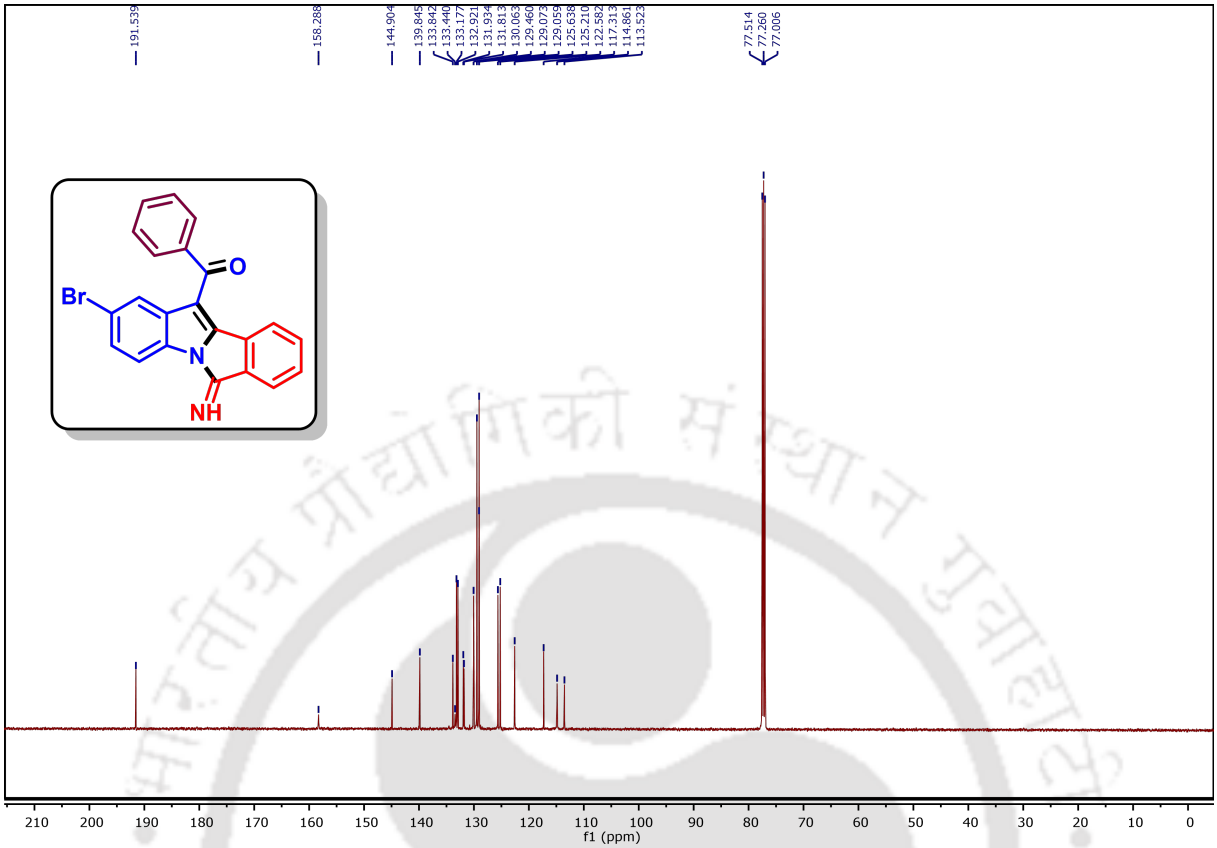

^{13}C{^{1}H} spectrum of compound **24bc** (125 MHz, $CDCl_3$)

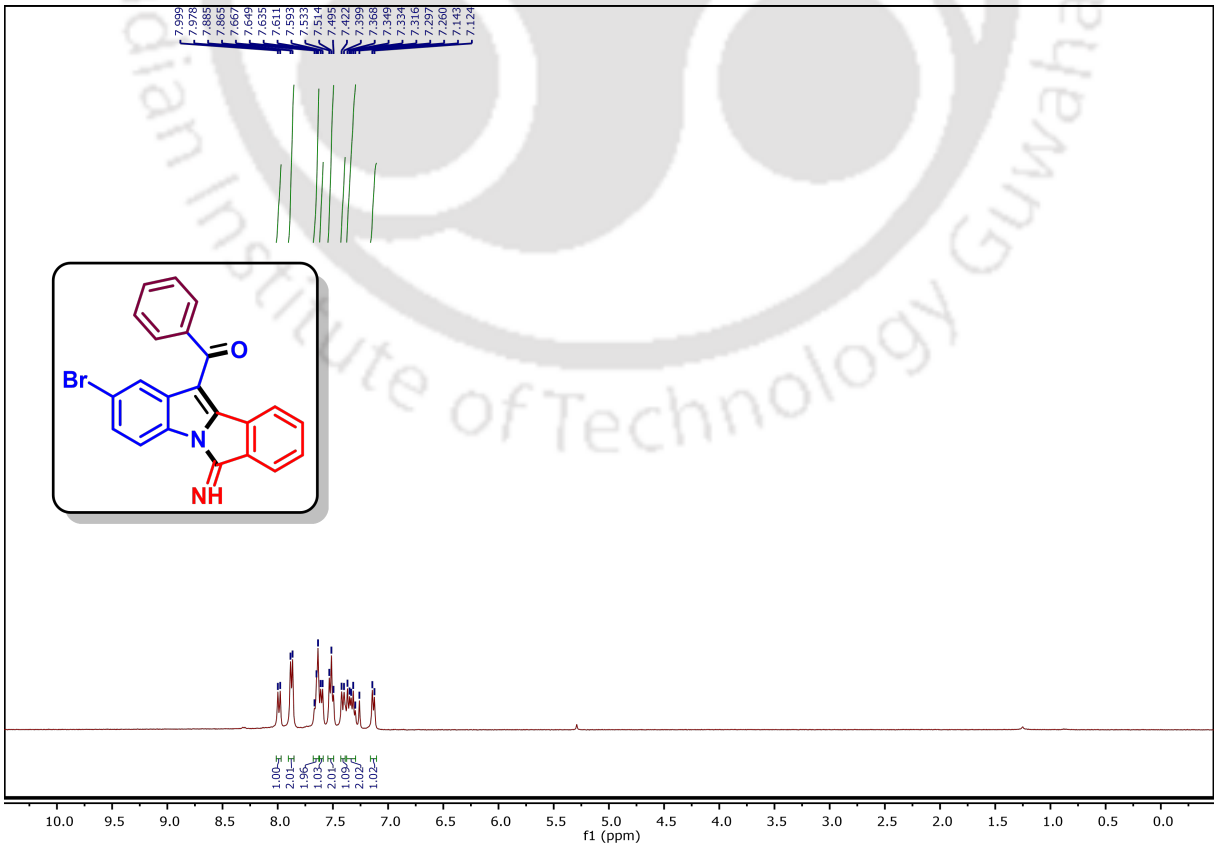

^{1}H spectrum of compound **25a** (500 MHz, $CDCl_3$)

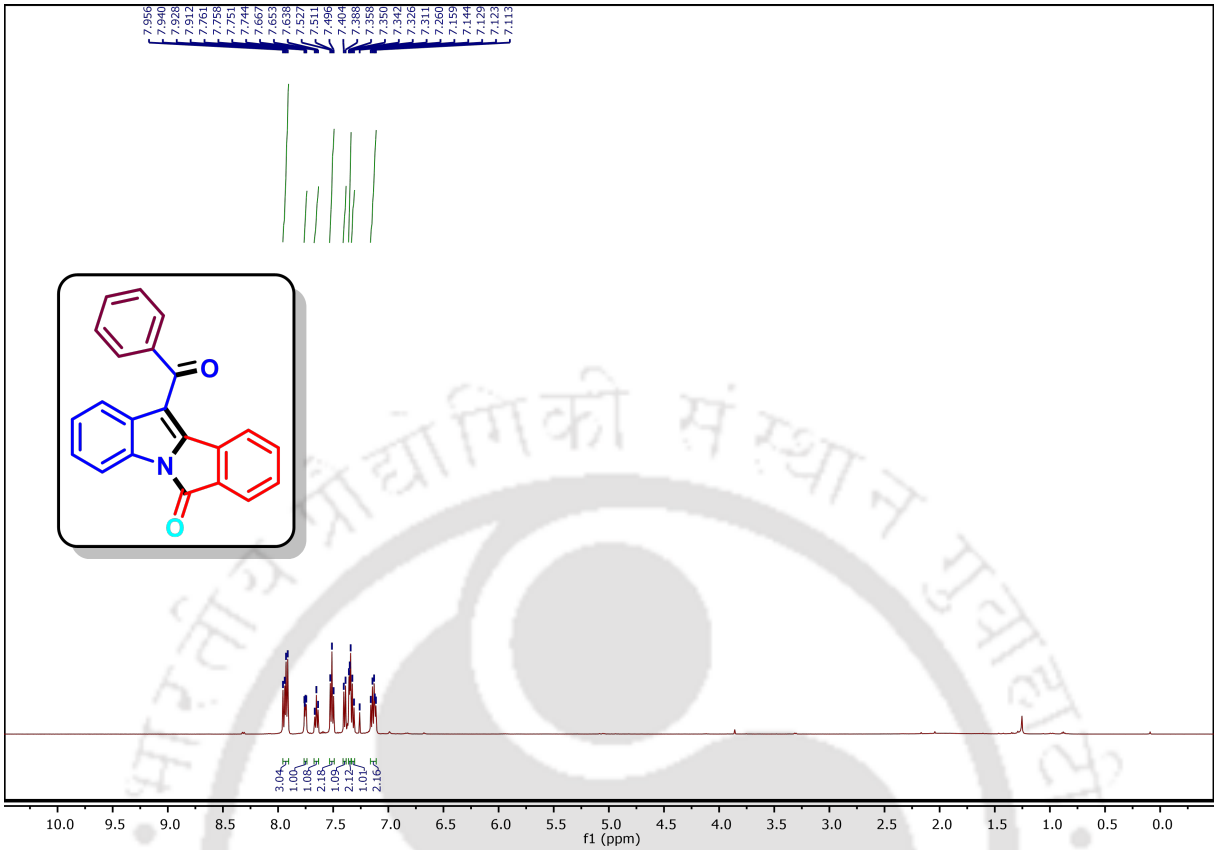

^{13}C{^{1}H} spectrum of compound **25a** (125 MHz, $CDCl_3$)

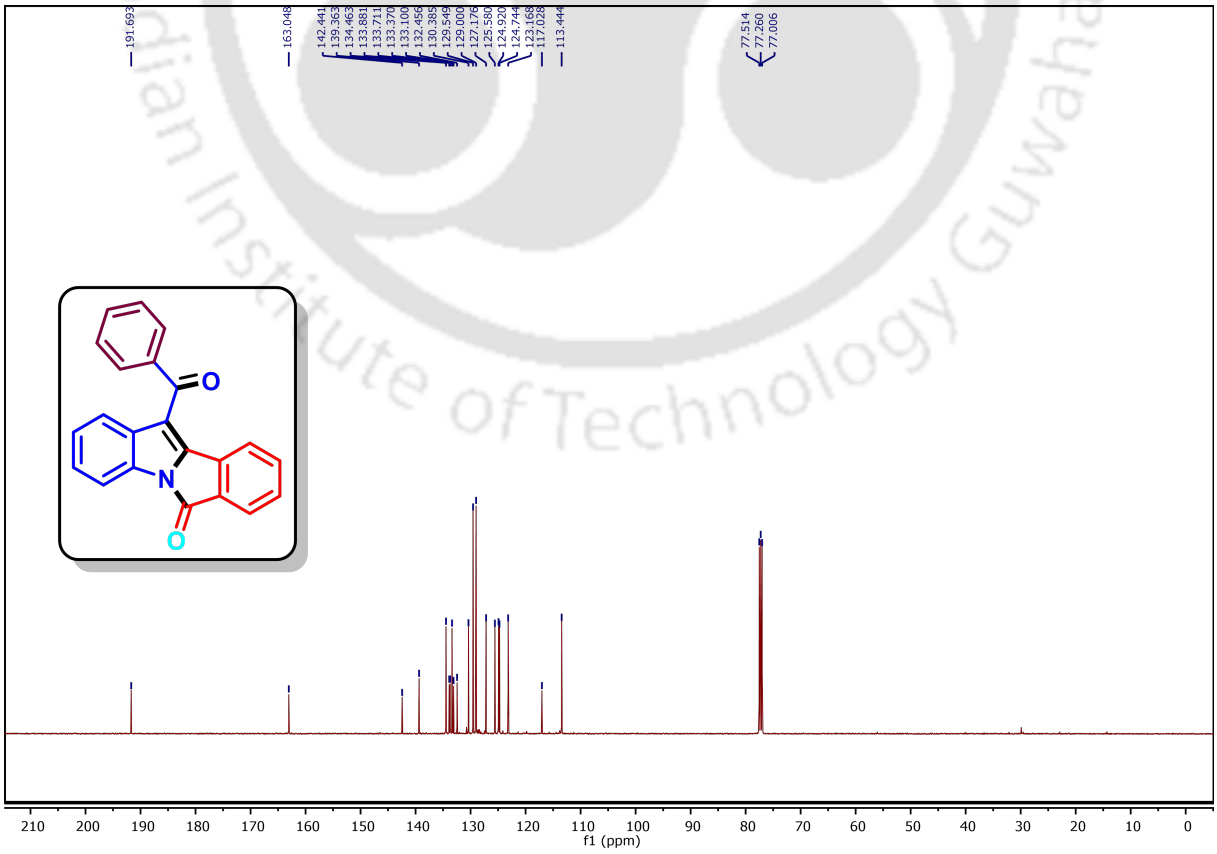

^{1}H spectrum of compound **25e** (500 MHz, $CDCl_3$)

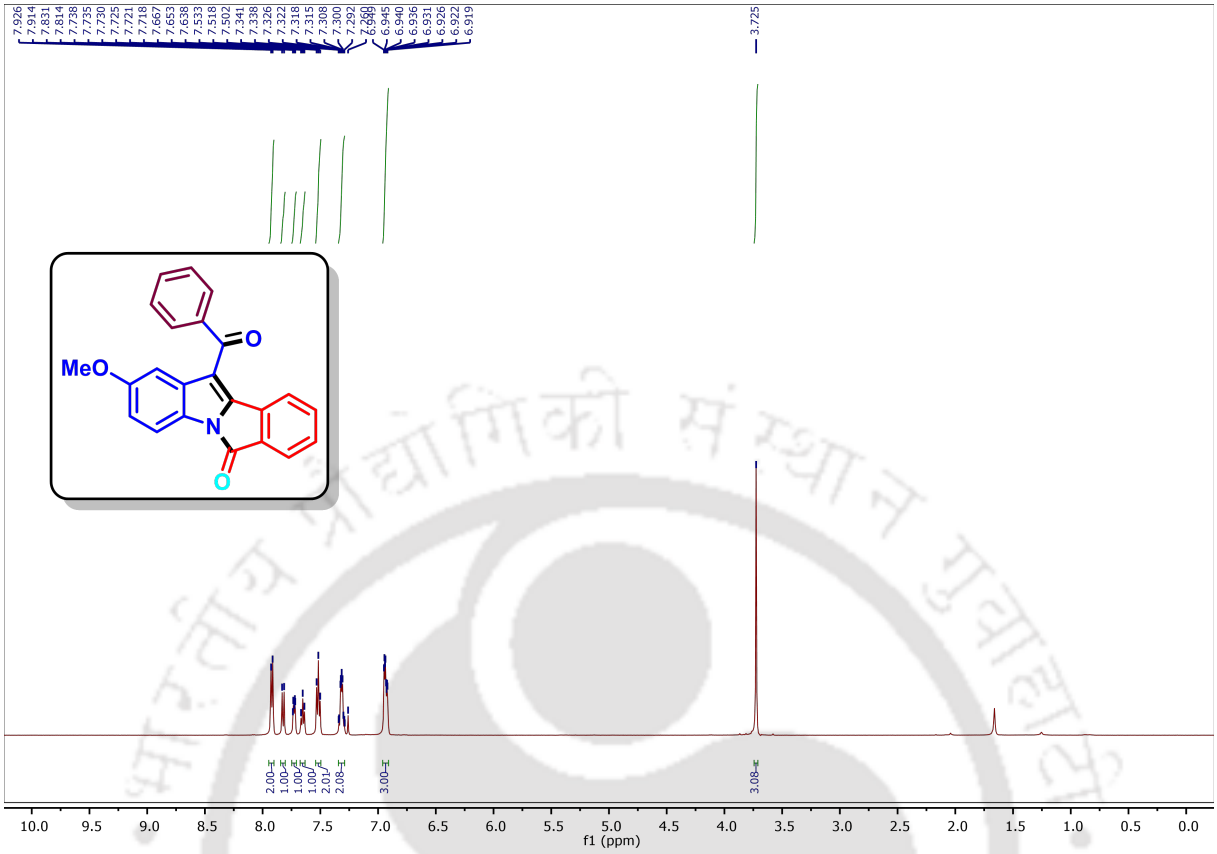

^{13}C{^{1}H} spectrum of compound **25e** (125 MHz, $CDCl_3$)

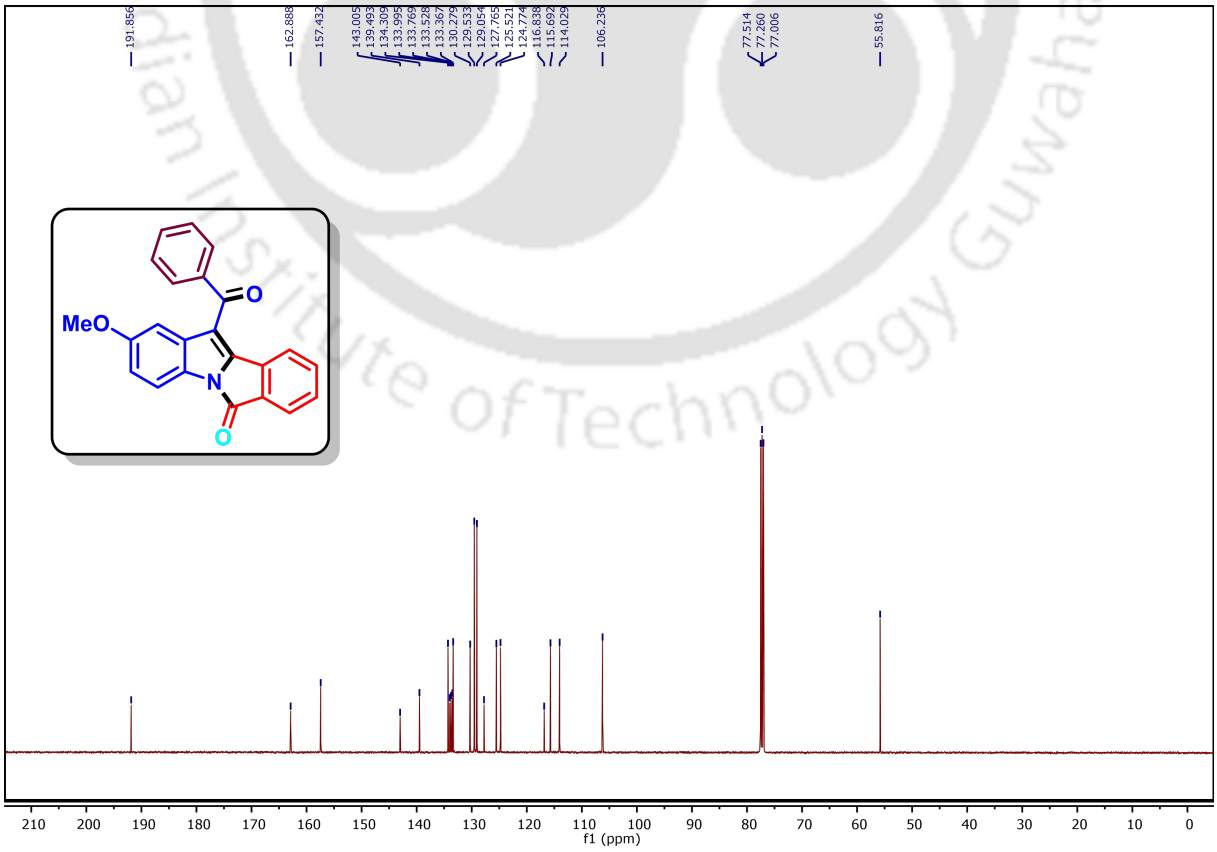

^{1}H spectrum of compound **27a** (500 MHz, $CDCl_3$)

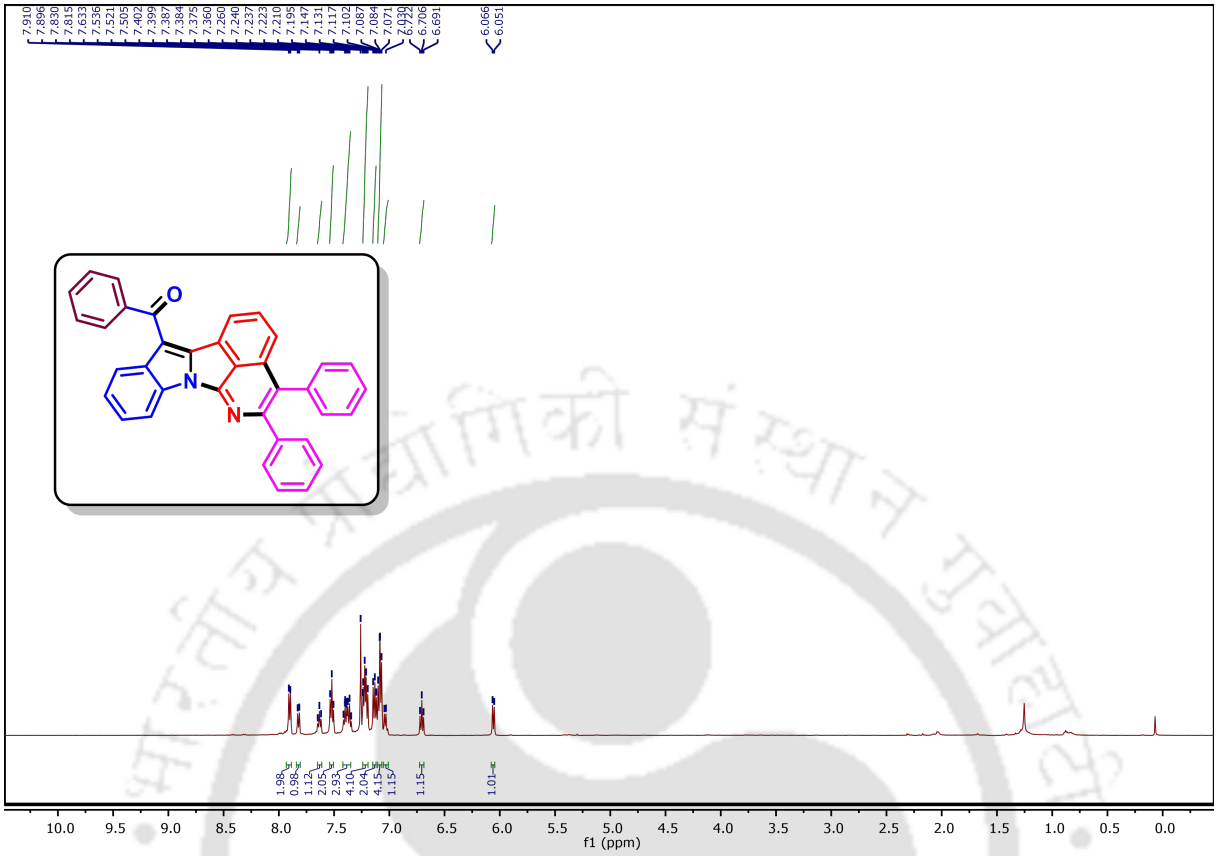

^{13}C{^{1}H} spectrum of compound **27a** (125 MHz, $CDCl_3$)

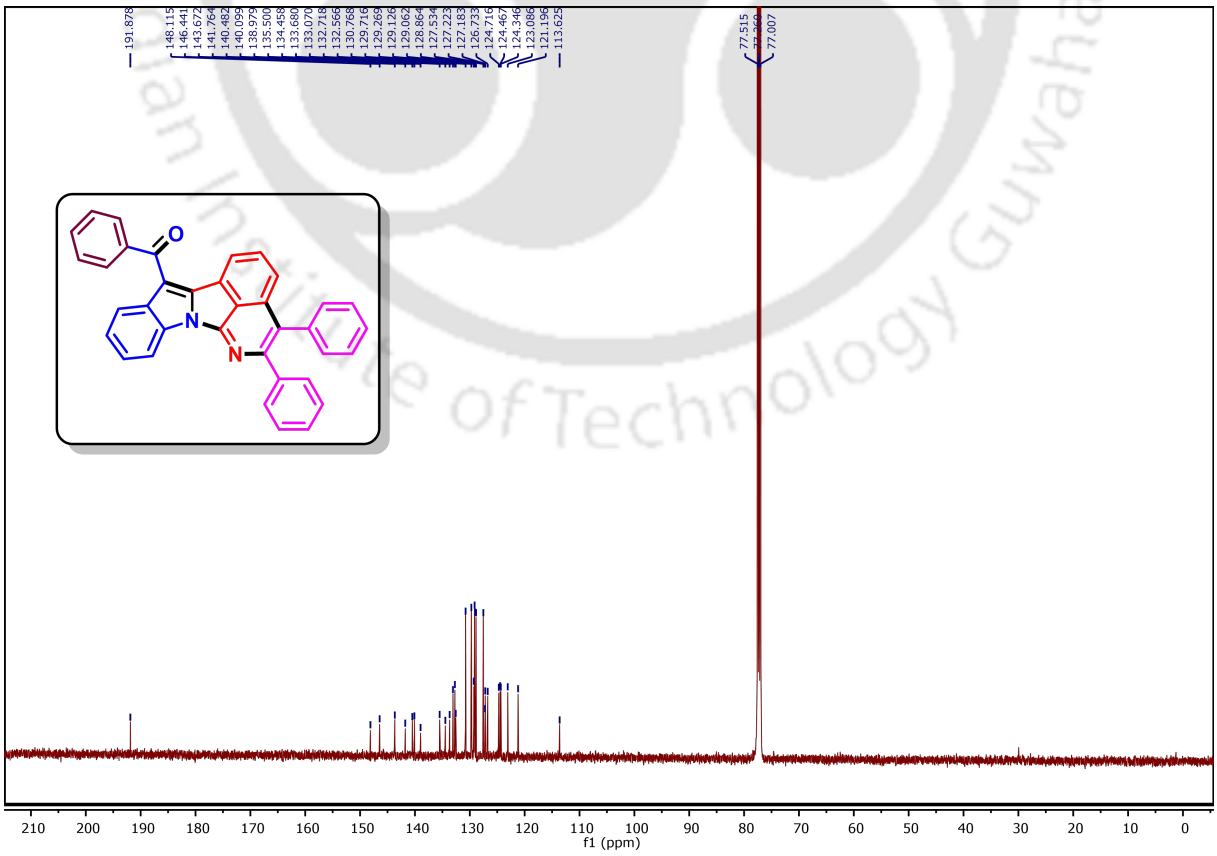

Chapter 4

Efficient Synthesis of Pseudoindoxyls from 2-Nitrobenzylidenemalonates and Indoles

Contents

Abstract: This chapter highlights a facile and efficient synthesis of structurally diverse pseudoindoxyls *via* indole-assisted Michael/Domino reaction of 2-nitrobenzylidenemalonates and indoles. The reaction is promoted by an inorganic base giving good to excellent yields. The reaction proceeds *via* Michael addition followed by nucleophilic addition-elimination and hydrolysis, where eco-friendly H_2O acts as an oxygen source in a cascade fashion. The developed methodology is a transition-metal-free novel and sustainable approach for the construction of pseudoindoxyl scaffolds with various functional group compatibility. The synthetic utility of the protocol was demonstrated by late-stage functionalization of the products, and photophysical properties have also been studied for some synthesized compounds.

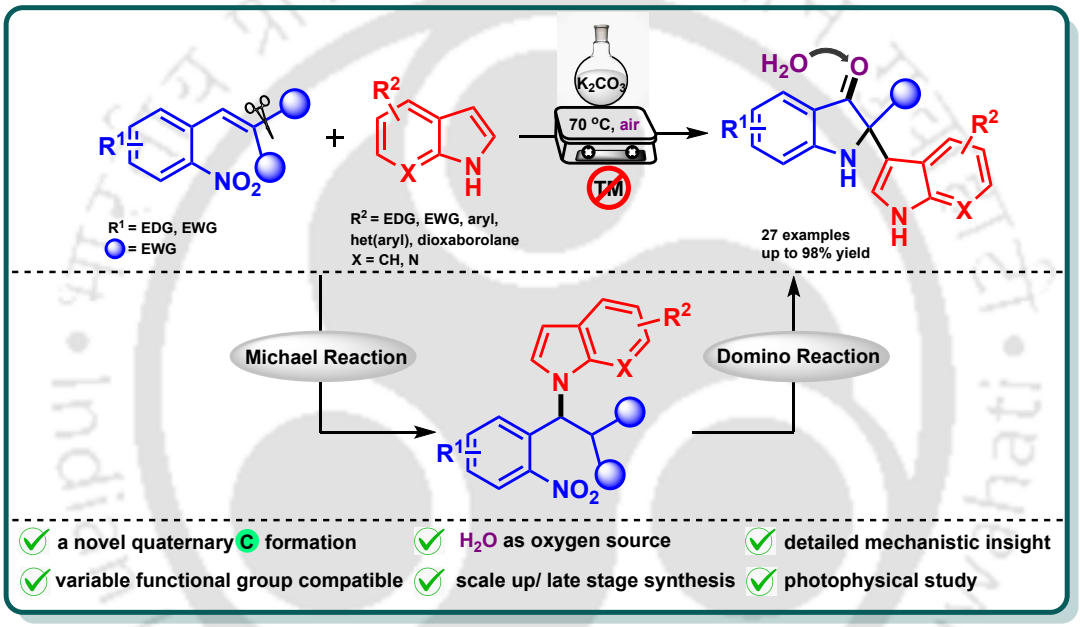

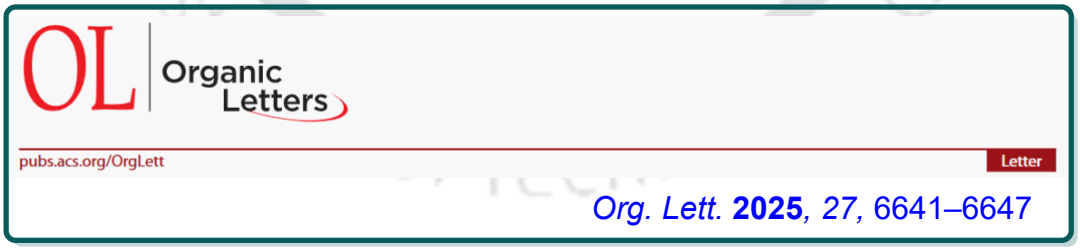

4.1 Introduction

Pseudoindoxyl (2,2-disubstituted indolin-3-one) derivatives that bear a quaternary stereocenter at the C2 position are a vital class of indole alkaloids having notable biological activities.[1] These scaffolds have drawn considerable attention due to their occurrence in a wide range of natural products such as halichrome A (**I**), isatisine A (**II**), austamide (**III**), cephalinone (**IV**), strobilanthoside A (**V**), and aristotelone (**VI**) (*Figure 4.1.1*).[2] Beyond their biological roles, pseudoindoxyls also have prominent applications in the fields of fluorescence labeling, optoelectronic materials, and solar cell technologies, highlighting their multipurpose utility.[3] The unique reactivity and functional versatility of pseudoindoxyls make them an attractive synthetic target in synthetic organic chemistry, enhancing extensive efforts towards developing efficient and enantioselective methods for their construction.

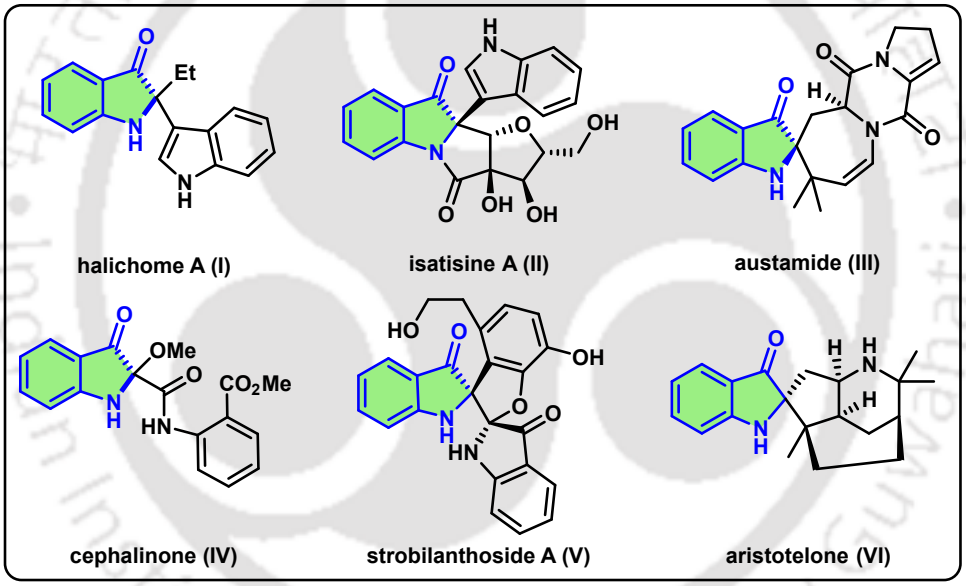

Figure 4.1.1. *Examples of biologically active pseudoindoxyls.*

4.2 Literature Survey on the Synthesis of Substituted Pseudoindoxyls

Owing to the structural complexity and diverse functionality of pseudoindoxyls (indolin-3-ones), enormous synthetic efforts[4] have been explored for the construction of these molecules, with various well-designed procedures being reported. Traditional synthetic approaches have largely relied on the oxidative rearrangement of indole derivatives,[5a] direct transformations from 3*H*-indol-3-ones or indolin-3-ones,[5b] and cyclization reactions from acyclic starting materials.[5c]

Here, a few examples for the synthesis of pseudoindoxyl derivatives have been presented:

Zhong and his group recently developed an enantioselective oxidative cross-coupling of 3-hydroxyindole esters **1** with various nucleophiles **2** to form functionalized 2,2-disubstituted indolin-3-ones **3** catalyzed by copper efflux oxidase (*Scheme 4.2.1*).[6] This H_2O_2-driven biocatalysis involving CueO offers simple operation, high atom economy, mild aqueous conditions, water as a by-product, and broad substrate scope.

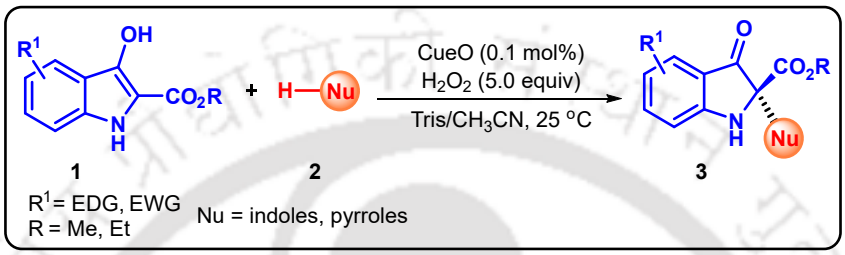

Scheme 4.2.1. *CueO-catalyzed synthesis of indolin-3-ones.*

Likewise, Baran and his colleague reported an oxidative coupling of 2-carboxymethyl-3-oxindole **4** with indoles/pyrroles **5** for the synthesis of substituted 2,2-disubstituted indolin-3-ones **6**, using CAN as the stoichiometric oxidant (*Scheme 4.2.2*).[7] The reaction proceeds under mild reaction conditions without pre-functionalization and tolerates diverse functional groups.

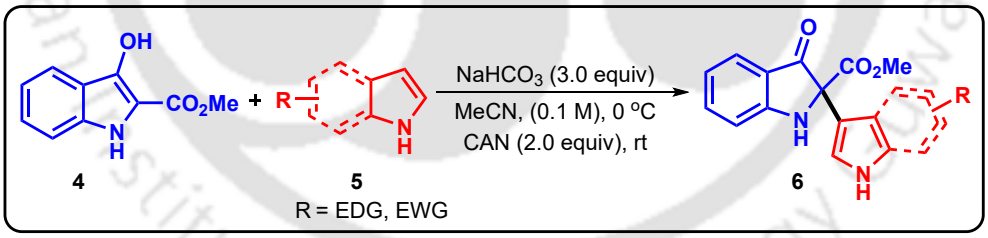

Scheme 4.2.2. *CAN-catalyzed synthesis of indolin-3-ones.*

In a recent development, West and co-workers introduced a dual catalytic action of $Cu(OTf)_2$ for azide–metallocarbene coupling of diazo–azide derivatives **7** with indoles **8** to synthesize 2-(3-indolyl)indolin-3-one scaffolds **9** (*Scheme 4.2.3*).[8] The overall process proceeds *via* a dual catalytic sequence at room temperature, where redox activation of $Cu(OTf)_2$ by indole generates Cu(I) for azide–metallocarbene coupling, while the resulting Brønsted acid catalyzes the C–C bond-forming indole addition step.

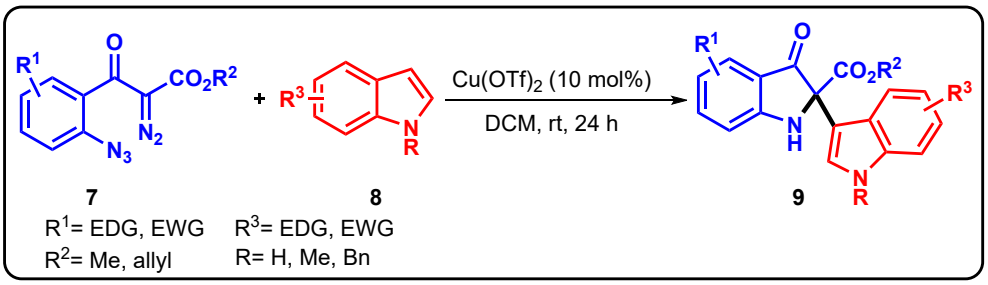

Scheme 4.2.3. *Cu-catalyzed synthesis of indolin-3-ones.*

Reddy and his group lately synthesized chiral indol-3-yl-3-indolinone-2-carboxylate derivatives **12** from indoles **11** and indolenines, derived *in situ* from 3-indolinone-2-carboxylates **10** using 3,3′-bis(triphenylsilyl)-1,1′-binaphthyl-2,2′-diyl hydrogen phosphate (BINOL phosphoric acid) as a catalyst (*Scheme 4.2.4*).[9] The reaction proceeds under mild conditions and provides chiral indol-3-yl-3-indolinone-2-carboxylate derivatives in good yields with excellent *ee* values.

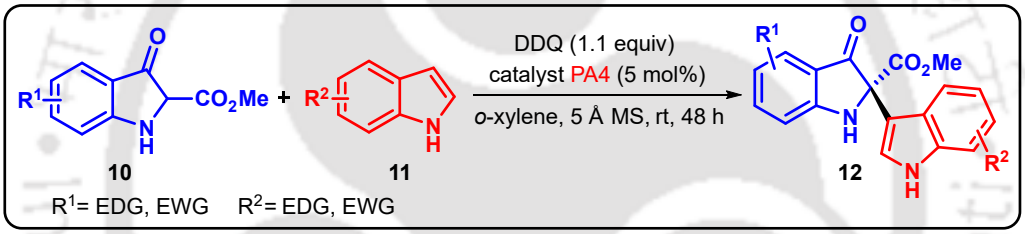

Scheme 4.2.4. *Chiral phosphoric acid-catalyzed synthesis of indolinone-2-carboxylates.*

Jia and colleagues developed a gold/chiral phosphoric acid dual-catalyzed enantioselective redox annulation of nitroalkynes **13** with indoles **14** to access *N*-hydroxy indolin-3-ones **15** (*Scheme 4.2.5*).[10] This method offers flexibility to yield the desired product through either a zwitterionic intermediate or a chiral ion pair. The subsequent reduction of the N-O bond to release the free amine was achieved with $N_2H_4{\cdot}H_2O$ as the reducing agent, resulting in the formation of indolin-3-ones **16**.

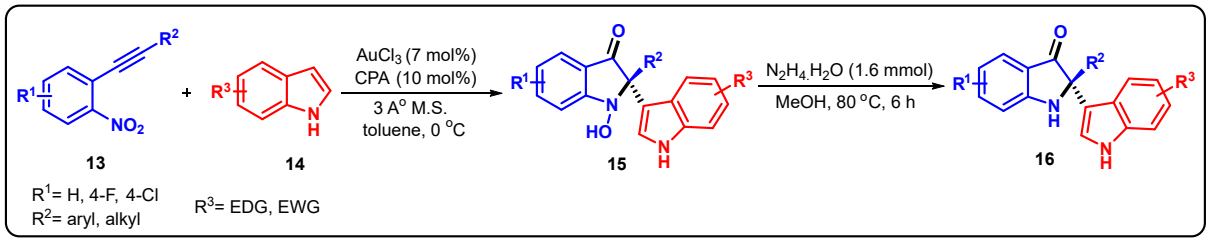

Scheme 4.2.5. *Gold/chiral phosphoric acid dual-catalyzed synthesis of indolin-3-ones.*

Zhao and co-workers unveiled a gold/copper-co-catalyzed one pot tandem reaction involving 2-alkynylanilines **17**, utilizing TBHP **18** as both the terminal oxidant and oxygen-atom source for the efficient synthesis of diverse 2,3′-bisindolin-3-ones **19** (*Scheme 4.2.6*).[11] This single-step process involves a tandem mechanism that comprises intermolecular nucleophilic addition, intramolecular cyclization, and oxidative cross-dehydrogenative coupling reactions.

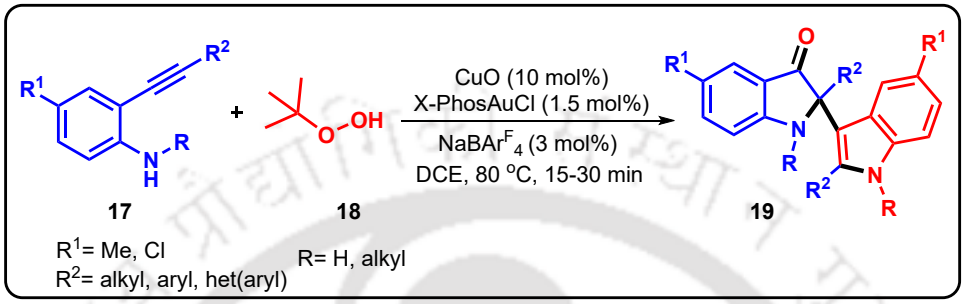

Scheme 4.2.6. *Gold/copper-co-catalyzed synthesis of bisindolin-3-ones.*

Fan and co-workers introduced a Cu(II)-catalyzed dimerization of 2-alkynylanilines **20** to synthesize 2-indolyl-3-oxoindolines **21** (*Scheme 4.2.7*).[12] The mechanistic pathway for producing 2-indolyl-3-oxoindolines involves a $Cu(OAc)_2/O_2$-promoted intramolecular cyclization of 2-alkynylaniline, yielding the essential indole and 3*H*-indol-3-one intermediates, followed by the indolylation of 3*H*-indol-3-one.

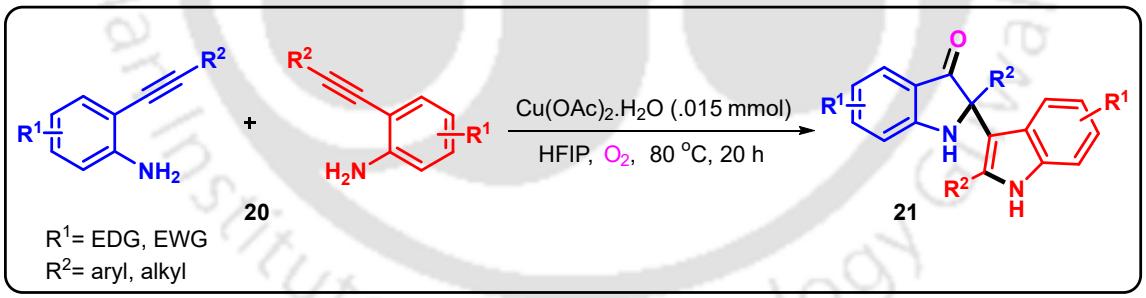

Scheme 4.2.7. *Cu(II)-catalyzed synthesis of 3-oxoindolines.*

4.3 Present Work

These literature findings suggest that these methods often suffer from certain drawbacks, including the need for harsh reaction conditions, the use of noble transition metals, or the necessity for multi-step synthesis of starting materials. As a result, there remains a strong demand for more straightforward, efficient, and sustainable synthetic approaches, particularly those that enable the direct formation of these

complex structures from readily available acyclic starting materials in a simple and cost-effective manner.

However, as per the existing literature report (*Scheme 4.3.1a*),[13] the reaction of 2-alkynylbenzylidene malonate with indole *via* base leads to the formation of 2,2-disubstituted 1*H*-indene scaffold through a tandem Michael addition followed by nucleophilic addition reactions. In this context, we assumed that the reaction of 2-nitrobenzylidene malonate with indole in the presence of a base would yield oxoindolinium moiety *via* Michael addition and subsequent tandem reactions (*Scheme 4.3.1b*). But, to our surprise, 2,2-disubstituted indolin-3-one was isolated from the proposed reaction.

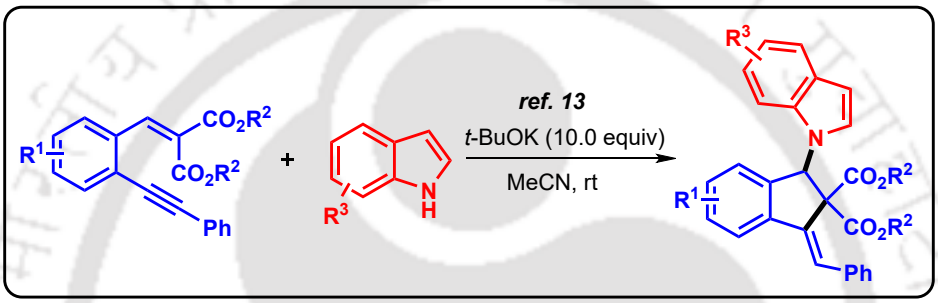

Scheme 4.3.1a. *Previous reports on the reactivity of 2-alkynylbenzylidene malonate with indole via base.*

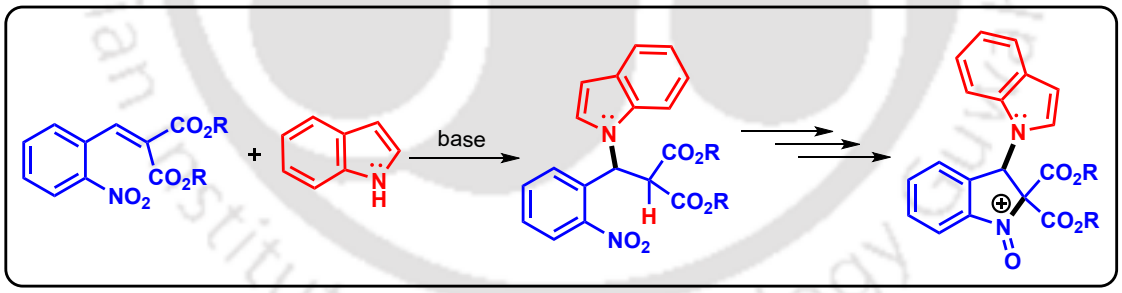

Scheme 4.3.1b. *Our hypothesis on the reactivity of 2-nitrobenzylidene malonate with indole via base.*

Thus, this chapter describes a simple methodology for the efficient synthesis of 2-(indol-3-yl)-indolin-3-one-2-carboxylate derivatives **24** that comprises of the reaction of 2-nitrobenzylidenemalonates **22** with indoles **23** in the presence of a mild base such as potassium carbonate (*Scheme 4.3.1c*).

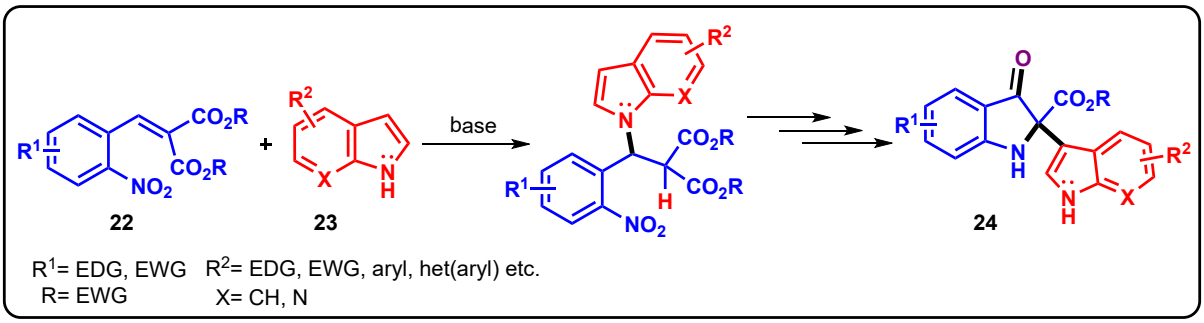

Scheme 4.3.1c. *Synthesis of indolin-3-ones via tandem reactions.*

4.4 Results and Discussion

4.4.1 Optimization of the Reaction

To explore our assumption, we initially took 2-diethyl 2-(2-nitrobenzylidene)malonate (**22a**) and 1*H*-indole (**23a**) as model substrates. In the beginning, **22a** (1.0 equiv) and **23a** (1.1 equiv) were subjected to react with K_2CO_3 (1.0 equiv) in acetonitrile (CH_3CN) at room temperature. After 6 h, intermediate **A** was isolated in a 75% yield (*Table 4.4.1.1,* entry 1). Structural analysis using NMR (^1H and $^{13}C\{^1H\}$) spectroscopy and HRMS confirmed the intermediate **A** as diethyl 2-((1*H*-indol-1-yl)(2-nitrophenyl)methyl)malonate. When the reaction was further performed by elevating the temperature to 70 °C, maintaining the other reaction conditions, we successfully isolated the product ethyl 2-(1*H*-indol-3-yl)-3-oxoindoline-2-carboxylate (**24aa**) in 74% yield within 2 h (*Table 4.4.1.1,* entry 2).

Next, we tried to optimize the reaction by screening different solvents, including 1,2-DCE, DCM, DMF, DMSO, 1,4-dioxane, and toluene (*Table 4.4.1.1,* entries 3–8). Out of them, 1,2-DCE and DCM were ineffective, yielding no product (*Table 4.4.1.1,* entries 3 and 4). However, DMF proved to be efficient, providing an improved yield of 80% (*Table 4.4.1.1,* entry 5). Other solvents, such as DMSO and 1,4-dioxane failed to increase the yield (*Table 4.4.1.1,* entries 6 and 7), while toluene led to decomposition of the starting materials (*Table 4.4.1.1,* entry 8). Again, when we tried to perform the reaction in a mixture of DMF and water (1:1) (*Table 4.4.1.1,* entry 9) and water (*Table 4.4.1.1,* entry 10), they were only able to deliver the intermediate **A** in 49 and 40%, respectively where the former one produced a trace amount of our desired product **24aa** also. Based on these observations, DMF was found to be the most suitable solvent for this transformation. Further, increasing the K_2CO_3 loading to 1.5 equiv increased the yield up to 85% (*Table 4.4.1.1,* entry 11) and again, increasing

Table 4.4.1.1. *Optimization of the reaction*[a]

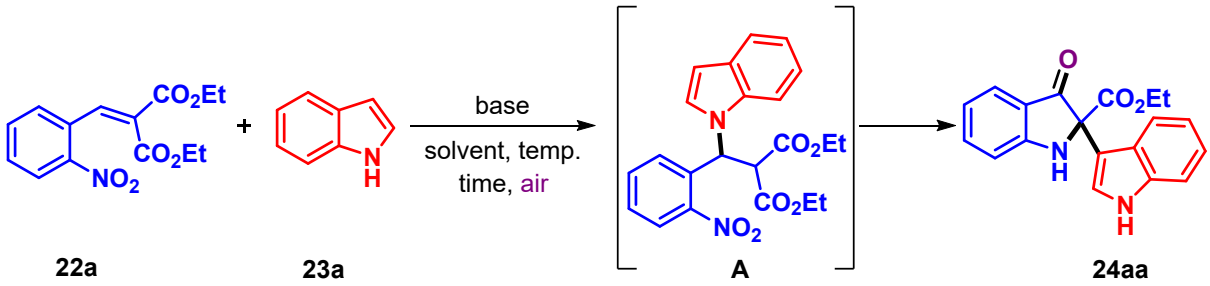

Entry[a]	Reagent (equiv)	Solvent	Temp (°C)	Time (h)	Yield (%)[b] (A)	Yield (%)[b] (24aa)
1.	K_2CO_3 (1.0)	CH_3CN	rt	6.0	75	-
2.	K_2CO_3 (1.0)	CH_3CN	70	2.0	-	74
3.	K_2CO_3 (1.0)	1,2-DCE	70	12.0	-	N.R
4.	K_2CO_3 (1.0)	DCM	70	12.0	-	N.R
5.	K_2CO_3 (1.0)	DMF	70	2.0	-	80
6.	K_2CO_3 (1.0)	DMSO	70	3.0	-	65
7.	K_2CO_3 (1.0)	1,4-Dioxane	70	3.0	-	63
8.	K_2CO_3 (1.0)	Toluene	70	0.5	-	_[c]
9.	K_2CO_3 (1.0)	DMF:H_2O	70	3.0	49	trace
10.	K_2CO_3 (1.0)	H_2O	70	0.5	40	-
11.	**K_2CO_3 (1.5)**	**DMF**	**70**	**1.0**	**-**	**85**
12.	K_2CO_3 (2.0)	DMF	70	1.0	-	78
13.	K_2CO_3 (1.5)	DMF	100	1.0	-	82
14.	K_2CO_3 (1.5)	DMF	50	4.0	-	70
15.	Cs_2CO_3 (1.5)	DMF	70	1.0	-	77
16.	KO^{t}Bu (1.5)	DMF	70	1.0	-	75
17.	NaH (1.5)	DMF	70	4.0	-	43
18.	DBU (1.5)	DMF	70	12.0	-	N.R
19.	K_3PO_4 (1.5)	DMF	70	2.0	-	71

[a]**22a** (0.34 mmol), **23a** (0.37 mmol), solvent 2.0 mL. [b]Isolated yield, [c]Decomposed product, N.R.= no reaction.

it to 2.0 equiv, resulting in a slight decrease in the yield (*Table 4.4.1.1,* entry 12). Additionally, a few reactions were also performed to improve the yield by adjusting the temperature to 100 °C as well as 50 °C, but both were unsuccessful in delivering a higher yield (*Table 4.4.1.1,* entries 13 and 14). Subsequently, we also tried various bases including Cs_2CO_3, KO^{t}Bu, NaH, DBU, and K_3PO_4 (*Table 4.4.1.1,* entries 15–19). Out of them, Cs_2CO_3 and KO^{t}Bu gave moderate yields of 77% and 75%, respectively, and NaH led to a significantly lower yield of 43% (*Table 4.4.1.1,* entries 15–17). Besides, DBU proved to be completely ineffective (*Table 4.4.1.1,* entry 18), and K_3PO_4 failed to improve the yield (*Table 4.4.1.1,* entry 19) for this transformation.

Considering all these observations, the optimized conditions for this reaction were determined to be K_2CO_3 (1.5 equiv) in DMF at 70°C (*Table 4.4.1.1,* entry 11), providing the maximum yield and efficiency for the reaction.

4.4.2 Substrate Scope

Using the established optimized reaction conditions, the substrate scope of the reaction was explored with a wide variety of 2-nitrobenzylidenemalonates **22** and 1*H*-indoles **23**. Initially, diethyl 2-(2-nitrobenzylidene)malonate was varied with both electron-donating as well as electron-withdrawing groups in the aromatic ring (R^1) as shown in *Scheme 4.4.2.1.* Moderate electron-withdrawing groups like –Cl, –Br, and –F on 2-nitrobenzaldehyde delivered their respective products **24ab-24ad**, with 80%, 79%, and 83% yields, respectively. However, strong electron-withdrawing groups like $-CF_3$ and $-CO_2Me$ were also well-tolerated, giving corresponding products **24ae** and **24af** in good yields (63-67%). The presence of two –Cl groups on the aromatic ring also furnished its respective product **24ag** smoothly, with a yield of 77%. On the other hand, electron-donating groups like –Me and –OMe were found to be effective, providing their respective products **24ah** and **24ai** in outstanding yields (91-95%). The introduction of two –OMe groups on the aromatic ring resulted in 97% yield of its product **24aj**. The high yields of products **24ah-24aj** might be due to the stabilization of the 1-oxoindolinium ion by electron-donating –Me and –OMe groups. In addition to this, the variations in the R group of the ester of 2-nitrobenzylidenemalonates **22** were also explored (*Scheme 4.4.2.1*). Substituting the –Et group with –Me and –^{i}Pr groups showed comparable reactivity, leading to 81% and 87% yields of products **24ak** and **24al**, respectively.

To further validate the versatility of this protocol, we also examined various substituents on 1-*H* indoles **23** (R^2) (*Scheme 4.4.2.2*). Moderate electron-withdrawing

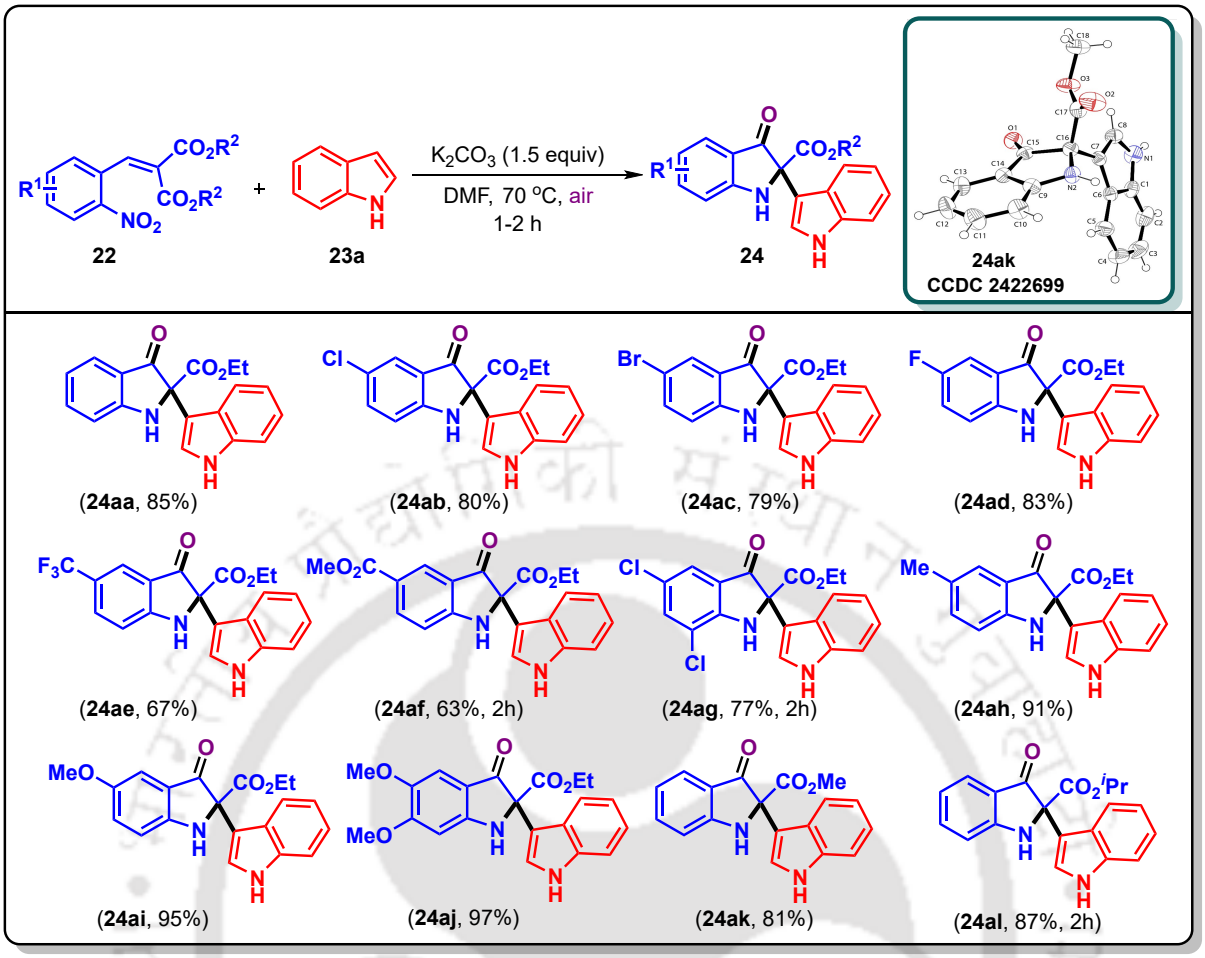

[a]Reaction condition: **22** (0.51 mmol, 1.0 equiv), **23a** (0.56 mmol, 1.1 equiv), solvent 4.0 mL. [b]Isolated yield of the product.

Scheme 4.4.2.1. *Scope of different functionalized 2-nitrobenzylidenemalonates.*[a,b]

groups afforded their respective products **24bb-24bd** in good yields (82-91%). Strong electron-withdrawing groups like $-NO_2$ and –CN were also well tolerated, delivering moderate yields of their respective products **24be** and **24bf** (75-76%). Electron-donating groups exhibited excellent reactivity towards this transformation. For example, a –Me group on 1-*H* indole afforded its product **24bg** in 95% yield, while strong electron-donating groups like –OMe and –^{t}Bu gave 98% yields of their products **24bh** and **24bi**, respectively. This might be due to the increase in nucleophilicity on the indole moiety by electron-donating –Me, –OMe, and –^{t}Bu groups. Furthermore, the introduction of 4,4,5,5-tetramethyl-1,3,2-dioxaborolane on 1-*H* indole provided 85% yield of its corresponding product **24bj**. Phenyl and heterocyclic thiophene rings also proceeded well under the reaction conditions, delivering 97% and 96% yields of their products **24bk** and **24bl**, respectively. Unfortunately, the reaction with 1-*H* indazole **23m** did not proceed, resulting in decomposition. This could be attributed to the electronegativity of an additional nitrogen atom, which reduces its nucleophilicity.

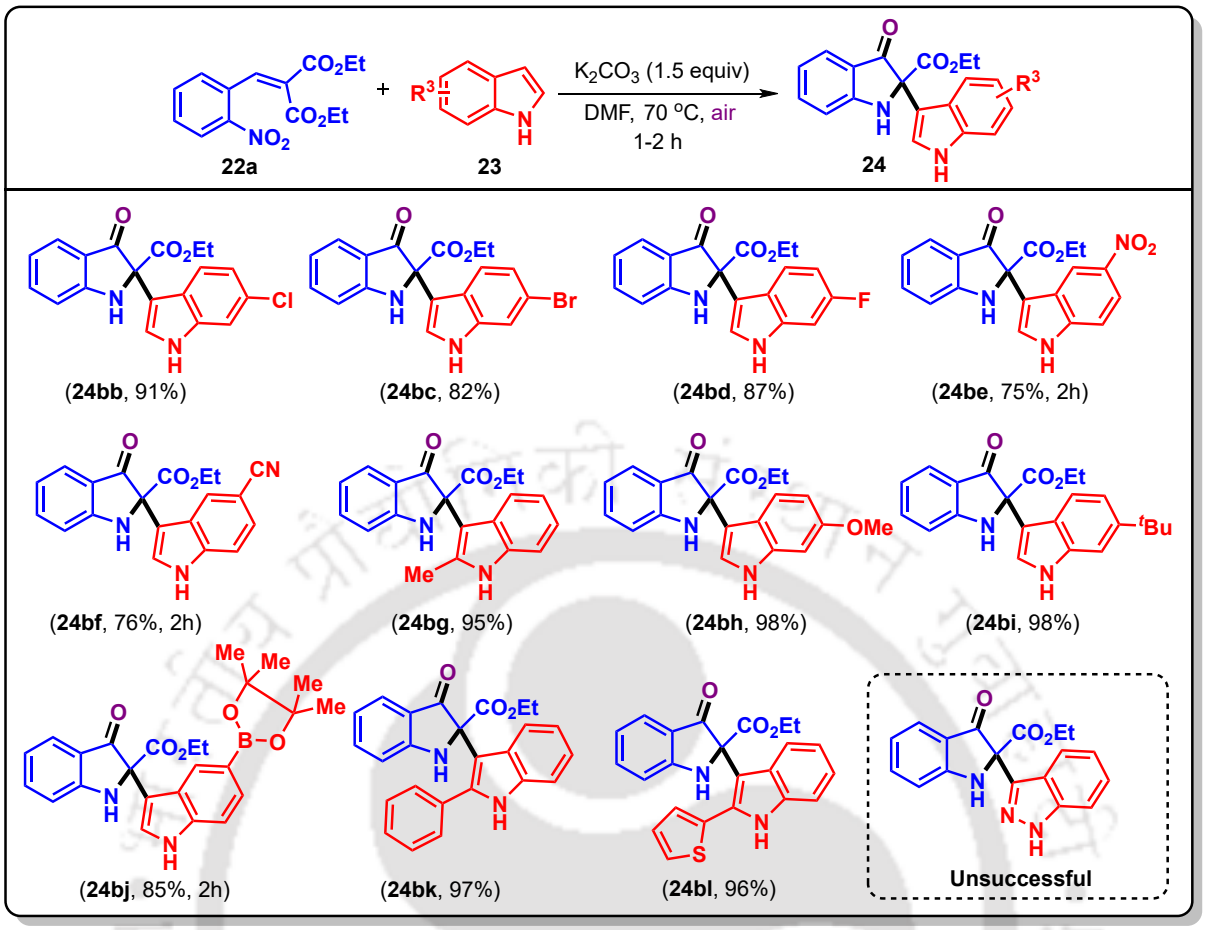

[a]Reaction condition: **22a** (0.51 mmol, 1.0 equiv), **23** (0.56 mmol, 1.1 equiv), solvent 4.0 mL. [b]Isolated yield of the product.

Scheme 4.4.2.2. *Scope of different functionalized indoles.*[a,b]

The protocol was also extended to 1*H*-pyrrolo[2,3-*b*]pyridine **23n** (*Scheme 4.4.2.3*). The reaction of **22a** with **23n** proceeded smoothly, providing product **24bn** in 93% yield. Further, functionalization with electron-withdrawing as well as electron-

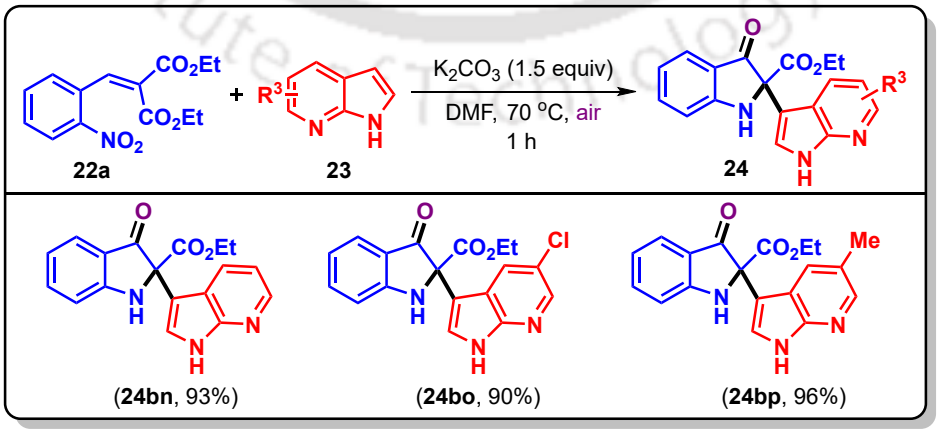

[a]Reaction condition: **22a** (0.51 mmol, 1.0 equiv), **23** (0.56 mmol, 1.1 equiv), solvent 4.0 mL. [b]Isolated yield of the product.

Scheme 4.4.2.3. *Scope of different functionalized pyrrolopyridines.*[a,b]

donating groups on the pyridine ring comfortably furnished their corresponding products **24bo** and **24bp** in excellent yields of 90% and 96%, respectively.

Additionally, when a reaction was performed using the starting material **22s**, prepared from an enantioenriched malonate L-menthol, the developed protocol produced its corresponding product **24as** in 61% yield as inseparable diastereomers with 1:1 ratio (*Scheme 4.4.2.4*).

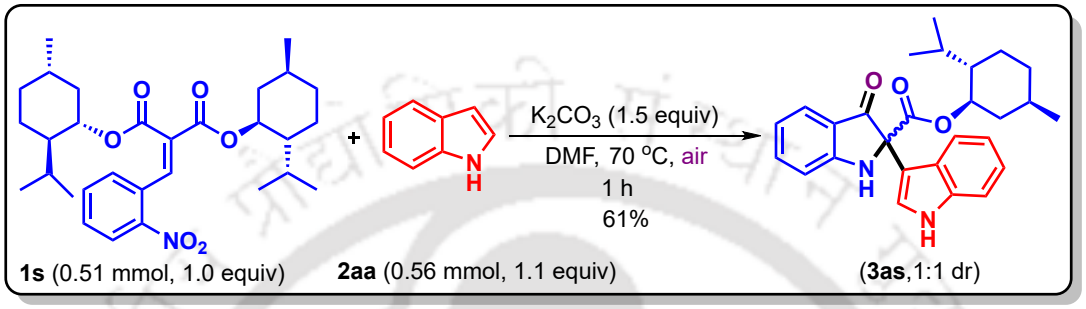

Scheme 4.4.2.4. *Reaction with L-menthol.*

In an interesting note, when the reaction was performed using a mixed malonate component, for example employing cyano ester (**22m**), keto ester (**22n** and **22o**) and sulfonyl ester (**22p**), the reaction predominantly delivered ethyl 2-(1*H*-indol-3-yl)-3-oxoindoline-2-carboxylate **24aa** but not any product having the other malonate component in the C2 position (*Scheme 4.4.2.5a*). Again, when the reaction was performed with malononitrile (**22q**), diketone (**22r**), and ethyl butyrate (**22t**), the reaction did not afford the desired product but did afford some decomposed by-products under the established reaction conditions (*Scheme 4.4.2.5b*).

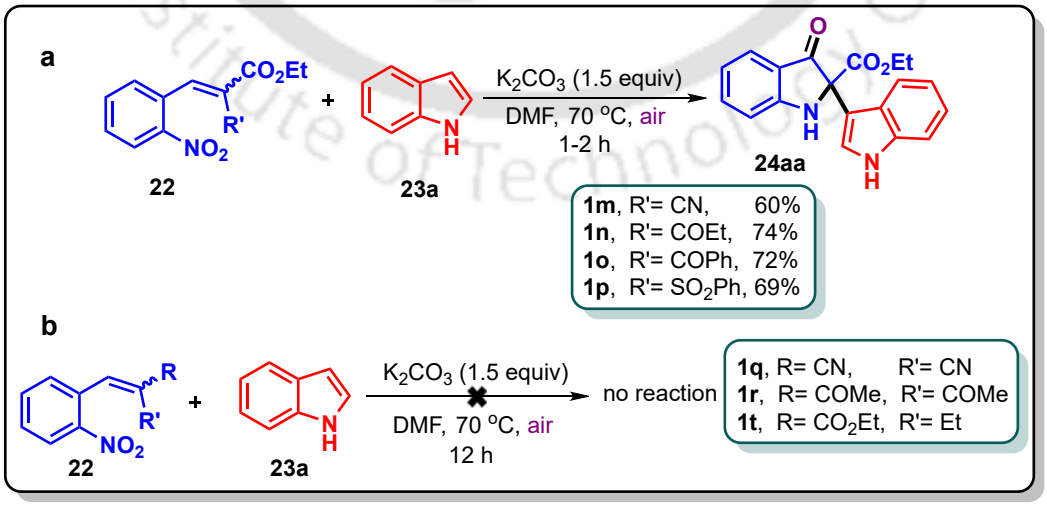

[a]Reaction condition: **22** (0.51 mmol, 1.0 equiv), **23a** (0.56 mmol, 1.1 equiv), solvent 4.0 mL.
[b]Isolated yield of the product.

Scheme 4.4.2.5. *Scope of different malonate components.*[a,b]

The structure of all the compounds was determined by ^{1}H and $^{13}C\{^{1}H\}$ NMR, IR spectroscopy, high resolution mass spectrometry (HRMS), and X-ray crystallographic analysis of the compound **24ak**.

4.4.3 Gram-Scale Synthesis

To further validate the applicability of this protocol, gram-scale synthesis was carried out (*Scheme 4.4.3.1*), wherein compound **22a** (1.00 g, 3.41 mmol) was allowed to react with compound **23a** (0.44 g, 3.75 mmol) under standardized reaction conditions. The outcome produced the target compound **24aa** in an impressive 80% yield (0.87 g), highlighting the potential of this method for large-scale applications.

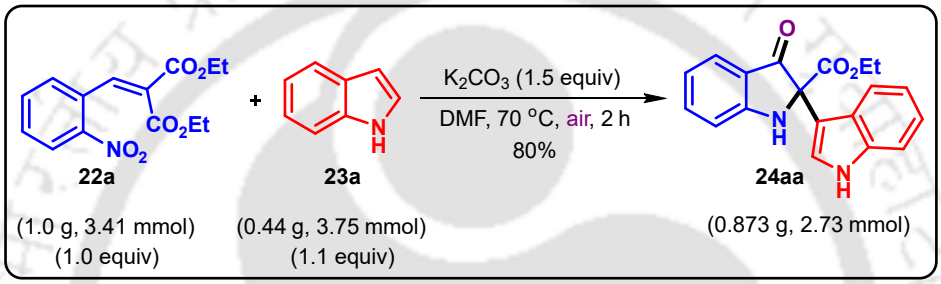

Scheme 4.4.3.1. *Gram-scale synthesis.*

4.4.4 Control Experiments

To explore the proposed mechanistic pathway, several control experiments were conducted (*Scheme 4.4.4.1*). Initially, a reaction was performed between **22a** and **23a** at room temperature in the presence of 1.0 equiv of K_2CO_3, and this resulted in the formation of intermediate **A** in 87% yield within 4 h (*Scheme 4.4.4.1a*). Subsequently, intermediate **A** was treated with an additional K_2CO_3 (1.0 equiv) at 70 °C, and gratifyingly desired product ethyl 2-(1*H*-indol-3-yl)-3-oxoindoline-2-carboxylate (**24aa**) was obtained in 83% yield (*Scheme 4.4.4.1a*). This confirms the initial formation of intermediate **A** during the reaction.

To further validate the reaction pathway, the reaction was performed separately in the presence of BHT and TEMPO under standard reaction conditions (*Scheme 4.4.4.1b*). When **22a** and **23a** were reacted in the presence of 2.0 equiv of TEMPO, the product **24aa** was isolated in 76% yield. Similarly, using 2.0 equiv of BHT resulted in 70% yield of **24aa**. Since neither TEMPO nor BHT radical scavenger inhibited the reaction, it suggests that the reaction proceeds *via* ionic mechanism.

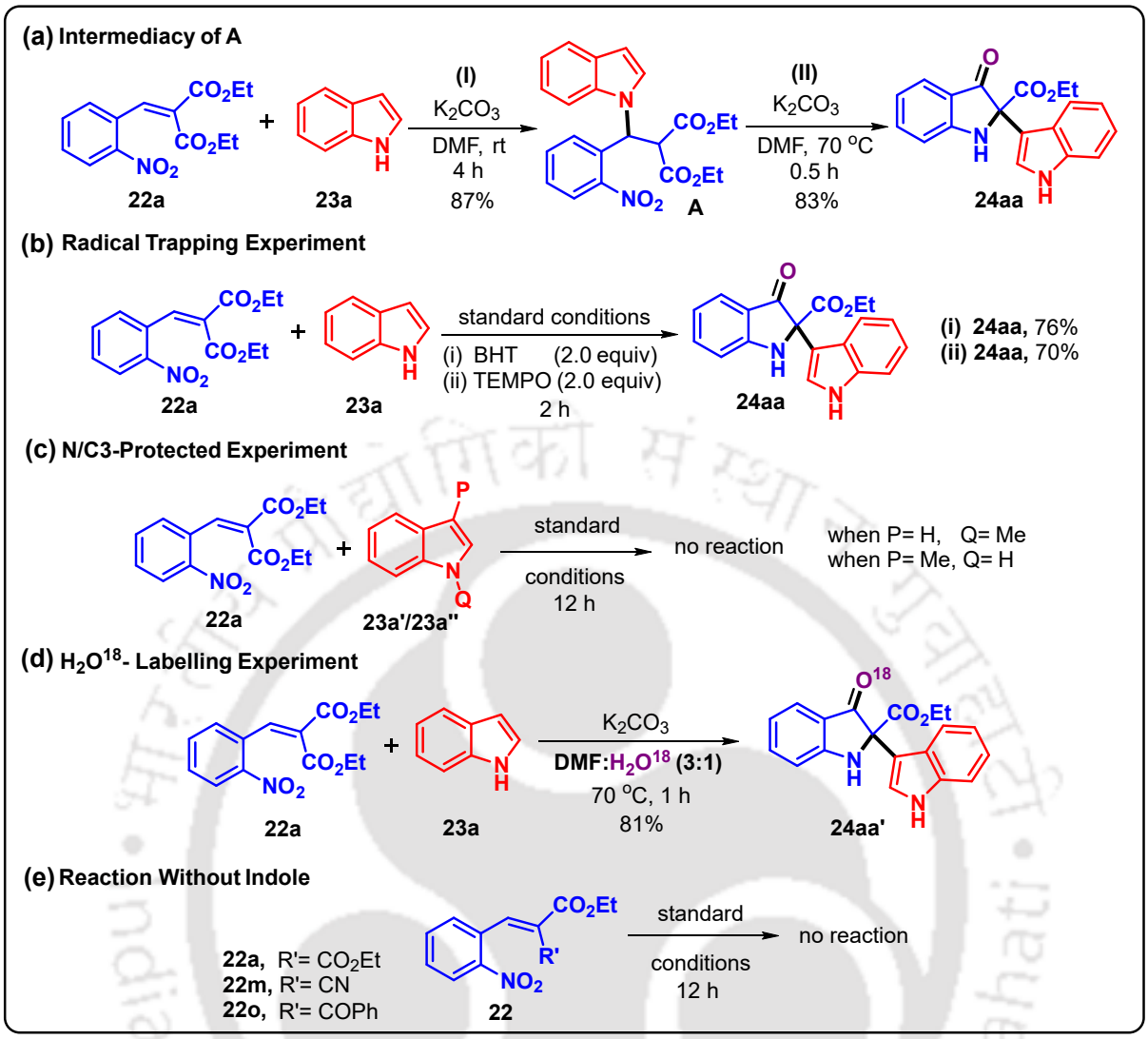

Scheme 4.4.4.1. *Control experiments.*

Besides, separate experiments were conducted between compound **22a** and indole derivatives protected at the N- and C–3 position by a –Me group, respectively (*Scheme 4.4.4.1c*). Both reactions failed to afford any product, confirming that the presence of hydrogen (H) atom at these positions is crucial for the reaction to proceed smoothly.

Again, to trace the oxygen source, a reaction between **22a** and **23a** was performed in a solvent mixture of DMF and isotopically labeled H_2O^{18} (3:1) (*Scheme 4.4.4.1d*). The resulting product **24aa'** (81% yield) was confirmed to contain O^{18} through HRMS and $^{13}C\{^1H\}$ NMR analysis (*Figure 4.4.4.1*). Thus, it demonstrates that H_2O serves as the oxygen source for the keto group formed in the reaction *via* hydrolysis.

Finally, another control experiment was performed by doing the reaction of **1a**, **1m** and **1o** under the optimized reaction conditions in the absence of indole

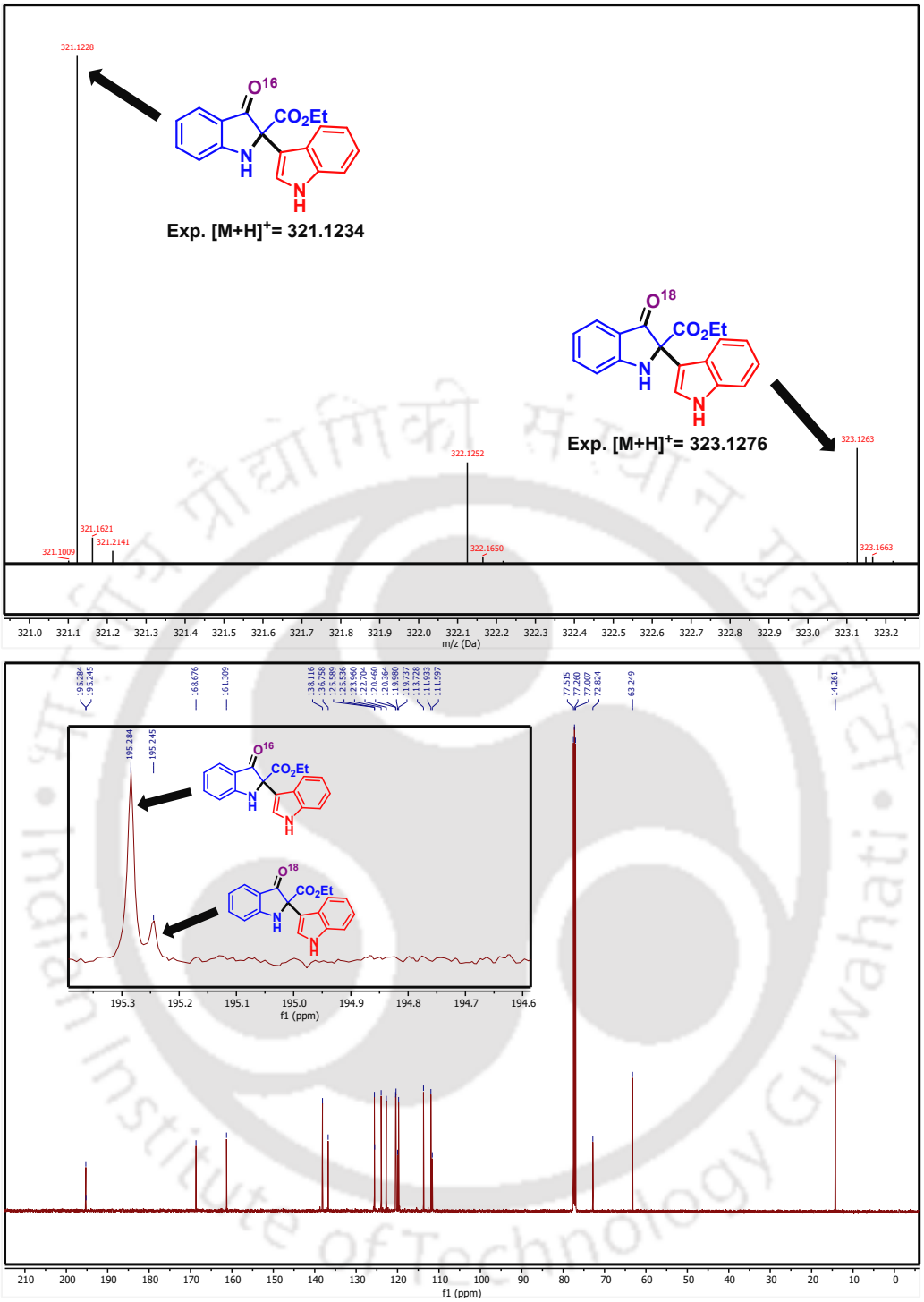

Figure 4.4.4.1. *HRMS and* $^{13}C\{^1H\}$ *spectra for compound* ***24aa'***.

(*Scheme 4.4.4.1e*). But no change was observed even after 12 h of reaction. This indicates that the indole moiety has an important role in the formation of indolin-3-one intermediate **K**.

4.4.5 Plausible Mechanism

Based on prior literature[14] and validated through our intricately designed control experiments, a plausible mechanism has been proposed (*Scheme 4.4.5.1*).

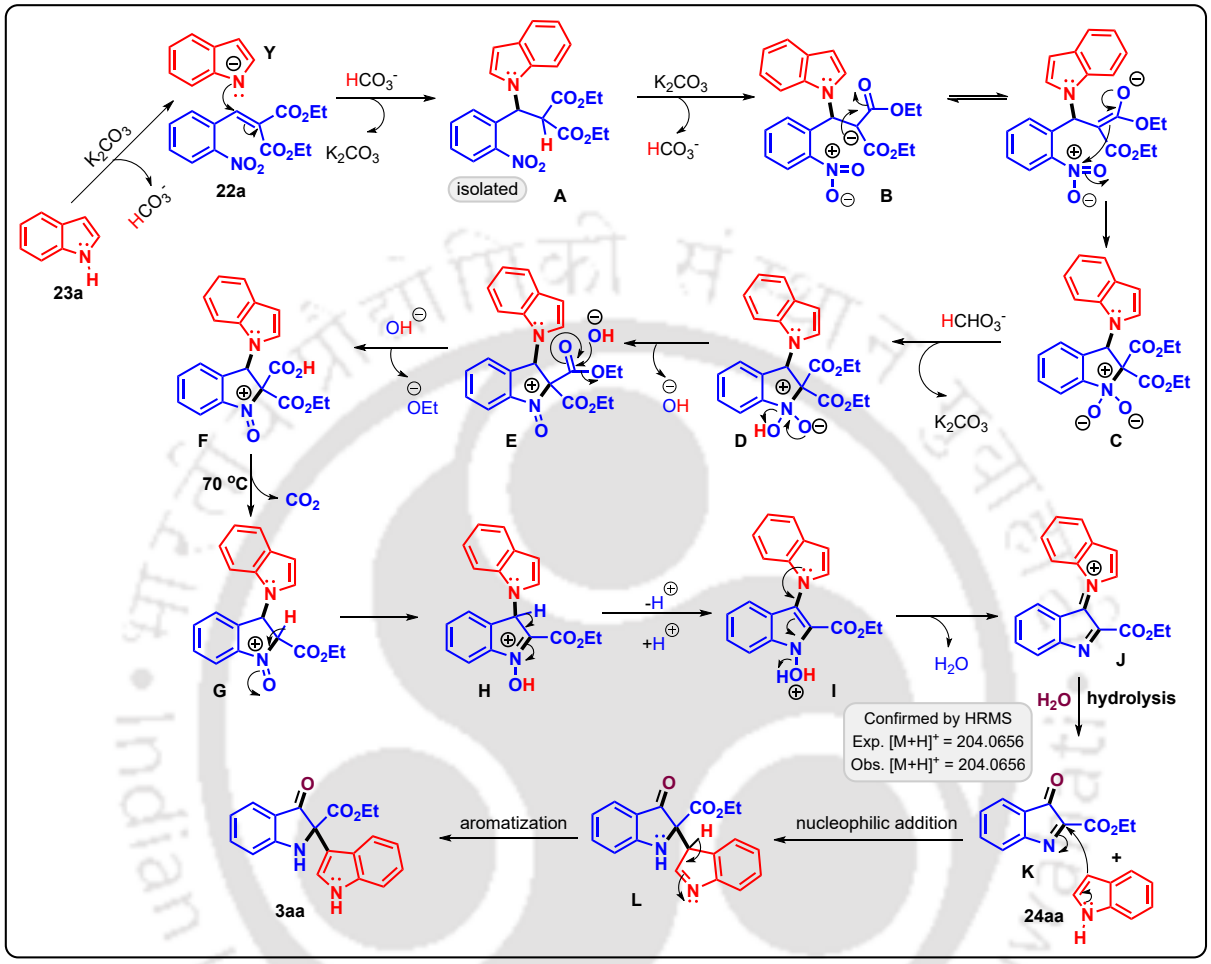

Scheme 4.4.5.1. *Plausible mechanism for the reaction.*

Starting with diethyl 2-(2-nitrobenzylidene)malonate **22a** and 1-*H* indole **23a** as model substrates, the process begins when a base K_2CO_3 deprotonates indole, turning it into a reactive nucleophile **Y**. This nucleophile **Y** rapidly involves in a Michael reaction with diethyl 2-(2-nitrobenzylidene)malonate, forming intermediate **A**, confirmed by both ^1H and $^{13}C\{^1H\}$ NMR spectroscopy and HRMS analysis. The base then abstracts the acidic proton of **A**, generating intermediate **B**, which then reacts with nitro group intramolecularly to form intermediate **C**. Next, intermediate **C** after protonation leads to intermediate **D**, which after the elimination of the hydroxide ion forms intermediate **E**. Subsequently, intermediate **E** undergoes hydrolysis to form acid intermediate **F**, which after decarboxylation at 70 °C converts to intermediate **G.** The intermediate **G** then rearranges to intermediate **H** which after proton elimination/

addition and subsequent water elimination forms intermediate **J**. Intermediate **J** upon hydrolysis gives intermediate **K** (which is confirmed by HRMS) and starting material **22a**. Finally, intermediate **K** and **22a** undergo nucleophilic addition reaction to give intermediate **L**, which, after aromatization, gives the product **24aa**. In the case of **22m-22p**, groups -CN, -COEt, -COPh and -SO_2Ph respectively, hydrolyze faster than -CO_2Et under the established reaction condition, resulting in the formation of the ester substituted product.

4.4.6 Post-synthetic Application

A few post-synthetic modifications were also instigated using different synthesized pseudoindoxyl derivatives (*Scheme 4.4.6.1*). First, compound **24aa** was converted into its thione derivative by replacing oxygen atom of the keto group with sulfur, using P_2S_5 (1.0 equiv) in toluene under reflux condition,[15a] yielding product ethyl 2-(1*H*-indol-3-yl)-3-thioxoindoline-2-carboxylate (**25**) in 71% within 30 min (*Scheme 4.4.6.1a*).

Additionally, two Suzuki cross-coupling reactions were implemented separately on **24bj** and **24ac**, respectively.[15b,c] The first between **24bj** and iodobenzene in the presence of K_2CO_3 (5.0 equiv) and $Pd(PPh_3)_4$ (5 mol%) using toluene:H_2O:EtOH (2:1:0.5) as solvent, afforded product ethyl 3-oxo-2-(5-phenyl-1*H*-indol-3-yl)indoline-2-carboxylate (**26**) in remarkable 90% yield (*Scheme 4.4.6.1b*).

The latter reaction between **24ac** and phenylboronic acid produced product ethyl 2-(1*H*-indol-3-yl)-3-oxo-5-phenylindoline-2-carboxylate (**27**) in an admirable 82% yield

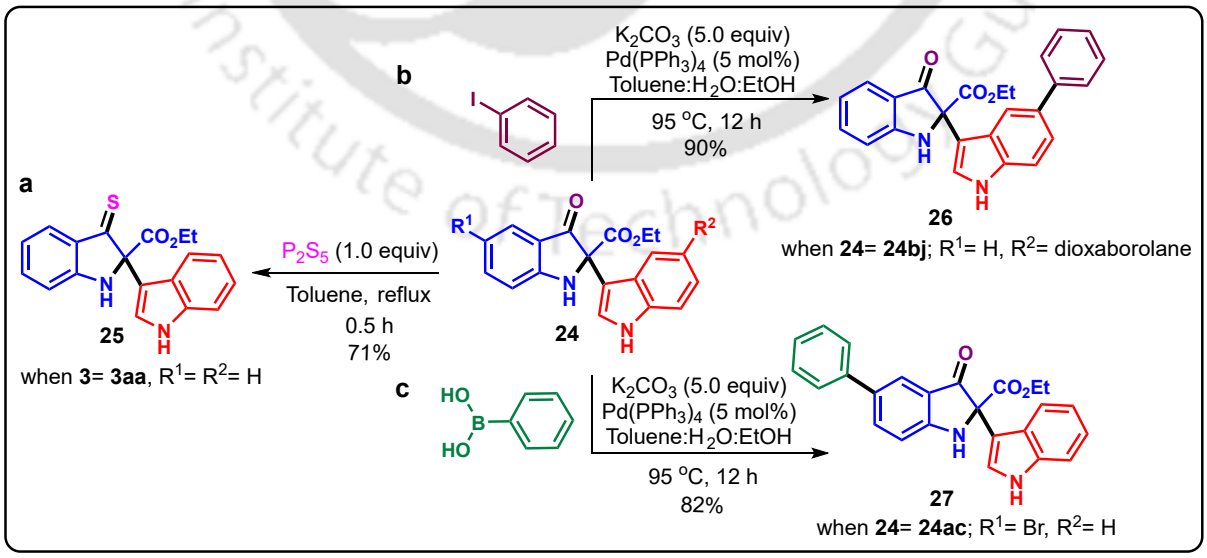

Scheme 4.4.6.1. *Post-synthetic modifications to thione and Suzuki adducts.*

under similar reaction conditions (*Scheme 4.4.6.1c*).

These late-stage modifications highlight the versatility and the synthetic utility of this protocol towards the synthesis of diverse nitrogen-based heterocycles in a concise and efficient manner.

4.5 Photophysical Studies

Building upon the established significance of pseudoindoxyls, these π-conjugated nitrogen-containing heterocyclic compounds continue to demonstrate remarkable potential in fluorescence-based applications. Their strong photophysical properties make them ideal candidates for advanced technologies such as fluorescent probes for bio-imaging, solar cells, and OLEDs.[16] In line with their potential in the photoelectronic field, ultraviolet absorbance (λ_{abs}) and fluorescence emission (λ_{em}) spectra and UV irradiation of some synthesized pseudoindoxyl moieties were studied in 10 μM dichloromethane solution, as shown in *Figure 4.5.1*. The absorption peaks (λ_{abs}) and calculated molar extinction coefficient (ϵ) are summarized in *Table 4.5.1*. Through detailed analysis in dichloromethane, compounds **24af**, **24bd**, **24bf**, **24bn**, **24bo**, and **24bp** exhibited a pair of fluorescent emission bands, covering the indigo (420–440 nm) and blue (440–490 nm) regions under 370–385 nm photoexcitation.

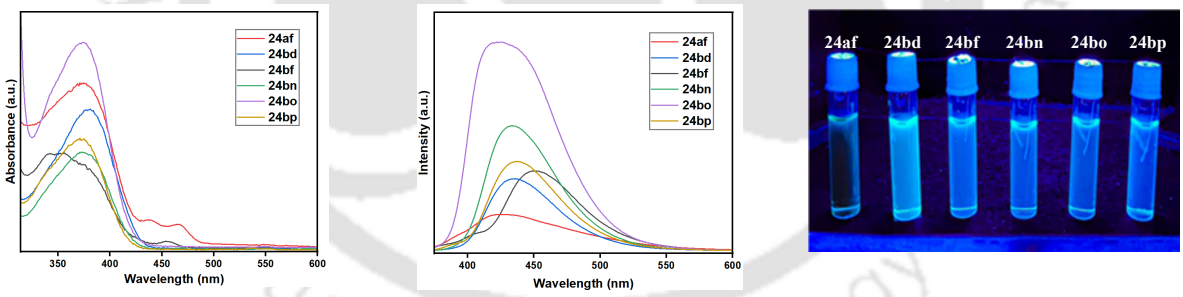

(a) (b) (c)

Figure 4.5.1. *(a) UV-visible, (b) fluorescence spectra, and (c) UV irradiation of* ***24af****,* ***24bd****,* ***24bf****,* ***24bn****,* ***24bo****, and* ***24bp*** *at 365 nm.*

Table 4.5.1. *UV-Vis and photoluminescence parameters*

entry	compound	λ_{max} (nm)[a]	absorbance at λ_{max}	ε (1×10^4 M^{-1} cm^{-1})	λ_{em} (nm)[b]
1	**24af**	371	0.189	1.89	421
2	**24bd**	381	0.159	1.59	436
3	**24bf**	356	0.110	1.10	451
4	**24bn**	373	0.111	1.11	434
5	**24bo**	374	0.235	2.35	423
6	**24bp**	371	0.127	1.27	440

[a]Absorption wavelengths. [b]Emission wavelengths in DCM at a concentration of 1×10^{-5} M.

4.6 Crystallographic Description

The structure of all compounds was confirmed from standard spectroscopic experiments and finally by *X*-ray crystallographic analysis of compound **24ak** (*Figure 4.6.1*).

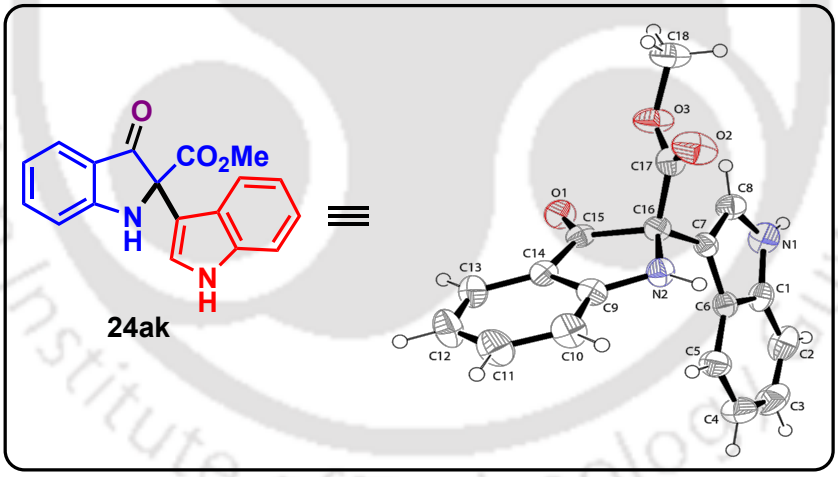

Figure 4.6.1. *ORTEP diagram of compound* ***24ak****, thermal ellipsoids are drawn on 50% probability level.*

Single crystal X-ray diffraction of compound **24ak** was obtained by slow evaporation of hexane and ethyl acetate solution (9:1). The detailed data collection and structure refinement are summarized in *Table 4.6.1*, where CCDC **2422699** of **24ak** contains the supplementary crystallographic data.

Table 4.6.1. *Crystal parameters of compound* ***24ak***

Compound 24ak	**CCDC 2422699**
Formula	$C_{18}H_{14}N_2O_3$
Formula weight	306.31
T/K	297(2)
Crystal system	Monoclinic
Space group	P 1 21/c 1
a/Å	11.9524(10)
b/Å	8.0432(7)
c/Å	15.4668(13)
a/°	90.0
β/°	92.424(2)
γ/°	90.0
V/Å^3	1485.6(2)
Z	4
Abs. Coeff./mm^{-1}	0.095
Abs. Correction	none
GOF on F^2	1.201
Final R indices [$I>2\sigma$(I)]	$R1 = 0.0863$ $wR2 = 0.1187$
R indices [all data]	$R1 = 0.0687$ $wR2 = 0.1269$

4.7 Conclusion

In conclusion, we have established a straight and streamlined protocol for synthesizing pseudoindoxyl derivatives in excellent yields *via* a base-mediated reaction of 2-nitrobenzylidenemalonates and indoles. This approach seamlessly provides pseudoindoxyl scaffolds in a metal-free tandem process. The scalability of the synthesis and subsequent modifications further underscore the practicality of this method. In

addition to this, the UV-visible, fluorescence, as well as UV-irradiation study of some synthesized pseudoindoxyls were also investigated.

4.8 Experimental Section

4.8.1 Reaction Procedure

4.8.1.1 General Experimental Procedure for the Synthesis of Starting Materials

The starting materials **22a**, **22b**, **22d**, **22k**, **22m**, **22q** and **22r** were synthesized according to the literature reports, and the spectroscopic data of the compounds are in good agreement with the literature data.[17]

4.8.1.1.1 General Experimental Procedure for the Synthesis of Compounds 22c, 22e–22j, 22l, 22n–22p, 22s and 22t

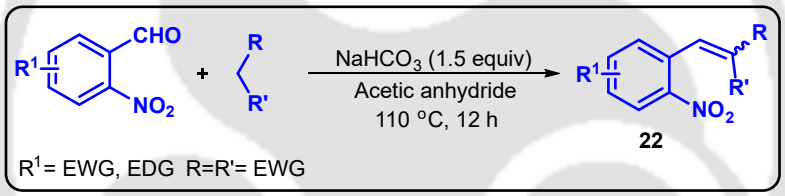

To a mixture of substituted 2-nitrobenzaldehyde derivative (1.32 mmol, 1.0 equiv) and sodium bicarbonate (1.98 mmol, 1.5 equiv), acetic anhydride (5 mL) was added under N_2 atmosphere. The reaction mixture was stirred for 5 min at room temperature, after which malonate component (1.32 mmol, 1.0 equiv) was added dropwise over a period of 2 min. The reaction mixture was then allowed to stir at 110 °C. The progress of the reaction was monitored by TLC analysis (using hexane/ethyl acetate = 9:1 as eluents). After completion of the reaction (12 h), it was allowed to cool to room temperature. The reaction mixture was then washed with saturated Na_2CO_3 and brine solution. The aqueous phase was extracted with ethyl acetate (3 × 10 mL). The combined organic layers were then dried over Na_2SO_4 and concentrated by using a rotary evaporator. The crude product was then purified by column chromatography over silica gel to provide the corresponding starting material **22**.

4.8.1.2 General Experimental Procedure for the Synthesis of Compounds 24aa–24al,24bb–24bl, 24bn–24bp and 3as

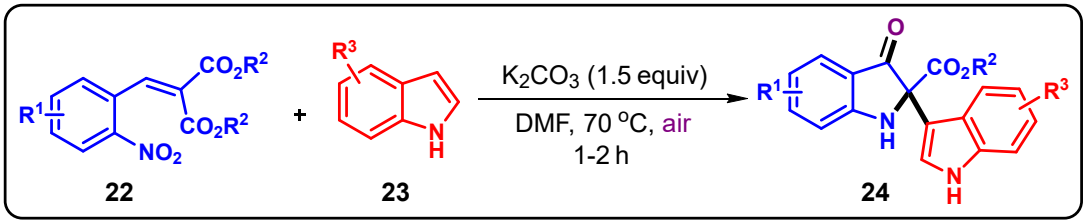

To a mixture of 2-nitrobenzylidenemalonate **22** (0.51 mmol, 1.0 equiv), indole **23** (0.56 mmol, 1.1 equiv), and K_2CO_3 (0.76 mmol, 1.5 equiv), DMF (4 mL) was added under air atmosphere. The reaction was then heated in an oil bath at 70 °C and monitored by TLC analysis (using hexane/ethyl acetate = 7:3 as eluents). After completion of the reaction (1–2 h), the reaction mixture was allowed to cool to room temperature and then diluted with ethyl acetate and brine solution. The organic phase was extracted with ice water (3 × 10 mL). The combined organic extracts were dried over anhydrous Na_2SO_4 and concentrated using a rotary evaporator. The crude product was subjected to column chromatography over silica gel to give the corresponding product **24**.

4.8.1.3 Experimental Procedure for the Gram-scale Synthesis of Compound 24aa

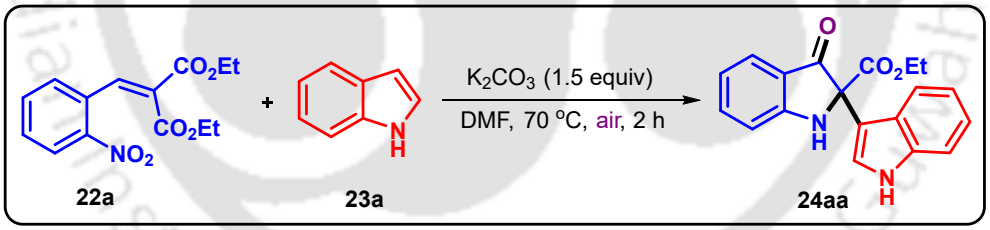

To a mixture of diethyl 2-(2-nitrobenzylidene)malonate **22a** (1.0 g, 3.41 mmol, 1.0 equiv), 1*H*-indole **23a** (0.44 g, 3.75 mmol, 1.1 equiv), and K_2CO_3 (0.71 g, 5.11 mmol, 1.5 equiv), was added DMF (10 mL) under air atmosphere. The reaction was then heated in an oil bath at 70 °C and monitored by TLC analysis. After completion of the reaction (2 h), the reaction mixture was allowed to cool to room temperature and then diluted with ethyl acetate and brine solution. The organic phase was extracted with ice water (3 × 20 mL). The combined organic extracts were dried over anhydrous Na_2SO_4 and concentrated using a rotary evaporator. The crude product was subjected to column chromatography over silica gel to give the corresponding product **24aa** in 80% yield (0.87 g).

4.8.1.4 Experimental Procedure for Control Experiments

4.8.1.4.1 Experimental Procedure for Intermediacy of A (a) Step I

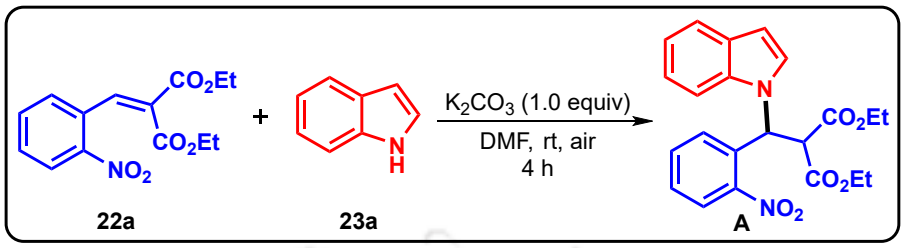

To a mixture of diethyl 2-(2-nitrobenzylidene)malonate **22a** (0.34 mmol, 1.0 equiv), 1*H*-indole **23a** (0.37 mmol, 1.1 equiv), and K_2CO_3 (0.34 mmol, 1 equiv), DMF (3 mL) was added under air atmosphere. The reaction was then allowed to stir at room temperature and monitored by TLC analysis (using hexane/ethyl acetate = 9:1 as eluents). After completion of the reaction (4.0 h), the reaction mixture was diluted with ethyl acetate and brine solution. The organic phase was extracted with ice water (3 × 10 mL). The combined organic extracts were dried over anhydrous Na_2SO_4 and concentrated using a rotary evaporator. The crude product was subjected to column chromatography over silica gel to give the intermediate **A** in 87% yield.

4.8.1.4.2 Experimental Procedure for Intermediacy of A (a) Step II

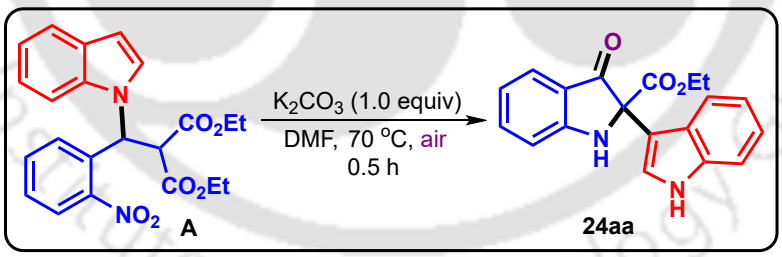

To a mixture of intermediate **A** (0.15 mmol, 1.0 equiv) and K_2CO_3 (0.15 mmol, 1 equiv), DMF (2 mL) was added under air atmosphere. The reaction was then allowed to stir at 70 °C and monitored by TLC analysis (using hexane/ethyl acetate = 7:3 as eluents). After completion of the reaction (0.5 h), the reaction mixture was allowed to cool to room temperature and then diluted with ethyl acetate and brine solution. The organic phase was extracted with ice water (3 × 10 mL). The combined organic extracts were dried over anhydrous Na_2SO_4 and concentrated using a rotary evaporator. The crude product was subjected to column chromatography over silica gel to give the product **24aa** in 83% yield.

4.8.1.4.3 Experimental Procedure for Radical Trapping Experiment (b)

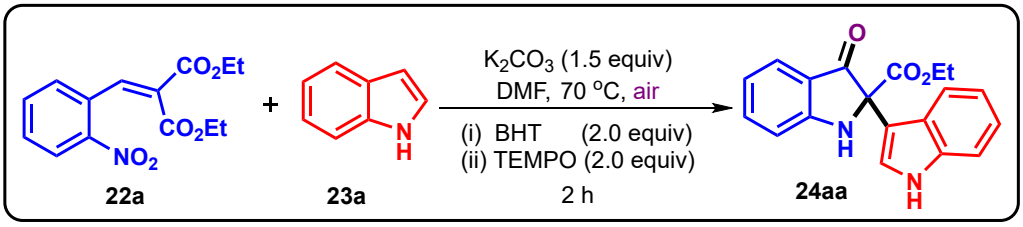

To a mixture of diethyl 2-(2-nitrobenzylidene)malonate **22a** (0.34 mmol, 1.0 equiv), 1*H*-indole **23a** (0.37 mmol, 1.1 equiv), K_2CO_3 (0.51 mmol, 1.5 equiv), and TEMPO or BHT (0.68 mmol, 2.0 equiv), was added DMF (3 mL) under air atmosphere. The reaction was then allowed to stir at 70 °C and monitored by TLC analysis. After completion of the reaction (1.0 h), the reaction mixture was allowed to cool to room temperature and then diluted with ethyl acetate and brine solution. The organic phase was extracted with ice water (3 × 10 mL). The combined organic extracts were dried over anhydrous Na_2SO_4 and concentrated using a rotary evaporator. The crude product was subjected to column chromatography over silica gel to give the corresponding product **24aa** in 76% yield for TEMPO and 70% yield for BHT. This observation suggests the non-involvement of any radical path in the reaction.

4.8.1.4.4 Experimental Procedure for N- and C3- Protected Experiment (c)

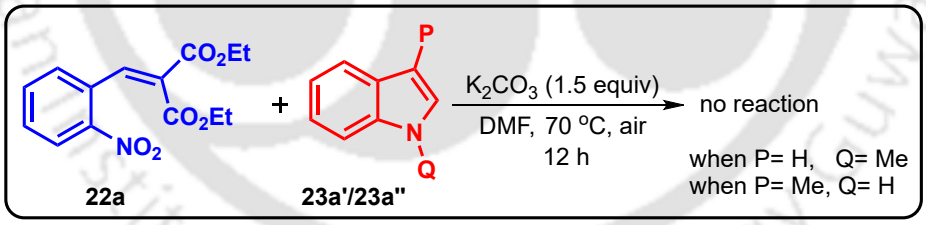

To a mixture of diethyl 2-(2-nitrobenzylidene)malonate **22a** (0.34 mmol, 1.0 equiv), 1-methyl-1*H*-indole or 3-methyl-1*H*-indole (**23a'**/**23a''**) (0.37 mmol, 1.1 equiv), and K_2CO_3 (0.51 mmol, 1.5 equiv), was added DMF (3 mL) under air atmosphere. The reaction was then allowed to stir at 70 °C and monitored by TLC analysis. No expected product was observed even after 12 h, highlighting the critical role of hydrogen (H) atoms at these specific positions.

4.8.1.4.5 Experimental Procedure for H_2O-Labelling Experiment (d)

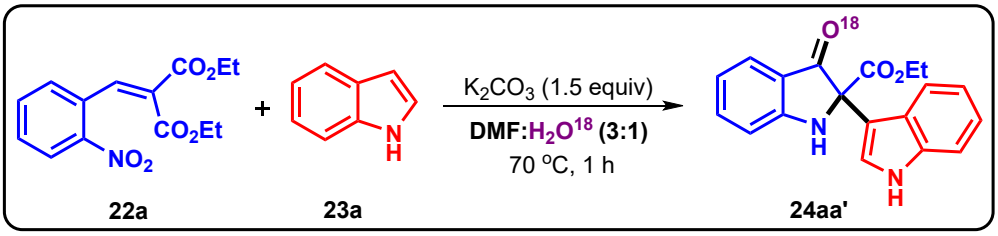

To a mixture of diethyl 2-(2-nitrobenzylidene)malonate **22a** (0.34 mmol, 1.0 equiv), 1*H*-indole **23a** (0.37 mmol, 1.1 equiv), K_2CO_3 (0.51 mmol, 1.5 equiv), was added DMF:H_2O^{18} (3:1) (DMF 1.5 mL, H_2O^{18} 0.5 mL) under air atmosphere. The reaction was then allowed to stir at 70 °C and monitored by TLC analysis. After completion of the reaction (1.0 h), the reaction mixture was allowed to cool to room temperature and then diluted with ethyl acetate and brine solution. The organic phase was extracted with ice water (3 × 10 mL). The combined organic extracts were dried over anhydrous Na_2SO_4 and concentrated using a rotary evaporator. The crude product was subjected to column chromatography over silica gel to give the corresponding O^{18} labelled product **24aa'** in 81% yield. In the HRMS analysis, two peaks at 321.1228 (for unlabelled **24aa'**) and 323.1263 (for O^{18} labelled **24aa'**) were observed, indicating the involvement of O^{18} labelled water in the reaction. Again, in $^{13}C\{^1H\}$ NMR spectrum one extra peak at 195.24 indicates the presence of O^{18} in the molecule, which also confirms the participation of O^{18} labelled water in the reaction.

4.8.1.4.6 Experimental Procedure for Reaction Without Indole (e)

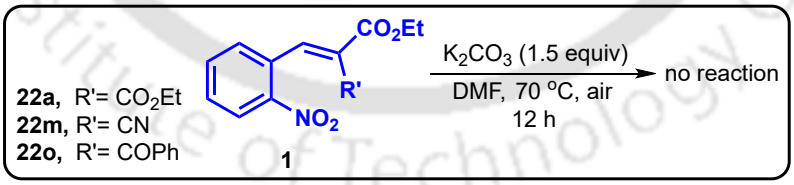

To a mixture of 2-nitrobenzylidenemalonate **22** (0.51 mmol, 1.0 equiv), DMF (4 mL) was added under air atmosphere. The reaction was then allowed to stir at 70 °C and monitored by TLC analysis (using hexane/ethyl acetate = 7:3 as eluents). No change was observed even after 12 h of the reaction, with starting materials remaining the same.

4.8.1.5 Experimental Procedure for the Synthesis of Compounds 25

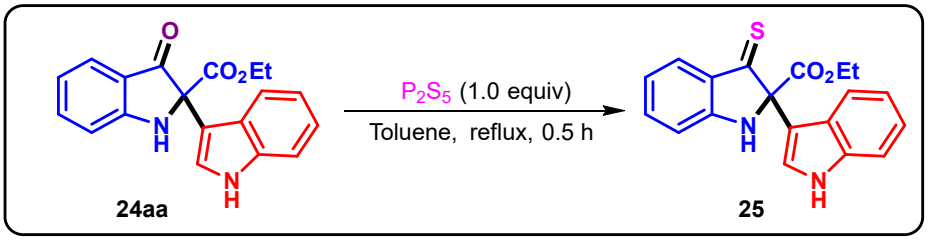

To a stirred suspension of compound **24aa** (50 mg, 0.15 mmol, 1.0 equiv) and P_2S_5 (33 mg, 0.15 mmol, 1.0 equiv), was added toluene (3.0 mL) under nitrogen atmosphere. The reaction mixture was then refluxed in an oil bath. The reaction was monitored by TLC analysis (using hexane/ethyl acetate = 7:3 as eluents), and after completion of the reaction (0.5 h), the solvent was removed under reduced pressure. The reaction mixture was then poured into water and extracted with EtOAc (3 × 10 mL). The combined organic extracts were dried over anhydrous Na_2SO_4 and concentrated using a rotary evaporator. The crude product was then purified using column chromatography over silica gel to get the corresponding product **25** in 71% yield.

4.8.1.6 Experimental Procedure for the Synthesis of Compounds 26

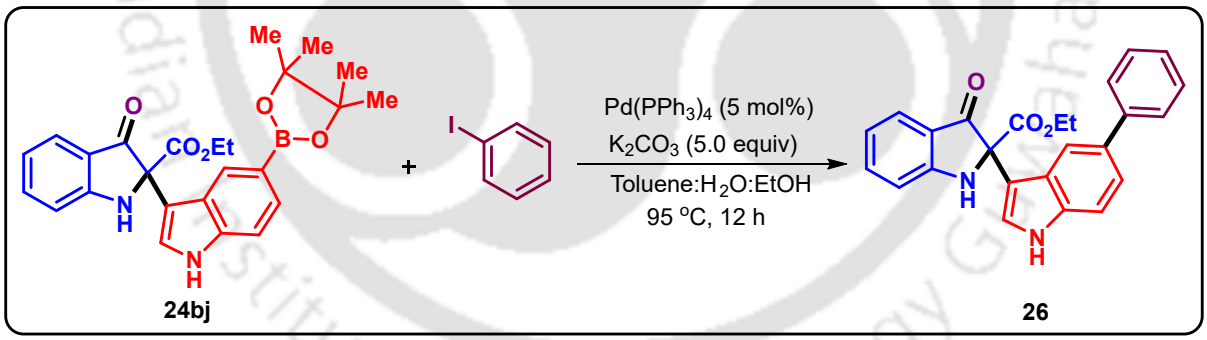

To an oven-dried Schlenk Tube containing a magnetic bar, iodobenzene (0.01 mL, 0.075 mmol, 1.0 equiv), compound **24bj** (50 mg, 0.11 mmol, 1.5 equiv), anhydrous K_2CO_3 (52 mg, 0.37 mmol, 5.0 equiv), $Pd(PPh_3)_4$ (4 mg, 0.004 mmol, 5 mol%), H_2O (1.0 mL), EtOH (0.5 mL), and toluene (2.0 mL) were added. The reaction vessel was charged with N_2 and sealed. After completion of the reaction, the reaction mixture was then heated to 95 °C using an oil bath and stirred for 12 h. The mixture was filtered over a small pad of Celite and diluted with DCM and H_2O and extracted with DCM (3 × 10 mL). The combined organic extracts were dried over anhydrous Na_2SO_4 and concentrated using a rotary evaporator. The crude product was then purified

using column chromatography over silica gel to get the corresponding product **26** in 90% yield.

4.8.1.7 Experimental Procedure for the Synthesis of Compounds 27

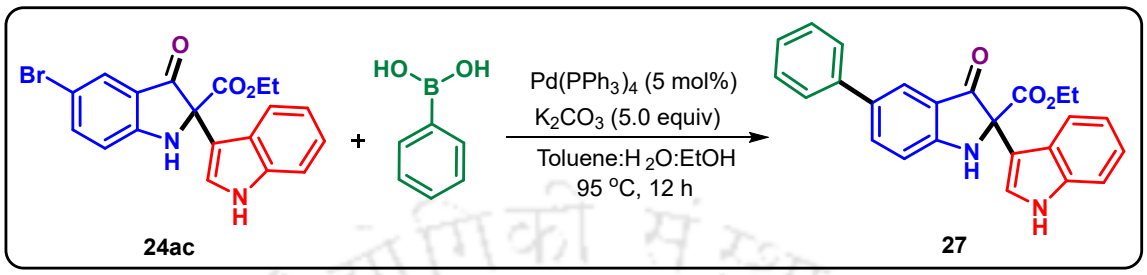

To an oven-dried Schlenk Tube containing a magnetic bar, compound **24ac** (50 mg, 0.12 mmol, 1.0 equiv), phenylboronic acid (23 mg, 0.18 mmol, 1.5 equiv), anhydrous K_2CO_3 (83 mg, 0.6 mmol, 5.0 equiv), $Pd(PPh_3)_4$ (7 mg, 0.006 mmol, 5 mol%), H_2O (1.0 mL), EtOH (0.5 mL), and toluene (2.0 mL) were added. The reaction vessel was charged with N_2 and sealed. The reaction mixture was then heated to 95 °C using an oil bath and stirred for 12 h. After completion of the reaction, the mixture was filtered over a small pad of Celite and diluted with DCM and H_2O and extracted with DCM (3 × 10 mL). The combined organic extracts were dried over anhydrous Na_2SO_4 and concentrated using a rotary evaporator. The crude product was then purified using column chromatography over silica gel to get the corresponding product **27** in 82% yield.

4.9 References

1. (a) Dhote, P. S.; Patel, P.; Vanka, K.; Ramana, C. V. *Org. Biomol. Chem.* **2021**, *19*, 7970–7994; (b) Andrade, M. T.; Lima, J. A.; Pinto, A. C.; Rezende, C. M.; Carvalho, M. P.; Epifanio, R. A. *Bioorg. Med. Chem.* **2005**, *13*, 4092–4095; (c) Cheng, G. G.; Li, D.; Hou, B.; Li, X. N.; Liu, L.; Chen, Y. Y.; Lunga, P. K.; Khan, A.; Liu, Y. P.; Zuo, Z. L.; Luo, X. D. *J. Nat. Prod.* **2016**, *79*, 2158–2166.

2. (a) Abe, T.; Kukita, A.; Akiyama, K.; Naito, T.; Uemura, D. *Chem. Lett.* **2012**, *41*, 728–729; (b) Liu, J. F.; Jiang, Z. Y.; Wang, R. R.; Zheng, Y. T.; Chen, J. J.; Zhang, X. M.; Ma, Y. B. *Org. Lett.* **2007**, *9*, 4127–4129; (c) Bhakuni, D. S.; Silva, M.; Matlin, S. A.; Sammes, P. G. *Phytochemistry* **1976**, *15*, 574–575; (d) Steyn, P. S. *Tetrahedron Lett.* **1971**, *12*, 3331–3334.

3. (a) Lee, J. H.; So, J. H.; Jeon, J. H.; Choi, E. B.; Lee, Y. R.; Chang, Y. T.; Kim, C. H.; Bae, M. A.; Ahn, J. H. *Chem. Commun.* **2011**, *47*, 7500–7502; (b) Matsumoto, S.; Samata, D.; Akazome, M.; Ogura, K. *Tetrahedron Lett.* **2009**, *50*, 111–114.

4. (a) Dolas, A. J.; Patel, A.; Shah, I. A.; Yadav, J.; Iype, E.; Kumar, I. *Org. Biomol. Chem.* **2025**, *23*, 2523–2538; (b) Ji, Y.; He, X.; Peng, C.; Huang, W. *Org. Biomol. Chem.* **2019**, *17*, 2850–2864; (c) Deeksha; Choudhary, D.; Gurjar, I. K.; Menon, A. P.; Deokar, A. R.; Singh, R. *Asian J. Org. Chem.* **2025**, *e202500102*; (d) Godfrey, R. C.; Green, N. J.; Nichol, G. S.; Lawrence, A. L. *Nat. Chem.* **2020**, *6*, 615–619; (e) Nandy, M.; Das, A.; Niyogi, S.; Khatua, A.; Jana, D.; Bisai, A. *Org. Lett.* **2024**, *26*, 10424–10429.

5. (a) Schendera, E.; Lerch, S.; von Drathen, T.; Unkel, L.-N.; Brasholz, M. *Eur. J. Org. Chem.* **2017**, *2017*, 3134–3138; (b) Guo, C.; Schedler, M.; Daniliuc, C. G.; Glorius, F. *Angew. Chem. Int. Ed.* **2014**, *53*, 10232–10236; (c) Fu, W.; Song, Q. *Org. Lett.* **2018**, *20*, 393–396.

6. Guo, H.; Sun, N.; Guo, J.; Zhou, T. P.; Tang, L.; Zhang, W.; Deng, Y.; Liao, R. Z.; Wu, Y.; Wu, G.; Zhong, F. *Angew. Chem. Int. Ed.* **2023**, *62*, e202219034.

7. Jessing, M.; Baran, P. S. *Heterocycles* **2011**, *82*, 1739–1745.

8. Atienza, B. J. P.; Jensen, L. D.; Noton, S. L.; Ansalem, A. K. V.; Hobman, T.; Fearns, R.; Marchant, D. J.; West, F. G. *J. Org. Chem.* **2018**, *83*, 6829–6842.

9. Yarlagadda, S.; Sridhar, B.; Subba Reddy, B. V. *Chem. Asian J.* **2018**, *13*, 1327–1334.

10. Liu, R.-R.; Ye, S.-C.; Lu, C.-J.; Zhuang, G.-L.; Gao, J.-R.; Jia, Y.-X. *Angew. Chem. Int. Ed.* **2015**, *54*, 11205–11208.

11. Li, Y.-J.; Yan, N.; Liu, C.-H.; Yu, Y.; Zhao, Y.-L. *Org. Lett.* **2017**, *19*, 1160–1163.

12. Jia, R.; Li, B.; Zhang, X.; Fan, X. *Org. Lett.* **2020**, *22*, 6810–6815.

13. Gao, K.; Wu, J. *Org. Lett.* **2008**, *10*, 2251–2254.

14. (a) Gao, K.; Wu, J. *Org. Lett.* **2008**, *10*, 2251–2254; (b) Ly, T. M.; Huynh, T. N.; Phan, N. H.; Dinh, P. T.; Nguyen, T. T. *J. Org. Chem.* **2024**, *89*, 17346–17354; (c) Keana, J. F. W.; Heo, G. S.; Gaughan, G. T. *J. Org. Chem.* **1985**,

50, 2346–2351; (d) Marien, N.; Reddy, B. N.; De Vleeschouwer, F.; Goderis, S.; Van Hecke, K.; Verniest, G. *Angew. Chem. Int. Ed.* **2018**, *57*, 5660–5664.

15. (a) Arandhara, P. J.; Behera, B. K.; Biswas, S.; Saikia, A. K. *Org. Biomol. Chem.* **2023**, *21*, 8772–8781; (b) Bulatov, E.; Lahtinen, E.; Kivijärvi, L.; Hey-Hawkins, E.; Haukka, M. *ChemCatChem* **2020**, *12*, 4831–4838; (c) Wu, X.; Lin, W.; Wang, L.; Li, N.; Tu, G.; Fu, Y.; Chen, D.-L.; Zhu, W.; Chen, G.; Zhang, F. *New J. Chem.* **2022**, *46*, 8575–8582.

16. Goriya, Y.; Ramana, C. V. *Chem. Commun.* **2013**, *49*, 6376–6378.

17. (a) Kleinmans, R.; Pinkert, T.; Dutta, S.; Paulisch, T. O.; Keum, H.; Daniliuc, C. G.; Glorius, F. *Nature* **2022**, *605*, 477–482; (b) Liu, Q.; Zhu, F.-P.; Jin, X.-L.; Wang, X.-J.; Chen, H.; Wu, L.-Z. *Chem. – Eur. J.* **2015**, *21*, 10326–10329; (c) Zhao, X. Z.; Smith, S. J.; Métifiot, M.; Johnson, B. C.; Marchand, C.; Pommier, Y.; Hughes, S. H.; Burke, T. R. J. *J. Med. Chem.* **2014**, *57*, 1573–1582; (d) Zhang, S.; Cheng, K.; Wang, X.; Yin, H. *Bioorg. Med. Chem.* **2012**, *20*, 6073–6079; (e) Liu, M.; Zhou, L.; Shi, W.; Hu, Y.; Liao, J.; Duan, Z.; Wang, W.; Wu, Y.; Zheng, B.; Guo, H. *Org. Lett.* **2021**, *23*, 7703–7707; (f) Zaytsev, S. V.; Villemson, E. V.; Ivanov, K. L.; Budynina, E. M.; Melnikov, M. Y. *Eur. J. Org. Chem.* **2017**, *2017*, 2814–2823.

4.10 Characterization Data

Diethyl 2-(5-bromo-2-nitrobenzylidene)malonate (22c):

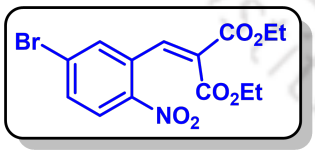

Yellow solid; R_f (Hexane/EtOAc, 9:1) 0.55; mp 73–75 °C. Yield 348 mg, 71%; ^{1}H NMR (500 MHz, $CDCl_3$) δ 8.31 (d, J = 2.0 Hz, 1 H), 8.03 (s, 1 H), 7.74 (dd, J = 8.5, 2.0 Hz, 1 H), 7.30 (d, J = 8.0 Hz, 1 H), 4.30 (q, J = 7.0 Hz, 2 H), 4.09 (q, J = 7.0 Hz, 2 H), 1.32 (t, J = 7.0 Hz, 3 H), 1.06 (t, J = 7.5 Hz, 3 H); ^{13}C{^{1}H} NMR (125 MHz, $CDCl_3$) δ 164.7, 163.3, 147.6, 139.9, 136.9, 131.6, 129.9, 129.4, 128.2, 123.7, 62.2, 61.8, 14.2, 13.9; IR (KBr, neat) 2983, 1722, 1528, 1343, 1249, 1213, 1064, 1020, 854, 761 cm^{-1}; HRMS (ESI) calcd. for $C_{14}H_{15}BrNO_6$ $(M + H)^+$ 372.0078, found 372.0078.

Diethyl 2-((5-((difluoro- λ³-methyl)-λ²-fluoraneyl)-2-nitrophenyl)methylene)malonate (22e):

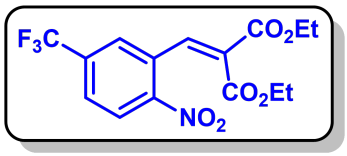

Pale yellow solid; R_f (Hexane/EtOAc, 9:1) 0.55; mp 80–82 °C. Yield 324 mg, 68%; ^{1}H NMR (500 MHz, $CDCl_3$) δ 8.40 (s, 1 H), 8.09 (s, 1 H), 7.87 (d, J = 8.0 Hz, 1 H), 7.56 (d, J = 8.5 Hz, 1 H), 4.28 (q, J = 7.0 Hz, 2 H), 4.03 (q, J = 7.5 Hz, 2 H), 1.29 (t, J = 7.0 Hz, 3 H), 0.99 (t, J = 7.0 Hz, 3 H); ^{13}C{^{1}H} NMR (125 MHz, $CDCl_3$) δ 164.2, 163.0, 147.2, 139.7, 134.2, 132.5 (q, J = 34.2 Hz), 131.3, 130.4, 130.3 (q, J = 3.5 Hz), 122.6 (q, J = 271.1 Hz), 122.3 (q, J = 4.0 Hz), 62.2, 61.8, 14.0, 13.7; ^{19}F NMR (470 MHz, $CDCl_3/C_6F_6$) δ –66.2 (s, –CF_3–); IR (KBr, neat) 2986, 1728, 1541, 1324, 1255, 1179, 1136, 1090, 1015, 907, 859 cm^{-1}; HRMS (ESI) calcd. for $C_{15}H_{15}F_3NO_6$ $(M + H)^+$ 362.0846, found 362.0848.

Diethyl 2-(5-(methoxycarbonyl)-2-nitrobenzylidene)malonate (22f):

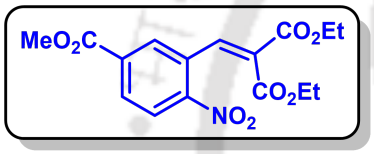

Yellow solid; R_f (Hexane/EtOAc, 9:1) 0.50; mp 53–55 °C. Yield 310 mg, 67%; ^{1}H NMR (400 MHz, $CDCl_3$) δ 8.12 (d, J = 8.4 Hz, 1 H), 8.09–8.06 (m, 1 H), 8.01–7.99 (m, 2 H), 4.23 (d, J = 7.2 Hz, 2 H), 4.03 (d, J = 7.2 Hz, 2H), 3.85 (s, 3 H), 1.25 (t, J = 7.2 Hz, 3 H), 1.00 (d, J = 7.2 Hz, 3 H); ^{13}C{^{1}H} NMR (125 MHz, $CDCl_3$) δ 164.6, 164.5, 163.2, 149.7, 139.8, 134.7, 131.5, 131.2, 130.6, 130.3, 125.2, 62.2, 61.8, 53.1, 14.2, 13.9; IR (KBr, neat) 2984, 1724, 1528, 1249, 1113, 1064, 1019, 986, 847, 744, 695 cm^{-1}; HRMS (ESI) calcd. for $C_{16}H_{18}NO_8$ $(M + H)^+$ 352.1027, found 352.1035.

Diethyl 2-(3,5-dichloro-2-nitrobenzylidene)malonate (22g):

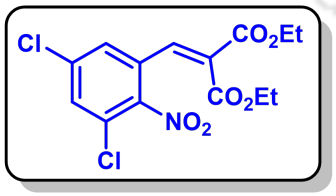

Yellow liquid; R_f (Hexane/EtOAc, 9:1) 0.50. Yield 347 mg, 73%; ^{1}H NMR (400 MHz, $CDCl_3$) δ 7.49 (d, J = 2.0 Hz, 1 H), 7.45 (s, 1 H), 7.33 (dd, J = 2.0, 0.8 Hz, 1 H), 4.21 (q, J = 7.2 Hz, 2 H), 4.16 (q, J = 7.2 Hz, 2 H), 1.23 (t, J = 7.2 Hz, 3 H), 1.13 (t, J = 7.2 Hz, 3 H); ^{13}C{^{1}H} NMR (125 MHz, $CDCl_3$) δ 163.9, 162.3, 146.6, 136.9, 133.3, 133.2, 131.3, 129.8, 127.5, 127.2, 62.3, 62.1, 13.9, 13.8; IR (KBr, neat) 2984, 1726, 1537, 1357, 1260, 1214, 1063, 1019, 861, 762 cm^{-1}; HRMS (ESI) calcd. for $C_{14}H_{14}Cl_2NO_6$ $(M + H)^+$ 362.0193, found 362.0173.

Diethyl 2-(5-methyl-2-nitrobenzylidene)malonate (22h):

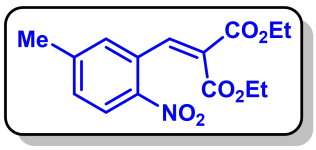

Yellow solid; R_f (Hexane/EtOAc, 9:1) 0.50; mp 68–70 °C. Yield 324 mg, 80%; ^{1}H NMR (500 MHz, $CDCl_3$) δ 8.10 (s, 1 H), 7.97 (s, 1 H), 7.41 (d, J = 7.0 Hz, 1 H), 7.29 (d, J = 7.5 Hz, 1 H), 4.29 (q, J = 7.0 Hz, 2 H), 4.08 (q, J = 7.0 Hz, 2 H), 2.44 (s, 3 H), 1.31 (t, J = 7.5 Hz, 3 H), 1.04 (t, J = 7.0 Hz, 3 H); ^{13}C{^{1}H} NMR (125 MHz, $CDCl_3$) δ 165.1, 163.6, 147.2, 141.4, 141.1, 134.6, 130.1, 129.0, 127.6, 125.5, 61.9, 61.6, 21.2, 14.2, 13.9; IR (KBr, neat) 2983, 1722, 1527, 1345, 1252, 1203, 1063, 1019, 852, 761, cm^{-1}; HRMS (ESI) calcd. for $C_{15}H_{18}NO_6$ $(M + H)^+$ 308.1129, found 308.1140.

Diethyl 2-(5-methoxy-2-nitrobenzylidene)malonate (22i):

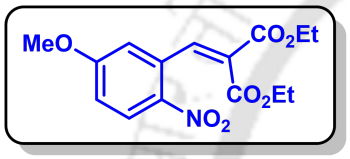

Brown liquid; R_f (Hexane/EtOAc, 9:1) 0.45. Yield 354 mg, 83%; ^{1}H NMR (500 MHz, $CDCl_3$) δ 8.12–8.08 (m, 2 H), 6.91 (dd, J = 9.0, 2.5 Hz, 1 H), 6.77 (d, J = 3.0 Hz, 1 H), 4.22 (q, J = 7.5 Hz, 2 H), 4.01 (q, J = 7.5 Hz, 2 H), 3.79 (s, 3 H), 1.24 (t, J = 7.0 Hz, 3 H), 0.96 (t, J = 7.0 Hz, 3 H); ^{13}C{^{1}H} NMR (125 MHz, $CDCl_3$) δ 164.7, 163.6, 163.2, 141.5, 139.9, 132.9, 128.8, 127.5, 114.96, 114.7, 61.8, 61.4, 56.1, 14.0, 13.6; IR (KBr, neat) 2983, 1722, 1577, 1512, 1338, 1233, 1210, 1065, 1021, 848, 835, 694 cm^{-1}; HRMS (ESI) calcd. for $C_{15}H_{18}NO_7$ $(M + H)^+$ 324.1078, found 324.1071.

Diethyl 2-(4,5-dimethoxy-2-nitrobenzylidene)malonate (22j):

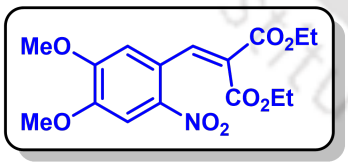

Orange solid; R_f (Hexane/EtOAc, 9:1) 0.45; mp 64–66 °C. Yield 391 mg, 84%; ^{1}H NMR (500 MHz, $CDCl_3$) δ 8.06 (s, 1 H), 7.66 (s, 1 H), 6.81 (s, 1 H), 4.22 (q, J = 7.0 Hz, 2 H), 4.04 (q, J = 7.0 Hz, 2 H), 3.89 (s, 3 H), 3.84 (s, 3 H), 1.25 (t, J = 7.0 Hz, 3 H), 1.01 (t, J = 7.0 Hz, 3 H); ^{13}C{^{1}H} NMR (125 MHz, $CDCl_3$) δ 165.2, 163.2, 153.1, 149.4, 141.0, 139.8, 128.2, 124.3, 111.4, 107.7, 61.6, 61.4, 56.4, 56.3, 13.9, 13. 7; IR (KBr, neat) 2982, 1723, 1519, 1333, 1281, 1211, 1065, 795, 764 cm^{-1}; HRMS (ESI) calcd. for $C_{16}H_{20}NO_8$ $(M + H)^+$ 354.1184, found 354.1178.

Diisopropyl 2-(2-nitrobenzylidene)malonate (22l):

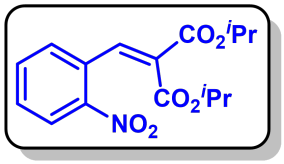

Brown solid; R_f (Hexane/EtOAc, 9:1) 0.50; mp 70–72 °C. Yield 322 mg, 76%; ^{1}H NMR (400 MHz, $CDCl_3$) δ 8.08 (d, J = 8.0 Hz, 1 H), 8.02 (s, 1 H), 7.56 (d, J = 7.6 Hz, 1 H), 7.48 (d, J = 8.0 Hz, 1 H), 7.36 (d, J = 7.6 Hz, 1 H), 5.09–5.03 (m, 1 H), 4.90–4.84 (m, 1 H), 1.22 (d, J = 6.4 Hz, 6 H), 0.95 (d, J = 6.4 Hz, 6 H); ^{13}C{^{1}H} NMR (125 MHz, $CDCl_3$) δ 164.3, 162.9, 147.1, 140.2, 133.7, 130.6, 130.2, 130.1, 130.1, 124.9, 69.7, 69.2, 21.7, 21.3; IR (KBr, neat) 2983, 1721, 1525, 1374, 1256, 1221, 1105, 1063, 929, 745, 697 cm^{-1}; HRMS (ESI) calcd. for $C_{16}H_{20}NO_6$ $(M + H)^+$ 322.1286, found 322.1296.

Ethyl-2-(2-nitrobenzylidene)-3-oxopentanoate (22n):

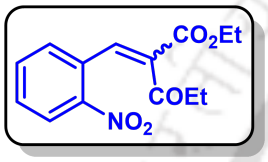

Brown liquid; R_f (Hexane/EtOAc, 4:1) 0.50. Yield 249 mg, 68%; ^{1}H NMR (400 MHz, $CDCl_3$) δ 8.12 (dd, J = 8.0, 1.2 Hz, 1 H), 7.98 (s, 1 H), 7.61–7.56 (m, 1 H), 7.54–7.50 (m, 1 H), 7.30 (d, J = 7.6 Hz, 1 H), 4.26 (q, J = 7.2 Hz, 2 H), 2.39 (q, J = 7.2 Hz, 2 H), 1.28 (t, J = 7.2 Hz, 3 H), 0.87 (t, J = 7.2 Hz, 3 H); ^{13}C{^{1}H} NMR (125 MHz, $CDCl_3$) δ 204.0, 163.9, 147.3, 138.5, 136.2, 133.9, 131.0, 130.3, 129.9, 125.0, 61.8, 37.1, 14.1, 7.5; IR (KBr, neat) 3476, 2983, 1699, 1523, 1343, 1252, 1138, 1029, 789 cm^{-1}; HRMS (ESI) calcd. for $C_{14}H_{16}NO_5$ $(M + H)^+$ 278.1023, found 278.1019.

Ethyl-2-benzoyl-3-(2-nitrophenyl)acrylate (22o):

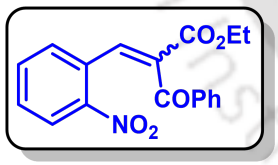

Yellow solid; R_f (Hexane/EtOAc, 4:1) 0.50; mp 97–99 °C. Yield 279 mg, 65%; ^{1}H NMR (400 MHz, $CDCl_3$) δ 8.30 (s, 1 H), 8.01 (d, J = 7.6 Hz, 1 H), 7.81 (d, J = 7.6 Hz, 2 H), 7.44 (t, J = 7.6 Hz, 2 H), 7.37 (t, J = 7.6 Hz, 2 H), 7.30 (t, J = 8.0 Hz, 2 H), 4.25 (q, J = 7.2 Hz, 2 H), 1.20 (t, J = 7.2 Hz, 3 H); ^{13}C{^{1}H} NMR (125 MHz, $CDCl_3$) δ 193.9, 164.3, 147.3, 139.9, 136.4, 134.2, 134.1, 133.9, 131.6, 130.3, 130.0, 129.1, 128.8, 125.0, 62.0, 14.2; IR (KBr, neat) 3466, 2986, 1672, 1523, 1344, 1247, 1092, 789 cm^{-1}; HRMS (ESI) calcd. for $C_{18}H_{16}NO_5$ $(M + H)^+$ 326.1023, found 326.1022.

Ethyl 3-(2-nitrophenyl)-2-(phenylsulfonyl)acrylate (22p):

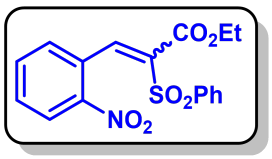

Yellow solid; R_f (Hexane/EtOAc, 3:2) 0.50; mp 124–126 °C. Yield 305 mg, 64%; ^{1}H NMR (500 MHz, $CDCl_3$) δ 8.68 (s, 1 H), 8.23 (d, J = 7.5 Hz, 1 H), 8.02 (d, J = 7.5 Hz, 2 H), 7.68–7.62 (m, 2 H), 7.60–7.54 (m, 3 H), 7.38 (d, J = 7.5 Hz, 1 H), 3.91 (q, J = 7.0 Hz, 2 H), 0.85 (t, J = 7.0 Hz, 3 H); ^{13}C{^{1}H} NMR (125 MHz, $CDCl_3$) δ 160.8, 146.9, 146.4, 139.4, 136.1, 134.0, 133.9, 130.6, 130.0, 129.9, 129.2, 128.8, 124.9, 62.2, 13.5; IR (KBr, neat) 3466, 2990, 1725, 1524, 1344, 1321, 1215, 1154, 1088, 687 cm^{-1}; HRMS (ESI) calcd. for $C_{17}H_{16}NO_6S$ $(M + H)^+$ 362.0693, found 362.0689.

1-((1*R*,2*S*,5*R*)-2-Isopropyl-5-methylcyclohexyl) 3-((1*S*,2*S*,5*S*)-2-isopropyl-5-methylcyclohexyl) 2-((*E*)-2-nitrobenzylidene)malonate (22s):

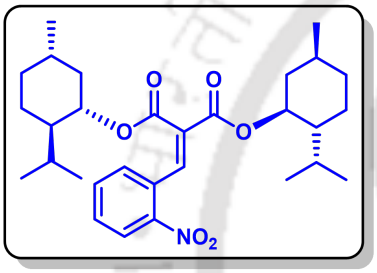

Pale yellow gummy; R_f (Hexane/EtOAc, 9:1) 0.60. Yield 386 mg, 57%; ^{1}H NMR (500 MHz, $CDCl_3$) δ 8.17 (d, J = 9.0 Hz, 1 H), 8.11 (s, 1 H), 7.59 (d, J = 8.0 Hz, 1 H), 7.53 (t, J = 8.0 Hz, 1 H), 7.46 (d, J = 8.0 Hz, 1 H), 4.83 (t, J = 8.5 Hz, 1 H), 4.60 (t, J = 9.5 Hz, 1 H), 2.11 (d, J = 12.5 Hz, 1 H), 1.92 (d, J = 8.0 Hz, 1 H), 1.68 (d, J = 11.5 Hz, 4 H), 1.60–1.49 (m, 3 H), 1.41–1.31 (m, 3 H), 1.20 (t, J = 12.0 Hz, 1 H), 1.10–0.99 (m, 2 H), 0.93–0.84 (m, 9 H), 0.81–0.76 (m, 6 H), 0.71 (d, J = 7.5 Hz, 3 H), 0.52–0.48 (m, 3 H); ^{13}C{^{1}H} NMR (125 MHz, $CDCl_3$) δ 164.9, 163.1, 147.2, 139.6, 133.9, 130.8, 130.6, 130.1, 125.0, 76.2, 75.9, 47.4, 46.6, 40.9, 40.2, 34.4, 34.1, 31.6, 31.4, 26.3, 25.8, 23.4, 23.2, 22.2, 22.1, 21.1, 20.9, 16.4, 16.1; IR (KBr, neat) 3473, 2956, 1714, 1527, 1345, 1253, 1218, 789, 529 cm^{-1}; HRMS (ESI) calcd. for $C_{30}H_{44}NO_6$ $(M + H)^+$ 514.3164, found 514.3169.

Ethyl 2-(2-nitrobenzylidene)butanoate (22t, inseparable mixture of isomers 3:1):

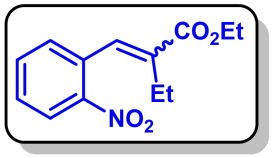

Yellow liquid; R_f (Hexane/EtOAc, 17:3) 0.50. Yield 230 mg, 70%; ^{1}H NMR (500 MHz, $CDCl_3$) δ 8.05 (d, J = 8.0 Hz, 1 H, major), 8.01 (d, J = 8.0 Hz, 1 H, minor), 7.79 (s, 1 H, major), 7.62 (t, J = 8.0 Hz, 1 H, major), 7.51 (t, J = 7.5 Hz, 1 H, minor), 7.47 (t, J = 8.0 Hz, 1 H, major), 7.39 (t, J = 8.0 Hz, 1 H, minor), 7.31 (d, J = 8.0 Hz, 1 H, major), 7.21 (d, J = 8.0 Hz, 1 H, minor), 7.04 (s, 1 H, minor), 4.23 (q, J = 7.5 Hz, 2 H, major), 3.86 (q, J = 7.5 Hz, 2 H, minor), 2.43 (q, J = 7.5 Hz, 2 H, minor), 2.23

(q, J = 7.5 Hz, 2 H, major), 1.28 (t, J = 7.0 Hz, 3 H, major), 1.12 (t, J = 7.5 Hz, 3 H, minor), 0.96 (t, J = 7.0 Hz, 3 H, major), 0.84 (t, J = 7.0 Hz, 3 H, minor); $^{13}C\{^1H\}$ NMR (125 MHz, $CDCl_3$) δ 167.4, 167.0, 147.6, 147.2, 136.9, 136.1, 135.1, 133.8, 133.3, 132.9, 131.8, 131.7, 130.8, 130.7, 128.9, 128.1, 124.7, 124.1, 60.8, 60.2, 27.1, 21.0, 14.1, 13.7, 13.4, 12.7; IR (KBr, neat) 3476, 2981, 1708, 1522, 1342, 1233, 1127, 1045, 787, 704 cm^{-1}; HRMS (ESI) calcd. for $C_{13}H_{16}NO_4$ $(M + H)^+$ 250.1074, found 250.1067.

Ethyl 2-(1*H*-indol-3-yl)-3-oxoindoline-2-carboxylate (24aa):

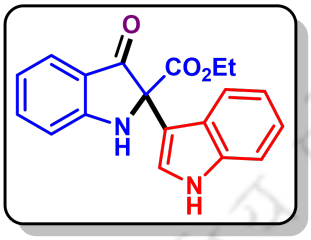

Yellow solid; R_f (Hexane/EtOAc, 7:3) 0.50; mp 173–175 °C. Yield 139 mg, 85%; ^1H NMR (500 MHz, $CDCl_3$) δ 8.37 (s, 1 H), 7.61 (d, J = 8.0 Hz, 1 H), 7.50 (d, J = 8.0 Hz, 1 H), 7.43 (t, J = 8.0 Hz, 1 H), 7.21 (d, J = 8.0 Hz, 1 H), 7.18 (d, J = 2.5 Hz, 1 H), 7.07 (t, J = 7.5 Hz, 1 H), 6.99 (t, J = 7.5 Hz, 1 H), 6.90 (d, J = 8.5 Hz, 1 H), 6.84 (t, J = 7.5 Hz, 1 H), 5.67 (s, 1 H), 4.18 (q, J = 7.0 Hz, 2 H), 1.14 (t, J = 7.0 Hz, 3 H); $^{13}C\{^1H\}$ NMR (125 MHz, $CDCl_3$) δ 195.3, 168.7, 161.3, 138.1, 136.8, 125.6, 125.5, 124.0, 122.7, 120.4, 120.3, 119.9, 119.7, 113.7, 111.9, 111.5, 72.8, 63.2, 14.2; IR (KBr, neat) 3357, 2983, 1733, 1615, 1467, 1325, 1231, 1013, 896, 749 cm^{-1}; HRMS (ESI) calcd. for $C_{19}H_{17}N_2O_3$ $(M + H)^+$ 321.1234, found 321.1249.

Ethyl 5-chloro-2-(1*H*-indol-3-yl)-3-oxoindoline-2-carboxylate (24ab):

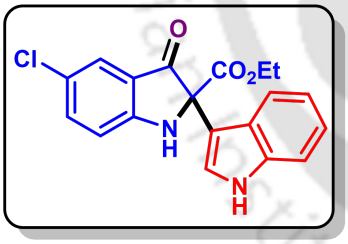

Yellow solid; R_f (Hexane/EtOAc, 7:3) 0.55; mp 170–172 °C. Yield 144 mg, 80%; ^1H NMR (400 MHz, $CDCl_3$) δ 8.52 (s, 1 H), 7.72 (d, J = 8.0 Hz, 1 H), 7.61 (d, J = 8.0 Hz, 1 H), 7.54 (t, J = 7.6 Hz, 1 H), 7.31 (d, J = 9.2 Hz, 1 H), 7.18 (t, J = 7.2 Hz, 1 H), 7.10 (t, J = 7.2 Hz, 1 H), 7.01 (d, J = 8.4 Hz, 1 H), 6.95 (t, J = 7.2 Hz, 1 H), 5.78 (s, 1 H), 4.29 (q, J = 7.2 Hz, 2 H), 1.24 (t, J = 7.2 Hz, 3 H); $^{13}C\{^1H\}$ NMR (125 MHz, $CDCl_3$) δ 195.1, 168.6, 161.3, 138.0, 136.7, 125.6, 123.8, 122.8, 120.5, 120.4, 120.1, 119.8, 113.8, 111.9, 111.8, 72.8, 63.3, 14.3; IR (KBr, neat) 3363, 2924, 1736, 1615, 1474, 1230, 1172, 890, 748 cm^{-1}; HRMS (ESI) calcd. for $C_{19}H_{16}ClN_2O_3$ $(M + H)^+$ 355.0844, found 355.0833.

Ethyl 5-bromo-2-(1*H*-indol-3-yl)-3-oxoindoline-2-carboxylate (24ac):

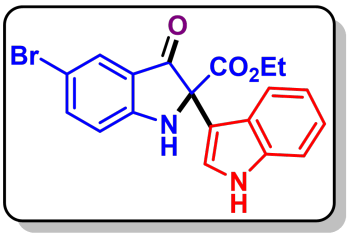

Yellow solid; R_f (Hexane/EtOAc, 7:3) 0.55; mp 164–166 °C. Yield 161 mg, 79%; ^{1}H NMR (500 MHz, $CDCl_3$) δ 8.50 (s, 1 H), 7.61 (dd, J = 12.5, 8.0 Hz, 2 H), 7.38 (d, J = 8.0 Hz, 1 H), 7.34–7.33 (m, 1 H), 7.25–7.23 (m, 1 H), 7.16 (t, J = 7.5 Hz, 1 H), 7.11 (dd, J = 8.5, 1.5 Hz, 1 H), 5.90 (s, 1 H), 4.35 (q, J = 7.0 Hz, 2 H), 1.31 (t, J = 7.0 Hz, 3 H); ^{13}C{^{1}H} NMR (125 MHz, $CDCl_3$) 194.0, 168.2, 161.4, 136.7, 133.5, 126.6, 125.4, 123.9, 122.8, 120.5, 119.7, 118.7, 116.5, 111.9, 111.2, 73.1, 63.4, 14.3; IR (KBr, neat) 3373, 2986, 1737, 1605, 1461, 1260, 1227, 914, 749 cm^{-1}; HRMS (ESI) calcd. for $C_{19}H_{16}BrN_2O_3$ $(M + H)^+$ 399.0339, found 399.0343.

Ethyl 5-fluoro-2-(1*H*-indol-3-yl)-3-oxoindoline-2-carboxylate (24ad):

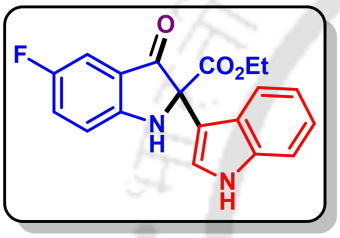

Pale yellow solid; R_f (Hexane/EtOAc, 7:3) 0.50; mp 161–163 °C. Yield 143 mg, 83%; ^{1}H NMR (500 MHz, $CDCl_3$) δ 8.37 (s, 1 H), 7.55 (d, J = 8.0 Hz, 1 H), 7.31–7.28 (m, 2 H), 7.24–7.22 (m, 2 H), 7.14 (t, J = 7.5 Hz, 1 H), 7.05 (t, J = 8.0 Hz, 1 H), 6.92 (dd, J = 9.0, 4.0 Hz, 1 H), 5.64 (s, 1 H), 4.23 (q, J = 7.0 Hz, 2 H), 1.19 (t, J = 7.0 Hz, 3 H); ^{13}C{^{1}H} NMR (125 MHz, $CDCl_3$) δ 194.9 (d, J = 3.5 Hz), 168.5, 157.90, 157.5 (d, J = 239.7 Hz), 136.7, 126.2 (d, J = 25.4 Hz), 125.5, 123.9, 122.8, 120.6 (d, J = 7.2 Hz), 120.5, 119.8, 115.1 (d, J = 7.5 Hz), 111.9, 111.4, 110.3 (d, J = 22.7 Hz), 73.9, 63.4, 14.2; ^{19}F NMR (470 MHz, $CDCl_3/C_6F_6$) δ –126.3 (s, –CF–); IR (KBr, neat) 3367, 2983, 1701, 1626, 1491, 1231, 1011, 746, 529 cm^{-1}; HRMS (ESI) calcd. for $C_{19}H_{16}FN_2O_3$ $(M + H)^+$ 339.1140, found 339.1134.

Ethyl 2-(1*H*-indol-3-yl)-3-oxo-5-(trifluoromethyl)indoline-2-carboxylate (24ae):

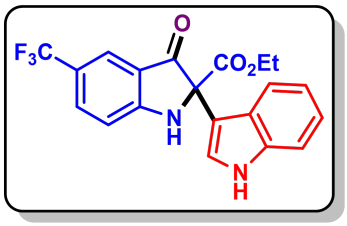

Brown solid; R_f (Hexane/EtOAc, 7:3) 0.55; mp 153–155 °C. Yield 133 mg, 67%; ^{1}H NMR (500 MHz, $CDCl_3$) δ 8.34 (s, 1 H), 7.77 (d, J = 8.0 Hz, 1 H), 7.59 (d, J = 8.0 Hz, 1 H), 7.35–7.32 (m, 2 H), 7.25 (s, 1 H), 7.19 (t, J = 7.5 Hz, 1 H), 7.14 (d, J = 8.0 Hz, 1 H), 7.10 (t, J = 7.5 Hz, 1 H), 5.93 (s, 1 H), 4.28 (q, J = 7.0 Hz, 2 H), 1.25 (t, J = 7.0 Hz, 3 H); ^{13}C{^{1}H} NMR (125 MHz, $CDCl_3$) δ 194.4, 168.0, 160.3, 139.05 (d, J = 32.0 Hz), 136.8, 126.4, 125.4, 124.7, 123.9, 123.0, 122.2, 120.6, 119.8, 116.9 (d, J = 3.4 Hz), 111.9, 111.1, 110.7 (d, J = 4.1 Hz), 73.3, 63.5, 14.3; ^{19}F NMR (470 MHz, $CDCl_3/C_6F_6$) δ –66.8 (s, –CF_3–); IR (KBr,

neat) 3381, 2924, 1737, 1634, 1459, 1340, 1259, 1131, 1057, 749 cm^{-1}; HRMS (ESI) calcd. for $C_{20}H_{16}F_3N_2O_3$ $(M + H)^+$ 389.1108, found 389.1101.

Ethyl 2-(1*H*-indol-3-yl)-5-methyl-3-oxoindoline-2-carboxylate–carbon dioxide (1/1) (24af):

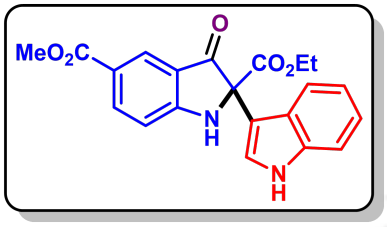

Brown solid; R_f (Hexane/EtOAc, 7:3) 0.50; mp 175–177 °C. Yield 121 mg, 63%; ^1H NMR (400 MHz, $CDCl_3$) δ 8.47 (s, 1 H), 8.38 (s, 1 H), 8.18 (dd, J = 8.4, 1.6 Hz, 1 H), 7.51 (d, J = 8.0 Hz, 1 H), 7.32 (d, J = 8.0 Hz, 1 H), 7.29 (s, 1 H), 7.17 (t, J = 6.8 Hz, 1 H), 7.07 (t, J = 8.0 Hz, 1 H), 6.95 (d, J = 8.4 Hz, 1 H), 6.15 (s, 1 H), 4.27 (q, J = 7.2 Hz, 2 H), 3.89 (s, 3 H), 1.23 (t, J = 7.2 Hz, 3 H); $^{13}C\{^1H\}$ NMR (125 MHz, $CDCl_3$) δ 193.9, 168.0, 166.5, 163.0, 139.2, 136.8, 128.4, 125.3, 124.0, 122.9, 122.0, 120.6, 119.5, 119.2, 112.5, 112.0, 110.9, 73.3, 63.4, 52.3, 14.3; IR (KBr, neat) 3355, 2924, 1705, 1618, 1435, 1012, 767, 745, 523 cm^{-1}; HRMS (ESI) calcd. for $C_{21}H_{19}N_2O_5$ $(M + H)^+$ 379.1289, found 379.1274.

Ethyl 5,7-dichloro-2-(1*H*-indol-3-yl)-3-oxoindoline-2-carboxylate (24ag):

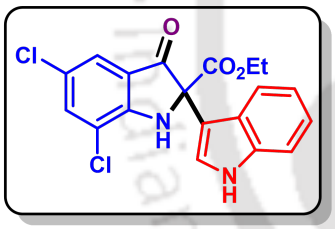

Pale yellow solid; R_f (Hexane/EtOAc, 7:3) 0.60; mp 157–159 °C. Yield 153 mg, 77%; ^1H NMR (500 MHz, $CDCl_3$) δ 8.46 (s, 1 H), 7.62–7.59 (m, 2 H), 7.57 (s, 1 H), 7.34 (d, J = 8.5 Hz, 1 H), 7.30 (s, 1 H), 7.21 (t, J = 7.5 Hz, 1 H), 7.14 (t, J = 7.5 Hz, 1 H), 5.91 (s, 1 H), 4.31 (q, J = 7.5 Hz, 2 H), 1.27 (t, J = 7.5 Hz, 3 H); $^{13}C\{^1H\}$ NMR (125 MHz, $CDCl_3$) δ 193.4, 167.6, 155.9, 136.7, 136.5, 125.5, 125.2, 124.0, 123.4, 122.9, 121.7, 120.6, 119.8, 119.4, 111.9, 110.6, 73.8, 63.6, 14.2; IR (KBr, neat) 3347, 2970, 1716, 1640, 1365, 1331, 1152, 1046, 865, 741 cm^{-1}; HRMS (ESI) calcd. for $C_{19}H_{15}Cl_2N_2O_3$ $(M + H)^+$ 389.0455, found 389.0430.

Ethyl 2-(1*H*-indol-3-yl)-5-methyl-3-oxoindoline-2-carboxylate (24ah):

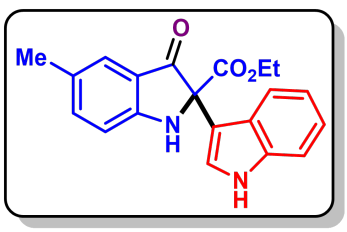

Brown solid; R_f (Hexane/EtOAc, 7:3) 0.50; mp 196–196 °C. Yield 155 mg, 91%; ^1H NMR (400 MHz, $CDCl_3$) δ 8.56 (s, 1 H), 7.59 (t, J = 8.4 Hz, 2 H), 7.28 (d, J = 8.0 Hz, 1 H), 7.23 (s, 1 H), 7.16 (t, J = 7.6 Hz, 1 H), 7.08 (t, J = 7.6 Hz, 1 H), 6.79–6.75 (m, 2 H), 5.70 (s, 1 H), 4.27 (q, J = 7.2 Hz, 2 H), 2.40 (s, 3 H), 1.23 (t, J = 7.2 Hz, 3 H); $^{13}C\{^1H\}$ NMR (125 MHz, $CDCl_3$) δ 194.6, 168.8, 161.8, 149.9, 136.7, 125.5, 125.3, 124.0, 122.6, 122.2, 120.2, 119.7, 117.7, 113.7, 111.9, 111.6, 73.1, 63.1, 22.7, 14.2; IR (KBr, neat) 3357, 2923, 1735, 1618, 1459,

1259, 1110, 986, 749 cm^{-1}; HRMS (ESI) calcd. for $C_{20}H_{19}N_2O_3$ $(M + H)^+$ 335.1391, found 335.1412.

Ethyl 2-(1*H*-indol-3-yl)-5-methoxy-3-oxoindoline-2-carboxylate (24ai):

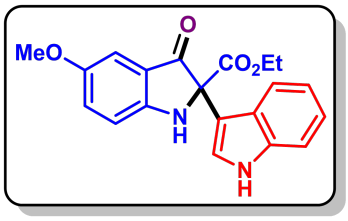

Yellow solid; R_f (Hexane/EtOAc, 7:3) 0.40; mp 200–202 °C. Yield 169 mg, 95%; ^{1}H NMR (500 MHz, $CDCl_3$) δ 8.35 (s, 1 H), 7.59 (d, J = 8.0 Hz, 1 H), 7.33–7.31 (m, 2 H), 7.22–719 (m, 2 H), 7.11 (d, J = 3.0 Hz, 1 H), 7.08 (d, J = 7.5 Hz, 1 H), 6.97 (d, J = 9.0 Hz, 1 H), 5.54 (s, 1 H), 4.27 (q, J = 7.0 Hz, 2 H), 3.79 (s, 3 H), 1.23 (t, J = 7.0 Hz, 3 H); ^{13}C{^{1}H} NMR (125 MHz, $CDCl_3$) δ 195.4, 168.8, 157.1, 154.6, 136.7, 128.7, 125.6, 123.8, 122.8, 120.5, 120.4, 119.8, 115.5, 111.9, 111.8, 105.2, 73.8, 63.3, 56.0, 14.3; IR (KBr, neat) 3363, 2925, 1730, 1693, 1493, 1337, 1222, 1025, 825, 747, 541 cm^{-1}; HRMS (ESI) calcd. for $C_{20}H_{19}N_2O_4$ $(M + H)^+$ 351.1340, found 351.1331.

Ethyl 2-(1*H*-indol-3-yl)-5,6-dimethoxy-3-oxoindoline-2-carboxylate (24aj):

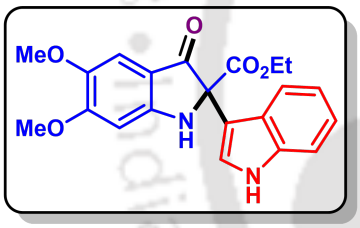

Dark yellow solid; R_f (Hexane/EtOAc, 3:2) 0.40; mp 203–205 °C. Yield 188 mg, 97%; ^{1}H NMR (400 MHz, $CDCl_3$) δ 8.52 (s, 1 H), 7.53 (d, J = 8.0 Hz, 1 H), 7.31–7.29 (m, 2 H), 7.15 (t, J = 7.2 Hz, 1 H), 7.08–7.04 (m, 2 H), 6.46 (s, 1 H), 5.64 (s, 1 H), 4.26 (q, J = 7.2 Hz, 2 H), 3.92 (s, 3 H), 3.84 (s, 3 H), 1.22 (t, J = 7.2 Hz, 3 H); ^{13}C{^{1}H} NMR (100 MHz, $CDCl_3$) δ 193.3, 169.1, 159.3, 159.1, 145.3, 136.7, 125.7, 124.0, 122.6, 120.3, 119.5, 111.9, 111.9, 111.7, 104.7, 96.0, 73.4, 63.2, 56.6, 56.4, 14.3; IR (KBr, neat) 3352, 2957, 1700, 1637, 1415, 1305, 1293, 1086, 1008, 797, 637 cm^{-1}; HRMS (ESI) calcd. for $C_{21}H_{21}N_2O_5$ $(M + H)^+$ 381.1445, found 381.1436.

Methyl 2-(1*H*-indol-3-yl)-3-oxoindoline-2-carboxylate (24ak):

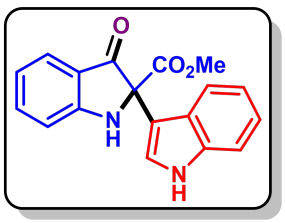

Brown solid; R_f (Hexane/EtOAc, 7:3) 0.50; mp 180–182 °C. Yield 126 mg, 81%; ^{1}H NMR (500 MHz, $CDCl_3$) δ 8.27 (s, 1 H), 7.70 (d, J = 7.5 Hz, 1 H), 7.58 (d, J = 8.0 Hz, 1 H), 7.53 (t, J = 7.5 Hz, 1 H), 7.35 (d, J = 9.5 Hz, 2 H), 7.19 (t, J = 7.5 Hz, 1 H), 7.10 (t, J = 7.5 Hz, 1 H), 7.00 (d, J = 8.5 Hz, 1 H), 6.93 (t, J = 7.5 Hz, 1 H), 5.73 (s, 1 H), 3.80 (s, 3 H); ^{13}C{^{1}H} NMR (125 MHz, $CDCl_3$) δ 195.0, 169.2, 161.3, 138.2, 136.7, 125.6, 123.8, 122.9, 120.6, 120.1, 119.7, 113.8, 111.9,

111.8, 72.6, 54.0; IR (KBr, neat) 3475, 3378, 3070, 2211, 1736, 1614, 1468, 1313, 1156, 1024, 748 cm^{-1}; HRMS (ESI) calcd. for $C_{18}H_{15}N_2O_3$ $(M + H)^+$ 307.1078, found 307.1087.

Isopropyl 2-(1*H*-indol-3-yl)-3-oxoindoline-2-carboxylate (24al):

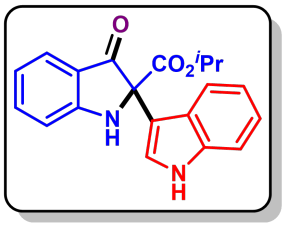

Dark brown solid; R_f (Hexane/EtOAc, 7:3) 0.55; mp 187–189 °C. Yield 148 mg, 87%; ^1H NMR (500 MHz, $CDCl_3$) δ 8.46 (s, 1 H), 7.69 (d, J = 8.0 Hz, 1 H), 7.60 (d, J = 8.0 Hz, 1 H), 7.52 (t, J = 7.5 Hz, 1 H), 7.30–7.25 (m, 2 H), 7.15 (t, J = 7.5 Hz, 1 H), 7.07 (t, J = 8.0 Hz, 1 H), 6.99 (d, J = 8.5 Hz, 1 H), 6.92 (t, J = 7.5 Hz, 1 H), 5.72 (s, 1 H), 5.15–5.08 (m, 1 H), 1.24 (d, J = 6.5 Hz, 3 H), 1.18 (d, J = 6.0 Hz, 3 H); $^{13}C\{^1H\}$ NMR (125 MHz, $CDCl_3$) δ 195.2, 168.1, 161.3, 137.9, 136.7, 125.6, 125.5, 123.9, 122.6, 120.4, 120.2, 120.0, 119.9, 113.7, 111.9, 111.7, 72.9, 71.2, 21.8, 21.7; IR (KBr, neat) 3386, 2931, 1737, 1619, 1466, 1370, 1275, 1260, 1100, 749 cm^{-1}; HRMS (ESI) calcd. for $C_{20}H_{18}N_2NaO_3$ $(M + Na)^+$ 357.1210, found 357.1216.

Ethyl 2-(6-chloro-1*H*-indol-3-yl)-3-oxoindoline-2-carboxylate (24bb):

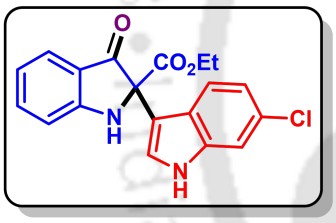

Yellow solid; R_f (Hexane/EtOAc, 7:3) 0.50; mp 172–174 °C. Yield 164 mg, 91%; ^1H NMR (500 MHz, $CDCl_3$) δ 8.58 (s, 1 H), 7.68 (d, J = 7.5 Hz, 1 H), 7.56–7.50 (m, 2 H), 7.24 (s, 2 H), 7.02 (dd, J = 8.0, 3.5 Hz, 2 H), 6.94 (t, J = 7.5 Hz, 1 H), 5.71 (s, 1 H), 4.27 (q, J = 7.0 Hz, 2 H), 1.23 (t, J = 7.0 Hz, 3 H); $^{13}C\{^1H\}$ NMR (125 MHz, $CDCl_3$) δ 195.2, 168.5, 161.3, 138.3, 137.2, 128.6, 125.7, 124.7, 124.1, 121.1, 120.9, 120.7, 119.9, 113.8, 111.8, 72.8, 63.4, 14.3; IR (KBr, neat) 3335, 2890, 1716, 1590, 1456, 1273, 1100, 1032, 872, 740 cm^{-1}; HRMS (ESI) calcd. for $C_{19}H_{16}ClN_2O_3$ $(M + H)^+$ 355.0844, found 355.0831.

Ethyl 2-(6-bromo-1*H*-indol-3-yl)-3-oxoindoline-2-carboxylate (24bc):

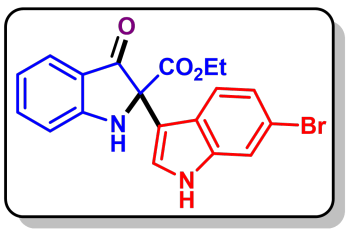

Brown solid; R_f (Hexane/EtOAc, 7:3) 0.50; mp 169–171 °C. Yield 167 mg, 82%; ^1H NMR (400 MHz, $CDCl_3$) δ 8.60 (s, 1 H), 7.68 (d, J = 7.2 Hz, 1 H), 7.53 (t, J = 7.6 Hz, 1 H), 7.46 (d, J = 8.4 Hz, 1 H), 7.40 (s, 1 H), 7.22 (s, 1 H), 7.15 (d, J = 8.4 Hz, 1 H), 7.01 (d, J = 8.4 Hz, 1 H), 6.94 (t, J = 7.6 Hz, 1 H), 5.71 (s, 1 H), 4.27 (q, J = 7.2 Hz, 2 H), 1.23 (t, J = 7.2 Hz, 3 H); $^{13}C\{^1H\}$ NMR (125 MHz, $CDCl_3$) δ 195.1, 168.4, 161.3, 138.3, 137.6, 125.7, 124.6, 123.6, 121.4, 121.3, 120.7, 119.9, 116.3, 114.8, 113.8, 111.9, 72.7, 63.4, 14.3; IR (KBr,

neat) 3372, 2900, 1737, 1620, 1473, 1249, 1122, 914, 756 cm^{-1}; HRMS (ESI) calcd. for $C_{19}H_{16}BrN_2O_3$ $(M + H)^+$ 399.0339, found 399.0351.

Ethyl 2-(6-fluoro-1*H*-indol-3-yl)-3-oxoindoline-2-carboxylate (24bd):

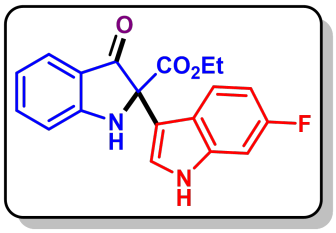

Brown solid; R_f (Hexane/EtOAc, 7:3) 0.55; mp 157–159 °C. Yield 150 mg, 87%; ^{1}H NMR (500 MHz, $CDCl_3$) δ 8.66 (s, 1 H), 7.70 (d, J = 8.0 Hz, 1 H), 7.49 (t, J = 8.0 Hz, 1 H), 7.20 (s, 1 H), 7.10–7.05 (m, 2 H), 6.94 (d, J = 8.5 Hz, 1 H), 6.88 (t, J = 7.5 Hz, 1 H), 6.79 (t, J = 7.5 Hz, 1 H), 5.89 (s, 1 H), 4.22 (q, J = 7.0 Hz, 2 H), 1.17 (t, J = 7.0 Hz, 3 H); ^{13}C{^{1}H} NMR (125 MHz, $CDCl_3$) δ 194.8, 168.7, 161.4, 156.1 (d, J = 240.8 Hz), 139.51 (d, J = 11.4 Hz), 138.3, 125.6, 124.1, 123.3 (d, J = 8.0 Hz), 120.0, 119.5, 114.8 (d, J = 20.7 Hz), 113.5, 110.2 (d, J = 2.6 Hz), 108.3 (d, J = 3.5 Hz), 105.3 (d, J = 20.0 Hz), 72.4, 63.2, 14.2; ^{19}F NMR (470 MHz, $CDCl_3/C_6F_6$) δ –124.6 (s, –CF–); IR (KBr, neat) 3463, 2982, 1701, 1459, 1366, 1203, 1011, 782, 701, 534 cm^{-1}; HRMS (ESI) calcd. for $C_{19}H_{16}FN_2O_3$ $(M + H)^+$ 339.1140, found 339.1142.

Ethyl 2-(5-nitro-1*H*-indol-3-yl)-3-oxoindoline-2-carboxylate (24be):

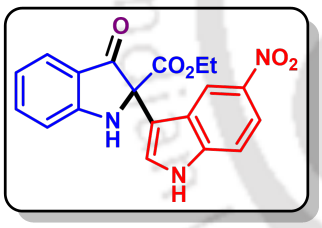

Dark brown solid; R_f (Hexane/EtOAc, 7:3) 0.55; mp 183–185 °C. Yield 140 mg, 75%; ^{1}H NMR (500 MHz, $CDCl_3$) δ 9.11 (s, 1 H), 8.78 (s, 1 H), 8.00 (d, J = 9.0 Hz, 1 H), 7.67 (d, J = 8.0 Hz, 1 H), 7.57 (t, J = 7.5 Hz, 1 H), 7.52 (s, 1 H), 7.29 (d, J = 9.0 Hz, 1 H), 7.10 (d, J = 8.5 Hz, 1 H), 6.97 (t, J = 7.5 Hz, 1 H), 5.84 (s, 1 H), 4.30 (q, J = 7.0 Hz, 2 H), 1.29 (t, J = 7.0 Hz, 3 H); ^{13}C{^{1}H} NMR (125 MHz, $CDCl_3$) δ 194.8, 168.1, 161.6, 142.2, 139.8, 138.5, 127.2, 125.7, 124.9, 121.1, 119.7, 118.3, 118.1, 114.1, 114.0, 111.9, 72.7, 63.7, 14.2; IR (KBr, neat) 3356, 2924, 1735, 1617, 1520, 1468, 1333, 1230, 1093, 897, 750 cm^{-1}; HRMS (ESI) calcd. for $C_{19}H_{16}N_3O_5$ $(M + H)^+$ 366.1085, found 366.1073.

Ethyl 2-(5-cyano-1*H*-indol-3-yl)-3-oxoindoline-2-carboxylate (24bf):

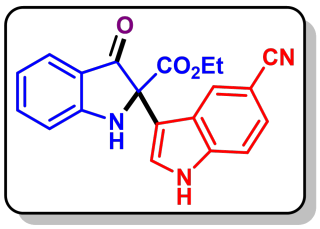

Dark brown solid; R_f (Hexane/EtOAc, 7:3) 0.50; mp 193–195 °C. Yield 134 mg, 76%; ^{1}H NMR (400 MHz, $CDCl_3$) δ 9.16 (s, 1 H), 8.10 (s, 1 H), 7.69 (d, J = 8.0 Hz, 1 H), 7.59 (t, J = 7.6 Hz, 1 H), 7.46 (s, 1 H), 7.34–7.28 (m, 2 H), 7.09 (d, J = 8.4 Hz, 1 H), 6.99 (t, J = 7.6 Hz, 1 H), 5.83 (s, 1 H), 4.31 (q, J = 7.2 Hz, 2 H), 1.29 (t, J = 7.2 Hz, 3 H); ^{13}C{^{1}H} NMR (125 MHz, $CDCl_3$) δ

194.9, 168.1, 161.5, 138.6, 138.5, 126.4, 126.4, 125.7, 125.3, 125.2, 121.1, 120.9, 119.6, 113.9, 112.8, 112.4, 103.2, 72.8, 63.6, 14.3; IR (KBr, neat) 3340, 2925, 2221, 1732, 1614, 1468, 1230, 1100, 897, 752 cm^{-1}; HRMS (ESI) calcd. for $C_{20}H_{16}N_3O_3$ $(M + H)^+$ 346.1187, found 346.1178.

Ethyl 2-(2-methyl-1*H*-indol-3-yl)- 3-oxoindoline-2-carboxylate (24bg):

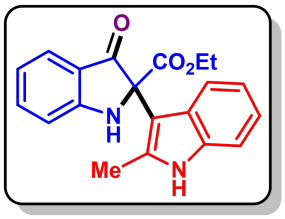

Yellow solid; R_f (Hexane/EtOAc, 7:3) 0.50; mp 199–201 °C. Yield 162 mg, 95%; ^{1}H NMR (500 MHz, $CDCl_3$) δ 8.22 (s, 1 H), 7.70 (d, J = 7.5 Hz, 1 H), 7.50 (t, J = 7.5 Hz, 1 H), 7.19 (d, J = 8.0 Hz, 1 H), 7.12 (d, J = 8.0 Hz, 1 H), 7.03 (t, J = 7.0 Hz, 1 H), 6.97 (t, J = 7.5 Hz, 1 H), 6.92 (d, J = 8.0 Hz, 2 H), 5.57 (s, 1 H), 4.35–4.26 (m, 2 H), 2.13 (s, 3 H), 1.24 (t, J = 7.5 Hz, 3 H); ^{13}C{^{1}H} NMR (125 MHz, $CDCl_3$) δ 195.9, 169.4, 161.3, 138.1, 135.1, 133.8, 127.2, 125.4, 121.6, 120.3, 120.1, 119.9, 118.4, 113.4, 111.1, 106.9, 73.5, 63.4, 14.2, 13.5; IR (KBr, neat) 3367, 2972, 1740, 1610, 1310, 1206, 1080, 847, 756 cm^{-1}; HRMS (ESI) calcd. for $C_{20}H_{19}N_2O_3$ $(M + H)^+$ 335.1391, found 335.1412.

Ethyl 2-(6-methoxy-1*H*-indol-3-yl)-3-oxoindoline-2-carboxylate (24bh):

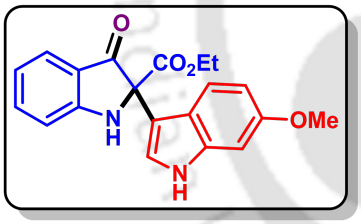

Brown solid; R_f (Hexane/EtOAc, 7:3) 0.45; mp 203–205 °C. Yield 175 mg, 98%; ^{1}H NMR (500 MHz, $CDCl_3$) δ 8.49 (s, 1 H), 7.68 (d, J = 7.5 Hz, 1 H), 7.44 (t, J = 8.0 Hz, 1 H), 7.08 (t, J = 8.0 Hz, 1 H), 7.00 (s, 1 H), 6.89 (dd, J = 13.5, 8.5 Hz, 2 H), 6.82 (t, J = 7.5 Hz, 1 H), 6.53 (d, J = 7.5 Hz, 1 H), 6.12 (s, 1 H), 4.20–4.12 (m, 2 H), 3.91 (s, 3 H), 1.12 (t, J = 7.5 Hz, 3 H); ^{13}C{^{1}H} NMR (125 MHz, $CDCl_3$) δ 195.9, 169.4, 161.3, 138.1, 135.1, 133.8, 127.2, 125.4, 121.6, 120.3, 120.1, 119.9, 118.4, 113.4, 111.1, 106.9, 73.5, 63.4, 14.2, 13.5; IR (KBr, neat) 3325, 2890, 1648, 1510, 1365, 1210, 986, 840, 744 cm^{-1}; HRMS (ESI) calcd. for $C_{20}H_{19}N_2O_4$ $(M + H)^+$ 351.1340, found 351.1331.

Ethyl 2-(6-(tert-butyl)-1*H*-indol-3-yl)-3-oxoindoline-2-carboxylate (24bi):

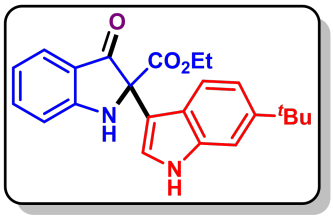

Dark brown solid; R_f (Hexane/EtOAc, 7:3) 0.50; mp 195–197 °C. Yield 188 mg, 98%; ^{1}H NMR (500 MHz, $CDCl_3$) δ 8.43 (s, 1 H), 7.68 (d, J = 8.0 Hz, 1 H), 7.54 (d, J = 8.5 Hz, 1 H), 7.50 (t, J = 7.5 Hz, 1 H), 7.32 (s, 1 H), 7.24 (s, 1 H), 7.18 (d, J = 8.5 Hz, 1 H), 6.96 (d, J = 8.0 Hz, 1 H), 6.91 (t, J = 7.5 Hz, 1 H), 5.74 (s, 1 H), 4.29–4.22 (m, 2 H), 1.33 (s, 9 H), 1.23 (t, J = 7.0 Hz, 3

H); $^{13}C\{^{1}H\}$ NMR (125 MHz, $CDCl_3$) δ 195.3, 168.7, 161.2, 146.1, 137.9, 137.0, 125.5, 123.6, 123.2, 120.3, 119.9, 119.2, 118.7, 113.6, 111.2, 108.1, 72.8, 63.1, 34.9, 31.9, 14.3; IR (KBr, neat) 3378, 2961, 1699, 1617, 1466, 1323, 1102, 898, 751, 651 cm^{-1}; HRMS (ESI) calcd. for $C_{23}H_{25}N_2O_3$ $(M + H)^+$ 377.1860, found 377.1859.

Ethyl 3-oxo-2-(5-(4,4,5,5-tetramethyl-1,3,2-dioxaborolan-2-yl)-1*H*-indol-3-yl)indoline-2-carboxylate (24bj):

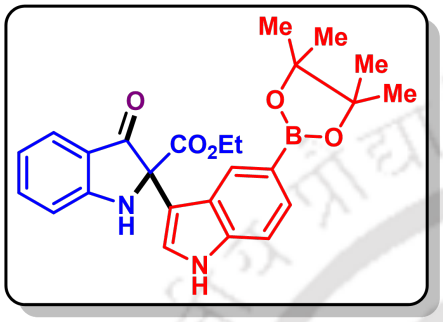

Dark brown solid; R_f (Hexane/EtOAc, 7:3) 0.40; mp 213–215 °C. Yield 193 mg, 85%; ^{1}H NMR (500 MHz, $CDCl_3$) δ 8.66 (s, 1 H), 8.10 (s, 1 H), 7.58 (d, J = 7.5 Hz, 1 H), 7.52 (d, J = 8.0 Hz, 1 H), 7.38 (t, J = 7.5 Hz, 1 H), 7.17–7.13 (m, 2 H), 6.84 (d, J = 8.0 Hz, 1 H), 6.79 (t, J = 7.0 Hz, 1 H), 5.78 (s, 1 H), 4.13 (q, J = 7.5 Hz, 2 H), 1.26 (s, 12 H), 1.11 (t, J = 7.5 Hz, 3 H); $^{13}C\{^{1}H\}$ NMR (125 MHz, $CDCl_3$) δ 195.2, 168.7, 161.4, 138.8, 138.0, 128.7, 127.3, 125.5, 125.4, 123.9, 120.2, 119.8, 113.7, 111.9, 111.4, 83.7, 72.5, 63.2, 25.0, 14.1; ^{11}B NMR (160 MHz, $CDCl_3$) δ –0.21 (bs, –CB–); IR (KBr, neat) 3363, 2978, 1776, 1615, 1468, 1355, 1230, 1145, 857, 751 cm^{-1}; HRMS (ESI) calcd. for $C_{25}H_{28}BN_2O_5$ $(M + H)^+$ 447.2086, found 447.2078.

Ethyl 3-oxo-2-(2-phenyl-1*H*-indol-3-yl)indoline-2-carboxylate (24bk):

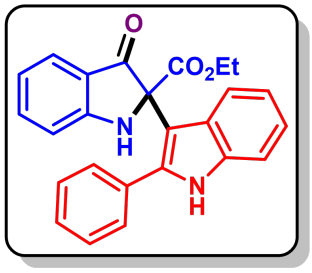

Dark yellow solid; R_f (Hexane/EtOAc, 7:3) 0.60; mp 207–209 °C. Yield 196 mg, 97%; ^{1}H NMR (500 MHz, $CDCl_3$) δ 8.46 (d, J = 14.0 Hz, 1 H), 7.50 (d, J = 7.5 Hz, 1 H), 7.42 (t, J = 8.0 Hz, 1 H), 7.30 (d, J = 7.0 Hz, 2 H), 7.24 (d, J = 7.0 Hz, 2 H), 7.20 (d, J = 7.0 Hz, 2 H), 7.14 (d, J = 8.0 Hz, 2 H), 7.03 (t, J = 7.5 Hz, 1 H), 6.91 (t, J = 8.0 Hz, 1 H), 6.82 (t, J = 7.5 Hz, 2 H), 5.54 (s, 1 H), 3.66–3.60 (m, 1 H), 3.38–3.31 (m, 1 H), 0.84 (t, J = 7.0 Hz, 3 H); ^{13}C{^{1}H} NMR (125 MHz, $CDCl_3$) δ 195.6, 168.5, 160.9, 138.1, 137.9, 135.7, 132.8, 129.6, 128.7, 128.4, 126.9, 125.3, 122.6, 120.4, 120.3, 120.2, 119.9, 113.4, 111.4, 107.9, 73.5, 62.8, 13.7; IR (KBr, neat) 3347, 2982, 1703, 1614, 1486, 1323, 1229, 1196, 895, 743, 699 cm^{-1}; HRMS (ESI) calcd. for $C_{25}H_{21}N_2O_3$ $(M + H)^+$ 397.1547, found 397.1545.

Ethyl 3-oxo-2-(2-(thiophen-2-yl)-1*H*-indol-3-yl)indoline-2-carboxylate (24bl):

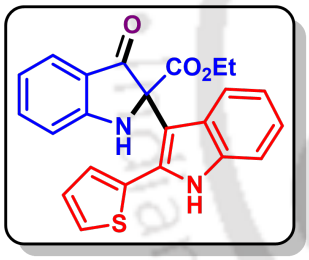

Dark yellow solid; R_f (Hexane/EtOAc, 7:3) 0.55; mp 203–205 °C. Yield 197 mg, 96%; ^{1}H NMR (500 MHz, $CDCl_3$) δ 8.55 (s, 1 H), 7.66 (d, J = 8.0 Hz, 1 H), 7.53 (t, J = 8.0 Hz, 1 H), 7.36 (d, J = 5.5 Hz, 1 H), 7.27 (d, J = 8.0 Hz, 2 H), 7.17–7.14 (m, 2 H), 7.02 (t, J = 7.5 Hz, 1 H), 6.99–6.97 (m, 1 H), 6.93 (t, J = 7.5 Hz, 2 H), 5.65 (s, 1 H), 3.94–3.87 (m, 1 H), 3.74–3.68 (m, 1 H), 1.04 (t, J = 7.0 Hz, 3 H); ^{13}C{^{1}H} NMR (125 MHz, $CDCl_3$) δ 195.4, 168.4, 160.9, 138.0, 135.8, 132.9, 130.6, 129.6, 127.5, 127.4, 126.7, 125.3, 123.1, 120.6, 120.4, 120.1, 120.1, 113.4, 111.5, 109.8, 73.4, 63.0, 13.8; IR (KBr, neat) 3345, 2925, 1702, 1615, 1467, 1229, 1013, 894, 746, 700 cm^{-1}; HRMS (ESI) calcd. for $C_{23}H_{19}N_2O_3S$ $(M + H)^+$ 403.1111, found 403.1101.

Ethyl 3-oxo-2-(1*H*-pyrrolo[2, 3-*b*]pyridin-3-yl)indoline-2-carboxylate (24bn):

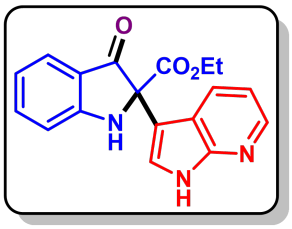

Brown solid; R_f (Hexane/EtOAc, 7:3) 0.40; mp 168–170 °C. Yield 152 mg, 93%; ^{1}H NMR (500 MHz, $CDCl_3$) δ 11.35 (s, 1 H), 8.27 (s, 1 H), 8.23 (d, J = 8.0 Hz, 1 H), 7.65–7.62 (m, 2 H), 7.51 (t, J = 7.5 Hz, 1 H), 7.07–7.01 (m, 2 H), 6.91 (t, J = 7.5 Hz, 1 H), 5.98 (s, 1 H), 4.28 (q, J = 7.0 Hz, 2 H), 1.26 (t, J = 7.0 Hz, 3 H); ^{13}C{^{1}H} NMR (125 MHz, $CDCl_3$) δ 194.7, 168.5, 161.4, 149.1, 143.0, 138.0, 130.2, 125.7, 124.4, 120.7, 119.9, 118.6, 116.2, 113.7, 110.4, 72.9, 63.4, 14.3; IR (KBr, neat) 3355, 2924, 1737, 1615, 1468, 1324, 1228, 896, 750 cm^{-1}; HRMS (ESI) calcd. for $C_{18}H_{16}N_3O_3$ $(M + H)^+$ 322.1187, found 322.1204.

Ethyl 2-(5-chloro-1*H*-pyrrolo[2,3-*b*]pyridin-3-yl)-3-oxoindoline-2-carboxylate (24bo):

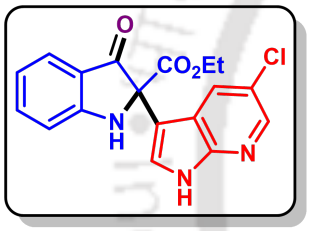

Brown solid; R_f (Hexane/EtOAc, 7:3) 0.45; mp 177–179 °C. Yield 163 mg, 90%; ^{1}H NMR (400 MHz, $CDCl_3$) δ 11.19 (s, 1 H), 8.36 (s, 1 H), 8.18 (s, 1 H), 7.66–7.62 (m, 2 H), 7.51 (t, J = 8.0 Hz, 1 H), 7.04 (d, J = 8.4 Hz, 1 H), 6.91 (t, J = 7.6 Hz, 1 H), 6.01 (s, 1 H), 4.29 (q, J = 7.2 Hz, 2 H), 1.29 (t, J = 7.2 Hz, 3 H); ^{13}C{^{1}H} NMR (125 MHz, $CDCl_3$) δ 194.5, 168.2, 161.5, 147.3, 141.6, 138.5, 130.1, 125.9, 125.8, 124.1, 120.9, 119.8, 119.4, 113.9, 110.2, 72.8, 63.6, 14.2; IR (KBr, neat) 3355, 2923, 1735, 1617, 1467, 1275, 1227, 896, 750 cm^{-1}; HRMS (ESI) calcd. for $C_{18}H_{15}ClN_3O_3$ $(M + H)^+$ 356.0797, found 356.0789.

Ethyl 2-(5-methyl-1*H*-pyrrolo[2,3-*b*]pyridin-3-yl)-3-oxoindoline-2-carboxylate (24bp):

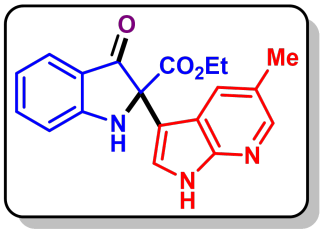

Brown solid; R_f (Hexane/EtOAc, 7:3) 0.40; mp 174–176 °C. Yield 164 mg, 96%; ^{1}H NMR (400 MHz, $CDCl_3$) δ 11.20 (s, 1 H), 8.24 (dd, J = 20.4, 4.8 Hz, 2 H), 7.61 (s, 1 H), 7.53 (d, J = 8.0 Hz, 1 H), 7.05 (dd, J = 8.0, 4.4 Hz, 1 H), 6.83 (s, 1 H), 6.74 (d, J = 8.0 Hz, 1 H), 5.85 (s, 1 H), 4.28 (q, J = 7.2 Hz, 2 H), 2.38 (s, 3 H), 1.26 (t, J = 7.2 Hz, 3 H); ^{13}C{^{1}H} NMR (125 MHz, $CDCl_3$) δ 193.9, 168.6, 161.9, 149.9, 149.1, 142.9, 130.2, 125.4, 124.4, 122.5, 118.7, 117.7, 116.2, 113.8, 110.6, 73.2, 63.3, 22.7, 14.3; IR (KBr, neat) 3358, 2924, 1729, 1617, 1463, 1333,

1227, 1109, 764, 613 cm^{-1}; HRMS (ESI) calcd. for $C_{19}H_{18}N_3O_3$ $(M + H)^+$ 336.1343, found 336.1340.

(1*R*,2*S*,5*R*)-2-isopropyl-5-methylcyclohexyl 2-(1*H*-indol-3-yl)-3-oxoindoline-2-carboxylate (24as, mixture of inseparable diastereomers 1:1):

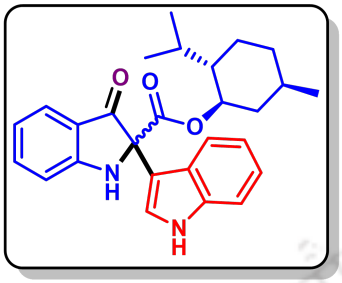

Pale red solid; R_f (Hexane/EtOAc, 7:3) 0.50; mp 210–212 °C. Yield 134 mg, 61%; ^{1}H NMR (500 MHz, $CDCl_3$) δ 8.27 (brs, 1 H, -NH, isomer 1), 8.24 (brs, 1 H, -NH, isomer 2), 7.70–7.67 (m, 2 H), 7.61–7.57 (m, 2 H), 7.53–7.49 (m, 2 H), 7.38 (d, J = 7.0 Hz, 2 H), 7.34 (d, J = 8.0 Hz, 2 H), 7.19–7.15 (m, 2 H), 7.11–7.05 (m, 2 H), 7.00 (d, J = 8.0 Hz, 2 H), 6.92 (t, J = 7.5 Hz, 2 H), 5.68 (brs, 2 H), 4.79–4.68 (m, 2 H), 1.95–1.93 (m, 2 H), 1.87–1.81 (m, 1 H), 1.65–1.53 (m, 6 H), 1.46–1.41 (m, 3 H), 1.32–1.26 (m, 2 H), 1.20–1.14 (m, 1 H), 1.09–0.98 (m, 1 H), 0.95–0.90 (m, 2 H), 0.86–0.78 (m, 9 H), 0.63 (d, J = 6.5 Hz, 3 H), 0.50 (d, J = 7.0 Hz, 3 H), 0.42 (d, J = 7.0 Hz, 3 H); ^{13}C{^{1}H} NMR (125 MHz, $CDCl_3$) δ 195.1, 194.9, 168.3, 168.2, 161.4, 161.2, 137.9, 137.8, 136.7 (2), 125.9, 125.7, 125.6, 125.5, 123.9, 123.6, 122.8, 122.7, 120.5, 120.4, 120.3 (2), 120.2 (2), 120.1, 119.8, 113.9, 113.7, 112.0, 111.9, 111.7 (2), 73.0, 72.9, 46.9, 46.8, 40.5, 40.4, 34.3, 34.2, 31.7, 25.9, 25.7, 23.4, 23.3, 22.1, 20.9, 20.6, 16.1, 15.9; IR (KBr, neat) 3352, 2925, 1705, 1615, 1468, 1226, 893, 741 cm^{-1}; HRMS (ESI) calcd. for $C_{27}H_{31}N_2O_3$ $(M + H)^+$ 431.2330, found 431.2326.

Diethyl (*S*)-2-((1*H*-indol-1-yl)(2-nitrophenyl)methyl)malonate (intermediate A):

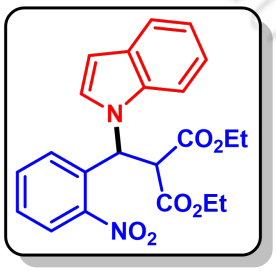

Brown Solid; R_f (Hexane/EtOAc, 9:1) 0.40; mp 126–128 °C. Yield 121 mg, 87%; ^{1}H NMR (500 MHz, $CDCl_3$) δ 7.86 (d, J = 8.0 Hz, 1 H), 7.61 (d, J = 7.5 Hz, 1 H), 7.59–7.54 (m, 3 H), 7.42 (t, J = 8.0 Hz, 1 H), 7.34 (d, J = 3.5 Hz, 1 H), 7.22–7.19 (m, 2 H), 7.08 (t, J = 7.5 Hz, 1 H), 6.56 (d, J = 3.5 Hz, 1 H), 4.60 (d, J = 2.0 Hz, 1 H), 4.09 (q, J = 7.0 Hz, 2 H), 3.90–3.87 (m, 1 H), 3.83–3.79 (m, 1 H), 1.09 (t, J = 7.5 Hz, 3 H), 0.87 (t, J = 7.0 Hz, 3 H); ^{13}C{^{1}H} NMR (125 MHz, $CDCl_3$) δ 166.1, 165.9, 149.3, 136.7, 133.3, 132.7, 129.5, 128.5, 128.4, 125.5, 125.1, 122.5, 120.9, 120.4, 110.6, 103.9, 62.5, 62.4, 57.4, 52.9, 13.9, 13.6; IR (KBr, neat) 2982, 1733, 1609, 1530, 1457, 1299, 1222, 1182, 1028, 741, 616 cm^{-1}; HRMS (ESI) calcd. for $C_{22}H_{23}N_2O_6$ $(M + H)^+$ 411.1551, found 411.1572.

Ethyl 2-(1*H*-indol-3-yl)-3-thioxoindoline-2-carboxylate (25):

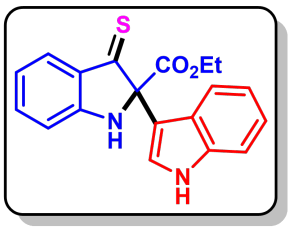

Dark brown solid; R_f (Hexane/EtOAc, 7:3) 0.60; mp 184–186 °C. Yield 36 mg, 71%; ^{1}H NMR (400 MHz, $CDCl_3$) δ 8.39 (s, 1 H), 7.61 (s, 1 H), 7.53 (d, J = 7.6 Hz, 1 H), 7.43 (d, J = 8.8 Hz, 1 H), 7.29 (d, J = 8.4 Hz, 1 H), 7.26–7.23 (m, 2 H), 7.15 (t, J = 7.6 Hz, 1 H), 7.06 (t, J = 7.6 Hz, 1 H), 6.91 (d, J = 8.4 Hz, 1 H), 5.74 (s, 1 H), 4.24 (q, J = 7.2 Hz, 2 H), 1.21 (t, J = 7.2 Hz, 3 H); ^{13}C{^{1}H} NMR (125 MHz, $CDCl_3$) δ 202.8, 170.6, 137.6, 136.2, 132.8, 129.6, 127.9, 126.6, 124.3, 123.4, 122.3, 121.1, 119.9, 113.2, 111.9, 111.3, 110.4, 68.2, 12.9; IR (KBr, neat) 3408, 2924, 1737, 1496, 1457, 1258, 1229, 1063, 748 cm^{-1}; HRMS (ESI) calcd. for $C_{19}H_{17}N_2O_2S$ $(M + H)^+$ 337.1006, found 337.1005.

Ethyl 3-oxo-2-(5-phenyl-1*H*-indol-3-yl)indoline-2-carboxylate (26):

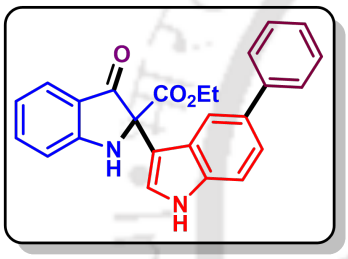

Yellow solid; R_f (Hexane/EtOAc, 7:3) 0.55; mp 200–202 °C. Yield 27 mg, 90%; ^{1}H NMR (500 MHz, $CDCl_3$) δ 8.34 (s, 1 H), 7.85 (s, 1 H), 7.70 (d, J = 8.0 Hz, 1 H), 7.58 (d, J = 7.5 Hz, 2 H), 7.52 (t, J = 7.5 Hz, 1 H), 7.45–7.38 (m, 5 H), 7.31 (t, J = 7.0 Hz, 1 H), 7.01 (d, J = 8.0 Hz, 1 H), 6.93 (t, J = 7.5 Hz, 1 H), 5.78 (s, 1 H), 4.28 (q, J = 7.0 Hz, 2 H), 1.24 (t, J = 7.0 Hz, 3 H); ^{13}C{^{1}H} NMR (125 MHz, $CDCl_3$) δ 195.0, 168.7, 161.3, 142.5, 138.1, 136.3, 133.9, 128.9, 127.6, 126.7, 126.2, 125.6, 124.5, 122.7, 120.6, 120.2, 118.4, 113.8, 112.3, 112.1, 72.7, 63.3, 14.3; IR (KBr, neat) 3365, 2924, 1735, 1615, 1468, 1240, 1102, 896, 752, 699 cm^{-1}; HRMS (ESI) calcd. for $C_{25}H_{21}N_2O_3$ $(M + H)^+$ 397.1547, found 397.1526.

Ethyl 2-(1*H*-indol-3-yl)-3-oxo-5-phenylindoline-2-carboxylate (27):

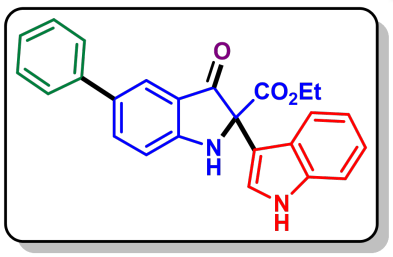

Yellow solid; R_f (Hexane/EtOAc, 7:3) 0.55; mp 211–213 °C. Yield 39 mg, 82%; ^{1}H NMR (600 MHz, $CDCl_3$(standard)/DMSO-d_6) δ 10.58 (s, 1 H), 7.78–7.77 (m, 1 H), 7.53 (d, J = 5.4 Hz, 1 H), 7.51–7.48 (m, 3 H), 7.42–7.38 (m, 1 H), 7.36 (dd, J = 8.4, 4.8 Hz, 1 H), 7.34–7.30 (m, 5 H), 7.21–7.19 (m, 1 H), 6.95 (dd, J = 8.4, 4.8 Hz, 1 H), 6.75–6.72 (m, 1 H), 4.18–4.14 (m, 2 H), 1.17–1.14 (m, 3 H); ^{13}C{^{1}H} NMR (150 MHz, $CDCl_3$(standard)/DMSO-d_6) δ 194.9, 167.9, 161.1, 141.8, 137.1, 135.9, 131.8, 128.0, 126.5, 125.6, 125.5, 124.3, 124.1, 120.8, 118.3, 118.2, 118.0, 112.4, 111.6, 110.5,

71.8, 61.7, 13.5; IR (KBr, neat) 3372, 2894, 1700, 1620, 1486, 1264, 1082, 920, 762, 705 cm^{-1}; HRMS (ESI) calcd. for $C_{25}H_{21}N_2O_3$ $(M + H)^+$ 397.1547, found 397.1527.

4.11 Representative Spectra

^{1}H spectrum of compound **24aa** (500 MHz, $CDCl_3$)

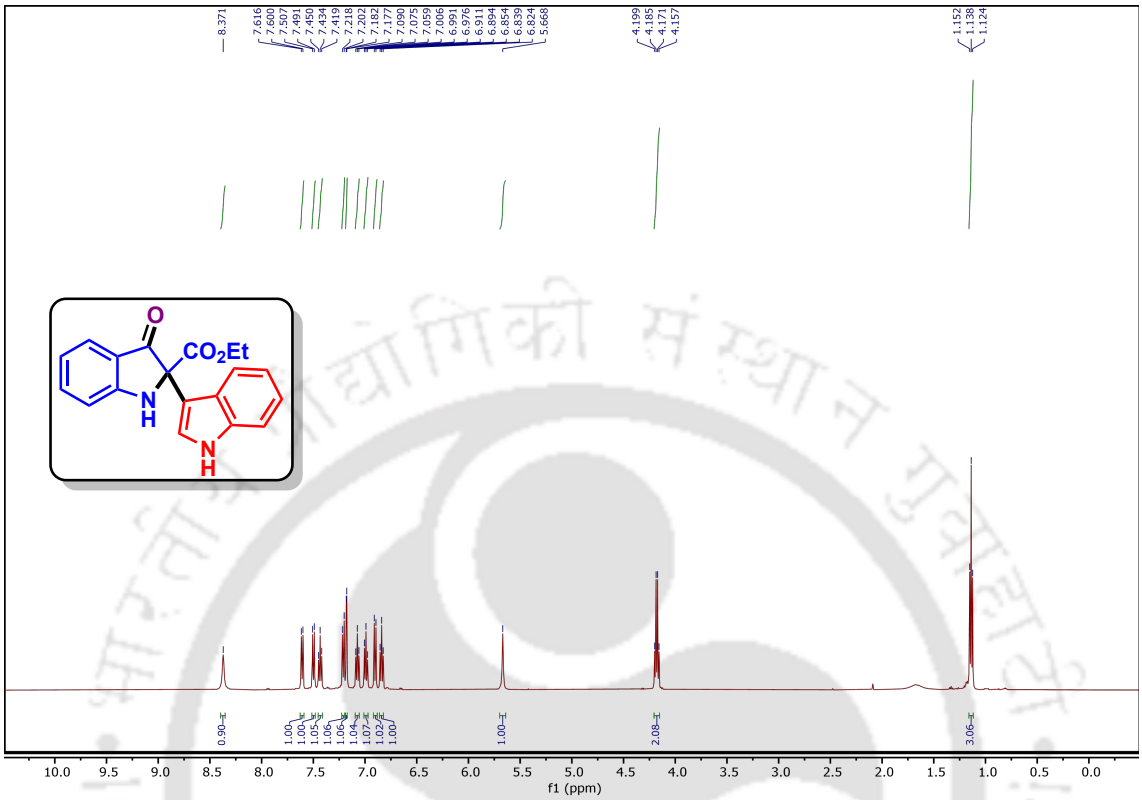

^{13}C{^{1}H} spectrum of compound **24aa** (125 MHz, $CDCl_3$)

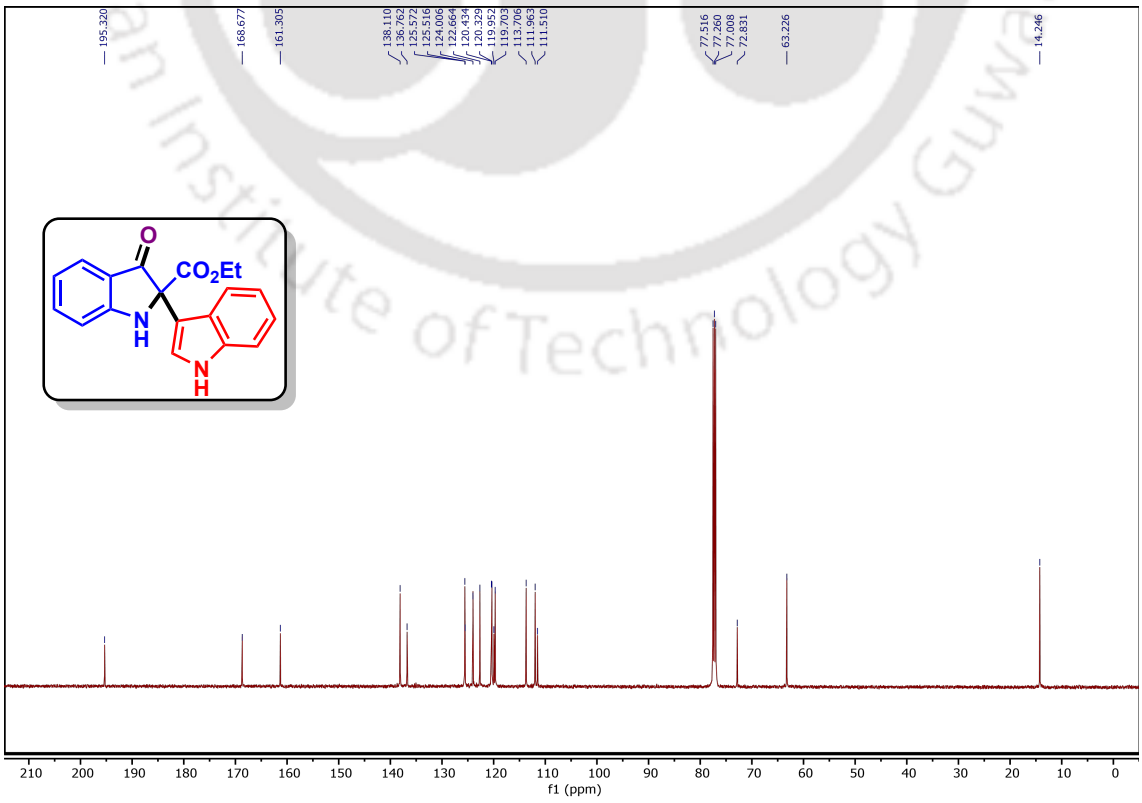

^{1}H spectrum of compound **24ag** (500 MHz, $CDCl_3$)

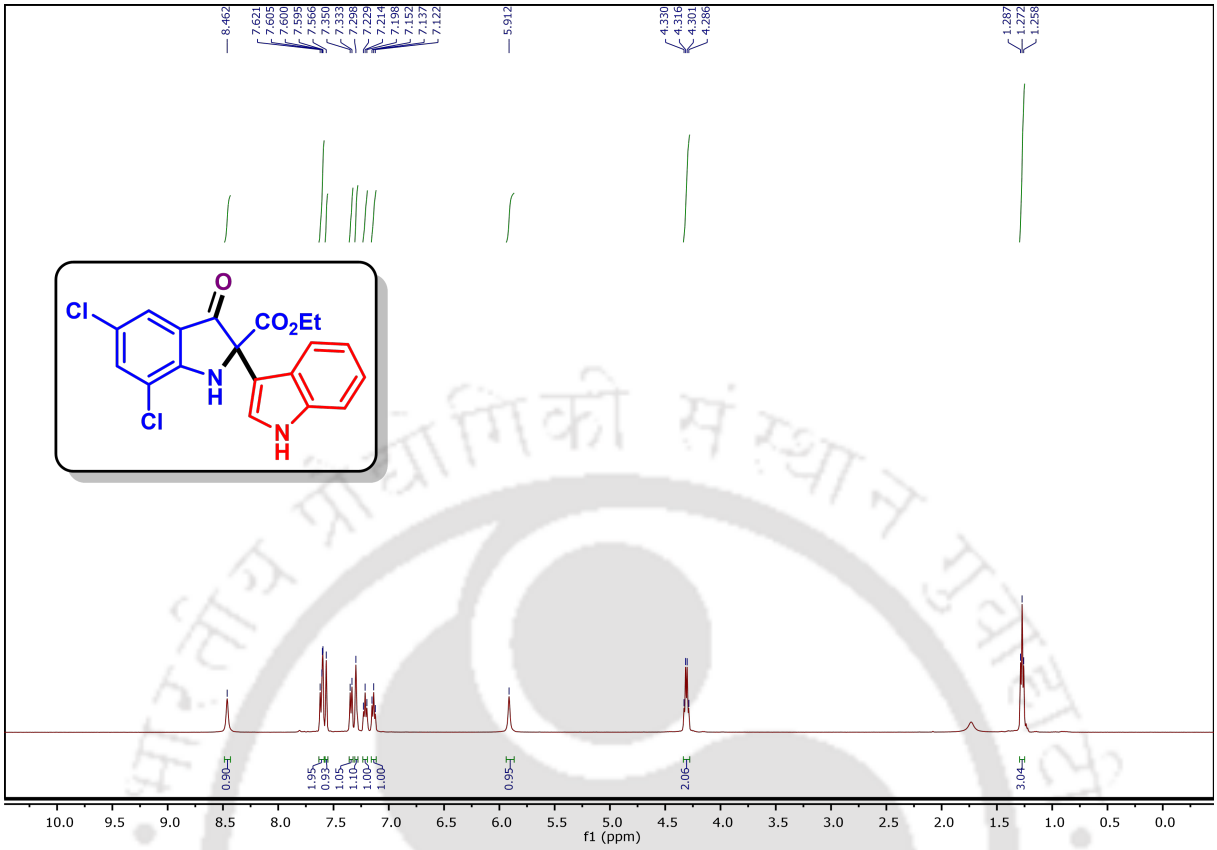

^{13}C{^{1}H} spectrum of compound **24ag** (125 MHz, $CDCl_3$)

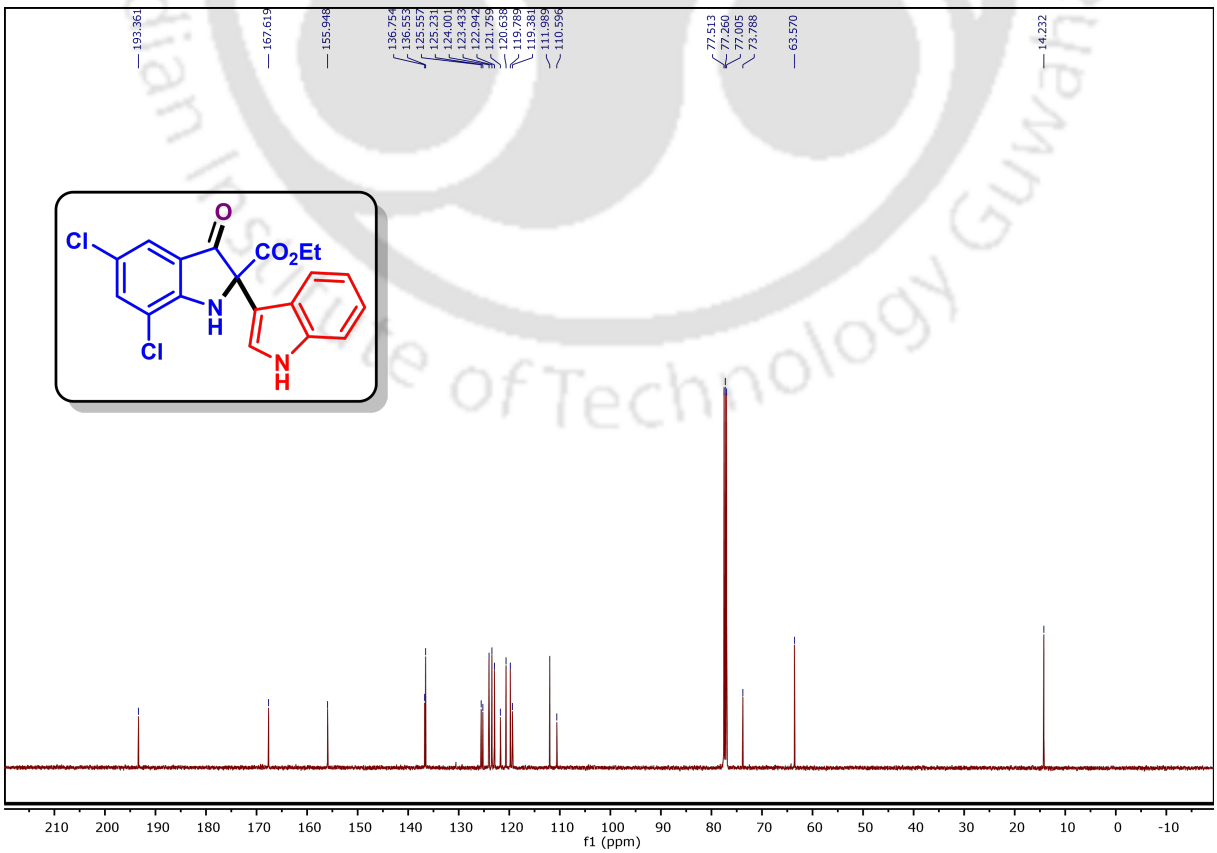

^{1}H spectrum of compound **24bi** (500 MHz, $CDCl_3$)

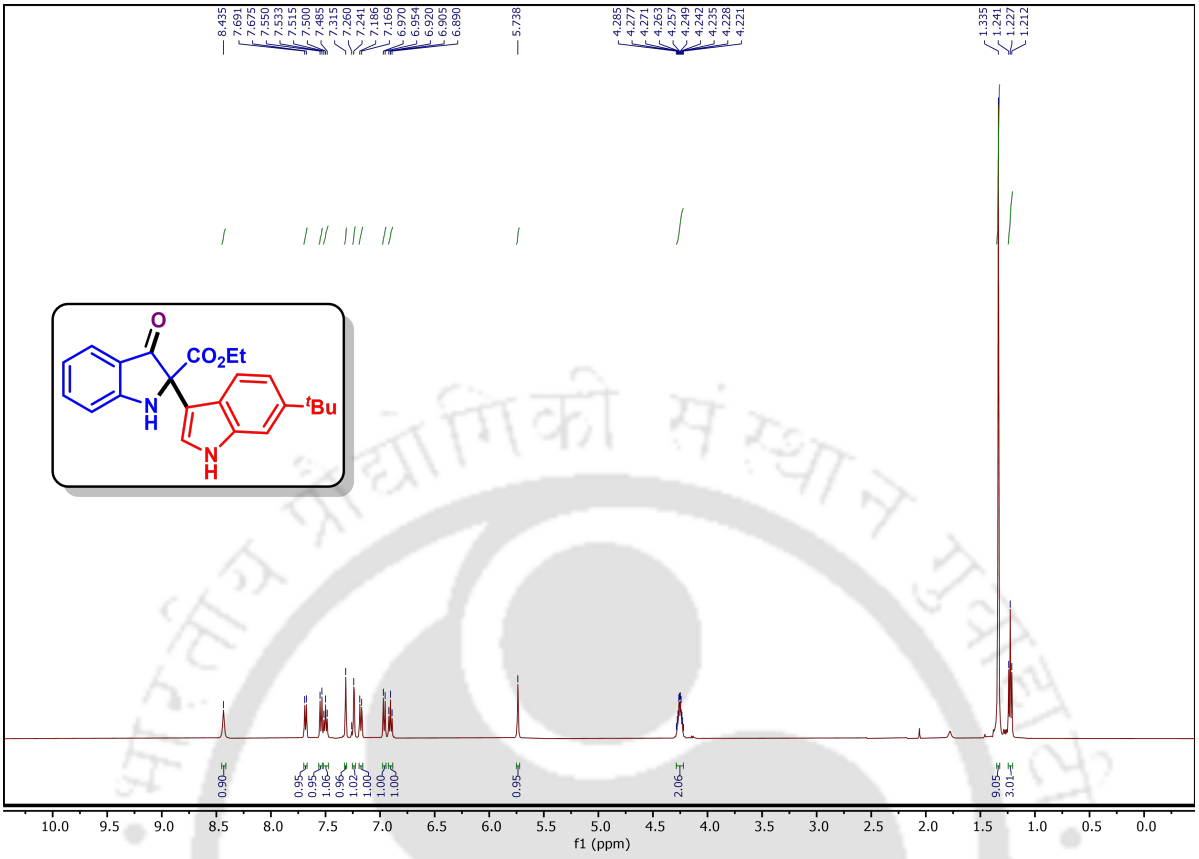

^{13}C{^{1}H} spectrum of compound **24bi** (125 MHz, $CDCl_3$)

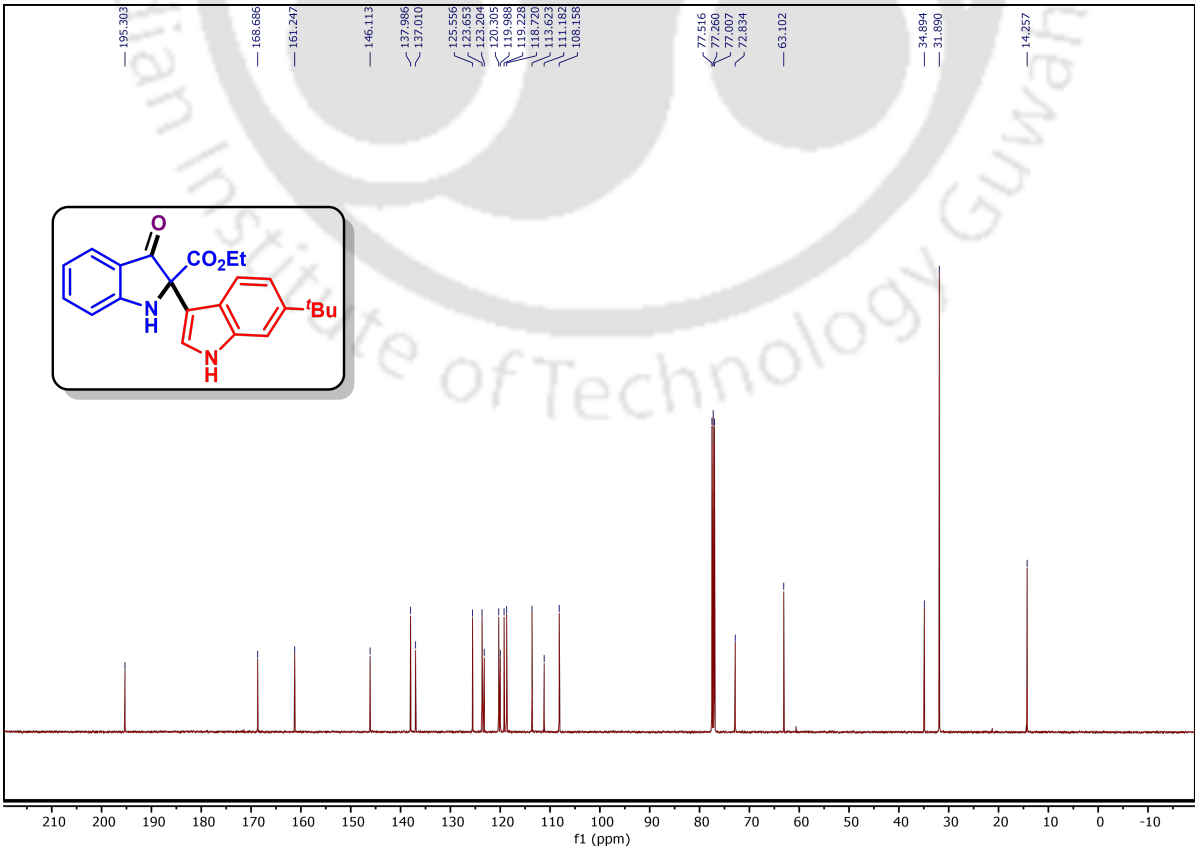

^{1}H spectrum of compound **24bn** (500 MHz, $CDCl_3$)

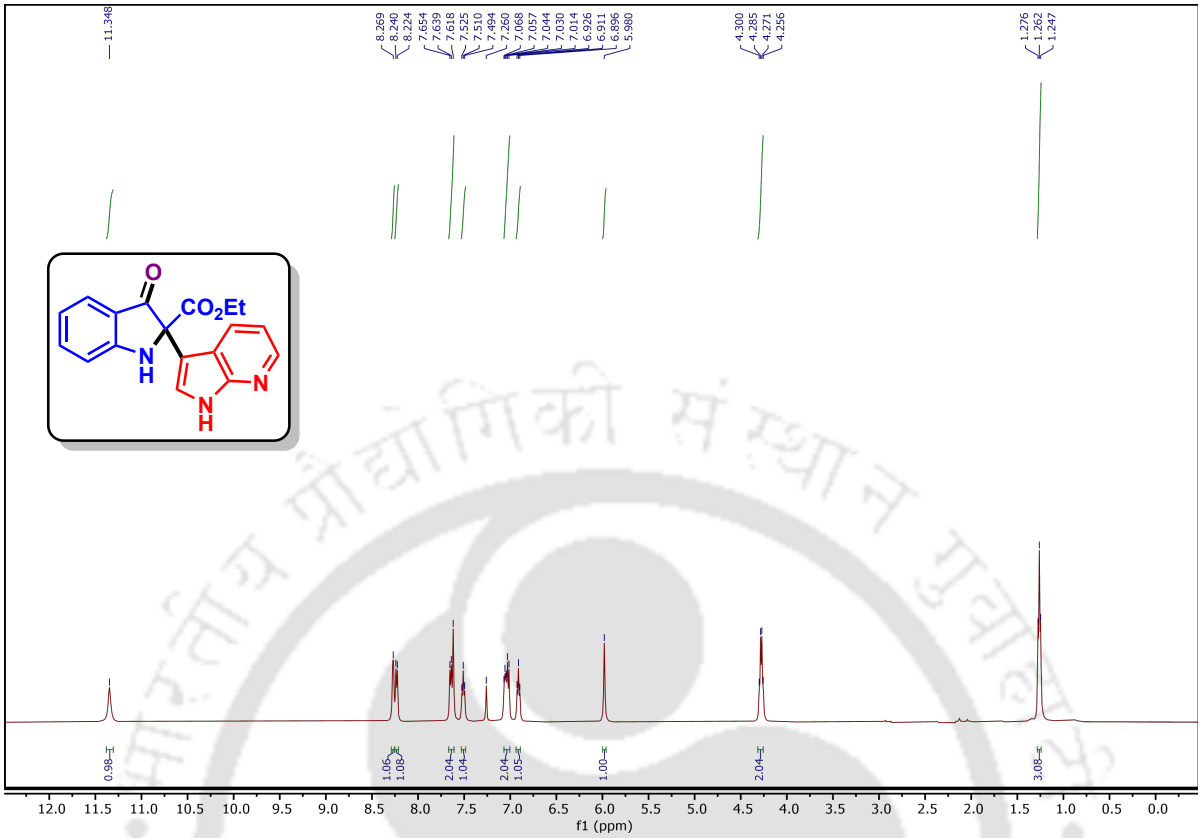

^{13}C{^{1}H} spectrum of compound **24bn** (125 MHz, $CDCl_3$)

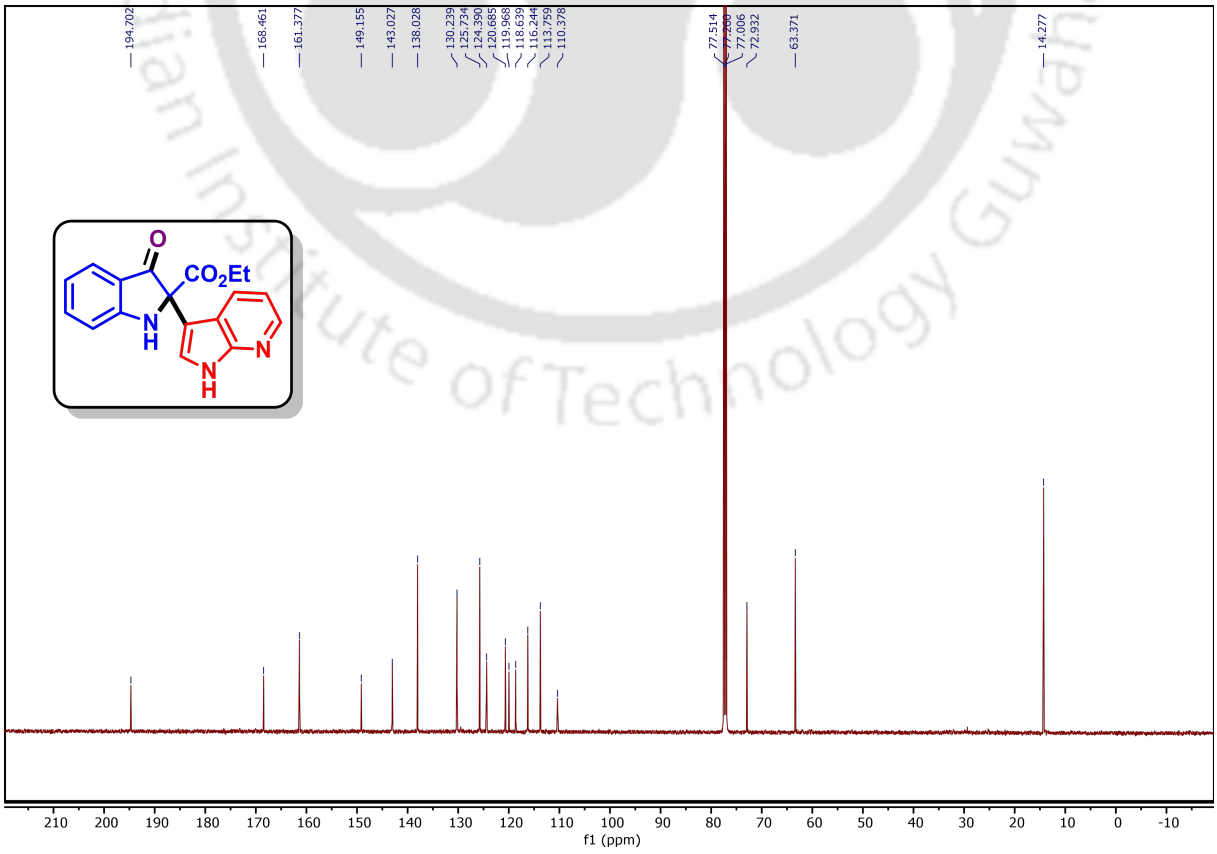

^{1}H spectrum of intermediate **A** (500 MHz, $CDCl_3$)

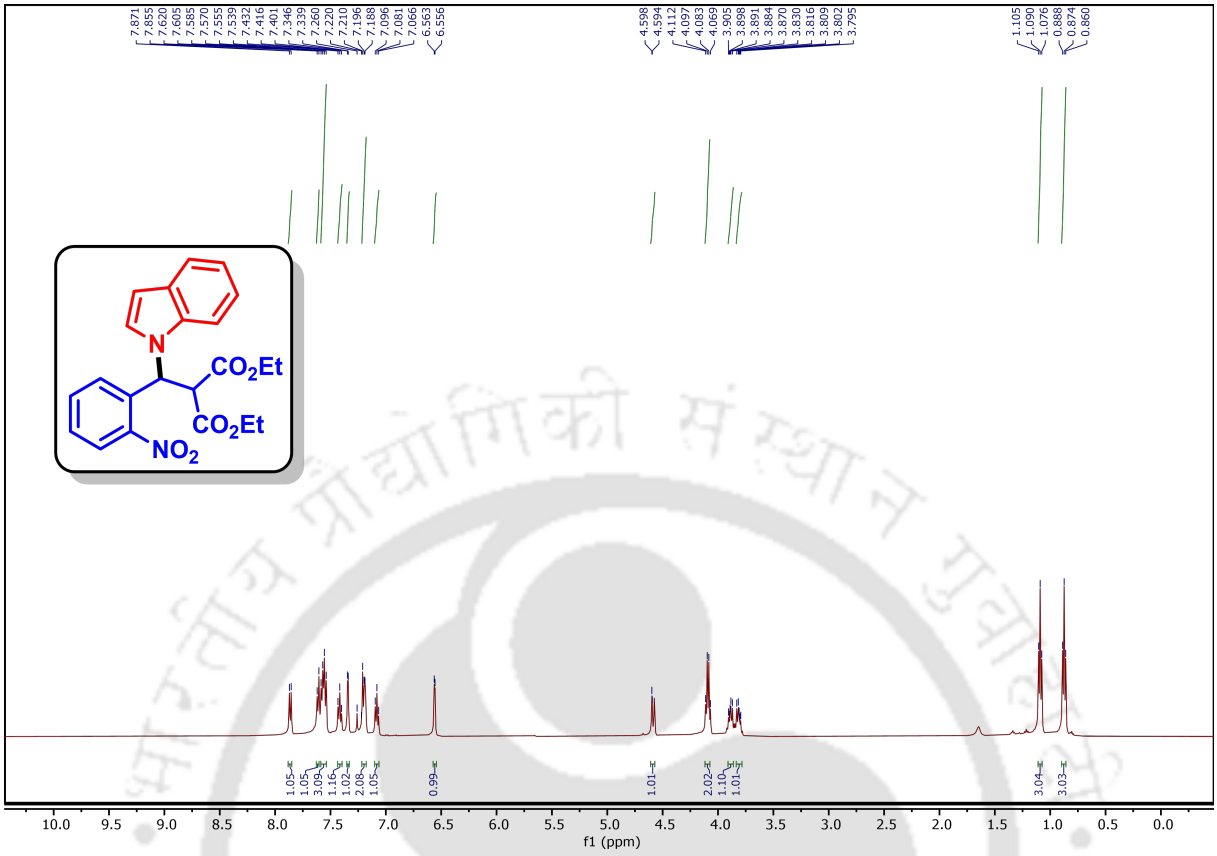

^{13}C{^{1}H} spectrum of intermediate **A** (125 MHz, $CDCl_3$)

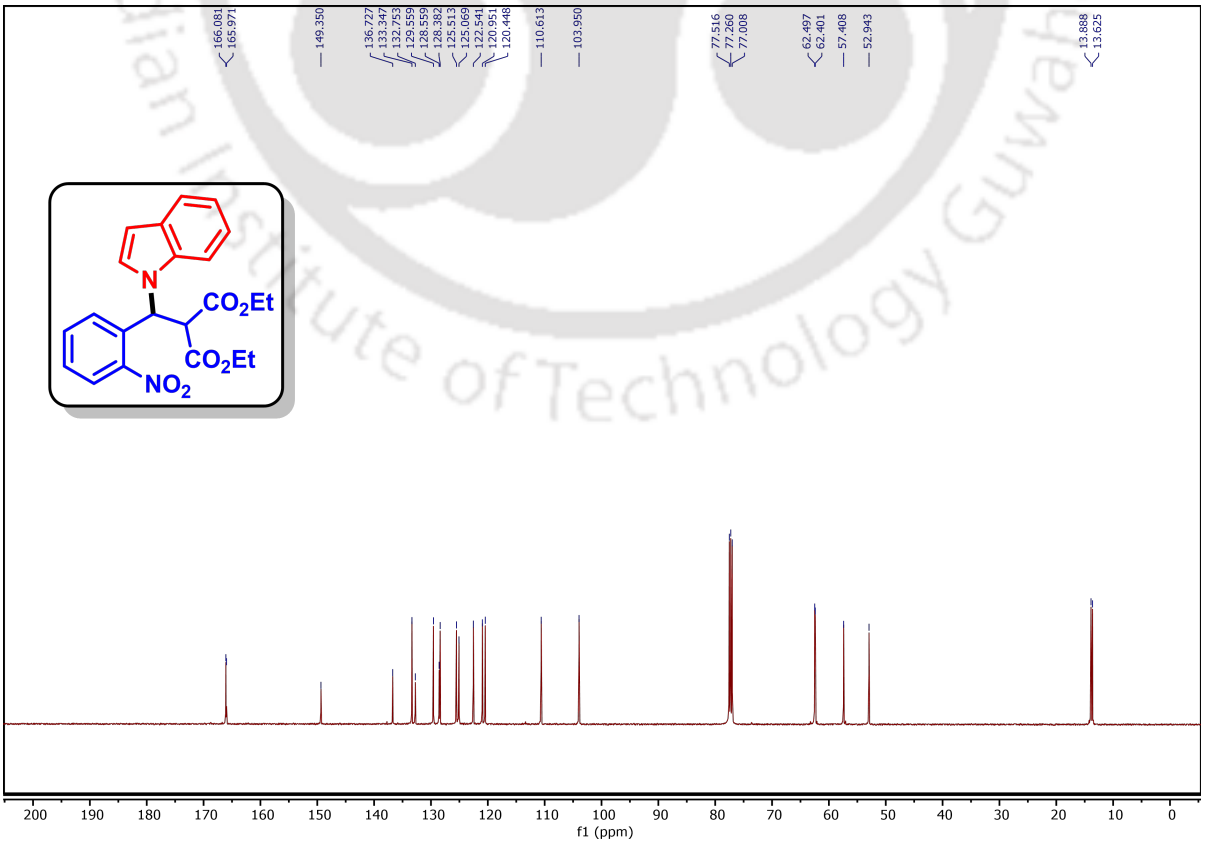

^{1}H spectrum of compound **25** (400 MHz, $CDCl_3$)

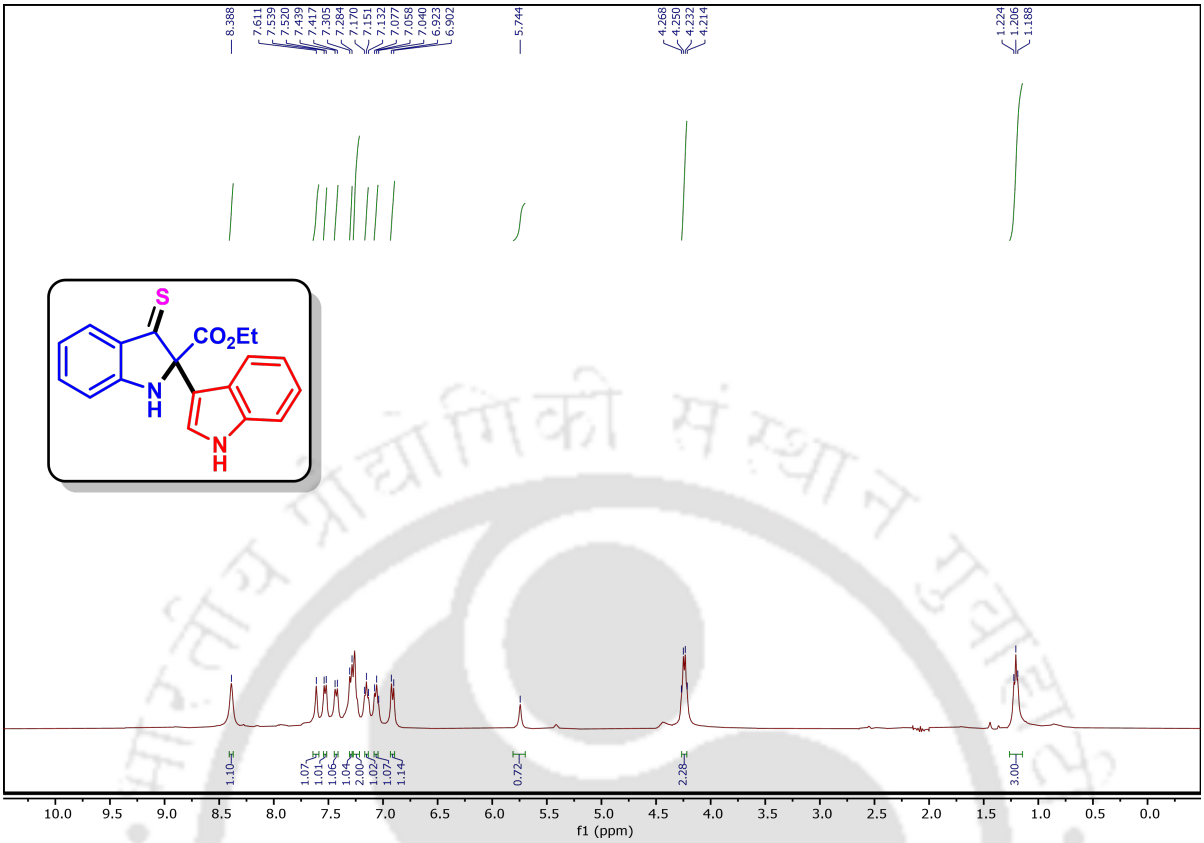

^{13}C{^{1}H} spectrum of compound **25** (125 MHz, $CDCl_3$)

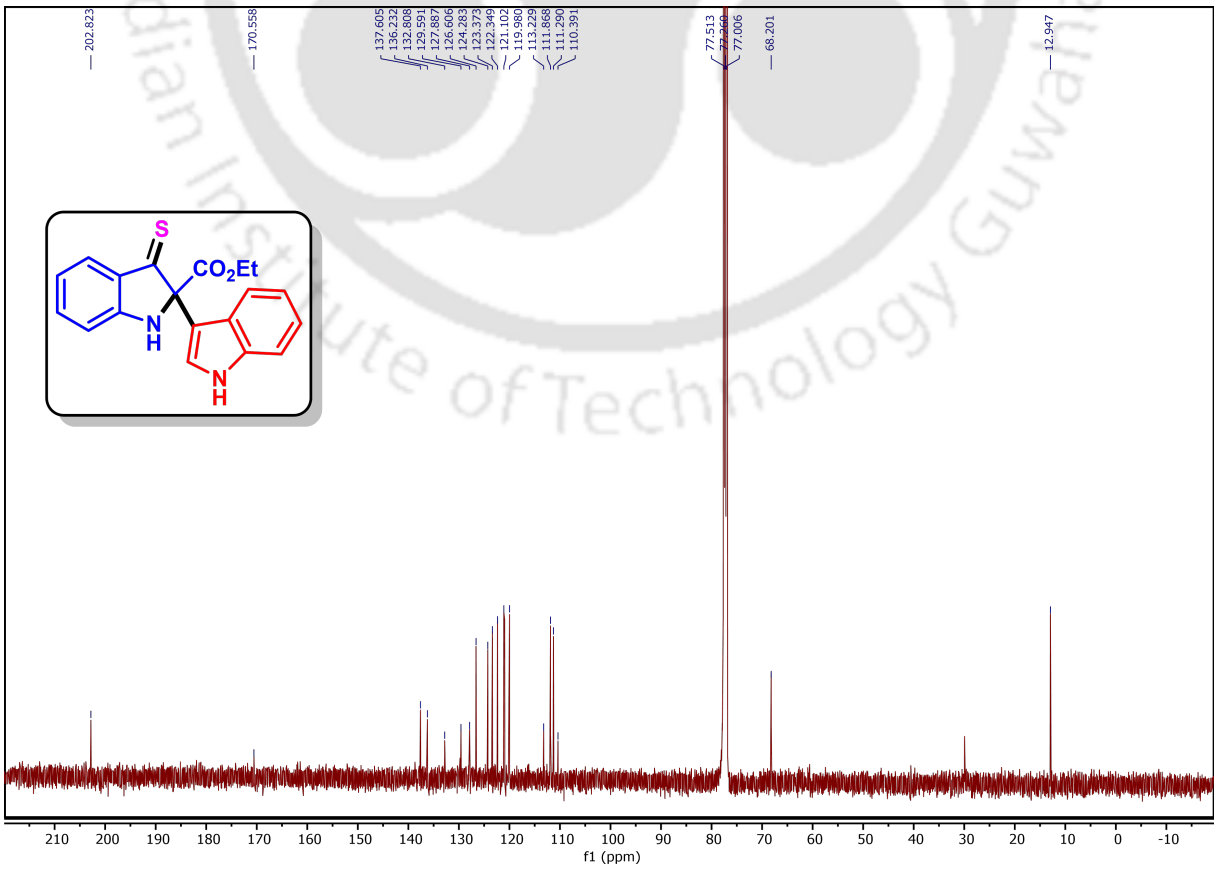

^{1}H spectrum of compound **27** (600 MHz, $CDCl_3$/DMSO-d_6)

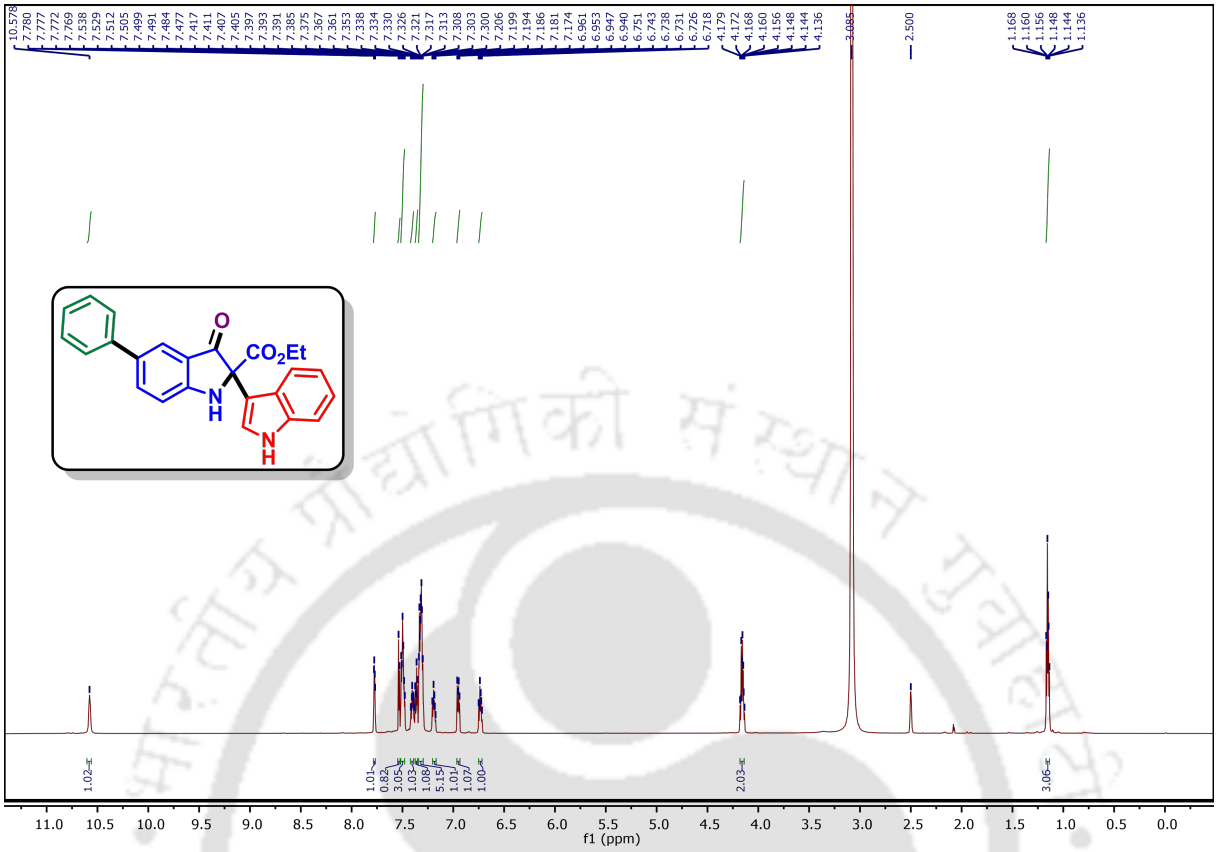

^{13}C{^{1}H} spectrum of compound **27** (150 MHz, $CDCl_3$/DMSO-d_6)

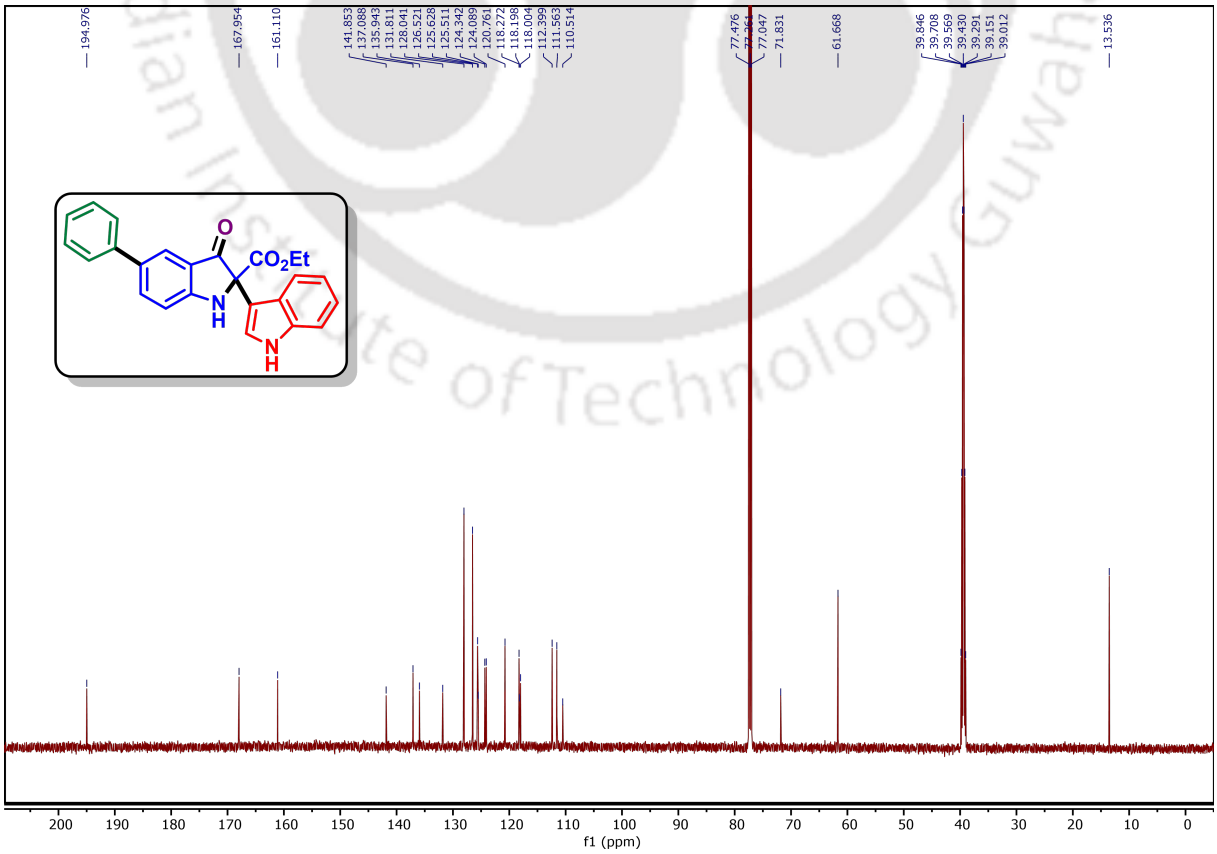

Chapter 5

Leveraging Cascade Annulation of 2-Alkynyl-cyclopropanes with Substituted Azides to Access Fused *N*-Heterocyclic Scaffolds

Contents

Abstract: This chapter represents a highly efficient and substrate-dependent methodology utilizing 2-alkynylcyclopropanes as a key substrate which undergoes tandem annulation with 2-azidobenzonitriles and 2-azidobenzaldehydes separately under Lewis acidic condition to provide 1,6-naphthyridine and isochromeno[4,3-*c*]quinoline frameworks, respectively, in excellent yields. Utilizing only a Lewis acid and readily available starting materials, it proficiently constructs highly fused *N*-heterocycles promising simplicity and advancement in the proposed protocol.

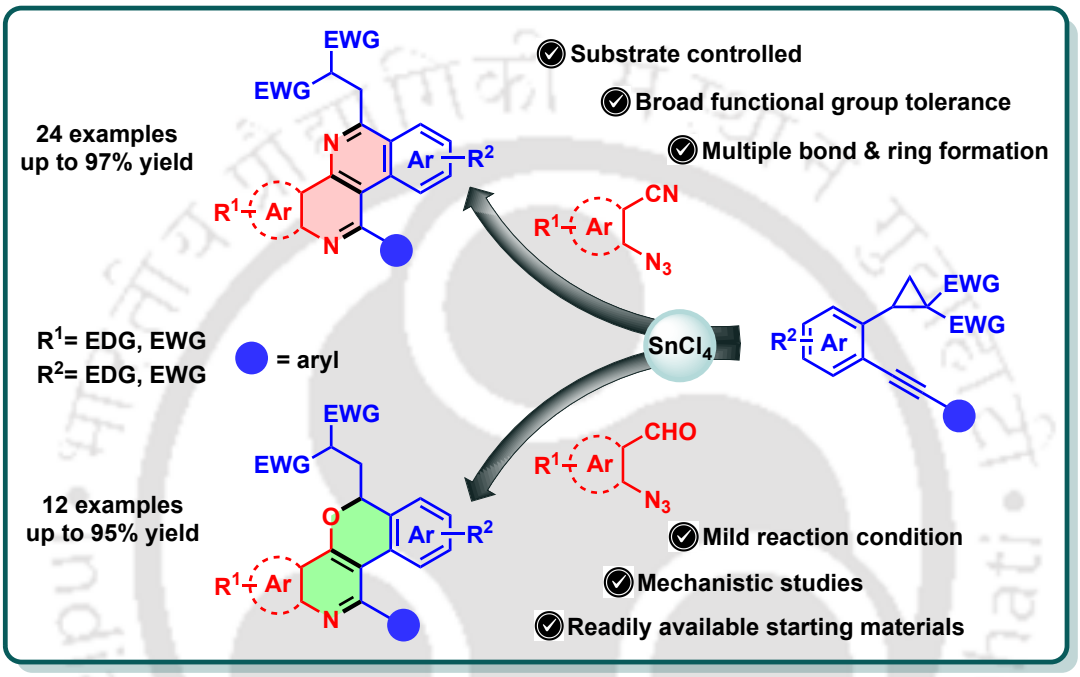

Manuscript Under Communication

5.1 Introduction

N-heterocycles, found in various organic compounds, have attained significant attention due to their diverse applications in drug development, pharmacological research, and material science.[1] They play a vital role in various biological processes and are a common motif in numerous medicinal compounds. Their structures facilitate interactions with biological systems, enhancing their therapeutic potential. Amid the abundance of *N*-heterocycles, naphthyridine and quinoline compounds are of much attraction to organic chemists as they possess several bioactivities and other fascinating properties.[2] Of particular interest are the 1,6-naphthyridine[3] and pyrano[3,2-*c*]quinoline[4] frameworks, which have emerged as powerful agents in medicinal and applied sciences, owing to their remarkable efficacy and multifaceted applications.

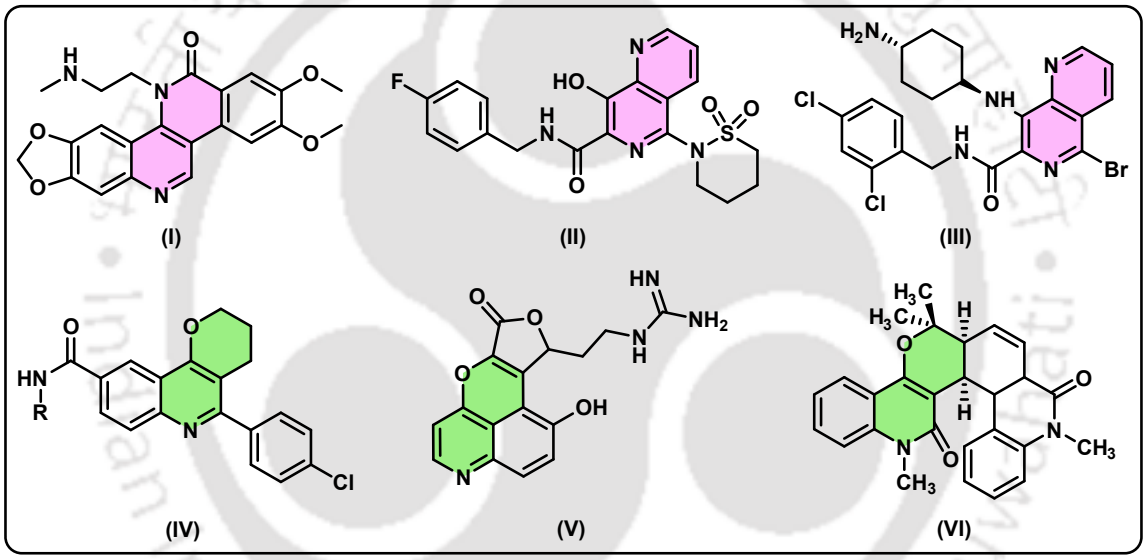

Figure 5.1.1. *Examples of biologically active 1,6-naphthyridines and pyrano[3,2-c]quinolines.*

1,6-naphthyridine-based molecules have been employed in the development of anticancer agents that selectively target cancer cells while minimizing side effects, making them as promising candidates for modern chemotherapy, for example, compound **I** inhibits lung and colon cancer. Besides, they also play crucial role as various bacterial and viral inhibitors, as compound **II** is a HIV-1 integrase inhibitor and compound **III** is a multikinase inhibitor (*Figure 5.1.1*).[5] Similarly, pyrano[3,2-*c*]quinoline derivatives have exhibited substantial activity against resistant bacterial strains and inflammatory conditions, adding to their versatility. For instance, compound **IV** is an acetylcholinesterase inhibitor, compound **V** has antifungal activity, and compound **VI** is a potential anticancer agent (*Figure 5.1.1*).[6] Beyond their biomedical implications,

these heterocyclic compounds play critical roles in fields such as chemical biology and materials chemistry, where they contribute to innovative sensor technologies and advanced functional materials.

5.2 Literature Survey on the Synthesis of Substituted 1,6-Naphthyridines and Isochromeno[4,3-*c*]quinolines

Due to their prominent bioactivity and notable synthetic applications, they are one of the major centers of attraction among chemists. Consequently, there is a concerted effort in organic chemistry to develop efficient synthetic methods for the construction of 1,6-naphthyridine and isochromeno[4,3-*c*]quinoline (analogue of pyrano[3,2-*c*]quinoline) scaffolds.

Here, a few examples for the synthesis of both 1,6-naphthyridine and isochromeno[4,3-*c*]quinoline derivatives have been presented:

5.2.1 Literature Survey on the Synthesis of 1,6-Naphthyridines

Okuma and co-workers reported a one-pot synthesis of dibenzo[b,*h*][1,6]naphthyridines **3** *via* an efficient four-condensation sequence starting from 2-acetylaminobenzaldehyde **1** and methyl ketones **2** under basic EtOH reflux conditions using NaOH (*Scheme 5.2.1.1*).[7] The reaction involves aldol, imination, aza-Morita–Baylis–Hillman, and intramolecular imination steps, seamlessly delivering the tetracyclic naphthyridine scaffold in a single operation.

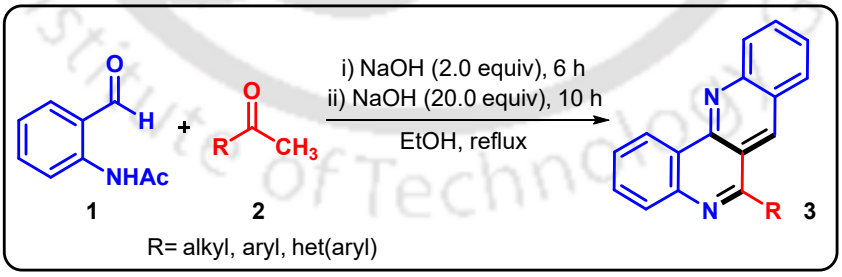

Scheme 5.2.1.1. *NaOH-mediated synthesis of 1,6-naphthyridines.*

Kumar and his group developed a palladium-catalyzed one-pot stepwise coupling/annulation methodology for the synthesis of benzo[*b*][1,6]naphthyridines **5**, starting from 2-chloroquinoline-3-carbonitriles **4** and nucleophiles such as sulfur and various amines (*Scheme 5.2.1.2*).[8] This cascade reaction features multiple bond-forming events such as C–S and C–N bond formation, cyclization, and if using primary amines,

hydroamination product forms, which after base-mediated cyclization reaction, afford the naphthyridine scaffold.

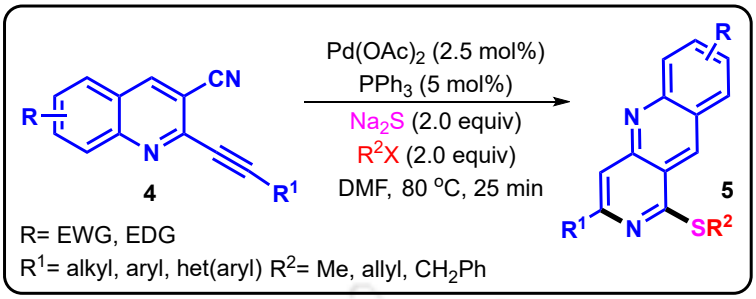

Scheme 5.2.1.2. *Pd-catalyzed synthesis of 1,6-naphthyridines.*

Abdulrahman *et al.* reported the synthesis of hexahydro-1,6-naphthyridine scaffolds **8**, known acetylcholinesterase (AChE) inhibitors, through a straightforward procedure. In this method, various bisarylmethylidene piperidones **6** reacted with 2-cyanoacetamide **7** in ethanol using a catalytic amount of sodium ethoxide (NaOEt) at room temperature (*Scheme 5.2.1.3*).[9]

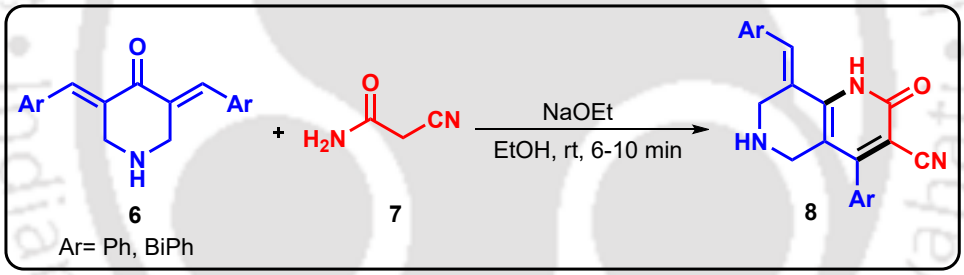

Scheme 5.2.1.3. *NaOEt-catalyzed synthesis of 1,6-naphthyridines.*

Ravi and his group developed a Brønsted acid-promoted cascade strategy for the synthesis of novel (*E*)-6-phenyl-7-styryl-5,6-dihydrodibenzo[*b*,*h*][1,6]naphthyridine derivatives **10** (*Scheme 5.2.1.4*).[10] In this approach, 2′-aminochalcone derivative **9**, obtained from the condensation of 2′-aminoacetophenone and benzaldehyde in

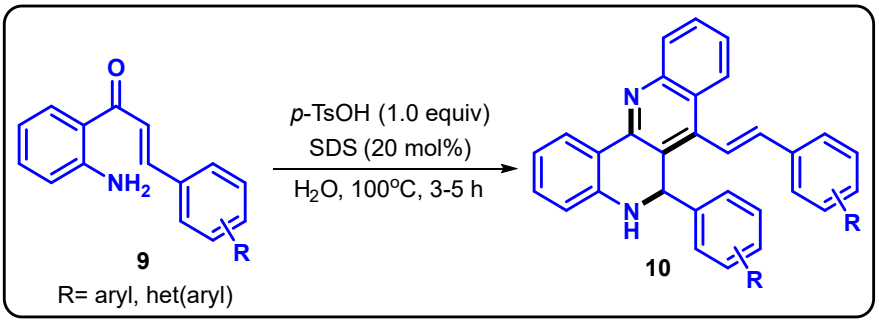

Scheme 5.2.1.4. *Brønsted acid-promoted synthesis of 1,6-naphthyridines.*

alkaline ethanol, underwent homodimerization in the presence of *p*-toluenesulfonic acid (*p*-TsOH) and 20 mol% sodium dodecyl sulfate (SDS) in water, yielding the corresponding 1,6-naphthyridine scaffolds.

Bahadur and colleagues reported a convenient one-pot domino sequence for the synthesis of dibenzo-fused 1,6-naphthyridines **14** using palladium catalyst (*Scheme 5.2.1.5*).[11] Initially, aldehydes **11** were condensed with various amines **12**, followed by reduction to afford the intermediate 2-chloroquinoline-3-carboxaldehyde amines **13**. Subsequent intramolecular C–H bond functionalization of compound **13** was carried out using palladium as the catalyst and sodium acetate (NaOAc) in DMA under nitrogen atmosphere, which leads to the oxidatively annulated product **14**.

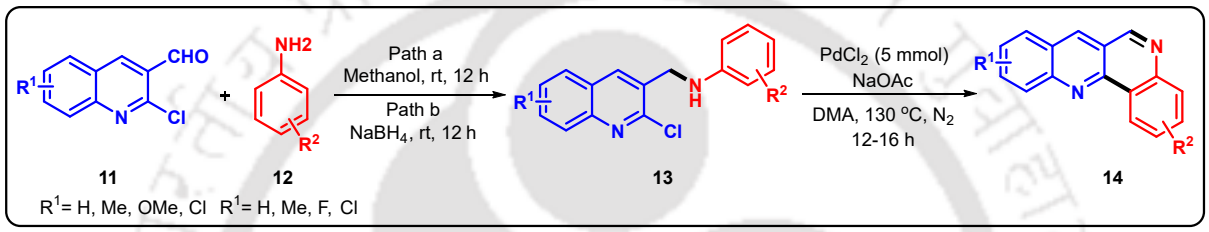

Scheme 5.2.1.5. *Pd-catalyzed synthesis of 1,6-naphthyridines.*

Akhilesh and co-workers demonstrated a silver-catalyzed tandem approach for the regioselective synthesis of highly functionalized 1,2-dihydrobenzo[1,6]naphthyridines **18** starting from *o*-alkynylaldehydes **15**, amines **16**, and ketones **17** under mild conditions (*Scheme 5.2.1.6*).[12] The formation of naphthyridine derivatives was achieved through a dual activation strategy involving both silver and the organocatalyst L-Proline within the same reaction system.

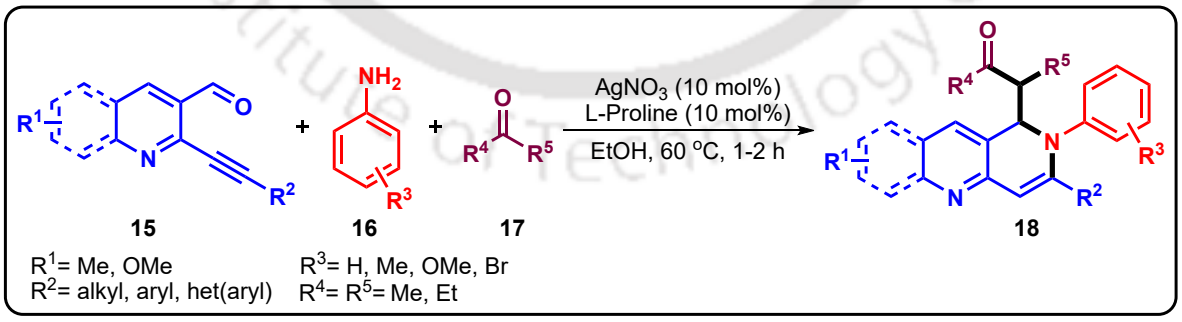

Scheme 5.2.1.6. *Silver/L-Proline-co-catalyzed synthesis of 1,6-naphthyridines.*

5.2.2 Literature Survey on the Synthesis of Isochromeno[4,3-*c*]quinolines

Recently, Saikia and co-worker reported an efficient cascade strategy combining alkynyl Prins cyclization with aza-Michael reaction to access regioselectively func-

tionalized isochromeno[4,3-*c*]quinoline scaffolds **21** (*Scheme 5.2.2.1*).[13] The one-pot sequence commences with an alkynyl Prins cyclization of suitably substituted *o*-alkynolanilines **19** and aldehydes **20**, leading to a reactive carbocation intermediate that subsequently undergoes an intramolecular aza-Michael addition to afford the isochromenoquinoline moieties.

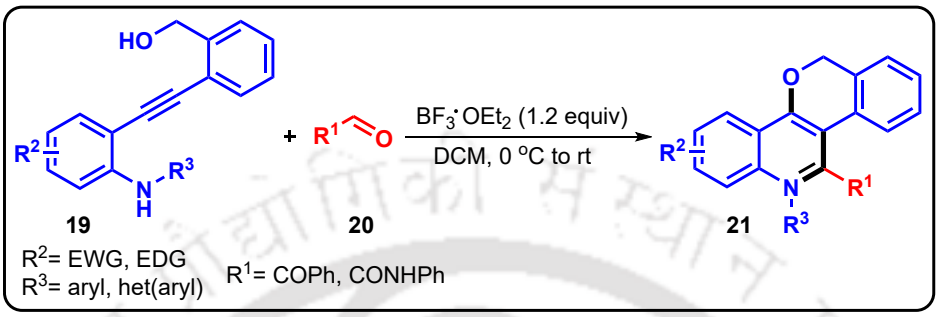

Scheme 5.2.2.1. *BF_3·OEt_2-mediated synthesis of isochromenoquinolines.*

Wu and his group presented a palladium-catalyzed tandem cyclization of functionalized diarylalkynes **22** with isocyanides **23**, affording isochromeno[4,3-*c*]quinoline frameworks **24** (*Scheme 5.2.2.2*).[14] This one-pot strategy begins with oxidative addition of the diarylalkyne to the palladium catalyst, followed by isocyanide insertion and intramolecular nucleophilic cyclization to form the heterocyclic core. Notably, the method offers excellent regio- and chemoselectivity, making it a streamlined and efficient route to these complex polycyclic systems.

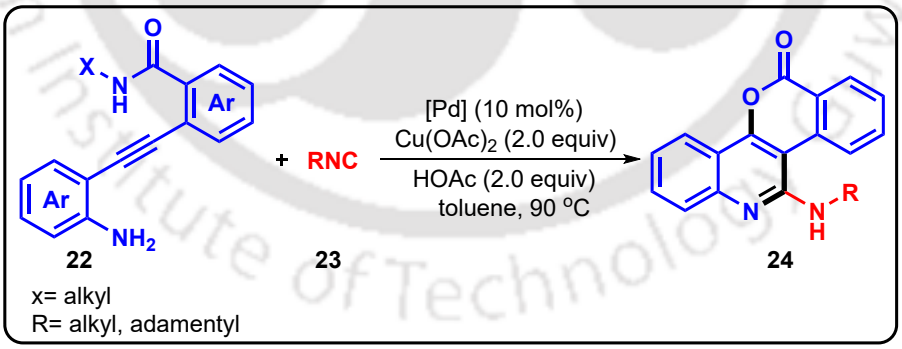

Scheme 5.2.2.2. *Pd-catalyzed synthesis of isochromenoquinolines.*

Liu and co-workers described a copper-catalyzed cascade annulation between alkynols **25** and 2-azidobenzaldehydes **26** to synthesize 6*H*-isochromeno[4,3-*c*]quinolines **27** in moderate to good yields (*Scheme 5.2.2.3*).[15] This one-pot transformation begins with an entropically disfavored intermolecular addition of the alkynol's hydroxyl to the azidobenzaldehyde, forming a hemiacetal intermediate. Subsequently, intramolecular

cyclization followed by aromatization in the resulting intermediate leads to the formation of the fused heterocycle.

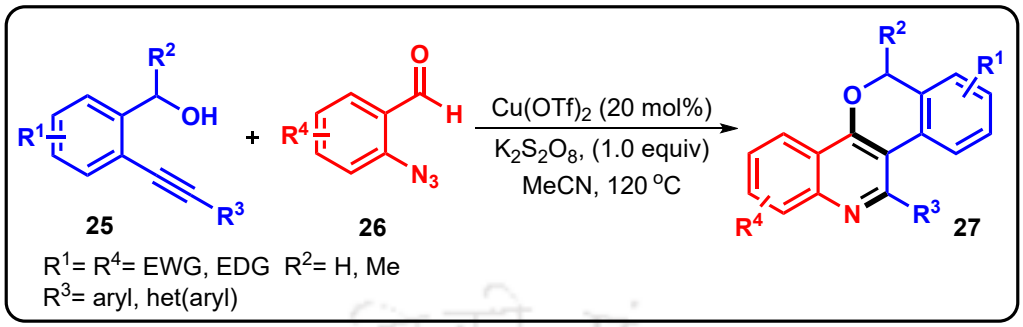

Scheme 5.2.2.3. *Cu-catalyzed synthesis of isochromenoquinolines.*

5.3 Present Work

From the above literature reports, it can be concluded that, despite the exceptional medicinal importance of these fused *N*-heterocycles, the synthesis of these core moieties remains very less explored. Therefore, there is an urgent need to develop novel and direct accessible synthetic methods to construct diversely functionalized 1,6-naphthyridine and isochromeno[4,3-*c*]quinolines scaffolds is a high value goal for synthetic and medicinal chemists. Besides, donor–acceptor (D–A) cyclopropanes (DAC) have attracted a lot of interest over the past two decades as useful building blocks in organic chemistry.[16] They are easy to make and show strong reactivity because of the strain in their three-membered ring. This reactivity is further increased by the presence of electron-donating and electron-withdrawing groups on the ring, known as the push–pull effect. By changing these groups, the reactivity of DAC can be varied in different reactions. One common reaction is the ring-opening of D–A cyclopropanes, which can be triggered by a Lewis acid or a nucleophile[17], leading to a variety of complex products.

In addition to this, the reactivity of D–A cyclopropanes in presence of Lewis acid to construct various *N*-heterocycles is well reported/explored (*Scheme 5.3.1a*), but the same for 2-alkynylcyclopropane (ACP) is very less explored. Recently, Yang and his group reported a gold/scandium bimetallic relay-catalyzed annulation strategy to construct tetracyclic indole scaffolds *via* formal [5+2] and [4+2] cycloadditions of 2-alkynylcyclopropanes with indoles (*Scheme 5.3.1b*).[18] Moreover, the utility of this newly developed ACP needs more exploration towards the synthesis of complex fused heterocycles.

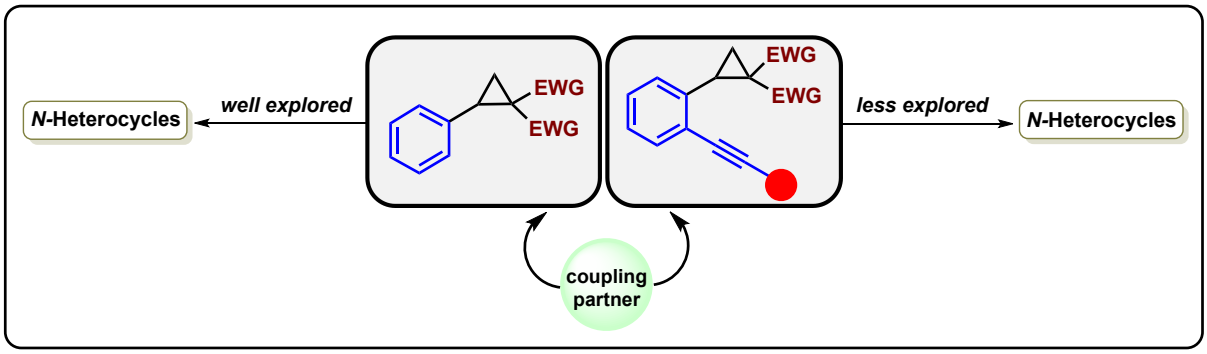

Scheme 5.3.1a. *Reactivity of DAC and ACP towards N-heterocycles.*

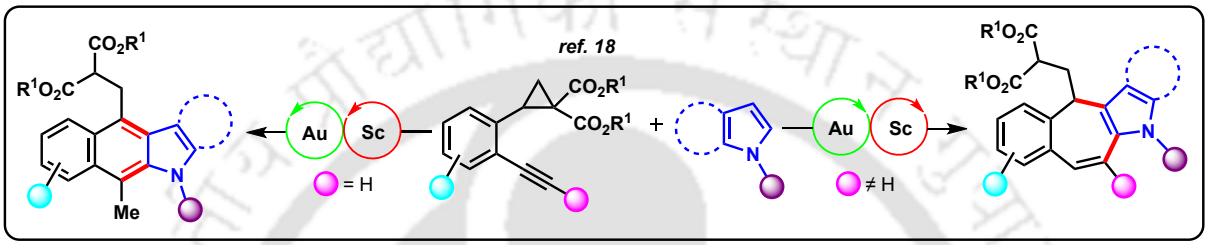

Scheme 5.3.1b. *Previous reports on the reactivity of ACP.*

Keeping all these in mind and encouraged by our previous works related to the synthesis of fused *N*-heterocycles, here in this chapter we have designed a highly efficient and substrate-controlled method utilizing 2-alkynylcyclopropanes **28** as a key substrate which undergoes tandem annulation with 2-azidobenzonitriles **29** and 2-azidobenzaldehydes **31** separately under Lewis acidic condition to provide 1,6-naphthyridine **30** and isochromeno[4,3-*c*]quinoline **32** frameworks, respectively in excellent yields (*Scheme 5.3.1c*).

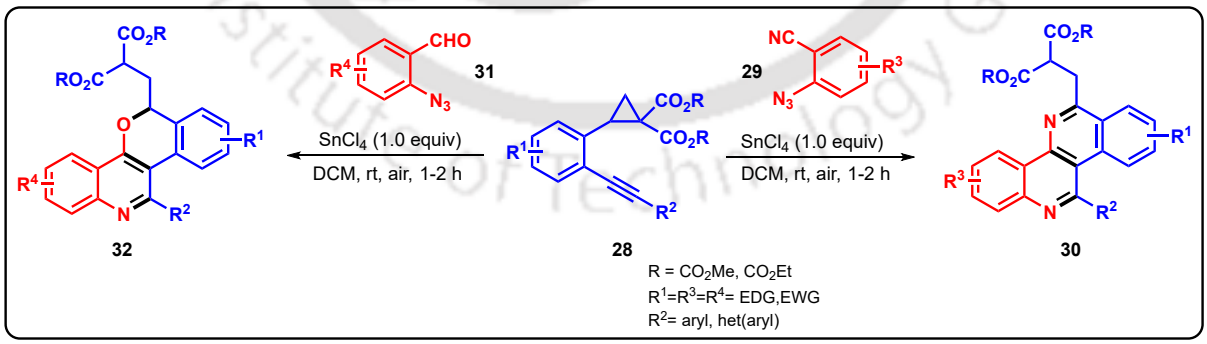

Scheme 5.3.1c. *Synthesis of 1,6-naphthyridines and isochromeno[4,3-c]quinolines from ACP.*

5.4 Results and Discussion

5.4.1 Optimization of the Reaction

The primary objective of our study is to identify the most effective reagent for the dual conversion. Therefore, a model reaction was conducted between diethyl 2-(2-(phenylethynyl)phenyl)cyclopropane-1,1-dicarboxylate (**28**) with 2-azidobenzonitrile (**29**) and 2-azidobenzaldehyde (**31**) separately using $BF_3{\cdot}OEt_2$ in 1,2-DCE under nitrogen atmosphere (*Table 5.4.1.1,* entry 1). To our dismay, neither reaction yielded any product, even after 12 h, with the starting materials remaining the same. Then we shifted to a strong acid $SnCl_4$ keeping other conditions sustained, and to our great satisfaction, both the reactions proceed gracefully providing their respective products diethyl 2-((11-phenyldibenzo[*c*,*h*][1,6]naphthyridin-6-yl)methyl)malonate (**30aa**) and diethyl (*S*)-2-((11-phenyl-6*H*-isochromeno[4,3-*c*]quinolin-6-yl)methyl)malonate (**32aa**) in outstanding yields of 88% and 79%, respectively within just 2 h with complete consumption of the starting materials (*Table 5.4.1.1,* entry 2). To achieve better yields of the products, several Brønsted/Lewis acids like TfOH, $In(OTf)_3$, $TiCl_4$, TMSOTf, $FeCl_3$, and $Cu(OTf)_2$ were screened, and out of them, only $TiCL_4$ afforded the products **30aa** and **32aa** in 65% and 69%, respectively. The rest of all reagents failed to give the corresponding products (*Table 5.4.1.1,* entries 3–8). Further, different solvents were also explored such as DCM, acetonitrile (CH_3CN), toluene and THF (*Table 5.4.1.1,* entries 9-12). In DCM, astonishingly the products **30aa** and **32aa** were obtained in incredible 93% and 88% yields, respectively, in just 1 h of reaction (*Table 5.4.1.1,* entry 9). However, in CH_3CN, the products' yields were comparatively low (*Table 5.4.1.1,* entry 10), and in toluene and THF, the reaction did not proceed with no change in the starting materials (*Table 5.4.1.1,* entries 11 and 12). Additionally, we performed another reaction using dry DCM under N_2 atmosphere. Interestingly, the reaction could afford 90% and 87% yields of the products **30aa** and **32aa**, respectively after 3 h (*Table 5.4.1.1,* entry 13), which is comparable to the yields obtained in entry 9 of *Table 5.4.1.1.* This indicates that there is no enhancement of yield under inert conditions. Again, the time of the reaction was also reduced to 30 minutes (*Table 5.4.1.1,* entry 14), which resulted in a comparatively lower 76% and 70% yields of their corresponding products **30aa** and **32aa**, respectively, with partial consumption of the starting materials. Besides, increasing and decreasing the equivalency of $SnCl_4$ leads to a slight and moderate decrease in the yields for both the products (*Table 5.4.1.1,* entries 15 and 16). From all these observations, $SnCl_4$ (1.0 equiv) in DCM was found to be the appropriate optimized condition for both the

transformations (*Table 5.4.1.1*, entry 9).

Table 5.4.1.1. *Optimization of the reaction*[a]

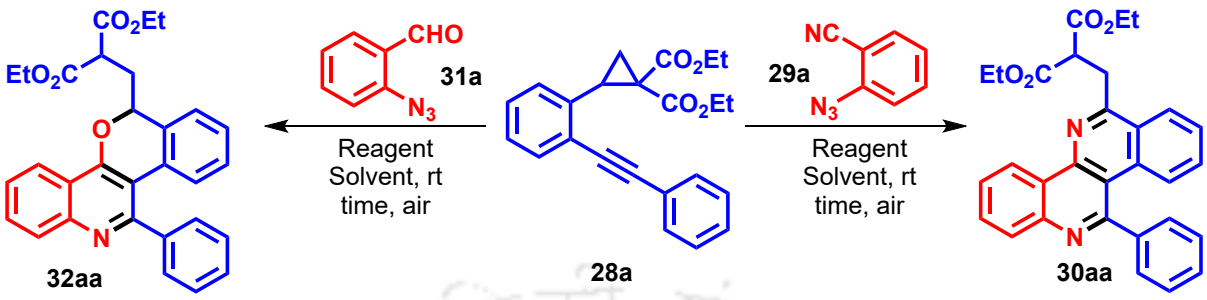

Entry[a]	Reagent (equiv)	Solvent	Time (h)	Yield (%)[b] (3aa)	Yield (%)[b] (5aa)
1.	$BF_3{\cdot}OEt_2$ (1.0)	1,2-DCE	12.0	N.R	N.R
2.	$SnCl_4$ (1.0)	1,2-DCE	2.0	88	79
3.	TfOH (1.0)	1,2-DCE	12.0	N.R	N.R
4.	$In(OTf)_3$ (0.3)	1,2-DCE	12.0	N.R	N.R
5.	$Cu(OTf)_3$ (0.3)	1,2-DCE	12.0	N.R	N.R
6.	$FeCl_3$ (1.0)	1,2-DCE	12.0	N.R	N.R
7.	$TiCl_4$ (1.0)	1,2-DCE	12.0	65	69
8.	TMSOTf (1.0)	1,2-DCE	12.0	N.R	N.R
9.	**$SnCl_4$ (1.0)**	**DCM**	**1.0**	**93**	**88**
10.	$SnCl_4$ (1.0)	CH_3CN	4.0	77	75
11.	$SnCl_4$ (1.0)	toluene	12.0	N.R	N.R
12.	$SnCl_4$ (1.0)	THF	12.0	N.R	N.R
*13.	$SnCl_4$ (1.0)	DCM	3.0	90	87
14.	$SnCl_4$ (1.0)	DCM	0.5	76	70
15.	$SnCl_4$ (1.2)	DCM	1.0	90	86
16.	$SnCl_4$ (0.5)	DCM	1.0	65	61

[a]**28a** (0.33 mmol), **29a**/**31a** (0.30 mmol), solvent 3.0 mL. [b]Isolated yield, N.R.= no reaction. *= Performed using dry solvent and under N_2 atmosphere

5.4.2 Substrate Scope

With the established optimized conditions in hand, the substrate scope of the reactions was broadly explored. For the 1,6-naphthyridine framework, different electron-withdrawing and donating groups were investigated in various positions of both 2-alkynylcyclopropane **28** and 2-azidobenzonitrile **29** (*Scheme 5.4.2.1*). Introducing electron-withdrawing groups like –Cl and –Br in the phenyl ring of the alkynyl part (R^2) of 2-alkynylcyclopropane afforded their corresponding products **30ab** and **30ac** in impressive yields of 88% and 90%, respectively. However, introducing electron-donating groups like –Me, –OMe, and –^{t}Bu afforded their respective products **30ad**–**30af** in excellent yields (93–97%). Furthermore, a substrate bearing an ortho-substituted bulky isopropyl group was investigated to assess the steric effect, and it successfully offered its corresponding product **30ag** in 81% yield. Altering the –Ph group of the alkynyl part with a naphthalene, phenanthrene and biphenyl group successfully delivered their respective products **30ah-30aj** in good yields. Introducing a heteroaryl thiophene group gratifyingly produced its corresponding product **30ak** in 80% yield. Again, variations in 2-azidobenzonitrile (R^3) were also performed. Substitution in the phenyl ring of 2-azidobenzonitrile with different moderate electron withdrawing groups like –Br, –F and strong electron withdrawing groups like –NO_2 and –CF_3 delivered their respective products **30al-30ao** in good yields from 82-90%. Similarly, electron donating groups like –Me and two –OMe groups in the phenyl ring afforded their respective products **30ap** and **30aq** in 93% and 85% yields. Now we replaced the –Et group in 2-alkynylcyclopropane (R) with a – Me group and we obtained its corresponding product **30ar** in 91% yield. Next, the variations in R^1 position of 2-alkynylcyclopropane was also explored with different electron withdrawing groups like –Cl, –Br, –F and –CO_2Me and we successfully isolated their corresponding products **30as-30aw** in moderate to good yield from 76-83%. An electron donating group –Me was also introduced and it provided its corresponding product **30ax** in excellent 91% yield. However, when the reaction was performed using 2-azidonicotinonitrile **29y** and cyclohexyl group in the alkynyl part **28z**, the reaction did not lead to their corresponding products **30ay** and **30az**, respectively. This might be due to the acid base reaction in the former one and instability of the carbocation **B** (*Scheme 5.4.5.1*) generated during the reaction for the latter one. It is interesting to note that, when a reaction was performed using a mixed malonate component in 2-alkynylcyclopropane, for example, employing ethyl 2-(2-(phenylethynyl)phenyl)-1-propionylcyclopropane-1-carboxy-late (**28aa'**), a keto ester having two chiral centers, the reaction failed to afford its desired product **30aa'**. This outcome may be attributed

to the fact that the ester–ester system allows enolization-assisted stabilization of the Sn–bound intermediate **A**, whereas the keto–ester system lacks this stabilization,

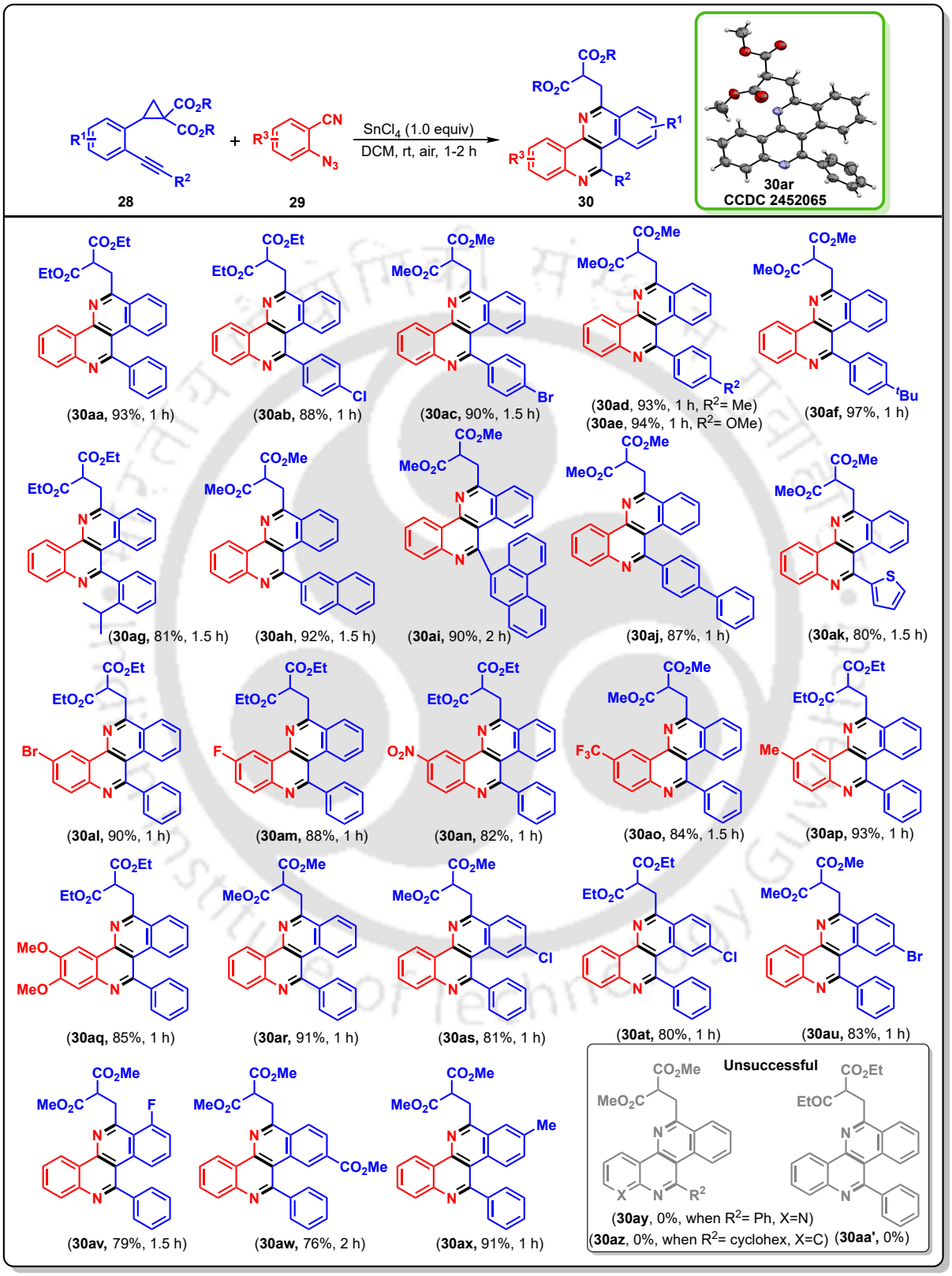

[a]Reaction condition: **28** (0.33 mmol, 1.0 equiv), **29** (0.30 mmol, 1.1 equiv), solvent 3.0 mL. [b]Isolated yield of the product.

Scheme 5.4.2.1. *Synthesis of 1,6-naphthyridine derivatives.*[a,b]

preventing effective activation of the cyclopropane.

For isochromeno[4,3-*c*]quinoline derivatives, we also explored different substituents in various positions of both 2-alkynylcyclopropane **28** and 2-azidobenzaldehyde **31** (*Scheme 5.4.2.2*). Initially, replacing the –Et group in 2-alkynylcyclopropane (R) with a –Me group delivered its corresponding product **32ab** in 85% yield. Subsequently, we introduced substituents on the phenyl ring of 2-azidobenzaldehyde (R^3), including moderate electron-withdrawing groups (–Br, –Cl), a strong electron-withdrawing group ($–CF_3$), and an electron-donating group (–Me). These substrates afforded the corresponding products **32ac**–**32ag** in moderate to good yields (73–90%). Similarly, introducing an electron donating –^{t}Bu group in the phenyl ring of R^2 offered its respective product **32ah** in 95% yield. We also varied the phenyl ring of 2-alkynylcyclopropane (R^1) with an electron withdrawing –Cl and electron donating –Me group and we favorably obtained 81% and 88% yields of their respective products **32ai** and **32aj**. Substituting the phenyl ring in the alkynyl part (R^2) of 2-alkynylcyclopropane with a biphenyl and heterocyclic thiophene ring were found to be tolerable under the proposed reaction condition producing 83% and 79% yields of their respective products **32ak** and **32al**.

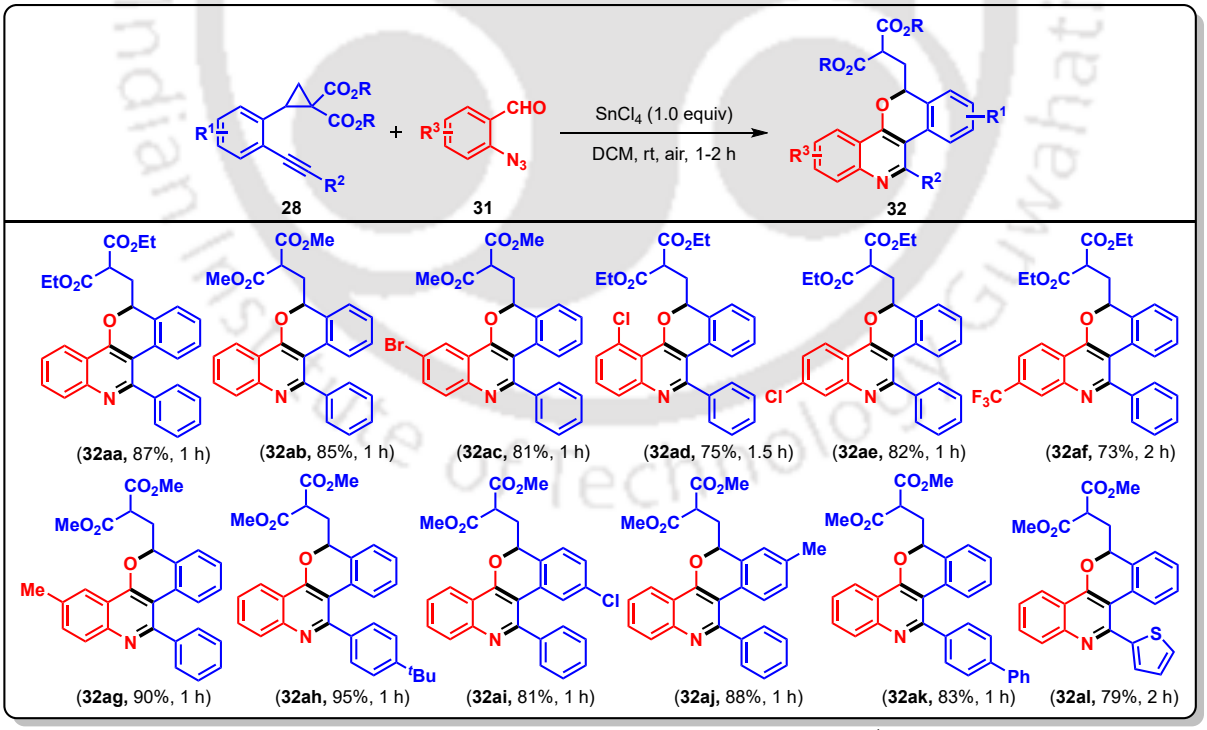

[a]Reaction condition: **28** (0.33 mmol, 1.0 equiv), **31** (0.30 mmol, 1.1 equiv), solvent 3.0 mL. [b]Isolated yield of the product.

Scheme 5.4.2.2. *Synthesis of isochromeno[4,3-c]quinoline derivatives.*[a,b]

The structures of all the compounds (**30aa–30ax**) and (**32aa–32al**) were determined by ^{1}H and $^{13}C\{^{1}H\}$ NMR, IR spectroscopy, high resolution mass spectrometry, and finally by X-ray crystallographic analysis of the compound **30ar**.

5.4.3 Gram-Scale Synthesis

To demonstrate the practical utility of our protocol, gram-scale reactions for both the substrates were performed separately (*Scheme 5.4.3.1*). The reactions were conducted using compound **28a** (1.00 g, 2.76 mmol) with both the compounds **29a**/**31a** (0.37 g, 2.51 mmol) under the standard optimized conditions separately. To our favor, both the reactions were successfully found to be applicable delivering 77% (0.925 g) and 71% (0.858 g) yields of their products **30aa**/**32aa**, respectively, highlighting the potential of this method for large-scale application.

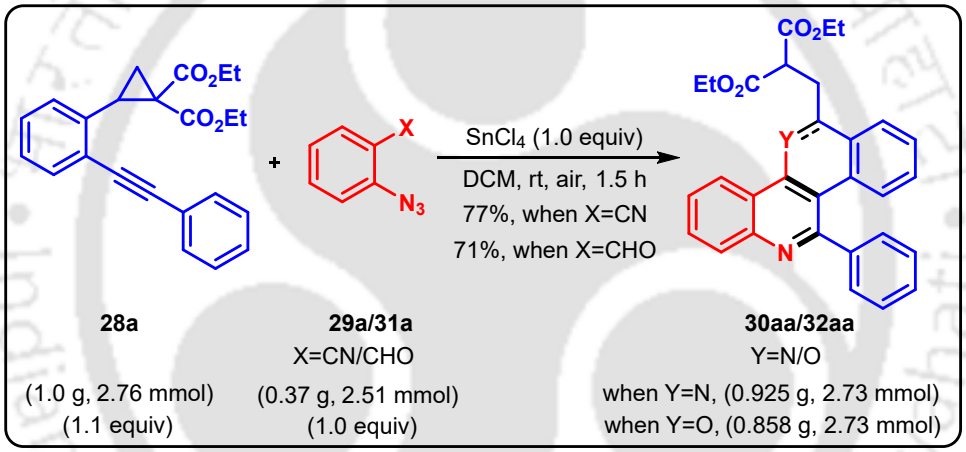

Scheme 5.4.3.1. *Gram-scale synthesis.*

5.4.4 Control Experiment

To investigate the reaction mechanism, some control experiments were carried out (*Scheme 5.4.4.1*). Initially, diethyl 2-(2-(phenylethynyl)phenyl)cyclopropane-1,1-dicarboxylate (**28a**) was subjected to react with phenylazide (**a′**) under the standard reaction condition (*Scheme 5.4.4.1a*). However, the proposed reaction did not proceed, and the starting materials remained unreacted after 12 h of the reaction.

Next, **28a** was subjected to react with cyanobenzene (**b′**) and *para*-chlorobenzaldehyde (**c′**) separately (*Scheme 5.4.4.1b* and *Scheme 5.4.4.1c*). In case of the former one (**b′**), the reaction leads to the formation of (*R*)-5-(3-ethoxy-2-(ethoxycarbonyl)-3-oxopropyl)-11-phenyl-11*H*-indeno[1,2-*c*]isoquinolin-6-ium (**33**) in 83% yield.

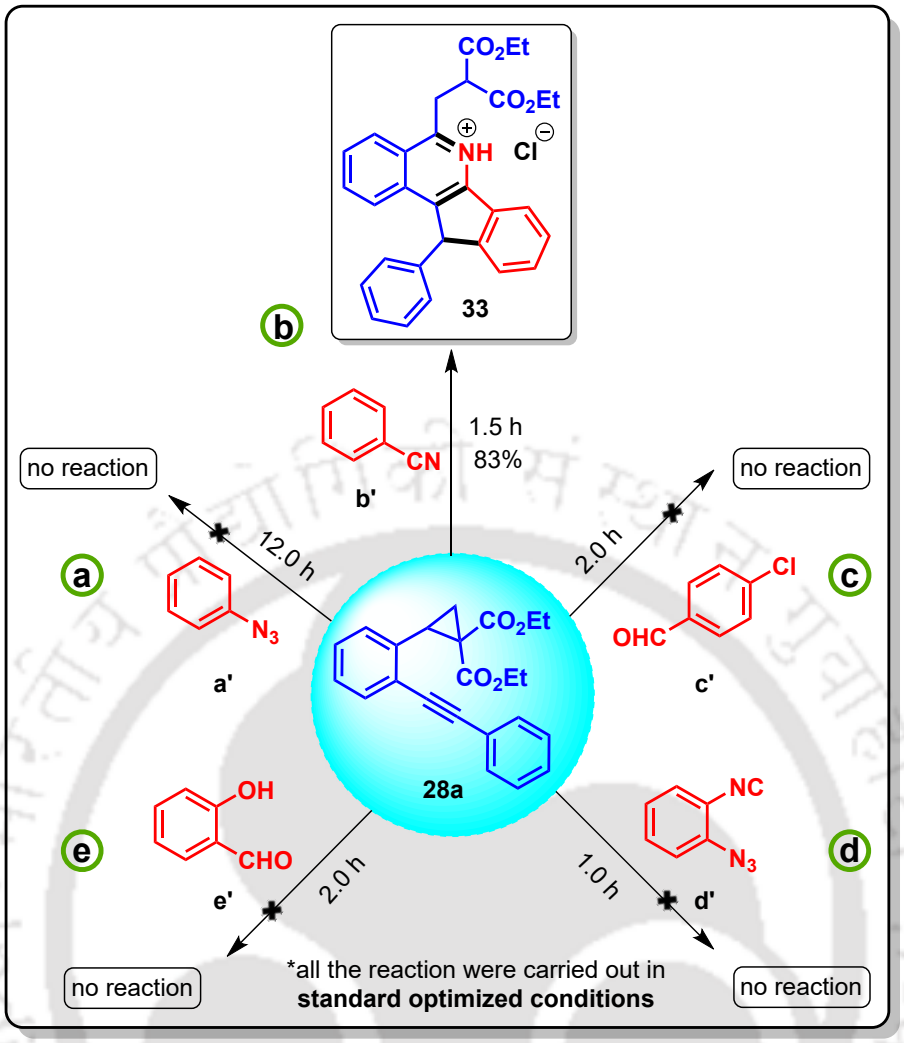

[a]Reaction conditions: 28a (0.33 mmol, 1.1 equiv), a'/b'/c'/d'/e' (0.3 mmol, 1.0 equiv), solvent 3.0 mL.

Scheme 5.4.4.1. *Control experiments.*

In contrast, with *para*-chlorobenzaldehyde (**c′**), no desired product was obtained, and the starting materials decomposed under the standard conditions. These results suggest that the reaction proceeds through a cascade pathway requiring the participation of both functionalities; otherwise, no product or undesired byproducts are formed.

Furthermore, when **28a** was treated with 1-azido-2-isocyanobenzene (**d′**), the reaction again failed to afford any product (*Scheme 5.4.4.1d*), indicating that replacing a –CN group with a –NC group disrupts the reaction.

Finally, a reaction of **28a** with salicylaldehyde (**e′**) was carried out to examine the influence of an ortho –OH group (*Scheme 5.4.4.1e*). This attempt also proved unsuccessful, with decomposition of the starting materials, demonstrating that the reaction cannot be initiated by an ortho –OH group adjacent to the benzaldehyde moiety.

5.4.5 Plausible Mechanism

Based on the control experiment and previously reported literature[19], a plausible mechanism is proposed (*Scheme 5.4.5.1*). Initially, in the presence of $SnCl_4$, the dicarbonyl compound **28** gets activated for the nucleophilic attack by 2-azidobenzonitrile **29** or 2- azidobenzaldehyde **31** to generate the enolized intermediate **A**. Then intramolecular nucleophilic attack by the alkyne group to the iminium/oxonium ion in intermediate **A** leads to the formation of intermediate **B**, which undergoes another intramolecular cyclization *via* the attack from the azide ion to form intermediate **C** (in case of 2-aminobenzonitrile)/**D** (in case of 2- azidobenzaldehyde), respectively. Finally, proton elimination/addition and subsequent N_2 elimination in **C**/**D** leads to the corresponding products **30**/**32**, respectively.

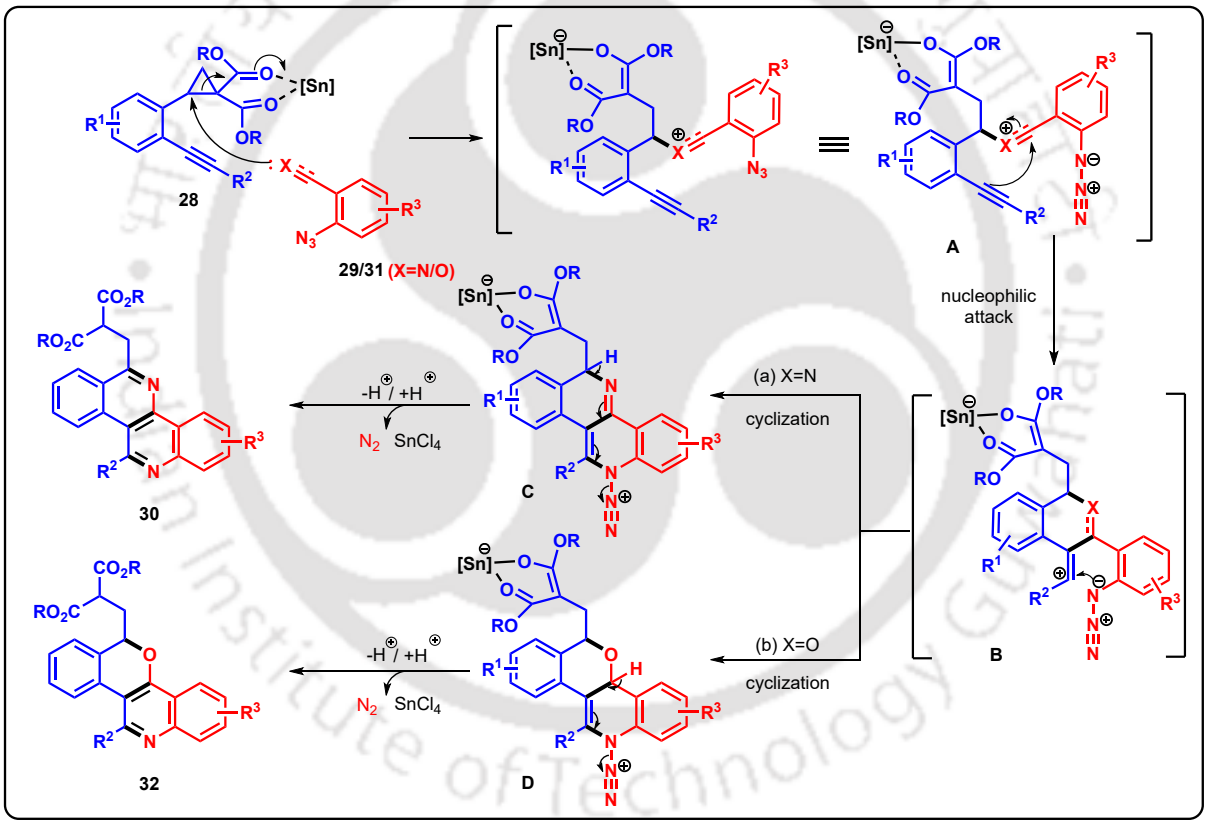

Scheme 5.4.5.1. *Plausible mechanism for the reaction.*

5.5 Crystallographic Description

The structure of all compounds was confirmed from standard spectroscopic experiments and finally by *X*-ray crystallographic analysis of compound **30ar** (*Figure 5.5.1*).

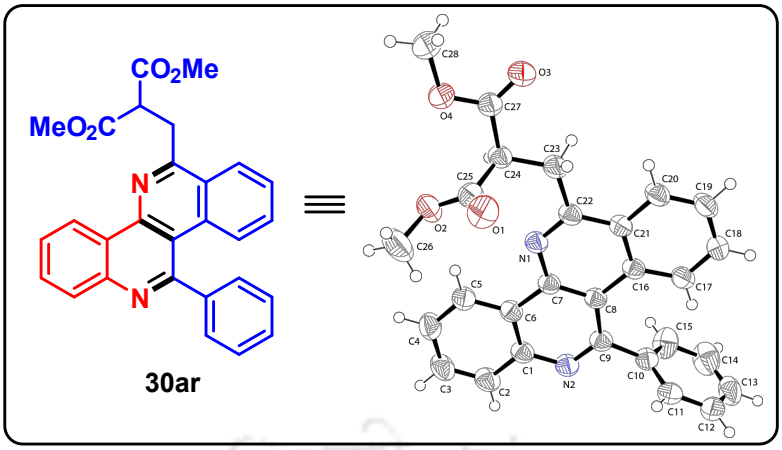

Figure 5.5.1. *ORTEP diagram of compound* ***30ar****, thermal ellipsoids are drawn on 50% probability level.*

Single crystal X-ray diffraction of compound **30ar** was obtained by slow evaporation of hexane and ethyl acetate solution (9:1). The detailed data collection and structure refinement are summarized in *Table 5.5.1,* where CCDC **2452065** of **30ar** contains the supplementary crystallographic data.

Table 5.5.1. *Crystal parameters of compound* ***30ar***

Compound 30ar	**CCDC 2452065**
Formula	$C_{28}H_{22}N_2O_4$
Formula weight	450.48
T/K	295(2)
Crystal system	Triclinic
Space group	P –1
a/Å	9.7302 (7)
b/Å	10.8770 (8)
c/Å	11.3278 (8)
a/°	108.364 (2)
β/°	92.134 (2)
γ/°	90.464 (2)
V/Å^3	1136.79 (14)
Z	23

Compound 30ar	CCDC 2452065
Abs. Coeff./mm^{-1}	0.130
Abs. Correction	none
GOF on F^2	1.419
Final R indices [$I > 2\sigma(I)$]	$R1 = 0.0516$ $wR2 = 0.1962$
R indices [all data]	$R1 = 0.0678$ $wR2 = 0.1754$

5.6 Conclusion

In conclusion, we have developed a substrate-controlled, efficient, and divergent synthetic strategy for the construction of valuable *N*-heterocyclic scaffolds 1,6-naphthyridines and isochromeno[4,3-*c*]quinolines from readily accessible 2-alkynylcyclopropanes. The protocol exhibits broad substrate scope, high functional group tolerance, and excellent yields along with demonstrated scalability. The ability to selectively access two different heterocyclic scaffolds under identical reaction conditions highlights the synthetic utility and mechanistic novelty of this approach, offering a powerful route for the streamlined synthesis of bioactive *N*-heterocycles.

5.7 Experimental Section

5.7.1 Reaction Procedure

5.7.1.1 General Experimental Procedure for the Synthesis of Starting Materials

The starting materials **28c**–**28e**, **28j**, **28k**, **28r**, **28s**, **28u**, **28v**, **28x**, **29a**, **29l**, **29n**, **29p**, **29q**, and **31a**–**31g** were synthesized according to the literature reports, and the spectroscopic data of the compounds are in good agreement with the literature data.[20]

5.7.1.1.1 General Experimental Procedure for the Synthesis of Compounds 28a, 28b, 28f–28i, 28t, 28w and 28z

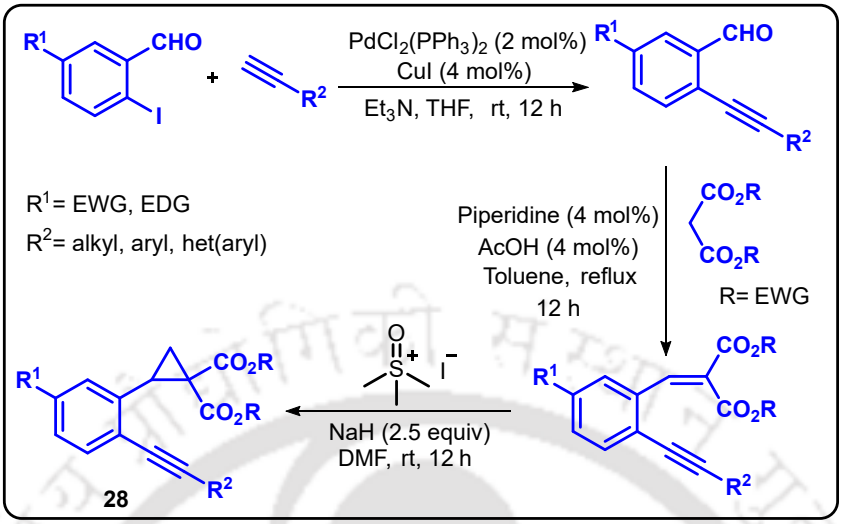

To a stirred suspension of $PdCl_2(PPh_3)_2$ (0.02 mmol, 2 mol %) and CuI (0.04 mmol, 4 mol %) in trimethylamine (5.0 mmol, 5.0 equiv) under nitrogen atmosphere was added 2-iodobenzaldehyde derivative (1.95 mmol, 1.0 equiv), and the reaction mixture was stirred for 10 min. Eventually, substituted acetylene derivative (2.15 mmol, 1.1 equiv) was added to the reaction mixture, and the mixture was allowed to stir at room temperature. The progress of the reaction was monitored by TLC (using hexane/ethyl acetate = 9:1 as eluents). After completion of the reaction (12 h), the excess triethylamine was evaporated using a rotary evaporator, and the reaction mixture was washed with saturated NH_4Cl and brine solution. The aqueous phase was extracted with ethyl acetate (3 × 10 mL). The combined organic layers were then dried over Na_2SO_4 and concentrated using a rotary evaporator. The resulting crude product underwent column chromatography over silica gel to isolate the corresponding Sonogashira adduct. After that, piperidine (0.04 mmol) and acetic acid (0.04 mmol) was added to a solution of Sonogashira adduct (1.94 mmol, 1.0 equiv) in toluene under N_2 atmosphere. The reaction mixture was stirred for 5 min at room temperature, after which malonate component (1.94 mmol, 1.0 equiv), was added dropwise over a period of 2 min. The reaction mixture was then allowed to stir at 110 °C. The progress of the reaction was monitored by TLC analysis (using hexane/ethyl acetate = 9:1 as eluents). After completion of the reaction (12 h), it was allowed to cool to room temperature. The reaction mixture was then washed with brine solution. The aqueous phase was extracted with ethyl acetate (3 × 10 mL). The combined organic layers were then dried over Na_2SO_4 and concentrated using a rotary evaporator. The

crude product was then purified by column chromatography over silica gel to provide the corresponding benzylidene malonate derivative. Next, sodium hydride (2.5 equiv) was added in a two-neck round bottom flask and washed 3-4 times with dry hexane to remove the mineral oil and subsequently trimethylsulphoxonium iodide (2.0 equiv) and dry DMF was added to it under N_2 atmosphere. Then the reaction mixture was allowed to cool to 0 °C and stir for 30 min. After that, a solution of benzylidene malonate derivative (0.86 mmol, 1.0 equiv) in dry DMF was added to it dropwise and allowed the reaction mixture to stir at room temperature. After completion of the reaction (monitored by TLC, using hexane/ethyl acetate = 9:1 as eluents), the reacion mixture was diluted with ethyl acetate, and washed with saturated ice cold solution of $NaHCO_3$ (2 × 10 mL), followed by ice cold brine solution (2 × 10 mL). The organic extracts were dried over Na_2SO_4 and concentrated using a rotary evaporator. The crude product was then purified by column chromatography over silica gel to provide the corresponding starting material **28**.

5.7.1.1.2 Experimental Procedure for the Synthesis of Compound 28aa':

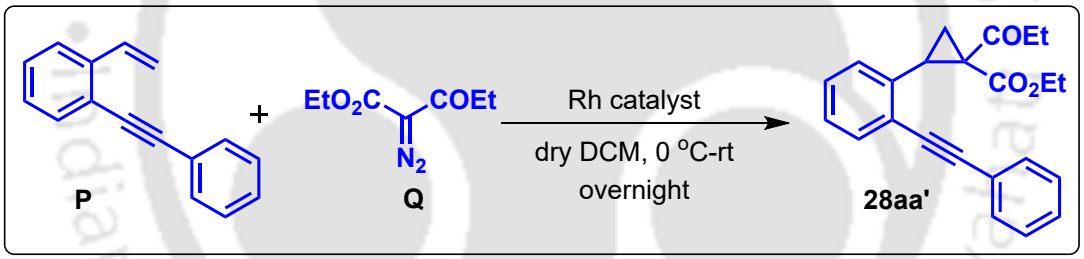

A solution of the corresponding 2-alkynylstyrene **P** (3.92 mmol, 1.0 equiv), $Rh_2(OAc)_4$ catalyst (0.5 mol%) in anhydrous dichloromethane was stirred under argon atmosphere at 0 °C. Diazomalonate **Q** (5.10 mmol, 1.3 equiv.) in dichloromethane was added dropwise over 30 min *via* syringe. Then, the cooling bath was removed, and the mixture was allowed to stir overnight at room temperature. After completion of the reaction, the solvent was removed *in vacuo*, and the crude product was purified by column chromatography to get the corresponding starting material **28aa'**.

5.7.1.1.3 General Experimental Procedure for the Synthesis of Compounds 29m, 29o, 29q and 29y

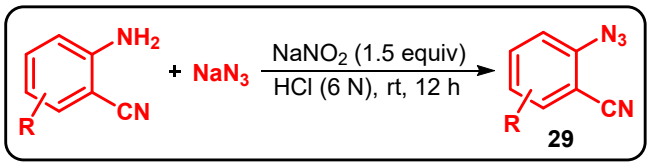

2-aminobenzonitrile derivative (1.65 mmol, 1.0 equiv) was dissolved in HCl (6 N) at 0°C. Sodium nitrite $NaNO_2$ (2.47 mmol, 1.5 equiv) was added slowly to the reaction mixture and stirred at 0°C for an additional 30 min. After that a solution of sodium azide, NaN_3 (2.47 mmol, 1.5 equiv) was added slowly at 0°C followed by stirring at room temperature for 12 h. After completion of the reaction, the reaction mixture was quenched with saturated NH_4Cl solution, and the organic layer was extracted with ethyl acetate (3 x 10 mL). The combined organic layers were further washed with brine solution, followed by drying over anhydrous Na_2SO_4. The organic phase was concentrated using a rotary evaporator to give the crude product, which was then subjected to column chromatography over silica gel to provide the desired starting material **29**.

5.7.1.2 General Experimental Procedure for the Synthesis of Compounds 30aa–30ax

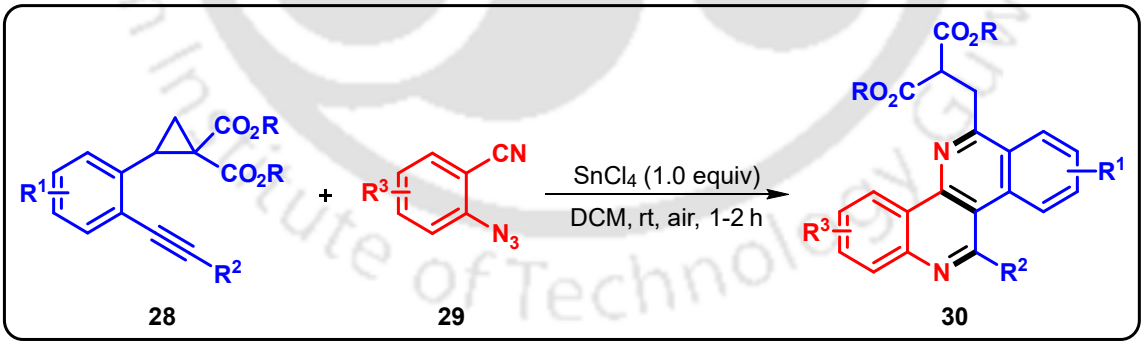

To a mixture of 2-alkynylcyclopropane **28** (0.33 mmol, 1.1 equiv) and 2-azidobenzonitrile **29** (0.3 mmol, 1.0 equiv) in DCM, $SnCl_4$ (0.3 mmol, 1.0 equiv) was added slowly at 0 °C under air atmosphere. The reaction was then allowed to stir at room temperature and monitored by TLC analysis (using hexane/ethyl acetate = 3:1 as eluents). After completion of the reaction (1–2 h), the solvent was removed under vacuo in a rotary evaporator, and then the residue was diluted with ethyl acetate, saturated $NaHCO_3$, and brine solution. The aqueous phase was extracted with ethyl

acetate (3 × 10 mL). The combined organic extracts were dried over anhydrous Na_2SO_4 and concentrated using a rotary evaporator. The crude product was subjected to column chromatography over silica gel to give the corresponding product **30**.

5.7.1.3 General Experimental Procedure for the Synthesis of Compounds 32aa–32al

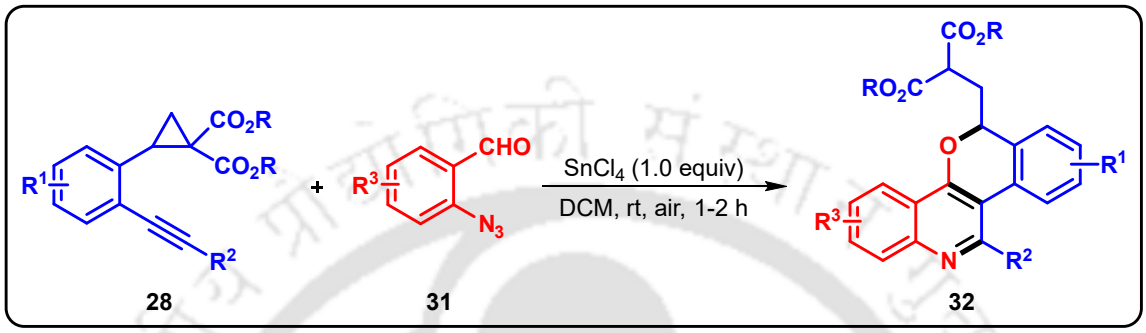

To a mixture of 2-alkynylcyclopropane **28** (0.33 mmol, 1.1 equiv) and 2-azidobenzaldehyde **31** (0.3 mmol, 1.0 equiv) in DCM, $SnCl_4$ (0.3 mmol, 1.0 equiv) was added slowly at 0 °C under air atmosphere. The reaction was then allowed to stir at room temperature and monitored by TLC analysis (using hexane/ethyl acetate = 7:3 as eluents). After completion of the reaction (1–2 h), the solvent was removed under vacuo in a rotary evaporator, and then the residue was diluted with ethyl acetate, saturated $NaHCO_3$, and brine solution. The aqueous phase was extracted with ethyl acetate (3 × 10 mL). The combined organic extracts were dried over anhydrous Na_2SO_4 and concentrated using a rotary evaporator. The crude product was subjected to column chromatography over silica gel to give the corresponding product **32**.

5.7.1.4 Experimental Procedure for the Gram-scale Synthesis of Compound 30aa

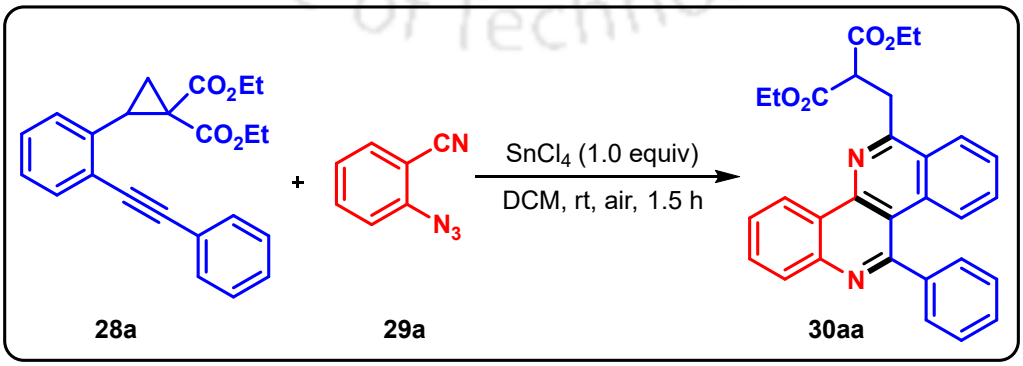

To a mixture of diethyl 2-(2-(phenylethynyl)phenyl)cyclopropane-1,1-dicarboxylate (**28a**) (1.0 g, 2.76 mmol, 1.1 equiv) and 2-azidobenzonitrile (**29a**) (0.37 g, 2.51 mmol, 1.0 equiv) in DCM, $SnCl_4$ (0.3 mL, 2.51 mmol, 1.0 equiv) was added slowly at 0 °C under air atmosphere. The reaction was then allowed to stir at room temperature and monitored by TLC analysis (using hexane/ethyl acetate = 3:1 as eluents). After completion of the reaction (1.5 h), the solvent was removed under vacuo in a rotary evaporator, and then the residue was diluted with ethyl acetate, saturated $NaHCO_3$, and brine solution. The aqueous phase was extracted with ethyl acetate (3 × 20 mL). The combined organic extracts were dried over anhydrous Na_2SO_4 and concentrated using a rotary evaporator. The crude product was subjected to column chromatography over silica gel to give the product **30aa** in 77% yield (0.925 g).

5.7.1.5 Experimental Procedure for the Gram-scale Synthesis of Compound 32aa

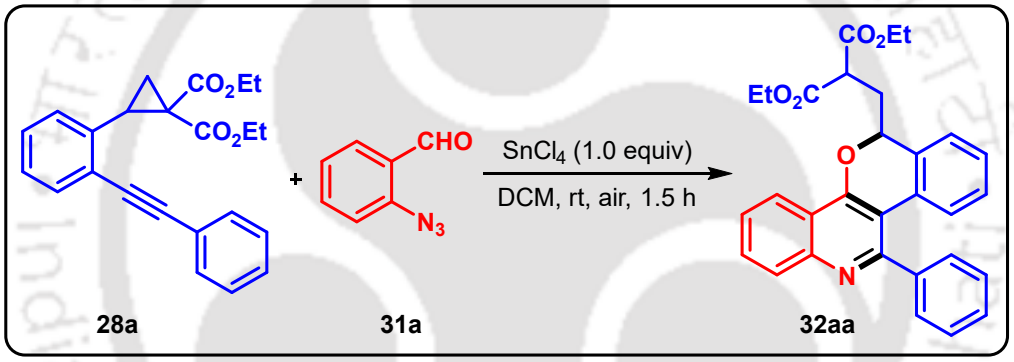

To a mixture of diethyl 2-(2-(phenylethynyl)phenyl)cyclopropane-1,1-dicarboxylate (**28a**) (1.0 g, 2.76 mmol, 1.1 equiv) and 2-azidobenzaldehyde (**31a**) (0.37 g, 2.51 mmol, 1.0 equiv) in DCM, $SnCl_4$ (0.3 mL, 2.51 mmol, 1.0 equiv) was added slowly at 0 °C under air atmosphere. The reaction was then allowed to stir at room temperature and monitored by TLC analysis (using hexane/ethyl acetate = 3:1 as eluents). After completion of the reaction (1.5 h), the solvent was removed under vacuo in a rotary evaporator, and then the residue was diluted with ethyl acetate, saturated $NaHCO_3$, and brine solution. The aqueous phase was extracted with ethyl acetate (3 × 20 mL). The combined organic extracts were dried over anhydrous Na_2SO_4 and concentrated using a rotary evaporator. The crude product was subjected to column chromatography over silica gel to give the corresponding product **32aa** in 71% yield (0.858 g).

5.7.1.6 Experimental Procedure for Control Experiments

5.7.1.6.1 Experimental Procedure for Reaction with Phenylazide (a)

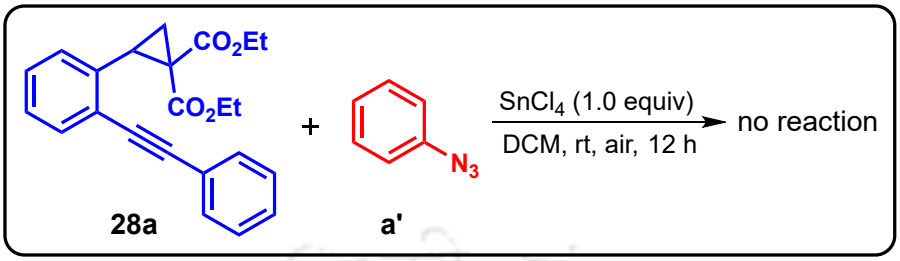

To a mixture of diethyl 2-(2-(phenylethynyl)phenyl)cyclopropane-1,1-dicarboxylate (**28a**) (0.33 mmol, 1.1 equiv) and phenylazide (**a'**) (0.3 mmol, 1.0 equiv) in DCM, $SnCl_4$ (0.3 mmol, 1.0 equiv) was added slowly at 0 °C under air atmosphere. The reaction was then allowed to stir at room temperature and monitored by TLC analysis. No expected product was observed even after 12 h, with the starting materials remaining unchanged.

5.7.1.6.2 Experimental Procedure for Reaction with Cyanobenzene (b)

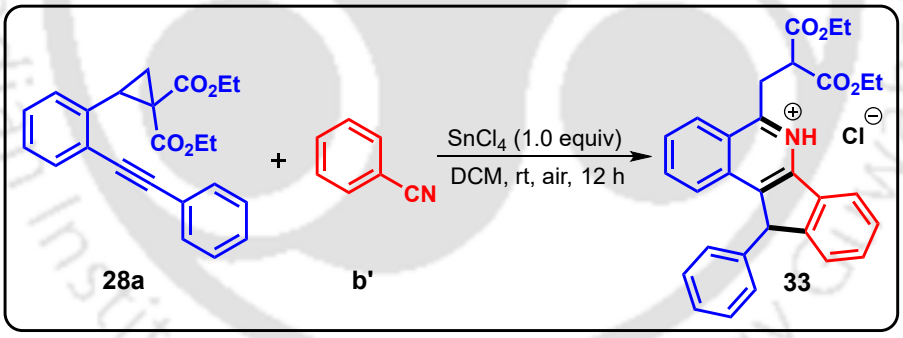

To a mixture of diethyl 2-(2-(phenylethynyl)phenyl)cyclopropane-1,1-dicarboxylate (**28a**) (0.33 mmol, 1.1 equiv) and cyanobenzene (**b'**) (0.3 mmol, 1.0 equiv) in DCM, $SnCl_4$ (0.3 mmol, 1.0 equiv) was added slowly in 0 °C under air atmosphere. The reaction was then allowed to stir at room temperature and monitored by TLC analysis. After 1.5 h, it leads to the formation of (*R*)-5-(3-ethoxy-2-(ethoxycarbonyl)-3-oxopropyl)-11-phenyl-11*H*-indeno[1,2-*c*]isoquinolin-6-ium (**33**) in 83% yield.

5.7.1.6.3 Experimental Procedure for Reaction with *p*-Chlorobenzaldehyde (c)

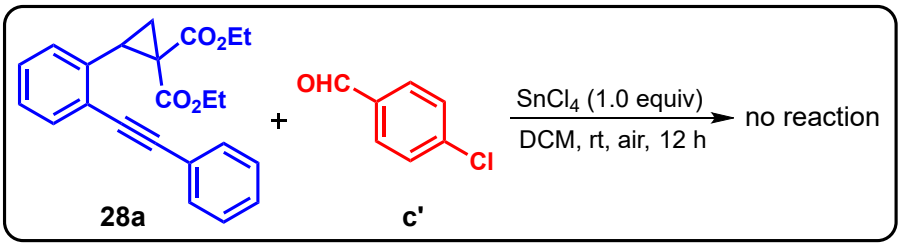

To a mixture of diethyl 2-(2-(phenylethynyl)phenyl)cyclopropane-1,1-dicarboxylate (**28a**) (0.33 mmol, 1.1 equiv) and *p*-chlorobenzaldehyde (**c'**) (0.3 mmol, 1.0 equiv) in DCM, $SnCl_4$ (0.3 mmol, 1.0 equiv) was added slowly in 0 °C under air atmosphere. The reaction was then allowed to stir at room temperature and monitored by TLC analysis. Unfortunately, the reaction did not proceed, and the starting materials decomposed under the proposed reaction conditions.

5.7.1.6.4 Experimental Procedure for Reaction with 1-azido-2-isocyanobenzene (d)

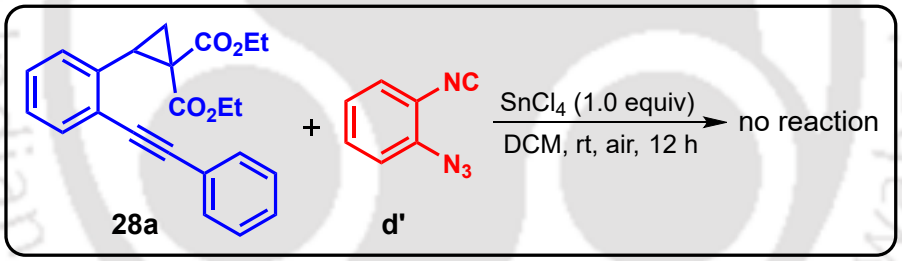

To a mixture of diethyl 2-(2-(phenylethynyl)phenyl)cyclopropane-1,1-dicarboxylate (**28a**) (0.33 mmol, 1.1 equiv) and 1-azido-2-isocyanobenzene (**d'**) (0.3 mmol, 1.0 equiv) in DCM, $SnCl_4$ (0.3 mmol, 1.0 equiv) was added slowly in 0 °C under air atmosphere. The reaction was then allowed to stir at room temperature and monitored by TLC analysis. Within 1 h of the reaction, the starting materials decomposed and did not lead to any product formation.

5.7.1.6.5 Experimental Procedure for Reaction with Salicylaldehyde (e)

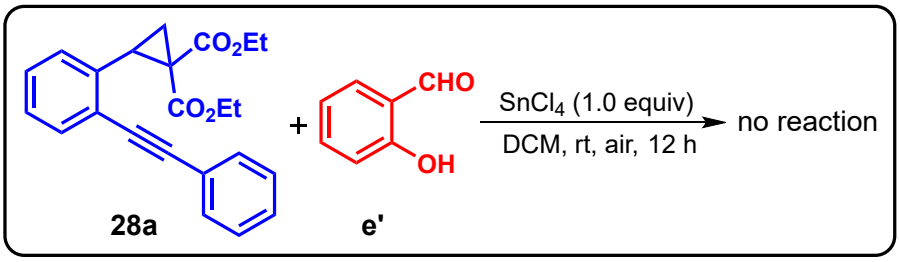

To a mixture of diethyl 2-(2-(phenylethynyl)phenyl)cyclopropane-1,1-dicarboxylate (**28a**) (0.33 mmol, 1.1 equiv) and salicylaldehyde (**e'**) (0.3 mmol, 1.0 equiv) in DCM, $SnCl_4$ (0.3 mmol, 1.0 equiv) was added slowly in °C under air atmosphere. The reaction was then allowed to stir at room temperature and monitored by TLC analysis. Replacing the $-N_3$ group with a –OH group in salicylaldehyde resulted in the decomposition of the starting materials instead of providing any product under the standard optimized reaction conditions.

5.8 References

1. (a) Atukuri, D.; Gunjal, R.; Holagundi, N.; Korlahalli, B.; Gangannavar, S.; Akkasali, K. *Drug Dev. Res.* **2021**, *82*, 767–783; (b) Dinodia, M. *Mini-Rev. Org. Chem.* **2023**, *20*, 735–747; (c) Amin, A.; Qadir, T.; Sharma, P. K.; Jeelani, I.; Abe, H. *Open J. Med. Chem.* **2022**, *16*, e187410452209010.

2. (a) Chabowska, G.; Barg, E.; Wójcicka, A. *Molecules* **2021**, *26*, 4324; (b) Wójcicka, A.; Mączyński, M. *Pharmaceuticals* **2024**, *17*, 1705; (c) Michael, J. P. *Nat. Prod. Rep.* **2003**, *20*, 476–493; (d) Michael, J. P. *Nat. Prod. Rep.* **2001**, *18*, 543–559.

3. (a) Lavanya, M.; Lin, C.; Mao, J.; Thirumalai, D.; Aabaka, S. R.; Yang, X.; Mao, J.; Huang, Z.; Zhao, J. *Top. Curr. Chem.* **2021**, *379*, 1–75; (b) Mostafa, M. A.; Bahig, E. E.; Hassanin, H. M. *Russ. J. Org. Chem.* **2024**, *60*, 1086–1106.

4. (a) Ibrahim, M. A.; Roushdy, N.; Atta, A. A.; Badran, A.-S.; Farag, A. A. M. *J. Mol. Struct.* **2024**, *1312*, 138660; (b) Zeyada, H.; El-Nahass, M.; El-Shabaan, M. *Synth. Met.* **2016**, *220*, 102–113; (c) Saeed, A. M.; AlNeyadi, S. S.; Abdou, I. M. *Heterocycl. Commun.* **2020**, *26*, 192–205.

5. (a) Kurtzberg, L. S.; Roth, S.; Krumbholz, R.; Crawford, J.; Bormann, C.; Dunham, S.; Yao, M.; Rouleau, C.; Bagley, R. G.; Yu, X.-J.; Wang, F.; Schmid,

S. M.; LaVoie, E. J.; Teicher, B. A. *Clin. Cancer Res.* **2011**, *17*, 2777–2787; (b) Zeng, L.-F.; Wang, Y.; Kazemi, R.; Xu, S.; Xu, Z.-L.; Sanchez, T. W.; Yang, L.-M.; Debnath, B.; Odde, S.; Xie, H.; Zheng, Y.-T.; Ding, J.; Neamati, N.; Long, Y.-Q. *J. Med. Chem.* **2012**, *55*, 9492–9509; (c) Wang, M.-S.; Zhuo, L.-S.; Yang, F.-P.; Wang, W.-J.; Huang, W.; Yang, G.-F. *Eur. J. Med. Chem.* **2020**, *185*, 111803; (d) Deady, L. W.; Rodemann, T.; Zhuang, L.; Baguley, B. C.; Denny, W. A. *J. Med. Chem.* **2003**, *46*, 1049–1054.

6. (a) Di Pietro, O.; Vicente-García, E.; Taylor, M. C.; Berenguer, D.; Viayna, E.; Lanzoni, A.; Sola, I.; Sayago, H.; Riera, C.; Fisa, R.; Clos, M. V.; Pérez, B.; Kelly, J. M.; Lavilla, R.; Muñoz-Torrero, D. *Eur. J. Med. Chem.* **2015**, *105*, 120–137; (b) Payne, D. J.; Hueso-Rodríguez, J. A.; Boyd, H.; Concha, N. O.; Janson, C. A.; Gilpin, M.; Bateson, J. H.; Cheever, C.; Niconovich, N. L.; Pearson, S.; Rittenhouse, S. *Antimicrob. Agents Chemother.* **2002**, *46*, 1880–1886; (c) Pearce, A. N.; Appleton, D. R.; Babcock, R. C.; Copp, B. R. *Tetrahedron Lett.* **2003**, *44*, 3897–3899; (d) Kamperdick, C.; Van, N. H.; Van Sung, T.; Adam, G. *Phytochemistry* **1999**, *50*, 177–181.

7. Okuma, K.; Koga, T.; Ozaki, S.; Suzuki, Y.; Horigami, K.; Nagahora, N.; Deshimaru, M. *Chem. Commun.* **2014**, *50*, 15525–15528.

8. Kumar, R.; Asthana, M.; Singh, R. M. *J. Org. Chem.* **2017**, *82*, 11531–11542.

9. Almansour, A. I.; Kumar, R. S.; Arumugam, N.; Basiri, A.; Kia, Y.; Ali, M. A. *Biomed. Res. Int.* **2015**, *2015*, 965987.

10. Ravi, M.; Chauhan, P.; Singh, S.; Kant, R.; Yadav, P. P. *RSC Adv.* **2016**, *6*, 48774–48778.

11. Singh, J. B.; Bharadwaj, K. C.; Gupta, T.; Singh, R. M. *RSC Adv.* **2016**, *6*, 26993–26999.

12. Verma, A. K.; Kotla, S. K. R.; Choudhary, D.; Patel, M.; Tiwari, R. K. *J. Org. Chem.* **2013**, *78*, 4386–4401.

13. Biswas, S.; Saikia, A. K. *J. Org. Chem.* **2024**, *89*, 14454–14471.

14. Gao, Q.; Wang, B.; Jiang, H.; Wu, W. *J. Org. Chem.* **2024**, *89*, 18370–18383.

15. Mao, X. F.; Zhu, X. P.; Li, D. Y.; Liu, P. N. *J. Org. Chem.* **2017**, *82*, 7032–7039.

16. (a) Reissig, H. U.; Zimmer, R. *Chem. Rev.* **2003**, *103*, 1151–1196; (b) Schneider, T. F.; Kaschel, J.; Werz, D. B. *Angew. Chem., Int. Ed.* **2014**, *53*, 5504–

5523; (c) Cavitt, M. A.; Phun, L. H.; France, S. *Chem. Soc. Rev.* **2014**, *43*, 804–818; (d) Ivanova, O. A.; Trushkov, I. V. *Chem. Rec.* **2019**, *19*, 2189–2208; (e) Banerjee, P.; Biju A. T. *Donor–Acceptor Cyclopropanes in Organic Synthesis*, John Wiley & Sons, **2024**; (f) Nareddy, R. R. *Synthesis and Reactions of Novel Donor–Acceptor Cyclopropanes*, Mississippi State University, **2016**; (g) Flisar, M. E. *The Application of Novel Donor–Acceptor Cyclopropanes in the Synthesis of Linearly Fused Tricyclic Triazoles*, The University of Western Ontario, Canada, **2014**.

17. (a) Qu, J.-P.; Liang, Y.; Xu, H.; Sun, X.-L.; Yu, Z.-X.; Tang, Y. *Chem. Eur. J.* **2012**, *18*, 2196–2201; (b) Zhu, J.; Liang, Y.; Wang, L.; Zheng, Z. B.; Houk, K. N.; Tang, Y. *J. Am. Chem. Soc.* **2014**, *136*, 6900–6903; (c) Xu, H.; Hu, J.-L.; Wang, L.; Liao, S.; Tang, Y. *J. Am. Chem. Soc.* **2015**, *137*, 8006–8009.

18. Xiao, J. A.; Peng, H.; Liang, J. S.; Meng, R. F.; Su, W.; Xiao, Q.; Yang, H. *Chem. Commun.* **2021**, *57*, 13369–13372.

19. (a) Sathishkannan, G.; Srinivasan, K. *Org. Lett.* **2011**, *13*, 6002–6005; (b) Pohlhaus, P. D.; Sanders, S. D.; Parsons, A. T.; Li, W.; Johnson, J. S. *J. Am. Chem. Soc.* **2008**, *130*, 8642–8650; (c) Pohlhaus, P. D.; Johnson, J. S. *J. Am. Chem. Soc.* **2005**, *127*, 16014–16015.

20. (a) Xiao, J. A.; Peng, H.; Liang, J. S.; Meng, R. F.; Su, W.; Xiao, Q.; Yang, H. *Chem. Commun.* **2021**, *57*, 13369–13372; (b) Zeng, L.; Li, J.; Cui, S. *Angew. Chem., Int. Ed.* **2022**, *61*, e202205037; (c) Puskov, G. I.; Shcherbakov, N. V.; Kukushkin, V. Y.; Dubovtsev, A. Y. *Adv. Synth. Catal.* **2025**, *367*, e202401051.

5.9 Characterization Data

Diethyl 2-(2-(phenylethynyl)phenyl)cyclopropane-1,1-dicarboxylate (28a):

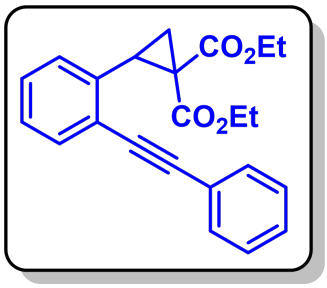

Pale yellow solid; R_f (Hexane/EtOAc, 9:1) 0.55; mp 93–95 °C. Yield 252 mg, 81%; ^{1}H NMR (500 MHz, $CDCl_3$) δ 7.46 (d, J = 7.0 Hz, 2 H), 7.41 (d, J = 7.0 Hz, 1 H), 7.25–7.20 (m, 3 H), 7.14–7.11 (m, 2 H), 7.00 (d, J = 7.0 Hz, 1 H), 4.11–3.99 (m, 2 H), 3.77–3.71 (m, 2 H), 3.52 (t, J = 8.5 Hz, 1 H), 2.20–2.17 (m, 1 H), 1.68–1.65 (m, 1 H), 1.07 (t, J = 6.5 Hz, 3 H), 0.75 (t, J = 6.5 Hz, 3 H); ^{13}C{^{1}H} NMR (125 MHz, $CDCl_3$) δ 169.9, 166.9, 136.9, 131.8, 131.7, 128.4, 128.3, 128.0, 127.4, 127.3, 125.6, 123.6, 94.7, 87.7, 61.6, 61.2, 37.2,

32.0, 18.8, 14.1, 13.8; IR (KBr, neat) 3015, 2210, 1726, 1345, 1213, 1138, 820, 676 cm^{-1}; HRMS (ESI) calcd. for $C_{23}H_{23}O_4$ $(M + H)^+$ 363.1591, found 363.1577.

Diethyl 2-(2-((4-chlorophenyl)ethynyl)phenyl)cyclopropane-1,1-dicarboxylate (28b):

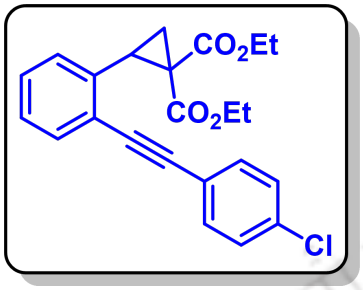

White solid; R_f (Hexane/EtOAc, 9:1) 0.50; mp 97–99 °C. Yield 237 mg, 76%; ^{1}H NMR (500 MHz, $CDCl_3$) δ 7.39 (d, J = 8.5 Hz, 3 H), 7.21 (d, J = 8.5 Hz, 2 H), 7.16–7.10 (m, 2 H), 7.00 (d, J = 7.0 Hz, 1 H), 4.12–4.01 (m, 2 H), 3.77–3.70 (m, 2 H), 3.49 (t, J = 8.5 Hz, 1 H), 2.18 (dd, J = 8.5, 5.0 Hz, 1 H), 1.65 (dd, J = 9.0, 5.0 Hz, 1 H), 1.09 (t, J = 7.5 Hz, 3 H), 0.74 (t, J = 7.5 Hz, 3 H); ^{13}C{^{1}H} NMR (125 MHz, $CDCl_3$) δ 169.8, 166.7, 136.9, 134.3, 132.9, 131.7, 128.7, 128.3, 127.4, 125.2, 122.1, 93.5, 88.6, 61.7, 61.1, 37.1, 31.9, 18.8, 14.1, 13.7; IR (KBr, neat) 3099, 2195, 1747, 1388, 1245, 1099, 817, 654 cm^{-1}; HRMS (ESI) calcd. for $C_{23}H_{22}ClO_4$ $(M + H)^+$ 397.1202, found 397.1192.

Dimethyl 2-(2-((4-(tert-butyl)phenyl)ethynyl)phenyl)cyclopropane-1,1-dicarboxylate (28f):

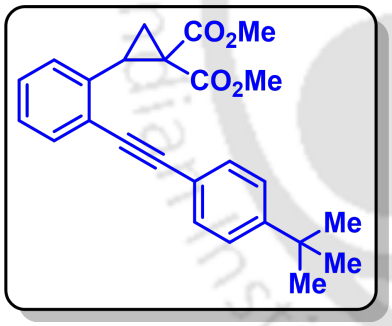

Brown gummy; R_f (Hexane/EtOAc, 9:1) 0.50. Yield 279 mg, 83%; ^{1}H NMR (500 MHz, $CDCl_3$) δ 7.51 (d, J = 6.0 Hz, 3 H), 7.39 (d, J = 7.5 Hz, 2 H), 7.24–7.21 (m, 2 H), 7.10–7.08 (m, 1 H), 3.72 (s, 3 H), 3.66 (t, J = 8.0 Hz, 1 H), 3.35 (s, 3 H), 2.33 (t, J = 6.0 Hz, 1 H), 1.84–1.80 (m, 1 H), 1.34 (s, 9 H); ^{13}C{^{1}H} NMR (125 MHz, $CDCl_3$) δ 170.2, 167.2, 151.6, 136.6, 131.7, 131.4, 127.8, 127.3, 127.0, 125.6, 125.3, 120.4, 94.9, 86.9, 52.7, 52.2, 36.9, 34.8, 31.3, 19.2; IR (KBr, neat) 3104, 2224, 1695, 1390, 1210, 1178, 890, 616 cm^{-1}; HRMS (ESI) calcd. for $C_{25}H_{27}O_4$ $(M + H)^+$ 391.1904, found 391.1929.

Diethyl 2-(2-((2-isopropylphenyl)ethynyl)phenyl)cyclopropane-1,1-dicarboxylate (28g):

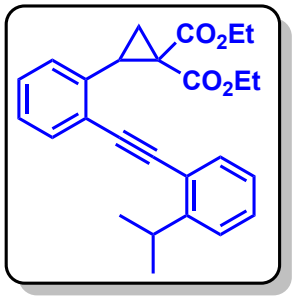

Yellow gummy; R_f (Hexane/EtOAc, 9:1) 0.55. Yield 268 mg, 77%; ^{1}H NMR (400 MHz, $CDCl_3$) δ 7.60 (d, J = 7.6 Hz, 1 H), 7.56–7.54 (m, 1 H), 7.34–7.32 (m, 2 H), 7.28–7.25 (m, 2 H), 7.22–7.18 (m, 1 H), 7.14–7.11 (m, 1 H), 4.20–4.11 (m, 2 H), 3.93–3.85 (m, 2 H), 3.68–3.58 (m, 2 H), 2.33 (dd, J = 8.0, 4.8 Hz, 1 H), 1.81 (dd, J = 9.2, 5.2 Hz, 1 H), 1.37 (d, J = 7.2 Hz, 6 H), 1.19 (t, J = 7.2 Hz, 3 H), 0.89 (t, J = 7.2 Hz, 3 H); ^{13}C{^{1}H} NMR (125 MHz, $CDCl_3$) δ 169.7, 166.8, 150.2, 136.5, 132.7, 131.9, 128.7, 127.9, 127.2, 127.0, 125.9, 125.5, 124.9, 122.2, 93.4, 91.2, 61.5, 61.1, 37.2, 31.8, 31.7, 23.2, 23.1, 18.7, 14.0, 13.7; IR (KBr, neat) 3163, 2199, 1713, 1447, 1367, 1182, 913, 657 cm^{-1}; HRMS (ESI) calcd. for $C_{26}H_{29}O_4$ $(M + H)^+$ 405.2061, found 405.2063.

Dimethyl 2-(2-(naphthalen-2-ylethynyl)phenyl)cyclopropane-1,1-dicarboxylate (28h):

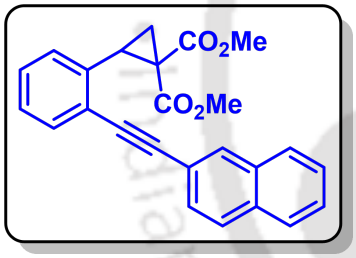

Brown solid; R_f (Hexane/EtOAc, 9:1) 0.55; mp 108–110 °C. Yield 234 mg, 71%; ^{1}H NMR (400 MHz, $CDCl_3$) δ 8.11 (s, 1 H), 7.88–7.83 (m, 3 H), 7.64–7.58 (m, 2 H), 7.54–7.51 (m, 2 H), 7.31–7.28 (m, 2 H), 7.15–7.13 (m, 1 H), 3.73 (s, 3 H), 3.72 (d, J = 8.8 Hz, 1 H), 3.40 (s, 3 H), 2.38 (dd, J = 8.4, 5.2 Hz, 1 H), 1.88 (dd, J = 9.2, 5.2 Hz, 1 H); ^{13}C{^{1}H} NMR (125 MHz, $CDCl_3$) δ 170.5, 167.4, 136.9, 133.2, 133.1, 131.9, 131.7, 128.6, 128.2, 128.1, 128.0, 127.9, 127.6, 127.3, 126.9, 126.7, 125.5, 120.9, 95.3, 87.9, 52.9, 52.4, 37.1, 32.7, 19.4; IR (KBr, neat) 3104, 2224, 1695, 1390, 1210, 1178, 890, 616 cm^{-1}; HRMS (ESI) calcd. for $C_{25}H_{21}O_4$ $(M + H)^+$ 385.1435, found 385.1443.

Dimethyl 2-(2-(phenanthren-9-ylethynyl)phenyl)cyclopropane-1,1-dicarboxylate (28i):

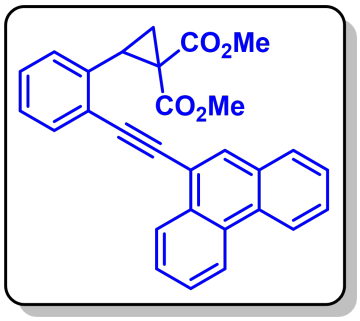

Brown gummy; R_f (Hexane/EtOAc, 9:1) 0.55. Yield 272 mg, 73%; ^{1}H NMR (500 MHz, $CDCl_3$) δ 8.71 (dd, J = 17.5, 8.0 Hz, 2 H), 8.62 (d, J = 7.5 Hz, 1 H), 8.16 (s, 1 H), 7.94 (d, J = 8.0 Hz, 1 H), 7.79–7.69 (m, 4 H), 7.65 (t, J = 7.5 Hz, 1 H), 7.35 (s, 2 H), 7.18 (s, 1 H), 3.81 (t, J = 9.0 Hz, 1 H), 3.58 (s, 3 H), 3.45 (s, 3 H), 2.42 (t, J = 6.5 Hz, 1 H), 1.91 (t, J = 6.5 Hz, 1 H); ^{13}C{^{1}H} NMR (125 MHz, $CDCl_3$) δ 170.3, 167.4, 136.8, 132.3, 131.5, 131.2, 130.5, 130.2, 128.8, 128.3, 127.7, 127.6, 127.3 (2), 127.2, 127.1, 125.6, 122.9, 122.8, 119.9, 93.1, 92.0, 52.8, 52.4, 37.3, 32.5, 19.3; IR (KBr, neat) 3029, 2194, 1725, 1331, 1270, 1129, 842, 763 cm^{-1}; HRMS (ESI) calcd. for $C_{29}H_{23}O_4$ $(M + H)^+$ 435.1591, found 435.1589.

Diethyl 2-(4-chloro-2-(phenylethynyl)phenyl)cyclopropane-1,1-dicarboxylate (28t):

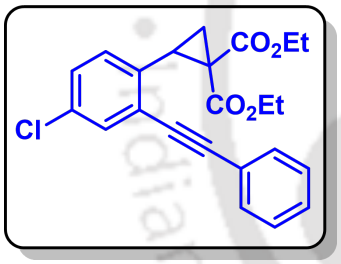

Brown gummy; R_f (Hexane/EtOAc, 9:1) 0.45. Yield 272 mg, 80%; ^{1}H NMR (400 MHz, $CDCl_3$) δ 7.56–7.52 (m, 2 H), 7.49 (d, J = 2.4 Hz, 1 H), 7.37–7.33 (m, 3 H), 7.21 (dd, J = 8.4, 2.4 Hz, 1 H), 7.02 (d, J = 8.0 Hz, 1 H), 4.22–4.10 (m, 2 H), 3.88 (q, J = 7.2 Hz, 2 H), 3.54 (t, J = 8.8 Hz, 1 H), 2.23 (dd, J = 8.0, 4.8 Hz, 1 H), 1.76 (dd, J = 9.2, 5.2 Hz, 1 H), 1.18 (t, J = 7.2 Hz, 3 H), 0.91 (t, J = 7.2 Hz, 3 H); ^{13}C{^{1}H} NMR (100 MHz, $CDCl_3$) δ 169.8, 166.8, 135.6, 133.2, 131.9, 131.5, 128.8 (2), 128.5, 128.2, 127.2, 123.1, 95.9, 86.3, 61.8, 61.4, 37.2, 31.4, 18.9, 14.2, 13.9; IR (KBr, neat) 2951, 2216, 1724, 1330, 1280, 1126, 820, 690 cm^{-1}; HRMS (ESI) calcd. for $C_{23}H_{22}ClO_4$ $(M + H)^+$ 397.1202, found 397.1206.

Dimethyl 2-(4-(methoxycarbonyl)-2-(phenylethynyl)phenyl)cyclopropane-1,1-dicarboxylate (28w):

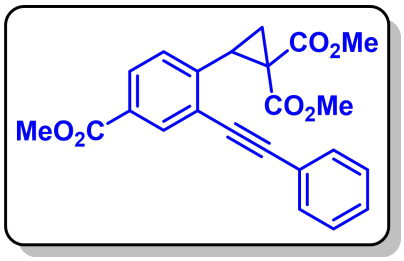

Pale yellow gummy; R_f (Hexane/EtOAc, 9:1) 0.45. Yield 259 mg, 77%; ^{1}H NMR (400 MHz, $CDCl_3$) δ 7.82 (dd, J = 8.0, 1.6 Hz, 1 H), 7.69 (s, 1 H), 7.48–7.45 (m, 3 H), 7.28–7.25 (m, 3 H), 3.81 (s, 3 H), 3.61 (s, 3 H), 3.51 (t, J = 8.8 Hz, 1 H), 3.28 (s, 3 H), 2.29 (dd, J = 8.0, 5.2 Hz, 1 H), 1.76 (dd, J = 9.2, 5.2 Hz, 1 H); ^{13}C{^{1}H} NMR (125 MHz, $CDCl_3$) δ 170.2, 167.1, 166.6, 137.0, 131.9, 131.6, 129.6, 129.5, 128.6, 128.1, 127.5, 127.2, 124.8, 93.9, 90.4, 52.8, 52.3, 52.2, 36.9, 32.3, 19.2; IR (KBr, neat) 2999, 2270, 1720, 1371, 1213, 1083, 880, 729 cm^{-1}; HRMS (ESI) calcd. for $C_{23}H_{21}O_6$ $(M + H)^+$ 393.1333, found 393.1360.

Dimethyl 2-(2-(cyclohexylethynyl)phenyl)cyclopropane-1,1-dicarboxylate (28z):

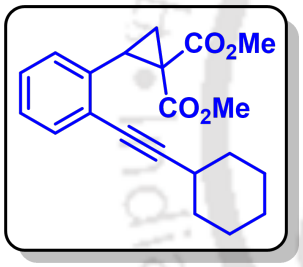

Pale yellow gummy; R_f (Hexane/EtOAc, 9:1) 0.60. Yield 202 mg, 69%; ^{1}H NMR (500 MHz, $CDCl_3$) δ 7.36 (dd, J = 8.0, 3.0 Hz, 1 H), 7.15 (dd, J = 6.5, 3.5 Hz, 2 H), 7.00–6.98 (m, 1 H), 3.77 (s, 3 H), 3.51 (t, J = 9.0 Hz, 1 H), 3.32 (s, 3 H), 2.58 (t, J = 10.0 Hz, 1 H), 2.27–2.24 (m, 1 H), 1.88 (d, J = 13.0 Hz, 2 H), 1.75 (s, 3 H), 1.56–1.48 (m, 3 H), 1.34 (s, 3 H); ^{13}C{^{1}H} NMR (125 MHz, $CDCl_3$) δ 170.2, 167.1, 136.3, 131.8, 127.2, 127.1, 126.8, 126.2, 99.9, 78.5, 52.6, 52.1, 36.8, 32.7, 32.6, 32.4, 29.9, 26.0, 25.1, 19.3; IR (KBr, neat) 2929, 2226, 1725, 1435, 1209, 1092, 754, 525 cm^{-1}; HRMS (ESI) calcd. for $C_{21}H_{25}O_4$ $(M + H)^+$ 341.1748, found 341.1720.

Ethyl 2-(2-(phenylethynyl)phenyl)-1-propionylcyclopropane-1-carboxylate (28aa'):

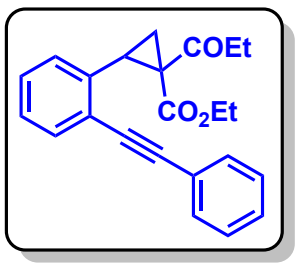

Colourless liquid; R_f (Hexane/EtOAc, 9:1) 0.50. Yield 272 mg, 20%; ^{1}H NMR (400 MHz, $CDCl_3$) δ 7.43–7.35 (m, 3 H), 7.28–7.23 (m, 3 H), 7.18–7.14 (m, 2 H), 7.05 (dd, J = 8.0, 2.4 Hz, 1 H), 3.80–3.64 (m, 2 H), 3.50 (t, J = 8.8 Hz, 1 H), 2.95–2.85 (m, 1 H), 2.65–2.55 (m, 1 H), 2.24 (dd, J = 8.4, 4.8 Hz, 1 H), 1.75 (dd, J = 8.8, 4.4 Hz, 1 H), 0.92 (t, J = 7.2 Hz, 3 H), 0.76 (t, J = 7.2 Hz, 3 H); ^{13}C{^{1}H} NMR (125 MHz, $CDCl_3$) δ 205.3, 168.4, 137.4, 131.9,

131.8, 128.5, 128.0, 127.9, 127.4, 125.6, 123.4, 94.9, 87.7, 61.2, 43.9, 35.7, 35.3, 21.4, 13.8, 8.2; IR (KBr, neat) 3061, 2978, 1722, 1692, 1314, 1177, 774, 690 cm^{-1}; HRMS (ESI) calcd. for $C_{23}H_{23}O_3$ $(M + H)^+$ 347.1642, found 347.1637.

2-Azido-3-fluorobenzonitrile (29m):

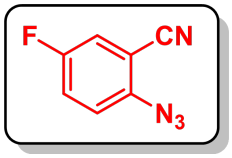

Brown solid; R_f (Hexane/EtOAc, 9:1) 0.55; mp 98–100 °C. Yield 216 mg, 81%; ^1H NMR (400 MHz, $CDCl_3$) δ 7.60 (td, J = 8.4, 6.0 Hz, 1 H), 7.06 (d, J = 8.0 Hz, 1 H), 6.95 (t, J = 8.4 Hz, 1 H); $^{13}C\{^1H\}$ NMR (100 MHz, $CDCl_3$) δ 163.9 (d, J = 257.5 Hz), 145.0 (d, J = 3.7 Hz), 135.3 (d, J = 10.0 Hz), 114.6 (d, J = 3.4 Hz), 111.9 (d, J = 19.8 Hz), 110.7, 93.7 (d, J = 18.8 Hz); ^{19}F NMR (470 MHz, $CDCl_3/C_6F_6$) δ –107.3 (s, –CF–); IR (KBr, neat) 3054, 2232, 2124, 1482, 1300, 1112, 830, 790, 623 cm^{-1}; HRMS (ESI) calcd. for $C_7H_4FN_4$ $(M + H)^+$ 163.0415, found 163.0410.

2-Azido-5-(trifluoromethyl)benzonitrile (29o):

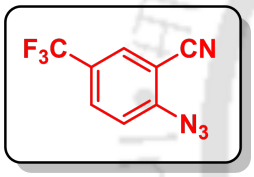

Brown gummy; R_f (Hexane/EtOAc, 9:1) 0.50. Yield 262 mg, 75%; ^1H NMR (500 MHz, $CDCl_3$) δ 7.79–7.77 (m, 2 H), 7.34 (d, J = 8.5 Hz, 1 H); $^{13}C\{^1H\}$ NMR (125 MHz, $CDCl_3$) δ 147.0, 131.3 (q, J = 3.7 Hz), 131.0 (q, J = 3.6 Hz), 127.6 (q, J = 34.2 Hz), 122.9 (q, J = 270.5 Hz), 119.6, 114.4, 104.7; ^{19}F NMR (470 MHz, $CDCl_3/C_6F_6$) δ –65.8 (s, –CF_3–); IR (KBr, neat) 3086, 2128, 1497, 1329, 1125, 828, 733, 629 cm^{-1}; HRMS (ESI) calcd. for $C_8H_4F_3N_4$ $(M + H)^+$ 213.0383, found 213.0379.

2-Azido-4,5-dimethoxybenzonitrile (29q):

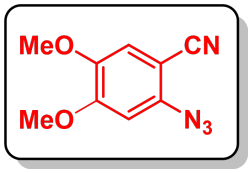

Brown solid; R_f (Hexane/EtOAc, 9:1) 0.60; mp 112–114 °C. Yield 293 mg, 87%; ^1H NMR (400 MHz, $CDCl_3$) δ 6.92 (s, 1 H), 6.61 (s, 1 H), 3.92 (s, 3 H), 3.83 (s, 3 H); $^{13}C\{^1H\}$ NMR (100 MHz, $CDCl_3$) δ 153.9, 146.6, 137.5, 116.1, 114.3, 101.9, 94.9, 56.5; IR (KBr, neat) 2923, 2221, 2112, 1498, 1281, 818, 774, 650 cm^{-1}; HRMS (ESI) calcd. for $C_9H_9N_4O_2$ $(M + H)^+$ 205.0721, found 205.0697.

2-Azidonicotinonitrile (29y):

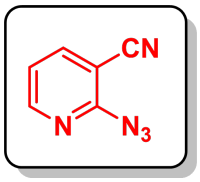

Dark brown solid; R_f (Hexane/EtOAc, 9:1) 0.45; mp 90–92 °C. Yield 170 mg, 71%; ^{1}H NMR (400 MHz, $CDCl_3$) δ 8.39 (dd, J = 4.4, 1.6 Hz, 1 H), 7.64 (dd, J = 8.8, 1.6 Hz, 1 H), 7.56 (dd, J = 8.4, 4.4 Hz, 1 H); ^{13}C{^{1}H} NMR (100 MHz, $CDCl_3$) δ 146.8, 141.5, 127.9, 126.8, 124.4, 114.5; IR (KBr, neat) 3056, 2131, 1728, 1449, 1310, 1157, 803, 752 cm^{-1}; HRMS (ESI) calcd. for $C_7H_4BrN_4$ $(M + H)^+$ 146.0462, found 146.0447.

Diethyl 2-((11-phenyldibenzo[*c*,*h*][1,6]naphthyridin-6-yl)methyl)malonate (30aa):

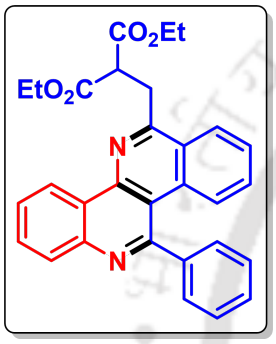

Yellow solid; R_f (Hexane/EtOAc, 3:1) 0.50; mp 183–185 °C. Yield 133 mg, 93%; ^{1}H NMR (500 MHz, $CDCl_3$) δ 9.24 (d, J = 8.0 Hz, 1 H), 8.33 (d, J = 8.0 Hz, 1 H), 8.23 (d, J = 8.5 Hz, 1 H), 7.82 (t, J = 7.5 Hz, 1 H), 7.73 (t, J = 8.0 Hz, 1 H), 7.68 (d, J = 8.5 Hz, 1 H), 7.61–7.58 (m, 3 H), 7.54–7.51 (m, 3 H), 7.39 (t, J = 8.0 Hz, 1 H), 4.81 (t, J = 7.5 Hz, 1 H), 4.37–4.26 (m, 4 H), 4.20 (d, J = 7.5 Hz, 2 H), 1.35 (t, J = 7.0 Hz, 6 H); ^{13}C{^{1}H} NMR (125 MHz, $CDCl_3$) δ 170.0, 161.2, 159.0, 145.8, 145.3, 143.8, 132.6, 130.1, 130.0, 129.4, 129.1, 128.9, 128.8, 127.5, 127.0, 126.7, 125.4, 125.3, 124.7, 114.6, 61.9, 49.5, 34.6, 14.4; IR (KBr, neat) 3461, 2981, 1729, 1355, 1150, 1025, 758, 699, 522 cm^{-1}; HRMS (ESI) calcd. for $C_{30}H_{26}N_2NaO_4$ $(M + Na)^+$ 501.1785, found 501.1765.

Diethyl 2-((11-(4-chlorophenyl)dibenzo[*c*,*h*][1,6]naphthyridin-6-yl)methyl)malonate (30ab):

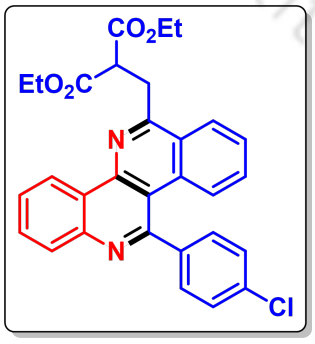

Pale yellow solid; R_f (Hexane/EtOAc, 3:1) 0.50; mp 173–175 °C. Yield 135 mg, 88%; ^{1}H NMR (400 MHz, $CDCl_3$) δ 9.23 (d, J = 8.8 Hz, 1 H), 8.36 (d, J = 8.0 Hz, 1 H), 8.21 (d, J = 8.0 Hz, 1 H), 7.83 (t, J = 8.4 Hz, 1 H), 7.77–7.71 (m, 2 H), 7.64 (t, J = 8.0 Hz, 1 H), 7.58 (d, J = 8.4 Hz, 2 H), 7.52–7.46 (m, 3 H), 4.80 (t, J = 7.2 Hz, 1 H), 4.35–4.26 (m, 4 H), 4.20 (d, J = 7.6 Hz, 2 H), 1.35 (t, J = 7.2 Hz, 6 H); ^{13}C{^{1}H} NMR (100 MHz, $CDCl_3$) δ 169.8, 161.3, 157.5, 145.6, 145.3, 142.0, 134.9, 132.1, 130.3, 130.2, 130.1, 129.4, 128.9, 127.5, 127.1, 126.6, 125.4, 125.2, 124.6, 114.2, 61.8, 49.3, 34.4, 14.2; IR (KBr, neat) 3417, 2954, 1709, 1361, 1220, 1152, 766, 700, 529 cm^{-1}; HRMS (ESI) calcd. for $C_{30}H_{25}ClN_2NaO_4$ $(M + Na)^+$ 535.1396, found 535.1384.

Dimethyl 2-((11-(4-bromophenyl)dibenzo[*c*,*h*][1,6]naphthyridin-6-yl)methyl)malonate (30ac):

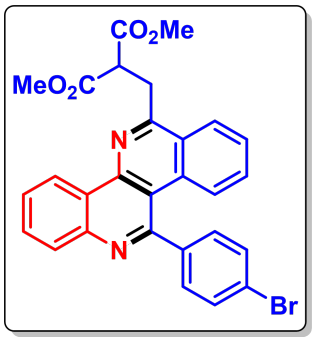

Yellow solid; R_f (Hexane/EtOAc, 3:1) 0.45; mp 150–152 °C. Yield 143 mg, 90%; ^{1}H NMR (500 MHz, $CDCl_3$) δ 9.20 (d, J = 8.5 Hz, 1 H), 8.36 (d, J = 8.0 Hz, 1 H), 8.20 (d, J = 8.5 Hz, 1 H), 7.83 (t, J = 7.5 Hz, 1 H), 7.78 (d, J = 9.0 Hz, 1 H), 7.75 (t, J = 8.0 Hz, 1 H), 7.68–7.63 (m, 3 H), 7.52–7.48 (m, 3 H), 4.82 (t, J = 7.5 Hz, 1 H), 4.22 (d, J = 7.5 Hz, 2 H), 3.86 (s, 6 H); ^{13}C{^{1}H} NMR (125 MHz, $CDCl_3$) δ 170.3, 161.3, 157.7, 145.9, 145.5, 142.8, 133.1, 132.6, 132.4, 130.8, 130.4, 129.2, 127.7, 127.4, 127.4, 126.7, 125.5, 125.4, 124.5, 123.3, 114.4, 53.1, 49.2, 34.8; IR (KBr, neat) 3412, 2987, 1725, 1360, 1202, 1176, 780, 699, 510 cm^{-1}; HRMS (ESI) calcd. for $C_{28}H_{21}BrN_2NaO_4$ $(M + Na)^+$ 551.0577, found 551.0553.

Dimethyl 2-((11-(*p*-tolyl)dibenzo[*c*,*h*][1,6]naphthyridin-6-yl)methyl)malonate (30ad):

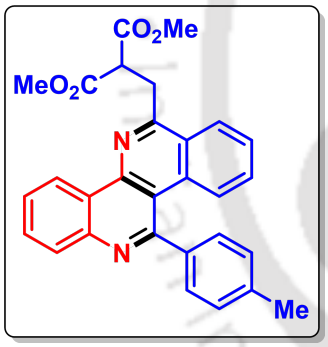

Pale yellow solid; R_f (Hexane/EtOAc, 3:1) 0.55; mp 192–194 °C. Yield 129 mg, 93%; ^{1}H NMR (500 MHz, $CDCl_3$) δ 9.30 (d, J = 8.0 Hz, 1 H), 8.36 (d, J = 8.0 Hz, 1 H), 8.26 (d, J = 8.0 Hz, 1 H), 7.84 (t, J = 7.5 Hz, 1 H), 7.77 (t, J = 8.0 Hz, 1 H), 7.64–7.59 (m, 2 H), 7.48–7.42 (m, 2 H), 7.39 (d, J = 9.0 Hz, 3 H), 4.84 (t, J = 7.0 Hz, 1 H), 4.23 (d, J = 7.5 Hz, 2 H), 3.87 (d, J = 4.5 Hz, 6 H), 2.02 (s, 3 H); ^{13}C{^{1}H} NMR (125 MHz, $CDCl_3$) δ 170.3 (2), 161.1, 159.1, 145.9, 145.0, 143.5, 135.6, 132.7, 131.2, 131.1, 130.1, 129.1, 128.9, 128.6, 127.6, 127.2, 127.1, 126.5, 125.9, 125.6, 125.5, 124.7, 115.3, 53.0, 49.2, 34.8, 19.8; IR (KBr, neat) 3450, 2931, 1746, 1514, 1250, 1080, 823, 648, 569 cm^{-1}; HRMS (ESI) calcd. for $C_{29}H_{24}KN_2O_4$ $(M + K)^+$ 503.1368, found 503.1351.

Dimethyl 2-((11-(4-methoxyphenyl)dibenzo[*c*,*h*][1,6]naphthyridin-6-yl)methyl)malonate (30ae):

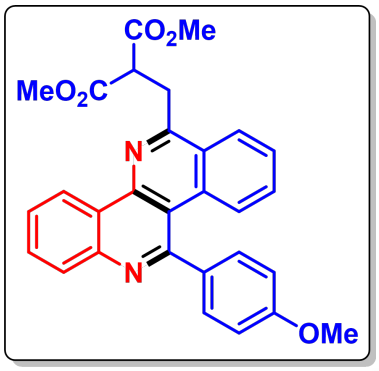

Pale yellow solid; R_f (Hexane/EtOAc, 3:1) 0.50; mp 198–200 °C. Yield 135 mg, 94%; ^{1}H NMR (600 MHz, $CDCl_3$) δ 9.18 (d, J = 8.4 Hz, 1 H), 8.32 (d, J = 8.4 Hz, 1 H), 8.20 (d, J = 8.4 Hz, 1 H), 7.84–7.79 (m, 2 H), 7.71 (t, J = 7.8 Hz, 1 H), 7.60 (t, J = 7.8 Hz, 1 H), 7.55 (d, J = 7.8 Hz, 2 H), 7.44 (t, J = 7.8 Hz, 1 H), 7.05 (d, J = 7.8 Hz, 2 H), 4.81 (t, J = 7.2 Hz, 1 H), 4.20 (d, J = 7.2 Hz, 2 H), 3.91 (s, 3 H), 3.86 (s, 6 H); ^{13}C{^{1}H} NMR (150 MHz, $CDCl_3$) δ 170.4, 160.9, 160.4, 158.7, 145.9, 145.4, 136.3, 132.8, 130.4, 130.1, 130.0, 129.0, 127.5, 127.4, 126.9, 126.7, 125.3, 125.2, 124.5, 114.8, 114.6, 55.7, 53.0, 49.2, 34.7; IR (KBr, neat) 3461, 2923, 1735, 1437, 1273, 1029, 823, 765, 528 cm^{-1}; HRMS (ESI) calcd. for $C_{29}H_{24}N_2NaO_5$ $(M + Na)^+$ 503.1578, found 503.1567.

Dimethyl 2-((11-(4-(tert-butyl)phenyl)dibenzo[*c*,*h*][1,6]naphthyridin-6-yl)methyl)malonate (30af):

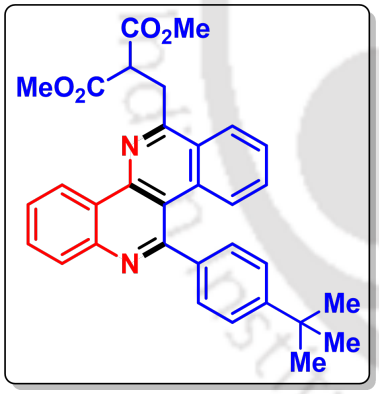

White solid; R_f (Hexane/EtOAc, 3:1) 0.55; mp 189–191 °C. Yield 147 mg, 97%; ^{1}H NMR (500 MHz, $CDCl_3$) δ 9.20 (d, J = 8.5 Hz, 1 H), 8.32 (d, J = 8.0 Hz, 1 H), 8.22 (d, J = 8.5 Hz, 1 H), 7.81 (t, J = 7.5 Hz, 1 H), 7.76 (d, J = 8.5 Hz, 1 H), 7.72 (t, J = 7.5 Hz, 1 H), 7.60 (t, J = 7.5 Hz, 1 H), 7.54 (s, 4 H), 7.40 (t, J = 8.0 Hz, 1 H), 4.82 (t, J = 7.0 Hz, 1 H), 4.21 (d, J = 7.5 Hz, 2 H), 3.86 (s, 6 H), 1.42 (s, 9 H); ^{13}C{^{1}H} NMR (125 MHz, $CDCl_3$) δ 170.4, 160.9, 159.2, 152.0, 145.9, 145.3, 140.9, 132.7, 130.1, 130.0, 129.1, 128.6, 127.6, 127.4, 127.0, 126.6, 126.3, 125.3, 125.2, 124.5, 53.0, 49.2, 35.0, 34.7, 31.6; IR (KBr, neat) 3392, 2917, 1716, 1498, 1310, 1066, 801, 798, 515 cm^{-1}; HRMS (ESI) calcd. for $C_{32}H_{30}N_2NaO_4$ $(M + Na)^+$ 529.2098, found 529.2094.

2-((11-(2-isopropylphenyl)dibenzo[*c*,*h*][1,6]naphthyridin-6-yl)methyl)malonate (30ag):

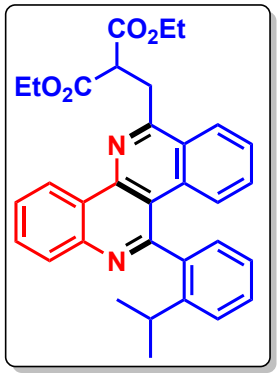

White solid; R_f (Hexane/EtOAc, 3:1) 0.60; mp 207–209 °C. Yield 126 mg, 81%; ^{1}H NMR (500 MHz, $CDCl_3$) δ 9.35 (d, J = 8.0 Hz, 1 H), 8.38 (d, J = 8.0 Hz, 1 H), 8.26 (d, J = 8.0 Hz, 1 H), 7.86–7.83 (m, 1 H), 7.79–7.76 (m, 1 H), 7.64–7.60 (m, 2 H), 7.56 (d, J = 4.5 Hz, 2 H), 7.45–7.42 (m, 1 H), 7.40–7.36 (m, 1 H), 7.29 (d, J = 7.5 Hz, 1 H), 4.84 (t, J = 7.5 Hz, 1 H), 4.37–4.28 (m, 4 H), 4.23 (d, J = 7.0 Hz, 2 H), 2.72–2.67 (m, 1 H), 1.37 (q, J = 7.0 Hz, 6 H), 1.13 (d, J = 7.0 Hz, 3 H), 0.90 (d, J = 7.0 Hz, 3 H); ^{13}C{^{1}H} NMR (125 MHz, $CDCl_3$) δ 170.1, 170.0, 161.2, 159.2, 146.1, 145.8, 145.0, 142.7, 132.7, 130.8, 130.1, 129.3, 129.1, 128.5, 127.5, 127.1, 126.74, 126.73, 125.6, 125.5, 124.9, 115.6, 61.9, 49.5, 34.7, 30.6, 24.5, 23.0, 14.4; IR (KBr, neat) 3343, 2945, 1701, 1567, 1319, 1132, 832, 801, 569 cm^{-1}; HRMS (ESI) calcd. for $C_{33}H_{32}N_2NaO_4$ $(M + Na)^+$ 543.2255, found 543.2226.

Dimethyl 2-((11-(naphthalen-2-yl)dibenzo[*c*,*h*][1,6]naphthyridin-6-yl)methyl)malonate (30ah):

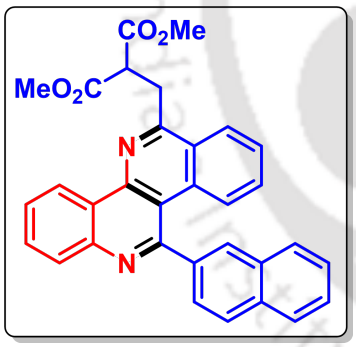

Pale yellow solid; R_f (Hexane/EtOAc, 3:1) 0.50; mp 191–193 °C. Yield 138 mg, 92%; ^{1}H NMR (500 MHz, $CDCl_3$) δ 9.24 (d, J = 8.5 Hz, 1 H), 8.33 (d, J = 8.0 Hz, 1 H), 8.27–8.24 (m, 2 H), 7.94 (q, J = 8.5 Hz, 3 H), 7.84 (t, J = 7.5 Hz, 1 H), 7.76 (t, J = 8.0 Hz, 2 H), 7.62–7.54 (m, 4 H), 7.30 (t, J = 8.0 Hz, 1 H), 4.84 (t, J = 7.0 Hz, 1 H), 4.23 (t, J = 6.5 Hz, 2 H), 3.88 (s, 6 H); ^{13}C{^{1}H} NMR (125 MHz, $CDCl_3$) δ 170.3, 161.1, 145.9, 141.3, 134.0, 133.6, 132.6, 130.2, 129.2, 128.9, 128.8, 128.2, 128.1, 127.6, 127.2, 127.0, 126.8, 126.7, 125.4, 125.3, 124.5, 53.0, 49.2, 34.7; IR (KBr, neat) 3336, 2952, 1732, 1433, 1275, 1152, 814, 762, 535 cm^{-1}; HRMS (ESI) calcd. for $C_{32}H_{24}N_2NaO_4$ $(M + Na)^+$ 523.1629, found 523.1626.

Dimethyl 2-((11-(phenanthren-9-yl)dibenzo[*c*,*h*][1,6]naphthyridin-6-yl)methyl)malonate (30ai):

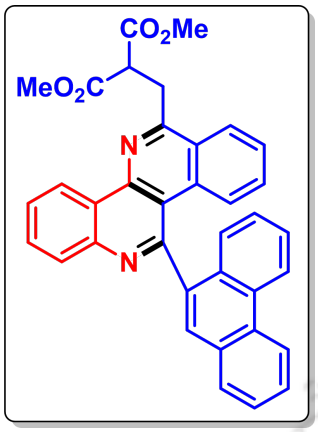

Pale yellow solid; R_f (Hexane/EtOAc, 3:1) 0.45; mp 203–205 °C. Yield 149 mg, 90%; ^{1}H NMR (500 MHz, $CDCl_3$) δ 9.38 (d, J = 8.5 Hz, 1 H), 8.84–8.82 (m, 2 H), 8.31 (dd, J = 18.5, 8.0 Hz, 2 H), 7.92–7.87 (m, 3 H), 7.83 (t, J = 8.0 Hz, 1 H), 7.76 (t, J = 8.0 Hz, 1 H), 7.72 (d, J = 9.0 Hz, 1 H), 7.67–7.63 (m, 2 H), 7.50 (t, J = 7.5 Hz, 1 H), 7.46 (d, J = 8.5 Hz, 1 H), 7.33 (t, J = 7.5 Hz, 1 H), 7.13 (t, J = 8.0 Hz, 1 H), 4.89 (t, J = 7.0 Hz, 1 H), 4.25 (d, J = 7.5 Hz, 2 H), 3.90 (d, J = 10.0 Hz, 6 H); ^{13}C{^{1}H} NMR (125 MHz, $CDCl_3$) δ 170.4, 170.3, 161.4, 158.0, 146.2, 145.2, 140.3, 132.2, 132.1, 131.3, 131.1, 130.8, 130.7, 130.3, 129.4, 129.3, 127.6, 127.5, 127.4, 127.3 (2), 127.2, 126.8, 126.7, 126.6, 125.8, 125.5, 124.8, 123.3, 122.9, 53.1, 49.2, 34.9; IR (KBr, neat) 3266, 2911, 1714, 1400, 1312, 1188, 786, 690, 521 cm^{-1}; HRMS (ESI) calcd. for $C_{36}H_{27}N_2O_4$ $(M + H)^+$ 551.1966, found 551.1967.

Dimethyl 2-((11-([1,1'-biphenyl]-4-yl)dibenzo[*c*,*h*][1,6]naphthyridin-6-yl)methyl)malonate (30aj):

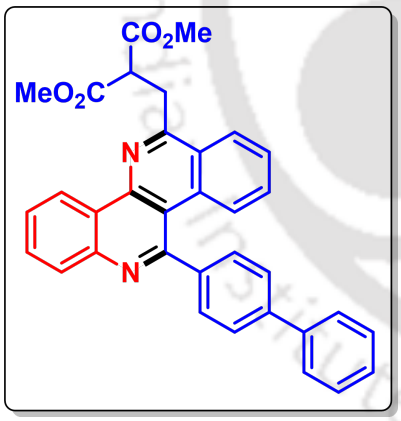

Pale yellow solid; R_f (Hexane/EtOAc, 3:1) 0.50; mp 200–202 °C. Yield 137 mg, 87%; ^{1}H NMR (500 MHz, $CDCl_3$) δ 9.22 (d, J = 8.0 Hz, 1 H), 8.36 (d, J = 8.5 Hz, 1 H), 8.25 (d, J = 8.0 Hz, 1 H), 7.91 (d, J = 8.5 Hz, 1 H), 7.84 (t, J = 7.5 Hz, 1 H), 7.78 (d, J = 8.0 Hz, 2 H), 7.75–7.69 (m, 5 H), 7.64 (t, J = 7.5 Hz, 1 H), 7.50 (t, J = 7.5 Hz, 2 H), 7.45 (d, J = 8.0 Hz, 1 H), 7.40 (t, J = 7.5 Hz, 1 H), 4.84 (t, J = 7.5 Hz, 1 H), 4.23 (d, J = 7.5 Hz, 2 H), 3.87 (d, J = 1.5 Hz, 6 H); ^{13}C{^{1}H} NMR (125 MHz, $CDCl_3$) δ 170.4, 161.1, 158.7, 145.9, 145.4, 142.8, 141.7, 140.8, 132.7, 130.3, 130.2, 129.5, 129.2, 129.1, 128.1, 127.8, 127.6, 127.4, 127.3, 126.7, 125.4 (2), 124.5, 114.6, 53.1, 49.2, 34.8; IR (KBr, neat) 3195, 2880, 1727, 1394, 1310, 1233, 810, 695, 544 cm^{-1}; HRMS (ESI) calcd. for $C_{34}H_{27}N_2O_4$ $(M + H)^+$ 527.1966, found 527.1966.

Dimethyl 2-((11-(thiophen-2-yl)dibenzo[*c*,*h*][1,6]naphthyridin-6-yl)methyl)malonate (30ak):

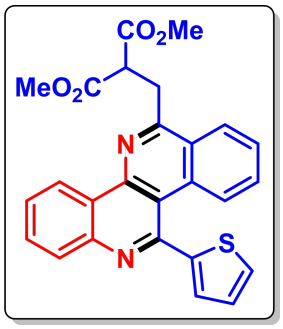

Brown solid; R_f (Hexane/EtOAc, 3:1) 0.55; mp 184–186 °C. Yield 109 mg, 80%; ^{1}H NMR (500 MHz, $CDCl_3$) δ 9.05 (d, J = 8.5 Hz, 1 H), 8.21 (d, J = 8.5 Hz, 1 H), 8.09 (d, J = 8.0 Hz, 1 H), 7.92 (d, J = 8.5 Hz, 1 H), 7.71 (t, J = 7.5 Hz, 1 H), 7.62 (t, J = 7.5 Hz, 1 H), 7.53 (t, J = 7.5 Hz, 1 H), 7.45 (d, J = 5.0 Hz, 1 H), 7.41 (t, J = 8.0 Hz, 1 H), 7.15 (s, 1 H), 7.05 (t, J = 4.5 Hz, 1 H), 4.69 (t, J = 7.0 Hz, 1 H), 4.09 (d, J = 7.5 Hz, 2 H), 3.76 (s, 6 H); ^{13}C{^{1}H} NMR (125 MHz, $CDCl_3$) δ 170.1, 160.9, 151.8, 145.6, 144.9, 132.3, 130.1, 129.9, 128.9, 128.3, 127.7, 127.6, 127.5, 127.2, 126.9, 126.5, 125.2, 125.0, 124.3, 114.9, 52.9, 48.9, 34.5; IR (KBr, neat) 3099, 2924, 1734, 1435, 1275, 1260, 843, 750, 530 cm^{-1}; HRMS (ESI) calcd. for $C_{26}H_{21}N_2O_4S$ $(M + H)^+$ 457.1217, found 457.1208.

Diethyl 2-((3-bromo-11-phenyldibenzo[*c*,*h*][1,6]naphthyridin-6-yl)methyl)malonate (30al):

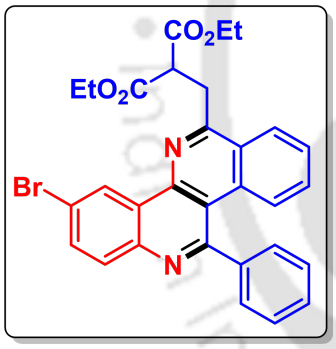

Brown solid; R_f (Hexane/EtOAc, 3:1) 0.50; mp 189–191 °C. Yield 150 mg, 90%; ^{1}H NMR (500 MHz, $CDCl_3$) δ 9.34 (s, 1 H), 8.36 (d, J = 8.0 Hz, 1 H), 8.07 (d, J = 8.5 Hz, 1 H), 7.87 (d, J = 8.5 Hz, 1 H), 7.70 (d, J = 9.0 Hz, 1 H), 7.63 (t, J = 7.5 Hz, 1 H), 7.60–7.58 (m, 2 H), 7.54–7.52 (m, 3 H), 7.42 (t, J = 7.5 Hz, 1 H), 4.76 (t, J = 7.5 Hz, 1 H), 4.42–4.31 (m, 4 H), 4.20 (d, J = 8.0 Hz, 2 H), 1.39 (t, J = 7.0 Hz, 6 H); ^{13}C{^{1}H} NMR (125 MHz, $CDCl_3$) δ 170.1, 161.8, 159.5, 144.4 (2), 143.6, 133.5, 132.4, 130.9, 130.3, 129.4, 129.1, 128.9, 127.9, 127.6, 127.1, 127.0, 126.7, 125.5, 121.4, 115.2, 62.0, 49.4, 34.6, 14.5; IR (KBr, neat) 3396, 2967, 1720, 1367, 1198, 1155, 796, 704, 523 cm^{-1}; HRMS (ESI) calcd. for $C_{30}H_{25}BrN_2NaO_4$ $(M + Na)^+$ 579.0890, found 579.0865.

Diethyl 2-((3-fluoro-11-phenyldibenzo[*c*,*h*][1,6]naphthyridin-6-yl)methyl)malonate (30am):

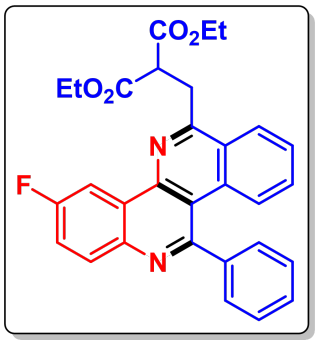

Yellow solid; R_f (Hexane/EtOAc, 3:1) 0.50; mp 180–182 °C. Yield 131 mg, 88%; ^{1}H NMR (400 MHz, $CDCl_3$) δ 8.34 (d, J = 8.4 Hz, 1 H), 8.03 (d, J = 8.0 Hz, 1 H), 7.74–7.69 (m, 2 H), 7.62–7.58 (m, 3 H), 7.53–7.50 (m, 3 H), 7.41–7.35 (m, 2 H), 4.96 (t, J = 7.2 Hz, 1 H), 4.29 (q, J = 7.2 Hz, 4 H), 4.14 (d, J = 7.2 Hz, 2 H), 1.32 (t, J = 7.2 Hz, 6 H); ^{13}C{^{1}H} NMR (100 MHz, $CDCl_3$) δ 170.2, 161.3, 161.1, 159.7 (d, J = 1.7 Hz), 158.7, 147.5, 145.2 (d, J = 8.0 Hz), 143.3, 132.2, 129.8, 129.6 (d, J = 9.5 Hz), 129.4, 129.1, 129.0, 127.7 (d, J = 17.8 Hz), 126.3 (d, J = 1.7 Hz), 125.4 (d, J = 4.3 Hz), 125.1, 115.1 (d, J = 1.5 Hz), 114.9 (d, J = 5.8 Hz), 113.9, 113.6, 61.8, 48.9, 34.3, 14.3; ^{19}F NMR (470 MHz, $CDCl_3/C_6F_6$) δ –110.8 (s, –CF–); IR (KBr, neat) 3421, 2854, 1711, 1493, 1154, 1079, 858, 731, 511 cm^{-1}; HRMS (ESI) calcd. for $C_{30}H_{25}FN_2NaO_4$ $(M + Na)^+$ 519.1691, found 519.1664.

Diethyl 2-((3-nitro-11-phenyldibenzo[*c*,*h*][1,6]naphthyridin-6-yl)methyl)malonate (30an):

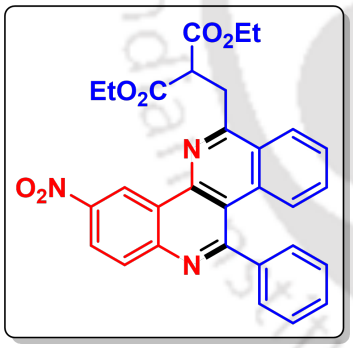

Brown solid; R_f (Hexane/EtOAc, 3:1) 0.40; mp 174–176 °C. Yield 129 mg, 82%; ^{1}H NMR (600 MHz, $CDCl_3$) δ 10.07 (d, J = 3.0 Hz, 1 H), 8.56 (dd, J = 9.0, 2.4 Hz, 1 H), 8.41 (d, J = 7.8 Hz, 1 H), 8.31 (d, J = 9.0 Hz, 1 H), 7.75 (d, J = 8.4 Hz, 1 H), 7.69 (t, J = 7.2 Hz, 1 H), 7.63 (dd, J = 7.2, 1.8 Hz, 2 H), 7.58–7.54 (m, 3 H), 7.47 (t, J = 7.2 Hz, 1 H), 4.82 (t, J = 7.2 Hz, 1 H), 4.44–4.39 (m, 2 H), 4.33–4.28 (m, 2 H), 4.24 (d, J = 7.2 Hz, 2 H), 1.36 (t, J = 7.2 Hz, 6 H); ^{13}C{^{1}H} NMR (150 MHz, $CDCl_3$) δ 170.1, 163.1, 162.8, 148.0, 146.3, 145.8, 143.0, 132.2, 130.8, 130.7, 129.7, 129.5, 128.9, 128.5, 127.6, 127.3, 125.7, 125.0, 123.9, 121.7, 62.1, 49.3, 34.6, 14.4; IR (KBr, neat) 3454, 2925, 1730, 1368, 1175, 1027, 757, 692, 515 cm^{-1}; HRMS (ESI) calcd. for $C_{30}H_{26}N_3O_6$ $(M + H)^+$ 524.1817, found 524.1815.

Dimethyl 2-((11-phenyl-3-(trifluoromethyl)dibenzo[*c*,*h*][1,6]naphthyridin-6-yl)methyl)malonate (30ao):

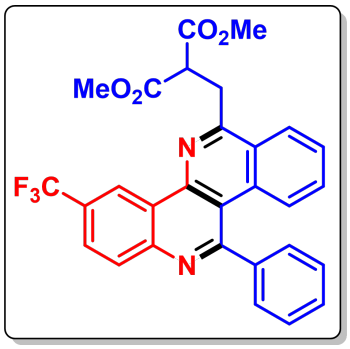

Yellow solid; R_f (Hexane/EtOAc, 3:1) 0.45; mp 201–203 °C. Yield 130 mg, 84%; ^{1}H NMR (400 MHz, $CDCl_3$) δ 9.53 (s, 1 H), 8.33 (dd, J = 16.0, 8.4 Hz, 2 H), 7.99 (d, J = 8.0 Hz, 1 H), 7.70 (d, J = 8.8 Hz, 1 H), 7.65 (t, J = 7.6 Hz, 1 H), 7.61–7.59 (m, 2 H), 7.55–7.53 (m, 3 H), 7.43 (t, J = 8.0 Hz, 1 H), 4.79 (t, J = 7.2 Hz, 1 H), 4.24 (d, J = 7.2 Hz, 2 H), 3.88 (s, 6 H); ^{13}C{^{1}H} NMR (125 MHz, $CDCl_3$) δ 170.5, 162.0, 161.3, 146.8, 145.3, 143.3, 132.3, 131.7, 130.4, 129.3, 129.2 (q, J = 73.9 Hz), 127.5, 126.9, 125.9 (q, J = 3.4 Hz), 125.5, 124.8, 123.6, 122.7 (q, J = 4.2 Hz), 115.4, 53.1, 48.9, 34.8; ^{19}F NMR (470 MHz, $CDCl_3$/C_6F_6) δ –64.7 (s, –CF_3–); IR (KBr, neat) 3392, 2801, 1723, 1517, 1126, 1034, 814, 720, 545 cm^{-1}; HRMS (ESI) calcd. for $C_{29}H_{22}F_3N_2O_4$ $(M + H)^+$ 519.1527, found 519.1545.

Diethyl 2-((3-methyl-11-phenyldibenzo[*c*,*h*][1,6]naphthyridin-6-yl)methyl)malonate (30ap):

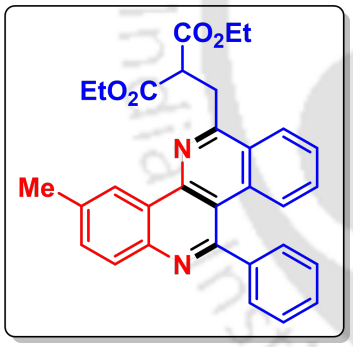

Pale yellow solid; R_f (Hexane/EtOAc, 3:1) 0.50; mp 193–195 °C. Yield 137 mg, 93%; ^{1}H NMR (400 MHz, $CDCl_3$) δ 9.10 (d, J = 8.4 Hz, 1 H), 8.30 (d, J = 8.0 Hz, 1 H), 8.01 (s, 1 H), 7.65 (d, J = 8.8 Hz, 1 H), 7.60–7.57 (m, 3 H), 7.55 (s, 1 H), 7.54–7.51 (m, 3 H), 7.37 (t, J = 8.0 Hz, 1 H), 4.79 (t, J = 7.2 Hz, 1 H), 4.36–4.26 (m, 4 H), 4.18 (d, J = 7.2 Hz, 2 H), 2.62 (s, 3 H), 1.36 (t, J = 7.2 Hz, 6 H); ^{13}C{^{1}H} NMR (150 MHz, $CDCl_3$) δ 170.1, 163.1, 162.8, 148.0, 146.3, 145.8, 143.0, 132.2, 130.8, 130.7, 129.7, 129.5, 128.9, 128.5, 127.6, 127.3, 125.7, 125.0, 123.9, 121.7, 62.1, 49.3, 34.6, 14.4; IR (KBr, neat) 3422, 2965, 1721, 1376, 1200, 1031, 701, 618, 532 cm^{-1}; HRMS (ESI) calcd. for $C_{31}H_{28}N_2NaO_4$ $(M + Na)^+$ 515.1942, found 515.1931.

Diethyl 2-((2,3-dimethoxy-11-phenyldibenzo[*c*,*h*][1,6]naphthyridin-6-yl)methyl)malonate (30aq):

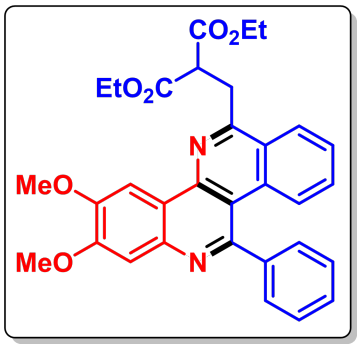

Brown solid; R_f (Hexane/EtOAc, 3:1) 0.50; mp 171–173 °C. Yield 137 mg, 85%; ^{1}H NMR (400 MHz, $CDCl_3$) δ 8.56 (s, 1 H), 8.29 (d, J = 8.0 Hz, 1 H), 7.67 (d, J = 8.8 Hz, 1 H), 7.58–7.55 (m, 4 H), 7.53–7.50 (m, 3 H), 7.38 (t, J = 7.6 Hz, 1 H), 4.68 (t, J = 7.6 Hz, 1 H), 4.27 (s, 3 H), 4.26–4.20 (m, 4 H), 4.16 (d, J = 7.2 Hz, 2 H), 4.05 (s, 3 H), 1.21 (t, J = 7.2 Hz, 6 H); ^{13}C{^{1}H} NMR (100 MHz, $CDCl_3$) δ 169.8, 160.7, 156.8, 152.7, 150.2, 144.5, 144.1, 142.5, 132.4, 130.0, 129.4, 128.9, 128.6, 127.3, 127.0, 126.2, 125.3, 120.3, 113.6, 108.5, 103.5, 61.8, 56.9, 56.4, 49.9, 34.7, 14.3; IR (KBr, neat) 3397, 2913, 1724, 1386, 1183, 1100, 787, 654, 516 cm^{-1}; HRMS (ESI) calcd. for $C_{32}H_{30}N_2NaO_6$ $(M + Na)^+$ 561.1997, found 561.1984.

Dimethyl 2-((11-phenyldibenzo[*c*,*h*][1,6]naphthyridin-6-yl)methyl)malonate (30ar):

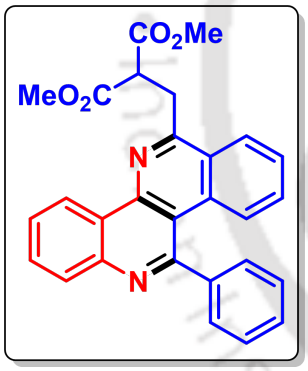

Red solid; R_f (Hexane/EtOAc, 3:1) 0.55; mp 195–197 °C. Yield 123 mg, 91%; ^{1}H NMR (500 MHz, $CDCl_3$) δ 9.19 (d, J = 8.0 Hz, 1 H), 8.29 (d, J = 8.5 Hz, 1 H), 8.23 (d, J = 8.0 Hz, 1 H), 7.81 (d, J = 8.0 Hz, 1 H), 7.73 (t, J = 8.0 Hz, 1 H), 7.66 (d, J = 8.5 Hz, 1 H), 7.60–7.57 (m, 3 H), 7.53–7.51 (m, 3 H), 7.38 (t, J = 8.0 Hz, 1 H), 4.80 (t, J = 7.5 Hz, 1 H), 4.19 (d, J = 7.0 Hz, 2 H), 3.86 (s, 6 H); ^{13}C{^{1}H} NMR (125 MHz, $CDCl_3$) δ 170.3, 161.0, 158.9, 145.7, 145.2, 143.7, 132.5, 130.1 (2), 129.3, 129.0, 128.9 (2), 127.4 (2), 127.1, 126.6, 125.3, 125.2, 124.4, 114.5, 52.9, 49.1, 34.7; IR (KBr, neat) 3406, 2925, 1734, 1435, 1275, 1156, 757, 694, 530 cm^{-1}; HRMS (ESI) calcd. for $C_{28}H_{22}N_2NaO_4$ $(M + Na)^+$ 473.1472, found 473.1468.

Dimethyl 2-((9-chloro-11-phenyldibenzo[*c*,*h*][1,6]naphthyridin-6-yl)methyl)malonate (30as):

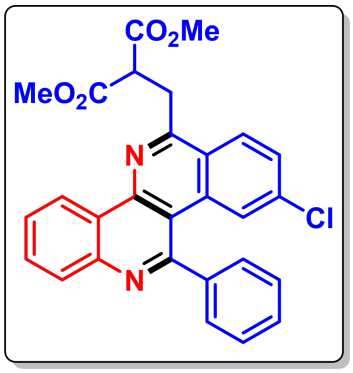

White solid; R_f (Hexane/EtOAc, 3:1) 0.50; mp 200–202 °C. Yield 118 mg, 81%; ^{1}H NMR (400 MHz, $CDCl_3$) δ 9.18 (d, J = 8.0 Hz, 1 H), 8.24 (dd, J = 9.6, 4.0 Hz, 2 H), 7.84 (t, J = 7.6 Hz, 1 H), 7.75 (t, J = 8.0 Hz, 1 H), 7.58–7.54 (m, 7 H), 4.79 (t, J = 7.2 Hz, 1 H), 4.16 (d, J = 7.2 Hz, 2 H), 3.86 (s, 6 H); ^{13}C{^{1}H} NMR (125 MHz, $CDCl_3$) δ 170.2, 160.7, 158.8, 146.0, 145.9, 143.0, 136.9, 133.8, 130.6, 129.6, 129.3, 129.2, 128.8, 128.1, 127.4, 127.2, 126.8, 125.2, 124.9, 124.6, 113.7, 53.1, 49.1, 34.7; IR (KBr, neat) 3453, 2920, 1717, 1395, 1199, 1102, 810, 721, 534 cm^{-1}; HRMS (ESI) calcd. for $C_{28}H_{22}ClN_2O_4$ $(M + H)^+$ 485.1263, found 485.1270.

Diethyl 2-((9-chloro-11-phenyldibenzo[*c*,*h*][1,6]naphthyridin-6-yl)methyl)malonate (30at):

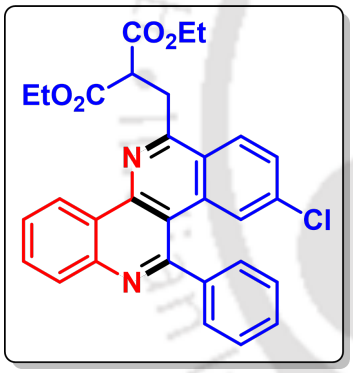

Pale yellow solid; R_f (Hexane/EtOAc, 3:1) 0.50; mp 208–210 °C. Yield 123 mg, 80%; ^{1}H NMR (600 MHz, $CDCl_3$) δ 9.22 (d, J = 7.8 Hz, 1 H), 8.24 (dd, J = 15.0, 9.0 Hz, 2 H), 7.84 (t, J = 7.2 Hz, 1 H), 7.73 (t, J = 7.2 Hz, 1 H), 7.58–7.54 (m, 7 H), 4.77 (t, J = 7.2 Hz, 1 H), 4.35–4.25 (m, 4 H), 4.14 (d, J = 7.2 Hz, 2 H), 1.35 (t, J = 7.2 Hz, 6 H); ^{13}C{^{1}H} NMR (100 MHz, $CDCl_3$) δ 169.9, 160.9, 158.8, 146.0, 145.9, 143.0, 136.8, 133.8, 130.6, 129.6, 129.2 (2), 128.8, 128.1, 127.3, 127.1, 126.9, 125.1, 124.9, 124.8, 113.7, 62.0, 49.4, 34.6, 14.4; IR (KBr, neat) 3400, 2975, 1728, 1401, 1165, 1076, 889, 754, 512 cm^{-1}; HRMS (ESI) calcd. for $C_{30}H_{26}ClN_2O_4$ $(M + H)^+$ 513.1576, found 513.1558.

Dimethyl 2-((9-bromo-11-phenyldibenzo[*c*,*h*][1,6]naphthyridin-6-yl)methyl)malonate (30au):

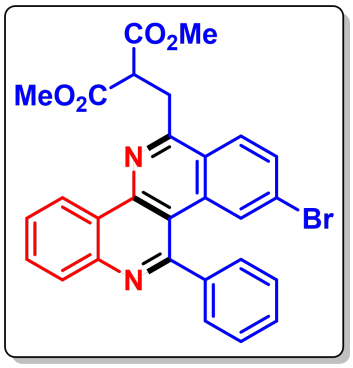

White solid; R_f (Hexane/EtOAc, 3:1) 0.55; mp 215–217 °C. Yield 132 mg, 83%; ^{1}H NMR (500 MHz, $CDCl_3$) δ 9.19 (d, J = 8.0 Hz, 1 H), 8.48 (s, 1 H), 8.25 (d, J = 8.5 Hz, 1 H), 7.85 (t, J = 7.5 Hz, 1 H), 7.76 (t, J = 7.5 Hz, 1 H), 7.60–7.54 (m, 6 H), 7.50 (d, J = 9.0 Hz, 1 H), 4.81 (t, J = 7.5 Hz, 1 H), 4.16 (d, J = 7.5 Hz, 2 H), 3.86 (s, 6 H); ^{13}C{^{1}H} NMR (125 MHz, $CDCl_3$) δ 170.2, 160.2, 158.2, 145.4, 133.5, 131.4, 130.6, 129.6, 129.2, 129.1, 128.9, 128.0, 127.9, 127.5, 125.2, 124.5, 121.9, 114.3, 53.1, 49.1, 34.7; IR (KBr, neat) 3412, 2960, 1722, 1390, 1186, 1099, 845, 720, 537 cm^{-1}; HRMS (ESI) calcd. for $C_{28}H_{22}BrN_2O_4$ $(M + H)^+$ 529.0758, found 529.0776.

Dimethyl 2-((7-fluoro-11-phenyldibenzo[*c*,*h*][1,6]naphthyridin-6-yl)methyl)malonate (30av):

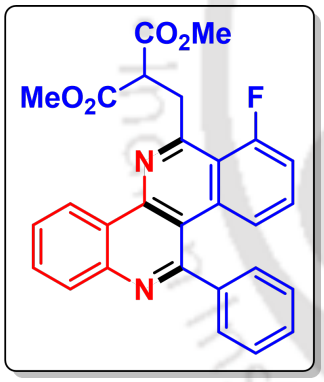

Off white solid; R_f (Hexane/EtOAc, 3:1) 0.50; mp 177–179 °C. Yield 111 mg, 79%; ^{1}H NMR (400 MHz, $CDCl_3$) δ 9.19 (d, J = 8.0 Hz, 1 H), 8.25 (d, J = 8.4 Hz, 1 H), 7.95 (dd, J = 9.2, 2.8 Hz, 1 H), 7.84 (t, J = 7.6 Hz, 1 H), 7.77–7.70 (m, 2 H), 7.62–7.54 (m, 5 H), 7.21–7.16 (m, 1 H), 4.82 (t, J = 7.2 Hz, 1 H), 4.15 (d, J = 7.6 Hz, 2 H), 3.87 (s, 6 H); ^{13}C{^{1}H} NMR (125 MHz, $CDCl_3$) δ 170.2, 162.0, 160.3 (d, J = 4.1 Hz), 160.0, 158.7, 145.8, 145.0, 143.7, 130.3, 130.2 (d, J = 8.0 Hz), 129.6, 129.5, 129.2 (d, J = 15.1 Hz), 128.9, 128.2 (d, J = 7.6 Hz), 127.4, 125.3, 124.4, 119.6 (d, J = 23.4 Hz), 114.4, 109.8 (d, J = 21.5 Hz), 53.1, 49.1, 34.7; ^{19}F NMR (470 MHz, $CDCl_3/C_6F_6$) δ –113.7 (s, –CF–); IR (KBr, neat) 3367, 2911, 1730, 1410, 1177, 1100, 829, 689, 511 cm^{-1}; HRMS (ESI) calcd. for $C_{28}H_{22}FN_2O_4$ $(M + H)^+$ 469.1559, found 469.1566.

Dimethyl 2-((9-(methoxycarbonyl)-11-phenyldibenzo[*c*,*h*][1,6]naphthyridin-6-yl)methyl)malonate (30aw):

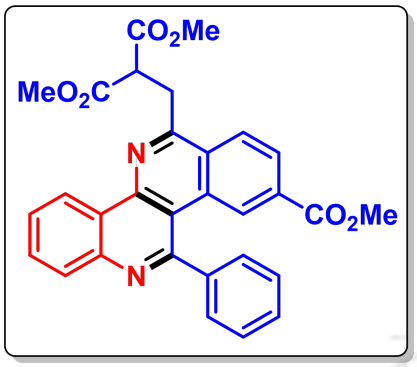

Yellow solid; R_f (Hexane/EtOAc, 3:1) 0.40; mp 208–210 °C. Yield 116 mg, 76%; ^{1}H NMR (500 MHz, $CDCl_3$) δ 9.20 (d, J = 8.5 Hz, 1 H), 9.03 (s, 1 H), 8.25 (d, J = 8.5 Hz, 1 H), 8.00 (d, J = 9.5 Hz, 1 H), 7.86 (t, J = 8.0 Hz, 1 H), 7.77–7.74 (m, 2 H), 7.61–7.59 (m, 2 H), 7.55–7.53 (m, 3 H), 4.83 (t, J = 7.5 Hz, 1 H), 4.28 (d, J = 7.0 Hz, 2 H), 4.00 (s, 3 H), 3.87 (s, 6 H); ^{13}C{^{1}H} NMR (125 MHz, $CDCl_3$) δ 170.2, 166.3, 161.9, 159.1, 146.5, 146.2, 143.3, 135.6, 130.9, 129.8, 129.6, 129.2, 129.0, 128.7, 127.8, 127.6, 127.5, 126.2, 125.1, 124.7, 114.2, 53.1, 52.8, 49.2, 34.8; IR (KBr, neat) 3396, 2944, 1726, 1402, 1170, 1107, 830, 709, 518 cm^{-1}; HRMS (ESI) calcd. for $C_{30}H_{25}N_2O_6$ $(M + H)^+$ 509.1708, found 529.1691.

Dimethyl 2-((8-methyl-11-phenyldibenzo[*c*,*h*][1,6]naphthyridin-6-yl)methyl)malonate (30ax):

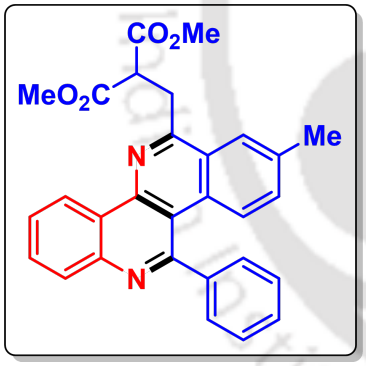

Yellow solid; R_f (Hexane/EtOAc, 3:1) 0.50; mp 199–201 °C. Yield 127 mg, 91%; ^{1}H NMR (500 MHz, $CDCl_3$) δ 9.20 (d, J = 8.0 Hz, 1 H), 8.20 (dd, J = 20.5, 8.0 Hz, 2 H), 7.81 (t, J = 7.5 Hz, 1 H), 7.73 (t, J = 7.5 Hz, 1 H), 7.58–7.53 (m, 5 H), 7.40 (d, J = 8.0 Hz, 1 H), 7.33 (s, 1 H), 4.79 (t, J = 7.5 Hz, 1 H), 4.15 (d, J = 7.0 Hz, 2 H), 3.86 (s, 6 H), 2.17 (s, 3 H); ^{13}C{^{1}H} NMR (125 MHz, $CDCl_3$) δ 170.4, 160.7, 159.2, 145.7, 145.4, 143.9, 140.4, 132.6, 130.0, 129.3, 129.1, 128.9, 128.7, 127.5, 127.0, 125.4, 125.1, 124.8, 124.5, 114.5, 52.9, 49.1, 34.6, 22.34; IR (KBr, neat) 3451, 2865, 1740, 1496, 1143, 1080, 894, 721, 568 cm^{-1}; HRMS (ESI) calcd. for $C_{29}H_{25}N_2O_4$ $(M + H)^+$ 465.1809, found 465.1790.

Diethyl (*S*)-2-((11-phenyl-6*H*-isochromeno[4,3-*c*]quinolin-6-yl)methyl)malonate (32aa):

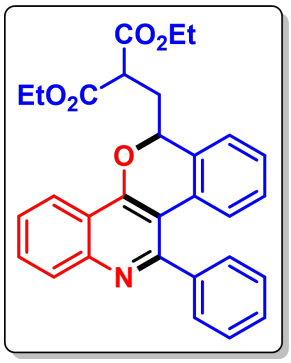

Brown gummy; R_f (Hexane/EtOAc, 7:3) 0.50. Yield 125 mg, 87%; ^{1}H NMR (400 MHz, $CDCl_3$) δ 8.11 (dd, J = 8.4, 1.2 Hz, 1 H), 8.00 (d, J = 8.4 Hz, 1 H), 7.62–7.58 (m, 3 H), 7.42 (ddd, J = 8.4, 6.8, 1.2 Hz, 1 H), 7.36–7.33 (m, 3 H), 7.16–7.09 (m, 2 H), 6.90 (ddd, J = 8.8, 6.8, 2.0 Hz, 1 H), 6.76 (d, J = 7.6 Hz, 1 H), 5.37 (dd, J = 8.4, 6.4 Hz, 1 H), 4.21–4.11 (m, 2 H), 4.07–3.99 (m, 2 H), 3.75 (t, J = 7.2 Hz, 1 H), 2.65–2.62 (m, 2 H), 1.18 (d, J = 7.2 Hz, 3 H), 1.10 (t, J = 7.2 Hz, 3 H); ^{13}C{^{1}H} NMR (125 MHz, $CDCl_3$) δ 169.0, 168.9, 157.8, 156.9, 148.1, 141.5, 132., 130.55, 129.7, 129.3, 129.0, 128.9, 128.3, 128.0, 127.6, 127.2, 126.3, 124.5, 121.8, 119.8, 112.7, 76.6, 62.0, 61.9, 48.7, 32.1, 14.2, 14.1; IR (KBr, neat) 3467, 2960, 1721, 1343, 1179, 1067, 787, 701, 536 cm^{-1}; HRMS (ESI) calcd. for $C_{30}H_{27}NNaO_5$ $(M + Na)^+$ 504.1782, found 504.1754.

Dimethyl (*S*)-2-((11-phenyl-6*H*-isochromeno[4,3-*c*]quinolin-6-yl)methyl)malonate (32ab):

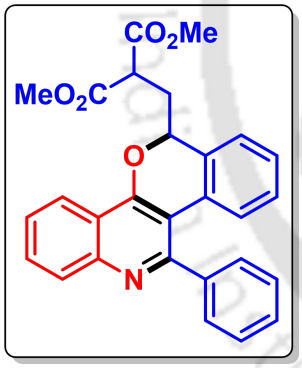

Yellow gummy; R_f (Hexane/EtOAc, 7:3) 0.50. Yield 115 mg, 85%; ^{1}H NMR (400 MHz, $CDCl_3$) δ 8.10 (d, J = 7.6 Hz, 1 H), 8.01 (d, J = 8.4 Hz, 1 H), 7.64–7.60 (m, 3 H), 7.44 (t, J = 8.0 Hz, 1 H), 7.37–7.34 (m, 3 H), 7.17–7.12 (m, 2 H), 6.94–6.90 (m, 1 H), 6.77 (d, J = 7.6 Hz, 1 H), 5.38 (t, J = 7.2 Hz, 1 H), 3.80 (t, J = 7.2 Hz, 1 H), 3.71 (s, 3 H), 3.59 (s, 3 H), 2.66 (t, J = 7.2 Hz, 2 H); ^{13}C{^{1}H} NMR (125 MHz, $CDCl_3$) δ 169.5, 169.4, 157.9, 156.9, 148.1, 141.5, 132.8, 130.6, 129.8, 129.3, 129.1, 128.9, 128.4, 128.1, 127.6, 127.3, 126.4, 124.5, 121.8, 119.8, 112.7, 76.6, 53.1, 53.0, 48.3, 32.2; IR (KBr, neat) 3396, 2918, 1730, 1367, 1150, 1088, 715, 686, 527 cm^{-1}; HRMS (ESI) calcd. for $C_{28}H_{23}NNaO_5$ $(M + Na)^+$ 476.1469, found 476.1442.

Dimethyl (*S*) -2-((2-bromo-11-phenyl-6*H*-isochromeno[4,3-*c*]quinolin-6-yl)methyl)malonate (32ac):

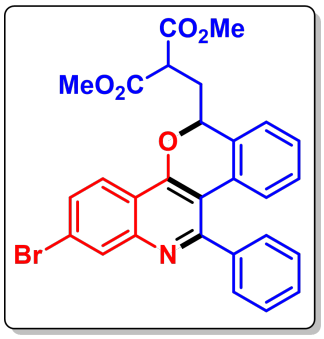

Yellow gummy; R_f (Hexane/EtOAc, 7:3) 0.55. Yield 129 mg, 81%; ^{1}H NMR (500 MHz, $CDCl_3$) δ 8.17 (d, J = 8.5 Hz, 1 H), 8.13 (d, J = 8.5 Hz, 1 H), 7.74 (d, J = 8.0 Hz, 1 H), 7.68–7.66 (m, 2 H), 7.55 (d, J = 7.5 Hz, 1 H), 7.47–7.45 (m, 3 H), 7.40 (s, 1 H), 7.13 (d, J = 8.5 Hz, 1 H), 6.69 (d, J = 8.5 Hz, 1 H), 5.42 (t, J = 7.5 Hz, 1 H), 3.89 (d, J = 7.0 Hz, 1 H), 3.81 (s, 3 H), 3.69 (s, 3 H), 2.71 (t, J = 7.0 Hz, 2 H); ^{13}C{^{1}H} NMR (125 MHz, $CDCl_3$) δ 169.3, 169.2, 157.6, 157.1, 134.8, 131.3, 131.1, 129.7, 129.4, 129.3, 129.1, 128.7, 127.6, 127.4, 126.7, 121.8, 121.7, 119.7, 112.1, 76.0, 53.2, 53.1, 48.2, 32.0; IR (KBr, neat) 3422, 2977, 1734, 1435, 1251, 1105, 886, 655, 529 cm^{-1}; HRMS (ESI) calcd. for $C_{28}H_{23}BrNO_5$ $(M + H)^+$ 532.0755, found 532.0760.

Diethyl (*S*)-2-((4-chloro-11-phenyl-6*H*-isochromeno[4,3-*c*]quinolin-6-yl)methyl)malonate (32ad):

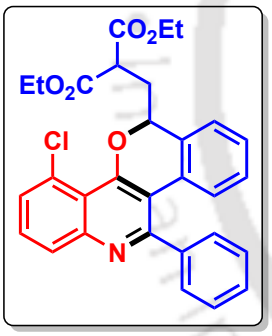

Yellow gummy; R_f (Hexane/EtOAc, 7:3) 0.45. Yield 116 mg, 75%; ^{1}H NMR (500 MHz, $CDCl_3$) δ 7.81 (d, J = 8.5 Hz, 1 H), 7.60–7.58 (m, 2 H), 7.55 (t, J = 8.0 Hz, 1 H), 7.36–7.33 (m, 3 H), 7.20–7.17 (m, 2 H), 7.14 (t, J = 7.5 Hz, 1 H), 6.91 (t, J = 7.5 Hz, 1 H), 6.76 (d, J = 8.0 Hz, 1 H), 5.34 (dd, J = 10.5, 3.5 Hz, 1 H), 4.24–4.19 (m, 2 H), 4.18–4.14 (m, 1 H), 4.08 (q, J = 7.0 Hz, 2 H), 2.73–2.67 (m, 1 H), 2.60–2.55 (m, 1 H), 1.21 (d, J = 7.0 Hz, 3 H), 1.15 (t, J = 7.5 Hz, 3 H); ^{13}C{^{1}H} NMR (125 MHz, $CDCl_3$) δ 169.5, 169.4, 158.4, 158.0, 149.8, 140.8, 136.2, 133.3, 129.9, 129.8, 129.3, 128.9, 128.2, 127.9, 127.8, 127.5, 126.5, 123.9, 116.4, 114.1, 113.0, 76.5, 61.93, 61.92, 48.4, 31.8, 14.3, 14.2; IR (KBr, neat) 3403, 2951, 1713, 1456, 1289, 1135, 867, 632, 519 cm^{-1}; HRMS (ESI) calcd. for $C_{30}H_{27}ClNO_5$ $(M + H)^+$ 516.1573, found 516.1567.

Diethyl (*S*)-2-((2-chloro-11-phenyl-6*H*-isochromeno[4,3-*c*]quinolin-6-yl)methyl)malonate (32ae):

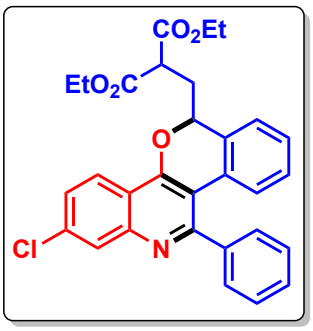

Pale yellow gummy; R_f (Hexane/EtOAc, 7:3) 0.45. Yield 127 mg, 82%; ^{1}H NMR (400 MHz, $CDCl_3$) δ 8.12 (dd, J = 8.4, 1.2 Hz, 1 H), 7.97 (d, J = 8.0 Hz, 1 H), 7.64–7.60 (m, 1 H), 7.59–7.57 (m, 2 H), 7.46–7.42 (m, 1 H), 7.34 (d, J = 8.4 Hz, 2 H), 7.18–7.15 (m, 2 H), 6.99–6.96 (m, 1 H), 6.80 (d, J = 8.0 Hz, 1 H), 5.38 (t, J = 7.2 Hz, 1 H), 4.22–4.11 (m, 2 H), 4.08–4.01 (m 2 H), 3.75 (t, J = 7.6 Hz, 1 H), 2.64 (t, J = 7.6 Hz, 2 H), 1.20 (t, J = 7.2 Hz, 3 H), 1.12 (t, J = 7.2 Hz, 3 H); ^{13}C{^{1}H} NMR (125 MHz, $CDCl_3$) δ 169.1, 169.0, 157.2, 156.5, 148.2, 140.0, 135.1, 133.0, 131.2, 130.7, 129.3, 129.1, 128.2, 128.1, 127.8, 127.1, 126.5, 124.7, 121.9, 119.9, 112.6, 76.7, 62.04, 62.03, 48.7, 32.1, 14.3, 14.2; IR (KBr, neat) 3319, 2901, 1745, 1411, 1307, 1173, 899, 656, 548 cm^{-1}; HRMS (ESI) calcd. for $C_{30}H_{27}ClNO_5$ $(M + H)^+$ 516.1573, found 516.1553.

Diethyl (*S*)-2-((11-phenyl-2-(trifluoromethyl)-6*H*-isochromeno[4,3-*c*]quinolin-6-yl)methyl)malonate (32af):

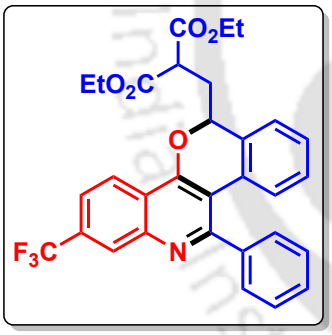

Brown gummy; R_f (Hexane/EtOAc, 7:3) 0.40. Yield 120 mg, 73%; ^{1}H NMR (400 MHz, $CDCl_3$) δ 8.32 (s, 1 H), 8.23 (d, J = 8.8 Hz, 1 H), 7.65–7.60 (m, 3 H), 7.41–7.37 (m, 3 H), 7.19–7.18 (m, 2 H), 6.98–6.93 (m, 1 H), 6.82 (d, J = 8.0 Hz, 1 H), 5.43 (t, J = 7.2 Hz, 1 H), 4.24–4.13 (m, 2 H), 4.09–4.03 (m, 2 H), 3.73 (t, J = 7.2 Hz, 1 H), 2.65 (t, J = 7.6 Hz, 2 H), 1.23 (d, J = 7.2 Hz, 3 H), 1.14 (t, J = 7.2 Hz, 3 H); ^{13}C{^{1}H} NMR (125 MHz, $CDCl_3$) δ 169.0, 168.9, 159.4, 156.7, 147.2, 141.1, 133.1, 132.2 (q, J = 32.4 Hz), 129.7, 129.5, 129.0, 128.30, 128.28, 127.9, 127.2 (q, J = 4.2 Hz), 125.3, 124.7, 123.2, 123.1, 121.9 (q, J = 3.4 Hz), 121.6, 120.9, 114.3, 62.14, 62.11, 48.7, 32.2, 14.3, 14.2; ^{19}F NMR (470 MHz, $CDCl_3/C_6F_6$) δ –65.9 (s, –CF_3–); IR (KBr, neat) 3400, 2889, 1712, 1454, 1369, 1171, 941, 689, 515 cm^{-1}; HRMS (ESI) calcd. for $C_{31}H_{27}F_3NO_5$ $(M + H)^+$ 550.1836, found 550.1817.

Dimethyl (*S*)-2-((3-methyl-11-phenyl-6*H*-isochromeno[4,3-*c*]quinolin-6-yl)methyl)malonate (32ag):

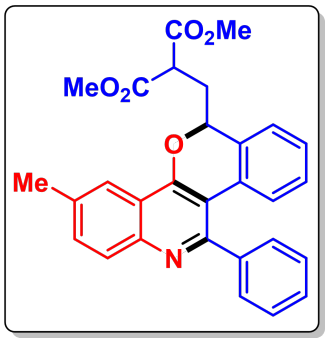

Brown gummy; R_f (Hexane/EtOAc, 7:3) 0.50. Yield 126 mg, 90%; ^{1}H NMR (500 MHz, $CDCl_3$) δ 8.19 (d, J = 8.0 Hz, 1 H), 8.09 (d, J = 8.5 Hz, 1 H), 7.71–7.68 (m, 3 H), 7.52 (t, J = 7.5 Hz, 1 H), 7.46–7.44 (m, 3 H), 7.11 (d, J = 6.5 Hz, 1 H), 7.01 (d, J = 7.5 Hz, 1 H), 6.59 (s, 1 H), 5.43 (t, J = 7.5 Hz, 1 H), 3.89 (d, J = 7.0 Hz, 1 H), 3.79 (s, 3 H), 3.68 (s, 3 H), 2.72 (t, J = 6.5 Hz, 2 H), 2.00 (s, 3 H); ^{13}C{^{1}H} NMR (125 MHz, $CDCl_3$) δ 169.5, 169.4, 157.9, 156.9, 148.0, 141.5, 137.5, 130.4, 130.0, 129.7, 129.3, 128.9, 128.8, 128.2, 128.0 (2), 126.2, 124.2, 121.7, 119.9, 112.7, 76.4, 53.0, 52.9, 48.3, 32.3, 21.4; IR (KBr, neat) 3402, 2917, 1714, 1488, 1293, 1110, 847, 651, 511 cm^{-1}; HRMS (ESI) calcd. for $C_{29}H_{25}NNaO_5$ $(M + Na)^+$ 490.1625, found 490.1612.

Dimethyl (*S*)-2-((11-(4-(tert-butyl)phenyl)-6*H*-isochromeno[4,3-*c*]quinolin-6-yl)methyl)malonate (32ah):

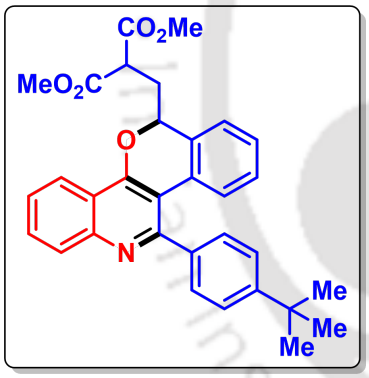

Brown gummy; R_f (Hexane/EtOAc, 7:3) 0.55. Yield 145 mg, 95%; ^{1}H NMR (500 MHz, $CDCl_3$) δ 8.09 (d, J = 7.0 Hz, 1 H), 8.00 (d, J = 8.0 Hz, 1 H), 7.60 (t, J = 7.5 Hz, 1 H), 7.54 (d, J = 7.0 Hz, 2 H), 7.42 (t, J = 8.0 Hz, 1 H), 7.37 (d, J = 7.5 Hz, 2 H), 7.17–7.11 (m, 2 H), 6.93 (t, J = 8.0 Hz, 1 H), 6.85 (d, J = 8.0 Hz, 1 H), 5.37 (t, J = 6.5 Hz, 1 H), 3.80 (t, J = 8.5 Hz, 1 H), 3.70 (s, 3 H), 3.59 (s, 3 H), 2.66 (t, J = 8.5 Hz, 2 H), 1.28 (s, 9 H); ^{13}C{^{1}H} NMR (125 MHz, $CDCl_3$) δ 169.5, 169.4, 157.9, 156.9, 152.2, 148.1, 138.6, 132.8, 130.5, 129.4, 129.3, 128.5, 128.1, 127.6, 127.3, 126.2, 125.9, 124.4, 121.7, 119.8, 112.7, 76.5, 53.1, 53.0, 48.3, 34.9, 32.2, 31.5; IR (KBr, neat) 3416, 2977, 1729, 1456, 1211, 1095, 836, 648, 533 cm^{-1}; HRMS (ESI) calcd. for $C_{32}H_{31}KNO_5$ $(M + K)^+$ 548.1834, found 548.1812.

Dimethyl (*S*)-2-((9-chloro-11-phenyl-6*H*-isochromeno[4,3-*c*]quinolin-6-yl)methyl)malonate (32ai):

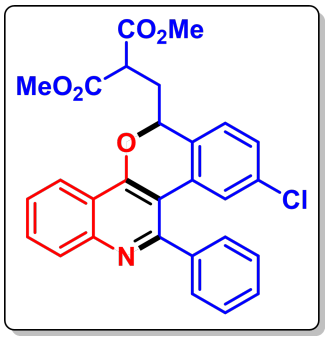

Brown gummy; R_f (Hexane/EtOAc, 7:3) 0.50. Yield 118 mg, 81%; ^{1}H NMR (400 MHz, $CDCl_3$) δ 8.18 (d, J = 8.4 Hz, 1 H), 8.13 (d, J = 8.4 Hz, 1 H), 7.74 (t, J = 7.2 Hz, 1 H), 7.68–7.66 (m, 2 H), 7.55 (t, J = 7.6 Hz, 1 H), 7.52–7.48 (m, 3 H), 7.21–7.16 (m, 2 H), 6.75 (s, 1 H), 5.45 (t, J = 7.2 Hz, 1 H), 3.87 (t, J = 6.8 Hz, 1 H), 3.80 (s, 3 H), 3.69 (s, 3 H), 2.71 (t, J = 7.2 Hz, 2 H); ^{13}C{^{1}H} NMR (150 MHz, $CDCl_3$) δ 169.4, 169.2, 157.7, 157.4, 148.2, 140.6, 134.2, 131.8, 131.1, 131.0, 130.1, 129.7, 129.5, 129.3, 129.1, 127.6, 127.2, 126.6, 125.8, 121.8, 119.7, 111.7, 76.2, 53.2, 53.1, 48.2, 32.2; IR (KBr, neat) 3417, 2954, 1709, 1435, 1220, 1025, 885, 766, 529 cm^{-1}; HRMS (ESI) calcd. for $C_{28}H_{22}ClNNaO_5$ $(M + Na)^+$ 510.1079, found 510.1054.

Dimethyl (*S*)-2-((8-methyl-11-phenyl-6*H*-isochromeno[4,3-*c*]quinolin-6-yl)methyl)malonate (rotamer ratio = 1:1, 32aj):

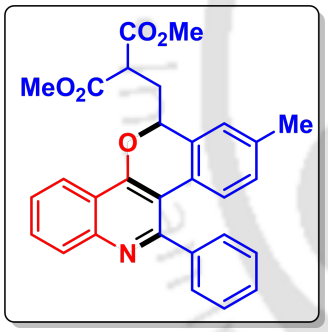

Brown gummy; R_f (Hexane/EtOAc, 7:3) 0.50. Yield 123 mg, 88%; ^{1}H NMR (400 MHz, $CDCl_3$) δ 8.23 (d, J = 8.4 Hz, 1 H), 8.10 (t, J = 7.6 Hz, 1 H), 7.72 (t, J = 7.2 Hz, 1 H), 7.59–7.52 (m, 2 H), 7.39–7.33 (m, 2 H), 7.23–7.18 (m, 3 H), 7.00–6.95 (m, 1 H), 6.75 (t, J = 8.8 Hz, 1 H), 5.50 (dd, J = 9.6 and 4.8 Hz, 1 H, rotamer 1), 5.43 (dd, J = 8.0 and 5.6 Hz, 1 H, rotamer 2), 3.91 (t, J = 7.6 Hz, 1 H), 3.80 (s, 3 H), 3.69 (s, 3 H, rotamer 1), 3.63 (s, 3 H, rotamer 2), 2.73–2.66 (m, 2 H, rotamer 1), 2.64–2.53 (m, 2 H, rotamer 2), 2.25 (s, 3 H, rotamer 1), 2.05 (s, 3 H, rotamer 2); ^{13}C{^{1}H} NMR (125 MHz, $CDCl_3$) δ 169.5, 169.4, 169.3, 169.2, 157.9, 157.8, 156.6, 155.9, 148.1, 147.9, 141.5, 141.3, 136.0, 135.5, 132.9, 132.8, 131.2, 130.9, 130.5, 129.7, 129.3, 129.2, 128.9, 128.8, 128.5, 128.4, 128.2, 127.9, 127.8, 126.9, 126.6, 126.4, 125.8, 125.1, 124.8, 124.4, 121.8, 121.7, 120.1, 119.9, 76.6, 76.3, 53.1, 53.0, 52.9, 48.2, 32.9, 32.5, 20.1, 19.8; IR (KBr, neat) 3396, 2910, 1726, 1456, 1289, 1125, 889, 628, 514 cm^{-1}; HRMS (ESI) calcd. for $C_{29}H_{25}NNaO_5$ $(M + Na)^+$ 490.1625, found 490.1613.

Dimethyl (*S*)-2-((11-([1,1'-biphenyl]-4-yl)-6*H*-isochromeno[4,3-*c*]quinolin-6-yl)methyl)malonate (32ak):

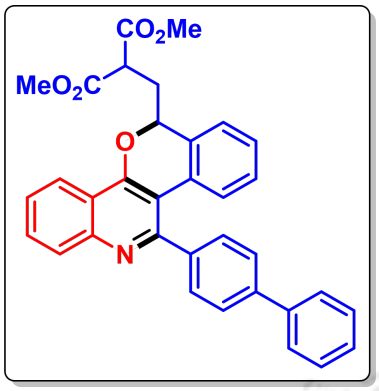

Brown gummy; R_f (Hexane/EtOAc, 7:3) 0.45. Yield 132 mg, 83%; ^{1}H NMR (500 MHz, $CDCl_3$) δ 8.24 (d, J = 8.5 Hz, 1 H), 8.15 (d, J = 8.5 Hz, 1 H), 7.84 (d, J = 8.0 Hz, 2 H), 7.77–7.71 (m, 5 H), 7.57 (t, J = 8.0 Hz, 1 H), 7.51 (t, J = 8.0 Hz, 2 H), 7.41 (t, J = 7.5 Hz, 1 H), 7.31–7.26 (m, 2 H), 7.10–7.04 (m, 2 H), 5.52 (t, J = 7.5 Hz, 1 H), 3.95 (t, J = 7.0 Hz, 1 H), 3.84 (s, 3 H), 3.73 (s, 3 H), 2.81 (t, J = 7.0 Hz, 2 H); ^{13}C{^{1}H} NMR (125 MHz, $CDCl_3$) δ 169.5, 169.4, 157.4, 157.0, 148.2, 141.7, 140.8, 140.4, 132.8, 130.6, 130.3, 129.4, 129.0, 128.4, 128.2, 127.8, 127.7, 127.6, 127.3, 126.4, 124.5, 121.8, 119.8, 112.7, 76.6, 53.1, 53.0, 48.3, 32.2; IR (KBr, neat) 3421, 2980, 1746, 1410, 1223, 1109, 836, 789, 560 cm^{-1}; HRMS (ESI) calcd. for $C_{34}H_{27}NNaO_5$ $(M + Na)^+$ 552.1782, found 552.1759.

Dimethyl (*S*)-2-((11-(thiophen-2-yl)-6*H*-isochromeno[4,3-*c*]quinolin-6-yl)methyl)malonate (32al):

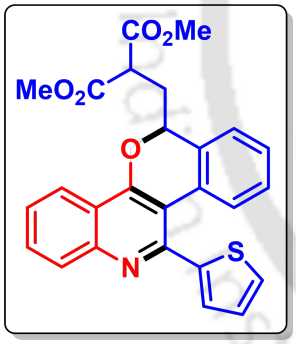

Brown gummy; R_f (Hexane/EtOAc, 7:3) 0.50. Yield 109 mg, 79%; ^{1}H NMR (500 MHz, $CDCl_3$) δ 8.13 (d, J = 8.5 Hz, 1 H), 8.02 (d, J = 8.5 Hz, 1 H), 7.68 (t, J = 7.5 Hz, 1 H), 7.51–7.46 (m, 2 H), 7.37–7.35 (m, 2 H), 7.29–7.26 (m, 2 H), 7.16–7.12 (m, 1 H), 7.06–7.03 (m, 1 H), 5.42 (t, J = 6.5 Hz, 1 H), 3.89 (t, J = 6.5 Hz, 1 H), 3.78 (s, 3 H), 3.68 (s, 3 H), 2.79–2.72 (m, 2 H); ^{13}C{^{1}H} NMR (125 MHz, $CDCl_3$) δ 169.5, 169.4, 156.9, 150.9, 148.2, 144.1, 132.9, 130.7, 129.3, 129.2, 128.4, 128.1 (2), 127.9, 127.7, 126.7, 126.4, 124.5, 121.7, 119.7, 112.8, 76.6, 53.1 (2), 48.4, 31.9; IR (KBr, neat) 3534, 2953, 1732, 1433, 1219, 1098, 758, 704, 518 cm^{-1}; HRMS (ESI) calcd. for $C_{26}H_{21}NNaO_5S$ $(M + Na)^+$ 482.1033, found 482.1005.

(*R*)-5-(3-ethoxy-2-(ethoxycarbonyl)-3-oxopropyl)-11-phenyl-11*H*-indeno[1,2-*c*]isoquinolin-6-ium (33):

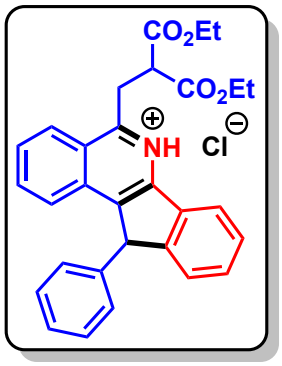

White Solid; R_f (Hexane/EtOAc, 4:1) 0.50; mp 143–145 °C. Yield 125 mg, 83%; ^{1}H NMR (500 MHz, $CDCl_3$) δ 8.27–8.25 (m, 1 H), 8.07 (d, J = 7.5 Hz, 1 H), 7.63–7.60 (m, 1 H), 7.52–7.51 (m, 2 H), 7.45 (t, J = 7.0 Hz, 1 H), 7.35–7.31 (m, 2 H), 7.29–7.24 (m, 4 H), 7.13 (d, J = 7.5 Hz, 2 H), 5.26 (s, 1 H), 4.68 (t, J = 7.5 Hz, 1 H), 4.37–4.26 (m, 4 H), 4.12–4.06 (m, 2 H), 1.34 (t, J = 7.5 Hz, 6 H); ^{13}C{^{1}H} NMR (125 MHz, $CDCl_3$) δ 170.3, 170.2, 158.3, 148.9, 141.2, 140.9, 133.5, 133.1, 130.4, 129.2, 128.3, 128.1, 127.7, 127.2, 126.5, 126.3, 126.0, 124.9, 124.4, 120.5, 61.73, 61.72, 52.1, 50.1, 33.7, 14.4; IR (KBr, neat) 3060, 2980, 1727, 1560, 1366, 1245, 1148, 1032, 754, 700 cm^{-1}; HRMS (ESI) calcd. for $C_{30}H_{28}NO_4$ $(M - Cl)^+$ 466.2013, found 466.2009.

5.10 Representative Spectra

^{1}H spectrum of compound **30aa** (500 MHz, $CDCl_3$)

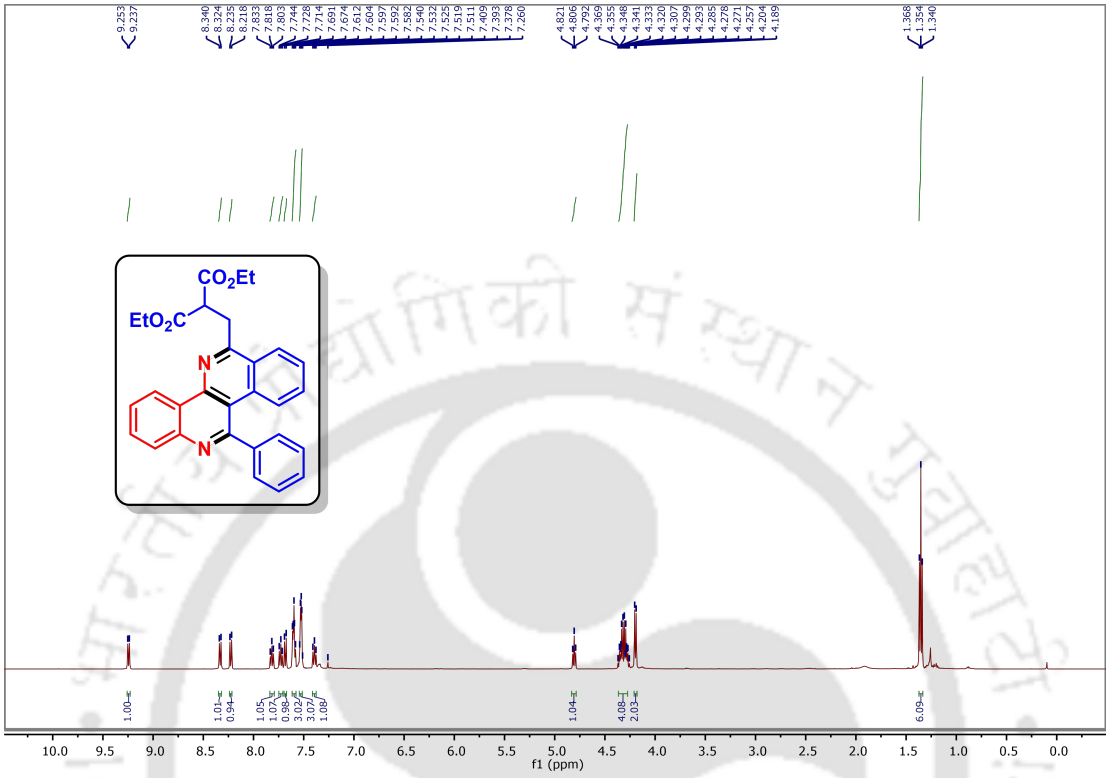

^{13}C{^{1}H} spectrum of compound **30aa** (125 MHz, $CDCl_3$)

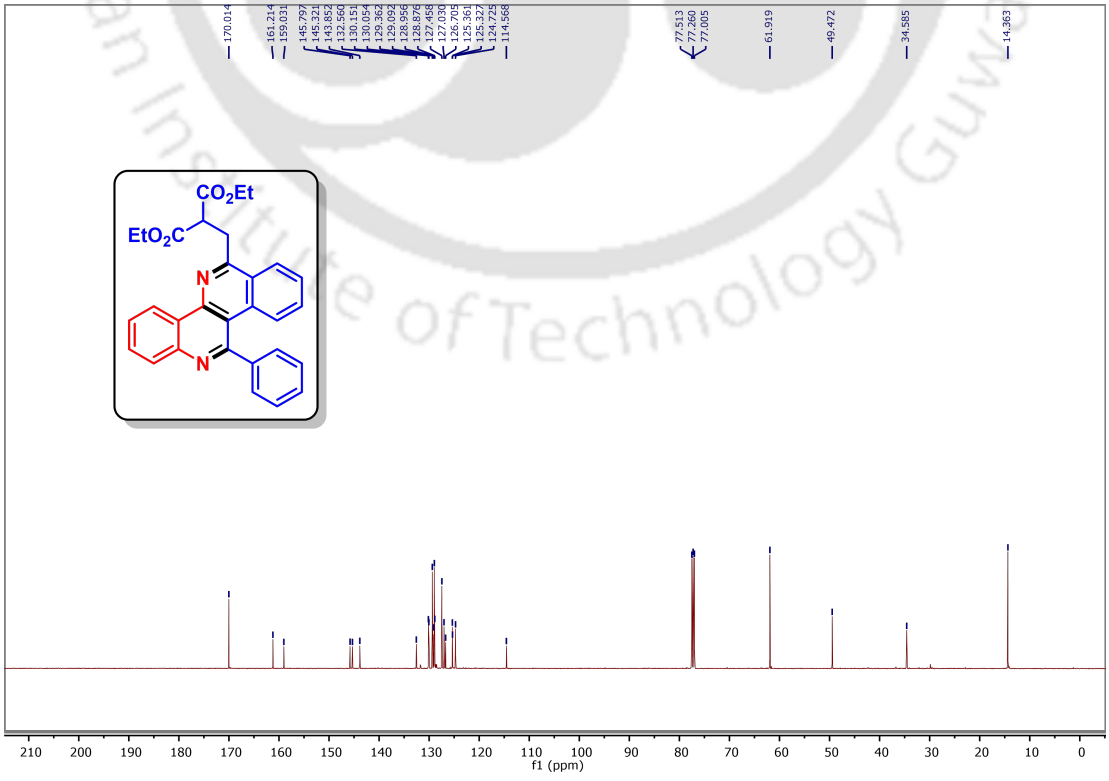

^{1}H NMR spectrum of compound **30ai** (500 MHz, $CDCl_3$)

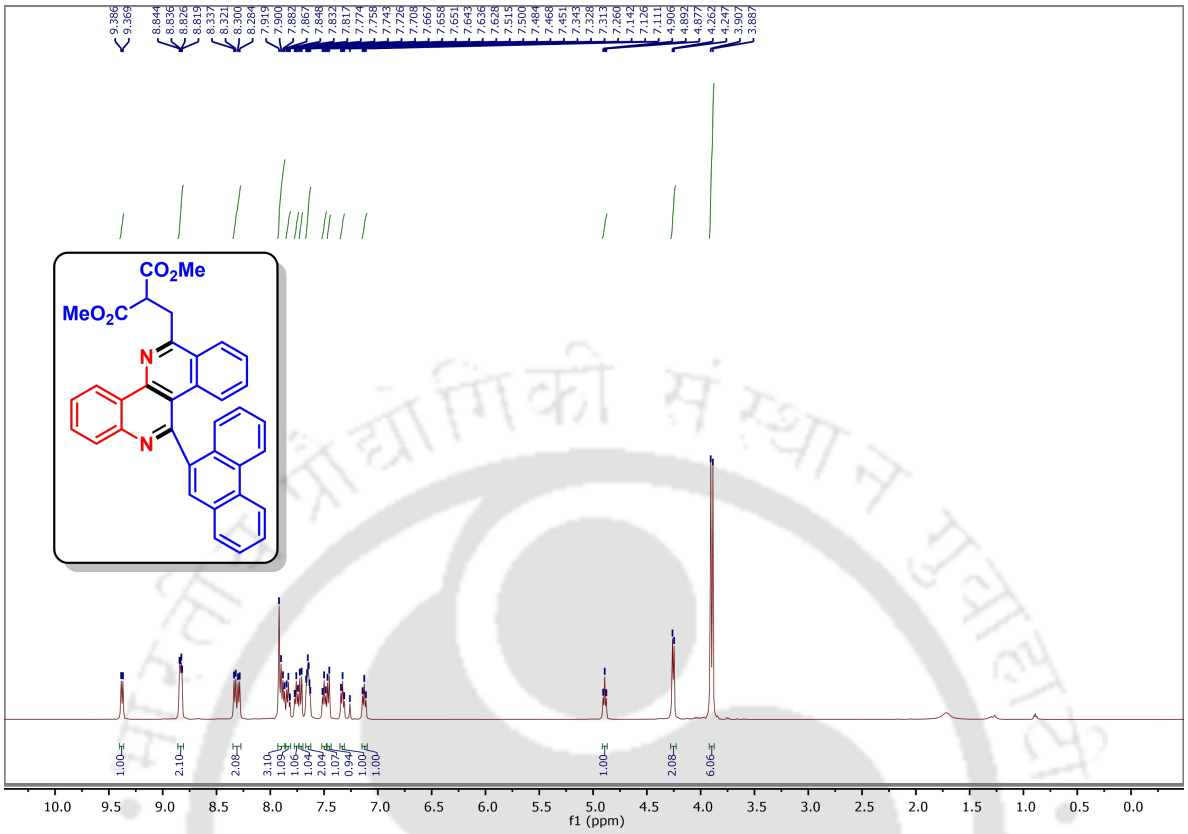

^{13}C{^{1}H} NMR spectrum of compound **30ai** (125 MHz, $CDCl_3$)

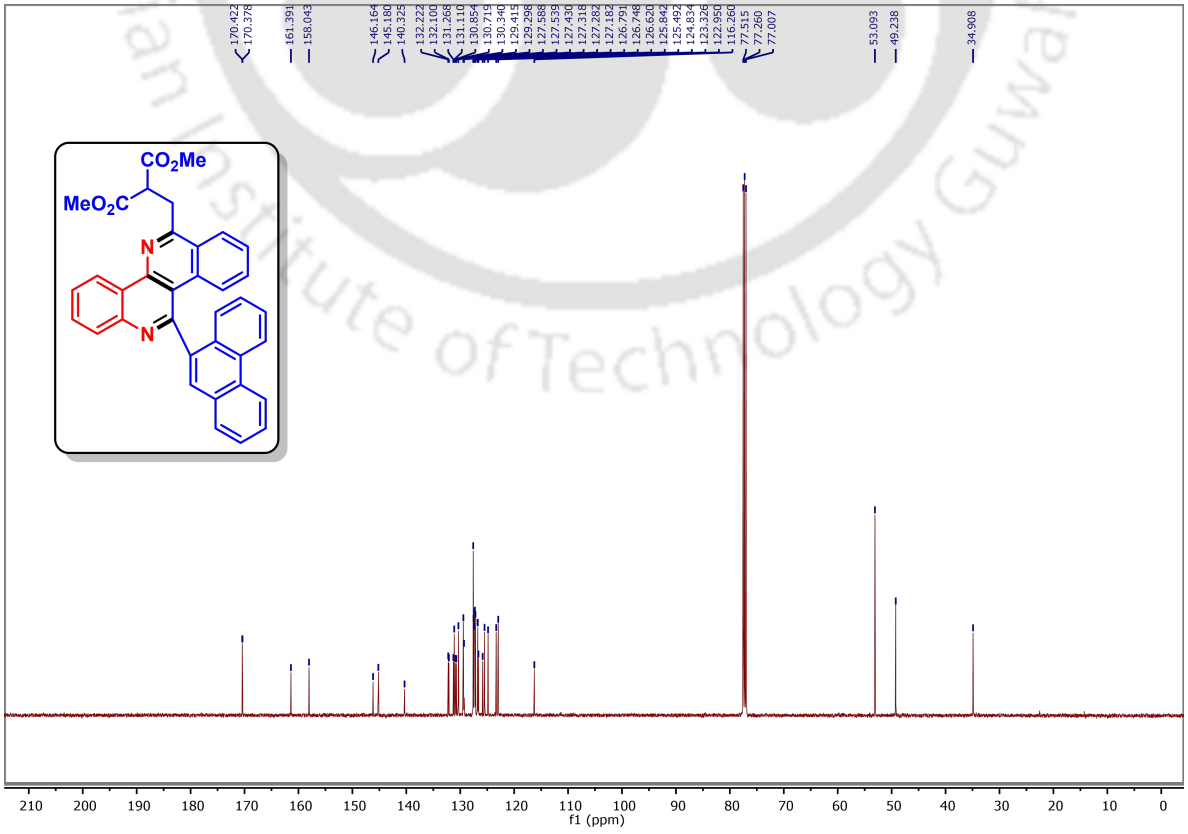

^{1}H NMR spectrum of compound **30aw** (500 MHz, $CDCl_3$)

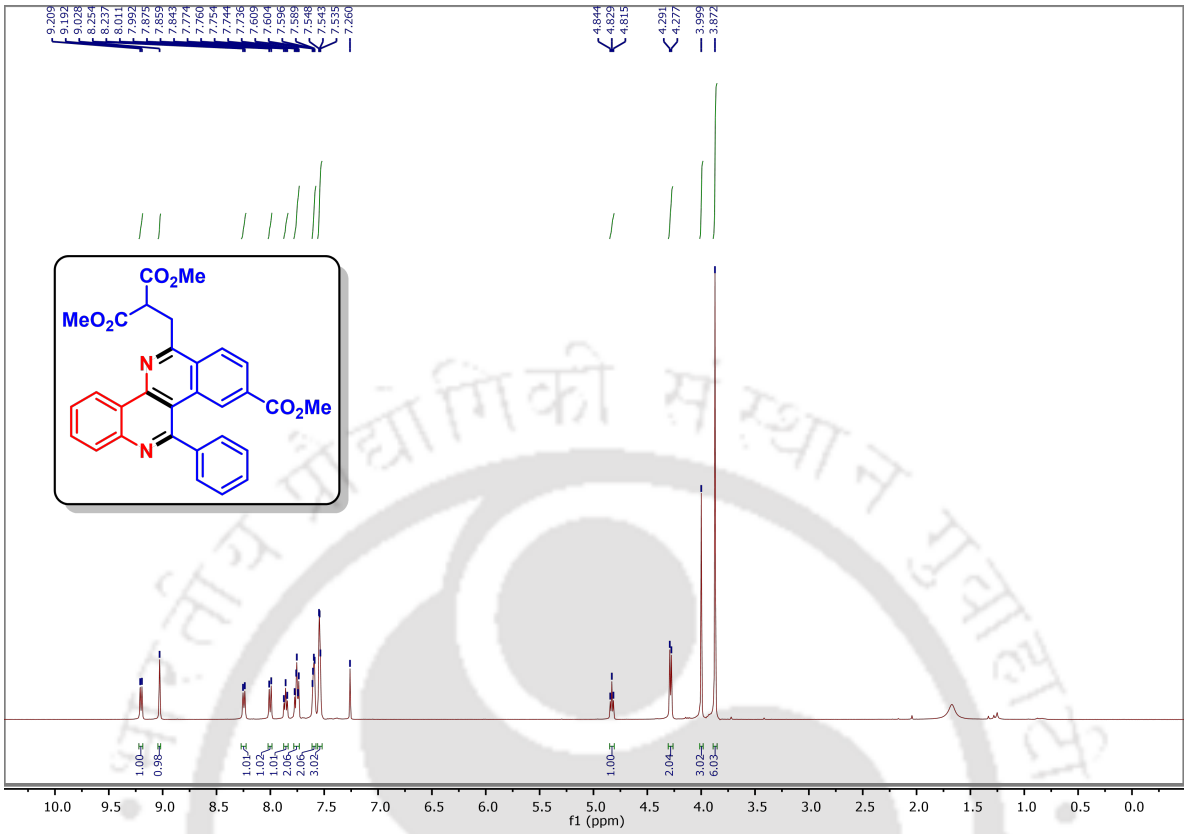

^{13}C{^{1}H} NMR spectrum of compound **30aw** (125 MHz, $CDCl_3$)

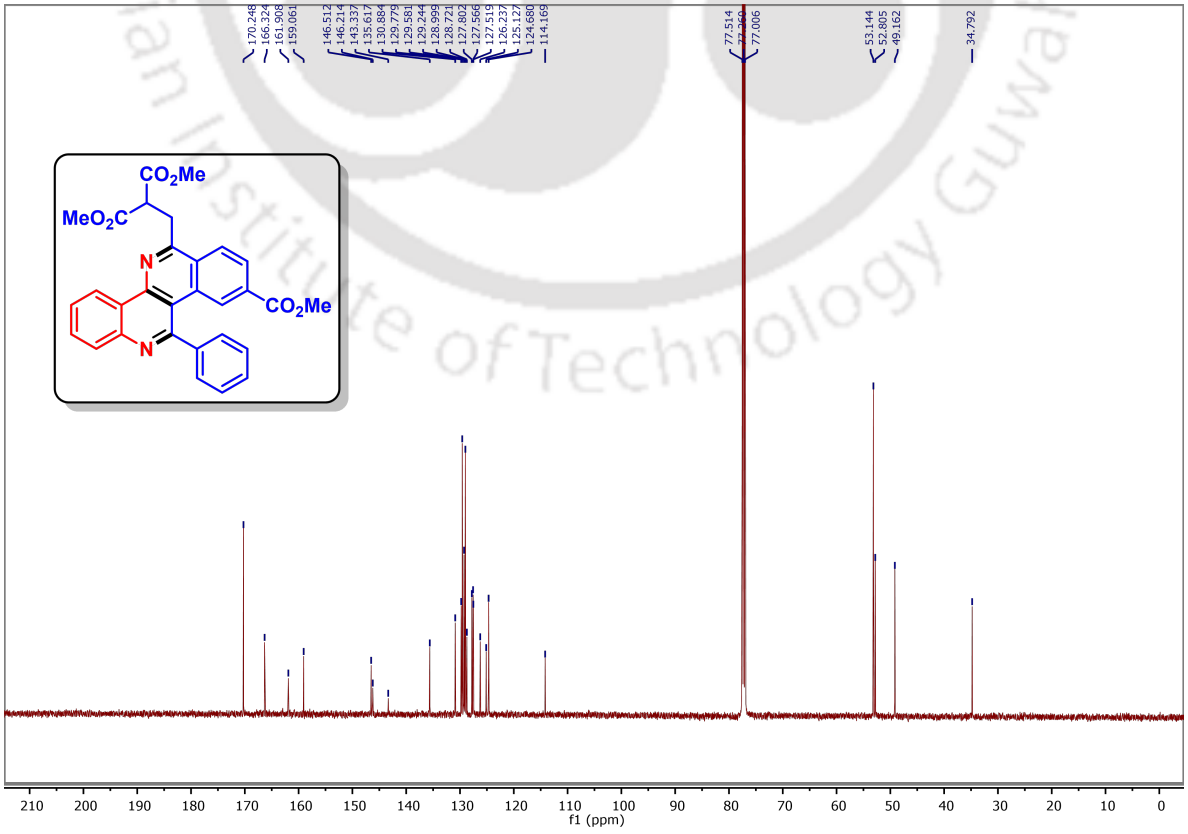

^{1}H NMR spectrum of compound **32aa** (400 MHz, $CDCl_3$)

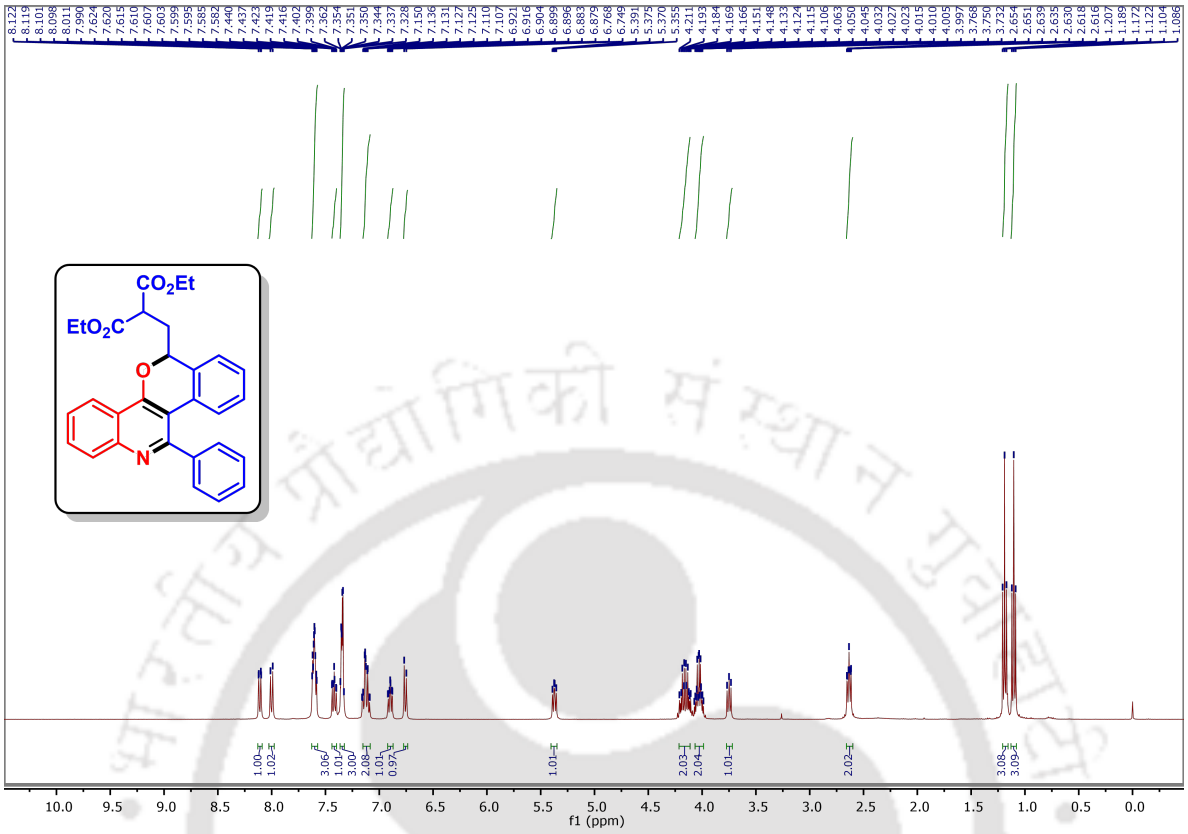

^{13}C{^{1}H} NMR spectrum of compound **32aa** (125 MHz, $CDCl_3$)

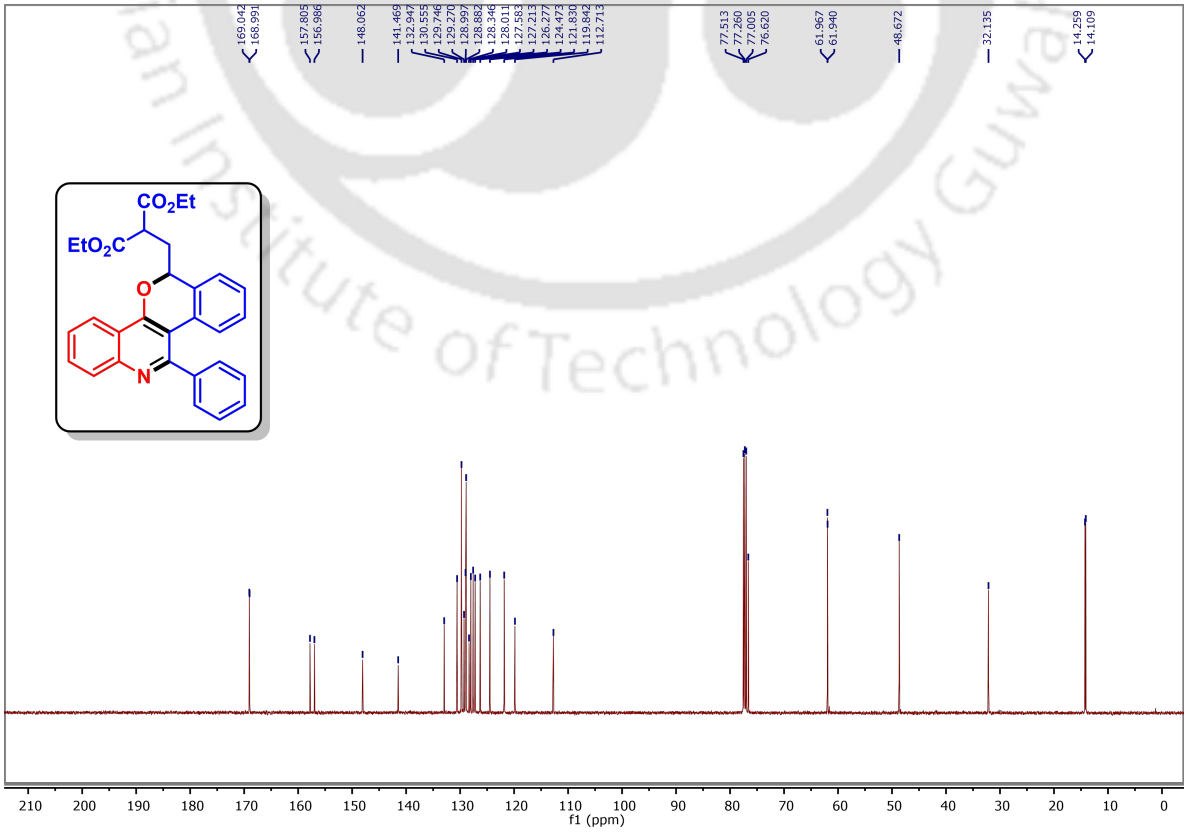

^{1}H NMR spectrum of compound **32ag** (500 MHz, $CDCl_3$)

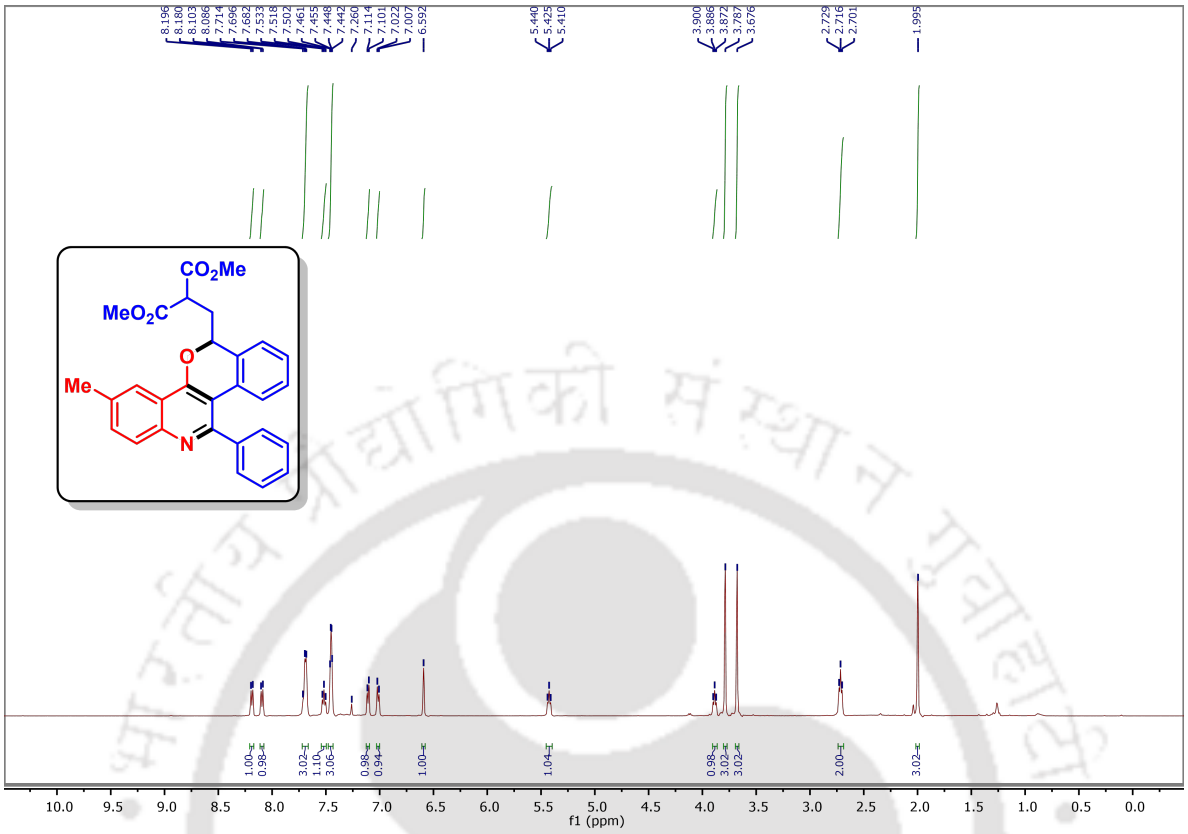

^{13}C{^{1}H} NMR spectrum of compound **32ag** (125 MHz, $CDCl_3$)

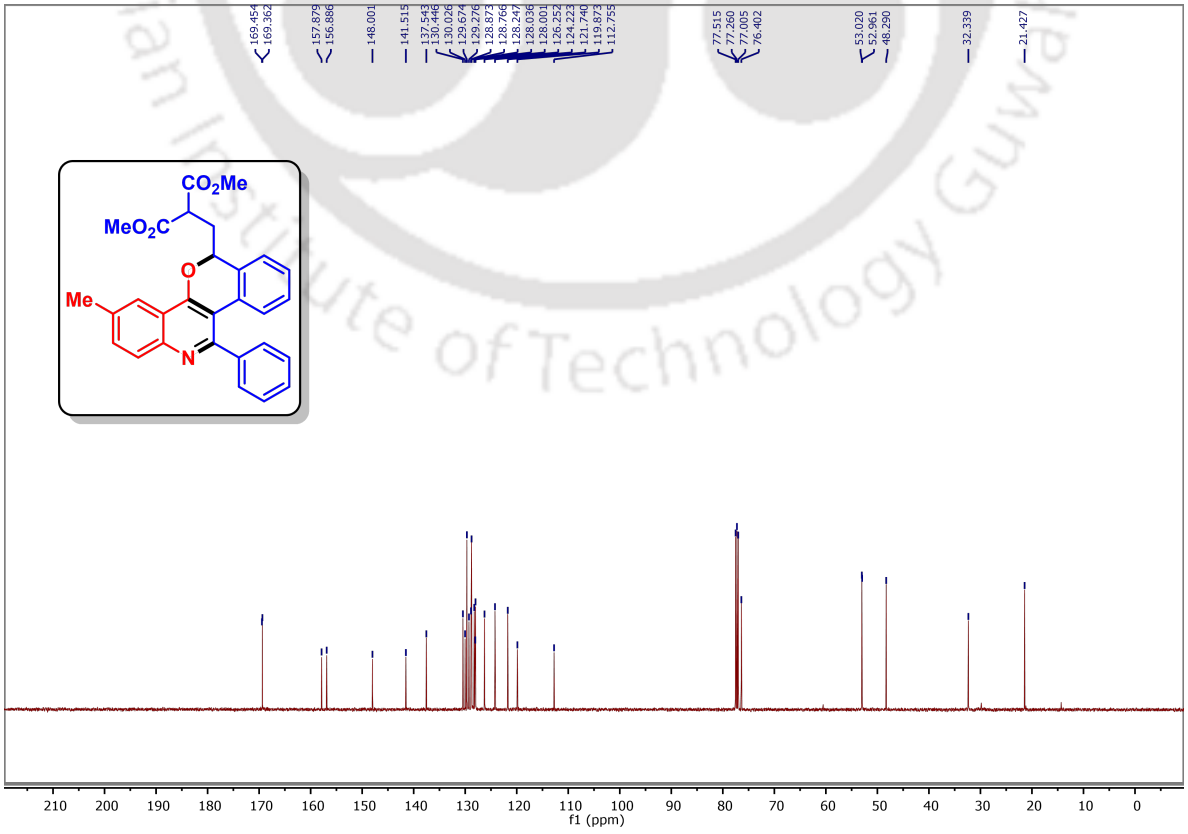

^{1}H NMR spectrum of compound **32al** (500 MHz, $CDCl_3$)

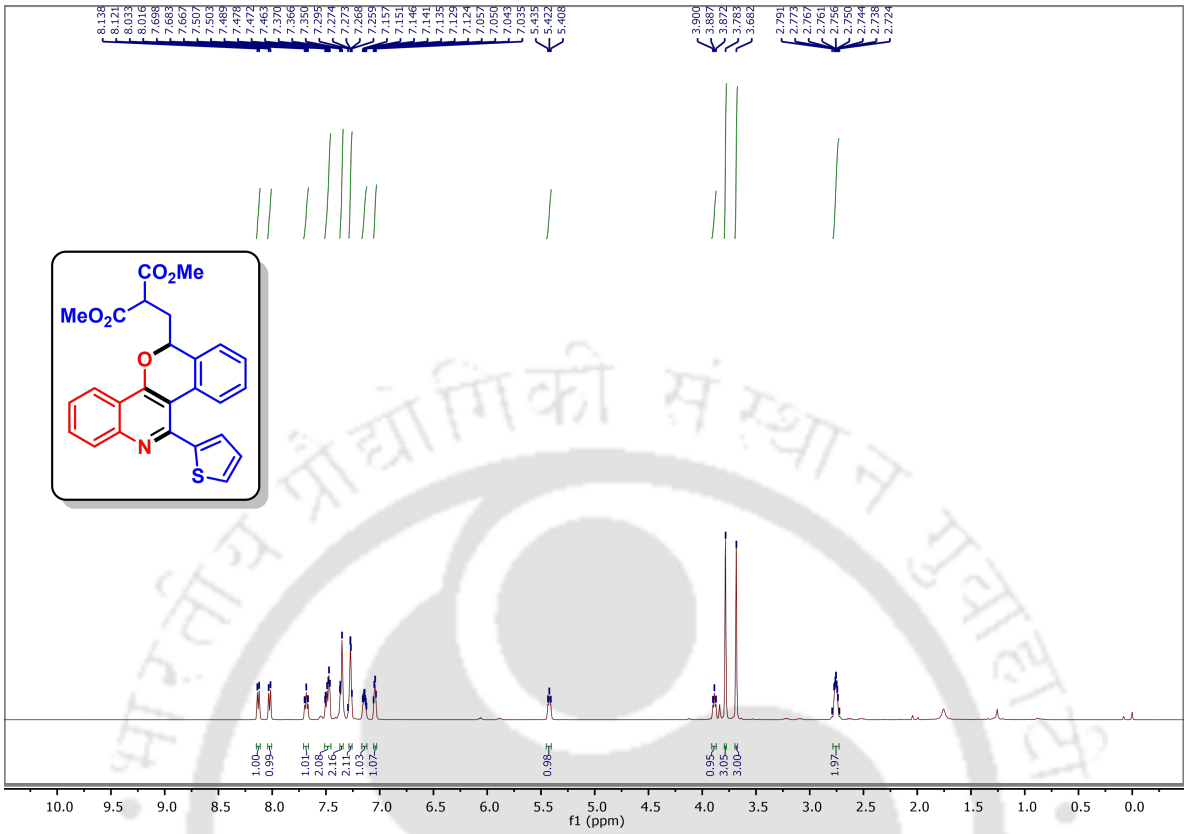

^{13}C{^{1}H} NMR spectrum of compound **32al** (125 MHz, $CDCl_3$)

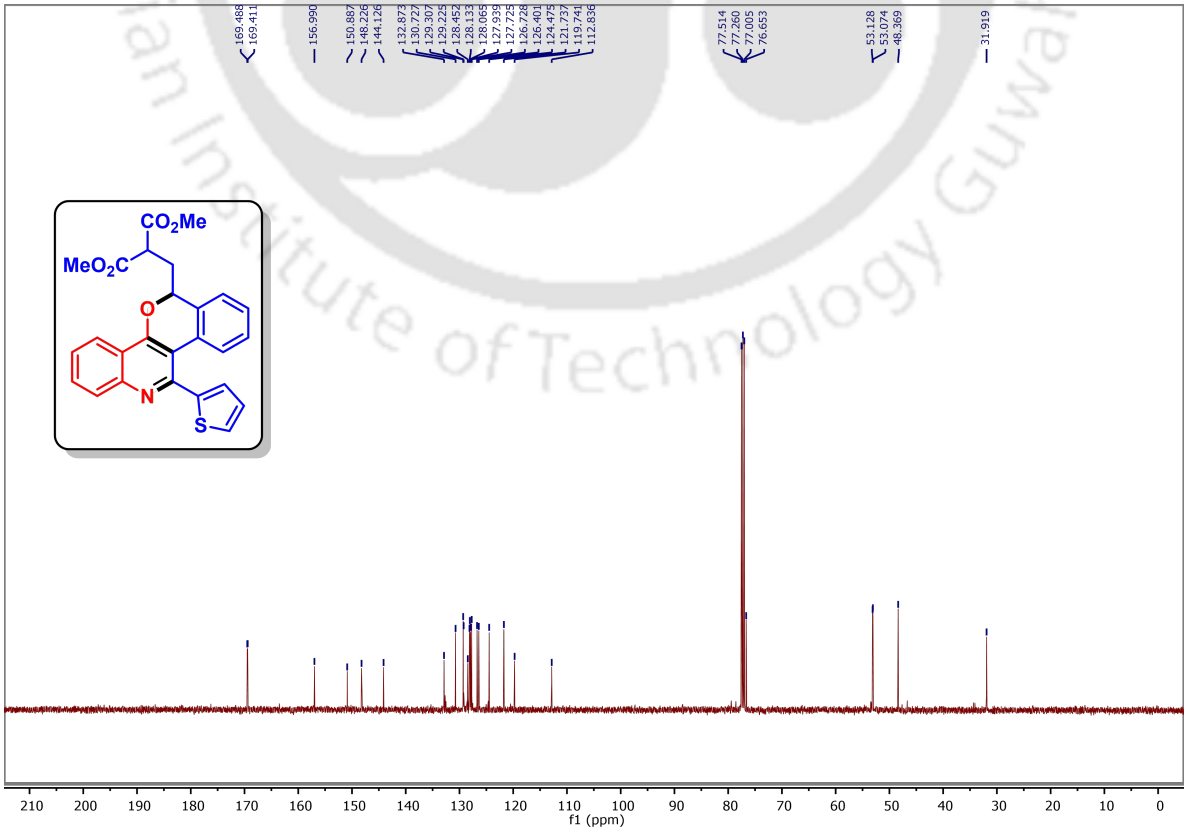

^{1}H NMR spectrum of compound **33** (500 MHz, $CDCl_3$)

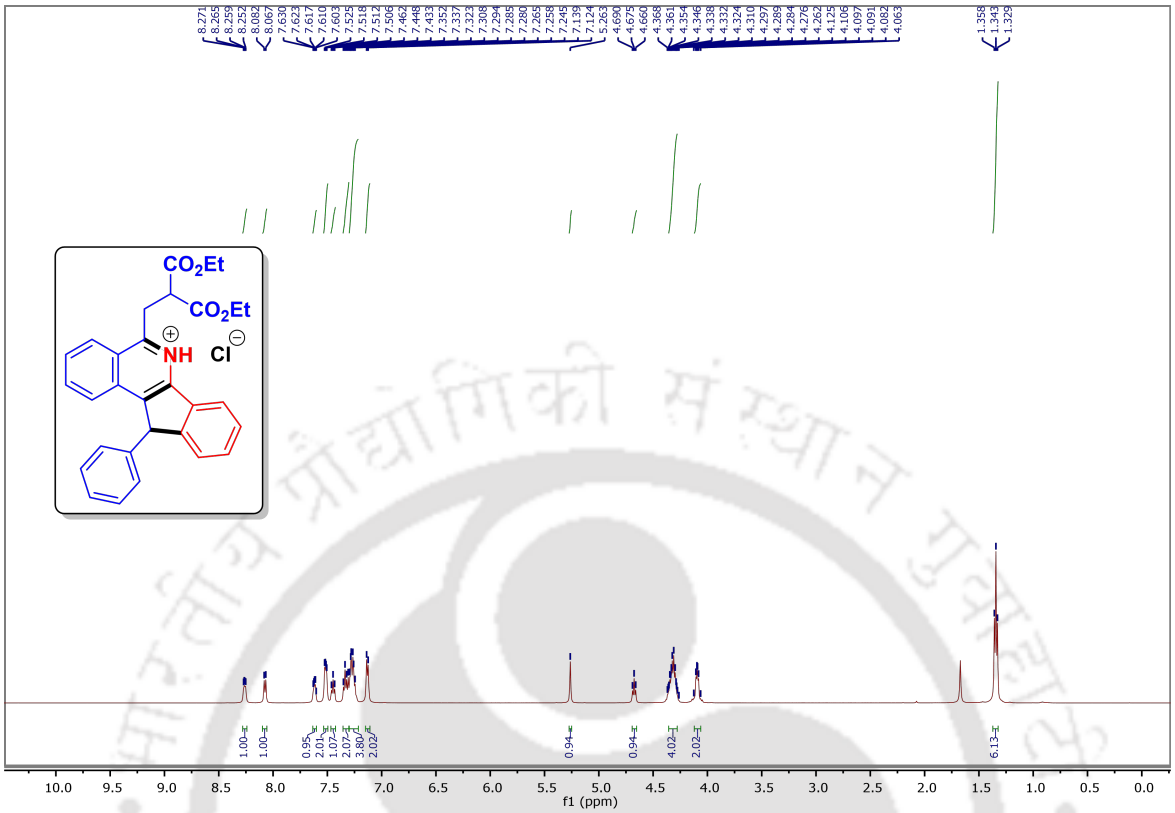

^{13}C{^{1}H} NMR spectrum of compound **33** (125 MHz, $CDCl_3$)

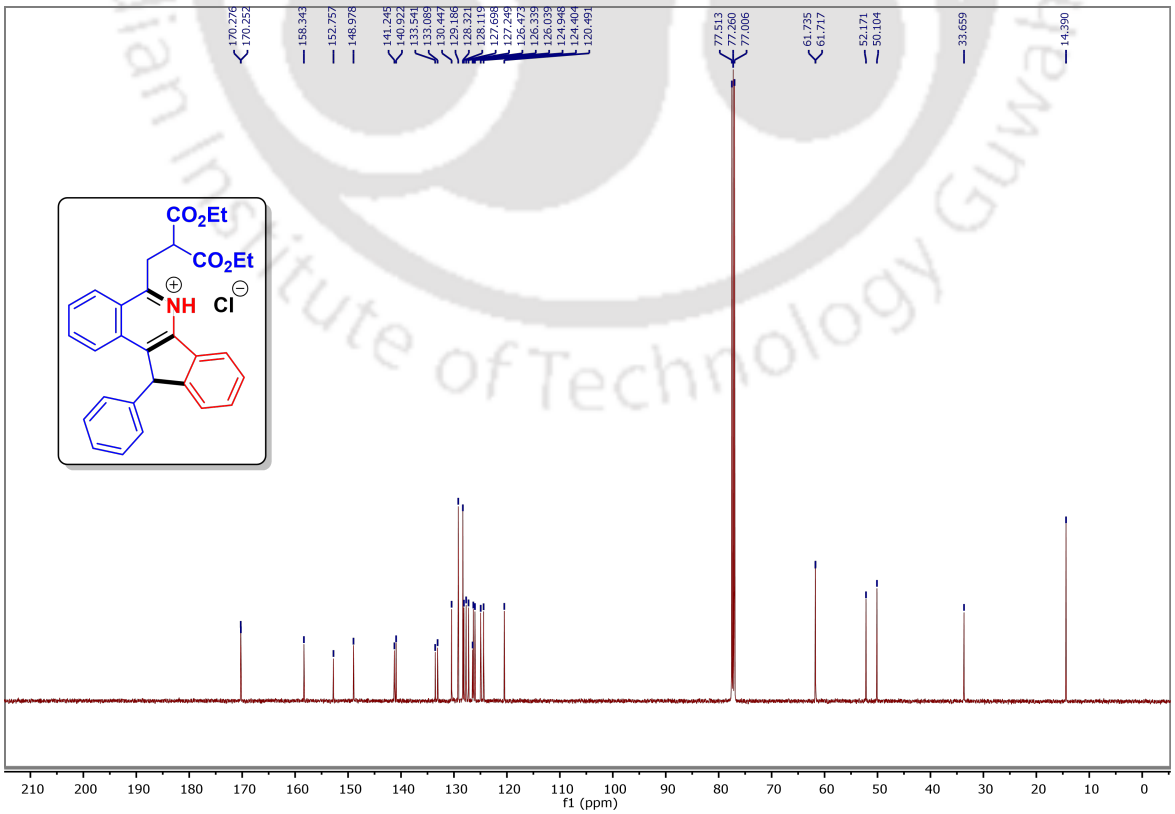

Chapter 6

Thesis Overview, Summary and Outlook, and Future Perspectives

Contents

भारतीय प्रौद्योगिकी संस्थान गुवाहाटी
Indian Institute of Technology Guwahati

Abstract: This chapter summarizes the key outcomes of the thesis, which focuses on the efficient and practical synthesis of diverse fused *N*-heterocycles of biological relevance. Various 1,2,3-triazole-fused isoindolone, isoindoloindolone, pseudoindoxyl, 1,6-naphthyridine, as well as isochromenoquinoline based frameworks were developed through metal-free, Lewis acid-catalyzed/mediated, and base-promoted reactions. The methods are straightforward, scalable, and follow a tandem reaction pathway. The structural features of these compounds offer opportunities for further modifications, biological evaluations, and potential applications in drug discovery and catalysis. The chapter also highlights future directions to expand the scope and impact of the present works.

भारतीय प्रौद्योगिकी संस्थान गुवाहाटी
Indian Institute of Technology Guwahati

6.1 Thesis Overview

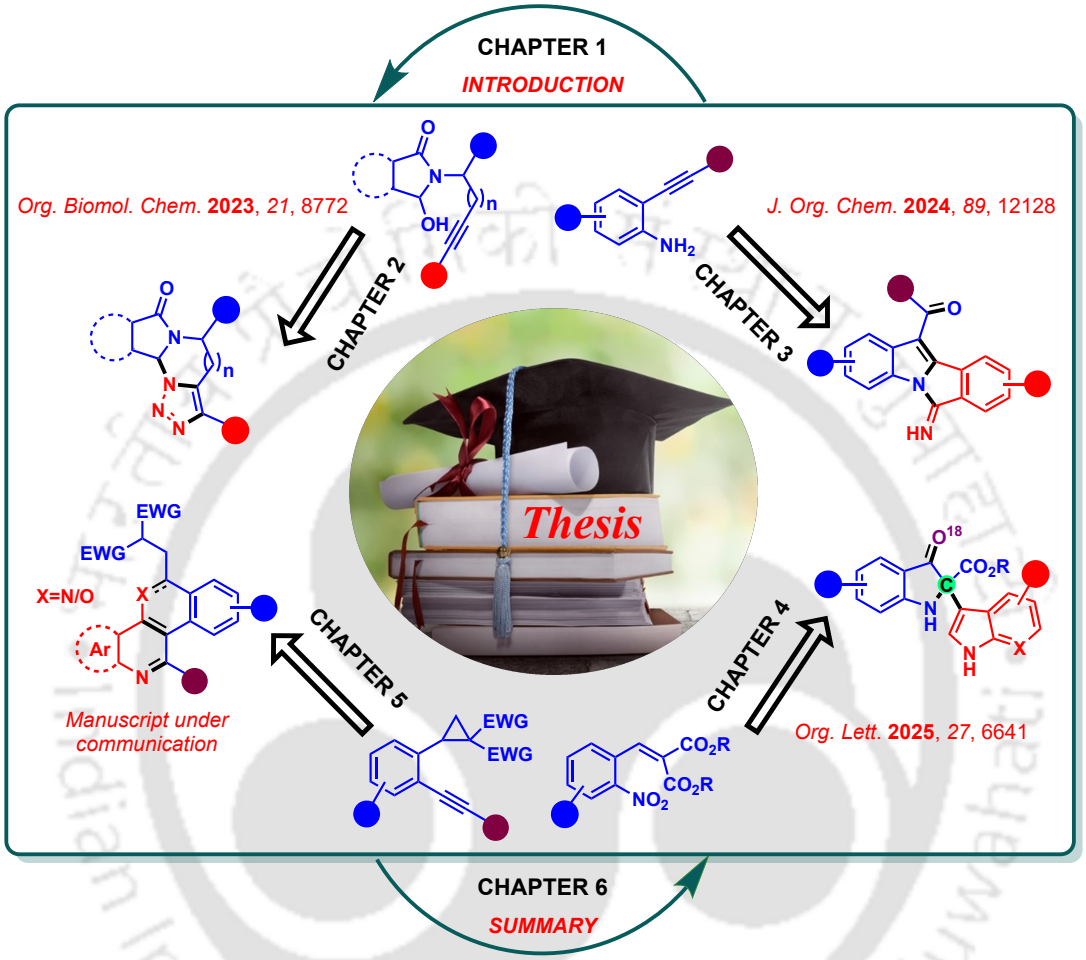

6.2 Summary and Outlook

This thesis focuses on the advancement of efficient and straightforward one-pot protocols for the synthesis of biologically relevant fused *N*-heterocycles *via* tandem cyclization of alkenyl or alkynyl functionalities. Key frameworks such as triazole-fused *N*-heterocycles, iminoisoindoloindolones, pseudoindoxyls, 1,6-naphthyridines, and isochromenoquinolines were synthesized using metal-free, Lewis acid-mediated/ catalyzed, or base-promoted protocols using readily available starting precursors. These one-pot tandem approaches not only demonstrate a wide range of substrate scope and functional group tolerance but also offer potential for structural modifications, and scale-up applications.

Chapter 1 provides an overview of heterocyclic chemistry with a focus on fused *N*-heterocycles. It highlights the significance of tandem reactions in constructing structurally diverse *N*-heterocyclic compounds and discusses the reactivity of alkenes and alkynes in acid-, base-, or metal-catalyzed cascade processes. The chapter outlines key strategies employing these unsaturated moieties to access complex, functionalized *N*-heterocycles, offering a foundamental understanding of their synthetic utility in organic chemistry.

Chapter 2 presents a transition-metal-free one-pot synthesis of dihydro[1,2,3]triazolo-pyrimidoisoindolones and dihydro[1,2,3]triazolo-diazepinoisoindolones from *N*-alkynyl-3-hydroxyisoindolinones and sodium azide, *via* *N*-acyliminium ion formation and Huisgen cycloaddition. The reaction, promoted by $BF_3{\cdot}OEt_2$ in DMF at 130 °C, offers a straightforward approach to 1,2,3-triazole-fused *N*-heterocycles in moderate to good yields. The methodology also enables the synthesis of its thione analogue through post-synthetic amide thionation.

Chapter 3 describes an efficient cascade synthesis of 6-iminoisoindoloindolones *via* a Lewis acid-catalyzed tandem alkynyl cyclization between 2-alkynylanilines and 2-formylbenzonitriles. Using TMSOTf as the catalyst, the protocol activates the nitrile group and employs water as a nucleophile under open-air conditions, delivering the fused *N*-heterocyclic scaffolds in excellent yields. The methodology is also applicable to the synthesis of bioactive isoindoloindolone and novel diphenylbenzopyrrolizinoisoquinolinone derivatives in good yields.

Chapter 4 outlines a facile and efficient transition-metal-free synthesis of structurally diverse pseudoindoxyls *via* an indole-assisted Michael/domino reaction between 2-nitrobenzylidenemalonates and indoles. Promoted by an inorganic base, the reaction proceeds through Michael addition, nucleophilic addition–elimination, and hydrolysis, with water serving as an oxygen source. The methodology offers good to excellent yields with broad functional group tolerance. Its synthetic utility is further demonstrated by late-stage functionalization and photophysical studies of some selected products.

Chapter 5 demonstrates a substrate-dependent, highly efficient cascade annulation of 2-alkynylcyclopropanes with either 2-azidobenzonitriles or 2-azidobenzaldehydes under Lewis acidic conditions to afford 1,6-naphthyridine and isochromeno[4,3-*c*]quinoline frameworks, respectively, in excellent yields. This protocol, employing only a Lewis acid and readily available substrates, offers a straightforward route to

highly fused *N*-heterocycles, highlighting both synthetic simplicity and methodological advancement.

6.3 Future Perspectives

The synthetic strategies and molecular frameworks developed in this thesis open up promising avenues for further research in the field of heterocyclic and medicinal chemistry. Key future directions are outlined below:

6.3.1 Pharmacological Exploration for Drug Design

The fused *N*-heterocycles synthesized in this thesis, such as triazole-fused isoindolones, iminoisoindoloindolones, pseudoindoxyls, 1,6-naphthyridines, and isochromenoquinolines hold significant potential for drug-discovery. Systematic screening for anticancer, CNS-active, antimicrobial, or enzyme-inhibitory properties could reveal promising candidates for therapeutic development.

6.3.2 Structural Modifications for Medicinal Chemistry

The scaffolds developed herein serve as valuable motifs for further structural modifications such as substitution at reactive nitrogen sites, functionalization of imines, or ring fusion may enhance key features for applications in the field of medicinal chemistry.

6.3.3 Scale-Up Potential for Industrial Applications

Several synthetic methodologies described in this thesis, including metal-free, base-promoted, and Lewis acid-catalyzed/mediated cascade reactions, proceed under mild or streamlined conditions. These operationally simple and environmentally benign features make them highly suitable for scale-up and sustainable synthesis in industrial applications.

6.3.4 Post-Synthetic Diversification for Novel Analogues

The presence of chemically versatile functional groups such as imines, triazoles, and ester functionalities in the synthesized molecules offers multiple avenues for diversification:

- Imines can undergo reduction to secondary amines or participate in multicomponent reactions, cycloadditions, and transition-metal coordination.
- Triazoles offer stability and synthetic flexibility, and may be further modified *via* *N*-alkylation, ring annulation, or metal complexation.
- Pseudoindoxyls may serve as privileged cores for late-stage functionalization or scaffold modifications for the utilization in medicinal chemistry.

6.3.5 Coordination and Catalytic Applications for Future Scope

The nitrogen-rich frameworks explored in this thesis, including 1,6-naphthyridines and triazole-fused isoindolones, exhibit excellent chelating ability with transition metals such as Cu, Zn, and Fe. This feature facilitates their use in the development of metal complexes with potential applications in catalysis, photophysical systems, or metallodrug design.

These future directions collectively aim to enhance the scientific utility, pharmaceutical relevance, and industrial scalability of the synthesized scaffolds, contributing to both academic advancement and translational research.

Appendix A

Lists of Publications in Peer Reviewed Journal and Posters Presented in Conferences

A.1 List of Publications

1. **Arandhara, P. J.**; Saikia, A. K. Efficient Synthesis of Pseudoindoxyls from 2-Nitrobenzylidenemalonates and Indoles. *Org. Lett.* **2025**, *27*, 6641–6647.

2. **Arandhara, P. J.**; Chutia, A.; Biswas, S.; Saikia, A. K. A Lewis Acid-Catalyzed Cascade Synthesis of Fused *N*-Heterocycles from 2-Alkynylanilines and 2-Formylbenzonitriles: Unveiling Iminoisoin-doloindolone and Its Derivatives. *J. Org. Chem.* **2024**, 89, 12128–12142.

3. Chutia, A.; **Arandhara, P. J.**; Saikia, A. K. Synthesis of Highly π-Extended Dihydrobenzo[*a*]Indenocarbazole Scaffolds via Tandem Benzannulation and Friedel–Crafts Reaction of 2-Alkynylanilines and 2-Alkynylbenzaldehydes Promoted by Lewis Acid. *J. Org. Chem.* **2024**, *89*, 11542–11557.

4. Biswas, S.; Bora, S. K.; **Arandhara P. J.;** Saikia, A. K. Regioselective Synthesis of Spiro Quinazolinones via Sequential Hydroalkoxylation and Intramolecular Amide-cyclization of Alkynol Ureas. *New. J. Chem.* **2024**, *48*, 10756-10761.

5. Chutia, A.; **Arandhara, P. J.**; Behera, B. K.; Pradhan, A.; Saikia, A. K. Synthesis of Benzodioxepinones and Benzoxazepinones via Tan-dem Oxidation and Iodolactonization of 2-O/N-Tethered Alkenyl Benzaldehyde Mediated by CuI/TBHP. *ACS Omega.* **2024**, *9*, 14217–14232.

6. Behera, B. K.; **Arandhara, P. J.**; Porashar, B.; Bora, S. K.; Saikia, A. K. Base-Promoted [4 + 2] Annulation Reaction of in Situ-Generated Azadienes from *N*-Propargylamines with Active Methylene Compounds: Access to Highly Functionalized 2-Pyridones. *J. Org. Chem.* **2023**, *88*, 15041–15059.

7. **Arandhara, P. J.**; Behera, B. K.; Biswas, S.; Saikia, A. K. Synthesis of 1,2,3-Triazole-Fused *N*-Heterocycles from *N*-Alkynyl Hydroxyiso-indolinones and Sodium Azide *via* the Huisgen Reaction. *Org. Bio-mol. Chem.* **2023**, *21*, 8772–8781.

8. Biswas, S.; Porashar, B.; **Arandhara, P. J.**; Saikia, A. K. Synthesis of pyrimido[2,1-*a*]isoindolone and isoindolo[2,1-*a*]quinazolinone via intramolecular aza-Prins type reaction. *Chem. Commun.*, **2021**, 57, 11701–11704.

9. **Arandhara, P. J.**; Chutia, A.; Saikia, A. K. Leveraging Cascade Annulation of 2-Alkynylcyclopropanes with Substituted Azides to Access Fused *N*-Heterocyclic Scaffolds. *(Manuscript under revision).*

A.2 List of Conferences

1. **Poster Presentation**

The 34th CRSI National Symposium in Chemistry (CRSI-NSC-34) and CRSI–RSC Symposium, Feb 6, 2025 -Feb 8, 2025, IISER Bhopal, Bhopal, Madhya Pradesh.

2. **Poster Presentation**

FICS 2024 - 7th International Conference on Frontiers in Chemical Sciences, Dec 2, 2024 -Dec 4, 2024, IIT Guwahati, Guwahati, Assam.

3. **Poster Presentation**

Research & Industrial Conclave - INTEGRATION 2023, May 14, 2023 -May 16, 2023, IIT Guwahati, Guwahati, Assam.